Interaction between Wnt and Androgen Receptor (AR) signalling pathways in prostate cancer

Khan, Ruhul Amin

Awarding institution:
King's College London

INTERACTION BETWEEN WNT AND ANDROGEN RECEPTOR (AR) SIGNALLING PATHWAYS IN PROSTATE CANCER

Mohammad Ruhul Amin Khan

Thesis for the Degree of
DOCTOR OF PHILOSOPHY

Supervised by
Dr Aamir Ahmed (Primary supervisor)
Professor Prokar Dasgupta (Clinical Supervisor)

Centre for Stem Cells & Regenerative Medicine
King's College London

August 2021

This thesis is dedicated to my father, whom I lost during the course of this journey

Declaration

I, Mohammad Ruhul Amin Khan, hereby declare that the work presented in this thesis is my own. I also certify that wherever the information is derived from other sources, this has been appropriately acknowledged in the thesis. Here, I would like to thank the following people for their contributions to this study:

- Prof Rui Henrique (University of Porto, Portugal), for providing human prostate tissue, insights into pathology and annotating human tissue samples.
- Michael Millar (University of Edinburgh), for performing the immunostaining of human tissue arrays.
- Chris Thrasivoulou and Tim Robson (University College London), for helping with the confocal imaging of immunofluorescence stained tissue arrays.

Abstract

Cells continuously respond to external and internal cues that can initiate signalling cascades that influence cell functions such as cell size, division, proliferation, survival, motility and differentiation. The signal is generally transduced and amplified within the cells by small molecules (e.g., Ca^{2+}_i) and proteins, that may also form complexes with other proteins. Dysregulation in cell signalling mechanisms play a key role in proliferative diseases such as cancer. Prostate cancer is the most common cancer in men worldwide with significant morbidity and mortality. Androgen deprivation therapy (ADT) is a first-line treatment for prostate cancer and initially regress the cancer, however, the cancer recurs and is termed castration resistant prostate cancer (CRPC).

Androgens and their metabolites (testosterone and 5α-dihydrotestosterone, DHT) are ligands for the androgen receptor (AR), an important cell signalling pathway in prostate cancer. Upon binding with its ligands (e.g., DHT), AR dimerizes and translocate into nucleus to activate gene transcription resulting in evasion of apoptosis. Dysregulation in AR signalling is one explanation for the development of CRPC. Another key cell signalling network is the Wnt pathway. Wnts (Wingless Integration Site) are a large family of secretory glycoproteins that bind to cell membrane receptors and ion channels to initiate an intracellular signal cascade. Free intracellular Ca^{2+} and β-catenin, a 92kDa cadherin that acts as transcription factor co-activator of genes including proto-oncogenes, act as intracellular transducers of Wnt signalling, regulating proliferation, survival and differentiation. Recently, Cx43 has also been shown as an accessory protein in Wnt signal transduction. Overactivation of Wnt signalling leads to cancer initiation and progression.

Individually, AR and Wnt pathways contribute towards carcinogenesis in prostate and other tissues. Although it is known that AR signalling pathway may be modulated by Wnt signalling, suggesting a close relationship between these key cell signalling mechanisms, little is known about (i) the pattern of co-expression of AR and Wnt related proteins in human prostate (ii) reciprocal activation of AR and Wnt signalling by their respective ligands and (iii) if there is a

physical interaction between the transducers of these signalling pathways. Close and reciprocal interaction and co-operativity between AR and Wnt pathways may have important implications for prostate carcinogenesis and therapy.

Here, I have investigated the expression of AR and Wnt related proteins in human prostate tissue and aimed to elucidate the interaction between these two key pathways at molecular and functional levels. I demonstrate, using *in situ* quantitative expression analysis, that AR expression decreases with increasing Gleason grade diagnosis (normal, Grade 3+3, Grade 4+4 and Grade 4+5/5+4), which is used to signify the aggressiveness of prostate cancer. Conversely, the expression of Wnt related proteins (β-catenin, TCF-1 and PYGO2) increases with increase in Gleason grading. These results indicate an antagonistic co-regulation of AR and Wnt signalling proteins in prostate cancer development. Interestingly, Cx43 expression, like that of AR, decreased in higher grade cancer compared to normal prostate. The expression of both AR and β-catenin show an increase in CRPC tissue compared to normal of different grades of prostate cancer.

Functional and molecular mechanisms of interaction between AR and Wnt signalling were investigated using *in vitro* cell culture and immunochemical techniques and prostate cancer cell lines LnCAP that expresses AR and PC3 which does not. I demonstrate for the first time that AR ligands induce stabilization and nuclear translocation of β-catenin and reciprocally, Wnt ligands induce translocation of AR into the nucleus. Wnt ligands also activated nuclear translocation of AR in $PC3^{(AR+)}$ (PC3 cells transfected with AR gene), validating the observations in LnCAP cells. Using co-immunoprecipitation, I also show for the first time that there is a physical interaction between androgen receptor and β-catenin.

The novel results presented here, show that in prostate cancer, AR and Wnt signalling pathways interact at functional and molecular levels and there is a reciprocity of signal activation that results in progression of prostate cancer and contributes towards the development of CRPC.

Acknowledgements

I would like to acknowledge my PhD supervisor, Dr Aamir Ahmed for his support and advice throughout this PhD and for providing me the opportunity to work in his laboratory. I am also grateful to Professor Prokar Dasgupta for his help and support. I am grateful for the support of PCRC charity who funded part of this project and also to King's College Development Fund for their financial support.

I am grateful for the help and insight of Professor Rui Henrique for providing the human tissue samples used in this study. I am grateful to Dr Christopher Thrasivoulou and Mr Tim Robson (University College London) and Mr Mike Millar (University of Edinburgh) for their technical support in imaging and staining experiments, respectively. I would like to thank my lab colleagues, Boyu Xie, Callum Arthurs, Bushra Kanwal, Marta Reyes Corral, Kevin Cao, Victoria Lopez-Cordony for their assistance at various stages of my research project.

Most of all I am grateful to my wife and my family for providing unstinting support throughout my PhD.

Table of Contents

List of Figures

List of Tables

List of Abbreviations

ADT	Androgen deprivation therapy
ACTB	β-actin gene
AIPC	Androgen independent prostate cancer
APC	Adenomatous polyposis coli
AR	Androgen Receptor
ARE	Androgen response element
ARR	Androgen regulatory region
ATP	Adenosine 5’-triphosphate
AU	Arbitrary unit
AUC	Area under curve
Bcl-2	B-cell lymphoma
BPH	Benign prostatic hyper plasia
BSA	Bovine serum albumin
Ca^{2+}_I	Free intracellular calcium
CamKII	Ca2+/calmodulin-dependent protein kinase II
cAMP	Cyclic adenosine monophosphate

Cat. No.	Catalogue number
CDKN1B	Cyclin-dependent kinase inhibitor 1B
CI	Cyclin D1 gen
Ck1α	Casein Kinase 1α
CK	Casein kinase
Cq	Quantitation cycle
CRPC	Castration resistant prostate cancer
CTNNB1	β-catenin gene
Cxn	Connexin
DAG	Diacylglycerol
DHT	Dihydrotestosterone
DKK	Dickkopf
DMSO	Dimethyl sulfoxide
dNTP	Nucleoside triphosphate
Dvl	Dishevelled
ELAC2	*ElaC Ribonuclease Z 2*
EMT	Epithelium to Mesenchymal Transition
ERGTA	Ethylene glycol tetra acetic acid
ER	Endoplasmic reticulum
ER	Oestrogen receptor
ETS	Erythroblast Transformation Specific
FGF	Fibroblast growth factor
FITC	Fluorescein isothiocyanate
FRA-1	FOS like antigen-1 (gene), also known as FOS like 1 AP-1 transcription factor subunit or FOSL1
FZD	Frizzled
g	Gravity
GSTP1	Glutathione S-transferase class π gene
GAPDH	Glyceraldehyde 3-phosphate dehydrogenase (gene)
GnRHAs	Gonadotropin releasing hormone
GPCR	G protein-coupled receptor
GSK-3β	Glycogen synthase kinase-3β
GTP	Guanosine 5’-triphosphate
HDAC	Histone deacetylase
HERG	Horse radish peroxidase
HH	Hedgehog
H&E	Hematoxylin & Eosin
HPC	Hereditary prostate cancer 1

ICC	Immunocytochemistry
Ig	Immunoglobulin
IHC	Immunohistochemistry
IP3	Inositol-1,4,5-triphosphate
IP3R	Inositol-1,4,5-triphosphate receptor
KLK3	Kallikrein 3
KGF or FGF-7	Keratinocyte growth factor
LBD	Ligand binding domain
LEF1	Lymphoid enhancer factor 1(gene)
LnCAP	Lymph node carcinoma of the prostate cell line
LOH	Loss of heterozygocity
LR	Likelihood ration
LRP5	Low density lipoprotein (LDL) receptor-related protein 5
LRP6	Low density lipoprotein (LDL) receptor-related protein 6
MAPK	Mitogen-activated protein kinase
MCF7	Michigan Cancer Foundation-7 cell line
mCRPC	Metastatic castration resistant prostate cancer
miRNA	Micro RNA
MMTV	Mouse Mammary Toumour Virus
MPRCs	Membrane potential regulating compounds
mRNA	Messenger ribonucleic acid
MW	Molecular weight
NA	Numerical aperture
NE	Nuclear envelope
NFAT	Nuclear factor of activated T cells
NLS	Nuclear localisation signal
NES	Nuclear export signal
NPC	Nuclear pore complex
NPT	Normal prostate tissue
PBS	Phosphate buffer saline
PC3	Prostate carcinoma cell line
PCa	Prostate cancer
PCP	Planar cell polarity
PFA	Paraformaldehyde
PIN	Prostatic Intraepithelial Neoplasia
PIP2	Phosphatidylinositol 4,5-bisphosphate
PKA	Protein kinase A
PKC	Protein kinase C

PLC	Phospholipase C
PP2A	Protein Phosphatase 2A
PSA	Prostate specific antigen
PTEN	Phosphatase and Tensin Homolog gene
qPCR	Quantitative polymerase chain reaction
PVDF	Polyvinylidene difluoride
PLC	Phospholipase C
RISC	RNA-induced silencing complex
ROI	Region of interest
RNaseL	Ribonuclease L
RPMI	Roswell Park memorial Institute Medium
TCF-1	T cell factor 1 (gene)
TMPRSS2-ERG	Transmembrane protease serine 2- *ETS-related gene*
TGF	Transforming growth factor
TRPM8	Transient receptor potential channel Member 8
UGE	Urogenital Epithelium
UGM	Urogenital mesenchyme
UGS	Urogenital sinus
WIF	Wnt inhibitory factor
Wnt	Wingless-related integration site
WISE	Wnt modulator in surface ectoderm

CHAPTER I

Introduction

1.1. Prostate

The vocable ‘‘prostate’’ is derived from the Ancient Greek word ‘"προστάτης: prohistani’ which means “to stand in front of”, "protector," or "guardian" and has been attributed to Herophilus of Alexandra, who used this expression in 335 B.C. to delineate the small organ located in front of the urinary bladder (Kirby et al., 1999). Although recognition of prostate as an organ has been recognised only with illustration of prostate and seminal vesicles by Regnier de Graaf around 1660 for over two decades, the accurate anatomical, physiological and pathological depiction of the gland did not seem to have appeared until the Renaissance (Kirby et al., 1999).

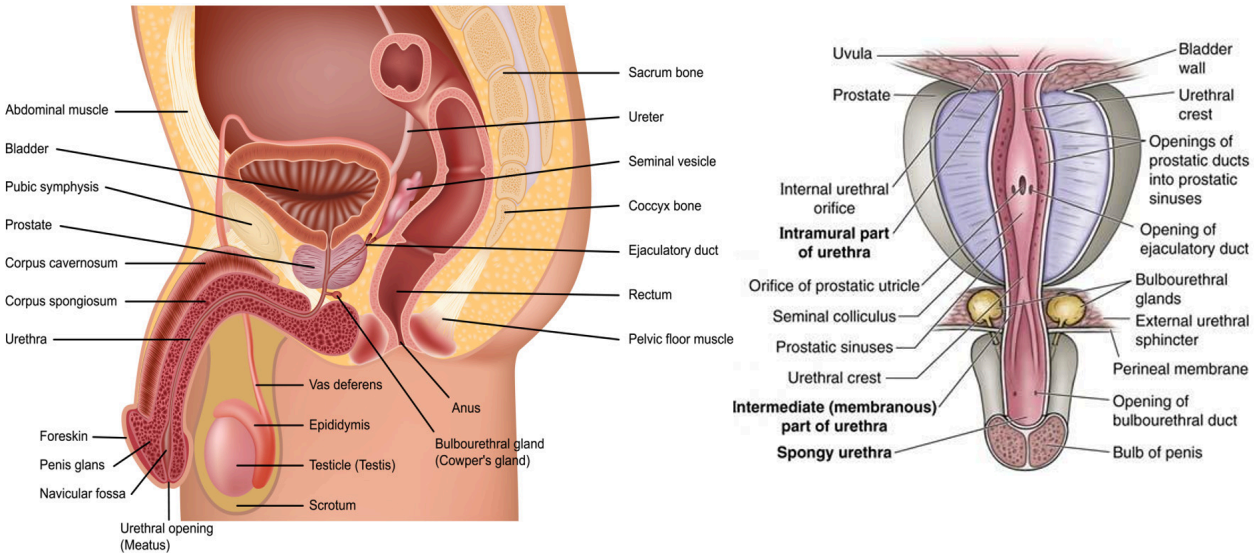

Figure 1.1. Schematic diagram of sagittal and frontal sections of the male urogenital complex illustrating the anatomical position of the adult prostate and associated structures (adapted from https://universityhealthnews.com/daily/prostate/what-is-the-prostate-gland/; accessed on: 12/03/2021).

The human prostate is a small walnut-sized organ shaped like an inverted pyramid, in which the base is the superior surface to the bladder and the apex inferior. The prostate measures between 3 and 4 cm at its widest portion and 4-6 cm long and weighs about 11 grams (range between 7 and 16 grams (Leissner and Tisell, 1979). Despite its size, the prostate gland is the largest male accessory gland, located posterior to the lower portion of the symphysis pubis, anterior to the rectum, and inferior to the urinary bladder in the sub-peritoneal compartment between the

pelvic diaphragm and the peritoneal cavity thus allowing DRE (digital rectal examination, an important, initial, diagnostic method for proliferative diseases of the prostate (Leissner and Tisell, 1979). The prostate surrounds the prostatic urethra, which runs through the prostate from base to apex.

1.2. Function of the prostate gland

The principal function of the prostate gland is to store and extravasate a slightly alkaline, milky or white fluid which contributes to the volume of the semen. The proteins in prostatic fluid are considered to provide nutrition to the seminal fluid. The secretions from the prostate constitute approximately 30% of the volume of semen, together with other 70% of spermatozoa and seminal vesicle fluid (Huggins and Clark, 1940). The alkalinity of semen is thought to neutralize the acidity of the vaginal tract to prolong the lifespan of sperm (Alahmar, 2019). Prostatic fluid is exudate in the first ejaculate fraction along with spermatozoa and the fluid of the seminal vesicle. Furthermore, prostatic fluid ameliorates the motility of spermatozoa, promotes their survival and preserve the distinctiveness of DNA (Alahmar, 2019).

1.3. Prostate anatomical features – a short history

The anatomical illustration of prostate as a male accessory sex gland is old and starts in 1543 (O'Malley and de CM Saunders, 1950). Gerard Blasius termed the mammalian accessory sex glands as ‘‘glandulae’’ surrounding the neck of the bladder in 1674 (Timms, 2008). William Cowper in 1699 first described the topology, structure and function and the glands were named after him as Cowper glands. Alkaline fluid secreted by this gland is thought to protect the sperm. After this, there is a long history of development and improvement leading to current understanding of the prostate and its pathologies (Timms, 2008). Prostate enlargement causing bladder neck obstruction as was suggested by Samuel Collins (Timms, 2008), and re-stablished by Giambattista Morgagni (Franks, 1954), who coined the term benign prostatic hyperplasia (BPH). As the prostate develops, paired bulbourethral glands (Fig. 1.1) sprout from the urethra just beneath the prostate.

In the late 19th century, research began on the anatomical features of embryological development of the accessory sex glands and urogenital structures. A novel procedure of tissue

section reconstruction called ‘‘plattenmodelliirmethode’’ described in 1883 by Born was applied for these anatomical studies. This method of employing wax models as a foundation for demonstrating prostate development has been depicted in different articles (Evatt, 1909) and (Dauge et al., 1986) reviewed by Timms (Timms, 2008). This model was an accurate, influential and anatomical descriptive reconstruction of serial histological sections. This influential model was used as a standard for describing the prostate anatomy in contemporary medical textbooks. McNeal interpreted the history of all the divergent perspectives surrounding this concept (McNeal, 1988b). In addition to this model, several alternative models of prostate anatomy were revealed during last 50 years shown here (Figs. 1.2 and 1.3.A-C) and reviewed extensively by Timms (Timms, 2008). The wider accepted concepts of prostate zones were eventually by McNeal (McNeal, 1988b).

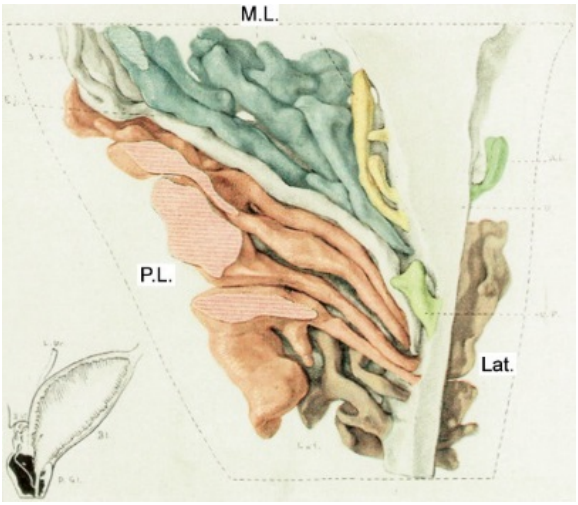

Figure 1.2. An illustration of a newborn male prostate derived from a wax model reconstruction. This sagittal view through the prostatic urethra shows the lobes described by Lowsley (1912). Anterior branches of lateral lobes (Lat.), posterior lobe (P.L.) and middle lobe (M.L.) indicated (Timms, 2008). Image adapted from (Timms, 2008) .

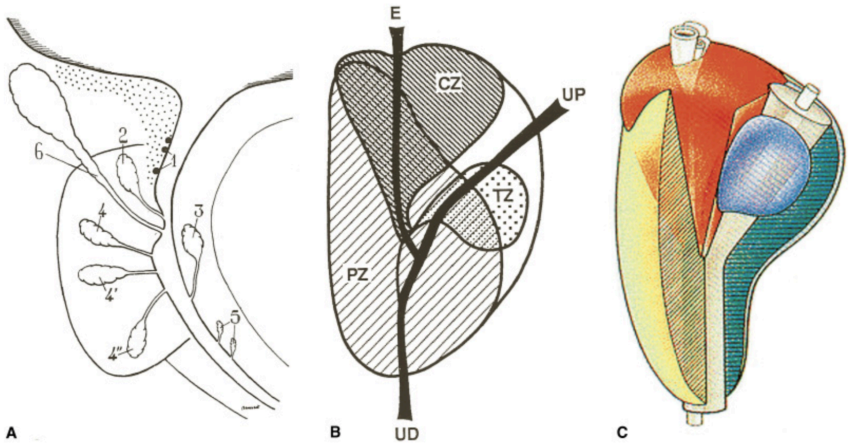

Figure 1.3. A. Sagittal sketching of human prostate showing regional classification of the gland described by (Vernet, 1953). 1 Intrasphincteric submucosal glands; 2 Middle portions of cranial gland; 3 Anterior lobe of the cranial; 4 Superior duct; 4´ Middle duct; 4´´inferior duct of the caudal gland; 5 glands of Littre; 6 ejaculatory duct (Timms, 2008); **B**. Sagittal diagram of adult human prostate showing distal urethra (UD), proximal urethra (UP) and ejaculatory duct (E). These structures showing relationship of three major glandular regions of the prostate described by McNeal (McNeal, 1988b). Central zone (CZ), peripheral zone (PZ) and transitional zone (TZ); **C.** Graphical three-dimensional representation of McNeal's three glandular zones of the prostate. Peripheral zone (yellow), central zone (red), transition zone (blue), anterior fibromuscular stroma (green) (Timms, 2008). Image adopted from (Timms, 2008).

1.4. Prostate development

The susceptibility of prostate to oncogenic transformation is significantly higher than other male secondary reproductive tissues, for instance, seminal vesicles (McNeal, 1988b). As a consequence, statistical investigation in man demonstrates that approximately one in seven will be diagnosed with prostate cancer during their lifetime (Siegel, 2016).

1.4.1. Embryonic development of the prostate

The prostate emerges from the primitive endodermal urogenital sinus (UGS), which give rise to caudal extension of the hindgut during embryogenesis, reviewed in (Timms, 2008).

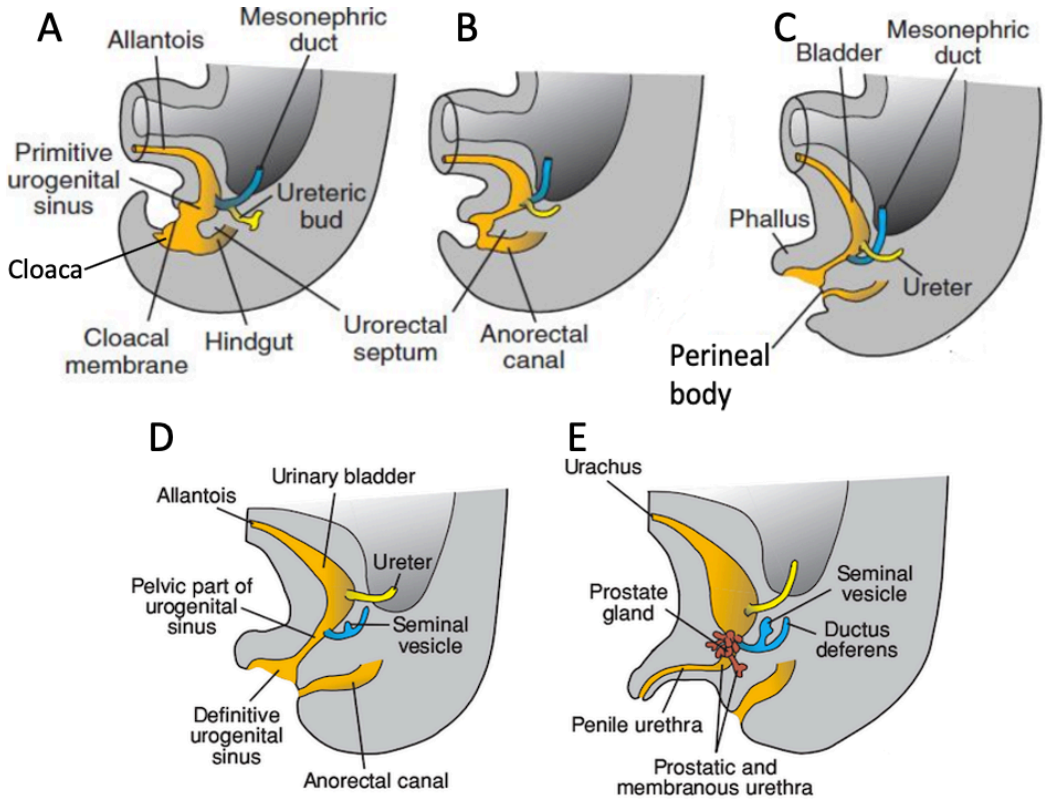

Figure 1.4. Division of the cloaca into the urogenital sinus, rectum and anal canal. **A**. Mid-sagittal view through the pelvis of a 5th week human foetus showing the cloaca, blind caudal extension of the hindgut. The cloaca has a ventral diverticulum, the allantois, extending up the anterior body wall and terminating in the umbilical cord. The urorectal septum grows caudally towards cloacal membrane to subdivide the cloaca. **B**. Mid-sagittal view through the pelvis of a 7th week human foetus showing division of the cloaca into the urogenital sinus ventrally and rectum and anal canal dorsally. **C**. The mesonephric duct is gradually absorbed into the wall of the urogenital sinus, and the ureters enter separately. **D**. Development of the urogenital sinus into the urinary bladder and definitive urogenital sinus. **E**. In the male the definite urogenital sinus develops into the penile urethra. The prostate gland is formed by budding from the urethra, and seminal vesicles are formed by budding from the ductus deferens (Cunha et al., 2004). Image adapted from (Sadler, 2018).

The UGS and hindgut are amalgamated as a single excretory tract at the embryonic cloaca, but the cloaca then divides into separate urogenital and anorectal tracts during 8 weeks of gestation in human (Cunha et al., 2018). The primitive urogenital sinus is subsequently subdivided into the bladder at its rostral end, the urogenital sinus (UGS) in the middle and penile urethra, caudally. The prostate forms through epithelial budding from the UGS, starts to form at approximately 10 weeks of gestation in humans (Cunha et al., 2018). The prostate organogenesis continues after the birth and prepubertal phases of development under the involvement of circulating androgens until the prostate approaches its mature stage during puberty.

Table 1.1. Stage of prostate organogenesis. Adapted from (Cunha et al., 2018).

Developmental event	Rat Age	Mouse age	Human Age	Human Crown-rump	Human Heal-toe
Pre-bud stage	14–18 dpc	13–15 dpc	8–9 wks	30–50 mm	2–5 mm
Initial budding	19 dpc	16–18 dpc	10–11 wks	50–60 mm	5–8 mm
Bud elongation & branching morphogenesis	1–50 dpn	1–40 dpn	11 wks & thereafter	70–80 mm (11wks)	11 mm (11wks)
Ductal canalization	~ 3–50 dpn	~ 3–50 dpn	11wks & thereafter	70–93 mm (11–12wks)	12–14 mm (11–12 wks)

dpc: days post-conception, dpn: days postnatal, wks: weeks.
Prostate organogenesis can be divided into four stages. Stage-1(Pre-bud stage); Stage-2 (Initial budding stage); Stage-3 (Bud elongation and branching morphogenesis stage): Stage-4 (Ductal canalization).

1.4.2. Cellular organisation

The mature prostate epithelium accommodates at least 3 types of cells that are morphologically distinct (i) luminal cells are tall columnar epithelial cells; (ii) below the luminal layer are non-secretory basal cells that line the basement membrane and functionally distinct neuroendocrine cells; (iii) neuroendocrine cells, which constitutes only a small proportion of total human prostatic epithelial cells originate from neural crest (Szczyrba et al., 2017). A layer of intermediate cells remains within the basal layer.

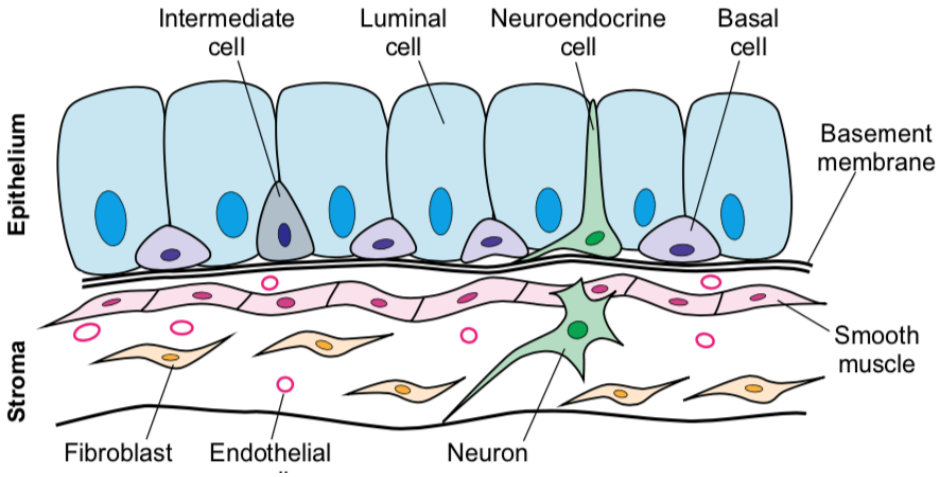

Figure 1.5. Schematic diagram of differentiated cell types of epithelial layer stroma and epithelial layers in adult prostate. The epithelial layers comprise basal cells that line on the basement membrane in between taller secretory luminal cells and sporadically intermediate and neuroendocrine cell populations. The epithelial duct is adjacent to a stromal compartment which possesses smooth muscle cells, fibroblasts, and vascular and neural components (Toivanen and Shen, 2017). The image adapted from (Toivanen and Shen, 2017).

There are a number of differentiated cell types in the mesenchyme (Fig. 1.5), for example, cells of the embryonic UGM form a layer of smooth muscle, lining the epithelium and show contractile activity facilitating the discharge of prostatic fluid into ejaculate (Hayward et al., 1996). Stroma

also includes blood vessels, smooth muscle fibroblast, macrophage, lymphocyte, extra cellular matrix, autonomic nerves, and immune cells.

1.4.3. Zonal structure of Prostate

The first studies of human prostate development described those epithelial buds emerge from the UGE in defined pairs, suggesting that the human gland consists of multiple lobes including anterior lobe (or isthmus), posterior lobe, lateral lobe and median lobe by Lowsley, O.S as reviewed in (Timms, 2008). The model that is now largely accepted was developed by McNeal (McNeal, 1988a and McNeal, 1988b) and comprises of four zones, namely, (1) the peripheral zone, (2) the central zone, (3) pre-prostatic region or transition zone, and (4) the anterior fibromuscular stroma (Fig. 1.6).

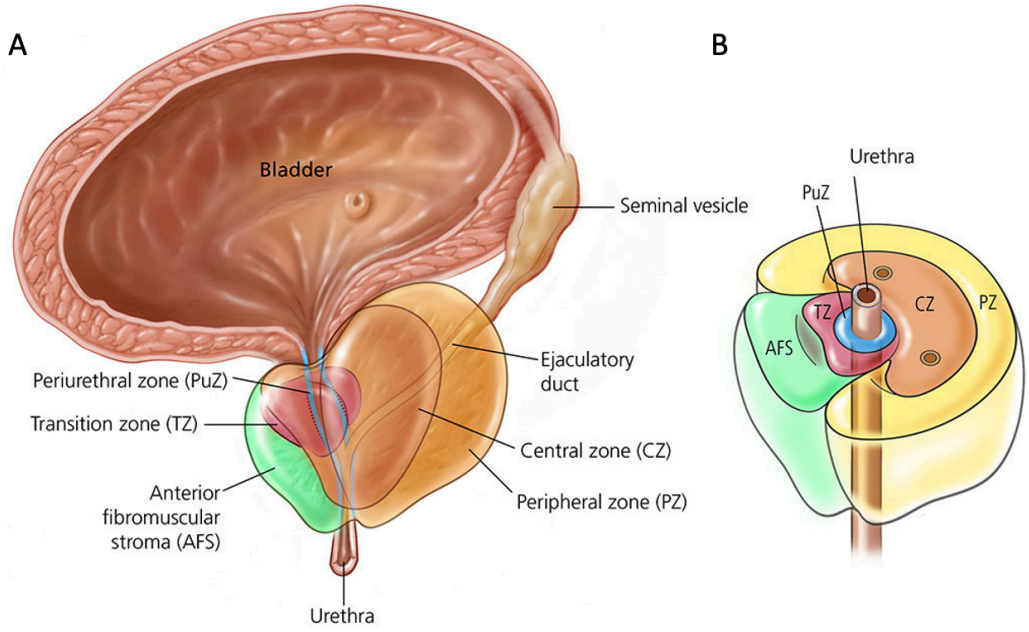

Figure 1.6. overview of prostate anatomy. (A) Coronal plane and (B) axial plane of an adult prostate showing the key structures and regions of the prostate are indicated (McNeal, 1969). Image adapted from Urology Care Foundation (https://www.urologyhealth.org/urology-a-z/p/prostatitis-(infection-of-the-prostate); accessed on 12/03/2021.

1. The peripheral zone: Constitutes ~70% of the glandular prostate volume. It forms a disc of tissue whose ducts originate laterally from the urethra lateral and distal to the verumontanum. The Peripheral zone is a common site of carcinoma.

2. The central zone: Comprises ~ 20% of the prostate. Its ducts arise close to the ejaculatory duct orifices and follow these ducts proximally. This zone branches anteriorly from the prostatic urethra to surround the ejaculatory duct. Its lateral border fuses with the proximal peripheral zone border, completing in continuity with the peripheral zone.

3. Transition zone or Periprostatic region: This zone encircles the urethra and contributes approximately 10% of the prostate formation. The urethral segment proximal to the verumontanum is linked anteriorly at a 35-degree angle to the distal segment. The Transition zone is associated with benign prostatic hyperplasia (BPH).

4. The anterior fibromuscular stroma: The above three categories are developed in epithelium. The human prostate also develops an anterior fibromuscular stroma that surround glandular tissue and fibrous capsule that protects the exterior of the organ.

1.5. Prostate organogenesis

Prostate organogenesis is a complex developmental process. Androgen dependent and other signalling pathways and those involved in mesenchymal-epithelial interactions. An overview of prostate development focusing on recent findings on sexual dimorphism, bud induction and branching morphogenesis and cellular differentiation is provided in the subsequent sections.

1.5.1. Prostate induction: sexual dimorphism in the urogenital sinus

The urogenital sinus can be transformed into either prostate in males or as a part of vagina in females (recently reviewed by (Toivanen and Shen, 2017).

Androgens are steroid hormones (e.g., testosterone, dihydrotestosterone and androstenedione) that are important for the development and maintenance of male characteristics in vertebrates by binding to androgen receptors (AR, see section 1.11). A major trigger for prostate development is testosterone, which is secreted in male embryos at substantially higher quantities than in female embryos, reviewed in (Toivanen and Shen, 2017). Leydig cells in the testes start

to release testosterone at approximately 9 weeks of gestation in humans. Testosterone is converted to dihydrotestosterone (DHT) by 5α-reductase in UGS which then bind to androgen receptor (AR), and translocate into the nucleus where it acts as transcription factor (Berman et al., 1995 and Ferraldeschi et al., 2015).

It has been suggested that the essential role of androgens on UGS means that sexual dimorphism is independent of genetics (Toivanen and Shen, 2017). For instance, XY embryos that have no active AR develop external female genitals and do not form prostate gland (Toivanen and Shen, 2017 and Lubahn et al., 1988). It should be noted that there are limitations to the ability of androgens to induce budding because UGS XX mice quickly lose androgen responsivity in grafts and organ culture on postnatal days P to P5, (reviewed in (Thomson, 2008).

Prostate induction and differentiation require AR expression and activity and AR plays a key role in UGM to induce prostate formation (Cunha et al., 2004). Subsequently, AR is a vital part in the epithelium for the expression of prostatic secretory proteins and for accelerating the differentiation of the surrounding mesenchyme into smooth muscle (Hayward et al., 1998 and Cunha et al., 2004).

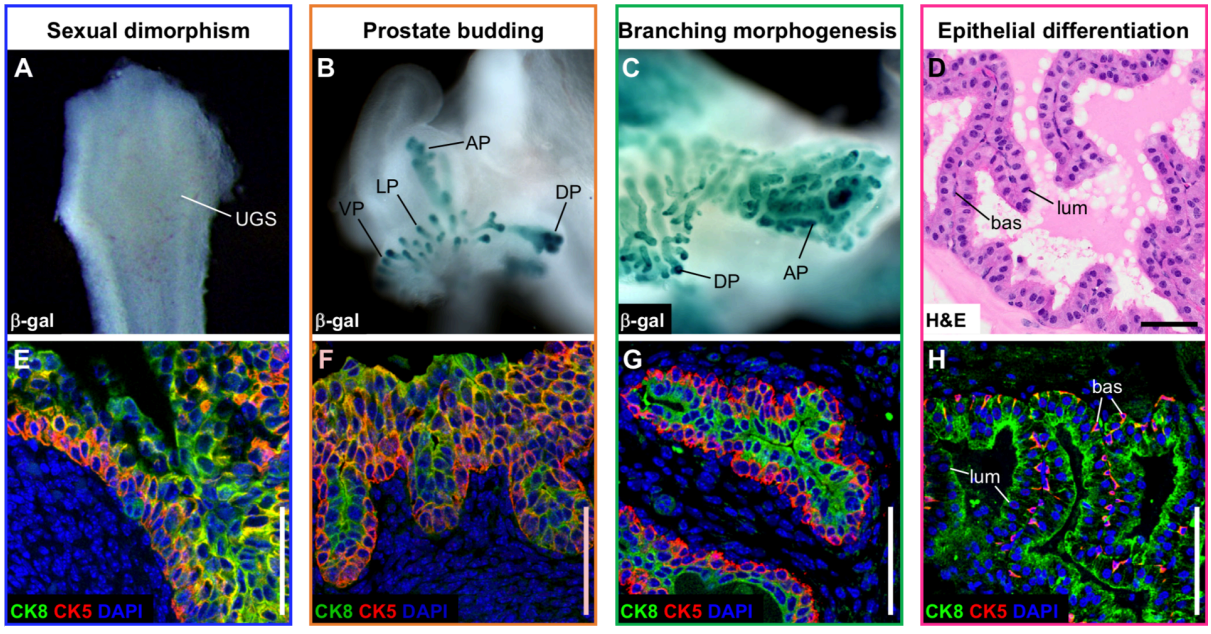

Figure 1.7. Prostate organogenesis illustrating four stages: (A) sexual dimorphism, (B) prostate budding, (C) branching morphogenesis and (D) epithelial differentiation. (**A**) Whole-mount images of *Nkx3.1*$^{lacZl+}$ male mouse UGS stained for β-galactosidase (β-gal) activity at 16.5 dpc showing lacking epithelial buds, (**E**) Immunofluorescence staining for cytokeratin 5 (CK5) and cytokeratin (CK8) showing expression of CK5 and CK8 in majority of urethral

epithelial progenitors. (**B**) Whole-mount images of *Nkx3.1*$^{lacZl+}$ male mouse UGS stained for β-galactosidase (β-gal) activity at P2 showing induction of androgen during epithelial budding resulting in the ductal structures of the four prostatic lobes, (**F**) Immunofluorescence staining for CK5 and CK8 expression of in which higher co-expression of CK5 and CK8 is observed. (**C**) Whole-mount images of *Nkx3.1*$^{lacZl+}$ male mouse UGS stained for β-galactosidase (β-gal) activity at P14 showing continuation of extensive branching morphogenesis during prostate development, (**G**) in which basal segregation of basal and luminal cells are observed. (**D**) Haematoxylin & Eosin (H&E) staining of the 8 weeks old mouse prostatic duct showing excretion in ductal lumen (**H**) displaying individual expression profile of cytokeratin in basal and luminal cells in spite of observation of subsets of intermediate cells. AP, anterior prostate; bas, basal; DP, dorsal prostate; LP, lateral prostate; lum, luminal; VP, ventral prostate. Scale bars: 50 µm. The Image adapted from (Toivanen and Shen, 2017).

1.5.2. Epithelial budding and specification

The outgrowth of the prostate tissue is initiated by the formation of UGE bud under the control of AR. While it is assumed that the expressed AR in the UGM induces UGE specification and differentiation (Toivanen and Shen, 2017). The mechanisms underlying mediating this inferential process are poorly described. The identity of the transitional signals from the UGM to the UGE is particularly ambiguous, and the mechanism of its control by AR signalling are not well understood.

There are two major hypothesis which describe the mechanism of androgens which mediate prostate epithelial induction and budding: the andromedin model and the smooth muscle model. These are illustrated below.

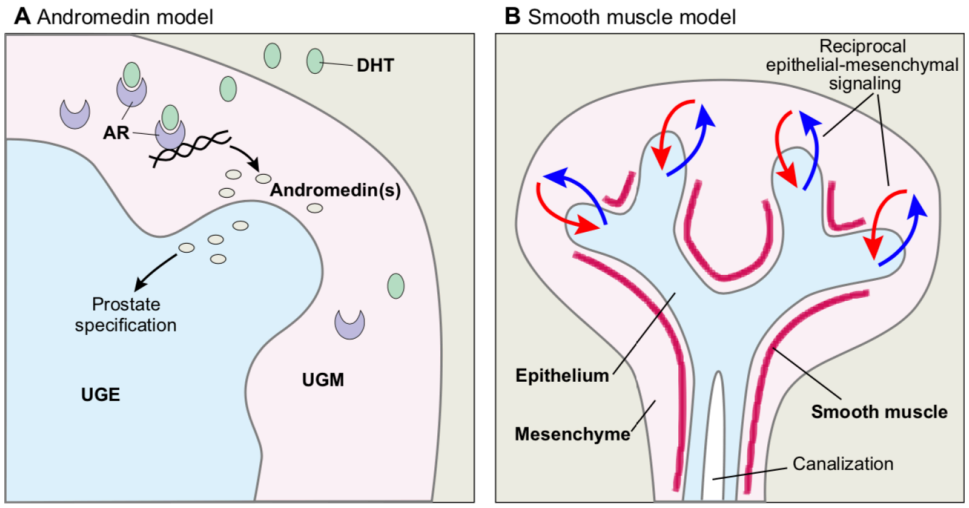

Figure 1.8. Models of prostate bud induction: (A) Andromedin model: This model showing AR expression through androgen signalling in the urogenital mesenchyme (UGM) results releasing one or more signalling factor (andromedins) to induce prostate budding in the adjacent urogenital epithelium (UGE). (B) Smooth muscle model: This model depicting constitutive epithelial budding induced by signal that is being controlled by androgen signalling

within mesenchyme. This model proposed androgen signalling regulates the differentiation of smooth muscle around the growing prostate ducts, thereby impeding further epithelial budding in the regions where smooth muscle has already formed (Toivanen and Shen, 2017). The Image adapted from (Toivanen and Shen, 2017).

1.5.3. Mechanisms and regulation of ductal outgrowth and branching morphogenesis

Following the formation of prostatic bud, ductal growth and branching morphogenesis are initiated with extensive proximal-distal outgrowth and branching of epithelium of a population of progenitor cells localized at the ductal tips, where the majority of proliferative cells are located and bifurcation of the branch points occurs (Sugimura et al., 1986). A number of cell signalling pathways have been implicated in this process including, e.g. Hedgehog (Hh) (Doles et al., 2006) and Activin (Cancilla et al., 2001).

1.5.4. Differentiation of the prostate epithelium

At an early phase of branching morphogenesis, the embryonic prostate is composed of solid epithelial cords, however, these eventually initiate ductal canalization to give rise to glandular formations, while the epithelial cells differentiate into basal, luminal and neuroendocrine lineages.

1.5.4.1. Mechanisms of epithelial canalization

The difference between adjacent seminal vesicle and prostate epithelium in prostatic emergence stage is that the seminal vesicle undergoes branching morphogenesis as hollow tubes and the prostate epithelium undergoes significant branching morphogenesis as solid buds, which then canalize during later stages of the development (Hayward et al., 1996). This has however not been well investigated in prostate although may involve process such as anoikis (Barker, 2014).

1.5.4.2. Lineage specificity during organogenesis, homeostasis and regeneration

Differentiation of stem cells is an important process in the development of an organ where stem cells give rise to specific lineages of cells within a tissue. For human prostate, there are not many reliable studies identifying the stem cells or their niche. Multiple stem/progenitor populations are thought to be localized in the prostate that give rise to specific distribution and functions during organogenesis and regeneration. A model of this is shown in Fig. 1.9.

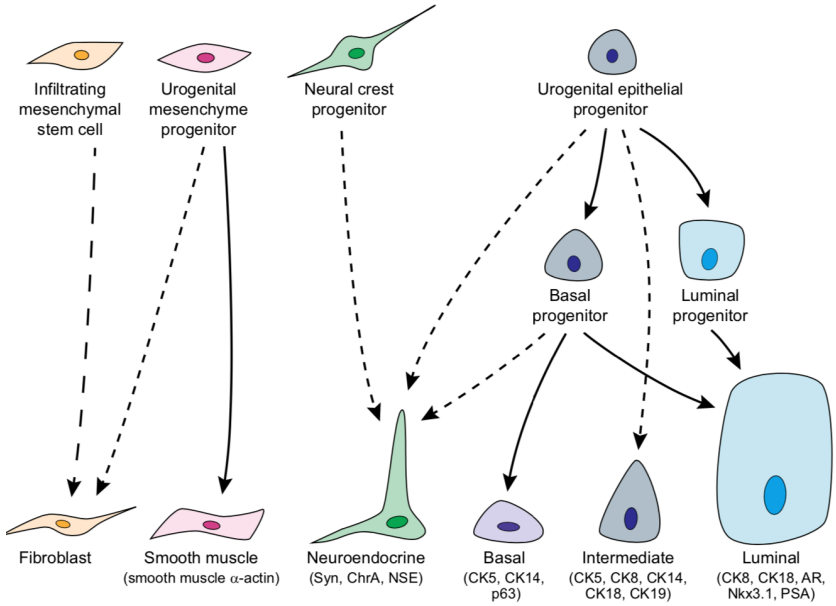

Figure 1.9. Lineage relationships between cell types during prostate organogenesis depiction. Solid arrows, dashed arrows indicate known and potential relationships respectively. Initiation of prostate budding, the urogenital epithelial progenitor produces basal progenitors with multipotent and unipotent functions and unipotent luminal progenitors. The neuroendocrine and intermediate cells seem to derive from urogenital epithelial progenitors, additionally neuroendocrine could be originated from neural crest progenitor. Urogenital mesenchyme progenitors give rise to differentiated smooth muscles in the prostatic stroma but origination of fibroblast from EGM progenitors and is still befuddle. ChrA, chromogranin A; NSE, enolase 2 (Eno2); Syn, synaptophysin (Syp). The Image adapted from (Toivanen and Shen, 2017).

1.6. Diseases of the prostate

Diseases of prostate glands are categorized into three distinct types: Prostatitis, Benign Prostatic Hyperplasia (BPH) and Prostate Cancer.

1.6.1. Prostatitis

Prostatitis is, an ill-defined inflammatory or infectious condition affecting the area around the prostate, an extremely common condition worldwide; around 2% - 10% of men are diagnosed with it during their lifetime (Krieger et al., 2002).

Prostatitis was primarily classified as acute bacterial prostatitis, chronic bacterial prostatitis, nonbacterial prostatitis and prostatodynia. In 1999, the National Institute of Digestive and Kidney Diseases (NIDDK) Chronic Prostatitis Workshop proposed a modified classification system of prostatitis syndromes (Krieger et al., 1999 and Krieger et al., 2002). The NIH categorizes these from I to IV:

I: acute bacterial prostatitis

II: Chronic bacterial prostatitis

III: Chronic nonbacterial prostatitis

IV: Asymptomatic inflammatory prostatitis

Pelvic region discomfort is a common symptom. Of these Category III is most prevalent (accounting for nearly 95% of all cases).

1.6.2. Benign Prostatic Hyperplasia (BPH)

A non-malignant enlargement of the prostate in men due to the excessive proliferation of stromal and glandular epithelial cells in the transition of the prostate and characterized by urethral obstruction, and lower urinary tract symptoms (Roehrborn, 2008 and Homma et al., 2011).

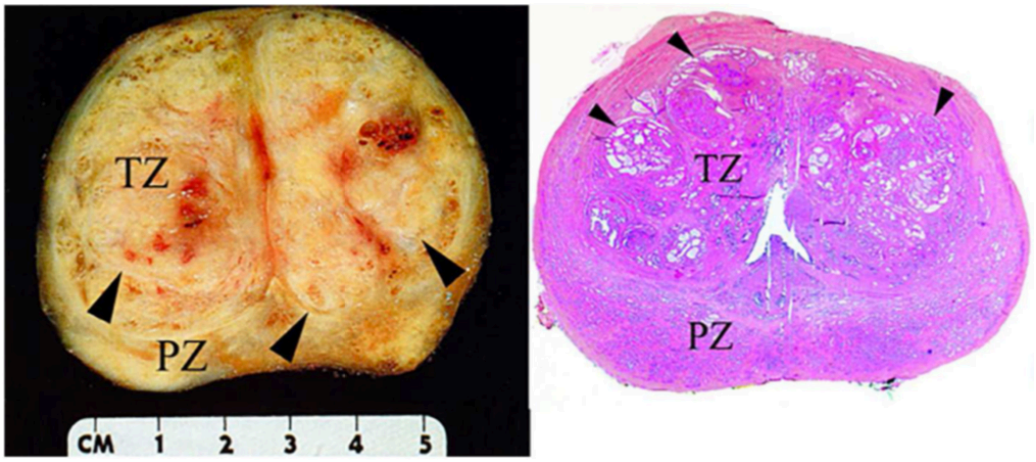

Figure 1.10. Left. Gross anatomy of prostate showing BPH in the transitional zone. Hyperplastic lump indicated by arrow, is observed in the transition zone (TZ) that absence in the peripheral zone (PZ). Right. Hematoxylin and eosin (H&E) stained wholemount cross-section of a human prostate showing the effect of BPH in TZ (Aaron et al., 2016). The image adapted from (Aaron et al., 2016).

Nearly 50% of men are diagnosed BPH by 50 years of age, and 90% of men are diagnosed with BPH when they are 70-79 years of age. Men with BPH experience great discomfort while urinating and often develop urinary tract infections (UTIs) and sometimes renal failure (Homma et al., 2011).

1.6.2.1. Aetiology of BPH

The detailed molecular aetiology of this hyperplastic disease is not yet known but may involve epithelial and stromal cell proliferation contributed by androgens, oestrogens, stromal-epithelial interactions, growth factors and cytokines, or to impaired programmed cell death or to impaired apoptosis leading to cellular accumulation (Roehrborn, 2008).

1.6.2.1.1. The role of androgens in BPH

Presence of testicular androgens is required during prostate development, puberty or aging (Sec. 1.5) (McConnell, 1995). Dihydrotestosterone (DHT) and androgen receptor remain highly expressed in prostate with aging, despite the fact that level of peripheral testosterone is reduced with aging (Harman et al., 2001). Once BPH has developed, withdrawal of DHT can shrink the BPH. Withdrawal of DHT, a ligand for AR, the androgen-sensitive tissue reduces protein synthesis resulting in an involution of BPH (Peters and Walsh, 1987). It is estimated that 90% of total prostatic androgen is derived from testicle is in the form of DHT while the rest from adrenal glands (Andriole et al., 2004). DHT bound AR translocates into the nucleus to activate gene transcription and eventually stimulation of the protein synthesis.

1.6.2.1.2. The role of Growth factor

Growth factors, e.g., bFGF (FGF-2), acidic FGF (FGF-1), Int-2 (FGF-3), keratinocyte growth factor (FGF-7), transforming growth factor (TGF-8) and epidermal growth have been associated in prostate growth. These are naturally occurring small peptide molecules that stimulate and in some cases inhibit cell proliferation and differentiations (Kyprianou and Isaacs, 1989). It has been proposed that cross interaction between growth factors and steroid hormones may alter the balance of cell proliferation versus cell death to produce (BPH) (Story et al., 1989).

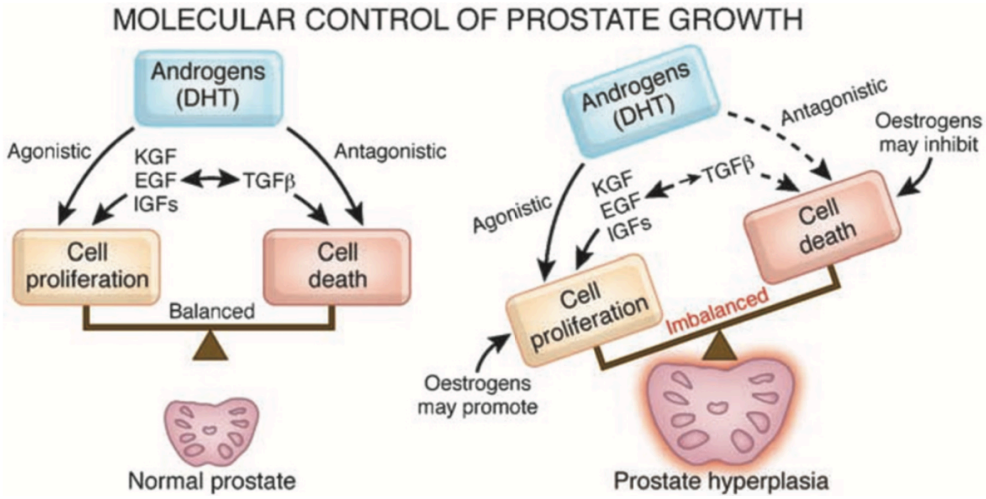

Figure 1.11. Displaying cellular homeostasis interacted by growth stimulatory and inhibitory factors in prostate gland in activated by testosterone and DHT. Right, depicting the imbalance and abnormal growth in BPH (Roehrborn, 2008). The figure adapted from (Roehrborn, 2008).

1.6.3. Prostate cancer

PCa was first described by the ancient Egyptians, while surgical procedures to remove the prostate were developed over 100 years ago (Capasso, 2005). A vast majority (~95%) of prostate cancers are adenocarcinomas arising from epithelial cells, (Bostwick, 1989b); of these nearly 70% of PCa are developed in the peripheral zone, 15-20% in the central zone, and 10-15% in the transitional zone. Some cancer grows slowly and other grows fast (Cancer, 2003). In the early stages, PCa is asymptomatic, however, patients with advanced PCa often suffer from painful urination, starting or stopping the urine flow, a frequent need to urinate, and blood in the urine (Cancer, 2003). Metastasized PCa commonly causes severe pain, mainly due because of metastases to the bone. PCa is a multifactorial disease, and several genetic and non-genetic factors are involved in its initiation and progression.

1.6.3.1. Epidemiology of PCa

PCa is the second most frequent malignancy and second leading cause of male cancer death worldwide. With an estimated 12,76,106 new cases and causing 3,58,989 deaths, 3.8% death of all death caused by cancer in men, have been recorded globally (Bray et al., 2018 and Ferlay et al., 2018b). There is a wide range in the incidences and mortalities of prostate cancer across the globe which increase with the increase of average age. The incidence rates are higher among the

African-American men compared to white men with 158.3 new cases diagnosed per 1,00,000 men and their mortality is approximately twice as white men (Panigrahi et al., 2019). Social, environment and genetic factors are the reasons for the discrepancy. New cases of projection have been estimated at 22,93,818 until 2040 by (Ferlay et al., 2019) and showed that there will be small variation, an increase of 1.05%, in mortality. A detail analysis of worldwide prostate cancer incidence, mortality rates as well as their temporal trends and survival rates based on GLOBOCAN 2018 estimates are presented here (Rawla, 2019).

1.6.3.1.1. Incidence of PCa

12,76,106 cases of global incidence of PCa representing 7.1% of all cancer in men was recorded in 2018 (Bray et al., 2018), but this incidence rate is highly variable (Bray et al., 2018) (Fig. 1.12). A major factor for this variability is likely to be the variability in PSA testing (Quinn and Babb, 2002).

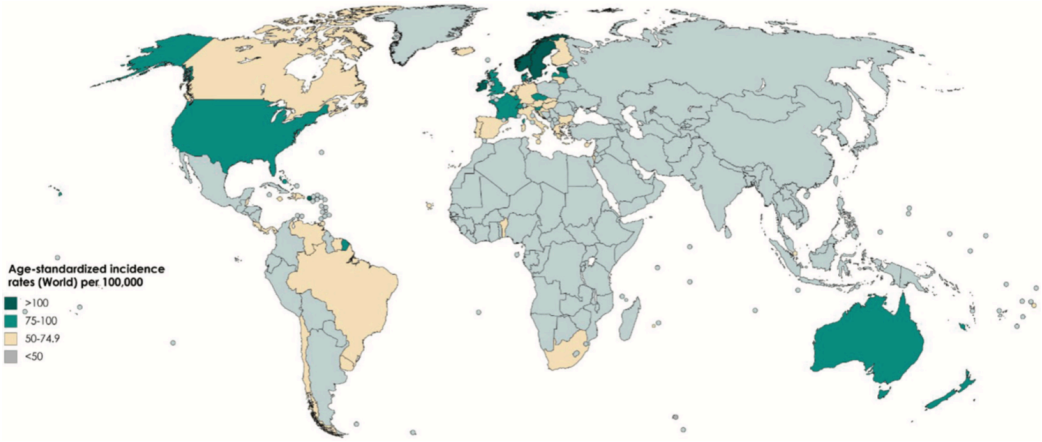

Figure 1.12. Map showing the global registered age-standardised incidence rates of prostate cancer in 2018 in men with variable ages. The map was obtained from (Rawla, 2019) created with mapchart.net with data obtained from GLOBOCAN 2018 (Bray et al., 2018).

The incidence age-standardized rate (ASR) appeared to be highest as 79.1/100000 people in Oceania, then 73.7/100000 people in North America and 62.1/100000 people in Europe followed by a lower incidence rate in Africa and Asia at 26.6 and 11.5 per 100000, respectively (Ferlay et al., 2018a). The incidences also fluctuated with population density for instance, the incidence rates were 190-fold higher at 189.1 in Guadeloupe and France than at 1.0 in Bhutan. The rate of PCa incidence increases correlatively with increase of age (Ferlay et al., 2018a). Only 1 in 350 men

under the age of 50 is diagnosed with PCa (Perdana et al., 2016) but the rate increases to 1 in every 52 men for ages 50 to 59 and further increases to 60% in men over the age of 65 years (Howlader et al., 2013).

1.6.3.1.2. Mortality statistics for PCa

Universal mortality rates for PCa also fluctuate worldwide (Fig. 1.13) (Ferlay et al., 2018c) . The PCa mortality rates were registered higher at 10.7 per 1,00,000 in Central America than Australia and New Zealand with 10.2 and Western Europe with 10.1 respectively (Ferlay et al., 2018c) . The lowest rate was reported in the countries of Asia (South-Central, 3.3; Eastern 4.7 and South-Eastern 5.4) and Northern Africa (5.8) (Fig. 1.13) (Ferlay et al., 2018c).

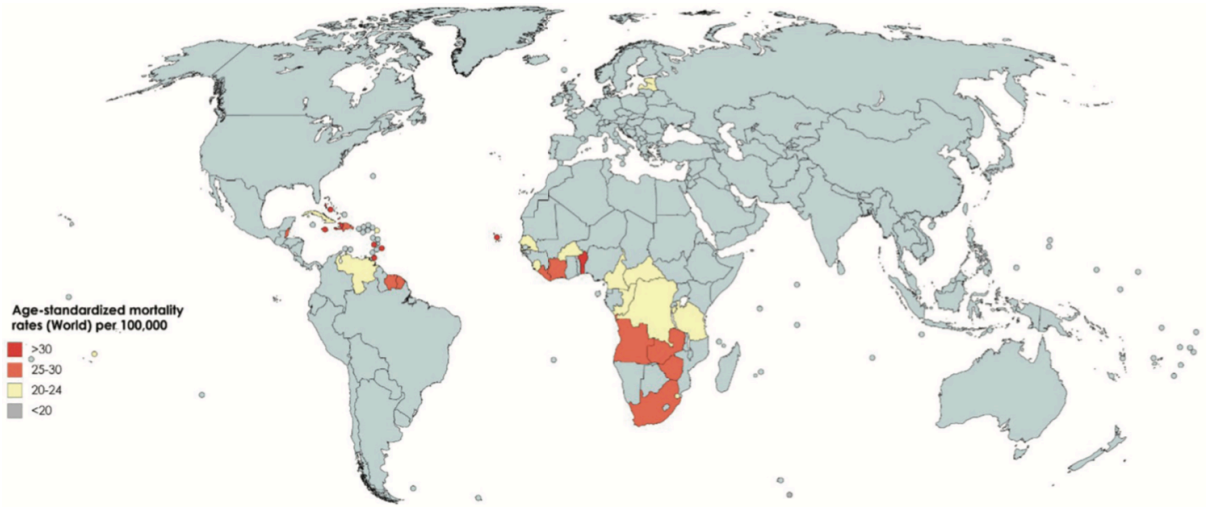

Figure 1.13. Map showing estimated age-standardised morality rates of PCa worldwide in 2018 in males including all ages. The map was obtained from (Rawla, 2019) created with mapchart.net with data obtained from GLOBOCAN 2018 (Bray et al., 2018).

1.6.3.1.3. Trends for PCa

An increasing trend of prostate cancer incidence is predicted with 1,017,712 worldwide which changes +79.7% overall till 2040 (Table 1.2) (Ferlay et al., 2019) . In Africa, the projected number of incidences for prostate is projected in 2040 to be at high as 97,663, that constitutes +120.6% followed by Latin America and the Caribbean with +101.1% and Asia with 100.9% and in Europe with lowest incidence as +30.1%.

Table 1.2. Estimation of incidence trend to increase from 2018 to 2040 for PCa in Males in all ages (Ferlay et al., 2019). The table adapted from (Ferlay et al., 2019).

		2018	2040			
		Number	Number	Demographic change	Change in risk	Overall change
Africa	Males (APC 0%)	80,971	178,634	97,663 (+120.6%)	97,663 (+120.6%)	97,663 (+120.6%)
Latin America and the Caribbean	Males (APC 0%)	190,385	382,808	192,423 (+101.1%)	192,423 (+101.1%)	192,423 (+101.1%)
North America	Males (APC 0%)	234,278	312,901	78,623 (+33.6%)	78,623 (+33.6%)	78,623 (+33.6%)
Europe	Males (APC 0%)	449,761	585,134	135,373 (+30.1%)	135,373 (+30.1%)	135,373 (+30.1%)
Asia	Males (APC 0%)	297,215	597,180	299,965 (+100.9%)	299,965 (+100.9%)	299,965 (+100.9%)

From 2018 to 2040, it is estimated that mortality will be double with 3,79,005 worldwide (Ferlay et al., 2019). The highest mortality rate is estimated to be in Africa with +124.4% followed by Asia with 116.7% while the lowest incidence will be recorded in Europe with +58.3% (Ferlay et al., 2019). Figs. 1.14 and 1.15 show incidence and mortality and region-specific incidence and mortality from PCa.

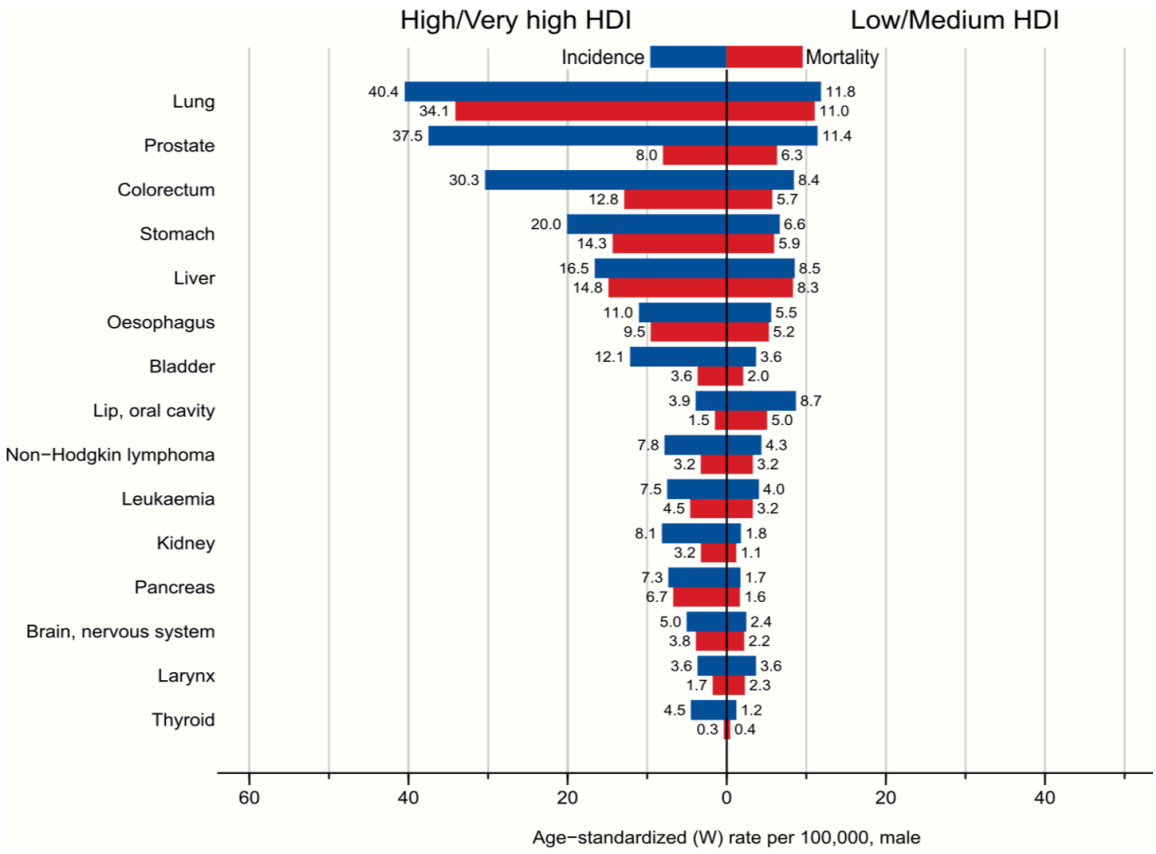

Figure 1.14. Bar charts of incidence and mortality at age-standardized rates in High/Very-High Human Development Index (HDI) regions vs Low/Medium HDI Regions among males in 2018. The most 15 common cancers world (W) in 2018 are shown in descending order of the overall age-standardized rate for males (Source: GLOBOCAN 2018) (Bray et al., 2018). The graph adapted from (Bray et al., 2018).

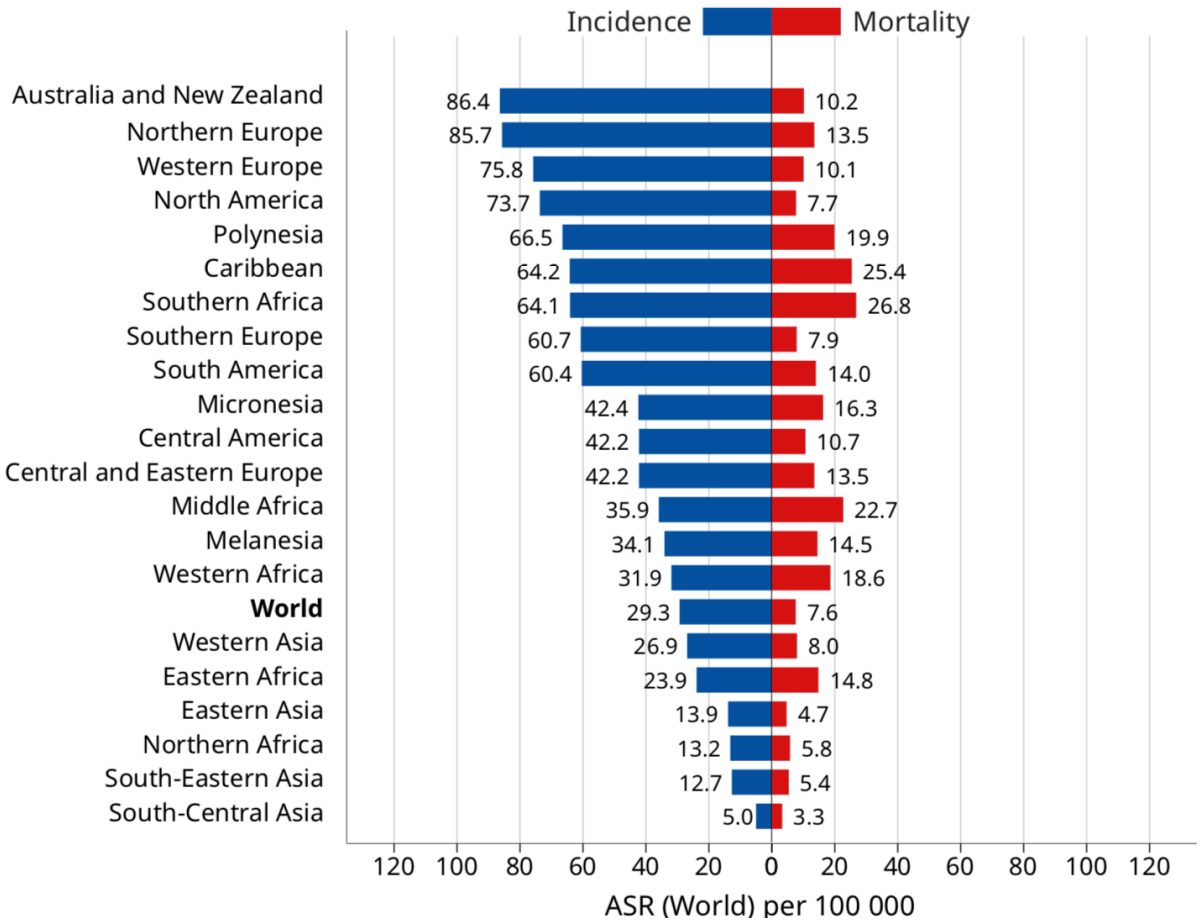

Figure 1.15. Dual Bar chart showing Region-Specific Incidence and Mortality Age-Standardized Rates for the PCa in 2018. Rates are shown in descending order of the world (W) age-standardized rate, and the highest national age-standardized rates for incidence and mortality are superimposed. Source: GLOBOCAN 2018 (Bray et al., 2018). The graph adapted from (Bray et al., 2018).

1.6.3.1.4. Survival rates after diagnosis of PCa

The prognosis is best when the cancer is confined to the organ and the rate for 5 year survival in the USA was reported to be about 98% (Howlader et al., 2016a). The incidence of PCa from 2003 to 2007 in Eurocare project (EUROCARE-5) showed that 5-year survival rates were 83% (Epidemiology of Prostate cancer in Europe, 2015). The survival rate fluctuates from 76% in Eastern countries to 88% in Southern and Central European countries. All over Europe the survival has increased over the period of 2003-2007, specifically with the greatest improvement being registered in the Eastern European countries (De Angelis et al., 2014).

1.7. Aetiology and risk factors for PCa

The aetiology of prostate cancer remains elusive, compared to other common cancers such as breast cancer (Shulewitz et al., 2006). The well-understood risk factors for PCa development are not limited to advanced age, ethnicity, genetic factors, family history (Bostwick et al., 2004a; Dagnelie et al., 2004; Bostwick et al., 2004b and Pienta and Esper, 1993). Other factors which are possibly associated with PCa including: obesity and physical inactivity, inflammation, hyperglycaemia, infections, environmental exposure to chemicals or ionizing radiation and diet involved in increased consumption of saturated animal fat and red meat, lower intake of fruits, vegetables, vitamins and coffee (Kolonel et al., 2004). Some of these are discussed below.

Age is considered a major risk factor for PCa. It is often suggested that PCa is a disease of older men (Bray et al., 2018). It is unusual in men younger than 40 years but PCa incidence increases in each decade after 40. The average age for PCa diagnosis is over 75 years old in the UK (Cancer Research UK, 2014b), 65 - 74 years in the USA (Surveillance, Epidemiology and End Results (SEER) 18, 2014). Around 30% of men who have died with different diseases other than PCa cancer, were found with histological diagnosis of PCa during autopsy (Scardino et al., 1992). Hence, it is often suggested that most men die 'with' PCa than 'of' PCa. The mortality rate can be reduced by clinical tests for the premalignant stage of PCa development and development of reliable, quantitative biomarkers for the prognostication of PCa are necessary to avoid unnecessary deaths due to PCa.

Ethnicity can also be characterized as a risk factor due to differential rates of diagnosis and death amongst various ethnicities and PCa development varies from one ethnic group to another (Ben-Shlomo et al., 2008). The risk of PCa development in men of Caucasian ethnicity, who have no familial history of prostate cancer, is increased after 50 years of age, but in black men or men with a familial history of prostate cancer PCa occurs after 40 years of age (Prostate Cancer. SEER, 2018). A significant ethnic variation occurs for the risk of PCa in United State, Africa and Caribbean (Parkin et al., 2014). In the UK, black men have a 3-fold higher risk of developing prostate cancer than white men (Ben-Shlomo et al., 2008), while Asian men have the lower risk

(National Cancer Intelligence Network and Cancer Research UK, 2009). Furthermore, in the USA the lowest incidence rate is observed in American Indian/Alaska men with 46.9, Native and Asian/Pacific Islander men with 52.4, followed by white men with 93.9 (Howlader et al., 2016b). The highest incidence rate is seen in African-American men with 157.6 (Howlader et al., 2016b). The incidence rates are quite varied from one region to other regions in the world which are associated with their socioeconomic conditions and biological factors (Hosain et al., 2011).

The blood levels of Prostate Specific Antigen (PSA), a protein encoded by *KLK3* gene, are known to be significantly higher in black men with/without PCa than white men (Kyle et al., 2004 and Vijayakumar et al., 1998). Existence of higher androgen levels in plasma, sensitivity of androgen receptors (due to reduced number of CAG or GGC repeats in exon 1) and altered insulin-like growth factor binding protein 3 (IGFBP-3) expressions in plasma may determine the biological differences among ethnicities (Ross et al., 1986). Furthermore, African-American men display a more aggressive form of the disease, which has also been associated with genetic and biological differences, although lack of adequate screening and delayed presentation was not excluded too (Wu and Modlin, 2012).

A family history of prostate cancer is another common risk factor for the development of prostate malignancies. This factor has persistently been associated with an increased risk of prostate cancer that varies according to the degree of the relationship, the number of relatives affected, and the age of diagnosis (Johns and Houlston, 2003 and Kiciński et al., 2011). Around 5-10% of PCa incidences are associated to family history and the inheritance of genes which are involved in development of PCa (Hemminki and Czene, 2002). Men with a family history of breast, ovarian cancers, Hodgkin's disease, leukaemia, liver cancer and melanoma are also at a higher risk of developing of PCa (Hemminki and Chen, 2005). Kral et al. reviewed the genetic determinants of prostate cancer and summarized the function of several candidate genes for the development of malignancy (Kral et al., 2011). The gene linkage studies reveal major susceptible genes for prostate carcinoma in younger men (<65 years) are located at seven different places on the chromosome. The *HPC1* (hereditary prostate cancer 1) gene located on 1q24-25, encodes enzyme ribonuclease L (RNaseL) (Chen et al., 2003), which is involved in the innate immune defence mechanisms and the interferon (IFN)-mediated signalling (Malathi et al., 2007). It plays

an important role in reducing antiviral activity and regulation of apoptotic cell death (Zhou et al., 1997). Mutation in RNase L in human prostate cancer samples become susceptible for retrovirus that reveal the importance of antiviral defences to PCa development (Miller et al., 2009). Furthermore, PCa with retroviral infections demonstrated the potential connection of chronic retroviral infection and resulting tissue inflammation (Eeles et al., 2008 and Schlaberg et al., 2009). The second HPC gene *HPC2/ELAC2* located on chromosome 17p11 encodes for a protein with poorly understood function (Camp and Tavtigian, 2002). ELAC2 protein is associated with PCa development by binding SMAD2 that up-regulate proliferation through activation of TGF-β signalling pathway (Noda et al., 2006). The third identified HPC genes is *MSR1* (macrophage scavenger receptor 1) located on chromosome 8p22 (Xu et al., 2002), which is involved in the initiation of inflammation and affects the induction and course of infection. However, no clear correlation has been found between these genes (Hemminki and Chen, 2005), and hereditary risk of prostate cancer (Andriole et al., 2004).

Diet has been extensively studied as a risk factor (Shimizu et al., 1991). Various constituents of diet including saturated fat, red meat (Alexander et al., 2010) and dairy (Gupta, 2007) have been studied but no equivocal evidence for their contribution to prostate carcinogenesis have been found. A high intake of calcium in the diet is associated with a higher risk of PCa (Wilson et al., 2015). Tomato and its constituent lycopene have controversial beneficial effects (van Breemen and Pajkovic, 2008). However, lycopene was found ineffective to provide clinical benefits in advanced PCa as found in an open phase II study (Taitt, 2018). Similarly, the role of vitamins (D and E) and micronutrients (e.g. selenium) remain a matter of debate (Mullins and Loeb, 2012 and Grant and Peiris, 2012).

Alcohol has also been associated with high risk of PCa (Hiatt et al., 1994). Intake of more than three drinks per day between wine, liquors or beer may be a possible risk factor for prostate and other cancers (Rizos et al., 2010). A weak correlation has been observed between alcohol intake and PCa mortality found in cohort studies (Schmidt and de Lint, 1972), but other studies did not find any correlation with increased risk (Adami et al., 1992).

The risks of PCa posed by dietary risks are compounded by obesity, as obesity is related to an increased risk of advanced and progressive PCa and increased PCa mortality (Discacciati et al.,

2012). High body mass index (BMI) is associated with more aggressive disease and worse outcomes (Freedland et al., 2005). Several meta-analysis have shown that obesity increases the risk of developing prostate cancer by 1% to 5% (Guh et al., 2009). The interpretation of the mechanism is that obese men contain altered circulating levels of metabolic and sex steroid hormones, which are considered to be linked in prostate development as well as oncogenesis (McBride, 2012) .

Obesity combined with physical inactivity promotes insulin resistance with reduced glucose uptake resulting in excessive insulin in the blood. The elevated insulin hormone is thought to promote prostate cancer initiation and/or progression (Kaaks and Stattin, 2010). A national data survey conducted in US populations showed that obesity is associated with more aggressive PCa and higher morality in spite of its lower incidence (Parekh et al., 2010). Exercise is supposedly one of the easiest modifiable risk factors to manage in a way to obtain many benefits and relatively few side effects when it comes to prostate cancer prevention. Indeed, Keogh and McLeod found that veterans who exercised had a significantly lower risk of prostate cancer (Keogh and MacLeod, 2012).

1.8. Prostate carcinogenesis

The transition from normal glandular cellular structure to malignancy happens through histological and molecular transformation (Isaacs, 1997). It is essential to understand the molecular mechanisms to gain a meaningful insight into the process of carcinogenesis that may eventually lead to better therapies for PCa.

1.8.1. Prostatic intraepithelial neoplasia (PIN): A route to prostate carcinogenesis

PIN is linked to progressive phenotypic and genotypic abnormalities between normal prostatic epithelial cells and cancer, suggesting a loss of cell differentiation and regulatory control as prostatic carcinogenesis progress (Nasir et al., 2002).

Premalignant prostatic lesions were first described in 1926 although they were not distinguished from PIN like lesions (Oertel, 1926). McNeal suggested these lesions as “intraductal dysplasia of the prostate’’ theorising that prostate carcinoma originated from active ductal/acinar epithelium and not from atrophic acini (McNeal, 1988b). McNeal’s interpretation, although not recognized

initially, was an important milestone in the description of PCa. McNeal and Bostwick explicitly defined its morphological parameters and developed a grading scale that closely anticipated invasive carcinoma association (McNeal and Bostwick, 1986), they provided a repeatable criteria for the diagnosis of "intraductal neoplasia'' and proposed its classification into 3 grades. Bostwick and Brawer (1987) later proposed the term Prostatic Intraepithelial Neoplasia (PIN) (Workshop on "Prostatic Dysplasia" (Bostwick and Brawer, 1987).

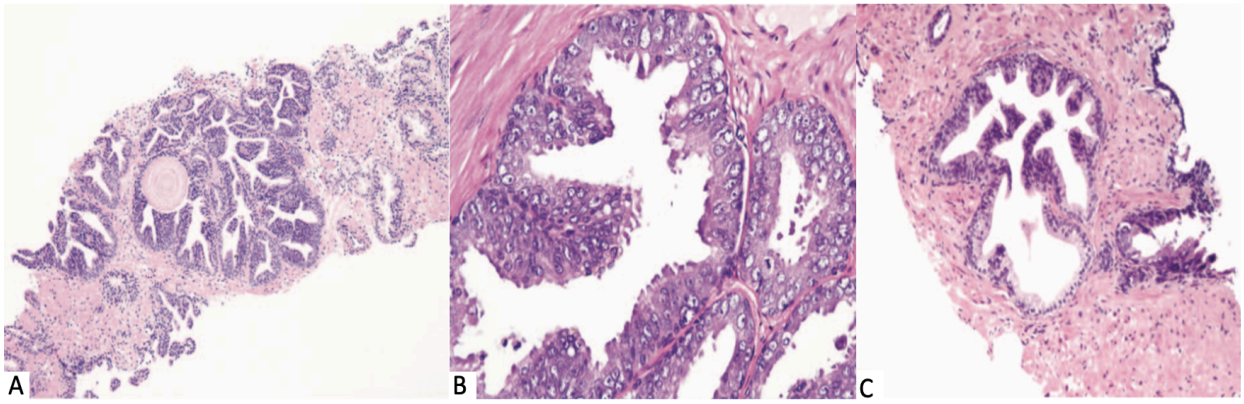

Figure.1.16. A H&E diagnosis of PIN is established by 3 essential observations at low magnification: (A) PIN at low-power view showing a cluster of glandular structures with hyperchromatic cells contrasting with adjacent normal glands (H&E, original magnification X40). The lining of the ductal structures is darker and thicker than the surrounding normal ducts, and a complex intraluminal growth pattern may exist. (B) PIN at high-power displaying the maximum number of cells contain stratified nuclear, enlarged nucleus, prominent nucleoli. There is a cytological triad at high magnification including: different degrees of nuclear-stratification enlargement, cells are hyperchromatic with darker nucleus, nucleolar is prominent. (C) PIN of core biopsy showing partial engagement of a gland. PIN is typically multifocal and includes clusters of glandular structures or can contain one particular gland in whole or in part. Image adapted from (Ayala and Ro, 2007).

The grading system (Sec. 1.9) was further refined and Grade 1 was changed to Low Grade PIN (LGPIN) and combined the Grades 2 and 3 to new name as High Grade PIN (HGPIN) (Bostwick, 1989a) on the basis of cytological characteristics of secretory cells (Fig. 1.17). LGPIN is characterised by cells with enlarged nuclei, variable size, normal or slightly increased chromatin content, small or inconspicuous nucleoli. HGPIN contains large nuclei of fairly uniform size, an increased chromatin content and prominent nucleoli that are similar to those of carcinoma cells. The basal-cell layer is usually intact in LGPIN but might have high degree of disruption in HGPIN.

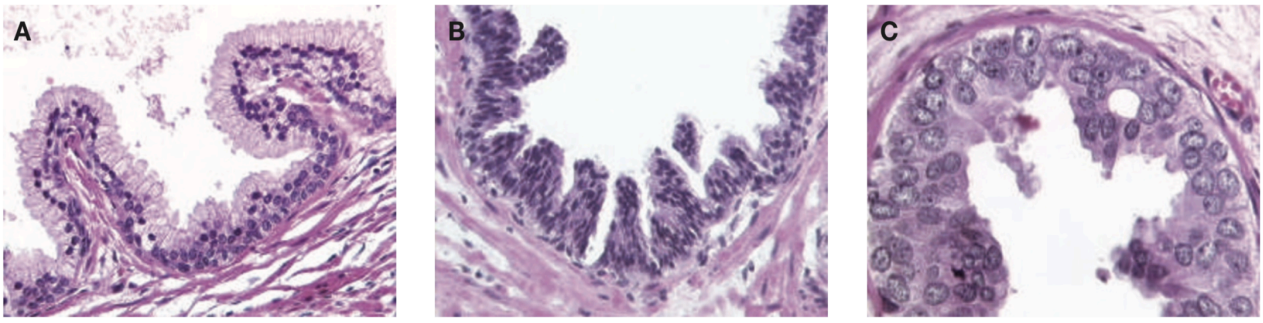

Figure 1.17. Morphological features of normal prostate, LGPIN and HGPIN. (A) normal prostate. (B) LGPIN with enlarged nuclei, varied in size. (C) HGPIN cells with large nuclei of fairly uniform size and prominent nucleoli that are similar to those of carcinoma cells. Image adapted from (Montironi et al., 2007).

LGPIN and HGPIN contain some similar cytological reproducible features whereas HGPIN show four different distinct histological architectural features (e.g., flat, tufting, micropapillary and cribriform (Bostwick and Cheng, 2008).

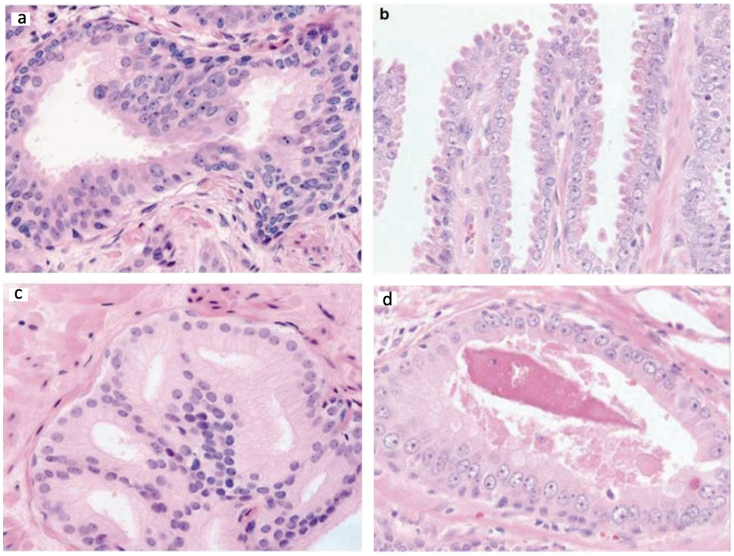

Figure 1.18. High Grade PIN with four distinct architectures: (a) tufting pattern: Epithelial cell crowding and stratification with prominent nuclei and nucleoli, (b) micropapillary, (c) cribriform pattern (d) Flat pattern. Image adapted from (Bostwick and Qian, 2004).

During the developmental process a number of lesions observed in the prostate have been considered as potential precursor lesions for prostate cancer, for instance, adenosis (atypical adenomatous hyperplasia) and proliferative inflammatory atrophy (PIA). Adenosis occurs in transition zone and could be considered a potential precursor to malignancy. These lesions which are often low grade are not considered to possess strong malignant potential (Merrimen et al., 2013).

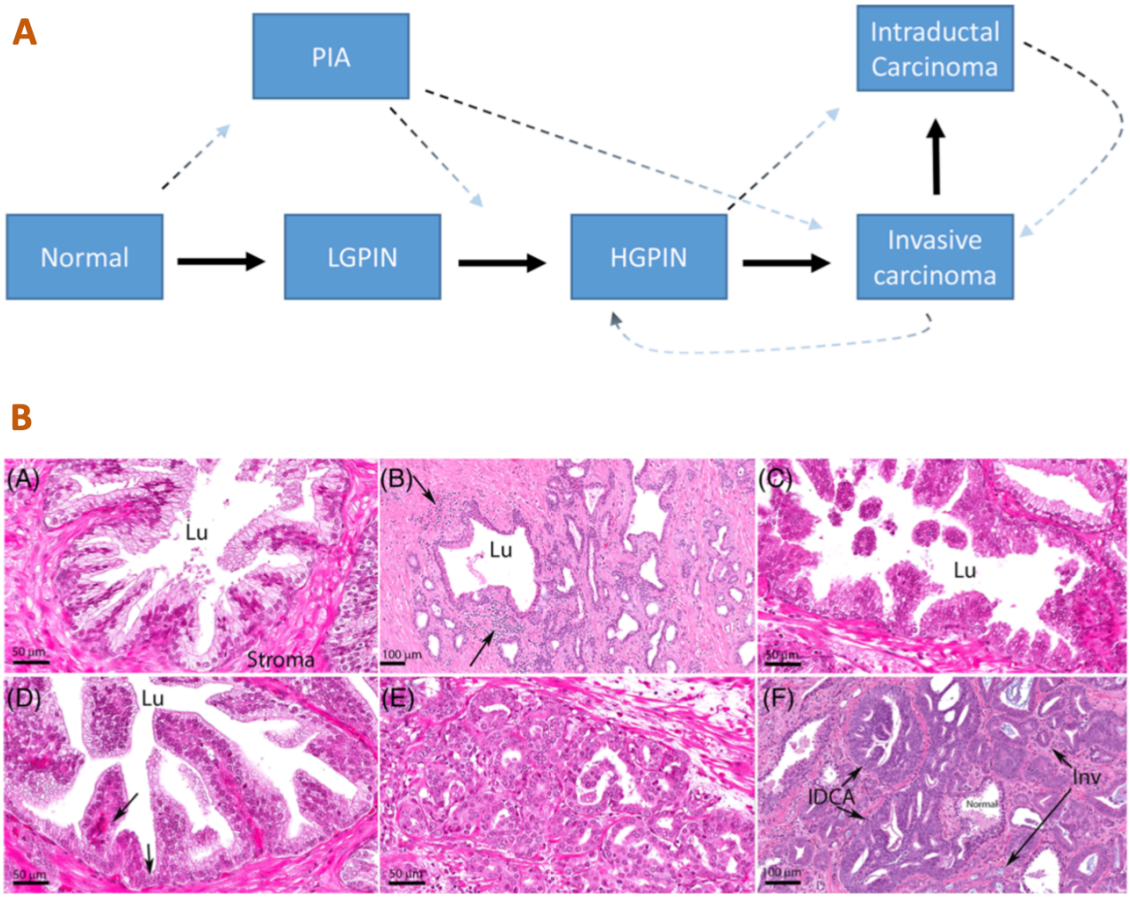

Figure 1.19. A process and histological changes in PCa progression. (A) A schematic diagram of the model of prostate cancer progression. PCa development from normal to LGPIN to HGPIN to carcinoma. Thicker black solid arrows represent canonical mechanism. Normal epithelium gives rise to PIA from where LGPIN or HGPIN and invasive carcinoma arises. The route from PIA to LGPIN or HGPIN is more common than directly to carcinoma. During the developmental process intraductal carcinoma is the final stage that arises after invasion but has been found to be present in prostates without invasion and thus may arise directly from HGPIN, however, not via invasive carcinoma. This suggests that lesions are morphologically not only identifiable as HGPIN arise prior to invasive carcinoma development, but also that lesions identifiable as HGPIN may also arise as retrograde spread from invasive carcinoma. (**B**) H&E images of morphologic entities. (A) normal tissue, (B) focal atrophy with PIA, (C) LG PIN, (D) HG PIN, (E) invasive adenocarcinoma (Gleason pattern 4+3=7, (F) intraductal carcinoma and adjacent invasive adenocarcinoma. Lu lumens of glands. Image adapted from (De Marzo et al., 2016).

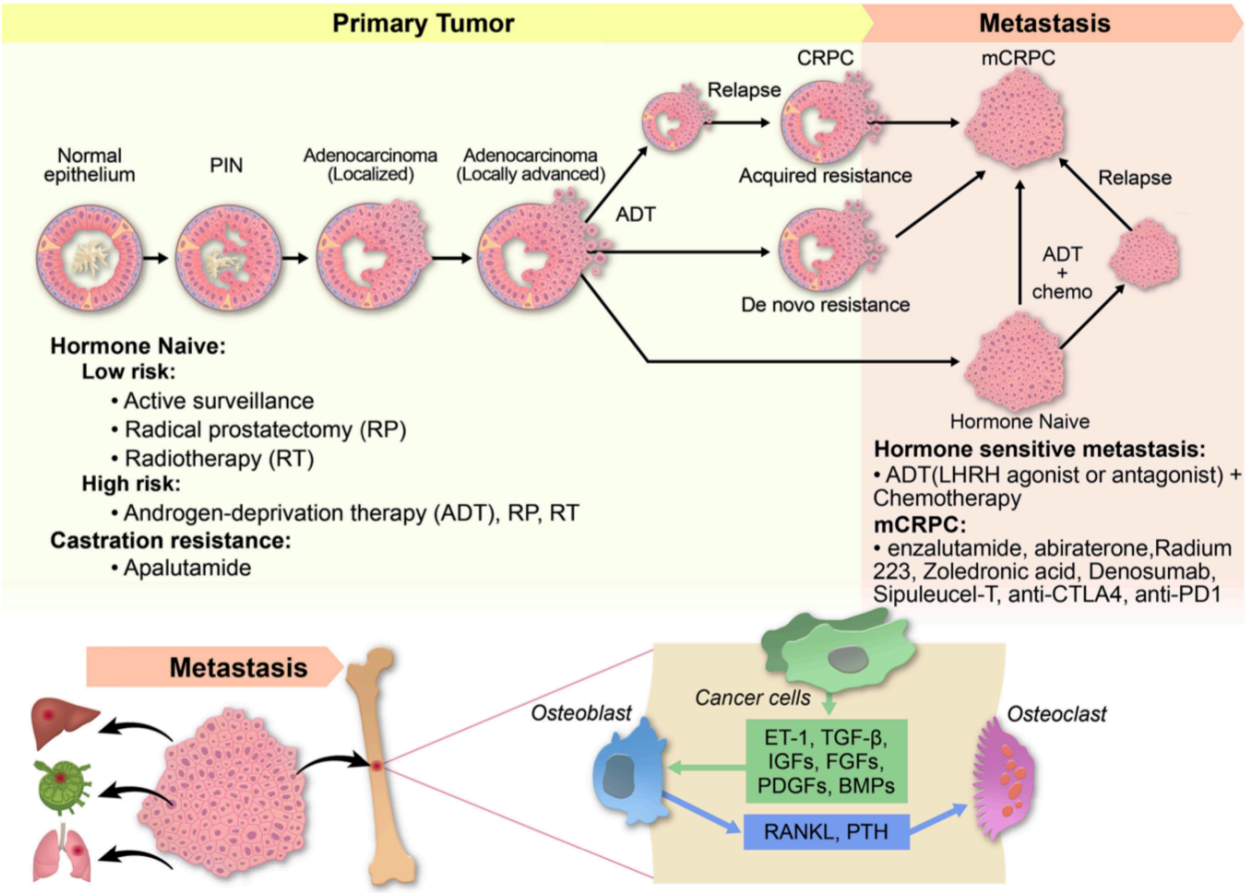

Figure 1.20. A model for PCa progression and mCRPC (castration resistant prostate cancer) development. PIN is characterised by the luminal cell proliferation with dysplasia along the canals. PIN, however, progress towards localized prostate adenocarcinoma, and then, as the basal cell layer degraded and cancer cells invade the basal lumina, it becomes locally invasive carcinoma. Locally advance prostate cancer metastasizes to lymph nodes and then to remote organs including bones, liver and lungs. AR-dependent localised advanced prostate adenocarcinoma may primarily respond to ADT (androgen deprivation therapy) and then advances to CRPC. Advances prostate adenocarcinoma may also demonstrate *de novo* tolerance to ADT. Likewise, AR-dependent hormone-naïve metastatic tumours primarily react to ADT and transit into mCRPC. AR-indifferent hormone naïve metastatic tumours show de novo resistance. The treatment choices for PCa relies on tumour stage and earlier treatments. Figure adapted from (Wang et al., 2018).

1.8.2. HGPIN as a PCa precursor

Association of HGPIN in relation to prostatic adenocarcinoma development is well documented, (Bostwick et al., 1996). The following discussion shows HGPIN may act as a precursor of PCa.

1.8.2.1. Clinicopathological evidence for HGPIN

The incidence of HGPIN increases with advancing age (Sakr et al., 1996), and its frequency in malignant prostate disease is significantly higher when compared with prostates without cancer

(Bostwick and Brawer, 1987). It has been reported that HGPIN was found in 82% prostate from patients suffering from cancer, whereas only 43% of benign prostate patients of similar age (Bostwick and Brawer, 1987). Other autopsy studies indicate that, similar to invasive carcinoma, the rates of HGPIN increase significantly with age. For instance, a prevalence of 7% to 8% has been seen in the third decade of life and upwards of 60% to 80% in the eight decades of life (Merrimen et al., 2013). PIN and PCa are mainly multifocal (multiple, distinct areas of malignancy exist within the prostate gland) (Arora et al., 2004) mostly in the peripheral zone (Haggman et al., 1997). Other authors documented a frequency of HGPIN in the transition zone above 1% (ranges 2-37%). Gaudin et al. suggested that the highest incidence of transition zone involvement (37%) was in cancer prostatectomy, the incidence in transurethral resection experiments was considerably lower (Gaudin et al., 1997).

1.8.2.2. Genetic and molecular evidence of HGPIN

HGPIN and PCa share similar genetic alternations (Qian et al., 1995) as a number of common molecular changes have been identified in these HGPIN and PCa. Micro-dissected HGPINs with identical incidence and pattern of chromosome loss of one allele from 8p12-21 (90%) in carcinoma and 63% in HGPIN relative to invasive adenocarcinoma were found by Emmert-Buck and colleagues (Emmert-Buck et al., 1995). They also suggested that 8p22 are displayed fewer LOH in PIN than carcinoma, suggesting that PIN is molecularly interlinked between normal and carcinoma. Qian et al. showed that PIN frequently harbours similar chromosomal alternations as invasive carcinomas (Qian et al., 1997). However, the idea is not universally accepted that PIN lesions also serve as a precursor due to similarity of molecular changes (Emmert-Buck et al., 1995). Telomere shortening is another somatic and genetic alteration found in both HGPIN and cancer (Meeker et al., 2002). Activation of telomerase enzyme has been found in 16% of HGPIN lesions and in 85% of invasive prostatic carcinoma. Telomerase activity could serve as an important biomarker in prostate carcinogenesis (Koeneman et al., 1998). The fusion gene TMPRSS2-ERG has also been detected in HGPIN in 5%-20% of men in European descent. This contrasts with a much higher frequency in carcinoma ($\backsim$50%) (Bostwick and Cheng, 2008).

1.8.3. Clinical importance of PIN

The prevalence of HGPIN in prostatic transurethral resection specimens is an important risk factor in PCa diagnosis (Gaudin et al., 1997). A study was conducted on 14 patients with HGPIN and BPH who were then followed up for next 7 years (mean, 5.9 years); of these 14 patients, 3 (21.4%) developed PCa (Moore et al., 2005). Patients that developed PCa were also found to have a higher PSA (8.1ng/ml), compared to those that did not (4.6ng/ml PSA). Because of the moderate development pace of prostate disease and considerable amount of time required for sufficient follow up in animal and human studies, the non-invasive precursor lesion HGPIN is an effective intermediate histological marker to indicate the possibility of cancer afterwards (Cheng et al., 2004).

1.9. Grading of PCa

Donald F. Gleason in 1966 created a grading system for prostatic carcinoma based on the pattern and architecture of the tumour (Gleason, 1966). Five grades or patterns were proposed based on morphological and architectural features in tissue sections, but not on cytological atypia, cell counts or mitotic rates. The proposed five patterns are described as follows:

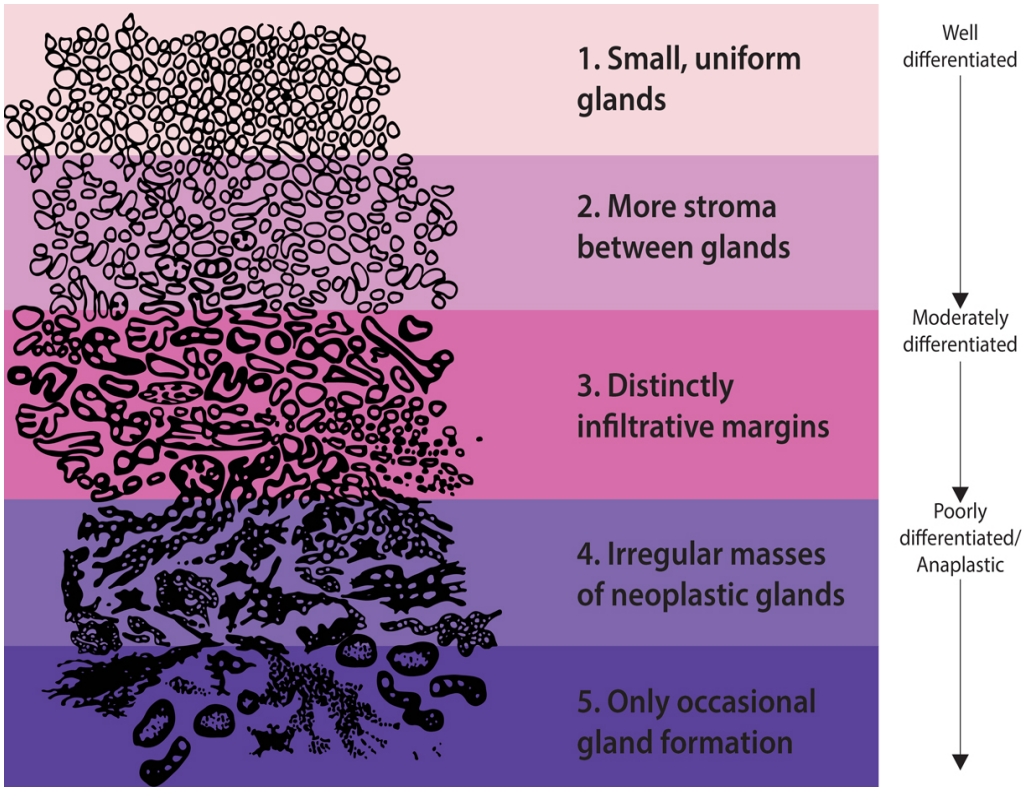

Figure 1.21. Gleason's original grading pattern proposed in 1966-1967 (Epstein et al., 2016b). (Image obtained from online on 06/06/2020).

Gleason proposed the following pattern based on studies of 270 patients (Epstein et al., 2005).

Pattern 1: Very well differentiated small and closely packed glands forming a circumscribed tumour mass.

Pattern 2: Similar to pattern 1 but with less well circumscribed glands showing greater variation in both size and shape. A mild degree of cribriform pattern may be present.

Pattern 3: This pattern shows a wide variation in morphology ranging from glands similar to those seen in pattern 2.

Pattern 4: Closely packed, large, pale polygonal cells that resemble renal cell carcinoma. There are some features of glandular differentiation and there is typical diffuse stromal infiltration.

Pattern 5: Undifferentiated carcinoma with little or no gland formation.

These have been periodically modified over the years starting in 1974 and 1977 (Samaratunga et al., 2016). In 2014 the International Society of Urological Pathology (ISUP) consensus formulated the Gleason grading pattern and finalised the following grading system which provided some degree of validation of grading (Epstein et al., 2016b).

An overall Gleason score is worked out by adding together two Gleason grades. The first is the most common grade in all the samples. The second is the highest grade of what's left. When these two grades are added together, the total is called the Gleason score. The modified Gleason's score are as follows:

Gleason score = the most common grade + the highest other grade in the samples (Shah and Zhou, 2016 and Epstein et al., 2016a).

Grade group 1: Gleason score 6 (3 + 3): All of the cancer cells found in the biopsy look likely to grow slowly.

Grade group 2: Gleason score 7 (3 + 4): Most of the cancer cells found in the biopsy look likely to grow slowly. There are some cancer cells that look likely to grow at a moderate rate.

Grade group 3: Gleason score 7 (4 + 3): Most of the cancer cells found in the biopsy look likely to grow at a moderate rate. There are some cancer cells that look likely to grow slowly.

Grade group 4: Gleason score 8 (3 + 5): Most of the cancer cells found in the biopsy look likely to grow slowly. There are some cancer cells that look likely to grow quickly.

Grade group 4: Gleason score 8 (4 + 4): All of the cancer cells found in the biopsy look likely to grow at a moderate rate.

Grade group 4: Gleason score 8 (5 + 3): Most of the cancer cells found in the biopsy look likely to grow quickly. There are some cancer cells that look likely to grow slowly.

Grade group 5: Gleason score 9 (4 + 5): Most of the cancer cells found in the biopsy look likely to grow at a moderate rate. There are some cancer cells that are likely to grow quickly.

Grade group 5: Gleason score 9 (5 + 4): Most of the cancer cells found in the biopsy look likely to grow quickly. There are some cancer cells that look likely to grow at a moderate rate.

Grade group 5: Gleason score 10 (5 + 5): All of the cancer cells found in the biopsy look likely to grow quickly.

1.10. Genetics of prostate carcinogenesis

Cancer is considered to have 'genesis in the genes'. Chromosomal aberrations, gene mutations and dysregulation of transcription that give rise to change in the function of genes such as inactivation tumour suppressor genes and activation of proto-onco and oncogenes (Paris et al., 2004) that ultimately manifest as uncontrolled cell proliferation. These genetic aberrations are acquired during development of the cancer or sporadically inherited from an ancestor resulting in predisposition to cancer. A brief discussion of this follows.

1.10.1. Hereditary Prostate Cancer

Hereditary cancers are usually distinguished from sporadic cancers by the descent, multifocality and earlier occurrence of family clustering and autosomal-dominant (Schulz et al., 2003). In most hereditary cancers, these cancers are characterised by an inherited mutation in one allele of a tumour suppressor gene. Somatic mutation of the second allele is then sufficient for tumour progressions. In sporadic cases, the inactivation of the same gene requires two successive mutations in the same cell. Many candidate genes and markers that co-segregate with prostate carcinoma have been identified for the families where prostate carcinoma occurs in multiple generations including one or more cases of early onset (Carter et al., 1992).

It has been recommended that at least seven loci of the genome possess an autosomal dominant gene for hereditary prostate cancer namely: 1q24-1q25 (*HPC1*), 1q42-q43 (*PCAP*), Xq27-q28

(*HPCX*), 1p36 (*CAPB*), 20q13 (*HPC20*), 17p11 (*ELCA2*) and 16q23 (Nwosu et al., 2001 and Bratt, 2002). Studies of this regions, three candidates familial PCa susceptibility genes have been identified: *HPC1* (hereditary prostate cancer 1) or RNase L gene (Carpten et al., 2002), *HPC2* (hereditary prostate cancer 2) or *ELAC2* gene (Rennert et al., 2005) and *MSR1* gene (Xu et al., 2002).

1.10.1.1. *HPC1* or *RNase L* gene

Three missense mutations, for instance Arg426Gln, Asp541Glu, and Ile97Leu were identified in the *HPC1* that may contribute to familial or sporadic PCa (Carpten et al., 2002). In the Spanish population, mutations in Arg426Gln were associated with worse prognosis (Alvarez-Cubero et al., 2012), whereas Asp541Glu mutation has been shown to increase the risk of PCa in some Japanese men (Nakazato et al., 2003). Functionally, *in vitro* studies have shown that the Arg426Gln mutation diminishes enzymatic activity of RNase L thereby decreasing the function of tumour suppressors that may enable tumour cells to escape apoptosis.

1.10.1.2. *HPC2* or *ELAC2* gene

Overexpression of this metal dependent hydrolase alters cell cycle progression (Korver et al., 2003) and men who inherit the same variant alleles are at increased risk of PCa (Suarez et al., 2001).

1.10.2. Chromosomal Loss, Amplification and Translocation

1.10.2.1. Chromosomal aberration

Whereas prostate carcinomas frequently remain euploid (e.g., 2 sets of chromosomes: 2x23 chromosomes) in the early stage, numerical and structural chromosome changes have been discovered. Chromosomal segment deletions as well as gains have been reported in advance cancers (Dong, 2001). Comparative genomic hybridization (CGH) has identified two primary characteristics in PCa. First, loss of the genetic material is more common than gains and amplifications (Visakorpi et al., 1995), indicating that tumour suppressor genes, thought to be within the deleted regions, are likely to play a significant role in prostate tumorigenesis. Second, many of the chromosomal losses can already be observed in the early stages of prostate cancer,

while gains and amplifications are found predominantly in CRPC, indicating that oncogenes are triggered at the late stage of the disease (Visakorpi et al., 1995). The identified gains and losses of chromosomal regions include gains at 8q and losses at 3p, 8p, 10q, 13q and 17p (Dong, 2001). Several key regulatory genes have been mapped within these chromosomal regions undergoing alteration and rearrangement which are associated with prostate carcinogenesis.

1.10.2.2. TMPRSS2-ERG

Gene fusion generated from chromosomal rearrangement are considered to play a key role in the initiation of tumorigenesis (Mitelman et al., 2007). An early example of this is the chromosomal rearrangements in prostate, *TMRSS2-ERG*, involving the 5'-promoter of transmembrane protease serine 2 (*TMPRSS2*), is fused with coding sequence of the erythroblastosis virus E26 (ETS) related gene (ERG) (Tomlins et al., 2005).

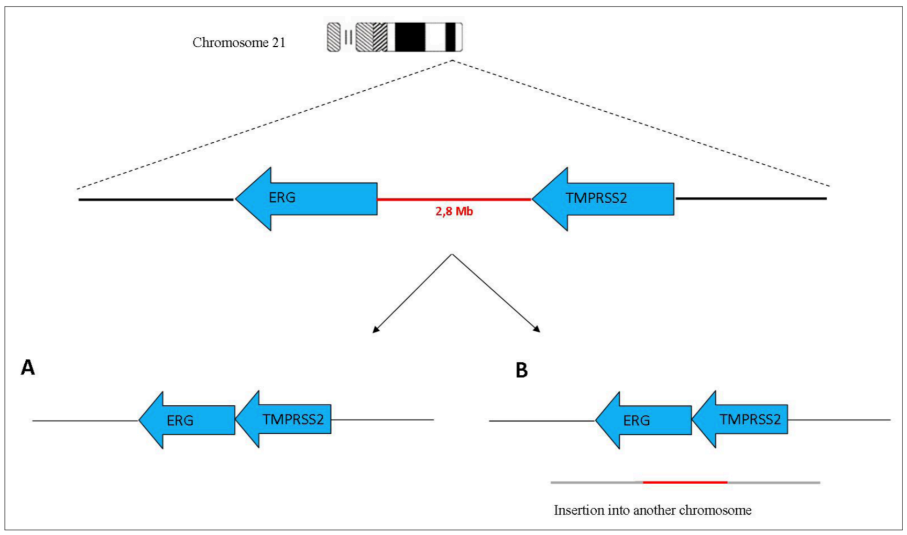

Figure 1.22. Schematic diagram of mechanism of fusion gene formation: (A) *TMPRSS2-ERG* fusion gene is produced by an interstitial omission, where 2.8mb (red line) segment is lost. (B) The *TMPRSS2-ERG* fusion gene is produced by the incorporation of the interstitial region into another chromosome in the genome. Adapted from (Burdova et al., 2014).

TMPRSS2 is a prostate-specific, androgen responsive gene, constitutively expressed under the transcriptional control of androgen through androgen responsive elements (ARE) in its 5'UTR. ETS family members are oncogenic transcription factors consisting of 27 members sharing a

conserved DNA binding domain that permits binding to purine rich DNA sequences containing a 5'-GGAA/T-3' core sequence (Basuyaux et al., 1997 and Williams et al., 2011) and N-terminal regulatory domain. The fusion of the genes results in the production of ETS transcription factors which are governed by TMPRSS2 androgen-sensitive promoter elements. This allows androgen receptors to bind these regions of TMPRSS2, resulting in the over expression of members of the ETS gene family. These ETS members can then induce their target gene expression (Tomlins et al., 2005). During *TMPRSS2-EFG* fusion, N-terminal of ETS is truncated but expression of C-terminal of ETS remain intact in the fusion protein remains under the control of the androgen-responsive promoter of *TMPRSS2*, because its C-terminal contains DNA binding ETS domain and transactivation domain (Clark et al., 2007). The frequency of these TMPRSS2-ERG fusions is 15% in high-grade PIN lesions and an approximately 50% in localized prostate cancer (Albadine et al., 2009). This indicates that the formation of this fusion gene takes place after cancer initiation. The emergence of chromosomal rearrangement may be an indirect result of AR function (Shen and Abate-Shen, 2010). Data from androgen-dependent LnCAP cells exhibit that AR binding induces chromosomal proximity between the *TMPRSS2* and *ERG* loci that promote the generation of TMPRSS2-ERG fusions following DNA damage (Mani et al., 2009).

ETS transcription factor is associated with diverse biological processes, including cell proliferation, apoptosis, differentiation, angiogenesis and invasion. The *TMPRSS2* also shows fusion with ETS isoforms such as ETV1, ETV2 and ETV5 in PCa (Helgeson et al., 2008). An investigation consisting of 27 patients with hormone-refractory metastatic prostate cancer patient samples; ten (37%) of them showed TMPRSS2-ERG mRNA expression and exhibited that the metastatic sites possessed a TMPRSS2-ERG fusion generated through interstitial deletion. *TMPRSS2-ERG* gene fusion contributes with periodic gene fusion in PCa, with a frequency of 40-70% (Rubio-Briones et al., 2010). Taking into account the pervasiveness of *TMPRSS2-ERG* fusion in PCa, and an increase in the incidence of PCa, further research of these fusions is important for understanding PCa biology. The relationship between this fusion and prognostic markers and disease aggressiveness could provide clinicians with a more informed way to classify PCa for prognostic and therapeutic purposes.

1.10.2.3. *MSR1* gene

MSR1 gene is found on chromosome 8p22 and encodes the macrophage scavenger receptor type A (Matsumoto et al., 1990). Linkage studies have implicated MSR1 in various diseases including growth of malignancy in prostate (Ostrander and Stanford, 2000). Various mutations have been depicted including Arg293X, Asp175Tyr, His441Arg, Val113Ala, and Ile54Val. Arg293X was first stated in the context of familial prostate cancer among the European descent while Asp175Tyr was found in a population of African-American origin (Xu et al., 2002).

1.10.2.4. *Nkx3.1*

Nkx3.1 located at 8p21 (He et al., 1997), encodes a prostate specific homeobox protein necessary for normal development of the prostate (Prescott et al., 1998). It is expressed in normal prostate epithelium and often show decreased expression in PIN lesions and in prostate cells (Bowen et al., 2000) and is the strongest candidate for the commonly observed 8p deletion in PCa. Although loss of *Nkx3.1* locus is often found in prostate cancer, no mutations have been identified in the remaining allele (Voeller et al., 1997). Nonetheless, the depletion of *Nkx3.1* expression has been found to be consistent with hormone-refractory and advanced tumour levels (Bowen et al., 2000). However, the absence of mutations on the remaining allele of *Nkx3.1* suggests haploinsufficiency (i.e., inactivation of only one allele) as the mechanism for removing the tumour suppressive activity of *Nkx3.1*. Many prostatic adenocarcinomas, including those of very high grade (Chuang et al., 2007) or metastatic, still exhibit substantial *Nkx3.1* protein level suggesting that *Nkx3.1* is not just a classical tumour suppressor gene. The fact that *Nkx3.1* is found in most prostate cancers and not in most other forms of tumour indicates *Nkx3.1* could be an excellent immunohistochemical marker for PCa (Ali et al., 2006).

1.10.2.5. Cyclin-dependent kinase inhibitor 1B (*CDKN1B*)

Cyclin-dependent kinase inhibitor 1B (*CDKN1B*) is a tumour suppressor gene that encodes p27 which is considered to be a somatic gene target for alteration during prostatic carcinogenesis. Disruption of Cdkn1b in mice contribute to prostatic hyperplasia. Mice with mutated *Pten* and *Cdkn1b* alleles developed localized prostate cancer (Di Cristofano et al., 2001). Decreased p27 expression is a characteristic of human prostate cancer cells, especially in prostate cancer cases

with poor prognosis (Cheville et al., 1998). Reduced expression of p27 has been reported in HGPIN (De Marzo et al., 1998) and in PIA lesions (Van Leenders et al., 2003).

1.10.2.6. *PTEN* gene

PTEN was recognised as a tumour suppressor gene located on chromosomal region 10q23 and is occasionally mutated and deleted in many cancers, including the prostate (Salmena et al., 2008). The *PTEN* gene encodes a dual-specificity phosphatase, converting phosphatidylinositol 3, 4, 5-trisphosphate (PIP3) into phosphatidylinositol 4, 5-bisphosphate (PIP2) (Maehama and Dixon, 1998). *PTEN* also acts as a direct antagonist of P13K enzyme which convert PIP2 into PIP3 which is accumulated on the cell membrane that leads to recruitment and activation of proteins containing pleckstrin homology (PH) domains 3-phosphoinositide-dependent protein kinase 1 (PDK1) and its substrate AKT. Active phosphorylated AKT modulates a number of downstream targets, including mTOR signalling, which inhibit apoptosis, cell cycle progression, cell proliferation, cell differentiation and invasion (Song et al., 2012). *PTEN* converts PIP3 into PIP2 and thus downregulate the function of AKT signalling pathway. The *PTEN* loss in prostate cancer was primarily deduced from its location, which regularly encounters allelic loss in prostate cancer and also from its reduction or loss of expression in prostate cancer (Dong et al., 2007).

1.10.3. Micro RNA: Role of miRNA in PCa

MicroRNAs (miRNAs) are a large class of endogenous short (approximately 18-22 nucleotides) noncoding single-stranded RNA molecules that act as posttranslational gene regulators (Ambros, 2004). Research findings have established that miRNAs play a crucial role in differentiation, proliferation, apoptosis and metabolic homeostasis in cellular pathways (Ruan et al., 2009). miRNAs may operate as either tumour suppressors or oncogenes, depending on whether they specifically target oncogenes or tumour suppressor genes (Volinia et al., 2006). The biogenesis of miRNAs follows a canonical multistep procedure that begins in the nucleus and ends in the cytoplasm and consists of three significant events: cropping, nuclear export and dicing is shown in Fig 1.23. Most mammalian miRNA genes are first transcribed into primary miRNAs (pri-miRNAs) which are 5’ capped and 3’ polyadenylated in the nucleus by RNA polymerase II or III (Cai et al., 2004).

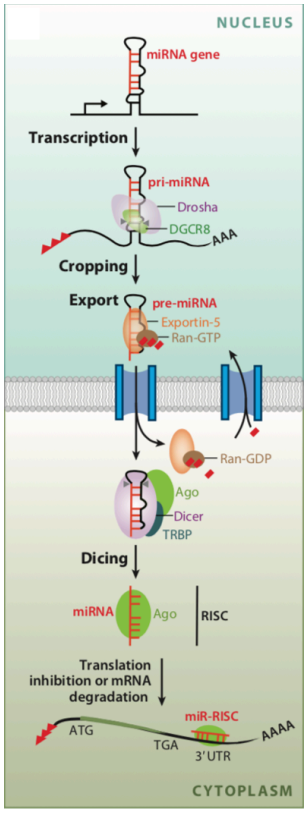

Figure 1.23. miRNA regulation in cancer. A schematic representation exhibiting the canonical miRNA biogenesis pathway. The miRNA biogenesis is composed of the following steps: transcription, nuclear cropping, export to cytoplasm and cytoplasmic dicing. MicroRNA genes are transcribed into capped and polyadenylated RNA transcripts (pri-miRNA) by RNA polymerase II and undergo a preliminary process by a nuclear enzyme of the RNAse III family, Drosha and produce hairpin loop RNAs (pre-miRNA) which are identified by the Exportin-5/Ran-GTP transporter and migrate into cytoplasm, where a second enzyme of the RNAse III family, Dicer catalyses the further processing named dicing, to generate miRNA duplexes. Dicer, TRBP and Argonaut (Ago) proteins mediate the processing of pre-miRNA and assembly of the RNA-induced silencing complex (RISC) in humans. One strand of each duplex remains on the Ago protein as the mature miRNA; the other strand is degraded. In both the dicing and RISC assembly phases, Ago is thought to be linked to Dicer. Image adapted from (Di Leva et al., 2014).

miRNAs were thought to have no role in cell function and be degraded, but over the past few years this view has changed. Recent data revealed that it can be used as an active strand and may play important biological roles (Yang et al., 2013). Some examples of this are shown in Fig. 1.24.

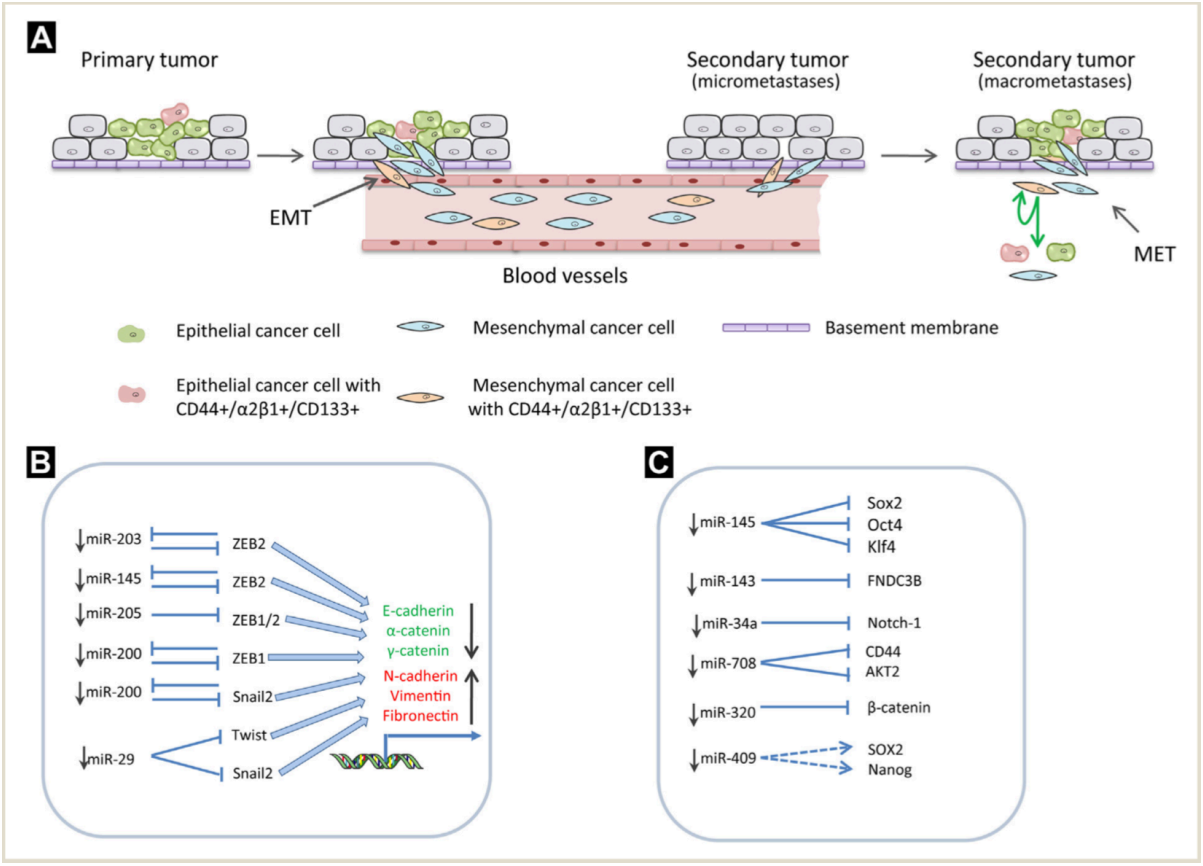

Figure 1.24. A model for representation of the role of MicroRNAs in Prostate Cancer Pathogenesis. miRNAs govern migration, invasion and outgrowth at a second site by regulatory frameworks of Epithelium to Mesenchymal Transition (EMT) and Mesenchymal to Epithelial Transition states and PCa stem cells (PCSCs). (A) EMT can bestow PCa cells with invasive and metastatic properties, consequently cancer cells with surrounding tissues migrate to distant sites. EMT phenotype cells that exhibit stem cell features require the capacity of self-renewal, which is necessary for the development of micro-metastases into macroscopic metastases. miRs such as miR-320 and miR-409 have been proposed to regulate EMT and PCSCs during this process. Numerous miRNAs that play an integral role in the EMT process and the cancer stem cell emergence are shown in (B) and (C). (B) miRNAs control transcription factors that suppress epithelial markers (E-cadherin, α-catenin and γ-catenin) and stimulate mesenchymal markers (N-cadherin, Vimentin, Fibronectin). (C) Modulating the process of stem cell creation and regulating stem cell markers, such as miRNAs (Wang et al., 2015). The image adapted from (Wang et al., 2015).

miRNAs are associated with cell cycle deregulation resulting in the increased proliferation of cells that exemplifies PCa, and loss of control of the cell cycle checkpoint promotes genetic destabilisation through a decrease of cyclin-dependent kinase (CDK) inhibitor p21 and elevation of cyclin D1 influx in PCa. Several miRNAs govern the extrinsic cell death pathway and are known to contribute to apoptosis resistance particularly in prostate cancer cells (Patron et al., 2012).

1.10.3.1. Invasion and Metastasis

The process of metastatic progression of the primary tumour into a metastatic lesion involves extracellular matrix changes, angiogenesis, tumour cell entry and exit from circulation (Nguyen et al., 2009). The tumour cell needs to overcome various physiological barriers to leave the tumour site and become metastatic either by aggregation of genetic and epigenetic modifications or through activation of proliferative cell signalling pathways. In a combinatorial example, miR-34a represses the expression of the transcription factor 7 (TCF7), is a known tumour repressor, and is known to be decreased in PCa (Yamamura et al., 2012). TCF7 is a strongly expressed Wnt signalling gene in PCa tissues, and it was a primary factor in bone metastasis (Chen et al., 2015b).

1.10.3.2. Androgen signal pathway and miRNA

AR-inducible miRs are conducted by androgens through androgen response elements (ARE) in the promotor regions. AR functions as a direct transcriptional regulator to miR-21 through the androgen-induced AR binding to the identified miR-21 promoter, named miPPR-21 (Ribas et al., 2009). Such miRs have been demonstrated to function as oncomirs, sometimes up regulated in PCa and promote tumour growth and proliferation, or to function as tumour suppressor, to display low PCa control and to prevent tumorigenesis.

1.10.4. Epigenetics effect on PCa

Genetically induced conditions such as mutations and epigenetic conditions lead to the malignancy of prostate cancer and its development. DNA methylation is one of the earliest reported features of epigenetic changes. Some other modification including histone modification is an epigenetically change that contributes to PCa development.

1.10.4.1. DNA methylation in PCa

DNA methylation is an epigenetic mechanism and plays a vital role in many molecular and cellular changes linked to the development and progression of prostate cancer (Li et al., 2005). DNA methylation refers to the addition of a methyl group through covalent bonding to the fifth carbon position of the cytosine pyrimidine (CpG) via DNA methyltransferase (Baylin, 2005). DNA methylation contributes to gene-silencing, by either hindering the entry of the target binding

sites for the transcriptional activators (Prendergast and Ziff, 1991) or by stimulation of the binding of methyl-binding domain proteins, which may facilitate suppression through association with histone deacetylases (HDACs) (Nan et al., 1998). DNA modifications such as hypermethylation and hypomethylation also play an integral role in the development of prostate carcinoma.

1.10.4.1.1. DNA hypermethylation in PCa

DNA hypermethylation is one of the most frequently identified epigenetic phenomenon in many cancers including prostate carcinoma. In addition, putative signalling pathways which are related to DNA damage repair, hormonal reaction, tumour cell invasion and cell cycle control are interrupted by CpG island hypermethylation.

Two examples of hypermethylation in prostate cancer are of Glutathione S-transferase class π gene (*GSTP1*) and oestrogen receptor. Malignant prostate epithelium almost universally does not express GSTPI due to hypermethylation in CpG island in the promoter region of the *GSTP1* gene (DeMarzo et al., 2003). In atypical, PIN tissue and in the urine and ejaculation of men with prostate cancer, an elevated CpG was detected (Nakayama et al., 2003). GSTP1 methylation is a potential epigenetic biomarker for prostate cancer because it is present in body fluids at detectable levels (DeMarzo et al., 2003).

Two forms of oestrogen receptors (ERs) are found in the prostate: ERα and ERβ. Missing or reduced expression of ERα and ERβ in PCa has been reported and their expressions were found unchanged to oestrogen therapy (Horvath et al., 2001). Hypermethylation has been shown to be the principal modification for the unresponsiveness of ER expression and also in advancement of PCa.

1.10.4.1.2. DNA hypomethylation in PCa

Demethylation (removal of methyl group) of normally methylated DNA is known as hypomethylation, prompting structural and functional alteration of a genome. Hypomethylation of a promoter region results in increased transcription and overexpression of downstream target genes.

Although DNA hypermethylation is well researched, hypomethylation also appears to play a critical role in PCa. For examples, hypomethylation of *PLAU* gene (urokinase plasminogen activator or uPA) which is associated with tumour invasion in PCa (Keer et al., 1991). The progressive expression of uPA from benign epithelium to primary organ-specific PCa, to PCa outside the prostatic capsule and to skeletal metastases is increased in immunohistochemical studies (Hoosein et al., 1991). PLAU promoter hypomethylation is significantly related to higher expression in hormone-independent prostate cancer cells, a greater *in vitro* potential and rising *in vivo* tumorigenesis (PAKNESHAN et al., 2003). CAGE (a new cancer/testis antigen gene), heparanase (HPSE), CYP1B1 and XIST are some other hypomethylated genes for PCa. HPSE, an endo-β-d-glucuronidase, and CYP1B1 are abundantly expressed but significantly hypomethylated in PCa opposed to the BPH samples (Tokizane et al., 2005 and Wang et al., 2007b).

A critical piece of early evidence driving this project in our laboratory was the discovery that Wnt5A is regulated by hypomethylation in prostate cancer tissue (Wang et al., 2007b). Using methylation specific PCR they confirmed the hypomethylation of the 5'UTR-regions of WNT5A and also CRIP1 and S100P. This results in over-expression of Wnt 5A protein in prostate cancer (Wang et al., 2010a). These data suggested that hypomethylation may be an important factor in prostate cancer as it targets key cell signalling pathways such as the Wnt network.

1.10.4.2. Histone modification

Histone acetylation is associated with transcriptional enhancement and histone deacetylation is connected to gene silencing (Hu and Lazar, 2000). PSA appears to be affected with histone methylation at its androgen response elements in 5'-regulatory regions. The H3-K4 methylation is connected to the transcriptional activation of the PSA gene in the prostate cell line LnCAP, with rapid reduce of H3 di- and trimethylated at lysine 4.

The following figure and table showing genes which contribute in PCa progression through epigenetic changes.

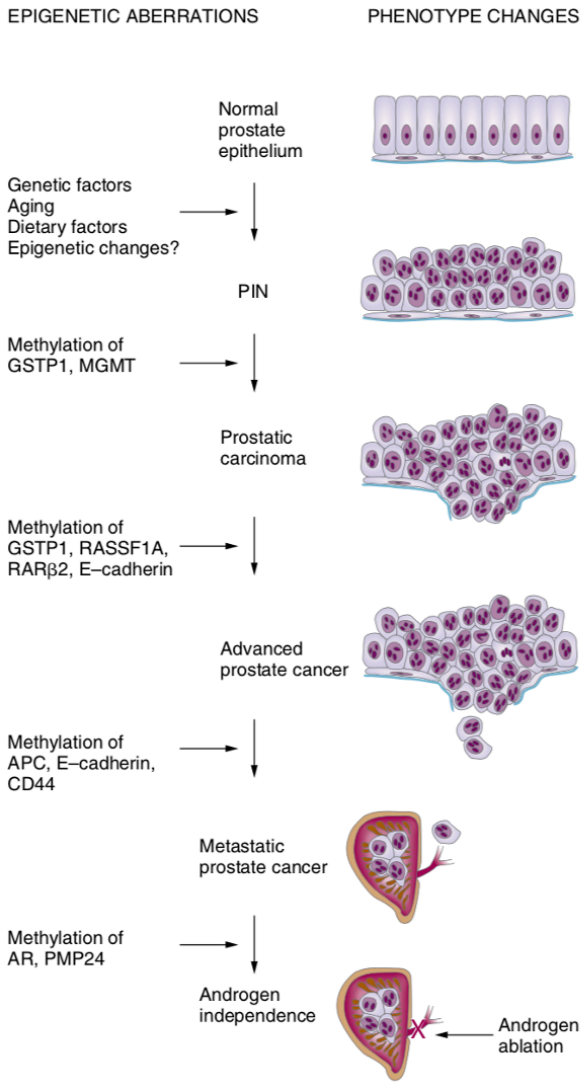

Epigenetic Changes in Prostate Cancer

Hypermethylation	Gene	Function
	Glutathione *S*-transferase P1 *(GSTP1)*	Detoxification if electrophilic compounds
	Ras association domain family protein isoform A *(RASSF1A)*	Unknown
	AR	Androgen effects +/–
	ER	Estrogen effects
	CCND2, CDKN2A, CDKN1A, SFN	Inhibit cyclin D–associated kinases, other cyclin dependent kinases
	CD44, CDH1, LAMA3, LAMB3	Cell architecture
	MGMT	DNA repair gene
	DAB2IP, EDNRB, RASSF1	Signal transduction
	PTGS2	Inflammatory response
Hypomethylation	*CAGE*	Novel testis antigen
	HPSE	Heparanase
	PLAU	Urokinase plasminogen activator
Histone modification	*VDR*	Vitamin D receptor
	CPA3	Carboxypeptidase A3
	RARB	Retinoic acid receptor β
	PSA	Prostate specific antigen
	DAB2IP	Tumor suppressor

Figure 1.25. Overview of epigenetic alteration in the development of prostate cancer. Epigenetic factors link in different steps in carcinogenesis by modifying genome with DNA methylation and histone modification. In the progression DNA methylation may be an early event causing inactivation of DNA repair genes such as GSTP1 and MGMT. Next phase of inactivation occurs in cell cycle control genes which contribute to advanced local prostate cancer. Then methylation in promoter region leads to loss of CD44 expression in PCa. DNA hypermethylation in AR resulting in inactivation that transform the PCa to androgen insensitive PCa and become metastasis. Adapted from (Li et al., 2004).

1.11. Androgen Receptor (AR) signalling in PCa

Huggins and his colleague first attributed the central role of androgen signalling in prostate cancer by showing that orchiectomy induces considerable regression of tumours (Huggins et al., 1941). Their discovery was recognised with a Nobel Prize in Physiology or Medicine in 1966. PCa depends upon androgen signalling. Indeed, a first line of therapy for PCa is termed Androgen

Deprivation Therapy (ADT). After this therapy PCa regresses but generally recurs after 4-5 years of ADT and termed CRPC (discussed in Chapter III in detail). In the following sections I discuss the structure and function of AR and signalling.

1.11.1. DHT synthesis in Leydig cell in testes

Testosterone and DHT are produced in Leydig cells in testes. It required more than a century to understand the principal steps associated in steroidogenesis in Leydig cell. Leydig cell investigation was initiated by a German zoologist and anatomist Franz von Leydig who identified the existence of interstitial cells in several mammalian experiments in 1850 (Leydig, 1850). Later it was proposed that the interstitial Leydig cells contain androgens. This was further investigated, and Baillie showed that 3β-hydroxysteroid dehydrogenase enzyme existed in those cells (Baillie, 1964). Around the same time the production of androgens was demonstrated *in vitro* and *ex vivo* cultures stimulated by pituitary gonadotropic hormones (Ewing and Eik-Nes, 1966). Hall and colleagues showed that cholesterol in the interstitial Leydig cells was converted to testosterone (Hall et al., 1969). A scheme of steroidogenesis in Leydig cells is shown in Fig. 1.26.

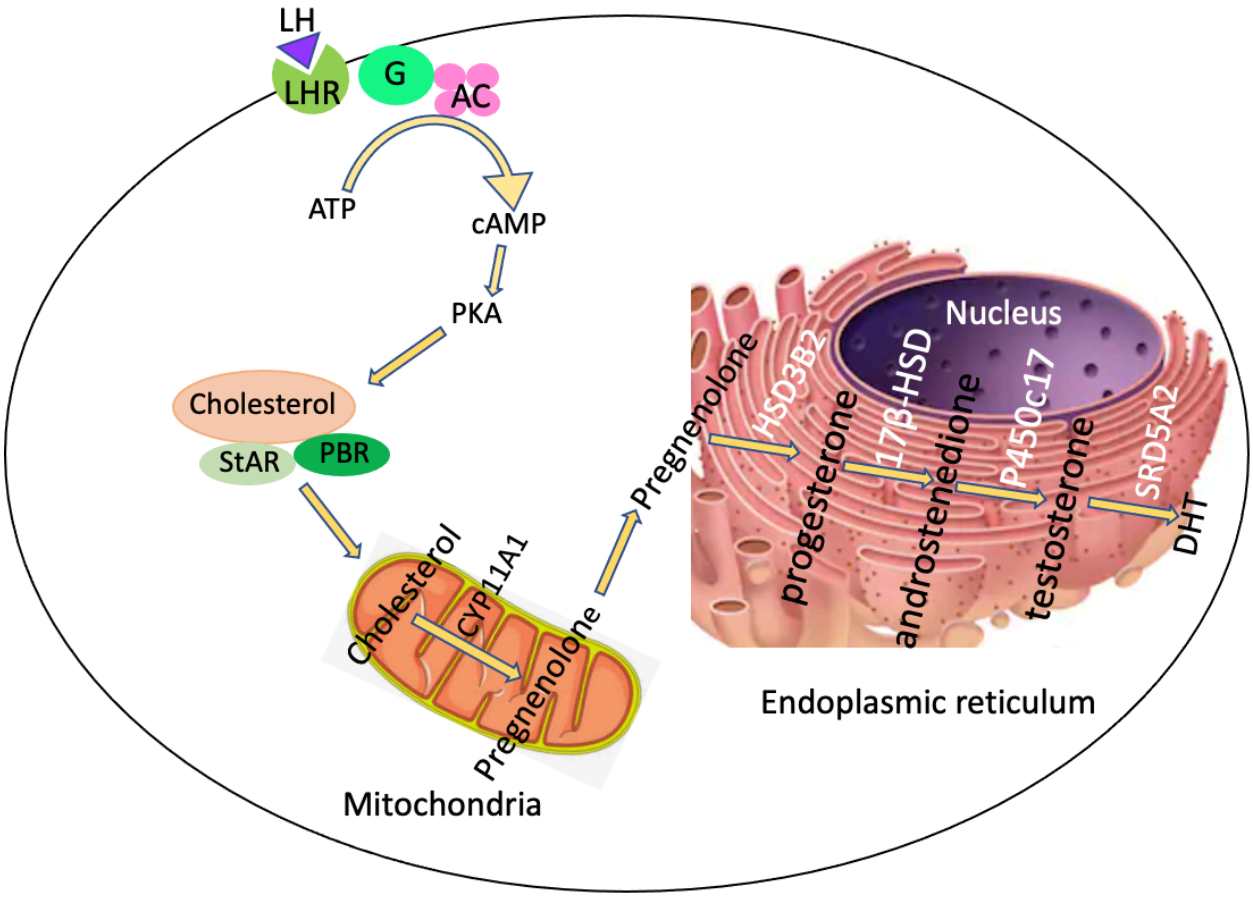

Figure 1.26. Schematic representation of Leydig cell displaying the steroidogenesis

Steroidogenesis in Leydig cells is critical phases of development and essential for homeostasis of key physiological functions. Steroidogenesis is a multi-step mechanism which is initiated with the secretion of Luteinizing hormone (LH) by the anterior pituitary gland in response to gonadotropin-releasing hormone (GnRH) from hypothalamus (Al-Agha and Axiotis, 2007). LH binds to its 7-transmembrane G-protein coupled receptor called LHCGR (luteinizing hormone/choriogonadotropin receptor) or LHR (luteinizing hormone receptor) on the cell membrane of Leydig cells and stimulates adenylate cyclase activity, resulting in increased cyclic adenosine 3', 5' monophosphate (cAMP) production (Dufau, 1998). cAMP activates the cAMP-dependent protein kinase (PKA) that phosphorylates serine, threonine amino acids on particular protein substrate (Hansson et al., 1999). Steroidogenesis is triggered by cAMP by temporally separate methods such as acutely (minutes) or chronologically (hrs). The translocation of cholesterol molecules from intracellular source into the inner mitochondrial membrane is normally considered to be the rate-determining step in steroidogenesis (Stocco and Clark, 1996).

The translocation mechanism of cholesterol involves an interaction between steroidogenic acute regulatory (StAR) protein and peripheral-type benzodiazepine receptor (PBR) (Stocco, 2000 and Papadopoulos, 2004). PBR has strongly affinity with the binding and movement of cholesterol from cytosolic donors into the inner mitochondrial membrane. StAR and PBR are strongly associated while translocating cholesterol into mitochondria where StAR acts as a cholesterol transport originator and PBR as a gateway to the entry pf cholesterol in mitochondria (Hauet et al., 2005). As soon as cholesterol is entered into mitochondria, it is transformed into pregnenolone catalysed by the C27 cholesterol side-chain cleavage cytochrome P450 enzyme (CYP11A1) and certain electron transferring proteins located on the matrix side of the inner mitochondrial membrane (Payne and Hales, 2004). Pregnenolone then leaves the mitochondria to the smooth endoplasmic reticulum, where it is converted by 3β-HSD to progesterone. This steroid is then metabolised by P450c17 to androstenedione, which is converted to testosterone by 17β-HSD (Payne and Hales, 2004). The testosterone is then converted into Dihydrotestosterone (DHT) by SRD5A2.

1.11.2. AR protein

The AR encoding gene is located on the chromosome Xq11-12 and consists of 8 exons. This gene spans 186587kb that encodes a 110kDa androgen receptor protein which consist of 919 amino acids (Heinlein and Chang, 2004). AR shows high structural homology with other steroid receptors such as progesterone receptor (PR), glucocorticoid receptor (GR), oestrogen receptor (ER), and thyroid receptor (TR) (Kuiper et al., 1989). The AR protein (termed AR) has four functional domains (Fig. 1.27) including: (1) N-terminal domain (NTD) - this domain is the most variable and poorly conserved domain. The NTD is encoded by exon 1 and accounts for more than half of the size of the AR. The NTD has an activation function 1 (AF-1) domain which includes two overlapping transcription activation units (TAUs) - TAU-1 (amino acids 1-370) assists AR transcriptional activity upon incitement by full agonist, and TAU-5 (amino acids 360-528) gives a constitutive movement to the AR without its ligand biding domain (LBD) (Fig. 1.27) (MacLean et al., 1997). Tau-1 possesses FQNLF motif (aa 23-27) and TAU-5 possesses WHTLF motif (aa 433-437), which are vital for modulating the ligand-dependent and interdomain interaction between

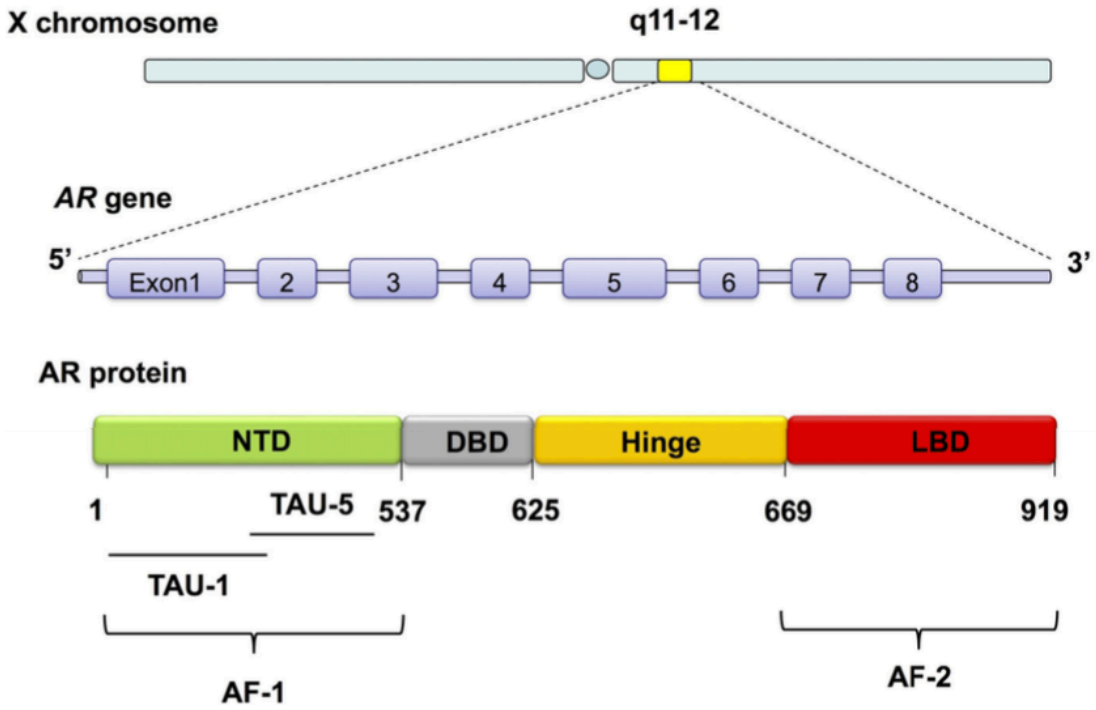

Figure 1.27. Schematic representation of AR gene and protein indicating specific motifs and domains. The *AR* gene on X chromosome contains 8 exons. The encoded AR proteins includes NTD, DBD, Hinge region and LBD as well as AF-1 and AF-2 and two transcription activation units (TAUs): TAU-1 and TAU-5. Adapted from (Pakula et al., 2017).

the NTD and LBD. Interplay of NTD-LBD is key for the sustainability of the AR dimer complex (Tan et al., 2015). (2) DNA-binding domain (DBD) is the most conserved region and is encoded by exon 2 and 3 and contains two zinc finger motifs which bind to androgen response elements of the target gene (Pakula et al., 2017). (3) Ligand binding domain (LBD) is encoded by exons 4-8 that binds to its ligands, testosterone and dihydrotestosterone (DHT). LBD domain along with activation function 2 (AF-2) domain is located in the carboxyl-terminal end of AR (Ferraldeschi et al., 2015). A majority of AR point mutations in PCa have been identified in the LBD implying their significance in aberrant AR signalling. (4) Hinge region is a short amino acid sequence located between the DBD and LBD. This region assists in the nuclear transport of the AR and in regulation of the transactivation potential resulting in post-translational modification. Interestingly, it performs as an integrator for signals coming from different pathways (Clinckemalie et al., 2012).

1.11.3. Variants of AR

Chang and colleagues cloned the full-length transcript of the AR gene (AR transcripts variant 1) (Lubahn et al., 1988). Two further variants were identified i.e., 110kDa and 87kDa AR proteins in

human genital skin fibroblast (Wilson and McPhaul, 1994), the former missing the N-terminal of the full length transcript. Endogenous AR variant in the prostate cancer cell lines was identified using immunoblotting of a lower molecular weight band when blots were screened for full-length AR (Gregory et al., 2001). Further finding demonstrated that the variants in the lower molecular weight band lacked the binding ligand domain (Tepper et al., 2002). It has been shown that aberrant expression of AR such as AR-Vs (AR-variants) is regulated by androgens (Nakata et al., 2016), which are found in PCa cells (e.g., LnCAP, VCAP, 22v1 and CWR-R1), human xenografts including LuCaP 86.2, LuCaP 136 and clinical PCa specimens. Several mechanisms have been described for the synthesis of AR-Vs including (1) Genomic alteration, (2) RNA alternative splicing, (3) Cofactor and signalling pathway.

1.11.3.1. Genomic alterations of AR

AR-GSRs (AR genomic structural rearrangements), sometimes on the same allele, underlie the generation of some of the AR-Vs (Kallio et al., 2018). A study conducted on tumours from multiple metastatic sites in the same patients showed similar patterns of deletion and duplication within the LBD of Arv567es variant that interpreted the dominant expression of Arv567es (Henzler et al., 2016). Androgen-dependent CWR22Pc cells harbour AR-GSR which is increased during castration and its existence is associated with elevated expression of AR-Vs (Li et al., 2011).

1.11.3.2. Alternative RNA splicing of AR transcript

RNA splicing of AR-Vs takes place at the transcriptional level (Paschalis et al., 2018). RNA splicing in AR-V7 involves inclusion of cryptic exon 3 (CE3) spanning intron 3. CE3 contains the canonical splice as well as 3'polyadenylation signal sequence and is recognised to be last exon of the AR-V7 transcript. A general splicing factor HNRNPA1 (heterogeneous nuclear ribonucleoprotein A1) was also reported to regulate AR-V7 expression in prostate cancer cells (Nadiminty et al., 2015). Activation of NFκB2/p52 and c-Myc signalling resulted in recruitment of HNRNPA1 to the splice site of AR pre-mRNA to promote AR-V7 expression (Nadiminty et al., 2015).

1.11.3.3. Cofactors regulating AR-Vs expression

The AKT, protein kinase, pathway regulates AR-V expression by modulating AR function and mediating survival signalling in CRPC (Szafran et al., 2017). Several kinases including Akt, Abl and

Src family kinases were shown to control the expression of AR-V7mRNA and the nuclear translocation of proteins (Szafran et al., 2017).

1.11.4. Overview of AR variants (AR-Vs) in PCa

More than 20 unique AR-Vs have been identified (with mRNA sequence cloned) from both prostate cancer cell lines and clinical CRPC specimens (Fig. 1.28) (Cao et al., 2016). AR-Vs have been categorized based on their transcriptional activity, including constitutively active AR-Vs (e.g., AR-V7, Arv567es), conditionally active AR-Vs (e.g., AR-V1, AR-V9), and inactive AR-Vs (e.g., AR-V13, AR-V14) (Hu et al., 2011). Every variant has an intact N-terminal domain but lack segments of the ligand-binding domain (LBD) whereas AR45 contains truncated N-terminal domain. Due to the truncated N-terminal domain (that generally contain two trans-activating regions, Tau1 and Tau5/AF5), AR45 does not to show its trans-activating ability and functions as a dominant-negative variant to nullify the function of the full-length AR (AR-FL) by forming a heterodimer with AR-FL (Ahrens-Fath et al., 2005).

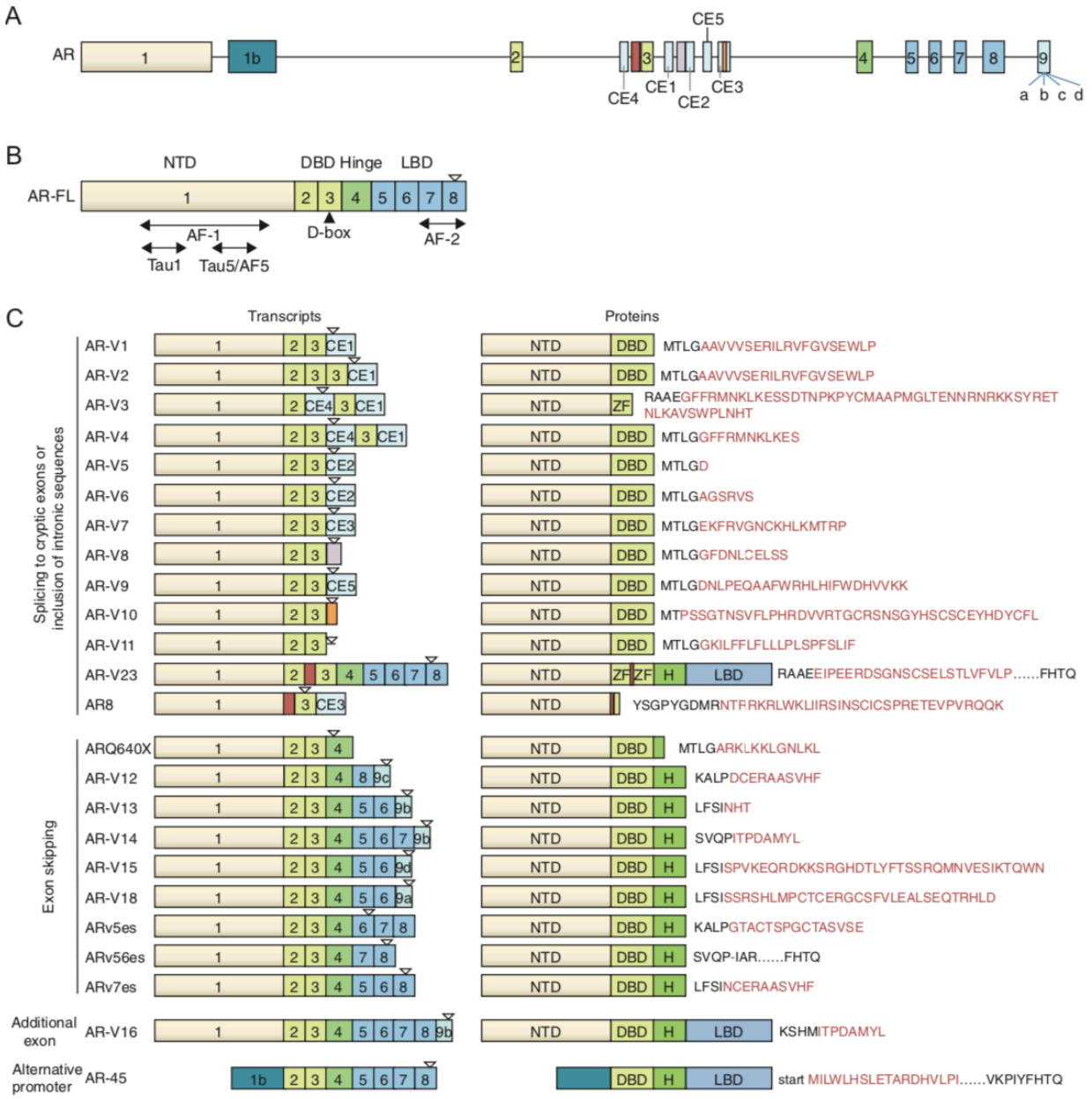

Figure 1.28. Schematic representation of the structure of AR-FL (AR full length) and AR-V transcripts and proteins. (A) genetic feature of AR gene with canonical exons and cryptic exons (CE). (B) AR-FL mRNA structure exhibiting exons encoding the N-terminal domain (NTD; exon 1), DNA-binding domain (DBD; exon 2 and 3), hinge region (part of exons 3 and 4) and ligand binding domain (LBD; exons 5-8). AF-1, Tau 1, Tau5/AF-5 and AF-2 are activation function domains. D-box indicated with black filled triangle mediating AR-V/AR-V, AR-V/AR-FL and AR-FL dimerization. (C) AR-Vs representing mRNA and protein structures. AR-V-specific peptides sequences are indicated in red, and the '-' in Arv56es indicates a unique junction. Inverted triangle indicating translation stop. Exon 9 contains four cryptic 3' splicing regions, the relating cryptic exons are indicated as 9a, 9b, 9c and 9d. Adapted from (Cao et al., 2016).

A majority of AR-Vs have a conserved DBD. Nevertheless, AR8 and AR-V3 (aka AR6) lack a functional DBD and second zinc finger in DBD respectively (Yang et al., 2011). As a consequence,

AR8 cannot act as a transcription factor because of the missing DBD (Yang et al., 2011), rather, AR, at the plasma membrane, stimulates EGF-induced Src activation and AR-FL phosphorylation and transactivation (Yang et al., 2011). Conversely, AR-V3, which still has the AR DNA-binding interface located in the first zinc finger of DBD may constitutively activate AR-responsive promoters in PCa cells (Dehm et al., 2008). The variant AR23 has in-frame insertions between the two zinc finger motifs, whilst preserving the intronic sequences portion. AR23 has been shown to exemplify cytoplasmic interaction, exclusively, enhancing transcriptional activity of the nuclear factor -kB while reducing activator protein-1 activity (Jagla et al., 2007). The insertion of intronic sequence is likely to abolish the DBD. The hinge region is encoded by exon 3 and 4 that has been shown to have the canonical signal of nuclear localization. For the variants to perform their trans-activation function, the nuclear localization property is essential. Some variants have no nuclear localization signal, but they remain primarily in the nucleus or have a basal level sufficient to achieve ligand independent transcriptional activity (Chan et al., 2012). Certain mechanisms for their nuclear localisation have been suggested, such as presence of a signal-like sequence, lack of nuclear export signal (Chan et al., 2012) or tyrosine phosphorylation in the the N-terminal domain (Karaca et al., 2015). However, these mechanisms seem unsuitable for all variants with predominant nuclear localisation and this was one motivation for conducting this project.

1.11.5. AR-Vs contributing to CRPC

The exact mechanism of the AR-Vs in development of CRPC remain to be elucidated. AR-V appears able to reactivate the AR transcriptional program in the absence of androgens and full-length AR (Liu et al., 2014). A number of findings suggest that every AR-V has a distinct transcriptional target in PCa cells (Hu et al., 2012). Studies found a set of genes including a number of cell-cycle-related genes are upregulated during overexpression of AR-V7 and AR-V12/ARv567es. Another report, using specimen of post hormone therapy PCa patients, showed that the expression of AR-V7 is correlated with expression of one of the cell-cycle-genes, UBE2C (Hu et al., 2012). These findings suggest that AR-Vs mediate a distinct profile of cell-cycle gene expression which is separate from full-length AR. Furthermore, similar studies have also shown that cell-cycle genes were upregulated in sample with AR variant expression (Hörnberg et al., 2011). AR-V7 resides in the nucleus under androgen-depleted conditions and is constitutively

active in response to androgens. This is similar to the mechanism of another key cell signalling pathway, namely Wnt signalling (see below) with β-catenin performing a function similar to AR as a transcription factor co-activator. Nearly 60% of colorectal cancer samples contain mutations in APC gene, coding for a β-catenin sequestering protein in the cytosol, resulting in β-catenin desequestration (release from the so-called destruction complex, see below) and nuclear accumulation and resulting activation in transcription of proto-oncogenes that drive the tumour (see below for details) (Kypta and Waxman, 2012).

The most common variant is AR-V7 with a 20 times higher expression in CRPC compared to hormone-naïve PCa. Prostate cancer cells that express full-length AR (AR-FL) and AR-Vs are independent of androgen and resistant to enzalutamide. Knockdown of AR variants in these cells suppress androgen-independent growth and confer enzalutamide responsiveness (Li et al., 2013). The AR-FL and AR-Vs are resistant to specific chemotherapeutic agent in CRPC such as abiraterone. A study on CRPC xenograft treated with abiraterone showed higher expression of AR-FL and AR-Vs (e.g., AR-V567es and AR-V7) (Mostaghel et al., 2011). Expression of AR-V1 and AR-V7 is higher in CRPC than in hormone-naïve bone metastasis. AR-V567es is expressed in CRPC bone metastasis but absence in hormone-naïve bone metastasis. Therefore, expression of AR-V567es and /or AR-V7 is correlatively associated with poor survival (Hörnberg et al., 2011). These changes of AR-V7 in circulating tumour cells could represent selective pressure from treatments on prostate cancer cells. The expression of AR-V7 in hormone-naïve prostate cancer is associated with a lower PSA from patients treated by androgen deprivation therapy. Therefore, AR-V7 could be used as a biomarker for the progression of hormone-naïve prostate cancer into CRPC (Li et al., 2018)

1.11.6. AR signalling in normal prostate

Testosterone is an endogenous androgen which is generated via hypothalamus-pituitary-Leydig cell axis (Radmayr et al., 2008). The hypothalamus releases LHRH (luteinizing hormone-releasing hormone) which in turn promotes the pituitary gland to release LH, which binds to Leydig cells of testes and enhance testosterone production (Radmayr et al., 2008). The secreted testosterone circulates in the blood stream where it binds to albumin and sex-hormone-binding globulin (SHBG), and the small fraction of it is dissolved freely in the serum. The free circulating

testosterone enters prostate cells; around 90% of testosterone is converted by 5α-reductase enzyme into its fivefold higher affinity form, dihydrotestosterone (DHT) than testosterone for AR binding (Radmayr et al., 2008). DHT binds to cytosolic AR where it remains sequestered binding with heat shock protein complexes consisting of Hsp70 (hsp70), Hsp(p60), Hsp90 and p23.

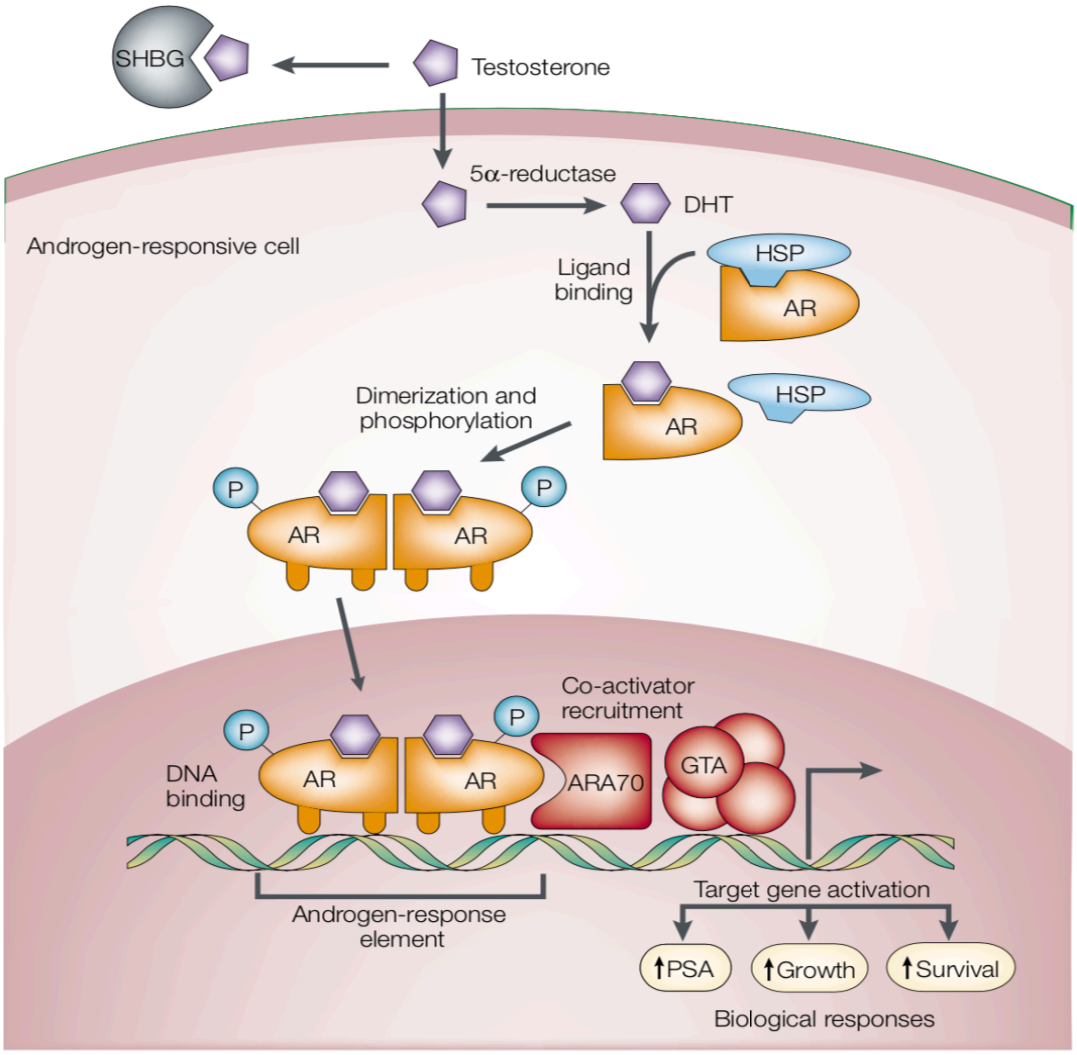

Figure 1.29. Preceptor and receptor-level modulation of androgen receptor (AR) action within the prostate cell. Mechanism is described in the text. Adapted from (Feldman and Feldman, 2001).

The key function of the complex is to maintain AR in a ligand binding conformation and to shield it from proteolysis (Prescott and Coetzee, 2006). Binding with DHT or testosterone induces a conformational change in the AR that leads to dissociation from the heat-shock proteins causing phosphorylation (Brinkmann et al., 1999), in part mediated by protein kinase A. The ligand-induced conformation shift promotes the formation of AR homodimer complexes which then

translocate into the nucleus where it binds to androgen response elements (AREs) in the promoter region of the target genes (Brinkmann et al., 1999). The activated DNA-bound AR homodimer complex deploy co-regulatory proteins, co-activators and co-repressors to the AR complex. The co-activators and co-repressors govern the AR complex to interact with the general transcription apparatus to enhance and inhibit transcription of target genes leading to biological responses including growth, survival and also the production of PSA (Lubahn et al., 1989 and Lee and Chang, 2003).

AR signalling is critical for normal prostate cell function and is also required for the growth and development of PCa cells. Prostate cancer prognosis depends on the balance of cells proliferating versus those dying. Androgens are the main controller of this ratio by both promoting proliferation and inhibiting apoptosis. So, prostate cancer is dependent on a level for androgenic escalation for growth and survival. Androgen depletion therapy (ADT) causes regression of cancer because without AR signalling, the rate of cell proliferation is lower and the rate of cell death increased, resulting in extinction of these cells (Denmeade et al., 1996). However, over time, some cancerous cells acquire specific molecular and cellular changes in order to activate AR signalling regardless to whether there a blockade of androgens. A number of mechanisms have been described in order to develop androgen independent PCa (AIPC).

1.11.7. Mechanism of development of AIPC

Intermittent androgen ablation is considered to cause selective pressure resulting mutation that cause AIPC. During androgen deprivation therapy (ADT), prostate cancer cells develop a variety of cellular pathways to survive and flourish in the androgen depleted environment. Postulated and documented mechanisms are as follows:

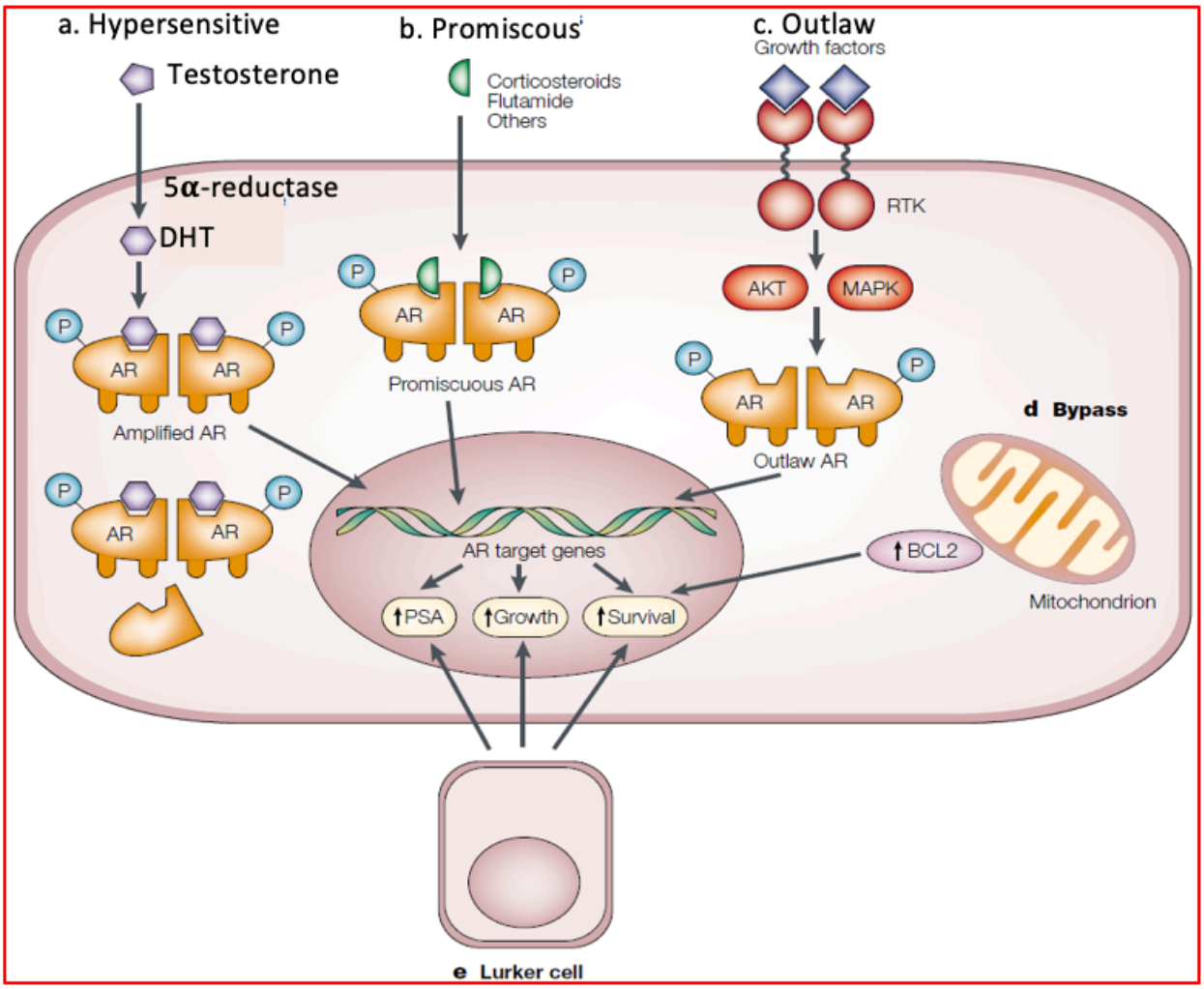

Figure 1.30. Five possible pathways for AIPC development. (a) hypersensitive pathway: AR stimulate sensitivity to balance low androgen levels. (b) promiscuous pathway: the ligand binding specificity of AR is extended to allow for the activation by non-androgenic compound present in the circulation. (c) outlaw pathway: Receptor tyrosine kinase (RTKs) are activated, and the AR is either phosphorylated by the AKT (protein kinase B) or by the mitogen-activated protein kinase (MAPK) pathway for generating a ligand-independent AR. (d) bypass pathway: parallel survival pathways which includes that containing the BCL2 (B-cell lymphoma 2) anti-apoptotic protein, avoid AR and its ligand. (e) lurker cell pathway: androgen-independent malignant cells that are evident in the prostate throughout its life. Image adapted from (Feldman and Feldman, 2001).

1.11.7.1. Hypersensitive pathway

The prostate cancer cells circumvent the effect of androgen ablation therapy by increasing its sensitivity to very low level of androgens (Chen et al., 2004a and Weber and Gioeli, 2004). Actually, in the classic sense the cancer cells do not become androgen independent, but rather become castration independent. Three mechanisms are proposed to explain how the cell could survive at lower level of androgen:

The first mechanism is increased expression of AR that facilitates increased ligand binding. Hormone refractory tumour cells not only increase expression of AR compared with androgen-dependent tumours (Chen et al., 2004a), but also androgen-independent cells are capable of surviving with 80% lower concentration of androgen than androgen-dependent cells for growth (Chen et al., 2004a).

The second mechanism is the increased sensitivity of AR to androgen during castration (Gregory et al., 2001). A study on AR mutated LnCAP demonstrated high levels expression of the AR, increased stability of the AR and enhanced nuclear localisation of AR in recurrent prostate tumours associated with an increased sensitivity to the growth promoting effects of DHT. A 4-fold lower concentration of DHT is required for growth stimulation of androgen independent cells than androgen dependent LnCAP cells (Gregory et al., 2001).

The third mechanism is increased local growth of androgens by PCa cells themselves. This may occur by an increased rate of conversion of testosterone to DHT by increasing 5α-reductase activity (Feldman and Feldman, 2001). This mechanism could be supported with evidence that in ethnic groups with higher level of 5α-reductase activity they have a higher rate of prostate cancer (Makridakis et al., 1997).

1.11.7.2. Promiscuous pathway

The AR signalling is activated by binding AR to its specified ligands testosterone or DHT. The specificity of AR is extended by mutations. Most mutations documented leading to binding promiscuity are aggregated in the ligand-binding domains of AR (Taplin and Balk, 2004). These mutations enable AR to interact with non-androgenic steroid molecules normally present in the circulation as well as antiandrogens (Debes and Tindall, 2004 and Chen et al., 2004a). As a consequence, the malignant cells continue to proliferate and avoid apoptosis by using other circulating hormones as substitute androgens when the level of androgen is low. The first identified AR gene mutation was in the hormone-dependent LnCAP cells (Veldscholte et al., 1992). The mutated AR binds to other steroid hormones as well as the androgen antagonist flutamide to activate the AR signalling to stimulate cell proliferation. The LnCAP cell line possesses a unique missense mutation of amino acid at position 877, which is located in the

ligand-binding domain. The result of this mutation is alanine replacement with threonine at position 877 (T877A), which is relatively common in patients with AIPC (Veldscholte et al., 1992). Though the presence of mutation in AR contracted its ligand specificity for DHT or testosterone thus broadening its specificity for progestins, oestrogens and many anti-androgens for activation of AR signalling (Veldscholte et al., 1992). This mutation would be of great benefit to a cancerous cell during ADT. Therefore, activation of this signal does not require androgens, but instead can utilize other common circulating hormones or molecules for its downstream signalling cascade.

1.11.7.3. Outlaw pathway

The AR signalling pathway involves AR and its androgen or non-androgen ligand activation. Apart from canonical ligand binding pathway, AR signalling elements can be activated for growth and proliferation in an alternative pathway, called outlaw pathway (Debes and Tindall, 2004). Cytosolic AR has been shown to interact with many molecules in a nongenomic role and activate various pathways. Deregulated growth factors, including insulin-like growth factor-1 (IGF-1), Keratinocyte growth factor (KGF), epidermal growth factor (EGF) and cytokines such as interleukine-6 (IL-6) have been reported to phosphorylate and activate the androgen receptor and thus activate downstream cascade (Culig et al., 2005). Receptor tyrosine kinases (RTK) are important signalling molecules that have been shown to be altered in various pathological conditions specially in cancers. The receptor-tyrosine-kinase pathway has been associated with the AR signalling pathway. For instance, overexpression of the receptor-tyrosine-kinase HER-2/neu has been reported to activate androgen receptor target genes in the absence of a ligand (Gioeli et al., 2002).

1.11.7.4. Bypass pathway

Administering ADT results in depletion of androgen supply to activate the AR signalling pathway for growth and proliferation. In such unfavourable circumstances, the PCa cells develop the ability to survive independent of ligand-mediated or non-ligand-mediated pathways for the activation of AR signalling pathway in AIPC cells. Additionally, complementary or alternative routes which can completely bypass AR may also be triggered. The best-known bypass mechanism involves modulation of apoptosis (Lorenzo et al., 2007). In androgen-dependent

prostate cancer cells, androgen receptor activation promotes cell proliferation and depletion of androgen leads to apoptosis of the cells. In spite of depletion of androgen, it has been observed that PCa cells gradually up-regulates antiapoptotic molecules (Raffo et al., 1995). The *BCL2* gene is considered to be a candidate bypass gene which can block apoptosis. *BCL2* is not generally expressed in secretory epithelial cells of the prostate. But *BCL2* is expressed quite often in premalignant Prostatic Intraepithelial Neoplasia (PIN) and in AIPC (Colombel et al., 1993). Moreover, A study showed an emergence of *BCL2* expression which was not expressed in the initial stages of PCa tumour development in xenografts from castrated mice. But the emergence of AIPC in a LnCAP xenograft was delayed while blocking the *BCL2* with antisense oligonucleotide (Gleave et al., 1999).

1.11.7.5. Lurker cell pathway

The efficacy of the ADT fails because of the dependence of cell growth on androgen supply turns into androgen independent growth. A study shown AIPC still develop after ADT (Isaacs et al., 1991). The reason could be that a subpopulation of androgen-independent tumour cells was present even before therapy was started. The putative epithelial stem cells of prostate are recognised to be autonomous of androgen for their proliferation and death (Isaacs et al., 1991).

Based on the description provided above, early detection of PCa that remain confined in prostate can be treated using drugs for a successful therapy. Transition of PCa from inert into aggressive forms require depletion of androgen production by radical prostatectomy called ADT. administration of ADT results in activation of other signalling pathway to compensate androgen supply to activate AR signalling pathways. This becomes more aggressive and metastasize to distal sites, eventually results in fatal outcome (Saraon et al., 2014). Identification of molecular aberration in APIC is extremely significant to perceive the disease and generate therapeutic target to enhance patient care.

1.12. Wnt signalling

The term Wnt is an amalgam of Wg (Wingless) and Int1 (integration 1) (Nusse et al., 1991). The gene Wingless (Wg) gene was genetically identified as a segment polarity gene in Drosophila in 1980 by (Nüsslein-Volhard and Wieschaus, 1980). The gene Int1 was originally identified as a

proto-oncogene in 1982 by Nusse and Varmus as a susceptible site for retroviral integration of the mouse mammary tumour virus (MMTV) in a mouse mammary cancer model (Nusse et al., 1991). The genes Wg and int1 were found homologous in Drosophila and mouse respectively (Rijsewijk et al., 1987).

1.12.1. Genes of Wnt signalling ligands

Nineteen Wnt genes have been discovered which are distributed over 10 chromosomes with an additional isoform described for human (Miller, 2001). A few, e.g. Wnt6 and Wnt 10A are positioned adjacently on the chromosome in the genome (Nusse et al., 1991). Wnt1 and Wnt10b are on chromosome 12 (~8.1kb), apart from each other. This is further illustrated in Table 1.3 and a phylogenetic tree showing evolutionary conservation is shown in Fig. 1.31.

Table 1.3. Representation of chromosomal locations of WNT genes in human and mouse. Location of genes distance from telomere indicating with cM (centimorgan). Accession number for Genebank GenBank (http://wwwx.ncbi.nlm.nih.gov/Genbank/index.html). Adapted from (Miller, 2001).

Human		Mouse		Accession numbers†	
Gene	Location	Gene	Location*	Human	Mouse
WNT1	12q13	*Wnt1*	15	X03072	K02593
WNT2	7q31	*Wnt2*	6 (4.2 cM)	X07876	AK012093
WNT2b/13	1p13	*Wnt2b/13*	3 (49.0 cM)	XM052111, XM052112	AF070988
WNT3	17q21	*Wnt3*	11 (63.0 cM)	AY009397	M32502
WNT3a	1q42.13	*Wnt3a*	11 (32.0 cM)	AB060284	X56842
WNT4	1p35	*Wnt4*	4	AY009398	M89797
WNT5a	3p14-p21	*Wnt5a*	14 (14.8 cM)	L20861	M89798
WNT5b	12p13.3	*Wnt5b*	6 (56.2 cM)	AB060966	M89799
WNT6	2q35	*Wnt6*	1	AY009401	M89800
WNT7a	3p25	*Wnt7a*	6 (39.5 cM)	D83175	M89801
WNT7b	22q13.3	*Wnt7b*	15 (46.9 cM)	AB062766	M89802
WNT8a/d	5q31	*Wnt8a*		AB057725, AY009402	Z68889
WNT8b	10q24	*Wnt8b*	19 (43.0 cM)	Y11094	AF130349
WNT10a	2q35	*Wnt10a*	1	AB059569	U61969
WNT10b/12	12q13.1	*Wnt10b*	15 (56.8 cM)	U81787	U61970
WNT11	11q13.5	*Wnt11*	7	Y12692	X70800
WNT14	1q42	-		AB060283	
WNT15	17q21	*Wnt15*	11	AF028703	AF031169
WNT16	7q31	*Wnt16*		XM031374, XM004884	AF172064

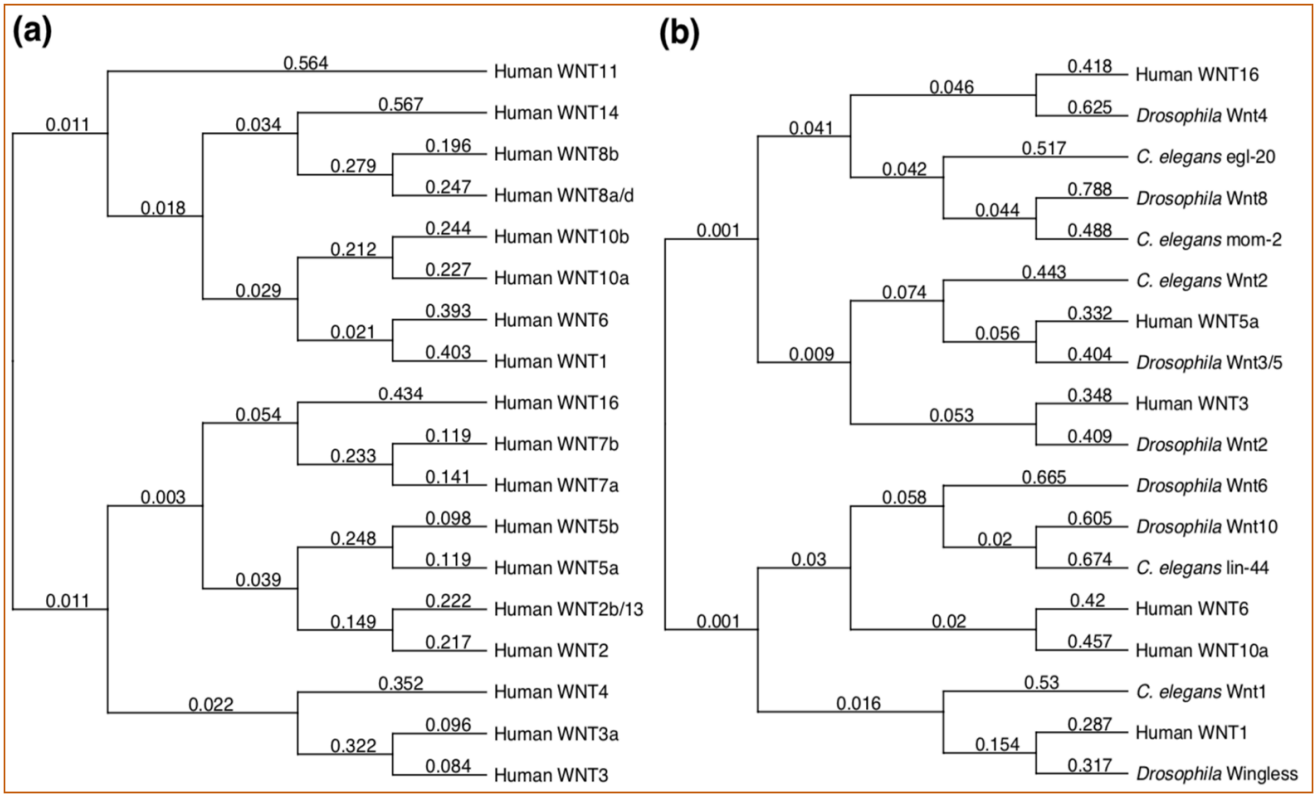

Figure 1.31. Phylogenetic tree predicted evolutionary relationships among the Wnt genes. (a) Anticipated 18 of 19 known human Wnt proteins sequences relationship in which Wnt15 was excluded due to unavailability of full sequence. (b) Predicted relationships between selected human Wnt proteins displaying each large grouping shown in (a) and Wnt proteins from mouse, Xenopus, Drosophila and Caenorhabditis elegans. Image adapted from (Miller, 2001).

Gai et al. reported 19 genes in mouse genome distributed over different chromosome demonstrated in the following figure (Fig. 1.32)

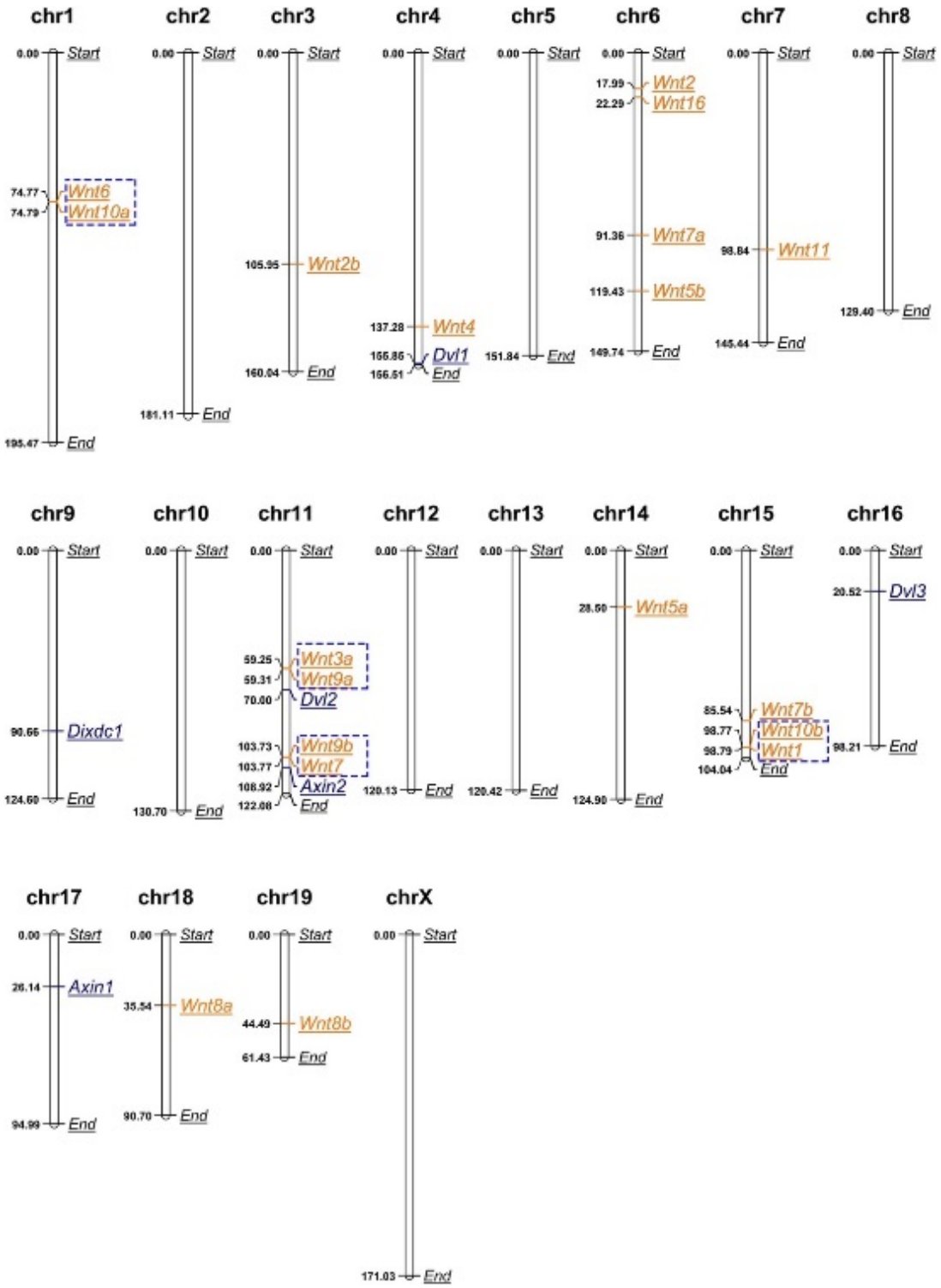

Figure 1.32. Distribution of mouse genes on chromosome. 19 Wnt genes located on certain chromosomes. Genes in blue boxes are tandem duplication genes. The unit of the length for all chromosome displayed here in megabases (Mb). The image adapted from (Gai et al., 2021).

1.12.2. Structure of Wnt Protein

Wnt proteins are secreted lipid-modified, cysteine-rich palmitoleated glycoproteins and predominantly connected with cell membrane and the extra-cellular matrix (ECM) (Reichsman et al., 1996). The molecular weight of human Wnt proteins varies from 39kDa (Wnt7a) to 46kDa (Wnt10a) (Miller, 2001). The proteins are composed of an N-terminal signal sequence of 350-400 amino acids, most of which forms intramolecular S-S bonding, including 22-24 of preserved cysteine residuals (Fig. 1.33). Following translation, the majority of the proteins are modified by glycosylation and lipidation.

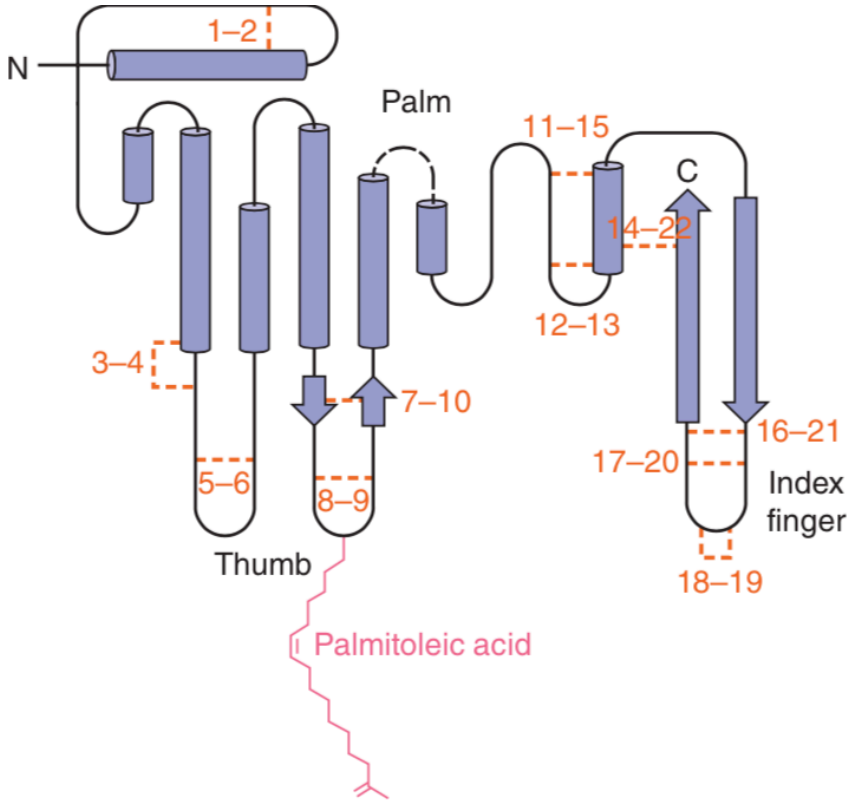

Figure 1.33. Schematic representation of secondary structure of Wnt. Orange colour: The conserved 22 cysteine residues are numerated to show the pairs forming disulfide bridge. Dashed line: The approximate position of linker region in which Wg (Wingless) insert approximately 80 amino acids. The image adapted from (Willert et al., 2003).

Although Wnt signalling is physiologically important, the bio-chemical understanding of Wnt protein function was poorly distinguished because of inherent difficulties in purifying its native forms (Willert et al., 2003 and Willert and Nusse, 2012). Although these obstacles have also prevented the analysis of the crystallography, co-expression of Xenopus Wnt8 protein with the

ligand binding domain, cysteine-rich domain (CRD), of the human Frizzled (Fzd) 8 receptor has allowed the crystallisation of these protein and some knowledge of the structure of Wnt proteins (Janda et al., 2012). This research concluded that Wnt proteins consist of two separate domains, a larger N-terminal domain (NTD) or D1, and a C-terminal domain (CTD) or D2. The NTD consists of six α-helices and two protruding β-hairpins, one of which has a preserved serum residue (Ser187 of Xenopus Wnt8) fastened to a chain of fatty acids which interacts with the Fz CRD in a lipid-in-groove manner (Willert et al., 2003). On the other hand, the Wnt8 CTD, consisting of one helix and two β-sheets, partially resembles the cysteine-knot growth factor hairpin loop; and Fz CRD also reacts with the tip of this hairpin. As a result, the Fzd CRD appears to be captivated by two distinct β-hairpin expeditions from the core of the Wnt protein (Willert et al., 2003).

1.12.3. Wnt protein Secretion

Subsequent to their translation, Wnt proteins are processed in the ER (endoplasmic reticulum) for post translational lipidation (Willert et al., 2003 and Takada et al., 2006). Nearly all Wnts are transformed by acyltransferase known as Porcupine (porcn), a member of the MBOAT family of transmembrane-bound O-acyltransferases (Takada et al., 2006). Following this modification, Wnt proteins are linked to a Wnt transporter protein, namely Wntless (Wls) and Evi or sprinter and then guided to a plasma membrane (Bänziger et al., 2006; Bartscherer et al., 2006; Goodman et al., 2006 and Coombs et al., 2010). However, there is some controversy about the necessity of secretory mechanisms for Wnt; for example, secretion and lipidation of ectopically expressed Wnt5b are inhibited in porcn-deficient zebrafish embryos, while the Wnt3a expression is less or not affected (Chen et al., 2012). Furthermore, ectopically expressed Wnt11 and Wnt3a are secreted apically and basolaterally in polarized epithelial culture cells, but recycling of Wls is required only for the basolateral secretion of Wnt3a but not for the apical secretion of Wnt11 (Yamamoto et al., 2013). These findings indicate that the pathway mediated by Porcn/Wls continues to secret Wnt according to the subtype of Wnt and cellular environment. Also, N-glycosylation often governs the route of Wnt secretion in polarised epithelial cell cultures (Yamamoto et al., 2013). However, once the proteins have been secreted, these can be integrated in secretory vesicles whereby Wls proceeds to connect Wnt proteins with their cognate Frizzled receptors (Routledge and Scholpp, 2019).

1.12.4. Wnt signalling ligands investigated in prostate cancer

The functional role of the ligands discussed below has been investigated in this thesis and the role of these and some other Wnt ligands has been previously investigated in PCa cells in our laboratory (Wang et al., 2007b; Wang et al., 2010a; Thrasivoulou et al., 2013 and Ashmore et al., 2019) discussed in detail in later chapters.

Wnt-3A

The human Wnt-3A consists of 352aa of which 24aa act as signal sequence and other 328aa are mature segments (Saitoh et al., 2001). It has 87% sequence identity to human Wnt-3. The mature region contains 24 cysteines and two sites of N-linked glycosylation. Mouse mature regions also contains 328aa and is recognized as secreted glycoprotein of 44kDa (Smolich et al., 1993). Both of the mature segments are 96%aa identical (GenBank Accession # Q9QXQ5) but these two proteins have individual expression patterns (Saitoh et al., 2001).

Wnt5A

Wnt5A, 343 amino acid long and arises from a 365aa precursor protein that makes a secreted glycoprotein of 49 kDa (Burrus and McMahon, 1995). Wnt5A contains 25 cysteine residues and 4 potential N-linked glycosylation sites and a 10aa Wnt-1 family (Wnt-1, 2, 5a) signature that composed of CKCHGVSGSC motif (Clark et al., 1993). Wnt-5a of mature mouse region consists of 342aa and is 99% identical to human. The signalling sequence of human Wnt-5A is 22aa which is shorter than the mouse signalling sequence of 37aa (Clark et al., 1993). Chromosomal location of human Wnt-5A and mouse Wnt-5A is different. Human Wnt-5A gene resides on chromosome 3 whereas mouse Wnt-5A is on chromosome 14 indicating chromosomal rearrangement at this locus during evolution (Lejeune et al., 1995). Wnt-5A is expressed in endometrial epithelium (Bui et al., 1997), stomach mesenchyme (Lickert et al., 2001) and embryonic fibroblast (Clark et al., 1993).

Wnt9B

Wnt9B has been cloned in both human and mouse, in which human Wnt9B composed of 357aa containing 22aa signalling sequence and a 335aa mature region (Kirikoshi et al., 2001). The

mature segment contains 24 cysteines residues and one potential N-linked glycosylation site. The human and mouse Wnt9B share 64% sequence identity and differences exist in the C-terminal only (Qian et al., 2003). Wnt9B is present in embryonic muscle, epidermis, and intestinal, enamel, and salivary gland epithelium (Lawson et al., 2001).

The secondary protein structure of other human Wnts shares high sequence homology and is given below:

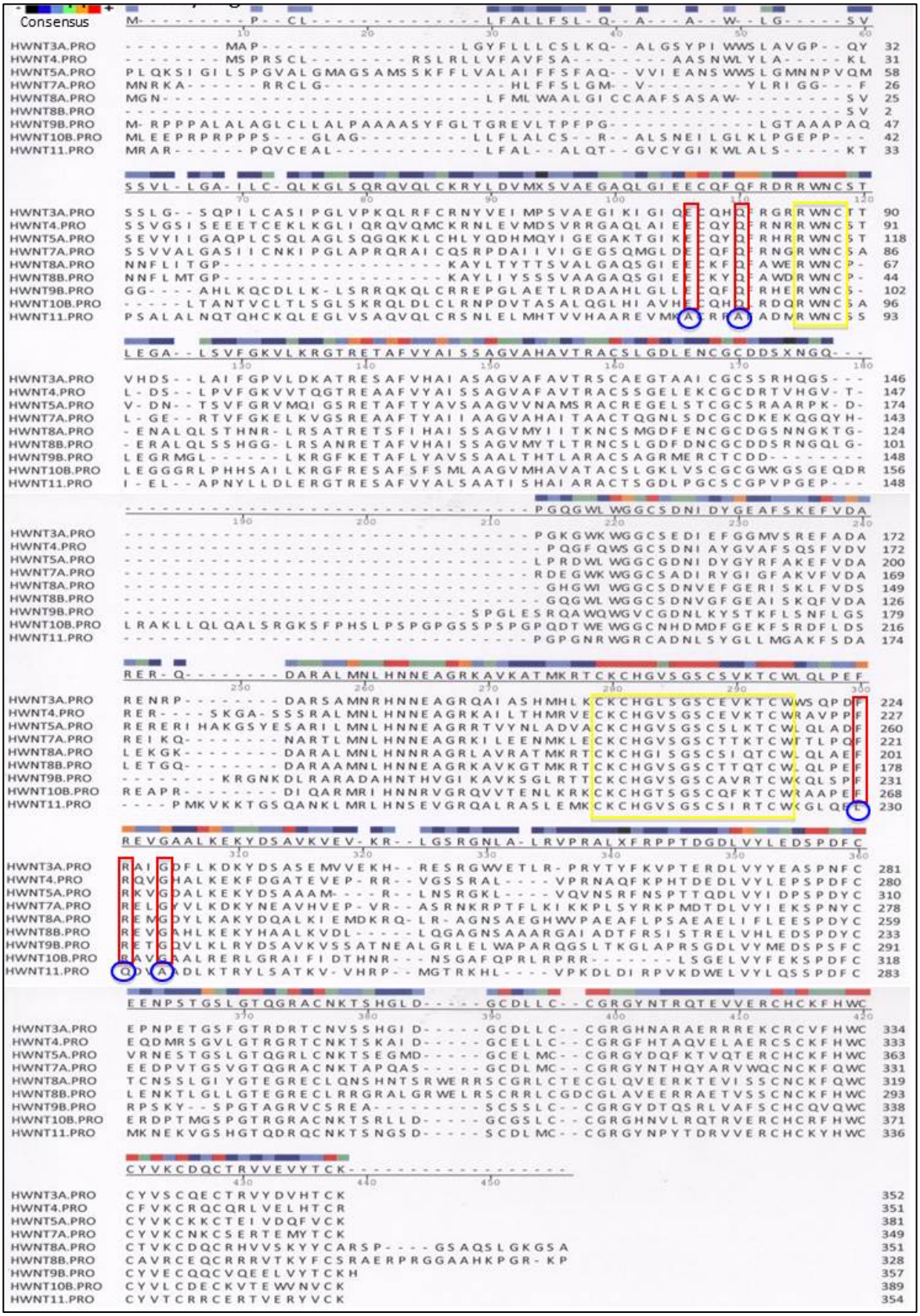
Consensus
HWNT3A.PRO
HWNT4.PRO
HWNT5A.PRO
HWNT7A.PRO
HWNT8A.PRO
HWNT8B.PRO
HWNT9B.PRO
HWNT10B.PRO
HWNT11.PRO

Figure 1.34. Sequence alignment of human Wnt (HWnt) proteins with ClustalW alignment algorithm using commercially available software (DNAstar). HWNT protein sequences were obtained from National Center for Biotechnology Information website (http://www.ncbi.nlm.nih.gov): Wnt3A, GenBank ID: BAB61052.1; Wnt4, BAC23080.1; Wnt5A, AAH74783.2; Wnt7A, BAA82509.1; Wnt8A, BAB60960.1; Wnt8B, CAA71994.1; Wnt9B, AAQ88584.1; Wnt10B, AAB51685.1; Wnt11, CAA73223.1. Aligned HWNT protein sequences (HWNTX.PRO) are listed from Wnt3A to Wnt11. Consensus amino acid sequence is given underneath the sequence similarity spectrum (no identity [-] = dark blue and consensus, complete identity [+] = red) is given on the top of the figure. Yellow boxes highlight conserved motifs in HWNT protein sequence. Blue boxes display the consensus motifs, identical in all HWNT protein sequences, with a circle signifying the amino acid substitution in Wnt11 sequence. Image adapted from (Thrasivoulou et al., 2013)

1.12.5. Classification of Wnt signalling pathways

Wnt signalling is a highly conserved cell signalling network. Wnt signalling is considered as an important mediator of vertebrate and invertebrate development to control cell proliferation, migration, cell polarity and cell fate determination and stem cell maintenance during embryonic development and tissue homeostasis (Nelson and Nusse, 2004 and Lien and Fuchs, 2014). Deregulation in Wnt signalling leads to carcinogenesis and progression of malignancies including intestine (White et al., 2012), skin (Sherwood and Leigh, 2016), breast (Shulewitz et al., 2006) and prostate (Davies et al., 2001 and Hu et al., 2016).

In the off state (Fig. 1.35A) where Wnt ligands are not bound to their receptors, levels of β-catenin in the cytoplasm remains low due to activity of ubiquitin-dependent proteasomal degradation process which is regulated by a molecular apparatus called β-catenin destruction complex (Stamos and Weis, 2013). The so-called destruction complex consists of scaffolding proteins Axin, APC, casein kinase-1-α (CK1α) and GSK3α/β. Recent evidence also indicates that in prostate cancer cell lines Connexin 43 may also form part of the destruction complex (Hou et al., 2019). The destruction complex acts in catalyzing the serine/threonine phosphorylation of a strongly preserved phosphor-degron at the N-terminus of β-catenin, preparing it for recruitment to the SCF-TRCP E3-ubiquitin ligase (Hart et al., 1999) and subsequent proteosome-mediated degradation (Hart et al., 1999).

The Wnt protein, as mentioned earlier, is a secreted glycoprotein that activates a signalling cascade by binding to the N-terminal extra-cellular cysteine-rich domain of a seven-pass transmembrane Frizzled (Fzd) receptors in the presence of co-receptor low-density-lipoprotein-related protein 5/6 (LRP 5/6). After binding of Wnt to the receptor complex, the signal transduces

to cytoplasmic Dishevelled (Dsh/Dvl). At the level of Dsh, the Wnt signal branches into two major cascades: 1. Canonical Wnt signalling pathway: Wnt/β-catenin dependent pathway and (2) Non canonical Wnt signalling pathways. Depending on activation domain of Dsh protein, the non-canonical is further divided into two, namely, planar cell polarity pathway and Wnt/Ca^{2+} pathway.

1.12.6. The canonical Wnt signalling pathway: Wnt/β-catenin pathway

This canonical pathway is the first intensively studied pathway and delineated from genetic screen in Drosophila, fly, worm, Xenopus and fish.

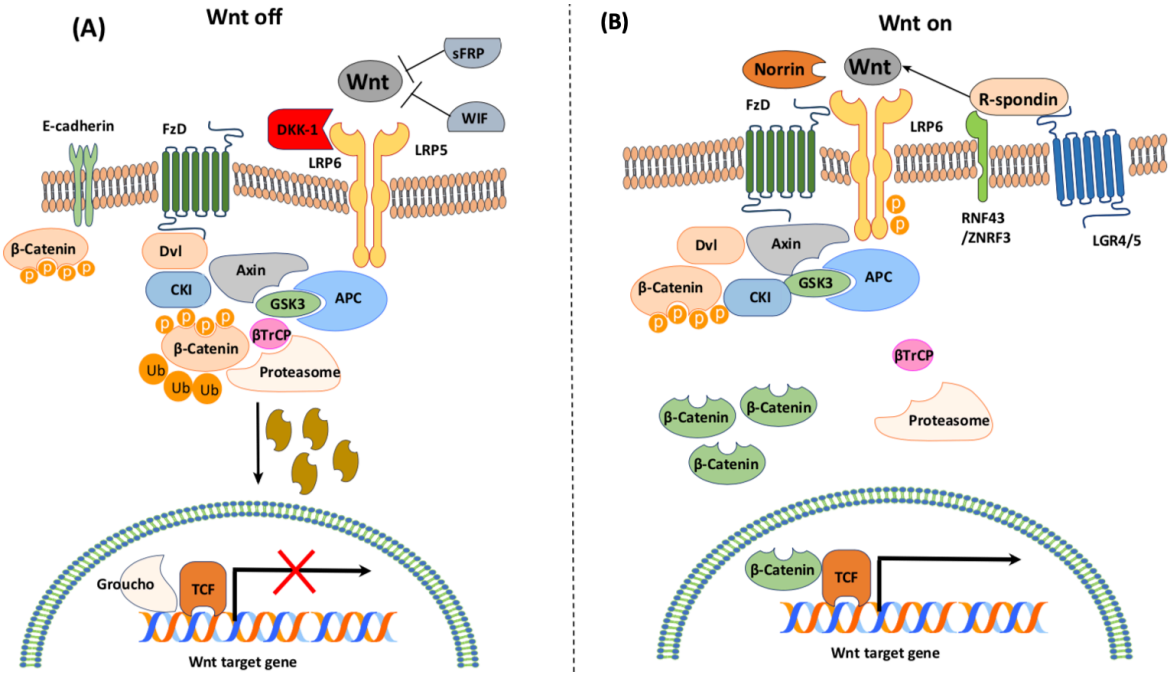

Figure 1.35. A schematic display of canonical Wnt signalling pathway. (A) left panel "Wnt off" state. In the absence of Wnt ligand the signal become inactivated. A destruction complex consists of Axin, APC, GSK3- β, and CK1 and β-catenin located in the cytosol. In this state β-catenin is dually phosphorylated by CK1 and GSK-3β and ubiquitinated by β-TrCP and targeted for proteasomal degradation. (B) Right ("Wnt on state"): Wnt ligand binds to Fzd receptor and LRP5/6 co-receptor complex. LRP5/6 receptors are then phosphorylated by CK1 and GSK-3β which recruits Dishevelled (DVL) proteins to the plasma membrane for polymerization and activation. Axin containing protein complex also migrate from cytosol to plasma membrane. DVL interacts with Fzd and Axin binds to phosphorylated LRP5/6. The newly formed complex induces in stabilization and accumulation of β-catenin in cytosol and subsequently translocates into nucleus where it complexes with Lef/Tcf proteins to mediate transcriptional induction of target genes. Image adapted from (Chae and Bothwell, 2018).

The central role of the pathway is the accumulation and translocation of the adherent's junction associated-protein, β-catenin, into the nucleus where it acts as a transcription factor co-activator in conjunction with proteins such as TCF and LEF (Huber et al., 1996). In the absence of the Wnt

signalling, cytoplasmic β-catenin is degraded by a β-catenin destruction complex, and comprises of scaffolding protein Axin, the tumour suppressor adenomatous polyposis coli gene product (APC), protein phosphatase 2A (PP2A), glycogen synthase kinase-3β (GSK-3β) and casein kinase 1α (CK1α) (Gordon and Nusse, 2006). Once the Wnt ligand (e.g., Wnt2, Wnt3, Wnt3A, and Wnt8A) binds to its receptor Fzd and co-receptor LRP5/6, this pathway become activated and triggers a series of steps that lead to inhibition of Axin-mediated β-catenin phosphorylation and consequently the stabilization and accumulation of β-catenin in cytoplasm (Davidson et al., 2005). β-catenin subsequently translocates into the nucleus where it interacts with members of the TCF/LEF DNA-binding transcription factors (Clevers, 2006) that binds to the promoter region of target genes such as c-MYC (He et al., 1998), CyclinD1 (Shtutman et al., 1999), CD44 (Bisson and Prowse, 2009), AR gene (Wan et al., 2012). These Wnt target genes, involved in organiser formation during embryogenesis such as c-MYC and Cyclin D1, are also important during carcinogenesis (Reya and Clevers, 2005).

Apart from the extracellularly residing Wnt ligands that activate the canonical Wnt signalling pathway, there are some extracellular proteins including sFRP family (secreted frizzled related protein; sFRP1, 2, 4 and 5) (Mii and Taira, 2011), WIF (Wnt inhibitory factor) (Bovolenta et al., 2008), the DKK family of proteins (e.g. DKK1-4 and DKKL1) (Niehrs, 2006), and the cysteine knot family proteins SOST (Semënov et al., 2005) and WISE (Lintern et al., 2009). These inhibitors attach to different receptors of the Wnt signalling pathways such as, sFRP bind to the Fzd receptor, DKK1 and SOST/WISE to LRP5/6 co-receptor, thus meddling with the complex ligand-receptor formation and blocking of Wnt.

1.12.7. The non-canonical Pathway

Whilst biomolecular and biochemical investigations were carried out on the canonical Wnt signalling pathway, non-canonical Wnt signalling e.g., Wnt/Ca^{2+} pathway was less concentrated. The best characterised non-canonical pathways included Wnt/Ca^{2+} signalling pathways, first described in vertebrate (Kühl et al., 2001) and PCP (Planar cell polarity) was first identified in drosophila (McEwen and Peifer, 2000). The WNT/JNK and WNT/Rho signage are other non-canonical pathways (Veeman et al., 2003).

1.12.7.1. Wnt/Ca^{2+} signalling pathway

This pathway plays diverse roles during embryogenesis including regulation of tissue separation and regulation of dorsal axis formation. This pathway (Fig. 1.36) is also activated by binding Wnt ligands (e.g., Wnt4, Wnt5a, Wnt5b, Wnt6, Wnt7a, and Wnt11) to receptor that recruits Dishevelled (DVL) and G protein that activate phospholipase C (PLC), leading to production of 1,2-diacylglycerol (DAG) and then activate protein kinase C (PKC) and inositol 1,4,5-triphosphate (IP3) which stimulate intracellular $[Ca^{2+}]_i$ from endoplasmic reticulum (ER) (Kohn and Moon, 2005). Excessive release of $[Ca^{2+}]_i$ activates calcineurin (CAN) and Ca^{2+}/calmodulin-dependent protein kinase II (CAMKII) and subsequently enhance overexpression of nuclear factor of activated T cells and obstruct Wnt/β-catenin dependent pathway through nemo-like kinase (NLK) (Ishitani et al., 2003).

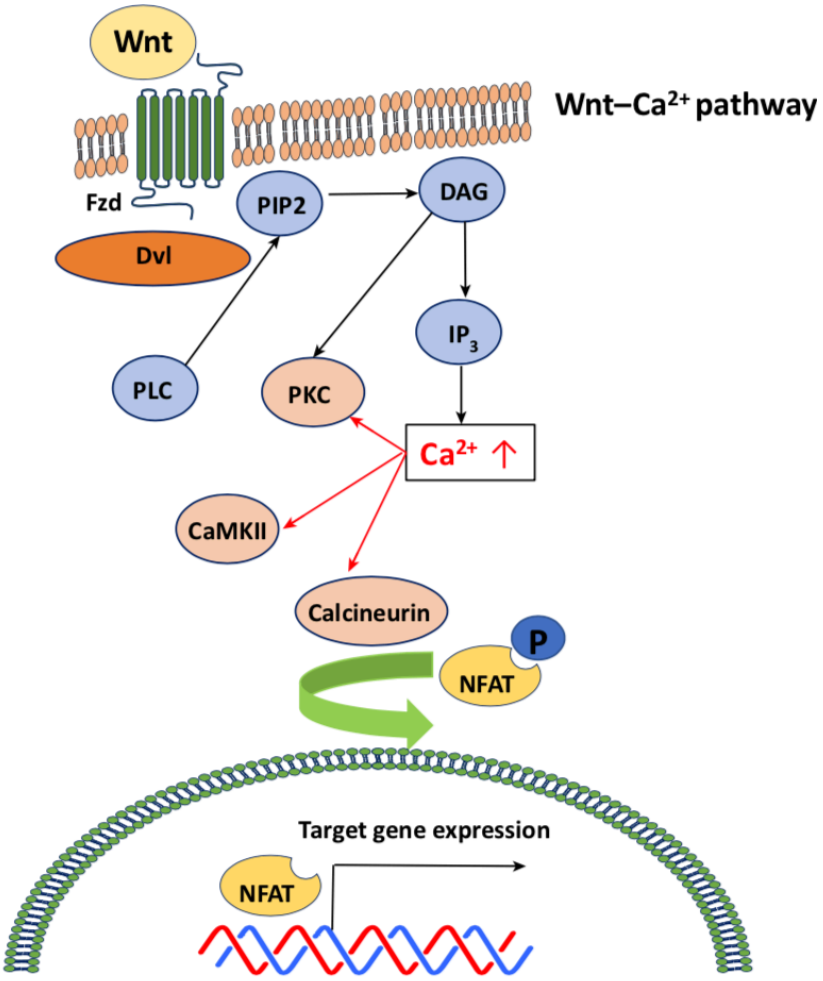

Figure 1.36. A schematic diagram of Wnt/Ca2+ signal transduction cascade. Activation of Wnt signal initiates by binding of Wnt ligands with Fzd receptor which directly interacts with DVL and activate specific domains such as PDZ and DEP of DVL (Komiya and Habas, 2008), additionally Fzd interacts with trimeric G-protein. DVL and G-protein may be co-stimulated in order to activate PLC or cGMP-specific PDE. Activated PLC cleaves PIP2 into DAG and IP3. IP3 binding with ER receptor releases Ca^{2+}. Increased Ca^{2+} and DAG stimulates PKC activate Cdc42 which is associated in ventral patterning. Furthermore, increased Ca^{+2} activates calcineurin and CamKII. CAMKII stimulates the transcription factor NFAT which regulates the gene that is associated in cell adhesion, migration and tissue separation (Komiya and Habas, 2008). Image adapted from (Chae and Bothwell, 2018).

1.12.7.2. Wnt-PCP signalling pathways

Wnt-PCP (planar cell polarity pathway, Fig. 1.37) is β-catenin independent pathway which has emerged from genetic studies in Drosophila in which mutations were discovered in Fzd and Dsh in Wnt signalling to reorganize the orientation of epithelial structures including cuticle hairs and sensory bristles (Seifert and Mlodzik, 2007). The activation of this signalling is mediated through Fzd, independent of the co-receptor LRP5/6 (He et al., 2004), using NRH1, Ryk, PTK7 and ROR2 to transduce the signal to Dsh protein which utilizes its PDZ and DIX domains to activate two parallel pathways that activate small GTPases Rho and Rac (Wallingford and Habas, 2005). The Rho pathway is activated by induction of Dsh-DAAM1 complex leading to activation of DAAM1 and consequently activation of the Rho GTPase through at least one Rho guanine exchange factor identified thus far, WGEF (Guanine Nucleotide Exchange Factor) (Habas et al., 2001 and Tanegashima et al., 2008).

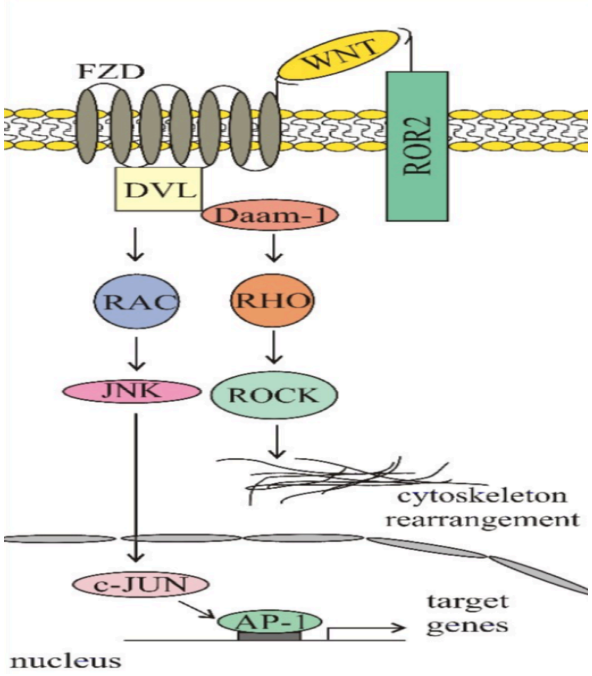

Figure 1.37. An overview of Wnt/planar cell polarity signalling pathway. The PCP is activated by binding to Fzd and ROR, then DVL is appointed, and DVL-Daam-1 is activated. Subsequently JNK and ROCK are activated, and cytoskeletal rearrangement occurs. Image adapted from (Gajos-Michniewicz and Czyz, 2020).

The Wnt/β-catenin dependent and Wnt/Ca^{2+} pathways were considered as non-interacting, linear and independent (Kohn and Moon, 2005) or antagonistic signalling pathways (Kühl et al., 2001). This view changed from a study in our laboratory (Thrasivoulou et al., 2013), describing the 'convergent model' in which interaction of these two pathways was proposed.

1.12.8. The convergent Wnt pathway in mammalian cells

Thrasivoulou et al. proposed a convergent model in which they demonstrated that Wnt/Ca^{2+} and Wnt/β-catenin pathways may act in a coordinated manner in mammalian cells (Fig. 1.38), dispelling the idea of canonical and non-canonical Wnt pathways, although this division still persists in some literature and has been used here in context.

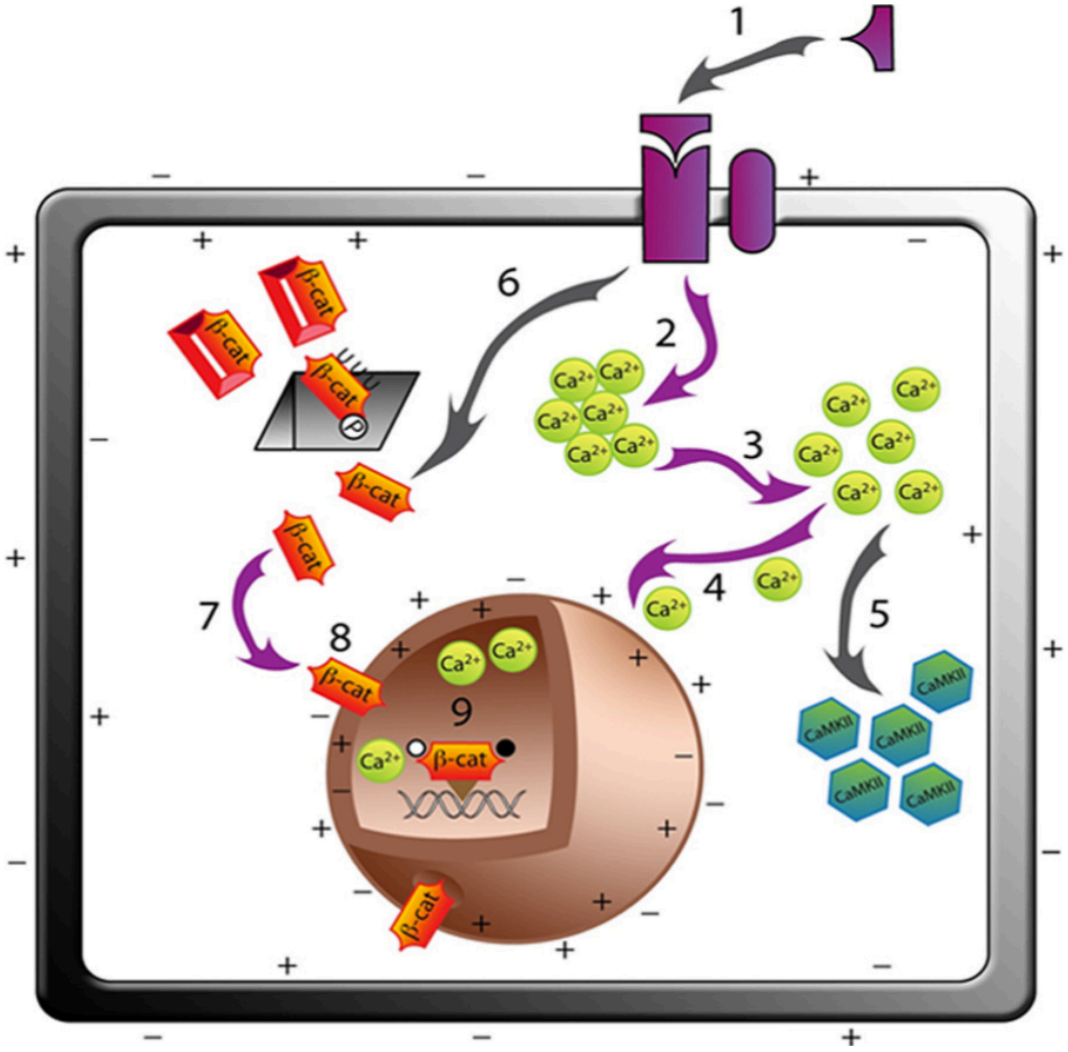

Figure 1.38. A study of convergence in mammalian cell lines for canonical (Wnt/β-catenin) and non-canonical (Wnt/Ca2+) Wnt signals. The following are the Wnt signalling proposed steps in mammalian cell:(1) Activation of Wnt signalling initiate by binding Wnt ligands (e.g., 3A, 4, 5A, 7, 9B, and 10B) binding to its known receptors (Frizzled, FZDs, LRP and SUMO) resulting in activation of intracellular $[Ca^{2+}]$i stores (2) that rises concentration of store operated free $[Ca^{2+}]i$ in cytosol (3). 1-3. The rise of free moving $[Ca^{2+}]_i$ depolarizes the nuclear membrane and as Ca^{2+} enter the nucleus (4), The NE is depolarized. (5) Free Ca^{2+} activates CamKII to stimulate cytoskeletal propagation in prostate cancer cells (Wang et al., 2010c). In canonical showed Wnt signalling activation (6) rescues the β-catenin from degradation in phosphorylation and ubiquitination and resulting in accumulation of β-catenin in cytosol (7) The β-catenin translocation is facilitated through depolarized NE (8) and Ca^{2+} is also increased in nucleus (9). β-catenin is co-localized in the nucleus where it binds to LEF/TCF proteins to inaugurate transcription of target genes. The image adapted from (Thrasivoulou et al., 2013).

A key question they were interested in was how does β-catenin, a 92kDa, negatively charged protein enter the nucleus as it lacked the conventional nuclear localization signal (NLS) or RAN GTPase activity? Their rational for proposing the convergent model was as follows: the nuclear envelope (NE) impedes macromolecular exchange between nucleoplasm and cytoplasm which

are larger than invagination of nuclear pore complex (NPC). The invaginations of NPC allow exchange of macromolecules with an upper limit of 10kDa (Mazzanti et al., 2001). Macromolecules (<10kDa) (Stehno-Bittel et al., 1995) are transported through the NPC into nucleoplasm but molecules greater than >10kDa require energy expenditure mechanisms such as GTPase RAN/transport receptor pathways to enter the nucleus. The transport of β-catenin (92-kDa) into nucleoplasm through NPC is not associated with simple diffusion (Suh and Gumbiner, 2003) or the RAN GTPase pathway (Eleftheriou et al., 2001) indicating that entry of β-catenin may encounter a considerable hurdle to transverse the NE. There is a trans-NE electrical potential which regulates Ca^{2+} and K^{+} concentration between cytoplasm and nucleoplasm (Mazzanti et al., 2001). $[Ca^{2+}]_i$ in cytoplasm regulates the concentration of $[Ca^{2+}]_i$ in nucleoplasm. An increase in nucleoplasmic $[Ca^{2+}]_i$ facilitates large macromolecules (>10kDa) to transverse NE (Sarma and Yang, 2011), whereas a decrease in nucleoplasmic $[Ca^{2+}]_i$ inhibits tans-NE macromolecular transport (Stehno-Bittel et al., 1995). Mazzanti et al. termed the nucleus as a ‘‘negatively charged sink’’ as it is largely composed of negatively charged DNA and nucleosome core protein (Luger et al., 1997 and Mazzanti et al., 2001). Incidentally, β-catenin is negatively charged at pH 7.0. So, the NE act as a physical as well as an electrical barrier for β-catenin transport into the nucleus, implying a physico-electrochemical mechanism for β-catenin translocation through the NE. Thrasivoulou et al. showed that the activation of the Wnt/β-catenin dependent pathway leads to increased cytosolic β-catenin, and simultaneously, Wnt mediated activated Wn/Ca^{2+} pathway release $[Ca^{2+}]_i$ which leads to an increase in the nucleoplasmic $[Ca^{2+}]_i$ and depolarises the NE that facilitates the passage of β-catenin across the NE. Upon translocation into the nucleus, β-catenin complexes with LEF/TCF family members (e.g., TCF1, TCF7) to mediate transcriptional induction of target genes (Thrasivoulou et al., 2013).

The convergent model was also further refined by work in our laboratory to suggest that a primary target for Wnt binding at the cell membrane in addition to its known Fzd and LRP receptors is an ion channel which is critical for initiating of the activation of Wnt mediated $Ca^{2+}{}_i$ release and may be a target for MPRCs (membrane potential regulating compounds) (Ashmore et al., 2019). This is discussed in later chapters in more detail.

1.13. Wnt signalling in diseases

The Wnt pathway is widely recognised for its participation in a variety of biological mechanisms. This pathway is involved in inherited familial adenomatous polyposis (FAP), where a mutated APC suppressor gene is unable to control β-catenin performance, enabling tumour cells to advance towards malignancy (Fodde, 2002). Mutations in the Wnt pathway interferes with the segment polarity in Drosophila embryos (Nüsslein-Volhard et al., 1984), which control cardiac development in mice and others developmental mechanisms in vertebrates and invertebrates (Logan and Nusse, 2004). Additionally, the Wnt pathway has been recognised as a major contributor to Alzheimer's and metabolic diseases. For instance, amyloid-β (Aβ) neurotoxicity in Alzheimer's disease leads to the downregulation of the Wnt signalling, which asserts that downregulated Wnt may have an important role in Alzheimer's disease pathogenesis (De Ferrari et al., 2003). Wnt signalling is also thought to be associated with metabolic disorders in which dysregulated Wnts are considered to be responsible for obesity and resistance to insulin (Sethi and Vidal-Puig, 2010).

Wnt signalling is also a crucial element for heart development, but dysregulation in Wnt signalling leads to heart and vascular disease (van Gijn et al., 2002). In addition, liver diseases such as, loss of β-catenin and other elements of the Wnt signalling pathways causes delayed liver regeneration following partial hepatectomy (Tan et al., 2006; Yang et al., 2014 and Planas-Paz et al., 2016), kidney disease (Zhou et al., 2012), lung disease (Tamamura et al., 2005), oral diseases (Queimado et al., 2007 and Foulkes, 1995), skin diseases (Adaimy et al., 2007; Bornholdt et al., 2009 and Gudjonsson et al., 2010).

Conversely, Wnt signalling pathway can also have positive effects on mammalian health as suggested by a number of studies. Chen and colleagues have highlighted the significant role of β-catenin in the early stage of fracture healing treatment (Chen et al., 2007). A number of Wnts including Wnt4, Wnt10B and LRP6 were expressed throughout the fracture recovery which showed that Wnt/β-catenin signalling was activated during fracture repair by a TCF-depended transcription reporter in bone and cartilage formations during fracture repair; others, however, concluded that activation of Wnt signalling is essential to regenerate hair follicles in wounded mice (Ito et al., 2007).

1.14. Wnt signalling in cancer

Wnt signalling pathway plays a complex role in cancer development. Mutation in major elements in Wnt signalling are strongly associated with various cellular processes including inexplicable and unmanageable cell proliferation, epithelial-mesenchymal transition (EMT) and metastasis (White et al., 2012).

1.14.1. Colorectal cancer (CRC)

The APC protein plays a crucial role in the formation of the destruction complex. Furthermore, APC is required for the swift transition of Axin immediately after Wnt stimulation and makes the combination of Axin with the LRP6/Arrow co-receptor in Drosophila (Tacchelly-Benites et al., 2018). Since APC adversely controls the canonical Wnt pathway, it probably can function as a tumour repressor (Senda et al., 2005). Against this background, the most common APC mutations within codon 1285 and 1513, termed mutation cluster region, representing just 10% of the entire coding region (Mori et al., 1992) with loss of functions and/or truncation was found in about 60-70% of colorectal cancer and adenomas (Christie et al., 2013 and Powell et al., 1992).

In addition to APC, mutations in the R-spondin/Lgr5/RNF43 modules are associated as drivers of Wnt-dependent tumour growth. Deleterious RNF43 mutations are mutually exclusive to APC mutations revealed in ~19% cases of colorectal cancer (Giannakis et al., 2014). Furthermore, R-spondin 3 mutations and fusion proteins expressed at a high level have been reported in 10% of cases of CRC (Seshagiri et al., 2012).

1.14.2. Breast cancer

Wnt signalling is activated in more than 50% of breast cancer patients and associated with reduced overall survival (Lin et al., 2000). The involvement of canonical Wnt signalling in the development and progression of triple negative breast cancer has been investigated intensively (Khramtsov et al., 2010 and Xu et al., 2015). Breast cancer subtypes contain higher level of β-catenin in the nucleus. Only a small proportion of tumours possesses somatic mutations of key Wnt signalling transducer such as β-catenin, while ligands and receptors of canonical Wnt signalling are frequently overexpressed in breast cancers, whereas secreted antagonists remain silent (Klarmann et al., 2008). Wnt signalling dysregulation and mutations have also been shown

Adrenocortical carcinoma (Chapman et al., 2011), ovarian cancer (Sauriol et al., 2020) and leukemia (Lento et al., 2013) , melanoma (Stolz et al., 1989) and hepatocellular carcinoma (Satoh et al., 2000).

1.15. Wnt signalling in prostate cancer

As suggested above, dysregulated Wnt signalling has been linked to the pathogenesis of many cancers and prostate cancer is no exception (Galluzzi et al., 2019 and Duchartre et al., 2016). β-catenin is the principal transducer of the canonical Wnt signalling pathway. β-catenin protein expression remains high in the cytoplasm and nucleus in prostate tumours (Kypta and Waxman, 2012). Genetic and epigenetic changes that activate Wnt/β-catenin signalling have been revealed to lead towards the progression of prostate cancer. A study revealed that 12% of CRPC samples showed recurring alteration in CTNNB1 (Beltran et al., 2013). A multi-institutional analysis of 150 metastatic CRPC tumours reported genomic alterations affect APC and CTNNB1 in 18% of samples (Robinson et al., 2015). Furthermore, the Wnt signalling gene analysis e.g. single nucleotide polymorphisms (SNP) exhibited links between APC genetic variations and decreased PSA-free survival and PCa advancement (Huang et al., 2010). Furthermore, various genes of the Wnt signalling pathway (CTNNB1 or β-catenin, APC, Fzds) show a high frequency of mutations in prostate cancer (COSMIC) (Grasso et al., 2012). Multiple studies show that Wnt/β-catenin signalling is involved in late-stage PCa and this signalling pathway is oncogenic, allows for castration-resistant growth, develop EMT (epithelial-to-mesenchymal transition) and stimulates NE (neuroendocrine) differentiation in PCa cells (Yokoyama et al., 2014 and Kypta and Waxman, 2012). Symes and his colleagues showed that protein targets of Wnt signalling were up regulated in human prostate cancer tissue (Symes et al., 2013).

Mouse and human cell systems were used to determine the consequences of stabilisation of β-catenin in non-malignant and malignant prostate cells and prostate cancer cells (Yokoyama et al., 2014 and Kypta and Waxman, 2012). Research in mouse showed that the Wnt/β-catenin activation leads to high-grade prostate intraepithelial neoplasia (PIN) while β-catenin remained stabilised, and APC was removed. The development of invasive carcinoma requires a second occurrence such as over expression of serine protease hepsin or deletion of phosphatase and tensin homologue (PTEN) (Francis et al., 2013).

Expression of the Wnt5A gene is significantly higher in prostate tissues and related cancer cell lines (Wang et al., 2007b). Wnt5A plays an important role in controlling cytoskeleton in prostate tissues through the Wnt/Ca^{2+}/CaMKII path and has been suggested to impede cell motility and wound healing process through inhibition of CaMKII (Wang et al., 2010b). Recent studies showed that increased non-canonical pathways activation of Wnt5a/Fzd2 is the most common mode of activation of WNT pathways in prostate cancer, causing increased EMT and metastasis. It emphasized the importance of the Wnt signalling pathway and EMT for prostate cancer development (Sandsmark et al., 2017).

1.16. Interaction between AR and Wnt signalling in PCa and emergence of CRPC

The individual roles of the Wnt and AR pathways in PCa have been described earlier (Secs. 1.11 and 1.12). Intracellular signalling pathways are often interconnected with considerable cross-talk between key cellular pathways (Schweizer et al., 2008a and Wang et al., 2008). Interaction between Wnt/β-catenin and AR signalling cascades has been proposed, particularly to play a role in the development of CRPC from hormone dependent PCa (Schweizer et al., 2008a). It has been suggested that the physical interaction between the elements of these two pathways are likely to take place in the first 6 of 12 armadillo repeats in a highly conserved central region of the β-catenin protein and N-terminal domain (NTD) and activation function 2 (AF2) in the ligand binding domain (LBD) (Ferraldeschi et al., 2015) of AR. Indeed, it has been suggested that β-catenin could directly bind to AR to boost its transcriptional activity by the stimulation of androgen. Yang et al. demonstrated that β-catenin preferentially and directly binds to the LBD of AR in the presence of DHT over several other steroid hormones such as estrogen receptor α, a progesterone receptor (Yang et al., 2002). β-catenin also binds to the AF2 region of the AR LBD and modulated the transcriptional effects of the AR N-terminal domain. Binding of β-catenin to ligand-engaged AR also facilitates the movement of β-catenin into the nucleus.

In addition, the Wnt/β-catenin signalling has been demonstrated to enhance AR gene expression through TCF/LEF-1 binding region in the AR promoter (Li et al., 2009). Wnt/β-catenin signalling, may therefore, acts as a synergistic regulator of androgen signalling in an androgen dependent manner in hormone-naïve PCa (Fig. 1.39). Conversely, the impact of the AR signalling on Wnt/β-catenin is more challenging. Preliminary studies in gonadotropin-releasing hormone neural cells

revealed that binding of DHT with AR suppressed β-catenin/TCF-responsive reporter gene activity (Pawlowski et al., 2002b). Treatment of AR^+ LnCAP cells with androgen (DHT/testosterone) suppress the expression of Wnt/β-catenin target genes while AR activity inhibition increases the Wnt/β-catenin-responsive transcription; this finding indicates that AR signalling suppresses the β-catenin/TCF-mediated transcription after activation with androgens (Lee et al., 2015) (Fig. 1.39.A). Generally, β-catenin act as a transcription co-activator of TCF4 to regulate transcription of Wnt/β-catenin target genes. But in hormone-naïve PCa cells, β-catenin may prefer AR interaction to that of TCF4. An increased interaction of β-catenin with TCF4 by avoiding AR leads to promote Wnt/β-catenin-target gene expression. Further study revealed that Wnt/β-catenin signalling could increase AR gene expression via the TCF/LEF-1 binding sites in the AR promoter (Li et al., 2009).

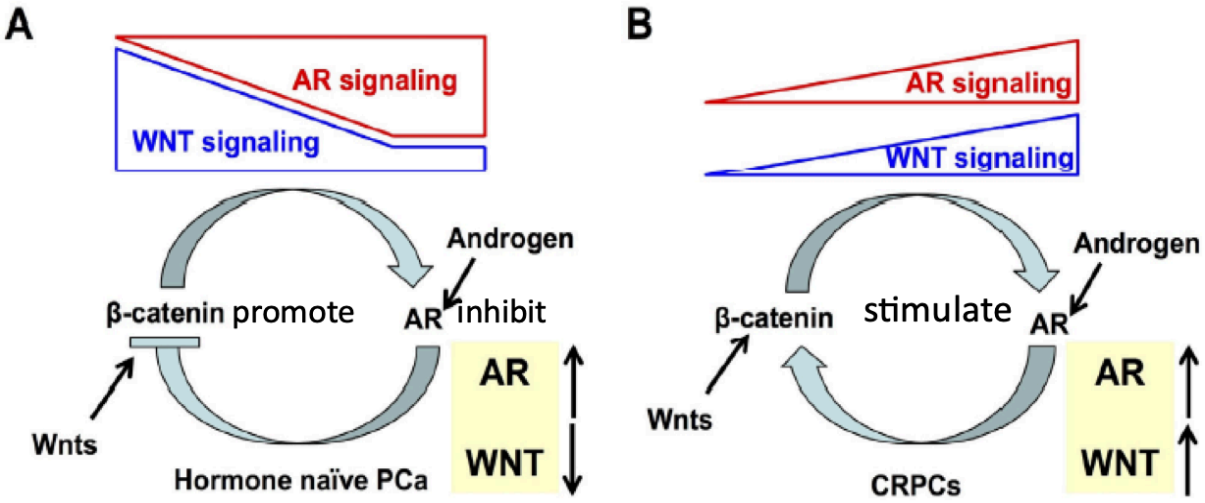

Figure 1.39. A representation of a standardized model of interaction of Wnt and AR signalling pathways in PCa initiation and progression. (A) In androgen dependent cells, AR signalling pathways suppress the Wnt/β-catenin signalling to hinder the expression of its target genes. Wnt (blue) and AR (red) signalling indicate the relative levels (equilibrium). (B) In CRPC, AR and Wnt/β-catenin signalling pathways mutually promote the activation of specific target genes for encouraging androgen-independent development and advancement of PCa. Wnt (blue) and AR (red) signalling implying relative level (e.g., synergistic relation). Image adapted from (Pakula et al., 2017).

The progression of PCa and conversion to CRPC has been associated with increased levels of AR gene and protein expression and their effects are transduced AR translocation to the nucleus and activation of gene transcription (Koivisto et al., 1997 and Schweizer et al., 2008a). Various studies have shown a close and functional interaction between AR and Wnt signalling pathways that accelerate the development of prostate tumours via over expression of AR (Schweizer et al.,

2008a; Takahashi et al., 2011 and de la Taille et al., 2003). AR may also activate a Wnt reporter gene to enhance promoter activity for Wnt target genes such as c-MYC, and cyclin D1 (Schweizer et al., 2008b). In addition, there is an increased growth in tumours in the transgenic mouse with overexpression of AR and stabilization of β-catenin (Lee et al., 2015).

It was discovered in our laboratory that in addition to the nuclear translocation of β-catenin, Cx43 protein (a gap junction protein which is associated with PCa development and progression) is also translocated into the nucleus in response to Wnt signalling activation (Hou et al., 2019). Therefore, as part of the investigations into the mechanisms of Wnt and AR interaction, I rationalized that the role of Cx43 should also be studied.

1.17. Connexin 43: A Gap Junction protein

Connexin 43 (Cx43) is a member of the GAP junction protein family that traverse the cell membrane and form complexes composed of hexamers that conduct the passage of ions, small metabolites and signalling molecules (of approximately 1 kDa, e.g., calcium and other ions, cyclic nucleotides, inositol phosphatase, ATP and prostaglandins) between adjacent cells (Goodenough et al., 1996). The communication is termed gap-junction-mediated intercellular coupling or communication (GJIC) (Wei et al., 2004 and Trosko, 2007). Gap junctions are involved in a wide range of physiological activities including, cellular development, growth and differentiation, cell apoptosis, tissue homeostasis (Sheridan and Atkinson, 1985), embryonic development (Guthrie and Gilula, 1989) and tumour suppression in maintaining cell differentiation and preventing transformation (Cronier et al., 2009).

1.17.1. Structure of Gap junction

Gap junctions and other structures (e.g., tunneling nanotubes (Tarakanov and Goncharova, 2009)) that connect the cytoplasmic chambers of adjacent cells allow the exchange of cellularinformation. Gap junctions are semicrystalline bundles of intercellular channels generated by alignment and docking of two hemi-channel counterparts belonging to adjacent cells and such connections allow the formation of multicellular networks. The hemichannel of each cell is known as a connexon which binds to a neighbouring connexon through non-covalent bonds of cysteine residues of the extracellular loops (Yeager and Nicholson, 1996).

Each connexon is composed of six molecules of the membrane spanning connexin proteins, encoded by a multigene family (Willecke et al., 2002). The connexin protein profile of the connexon determines the gap junction channel as homomeric or heteromeric and homotypic or heterotypic. Homomeric/homotypic are normally composed of the same type of connexin, whereas heteromeric channels are formed of two different connexins and heterotypic channels are composed of two different connexons.

1.17.2. Structure of connexin protein

The members of connexin family share a similar structural topology (a conserved tertiary structure). Connexins have cytoplasmic amino-terminal and carboxyl-terminal (CT) ends, four membrane-spanning domains (M1, M2, M3 and M4) that constitute the wall/pore of the channel and these domains are connected by two extracellular loop domains (E1 and E2) that partake in cell-cell identification and docking, and one cytoplasmic loop domain. The E1 extracellular loop connects transmembrane domains M1 and M2, and E2 connects M3 and M4 domains. The cytoplasmic loop links the M2 and M3 membrane domains. Even though the amino acid sequences of the 21-connexin isoforms are highly similar, variations in the cytoplasmic loop and CT domains exist. The CT domains is shown to act as a scaffold, interacting with and integrating signalling from protein kinase C, MAPK, β-catenin, integrins, proto-oncogene tyrosine-protein kinase Src and tight junction protein ZO-1 (Toyofuku et al., 1998 and Plotkin et al., 2002). These interactions may affect the role of the binding partner; for example, the binding of Cx43 to β-catenin may reduce β-catenin translocation into the nucleus.

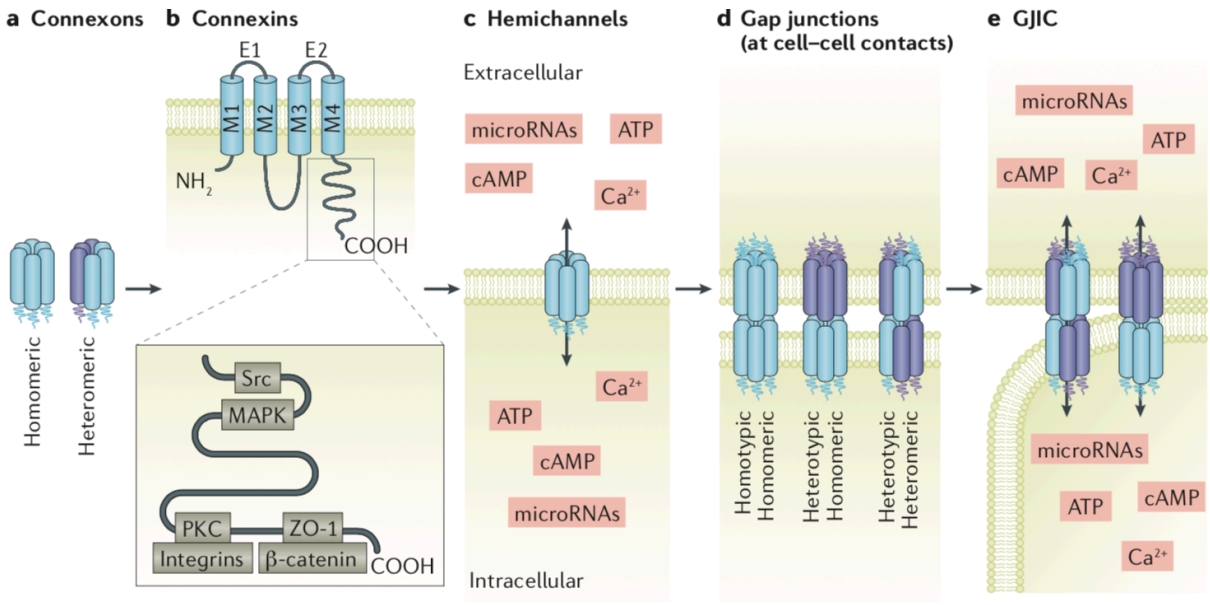

Figure 1.40. Gap junction with connexons and connexins. A. Hexamers of connexin form connexons which can be homomeric, consist of six monomers of same connexins, or heteromeric, composed of different connexins. B. Connexin contains four transmembrane domains (M1, M2, M3 and M4), two extracellular loops, a cytoplasmic loop and an intracellular carboxyl terminus interact with proto-oncogene tyrosine-protein kinase Src, MAPK, PKC, β-catenin and integrins. C. Connexon/hemichannels assist the flux of small molecules to pass through plasma membrane. D. Gap junction: Hemi-channels of each adjacent cell form gap junctions by interacting in homotypic or heterotypic joining. E. Gap junction construct passage for intercellular communication. Adapted from (Donahue et al., 2018).

The connexin protein is denoted Cx and designated according to the species from which the protein was derived and its theoretical molecular mass (in kDa). For instance, hCx43 or mCx43 means Cx43 was derived from human (h) or mouse (m) and the protein of about 43 kDa. Connexins are categorized into α, β or γ in regarding to the extent of sequence similarity and size of the cytoplasmic loop (Eiberger et al., 2001). Connexins are abbreviated with “Gj” for gap junction and numbered according to the order of discovery. For instance, mCx43 was the first discovery of the α-group (Gja1) and mCx32 was the first discovery of the β-group (Gjb2). So far, 21 genes in the human genome and 20 genes in the mouse genome have been discovered. The discrepancy between each nomenclature has to be clarified once all the connexin genes have been unambiguously recognized.

Table 1.4. The members of the connexin gene family and its chromosomal location in mouse and human. The table shows the current state of the sequence information available from the NCBI database (http://www.ncbi.nlm.nih.gov/genomes/static/ euk_g.html) (Eiberger et al., 2001).

Mouse connexin			Human connexin		
Cx	GJ	chr	chr	GJ	Cx
mCx23		10	6		hCx23
			6		hCx25
mCx26	Gjb2	14	13	GJB2	hCx26
mCx29	Gje1	5	7	GJE1	hCx30.2 (hCx31.3)
mCx30	Gjb6	14	13	GJB6	hCx30
mCx30.2	Gja11	11	17	GJA11	hCx31.9
mCx30.3	Gjb4	4	1	GJB4	hCx30.3
mCx31	Gjb3	4	1	GJB3	hCx31
mCx31.1	Gjb5	4	1	GJB5	hCx31.1
mCx32	Gjb1	X	X	GJB1	hCx32
mCx33	Gja6	X			
mCx36	Gja9	2	15	GJA9	hCx36
mCx37	Gja4	4	1	GJA4	hCx37
mCx39		18	10		hCx40.1
mCx40	Gja5	3	1	GJA5	hCx40
mCx43	Gja1	10	6	GJA1	hCx43
mCx45	Gja7	11	17	GJA7	hCx45
mCx46	Gja3	14	13	GJA3	hCx46
mCx47	Gja12	11	1	GJA12	hCx47
mCx50	Gja8	3	1	GJA8	hCx50
			1	GJA10	hCx59
mCx57	Gja10	4	6		hCx62
Σ 20					Σ 21

1.17.3. Genomic structure of connexin

The 5'-untranslated region (5'-UTR) lies in exon 1 which is separated from the complete connexin coding region and the subsequence 3'-UTR located in exon 2. Based on the splicing, this structure is categorized into two: (i) this category includes variations when different 5'-UTRs are spliced in a consecutive or alternative manner. This could be related to variation in the transcription pattern caused by different promoter utilization. (ii) the second category belongs to connexins when coding regions are interrupted by introns, e.g., mCx36, hCx36, mCx39, Cx40.1 and mCx57.

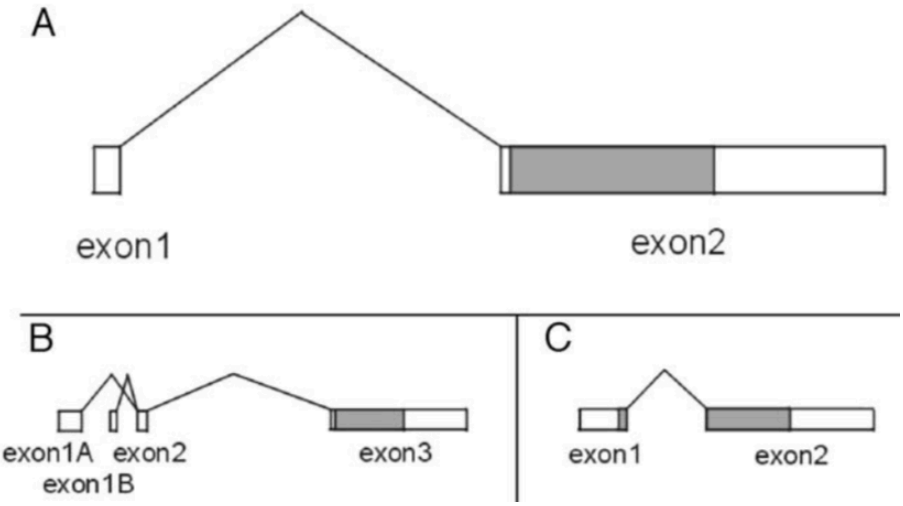

Figure 1.41. Structures of mouse connexin genes. (A) conventional gene structure. 5'-UTR is separated by an intron of different length from complete coding regions containing exon 2 (shaded box) and the subsequent 3'-UTR. (B) Various 5'-UTRs can be spliced alternatively and/or consecutively to the exon containing the region. (C) The coding region is spliced in mCx36, hCx36, mCx39, hCx40.1 and mCx57. Adapted from (Willecke et al., 2002)

1.17.4. Gap junction in disease

Gap junction channels formed by different connexins are functionally unique in terms of gating, conductance and permeability characteristics. Almost all cell types produce more than one connexin at a particular time, as demonstrated by keratinocytes expressing Cx26, Cx30, Cx30.3, Cx31, and Cx43. Dysregulation of connexins is associated with numerous genetic diseases. Mutation in Cx26 results in eight disorders and mutation in Cx43 in six diseases (Table 1.5).

Table 1.5. Genetic disorders caused by human connexin mutations (Srinivas et al., 2018).

Gene	Chromosome	Protein	Disorder(s)	OMIM
GJA1	6q22.31	Cx43	Craniometaphyseal dysplasia, autosomal recessive	218400
			Erythrokeratodermia variabilis et progressiva	133200
			Oculodentodigital dysplasia	164200
			Oculodentodigital dysplasia, autosomal recessive	257850
			Palmoplantar keratoderma with congenital alopecia	104100
			Syndactyly, type III	186100
GJA3	13q12.11	Cx46	Cataract	601885
GJA4	1p34.3	Cx37		
GJA5	1q21.2	Cx40	Atrial fibrillation, familial, 11	614049
			Atrial standstill, digenic (*GJA5/SCN5A*)	108770
GJA8	1q21.2	Cx50	Cataract	116200
GJA9	1p34.3	Cx59		
GJA10	6q15	Cx62		
GJB1	Xq13.1	Cx32	Charcot-Marie-Tooth neuropathy, X-linked 1	302800
GJB2	13q12.11	Cx26	Bart-Pumphrey syndrome	149200
			Deafness, autosomal dominant 3A	601544
			Deafness, autosomal recessive 1A	220290
			Hystrix-like ichthyosis with deafness	602540
			Keratitis-ichthyosis-deafness syndrome	148210
			Keratoderma, palmoplantar, with deafness	148350
			Vohwinkel syndrome	124500
			Porokeratotic eccrine ostial and dermal duct nevus	
GJB3	1p34.3	Cx31	Deafness, autosomal dominant 2B	612644
			Deafness, digenic, (*GJB2/GJB3*)	220290
			Erythrokeratodermia variabilis et progressiva	133200
GJB4	1p34.3	Cx30.3	Erythrokeratodermia variabilis et progressiva	133200
GJB5	1p34.3	Cx31.1		
GJB6	13q12.11	Cx30	Deafness, autosomal dominant 3B	612643
			Deafness, autosomal recessive 1B	612645
			Deafness, digenic (*GJB2/GJB6*)	220290
			Ectodermal dysplasia 2, Clouston type	129500
GJB7	6q14.3-q15	Cx25		
GJC1	17q21.31	Cx45		
GJC2	1q42.13	Cx47	Leukodystrophy, hypomyelinating, 2	608804
			Spastic paraplegia 44, autosomal recessive	613206
			Lymphedema, hereditary, IC	613480
GJC3	7q22.1	Cx30.2		
GJD2	15q14	Cx36		
GJD3	17q21.2	Cx31.9		
GJD4	10p11.21	Cx40.1		
GJE1	6q24.1	Cx23		

1.17.5. Cx43 in disease

Cx43 is the most ubiquitous connexin, expressed in many organs, tissues, and cell types, including heart, brain and kidney. Mutation in GJA1 gene causes autosomal dominant oculodentodigital dysplasia (ODDD) (Paznekas et al., 2003), and is inherited in an autosomal recessive pattern. ODDD is characterised by syndactyly (webbing of skin between fingers), microphthalmia (small eyes), craniofacial and dental abnormalities. Mutations in Cx43 are also associated with craniometaphyseal dysplasia (CMDR) and major symptoms include thickening of bones in the skull and abnormalities at the end of long bones of the limbs (Hu et al., 2013). Symptoms of ODDD are absent in patients with CMDR (Elçioglu and Hall, 1998), however, CMDR symptoms include distinctive facial features including a prominent forehead, wide nasal bridge, wide-set eyes and a prominent jaw.

1.17.6. Cx43 and Wnt signalling

Connexons interact with submembrane assemblies of cytoskeletal and signalling molecules, which are cumulatively referred to gap junction proteins (Mroue et al., 2011).). Cx43 interact with structural proteins, such as tubulin, N-cadherin, α-catenin and β-catenin and tight junction proteins, all of which stabilize the gap junction structure (Mroue et al., 2011 and Xu et al., 2001). These interactions also mediate channel-independent effects of connexins and connexon on cell adhesion and directed motility (Francis et al., 2011).

Cx43 is also modulated by interaction of β-catenin. β-catenin is an intracellular transducer protein in the Wnt signal transduction cascade (Chap-I, Sec. 1.12.6). β-catenin is a multi-functional protein whose activity depends on its subcellular localization. β-catenin at the plasma membrane is a component of cell adhesion junctions, while cytosolic accumulation leads to increase nuclear localization and transcriptional activity (Xing et al., 2008, and Spagnol et al., 2018). Hou et al. showed that subsequent to Wnt signalling activation Cx43 is translocated into the nucleus in a similar manner to that of β-catenin. It was further shown that Cx43 interacts with proteins associated with the so-called β-catenin destruction complex (Hou et al., 2019). It is therefore likely that there is cross talk between Wnt signalling and Cx43, with Wnt signal activation modulating intracellular Cx43 movement. It is clear that there is a close and physical interaction

between β-catenin, a transducer of Wnt signalling, and Cx43. For these reasons it was critical that the expression and functional relationship between Wnt and AR was also investigated from the perspective of gap junctions with Cx43 as a paradigm protein (in some experiments, another member of gap junction proteins, namely Cx31, was also investigated (Chap-V, Sec. 5.4.1.4-7).

1.18. Prostate cancer cell lines

In situ expression in human tissue is a first important step in understanding what molecular changes are occurring during the development of disease. However, human tissue obtained at biopsy or surgery cannot be used to understand detailed mechanisms of signalling. To elucidate mechanistic information, it is essential to use cell based models. Furthermore, an important first step towards the development of successful therapies is to understand the molecular perturbations regulating the oncogenesis and associated tumorigenesis in *in vitro* cell models of disease.

Cell based models also offset significant drawbacks including ethical concerns regarding use and treatment and housing costs in adopting an animal model for research have forced researchers to develop *in vitro* models that mimic tumorigenesis. As a consequence of the efforts, several cancer cells lines have been developed and used for determining mechanisms underlying cancer tumorigenesis and for identifying markers of therapeutic response (Masters, 2002). Cancer cell lines have several benefits, including the ability to proliferate and screen for high-performance medications (McDermott et al., 2007). A number of PCa cell lines from primary PCa tumours, PCa metastases and PCa xenograft models have now been generated.

In addition to using human prostate tissue (Chap-III and IV) I used prostate cancer cell lines which are in common use in this type of research. A summary of original PCa cell lines generated from PCa tumours, metastases, xenograft tumours and treatment resistant PCa sublines are given below. LnCAP and PC3 are considered to constitute gold standard of PCa cell culture lines. Two of these, LnCAP and PC3 were used extensively in my research (Chap-V).

PC3 cell line

In 1979, PC3 cell line was first extracted from a 62 year-old white man's metastatic lumbar prostate tumour which entirely consisted of carcinoma cells (Koochekpour et al., 2004). This cell

line is similar to DU-145 cells in that this cell is hormone-insensitive and does not express AR and PSA mRNA and protein but expresses TGF-α and EGFR mRNA (Ching et al., 1993). This cell line has 4 sublines which were generated from a PC3 xenograft tumour in athymic mouse and are more metastatic than the parental PC3 cell line (Kozlowski et al., 1984). The sublines are PC-3 ML cell line that preferentially metastasizes to the lumbar vertebrate, PC-3 MC cell line that metastasizes to mandibular region of the right cheek, PC-3 MR cell line that metastasizes to rib cartilage and PC-3 MK cell line what metastasize to right front knee bone in SCID mice (Wang and Stearns, 1991). Latest investigations have demonstrated that PC3 cells have neuroendocrine or small cell carcinoma characteristics in comparison with adenocarcinoma (Marchiani et al., 2010 and Tai et al., 2011).

LnCAP cell line

LnCAP cell line was first established in 1980 from a needle aspiration biopsy of a lymph node metastatic lesion obtained from a 50-year-old Caucasian male patient with stage D PCa (Horoszewicz, 1980). LnCAP cells grow well in media supplemented with 2.5-10% foetal calf serum (FCS) which regulates the mean population doubling time which is approximately 60hrs. The LnCAP cell is androgen dependent because the cell express AR and PSA mRNA as well as protein (Horoszewicz et al., 1983). The cell demonstrates aberrant response to steroid ligand due to possession of point mutation at T877A in the ligand-binding domain of AR. In addition, the LnCAP cells also express CK-8, CK-18 and CK-20 and contain a wild-type (WT) TP53 gene (Isaacs et al., 1991 and Carroll et al., 1993). The LnCAP cell line was further subcultured (e.g., LnCAP-abl) parental LnCAP cells through long-term androgen deprivation, anti-androgen and chemotherapeutic agent treatment, stable transfection and selection of metastatic cell lines by serial passing in mice.

A detailed description of other prostate cancer cell lines in the literature is given in Appendix.

1.19. Hypothesis

AR and Wnt signalling pathways are known to play a central role in cancer. Despite our knowledge regarding the roles of AR and Wnt signalling in prostate cancer, there is little information on how these pathways may interact and how such an interaction may impact development of prostate

cancer. Key questions remain, for example (a) is there any co-regulation of protein and RNA expression for AR and Wnt signalling targets in low and high Gleason grade human prostate cancer tissue and does it alter in castrate resistant disease? At a cellular, functional and molecular level (b) is there any reciprocity at the ligand binding and activation between AR and Wnt signalling pathways in prostate cancer cells and do transducers of these critical carcinogenic pathways interact with each other? Such and interaction may result in amplification of the carcinogenic signal.

The following hypotheses were tested in this research project:

(i) There is co-regulation of AR and Wnt signalling targets in cancer and this could be assessed by quantitatively measuring protein and RNA expression in normal, low and high Gleason grade prostate cancer and CRPC tissue obtained from prostate cancer patients.

(ii) There is close interaction and co-operativity between AR and Wnt signalling mechanisms in prostate cancer cells.

1.20. Aim

The overall aim of the project was to investigate the expression of Wnt and AR related proteins and mechanism of interactions in normal, low and high grade and castration resistant human prostate cancer tissue and cancer cell lines.

1.21. Objectives

In this thesis, I wished to address two key areas that in my view have not been tackled previously:

1. To elucidate the role of Wnt and AR pathways in PCa, it is crucial to determine the level of expressions and interactions of Wnt and AR signalling genes and proteins *in situ*. Our laboratory has developed and refined unbiased, quantitative immunohistochemistry (qIHC) to identify and characterize various biomarkers and proteins in PCa and other cancers (Symes et al., 2013; Arthurs et al., 2020; Arya et al., 2015 and Cao et al., 2018).

(i) To determine the expression of Wnt and AR target proteins in normal, low and high Gleason grade cancer using single label chromogenic staining and quantitative immunohistochemical techniques

(ii) To determine the RNA expression of Wnt and AR signalling genes and proteins and also quantitative protein colocalization in non-CRPC and CRPC in order to understand the interaction of AR and Wnt signalling *in situ* using single molecule RNA measurement and multi-label qIHC techniques

2. To investigate functional and molecular interaction between AR and Wnt signalling at the cellular level. The role of Wnt and AR signalling in PCa and the interaction of Wnt and AR signalling in PCa were carried out. To better understand the roles and interaction between Wnt and AR signalling in prostate cancer, I have conducted functional analysis using Western blot, immunocytochemistry, co-immunoprecipitation and quantitative PCR ±DHT ±Wnt in LnCAP, PC3 and PC3$^{(AR+)}$ prostate cancer cell lines, to determine:

(i) the expression of Wnt related (e.g., β-catenin, c-MYC and Cx43) and AR target proteins (e.g., AR, TMPRSS2, KLK3, PSA and Nkx3.1)

(ii) the translocation into the nucleus and co-localization of β-catenin, Cx43, AR

(iii) the physical interaction between β-catenin, AR and Cx43

(iv) gene expression for Wnt and AR signalling targets

CHAPTER II

Materials and Methods

2.1. Chemicals

Chemicals and antibodies used for immunohistochemistry and immunocytochemistry (IHC/ICC) in this project were purchased from various suppliers. The list of these antibodies along with their suppliers and catalogue numbers is provided in Table 2.1.

2.1.1. Immunohistochemical reagents

The following reagents were used in immunohistochemical technique

Table 2.1. Reagents for immunohistochemical staining. The reagents with catalogue and manufacturer's name are given the following table.

Name of the reagents	Catalogue	**Name of the manufacturer**
Ethanol	Cat: 458600	Sigma-Aldrich
Methanol	Cat: 34860	Sigma-Aldrich
Eosin Y solution	Cat: 318906	Sigma-Aldrich
SDS	Cat: 71729	Sigma-Aldrich
HCL	Cat: 258148	Honeywell Fluka
Tween® 20	Cat: P2287	Sigma-Aldrich
Triton™X-100	Cat: T9284	Sigma-Aldrich
Glycerol	Cat:444485B	VWR BDH chemical
DPX Mountant	06522	Sigma-Aldrich
Acetic acid	34254	Honeywell Fluka™ 34254
Hematoxylin Solution	GHS332	Sigma-Aldrich
Acetone	32201	Honeywell
H_2O_2	216763	Sigma-Aldrich
Paraformaldehyde	158127	Sigma-Aldrich
Embedding media		
Isopropyl alcohol	W292907	Sigma-Aldrich
Paraffin wax	12634077	Thermo scientific
Xylene	534056	Sigma-Aldrich
3,3'-Diaminobenzidine (DAB)	D3939	Sigma-Aldrich

2.1.2. Cell culture reagents

The following cell culture reagents were used. Details of usage are provided in individual sections below.

Table 2.2. Reagents for cell culture

Name of the reagents	Catalogue	Name of manufacturer	Specificity/Composition
RPMI 1640: Roswell Park Memorial Institute (RPMI) 1640 Medium	31870074	ThermoFisher Scientific	w/o: L-glumanine, Phenol red
FBS: Foetal Bovine Serum	A4766801	ThermoFisher Scientific	Endotoxin level: ≤ 1 EU/mL Hemoglobin level: ≤ 15 mg/dL
L-Glutamine (200 mM)	25030123	ThermoFisher Scientific	100x
PBS (Phosphate Buffer Saline)	10728775	Gibco, ThermoFisher Scientific	1x
Trypsin (10x)	59427C	Sigma-Aldrich	10x
Versene	15040066	ThermoFisher Scientific	1x Gibco Versene Solution (0.48 mM) is formulated as 0.2 g EDTA(Na4) per litre of Phosphate Buffered Saline (PBS)
DMSO (Dimethyl sulfoxide)	D4540	Sigma-Aldrich	Linear Formula: (CH3)2, ≥99.5% (GC), suitable for plant cell culture
Trypan Blue Solution	15250061	ThermoFisher Scientific	0.4%, 2,7-Naphthalenedisulfonic acid, 3,3-[(3,3-dimethyl [1,1-biphenyl]-4,4 diyl) bis(azo)] bis [5-amino4-hydroxy tetrasodium salt 72-57-1(0.1-1)

2.1.3. Ligands of Wnt and AR signalling pathways

The following protein ligands were used in this project.

Table 2.3. Wnt and AR signalling ligands. The following Wnt and AR signalling ligands were used.

Name of the ligands	Catalog and Source	Stock concentration	Working concentration
Wnt-3A	Cat: CSB-EP026136HU1, CUSABIO	1 µg/µl	10 nM
Wnt-5A	Cat: 645-WN-010, R&D systems	0.1 µg/µl	10 nM
Wnt-9B	Cat: 3669-WN-025, R&D system)	0.1 µg/µl	10 nM

DHT	Cat: D-073, Sigma-Aldrich	1 mg/ml	15 nM

2.1.4. Cell lysis reagents

The following reagents used in cell lysis procedure

Table 2.4. Reagents for cell lysis

Name of the reagents	Catalogue	Name of Manufacturer	Stock concentration/Composition
RIPA (Radio Immunoprecipitation Assay)	9806	Cell Signalling Technology	1x, 20 mM Tris-HCl (pH 7.5), 150 mM NaCl, 1 mM Na2EDTA 1 mM EGTA, 1% NP-40, 1% sodium deoxycholate, 2.5 mM sodium pyrophosphate 1 mM b-glycerophosphat, 1mM Na3VO4 and 1µg/ml leupeptin.
cOmplete™, Mini, EDTA-free Protease Inhibitor Cocktail Protease Inhibitor Cocktail Tablets provided in a glass vial, Tablets provided in a glass vial	11 836 170 001	Roche, Sigma-Aldrich	7x, For the inhibition of serine, cysteine, but not metalloproteases.
Phosphatase Inhibitor Cocktail Tablets provided in *EASYpacks*	04 906 837 001	Roche, Sigma-Aldrich	14x, The PhosSTOP Phosphatase Inhibitor Cocktail Tablets inhibit a broad spectrum of phosphatases such as acid and alkaline phosphatases, as well as serine/threonine (PP1, PP2A, and PP2B) and tyrosine protein phosphatases (PTP).

2.1.5. Western blotting reagents

The following reagents were used in Western blotting technique

Table 2.5. Reagents for Western blot experiment

Name of the reagents	Catalogue	Name of Manufacturer	Stock concentration/Composition
Alfa Aesar™ TRIS-buffered saline (TBS, 20X), with 2% Tween 20	15493269	Fisher Scientific part of ThermoFisher Scientific	1.0M Tris-HCl, 3.0M NaCl, pH 7.4 ± 0.1 with 2.0% Tween-20
Laemmli 4x	161-0747	BioRad	62.5 mM Tris-HCl, pH 6.8, 10% glycerol, 1% LDS, 0.005% Bromophenol Blue
Tris/Glycine/SDS	1610772	BioRad	10x premixed electrophoresis buffer, contains 25 mM Tris, 192 mM glycine, 0.1% SDS, pH 8.3 following dilution to 1x with water
Precision Plus Protein™ Dual Colour Standards	1610374	BioRad	Mixture of 10 recombinant proteins (10–250 kD), 8 blue-stained bands, and 2 pink reference bands (25 and 75 kD)
Colour Prestained Protein Standard (Broad Range, 11–245 kDa)	P7712	New England Biolab	Mixture of highly purified, pre-stained proteins, covalently coupled with a blue chromophore, and two reference bands (one orange and one green at 80 kDa and 25 kDa, respectively), that resolves into 12 sharp bands when electrophoresed.
Colour Prestained Protein Standard, Broad Range (10-250 kDa)	P7719	New England Biolab	Mixture of highly pure, recombinant, pre-stained proteins, covalently coupled with a blue chromophore, and two reference bands (one orange and one green at 72 kDa and 26 kDa, respectively), that resolves into 11 sharp bands when electrophoresed.

2.2. Methodological introduction: a short background of the techniques used

2.2.1. Immunohistochemistry (IHC)

IHC is a generic term for multiple methodologies used to detect different components of tissues as antigens *in situ* by means of interacting fluorophore or chromogen-tagged antibodies, typically (though not always) originated from another species (Taylor and Burns, 1974). IHC is a commonly used technique in pathology, particularly in oncology, neuropathology and hematopathology and surgical pathology (Garcia and Swerdlow, 2009 and Leong and Wright, 1987).

The development of immunostaining approaches began in the early 1940s, when Albert H. Coons at the Harvard Medical School in Boston, USA, showed that antigen can be localised in the tissue sections with fluorescein isothiocyanate (FITC)-labelled antibody (Coons et al., 1942). Formalin-Fixed Paraffin Embedded (FFPE) tissues was developed by Taylor and Burns (1974) (Taylor and Burns, 1974). In 1975, the hybridoma technique was introduced by Kohler and Milestein to generate monoclonal antibodies (mAbs) (Köhler and Milstein, 1975). The hybridoma mechanism has made it possible to use mAbs in IHC with a wide range of antigens and great quality of staining. With expansion and development of IHC technique, enzyme labels for instance, peroxidase (NAKANE and PIERCE JR, 1966) and alkaline phosphatase have been introduced (Mason and Sammons, 1978 and Fowler et al., 2011).

In 1982, Hsu and Soban used a series of metals including copper, nickel, cobalt etc., to produce different colour in DAB reaction, enabling the use of avidin biotin and a PAP to detect two different antibodies on the same slide. DAB substrate and methods labelled with enzymes were commonly used in the mid-1980s (Hsu and Soban, 1982).

However, the IHC staining paved the way for detecting antigens by causing minimal damage to tissue and cells and using minimum amount of antibodies which can determine tumour types and markers.

2.2.1.1. Tissue Array (TA)

Wan and colleagues first introduced TA in which tissues are transferred by punching from formalin-fixed, paraffin-embedded tissue blocks to recipient blocks (Wan et al., 1987). Kononen et al. (1998) improved the technique further. A single TA slide can accommodate different histological types of tumours which have to be compared or same type but different characteristics (such as, radio-resistant, radio-sensitive, high grade, low grade, metastatic and non-metastatic etc). The slide is prepared by transferring a minute cylindrical core from donor paraffin block to recipient block. The cores on the block are adroitly arranged in recognizable positions in rows and columns (hence the name “array”). The position of each tissue in the slide is systematically catalogued. Within the last few years, high-density TAs were evolved and turned to a standard laboratory method to diagnose and confirm diagnostic and prognostic biomarkers

for a range of diseases including gastrointestinal tumours, breast cancer, lung cancer and PCa (Fowler et al., 2011 and Kononen et al., 1998).

2.2.1.2. Tissue fixation

Tissue fixation: The objective of fixation is to stabilise the tissue to be impervious to further changes.

The following two types of fixations are used:

A. Coagulation fixation: Coagulative fixatives include organic and nonorganic solutions that coagulate proteins and restore them insoluble. This method preserves tissue structure at the light microscopic level very well, but consequences in cytoplasmic flocculation and low mitochondrial and secretory granules conservation.

B. Cross-linking fixation: Cross-linking fixatives undergo cross links within and between proteins, within and between nucleic acids and between nucleic acids and proteins. The most popular types in regular histology are acetone, formalin and aldehydes (e.g., formaldehyde, glutaraldehyde, chloral hydrate and glyxal), used with neutral buffered formaldehyde (Ramos-Vara et al., 2008). Formalin-fixed tissue sections are also popularly used in IHC because formalin-fixed paraffin-embedded tissue can be stored for many years. It is very convenient to use archived paraffin- embedded tissue to carry out IHC.

2.2.1.3. Deparaffinization of tissue

The tissue Deparaffinization is to remove the paraffin penetrated into the tissue. It is essential in order to prepare the sample for convenient of antigen retrieval. Multiple factors are involved in FFPE (Formalin Fixed Paraffin Embedded) tissue molecular cell profiles, for instance the pre-fixation time, the properties of the fixatives and the post-fixative storage parameters (Bass et al., 2014). Thus, deparaffinization procedures are believed to have significant impacts on antigen quality and quantity (Sengüven et al., 2014). The deparaffinization process is achieved by incubating the paraffinized tissue in a series of different concentration of xylene.

Xylene is a sweet, colourless, aromatic liquid or gas hydrocarbon present intuitively in coal, oil and wood tar. Xylene is favoured by many histologists because they easily extract alcohol from

the tissues and allow the tissue to become translucent and make paraffin penetration easier to deparaffinize the tissues (Pandey et al., 2014 and Sengüven et al., 2014). Following removal of paraffine, xylene is removed with 100% ethanol. Tissues are hydrated in a series of graded alcohols until water is used (Kalantari et al., 2016).

2.2.1.4. Antigen retrieval (ARE) of tissues

ARE method has been extensively employed in surgical pathology and research fields since its introduction in 1991 from the 1940s biochemical studies of protein and formaldehyde crosslinking (Shi et al., 1991 and Fraenkel-Conrat and Olcott, 1948). Numerous studies of the efficacy of ARE in immunohistochemistry (IHC) on a wide range of antibodies have shown that ARE is a single and reliable method for routine IHC, characterised by a significant increase in immunostaining intensity and a reduction of non-specific background staining on formalin-fixed paraffin-embedded tissue sections (Fraenkel-Conrat and Olcott, 1948).

The most formalin-fixed tissue necessitate ARE before proceeding to immunohistochemical staining. This is due to the formation of methylene bridge during fixation, which cross-link proteins and hence mask antigenic sites. The two methods used to retrieve the antigens are Heat method (Heat-Induced-Epitope-Retrieval: HIER) and Non-Heat method. Both methods function to break the bridges in methylene and expose the antigenic sites to enable antibodies to interaction.

2.2.1.5. 'Blocking' to eliminate non-specific binding

The blocking of antibodies and other tissue reagents is crucial to the elimination of non-specific binding. Even though the antibodies are highly target specific, intermolecular factors may encourage non-specific interaction to other molecules. Non-specific interaction thus excludes the appearance of the antigen-antibody binding of interest. A blocking step has to be conducted to prior to primary antibody incubation to lessen non-specific interaction.

2.2.1.5.1. Protein Blocking

Antibodies are highly charged molecules and bind to the reciprocal charged constituents in tissues resulting non-specific bindings of antibodies. Serum of same species in which secondary

antibody has been originated and bovine serum albumin (BSA) are used to musk hydrophobic side chains of proteins remain in the tissue. During conducting several staining using secondary antibodies from various species, it is essential to use blocking sera from the species of both secondary antibodies (Kim et al., 2003 and Taylor et al., 2013).

2.2.1.5.2. Endogenous enzyme blocking

This block is an antagonist that halt a substrate reaction from an enzyme remain in cells or tissues so that colourless chromogens do not convert into coloured end compound (Taylor et al., 2013).

a. Endogenous peroxidase blocking

Tissues for instance, liver, kidney and vascular tissue contain endogenous peroxidase which turn into brown if incubated with DAB substrate. Peroxidases generate high background while detect with HRP. The incubation of slides in 3% H_2O_2 containing methanol quench endogenous peroxidase reaction. Two other methods are seldomly used such as Glucose oxidase method and Acid hematin method (Taylor et al., 2013).

b. Biotin blocking

Blocking of endogenous biotin is required when a biotin-based detection system is implanted. It is normally found in brain, kidney and liver. It is to be blocked with avidin prior to incubate with biotin to block rest of the biotin binding sites on the avidin compound (Taylor et al., 2013).

c. Alkaline phosphatase (AP)

Tissue may contain endogenous peroxidase, pseudoperoxidase, and/or alkaline phosphatase activity which generate background signal when an alkaline phosphatase and/or peroxidase detection system and commensurate substrates are used. AP is present in placenta, intestine, lymphoid tissue and osteoblasts. Frozen tissue contains higher AP activity. AP in tissue is diagnosed with blue colour which is produced by incubating tissue with Alkaline Phosphatase chromogen (Taylor et al., 2013).

2.2.1.6. Detection method

The Ag-Ab reaction is not visible under the light/fluorescence microscope until it is labelled with a chromogen or a fluorophore. The primary, secondary and tertiary abs are labelled in a detection system that enable to visualise the immune reaction. A number of labels have been used, for instance fluorescent compound, metals and enzymes (Lucocq, 1985) and (Taylor et al., 2013). Enzymes such as alkaline phosphatase, peroxidase and glucose oxidase are still the most widely used labels. Detection systems are classified as direct or indirect methods.

2.2.1.6.1. Direct detection method

This is the easiest approach of one-step method with primary antibody tagged with signal compound (label). The reporter compounds are enzymes, fluorochrome, biotin and colloidal gold (Polak and Van Noorden, 1997).

2.2.1.6.2. Indirect method

Indirect detection method involves a two-step process:
The indirect is more sensitive to detect antigens in two step methods which was originally promoted by Coons (Coons et al., 1955). The first step involves unlabelled Ab, but the second step used Ab, that is raised against primary, is labelled. The indirect method is more sensitive and generate stronger signal to detect smaller number of antigens (Polak and Van Noorden, 1997).

A. Tyramide Signal Amplification method (TSA)

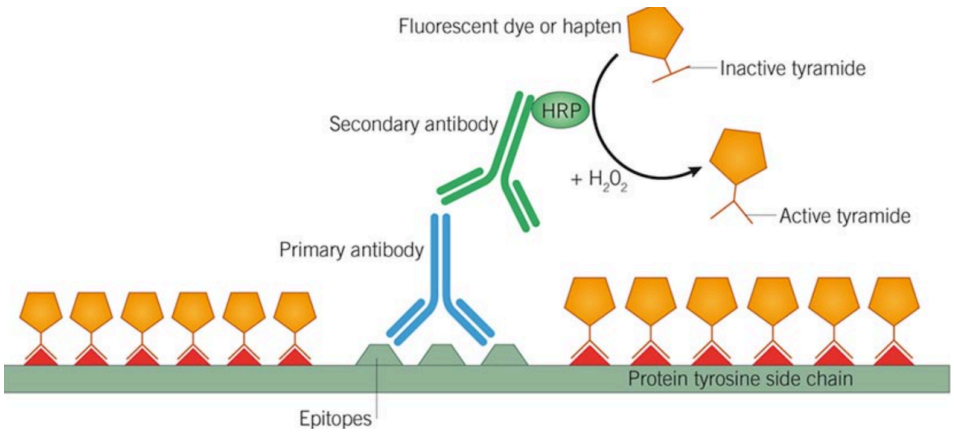

Figure 2.1. Schematic representation of principles of tyramide Signal Amplification. The tissue samples were labelled with primary and secondary antibodies. The secondary antibody was conjugated with horseradish peroxidase (HRP)

which was able to catalyse inactive labelled tyramide to convert into a reactive tyramide radical. The tyramide radical covalently binds to proximal tyrosine residues, thus providing signal amplification. Adapted from www.tocris.com/product-type/tyramide-signalling-amplification-tsa, accessed on 01/02/2021.

TSA has been demonstrated to be a versatile and efficient enzyme amplification tool for enhanced IHC staining. Conventional enzymatic staining method exploit the capacity of horseradish peroxidase (HRP) and alkaline phosphatase (AP) to transform a chromogenic substrate into a colourful reaction product precipitating at the site of enzyme activity (Roth and Perry, 2005). The TSA is based upon the performance of HRP on biotin or fluorophore conjugated tyramide substrate. The HRP binds with a hydrogen peroxide and phenolic component of tyramide to build highly responsive tyramide radicals, then bind together in covalence to electron-rich moieties (e.g., tyrosine) within tissue (Bobrow et al., 1989).

B. Chromogenic staining method

This approach of staining involves enzymes such as HRP and AP conjugated to secondary antibody which couples with primary antibody against the target protein. Enzymes can also bind to primary antibody directly to yield identifiable colour.

Two types of chromogen reactions are normally used: 1. Chromogens for HRP and 2. Chromogen for AP.

1. Chromogen for HRP

DAB (3,3'-diaminobenzidine) is oxidised in the presence of peroxidase and hydrogen peroxide which leads to the accumulation of a brown, water and alcohol-insoluble precipitate at the functional site of enzyme. The DAB reaction product is discretely localized at HRP-label sites, providing high resolution images of subcellular antigen distribution (Milde et al., 1989).

AEC (3-Amino-9-Ethylcarbozole) is another substrate for HRP which is converted into dark red in the positive area. The product derived from AEC is soluble in organic solvent and cannot be stored on a long-term basis.

2. Chromogens for AP

BCIP (5-Bromo-4-chloro-3-indolyl phosphate)/NBT (nitro blue tetrazolium) is a chromogenic substrate commonly recognised in the AP-based immunostaining. The substrate changes into the blue/violet colour following exposure to AP.

Other staining methods are:

Immuno-rolling circle amplification

Peroxidase-anti peroxidase (PAP) method

2.2.1.7. Counterstaining of tissue

DAPI (4',6-diamidino-2-phenylindole) and Hoechst are widely used nuclear dyes in IHC fluorescence, as they intercalate into the DNA to give a high UV excitement blue colour. The following dyes also use to stain nuclei.

Table 2.6. Immunostaining dye with target and colour products

Type	Dye	Target	Colour
Chromogenic	Haematoxylin	Nuclei	Blue to violet
Chromogenic	Nuclear fast red (Kernechtrot)	Nucleic acids	Red
Chromogenic	Methyl green	Nucleic acids	Green
Fluorescent	Hoechst stain	Nucleic acids	Blue
Fluorescent	DAPI	Nucleic acids	Blue

2.2.2. RNAscope

RNAscope® was developed by Advanced Cell Diagnostics (ACD) and is a substantial improvement of RNA *in situ* hybridization (ISH), which effectively resolves the conventional RNA ISH while presenting spatial and morphological background for single cell resolution (Wang et al., 2012 and Wang et al., 2014). It uses a specific signal amplification technique to view target RNA as punctate dots where each dot represents a single RNA molecule. The principal advantages of the RNAscope test are high sensitivity because of its high signal amplification technique, high precision due to its probe design technique to minimize non-specific off-target signals, and spatial and morphological RNA detection and quantification. Advancement of an automated RNA ISH assay would dramatically boost the clinical usability of RNA ISH by allowing for the standardisation of

more samples with decreased inter-user variability, reduced time which would allow for more reliable reproducible results. Subsequently automated version of RNAscope technology has been developed. Automated version of RNAscope was first used to detect HER2 in invasive breast carcinoma (Wang et al., 2013).

Standard and non-standard RNA ISH probe pools are designed by ACD following singleplex, duplex, multiplex configurations. Singleplex is very robust and give high-definition staining results which can be stored permanently due to the permanent staining. RNAscope duplex is applied to detect two RNA species and their co-localization to map co-expression within the same cellular context. ACD has employed the naming convention of channel 1 (C1) to refer to green and channel 2 (C2) to fast red. RNAscope multiplex assay allows single molecule detection of upto four RNA targets simultaneously.

2.2.2.1. RNAscope design strategy

The RNAscope method applies a probe design strategy in which two independent probes (double Z probes) must hybridize to the target sequence in tandem to enable signal amplification to take place. As it is pretty unlikely that two independent probes will hybridize to a non-specific target right next to each other, this proposed design assure the selective amplification of target-specific signals. For each RNA target, ~20 double Z target probe pairs are developed to specifically hybridize to the target molecule, but not to non-targeted molecules.

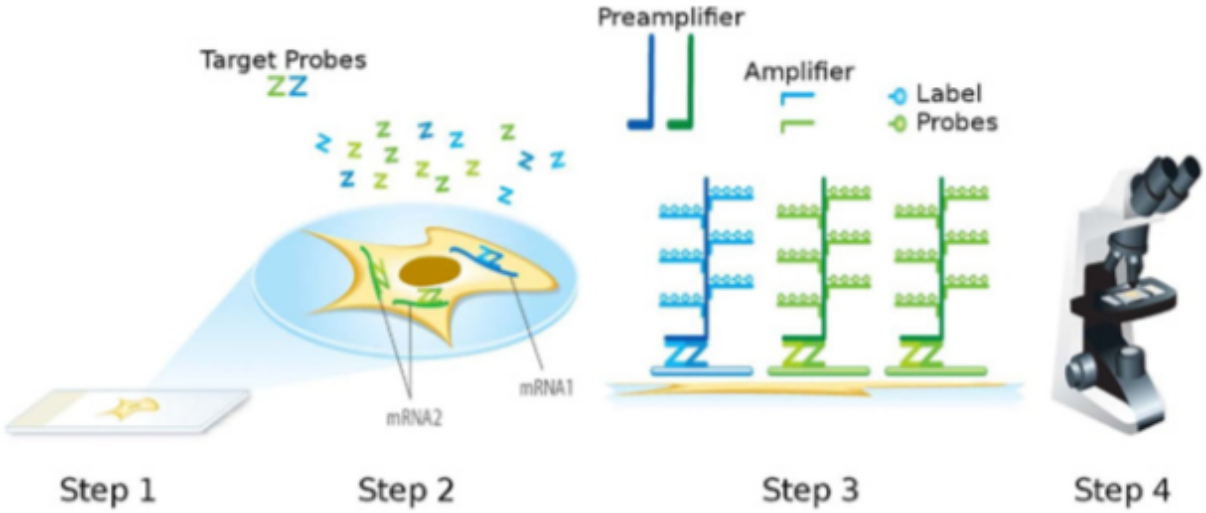

Figure 2.2. Stepwise Schematic representation of the RNAscope assay. Step-1: tissues are fixed and permeable to be exposed to target probes. Step-2: target RNA-specific oligonucleotide probes (Z) are hybridized in pairs (ZZ) to multiple RNA targets. The preamplifier binds to the upper regions of the Z probe pairs. Step-3: Multiple amplifiers in each pre-amplifier are hybridized. The label probes in each amplifier are also hybridized. Each label probe is conjugated with fluorophores or enzyme to generate a punctate dot for each RNA target. Step-4: Signals are detected using NanoZoomer 2.0-HT slide scanner by Hamamatsu Photonics or Carl Zeiss introduces Axio Scan.Z1 Digital Slide Scanner. Image adapted from (Wang et al., 2012).

The double Z probe design prevents background and increases the signal to noise ratio exponentially. Single Z probes binding to nonspecific site will not produce a binding site for the pre-amplifier, thus further preventing amplification of non-specific signals, enhancing specificity. Each of the target probes includes a region from 18-25 bases complementary to the target RNA, a spacer sequence and a 14-bases tail sequence (contemplated as Z). The double Z probe contains different form of tail sequence and hybridize contiguously to a target region (50 bases). The two tells sequence combine to form a 28-base preamplifier hybridization site which includes 20 binding regions for an amplifier, which possess also 20 binding sites for the label probe. A 1kb region of RNA sequence is usually targeted by 20 probes pairs; consequently, up to 8000 labels can be produced for every target RNA molecule by successive hybridization with a preamplifier, amplifier and label prob e.
The label probes were conjugated to, HRP labelled probe that produces green colour with DAB in C1 channel in the chromogenic reactions whereas, alkaline phosphatase (AP) labelled probe that yield fast red colour with DAB in C2 channel in chromogenic reactions.

2.2.3. Western Blotting (WB)

The transfer of proteins or nucleic acids to microporous membranes is termed as “blotting”. Proteins that are resolved on sodium dodecyl sulfate-polyacrylamide gel electrophoresis (SDS-PAGE) gels are generally transferred to Polyvinylidene difluoride (PVDF) membrane under the conduction of an electric current in a method recognised as western blotting (WB) or protein blotting (Towbin and Gordon, 1984 and LeGendre, 1990).

Western blotting is also called protein blotting and immunoblotting. The evolution of Western blot technique was first published by Renart and colleagues from the group of George Stark on July 1, 1979 in PNAS (Renart et al., 1979 and Marcus and Oransky, 2012). This same group had

already invented the RNA blotting method named as “Northern blot” two years prior. Later, W. Neal Burnette published the procedure naming “Western blotting” (Burnette, 1981). The lab of Burnette and Stark was on the western coast of the USA at the time, therefore, the method was called “Western blot” (Mukhopadhyay, 2012 and Moritz, 2020).

Western blotting is an universal and periodic technique implemented throughout laboratories for medical diagnostics including HIV, Lyme disease and Hepatitis B, therapeutic test and research in life science to investigate regulatory molecular events underpinning energy metabolism, protein turnover and chronic physiological adaptations such as investigation of protein abundance, kinase activity, cellular localisation, protein-protein interactions and or monitoring of post-translational modifications, ubiquitinoylation, glycosylation; methylation and SUMOylation (Moritz, 2020 and Kurien and Scofield, 2015).

WB consists of the following steps: a. extraction of cellular protein proteins from cells, b. quantification of protein concentration in cell lysate; c. SDS-PAGE; d. transfer of protein from gel to PVDF; e. blocking of PVDF; f. incubation of protein on PVDF by primary antibody; g. incubation of protein on PVDF by secondary antibody; h. detection of protein; i. quantification of the resulting bands using ImageJ software; j. Stripping the membrane and reprobe with primary antibody of target protein (Moritz, 2020 and Kurien and Scofield, 2015).

2.2.3.1. Cell Lysis

The extraction of proteins from cells and tissues requires lysis and disruption of cell membranes using homogenization techniques for instance, typically in the form of mechanical, sonication, and/or chemical approaches.

Proteins are extracted from cells by lysis and homogenisation with buffer. A vast array of cell lysis buffer is available. Particular buffer is optimally designed to extract protein of interest such as an appropriate detergent for protein extraction and solubilisation. For instance, integrin receptors are integral membrane proteins which are extracted enormously by Nonidet P-40 (NP-40). Radioimmunoprecipitation assay (RIPA) lysis buffers, which contains ionic detergents sodium deoxycholate as well as a non-ionic detergent NP-40/Ttriton X-100, is efficient of denaturing

proteins, breaking enormous protein interactions and releasing most cellular proteins (MacPhee, 2010).

2.2.3.2. Protein quantification

An accurate protein quantification is critical for protein purification and identification studies. A wide array of different methodologies has been proposed to quantify both complex protein mixtures and individual proteins. Four methods including Bradford (Bradford, 1976) and Bicinchoninic assay (BCA) assay (Smith et al., 1985), UV absorption at 280 nm (Desjardins et al., 2009) and Lowry methods (Lowry et al., 1951) which are commercially available.

2.2.3.2.1. Bicinchoninic acid (BCA) assay

The bicinchoninic acid (BCA) assay is a colorimetric method that was invented in 1985 by Paul K. Smith at Pierce Chemical Company, the major distributor of this assay, to measure the concentration in a sample (Smith et al., 1985).

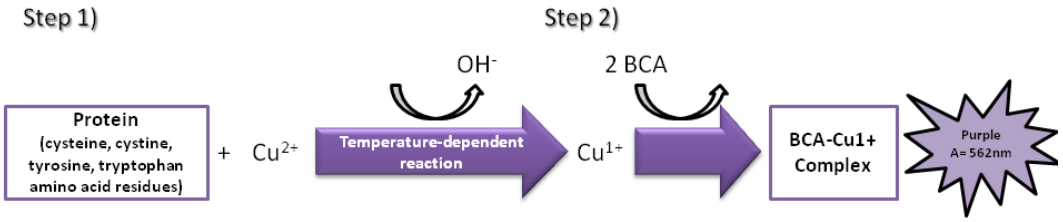

Figure 2.3. Schematic representation of BCA assay

This is a detergent-compatible formulation relied on bicinchoninic acid (BCA) for the colorimetric detection and quantitation of the total protein. This procedure integrates two reactions:

1. The peptide bonds in the protein sample is converted from Cu^{2+} to Cu^{1+} in an alkaline medium, called biuret reaction and this cuprous cation (Ch^{1+}) can be detected using highly sensitive and selective colorimetric procedure using a unique reagent containing bicinchoninic acid (Smith et al., 1985). The amount of Cu^{2+} reduced is proportional to the amount of protein present in the solution.

2. BCA is a particular chromogenic chelating agent for Cu^{1+}. Two molecules of BCA chelate with one Cu^{1+} ion. The decreased level of Cu^{2+} is a protein concentration result that can be spectrometrically measured by changing the colour of the sample solution from green into purple

which absorbs light at 562 nm that is nearly linear with increasing protein concentration that can be estimated by comparing with a known protein standard such as bovine serum albumin (BSA) with broad working range (20-2000 µg/ml). The macromolecular protein structure which are peptide bonds and four specific amino acids, such as cysteine, cystine, tryptophan and tyrosine, are recorded to be responsible for forming colour with BCA (Kong et al., 2016).

2.2.3.3. Sample preparation and SDS-PAGE system

SDS-PAGE (sodium dodecyl sulfate-polyacrylamide gel electrophoresis) is a simple and inexpensive method for the qualitative characterisation of proteins in complex mixture. Electrophoresis refers to migration of charged soluble molecules such as proteins based on molecular weight (MW) through a medium during exposure to an electric field. Electrophoresis in polyacrylamide gel termed as is PAGE, which was first introduced by Raymond & Weintraub (Kong et al., 2016), is formed by copolymerization of acrylamide and bis-acrylamide ("bis", N,N-methylene-bis-acrylamide). The reaction is a polymerization of vinyl supplements introduced by a free radical-generating system (Chrambach, 1985). Polymerization is initiated by ammonium persulfate and tetramethyl ethylenediamine (TEMED). TEMED enhances the rate of formation of free persulfate radicals, which in turn catalyses polymerization. The persulfate free radicals convert acrylamide monomers into free radicals that react with inactivated monomers to trigger a polymerization chain reaction (Shi and Jackowski, 1998) . The elongating chains of acrylamide are built up being crosslinked by introduction of bis-acrylamide forming a mesh like structure in which the holes of the mesh represent the pores (Bio-Rad, 2012).

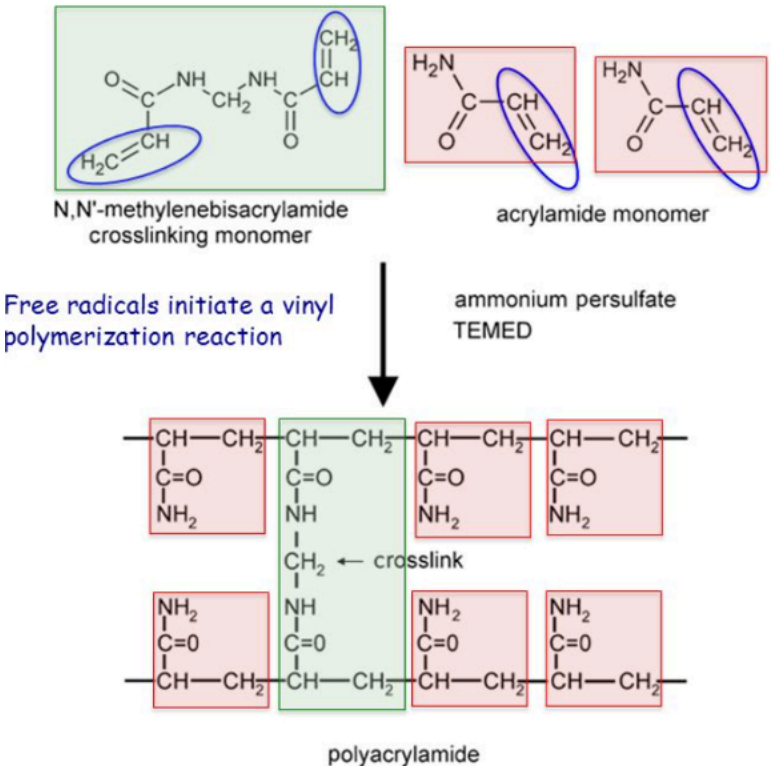

Figure 2.4. Formation of polyacrylamide

Laemmli introduced the reducing detergent sodium dodecyl sulfate (SDS) into a discontinuous denaturing buffer system and developed the most popular form of protein electrophoresis called SDS-PAGE (Laemmli, 1970). In SDS-PAGE procedure, the strongly anionic detergent SDS is used in combination with heat to unfold and break the many noncovalent bonds and proteins are stabilised. The presence of β-mercaptoethanol enhances to break any covalent bonds between cysteine residues. SDS binds noncovalently to proteins in a manner that imparts:

A. proteins are negatively charged. Since SDS is negatively charged and act as a surfactant. It masks the intrinsic charge of the proteins which it binds.

B. SDS binds to the hydrophobic region of the denatured protein at a consistent rate of 1.4 g of SDS per 1 g protein which keep consistent charge-to-mass ratio regardless of protein type. The quantity of SDS found is almost always proportional to the molecular mass of the polypeptide and is independent of its sequence.

C. Detergent molecules coat the unfolded protein chain which adopts a rod-shape as a consequence of electrostatic repulsion (Bio-Rad, 2012).

The protein-SDS complex contains net negative charges, hence migrate towards the anode and the separation is based on the size of the polypeptide.

2.2.3.4. Transfer of protein from gel to membrane

Following the separation on SDS-PAGE, the proteins are electrophoretically transferred onto a membrane resulting in immobilization of separated proteins that allow to probe with antibodies and provide additional longevity compared to gels (Bass et al., 2017).

The efficiency of protein transfer depends vastly on the nature of the gel, the molecular mass of the proteins being transferred, and the membrane being used. Thinner gels provide complete and accelerate transfer. 0.4mm thickness represent the lower practical limit (Harlow and Lane, 1988). The efficiency of protein transfer has also been facilitated with heat, special buffers and partial proteolytic digestion of the proteins prior to transfer (Kurien and Scofield, 2006).

The efficiency of protein transfer also depends on binding ability of protein to membrane. Nitrocellulose, polyvinylidene (PVDF), activated paper or activated nylon have been efficiently used to bind transferred proteins. Nitrocellulose is the most widely used substrate of the membrane, but it is not hydrophobic and does not bind protein covalently and becomes brittle when dries. A considerable quantity of proteins tends to migrate through nitrocellulose membrane, and only a small fraction of total count truly binds (Kurien and Scofield, 2006 and Bass et al., 2017).

Techniques to transfer proteins from gel to membrane: Protein transfer from SDS-PAGE gel to PVDF membranes has been acquired in three different ways:

(1) simple diffusion

(2) vacuum-assisted solvent flow and

(3) Electroblotting or electrophoresis elution.

Electroblotting is the most commonly used procedure to transfer proteins from gel to a membrane. Proteins are transferred in this technique more quickly and completely in compared to the diffusion and vacuum blot. This electroelution is conducted into two procedures:

A. Wet transfer: The gel-membrane sandwich is completely immersed in a buffer tank with platinum wire electrodes that was designed by (Towbin et al., 1979 and Kurien and Scofield, 2006).

B. Semi-dry transfer: This Western blot is also named as “horizontal blotting” which is an effective and widely used method in research and diagnostic laboratories. In this procedure, gel-membrane sandwich is placed between two carbon plates electrodes, a uniform electrical field in which up to six gel/membrane/filter are assembled and soaked well with transfer buffer. The assembly is clamped, and proteins are transferred with the activation of electrode plate by electricity.

2.2.3.5. Blocking of PVDF membrane

Following transfer of protein, unoccupied of binding sites of nitrocellulose or PVDF membrane are blocked to prevent non-specific binding of antibodies (primary and/or secondary antibody) to the membrane. Membranes have a high affinity for binding proteins which bind to antibody resulting in non-specific background. Blocking a blot has two crucial functions. The first is quite well established since it can assist to mask all possible non-specific binding sites on the membrane. The second objective is less documented and probably even less interpreted but blocking membrane can encourage the denaturation of antigenic sites. Nevertheless, prolong blocking times have (>24 h) have been recorded to effectively remove antigens (Bass et al., 2017 and MacPhee, 2010).

2.2.3.6. Primary antibodies and determining specificity

The WB principle has been established based on the detection of proteins through the binding and recognition of antibodies (AB) on one or more targets. This interaction is highly specific and occurs between a segment of the antigen (epitope) and the specific recognition sites located in the fragment antigen-binding fragment (Fab) region of the antibody called paratope. The primary antibody is specific and sensitive enough to interact and identify the intended target proteins. It is crucial to examine that the antibody is unique to the indigenous or denatured protein, as denaturisation of protein prior to load on SDS-PAGE may disrupt the exposure and accessibility

of the epitope, hinder the interact ability of the antibody. In some cases, indigenous/native-specific monoclonal antibodies may need to be used (Bass et al., 2017).

Specificity can be validated by testing against positive lysate or purified protein control, giving a detectable band at the correct molecular weight and a negative sample of tissue known not to express the designated target ([Human Atlas provides reliable protein expression data (http:/www.proteinatlas.org)], likely to result in no detectable band). Positive and negative controls will play a role in determining the degree of non-specific binding and potential false-positive bands, together with affirmation of increased/decreased protein expression, offering credibility that the highlighted band is always the correct one (Bass et al., 2017 and MacPhee, 2010).

2.2.3.7. Secondary antibody incubation

A Secondary antibody (2°Ab) is an important molecule for detection, sorting and purification of target antigens. 2°Ab allow the detection of protein of interest due to their specificity for the primary antibody species and isotype. Typically, 2°Ab conjugated with reporter signalling such as horseradish peroxidase (HRP) or certain fluorophores is able to bind to the fragment crystallizable (Fc) region on the 1°Ab which is detected by a camera or imaging device.

During WB procedure 2°Ab may cross react with other separated proteins or those used in blocking solution due to presence of similar peptide sequence. Non-specific binding for 2°Ab has to be checked by conducting procedure omitting 1°Ab incubation as negative control. 2°Ab solutions are generally made up with same buffer as prepared for blocking solution to reduces background followed by incubation at room temperature for 1-2 h as longer incubation generates a higher background. Concentration and incubation are changeable depends on nature of the proteins being investigated (Bass et al., 2017).

2.2.3.8. Detection of signal

Proteins on immunoblots have been detected by utilizing of organic dyes (Ponceau red, amido black, fast green and Coomassie Brilliant Blue (CBB), fluorescent labels (fluorescamine and coumarin), various silver staining methods and colloidal particles such as gold, silver, copper, iron or India ink. Two methods are generally used in which 2°Ab are conjugated with

(1) a labelled compound such as radio-isotope or fluorophore.

(2) enzyme-linked reagent for detection of protein on immunoblot.

Recent decades, a radioactive isotope or enzyme was exposed to X-ray film for detection of proteins on the blot, but recently enzyme and fluorophore are being detected by Camera.

The most commonly used enzymes are alkaline phosphatase (AP) (Bronstein et al., 1989) and Horseradish peroxidase (HPR) which are utilised for colorimetric and chemiluminescent detection.

In colorimetric detection, a substrate (i. e., 3,3'-diaminobenzidine) of HRP is oxidized to form a brown insoluble product. A scan of the blot by a specialised imager or traditional office scanner can then be done to quantify them using freely available software such as Image J (http://ImageJ.nih.gov/ij/). The main disadvantage of this type of identification is that the chemical reaction must be blocked and therefore, optimal reaction conditions (e. g. reaction time and temperature) must be assessed leading up to quantification (Bass et al., 2017 and MacPhee, 2010).

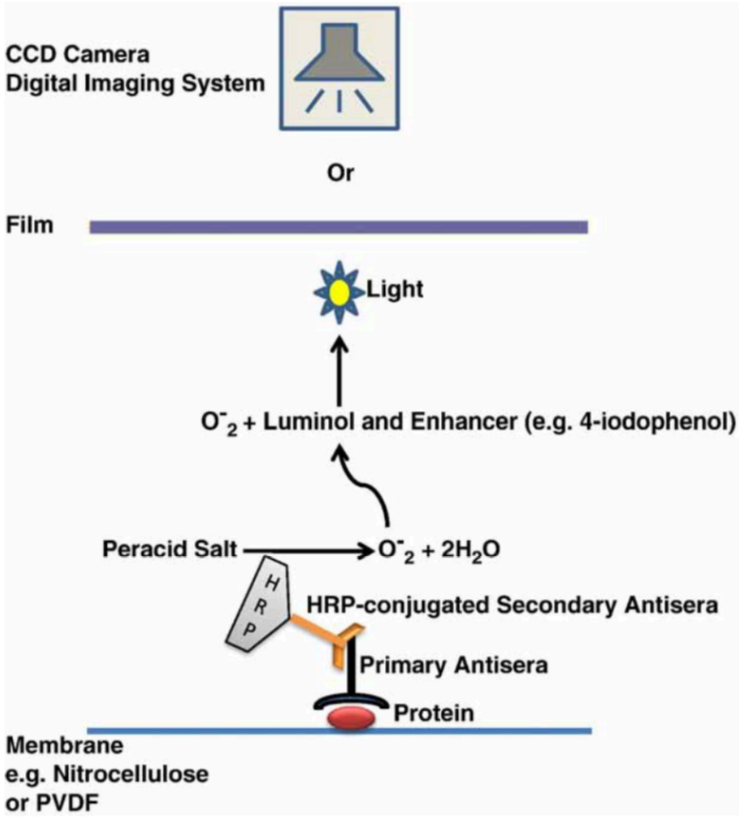

Figure 2.5. A schematic diagram of the detection of antigen using ECL reactions. Adsorption of proteins by membrane support are identified as primary antiserum followed by complexation of HRP-conjugated secondary antiserum to the complex. The HRP catalyses the reaction to oxidize the phenolic stimulant that react with 5-amino-2,3-dihydro-1, 4- phthalazinedione (luminol). The final result is the development of light that can be captured on film or by a digital imaging system. Image adapted from (MacPhee, 2010).

Enhance chemiluminescence (ECL), the upgrade version of Chemiluminescent detection is by far the most reliable technique of detection of antigens in Western blot. In ECL method, for instance, such as 5-amino-2,3-dihydro-1,4- phthalazinedione (luminol) is oxidized by hydrogen peroxidase and emit light at 425 nm during the chemical reaction (Bass et al., 2017).

2.2.3.9. Stripping and re-probing of the membrane

The stripping and re-probing the PVDF membranes allows to detect multiple antigens in a single run gel and thus saving the time and maximising efficiency. The blot This also provides confirmation of data obtained from the initial analysis of protein (e.g. different 1°Ab specific to another epitope on the same protein). The membrane allows another 1°Ab to bind to the target antigens, thus allowing detection of another proteins (Bass et al., 2017).

2.2.3.10. Analysis of signal

Analysis of the protein bands of interest on the blot is based on the nature of detection and the availability of imaging systems which can perform image acquisition and quantification. In spite of utilizing different methods of quantification by each of the software package but every system normally uses peak height or area of bands (Gassmann et al., 2009). It is significant to emphasize throughout quantification that target bands are within the linear range of detection, given that pixel saturating on image sensor can take place in highly abundant targets (Mollica et al., 2009). The software, such as ImageJ is able to detect saturation automatically. While analysis is conducted, clearest bands have to be produced by background subtraction (Gassmann et al., 2009). Inevitably, the choice of analysis must reflect the visualised blot and the linear detection within the range of the tool used for the imaging (Bass et al., 2017).

2.2.3.11. Normalization of Western Blot data

Target protein normalisation is done best when a single blot has been identified with target protein and ILC (internal loading control) in the same lane. Normalisation of sample to eliminate

variations in sample/gel is essential for accounting of potential errors in the preparation and loading of samples. The endogenous housekeeping proteins (HKP) such as glyceraldehyde 3-phosphate dehydrogenase (GAPDH), β-actin and α-tubulin are used as internal loading control (ILC) as their expression remain stable under various experimental conditions such as the HKP stay constant between control and experimental sample and shows unaffected by the treatment or intervention undertaken (Bass et al., 2017 and Pillai-Kastoori et al., 2020).

2.2.4. Immunocytochemistry (ICC)

Immunocytochemistry is a detection and visualisation technique to identify biomolecules in cells in situ by means of a specific antigen-antibody interaction where the antibody has been tagged with visible label. The is a powerful immunostaining technique to demonstrate both the existence and subcellular location of a particular molecules of interest. A.H. Coons first introduced immunofluorescence in 1941 in tissues in which he has used specific antibodies labelled with a fluorescent dye to localize antigens. The technique consists of first selecting a tissue containing the target antigen. The tissue is then processed to extract the cells and the cells is then fixed and attached to the slide followed by exposure to antibody or diluted serum. Secondly, a secondary antibody with attached visible or fluorescent trace the localization of any bound antibodies from patient serum. If the serum contains antibodies to a tissue protein, they will anatomically adequately bind to the tissue section (Mao et al., 1999 and Pestronk and Lopate, 2005).

Immunocytochemistry is an inexpensive and a quick technique, which makes it particularly useful for initial qualitative investigation of protein expression. Immunocytochemistry examination of nuclear antigens is frequent. Immunohistochemistry is largely advantageous when target antigens are complicated to purify target antigens in the amounts required for other methods of research. Low specificity may be a huge issue with ICC. Numerous distinct antigens can have identical cell distributions, allowing antibodies to be mistaken for each other. Therefore, findings established using this technique alone may not be unique to specific antigen, but still possible to determine co-localization of two or three proteins in the cells using different fluorescent attached secondary antibody (Mao et al., 1999 and Pestronk and Lopate, 2005).

2.2.5. quantitative PCR (qPCR)

qPCR (quantitative-Polymerase Chain Polymerase) is a powerful technique capable of providing reliable and quantitative data representing the biology of the experimental characteristics examined. PCR was developed in the early 1980 by Mullis and colleagues who were awarded the 1993 Nobel Prize for chemistry. PCR is generally defined as a simple, sensitive, faster method which uses oligonucleotide primers, dNTPs and heat tolerant Taq polymerase to amplify DNA. The system removed a significant barrier towards "fully quantitative" by discovering real time PCR. The inclusion of an initial reverse transcription (RT) step generated the complementary RT-PCR, a robust way to amplify any form of RNA. Currently, quantitative-PCR universally used in research and diagnostics. The qPCR was soon recognised as the "gold standard" in the quantitative analysis of nucleic acid due to its high specificity, sensitivity, simplicity, excellent reproducibility and wide range of dynamic quantification (Pfaffl and Berg, 2010).

qPCR has significant benefits in quantifying low target copy numbers from small quantities of tissue or in detecting slight variations in mRNA or microRNA expression levels in samples with low RNA concentrations or from single cell analysis. qPCR is a pioneer in comprehensive research to create new and improved applications due to its extensive quantifying ability in all kinds of biological matrix (Pfaffl and Berg, 2010).

2.3. Methods

2.3.1. Immunohistochemistry (IHC)

Ethics approval

Tissue was collected for pathological analysis at the University of Porto by Professor Rui Henrique under local ethics committee approval. Ethical approval of the use of human tissue for research in London was given by the joint University College London/University College London Hospital committees on the ethics of human research. Ethics approval was under REC Reference: 13/ES/0092 to Dr Aamir Ahmed.

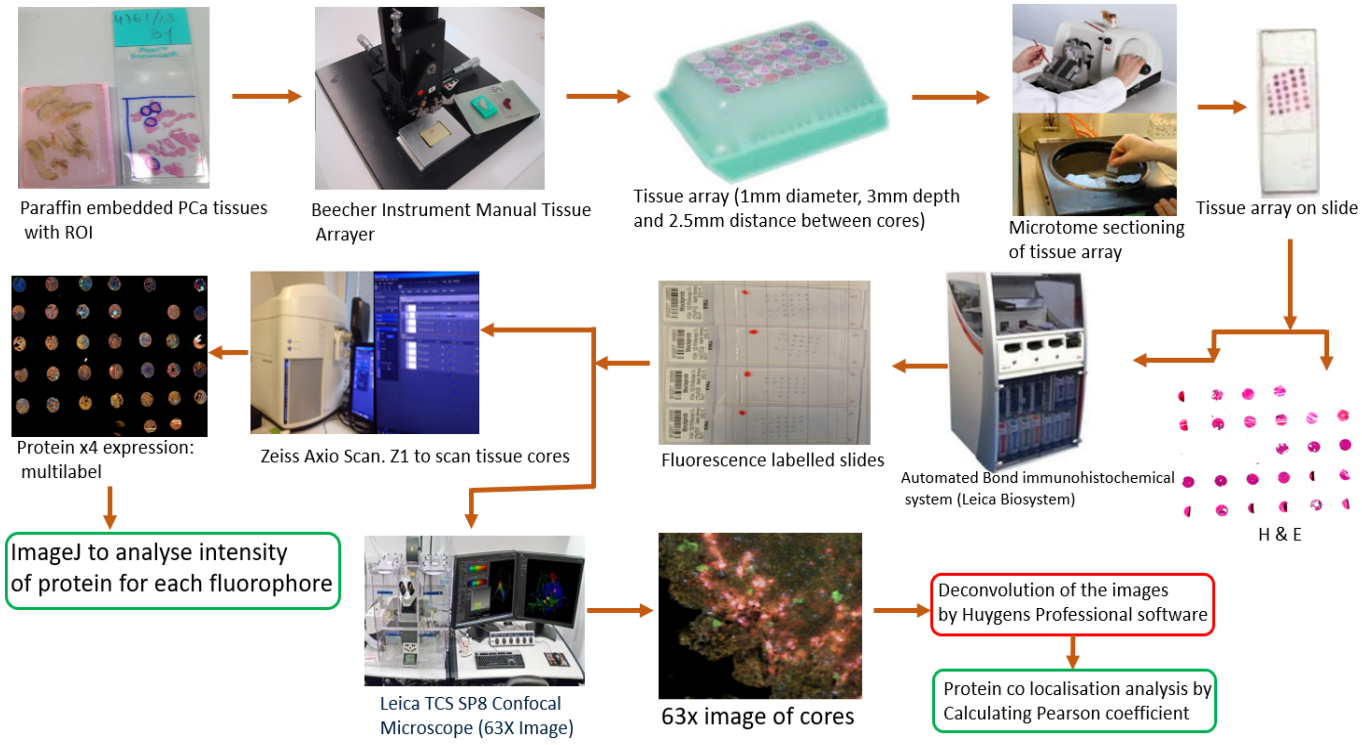

Figure 2.6. A flow chart of the steps of experimental procedure of IHC to determine the expression of Wnt and AR signalling proteins.

Collection of PCa and CRPC tissues

Eighty-six sample blocks of formalin fixed paraffin embedded (FFPE) normal prostate, benign prostatic hyperplasia (BPH) and different grades of PCa and castration resistance prostate cancer (CRPC) tissues were obtained from Rui Henrique, Guest Professor, Department of Pathology and Molecular Immunology Abel Salazar Institute of Biomedical Sciences University of Porto, Portugal.

Treatment of Patient with CRPC

The CRPC tissues were supplied from Institute of Portuguese Oncology Porto (IPO PORTO). At IPO Porto, CRPC patients with advanced metastasized PCa (which is the most common scenario) are admitted into enzalutamide or abiraterone therapy pathways. If the patient is very symptomatic (bone pain, for instance), alternatively, chemotherapy with docetaxel is administered (10 cycles).

2.3.1.1. Haematoxylin and Eosin (H&E) staining

H&E is most effective and common tool for tumour and cancer histological analysis in pathology (Chan, 2014).

The pathologist provided a clearer description for whole-mount tissue regions, where the cross-section of tissue from the gross section is mounted on the slide. The embedded tissues were sectioned with 6 μm and captured on poly-L-lysine coated glass slide followed by heating in an oven for 30 min at 60°C to melt the paraffin off the slides. The tissues were de-waxed by dipping in hydrophobic xylene three times with 5 min each followed by rehydration of tissues using a series of ethanol, 100% ethanol (2x10 min), 95% ethanol (2x10 min), 70% ethanol (2x10 min), 50% ethanol (2x10 min) and distilled water (2x5 min). While sections were in distilled water, haematoxylin was skimmed to remove oxidized particles. The tissue sections were dipped in haematoxylin solution (Sigma-Aldrich, UK) for 35 secs and immediately rinsed in deionized water followed by immersion of tissue sections in acid alcohol solution (1% HCl in 70% EtOH) for 8 secs to attain differentiation (removal of cytoplasmic staining). The tissues were then rinsed in running tap water for 2 min prior to 'blueing' in Scott's solution, which contains magnesium sulphate ($MgSO_4$) and sodium bicarbonate ($NaHCO_3$) in optimal proportions diluted in water for 2 min and further wash in running tap water for 2 min. Slides were evaluated at this stage to assure that sufficient nuclear staining was obtained using a light microscope. Dark stained sections were re-immersed in acid alcohol and lighter areas were re-immersed in haematoxylin. Tissue sections were submerged in 1% Eosin Y solution (Sigma-Aldrich, UK) for 2 min and rinsed in running tap water and dehydrated using a series of alcohols, 70% (2 min), 90% (2 min), 100% (2x5 min). Following dehydration, the tissues sections were then dipped in xylene for 15 min to remove alcohol and mounted with coverslips using DPX (Sigma-Aldrich, UK).

2.3.1.2. Identification of region of interest

The H&E stained tissue sections were sent to Rui Henrique (Pathologist) Guest Professor, Portugal to identify possible multiple tumour areas in the tissue sections. A tumour area was specified as an adjacent area containing specific tumour and manually annotated outline of the area covering each tumour region was illustrated. If cancerous regions of interest (ROI) can be

reliably and precisely contoured on entire mount whole slide image in the radical prostatectomy sections, this would facilitate quantitative recording of tumour size, region, aggression, metastasis and grade (Soetemans, 2017).

Pathologist followed the grading and scoring guideline of the International Society of Urological Pathologists (ISUP) to stratify the tumour and PCa tumour in tissue section (Epstein et al., 2016a) which have been described in Chap-I (Sec. 1.9).

2.3.1.3. Tissue array construction (TA)

Paraffin embedded 86 samples with their exam number and block references were obtained from Rui Henrique (Pathologist, Portugal). Following H&E, the samples were categorized in normal prostate tissues (NPT): 36 samples, benign prostatic hyperplasia (BPH): 10 samples, Gleason grade 3+3: 5 samples, Gleason grade 4+4: 5 samples, Gleason grade 4+5/5+4: 5 samples and CRPC: 20 samples, by pathologist using the grading and scoring guideline of the International Society of Urological Pathologists (ISUP) (Pierorazio et al., 2013 and Epstein et al., 2016a) . Total 171 cores composed of normal tissue cores: 66, BPH: 10, Gleason grade 3+3: 25, Gleason grade 4+4: 15, Gleason grade 4+5/5+4:15, CRPC cores: 40 were distributed over the 5 slides including RH16, RH17, RH18, RH19 and RH20_CRPC. The details of tissue catalogue, sample duplication and design of slide preparation presented in Appendix (Appx. 2).

The recipient paraffin block was prepared by pouring liquid paraffin into a stainless-steel base mould and allowed to cool. The recipient block was removed and assessed the paraffin surface for any bubble or holes. Excess paraffin was trimmed from the plastic cassette. ROIs on the donor tissue blocks were marked by pathologist. TA layout was determined and recorded all of the pertinent information about the tissue cores in the array. The recipient block was placed on the block holder. The identical circular indents were made by the small (recipient) and large (donor) punches. The depth of each punch was 3 mm in paraffin block and then donor block was placed on the array block holder, and punch was pushed downward on the sample to retrieve the tissue core, then donor tissue block was removed and replaced with recipient block in which punch was pushed downward until its tip reaches the top of the hole in the recipient array block. The large punch stylate was used to inject the tissue core into the hole created by smaller punch. The

diameter of core 1 mm and distance between two cores was 2.5 mm. Once the array is constructed, the TA block was pressed lightly on a flat surface to settle the tissue cores. The TA block was incubated in microwave oven at 37°C for 30 min by applying light and even pressure to the surface of the block with a clean glass slide to level the core heights. The TA slide was then transferred into fridge for further use.

2.3.1.4. Tissue dewaxing

The tissue sections were deparaffinized in three changes of xylene for 5 min and rehydrated by immersion in serial graded of alcohol solution which have been described elsewhere (Sec. 2.3.1.1) Following rehydration, the tissues sections were rinsed in running water.

2.3.1.5. Antigen retrieval

Antigen retrieval was conducted to allow binding of the paratope of primary antibody to the epitope of the antigen which was masked during the preparation of tissue for staining. Heat-Induced Epitope Retrieval (HIER) was used in which epitope retrieval solution (Cat: RE7116, Novocastra ^{TM}) was used. Pre-treatment can lead to a drastic improvement of immunoreactivity. The retrieval solution (10x) was diluted into 1x by adding 9 part of deionized water and was heated to boiling temperature (92-95°C) in a pressure cooker covering the lid without locking the lid. The slides were placed into metal staining racks which was immersed completely in the pressure cooker and the lid was locked. The pressure cooker reached at operating temperature after several min. Following removal of pressure cooker from the source heat, the slide was run under cold water keeping lid on. Lid was opened when the pressure was released observed by indicator. The slides were removed and placed immediately in cool tap water followed by rinse with PBS and proceeded for blocking

2.3.1.6. Blocking of non-specific binding sites

The tissue section was incubated in 3% H_2O_2 menthol solution for 30 min to neutralise the endogenous peroxidase activity and rinsed in running water for 10 min. The non-specific binding sites was blocked by incubation with 10% normal serum and 1% BSA in PBS for 1 h at room temperature. Normal serum was obtained from the species in which secondary antibody was

raised. This strategy minimises the cross reactivity of secondary antibody with endogenous immunoglobulins.

2.3.1.7. Determination of specificities of antibodies

A series of antibodies (Table 2.7 and Table 2.8) used in immunostaining were checked were checked. Initial antibody optimisation involved testing the antibodies on a suitable positive control tissue under a range of conditions (Symes et al., 2013 and Giuliano et al., 2016). This typically involved a titre run looking at different antibody dilutions (1:50, 1:100, 1:250, 1:500, 1:5000) along with a negative control (omission of primary antibody). The negative control was used to assess whether the secondary antibodies produce any nonspecific band. Staining was performed using well established automated immunostaining robots (Leica Bond Max/RX). Polymer based HRP detections were utilised due to their high sensitivity and specificity using a colorimetric DAB endpoint with Haematoxylin counterstain. Heat Induced Epitope Retrieval (HIER) was performed during antibody optimisation using a standard pH 6 (0.01M citrate buffer) and non HIER conditions were also assessed (Arya et al., 2015 and Toth and Mezey, 2007).

2.3.1.8. Immunostaining of prostate and PCa tissues

Wnt, AR and Connexin signalling proteins were investigated to measure their expression in normal prostate tissue (NPT), benign prostatic hyperplasia (BPH), Grade 3+3 PCa, Grade 4+4 PCa and Grade 4+5/5+4 PCa and castration resistant prostate cancer (CRPC) using two methods: 1. Chromogenic (DAB: 3,3'-Diaminobenzidine) and 2. Immunofluorescence staining methods.

2.3.1.8.1. Immunostaining of prostate and PCa tissues using chromogenic staining method

Chromogenic (DAB: 3,3'-Diaminobenzidine) staining implicit the expression of single protein in tissue *in situ*. The DAB staining was aimed to determine the sole expression of a protein of Wnt and AR and Connexin signalling pathways in prostate and PCa tissues. 30 samples of 15 NPT, 5 Grade 3+3, 5 Grade 4+4 and Grade 4+5/5+4 was used to construct three slides (e.g., RH16, RH17 and RH18) of TA. Each of the slides contain 30 cores of 15 cores (15 NPT), 5 cores (Grade 3+3), 5 cores (Grade 4+4) and 5 cores (Grade 4+5/5+4). The cores on RH19 and RH20_CRPC were also stained with anti-AR and anti-Cx43 antibodies. The tissue core combination and layout have been described in appendix (Sec. 2).

The AR signalling target protein e.g., AR, Wnt signalling targets, e.g., TCF-1, FRA-1 and β-catenin, Connexin signalling target, e.g., Cx43 protein were investigated to measure the expression using the antibodies as follows in the table:

Table 2.7. A list of antibodies. The following table contains the six antibodies, their host and dilution used in chromogenic technique

Primary antibody		Host	Cat and Manufacturer	Dilution	Cores on the slide were Stained
Anti-AR antibody		Rabbit	Ab133273, ABCAM	1:400	RH16, RH17, RH18 & RHC1, RH19, RH20_CRPC
Anti-β-Catenin antibody		Mouse	Ab22656, ABCAM	1: 200	RH16, RH17, RH18 & RHC1
Anti-FRA-1 antibody		Rabbit	ab252421, ABCAM	1:1000	RH16, RH17, RH18 & RHC1
Anti-TCF-1 antibody		Rabbit	2203S, Cell signalling technology	1:100	RH16, RH17, RH18 & RHC1
Anti-PYGO2 antibody		Rabbit	ab99274, ABCAM	1:200	RH16, RH17, RH18 & RHC1
Cx43		Rabbit	C6219: Sigma	1:1000	RH16, RH17, RH18 & RHC1, RH19, RH20_CRPC
Secondary antibody	Peroxidase AffiniPure Donkey Anti-Mouse IgG (H+L)	Donkey	715-035-151, Jackson Immunoresearch Laboratory (JIL)	1:500	Used against Ant-mouse primary antibody
	Peroxidase AffiniPure Donkey Anti-Rabbit IgG (H+L)	Donkey	711-035-152, Jackson Immunoresearch laboratory (JIL)	1:500	Used against Anti-rabbit primary antibodies

The tissue sections were stained with anti-AR, -β-Catenin, -FRA-1, -TCF-1, -PYGO2, and -Cx43 antibodies (Table 2.7) using Bond automated systems (Leica Biosystems, Milton Keynes, UK) according to manufacturer's protocol. For staining, the tissue sections were deparaffinised with Xylene and incubated with serial dilution of EtOH followed by hydration with water. The endogenous peroxidase activity was quenched with 0.6% H_2O_2 in methanol for 15 min and washed with PBS (2 x 3'). The tissues were blocked with serum by incubating 30 min. Following washing up, the tissue was incubated with primary antibodies listed in the Table 2.7 with corresponding dilutions and washed prior to incubation with secondary antibodies (Table 2.7). Following washing with PBS, the tissue sections were incubated chromogenic reaction buffer

(DAB) and co-inter-stained with haematoxylin. The tissue sections were dried and rehydrated with a serial dilution of EtOH and water. Slides were left in xylene until they are cover slipped. The slides were mounted, and coverslips were remained until harden.

A. Imaging and signal quantitation

Single Ab-labelled DAB-stained cores were scanned using NanoZoomer-RS Scanner (Type: C10730-02) with a resolution of 0.23µm/pixel (40x high resolution mode) (Hamamatsu Photonics UK Ltd, Welwyn Garden City, UK) and the image of an individual core was segregated and compiled and indexed according to the configuration of TA (Appx. 2). A semiautomated and unbiased quantitative method, ImageJ software (Schneider et al., 2012) where an algorithm developed in our lab was incorporated (Arya et al., 2015 and Symes et al., 2013). DAB stain (brown) on the tissue core was segmented on hue, saturation and brightness. Area containing tissue were identified on the duplicate image by conversion to 8-bit and application of a threshold to. Only pixel that are not the same intensity as the background are measured. Thresholds were optimised on a training set of images prior to application to the experimental set of images for quantitation. A macro was compiled for an unbiased quantitation to measure both the amount of DAB signal and the amount of tissue. Area of folded tissue and fitted to a probit regression (Area Fraction, AFperAMT).

B. Statistical analysis

The data was plotted as box plots (demonstrating a range of protein expression), mountain plots (to measure AUC) and ROC curves (for sensitivity and specificity of proteins for normal vs cancer or different grades of cancer). Logistic regression model for all possible combinations of proteins was performed using Medcalc software.

The area fraction data was transformed into probit and fitted to a Gaussian function. AUC values of 1.0 for an ROC curve mean high selectivity and sensitivity, whereas 0.5 suggests that the tested marker cannot distinguish between condition A vs B. Median selection and statistical test (significance of differences) were performed using Mann-Whitney U test (ns $P>0.05$; *$P<0.05$; **$P<0.01$; ***$P<0.001$; ****$P<0.0001$) (GraphPad Prism, version 8.0.0).

2.3.1.8.2. Immunostaining of prostate and PCa tissue using fluorescence staining method

Wnt, AR and Connexin signalling proteins were investigated to measure the expression and co-localization in normal prostate, benign prostatic hyperplasia, Grade 3+3 and CRPC tissues. A multiplex experiment was carried out to measure the expression and co-localisation of Wnt and AR signalling targets proteins using immunofluorescence staining. Second experiment (uniplex-1) was involved in DAB staining to investigate expression Wnt and AR target proteins. Immunofluorescence staining was conducted using an automated Bond Max automated staining system (Leica Biosystems, Milton Keynes, UK) using a protocol adapted from (Toth and Mezey, 2007). The staining protocol is described elsewhere (e.g., (Arya et al., 2015)), briefly reiterated below.

Multilabel experiment was conducted on RH19 and RH20_CRPC TAs which were stained with four antibodies on the same slide to conduct analysis of protein in Wnt and AR signalling pathways where anti-β-catenin antibody for the principal component, β-catenin, of Wnt signalling pathway, anti-FRA-1 and anti-c-MYC antibodies used for β-catenin targets FRA-1 and c-MYC respectively. All of these antibodies have been previously optimized for prostate and other human tissues for specificity (Symes et al., 2013; Arya et al., 2015; Giuliano et al., 2016 and Arthurs et al., 2017). Anti-AR antibody was used for AR, a major component of AR signalling pathway. The four target antibodies were re-coded so that their identity was unknown to the experiments when experiments were conducted.

Table 2.8. A list of antibodies. The table representing the antibodies and their corresponding host, catalogue, manufacturer and dilution used in the experiment.

Primary antibody	Fluorophores (Laser/excitation-emission nm)	Host	Cat and Source	Dilution
Fra-1	Tyr-Alexa 405 (405/415-480)	Rabbit	ab252421: ABCAM	1:200
β-Catenin	Tyr-FITC (488/500-550)	Mouse	Ab22656, ABCAM	1: 200
AR	Tyr-Cy3 (559/575-620)	Rabbit	Ab133273, ABCAM	1:250
c-MYC	Tyr-Cy5 (635/645-740)	Rabbit	C3956, Sigma	1:200
Secondary antibody	Peroxidase AffiniPure Donkey Anti-Mouse IgG (H+L)	Donkey	715-035-151: Jackson Immunoresearch Laboratory (JIL)	1:500

	Peroxidase AffiniPure Donkey Anti-Rabbit IgG (H+L)	Donkey	711-035-152: Jackson Immunoresearch laboratory (JIL)	1:500

The blocked tissue sections were incubated with four antibodies sequentially, similar to the techniques described elsewhere (Arya et al., 2015). The tissue sections were incubated with anti-β-Catenin antibody for 2 h at room temperature at 1: 200 dilution in TBST followed by TBST wash (3 x 5'). The array sections were incubated with secondary antibody Peroxidase AffiniPure Donkey anti-Mouse IgG (H+L) (cat:715-035-151, JIL) at 1:500 dilution for 30 min at RT followed by further TBST washes. The tissue sections were then incubated with Tyr-FITC for 10 min, subsequent to two washes with TBST and 10 min HIER using epitope retrieval buffer solution 1 (EP1) in Bond Automated System. The tissue sections were then incubated with anti-AR antibody for 2 h at RT followed by TBST wash (3x5') and incubated with secondary antibody for 30 min and washed with TBST prior to incubation with visualising reagent Tyr-Cy3 for 10 min. Following TBST wash and 10 min HIER with EP1, anti-c-MYC antibody was applied for 2 h followed by subsequent TBST wash (3x5') and secondary antibody incubation for 30 min. Following TBST wash, the visualising reagent Tyr-Cy5 was employed for 10 min and was washed with TBST. Sequentially, 10 min HIER incubation with EP1 and 2 h incubation with anti-FRA-1 antibody, the tissues sections were washed as usual incubated with secondary antibody followed by wash with TBST and subsequent incubation with fluorescence dye Tyr-Alexa 405 for 10 min followed by TBST wash and coverslip placement with Permafluor.

A. Fluorescence imaging of antibodies β-catenin, AR, c-MYC and FRA-1 signal

Each of the tissue cores on RH19 and RH20 TAs was imaged using Zeiss Axioscan Z.1 slide scanner (Carl Zeiss) at 20x magnification (Arya et al., 2015). The fluorescent signals were optimised prior to conducting Axioscan to avoid oversaturation of signal faint for each antibody. For a standardized comparison, the power of Colibri.2 LED lights and integration times of the Hamamatsu ORCA Flash4 camera (Hamamatsu Photonics) were kept constants for all samples. The imaging of the slides was carried out at the same time sequentially with identical image acquisition settings. Montages of each core were automatically generated and accumulated from

multiple 2048x2048 pixel with 16 bit gray level which were compiled locally on the acquisition computer.

B. Quantitation of the expression of Wnt and AR signalling proteins

To quantify the expression of each protein, an unbiased, reproducible and automated analysis was employed to quantify the intensity of each fluorophore used in the tissue micro array to measure the amount of expression of each antibody in prostate normal and malignant tissues. A plugin adapted to ImageJ has already been scripted to semi-automatically discriminate the whole TA, largely based on a threshold segmentation routine, was used. Lower and upper threshold parameters was standardised prior to include the median to maximum gray value of a range of samples across the whole sample set. These values were then used to perform a batch analysis of the entire sample set, where the mean gray values per TMA core was calculated (Wang et al., 2010a and Symes et al., 2013).

C. Quantitative co-localization of Wnt and AR target protein using High resolution confocal microscopy

In addition to the changes in expression in diseases such as cancer where the translation machinery is overactive (Arthurs et al., 2017), there may also be changes in the localization of proteins. This could be compared by measuring colocalization of two protein signals, subsequent to deconvolution to eliminate the noise, and may serve as a further biomarker for disease or for disease stratification (Symes et al., 2013; Arya et al., 2015 and Giuliano et al., 2016). To do this, 40 cores of control and malignant tissues were used in which 3 smaller regions of interest (ROIs) in each core were selected and imaged with confocal Microscope Leica TCS SP8 using oil emersion 63X 1NA objectives with zoom 6x. The images were saved as a lif file which were imported to Huygens Professional Software for deconvolution. The deconvolved images were saved as Huygens specific (HDF5) files for each channel (excitation/emission nm). The antibodies (Table 2.8) were fluorescently labelled with Tyr-FITC (488/500-550: Green), Tyr-Cy3 (559/575-620: Orange), Tyr-Cy5 (635/645-740: Red), Tyr-Alexa 405 (405/415-480: Blue). The HDF5 files were used to calculate Pearson coefficient for co-localisation using a written script adapted to Huygens pro (Arya et al., 2015).

D. Statistical analysis

Mountain plot and Box were constructed using GraphPad Prism, version 8.0.0 (GraphPad Software, San Diego, California USA. Median selection and statistical test (significance of differences) were performed using Mann-Whitney U test (ns P>0.05; *P<0.05; P**<0.01; ***P<0.001; ****P<0.0001) (GraphPad Prism, version 8.0.0).

2.3.2. RNAscope of mRNA analysis of Wnt and AR target proteins

Single molecule RNA detection combined with protein expression for the products of the same RNA molecules could provide a powerful correlation and a clear picture of transcriptional and translational changes that may occur during different stages of a disease. The ultimate objective is to conduct both single molecule RNA and protein expression on the same slide; to establish this technique, however, I have designed these experiments to be conducted on different tissue array slides.

2.3.2.1. Application of positive and negative control to verify RNA quality and specificity

A good and consistent quality control practice has to be implanted before carrying out experiments. To verify the target quality and specificity of target, a low-copy housekeeping gene positive control probe and a non-specific bacterial negative control probe are used to optimise the specific pre-treatment conditions for optimal RNA exposure and detection in the tissue samples before performing experiments. When the assay is run properly, there will be strong signal for positive control probe staining and clean background for negative control probe staining.

Peptidylprolyl Isomerase B (PPIB) and RNA Polymerase II Subunit A (POLR2A) were used to assess the quality of RNA expression of PPIB and POLR2A in each core of the slides. A universal negative control with probes targeting the Dap B gene from the soil born bacterium*, Bacillus subtilis* strain SMY was used to observe the background staining.

2.3.2.2. RNAscope staining

Four Wnt signalling targets including β-catenin, PYGO2, FRA-1. and TCF-1 were selected to determine their RNA expression based on the contribution in PCa development. Tissue cores of

normal prostate, BPH, Gleason score 3+3, Gleason score 4+4, Gleason score 4+5/5+4 and CRPC distributed over slides RH16, RH17, RH18, RH19 and RH20_CRPC (Appx. 2) were undertaken into the experiment. RNA probes were designed to hybridize the target RNA molecules of Wnt targets including β-catenin, PYGO2, FRA-1 and TCF-1. This protocol was conducted by Mike Millar at the University of Edinburgh.

Two control probes used in this analysis have unique properties, often assessed by quantitative gene expression methods (Hruz et al., 2011). The first control probe, POLR2A, encoding RNA II's major subunit, is a low copy stringent positive control that may be necessary for very low targets. The housekeeping gene PPIB encoding peptidyl-prolyl isomerase B functions in tissue proliferation such as tumour and other tissues that are not tumorous. It is expressed at adequately low level so as to provide robust consistency.

Microtome dissected FFPE tissue sections (5 µm thickness) were baked in a dry oven for 1 h at 60°C. The tissues were deparaffinized in xylene 2 x 5' followed by incubation in 100% EtOH for 2 x 1'. The tissues were left for air dried for 5 min at RT. Hydrogen Peroxide was applied to tissue arrays for 10 min at RT and the rack was submerged in distilled water and washed by moving the rack up and down 3-5 min and finally with fresh distilled water. The tissue slides were submerged in the boiling targeted retrieval solution (cat: 322452, ACD) and transferred to staining dish containing distilled water. The tissue slide was washed in distilled water by moving the rack up and down 3-5 times and completed with wash with fresh distilled water followed by washing up in fresh 100% by moving the rack up and down 3-5 times and dried in air. Hydrophobic barrier was created by drawing 2-4 times around the tissue using the image TM hydrophobic barrier pen and the tissue slide was dried for ~2 min at RT. ~5 drops of protease plus was applied to the tissue section and it was placed in prewarmed humidified control tray and incubated for 30 min at 40°C. The tissue slide was washed with distilled water by moving the rack up and down 3-5 times and finished washing with fresh water.

The probes, C1 and C2, were warmed at 40°C for 10 min and cooled to RT and centrifuged briefly followed by mixing the C2 and C1 at 1:5 ratio in a tube. Excess liquid was removed from the slides and ~4 drops of probe was added to the section. The slide was placed on tray and sealed and incubated for 2 h at 40°C in prewarmed oven at 40°C.

Following washing with wash buffer for 2 min at RT, ~4 drops of Amp1 was applied to the tissues section. The slide was placed on a tray and sealed and placed in a prewarmed oven for 30 min at 40℃ followed by washing with wash buffer for 2 min at RT. Excess liquid was removed from slides and ~4 drops of Amp2 was applied to tissue sections and incubated in a sealed tray by placing in a prewarmed over for 15 min at 40℃ and was washed with wash buffer for 2 min at RT and finished washing with fresh distilled water. Following removal of excess liquid, ~4 drops of Amp 3 was applied to the tissue sections and was incubated for 30 min at 40℃ and was washed and excess liquid was removed. ~4 drops of Amp 4 was applied to the tissue sections and incubated for 15 min at 40℃ in a prewarmed oven followed by washing up for 2 min at RT and excess liquid was removed and thus Amp 5 was applied and incubated for 30 min at RT and Amp 6 was added and incubated for 15 min at RT followed by washing up for 2 min at RT.

2.3.2.3. Detection of signal of RNAscope probes

The solution RED-B and RED-A were mixed at 1:60 ration and applied to the tissue section and incubated for 10 min at RT and washed with wash buffer for 2 min at RT. Following removal of excess liquid, ~4 drops of Amp 7 was applied to the tissue and incubated for 15 min at 40℃ and washed for 2 min. Subsequently, ~4 drops of Amp 8 was added and incubated for 30 min at 40℃. Following finishing of post application process, ~4 drops of Amp 9 was applied to the tissue sections and incubated for 30 min at RT and washed for 2 min at RT and ~4 drops of amp 10 was applied to tissue section and incubated for 15 min at RT and washed for 2 min at RT. The Green-B and Green-A solutions were mixed at 1:50 ratio and applied to the tissue section and incubated for 10 min at RT and washed for 5 min followed by washing and rinsing the tissue with distilled water. The slide was placed in 50% haematoxylin for 30 sec at RT and washed 3-5 times at tap water. The slide was then washed 10 secs in 0.02% Ammonia water and then washed 3-5 times in tap water. The slide was dried in an oven at 60℃ for 15 min and dipped in pure xylene and 1-2 drops of EcoMount was applied on slide before the xylene was dried. A coverslip was placed over the tissue section and dried in air for 30 min.

2.3.2.4. Imaging

RNAscope slides were scanned with automatically performed by Carl Zeiss Axioscan using 40x, 20x and 10x magnifications fitting bright field. Stained tissue cores were also scanned using NanoZoomer-RS Scanner (Type: C10730-02) with resolution 0.23µm/pixel (40x high resolution mode) (Hamamatsu Photonics UK Ltd, Welwyn Garden City, UK) for analysis purposes. Python software with Jupyter notebook was used to quantitate the expression of RNA. Prior to quantitation, threshold was applied for each image using hue, saturation and brightness. Each of the punctate dot indicate each RNA molecules. The quantified number was used to construct box to measure the expression of each single RNA molecule.

2.3.2.5. Statistical analysis

Mountain plot and Box were constructed using GraphPad Prism, version 8.0.0 (GraphPad Software, San Diego, California USA. Median selection and statistical test (significance of differences) were performed using Mann-Whitney U test (ns $P>0.05$; *$P<0.05$; P**<0.01; ***$P<0.001$; ****$P<0.0001$) (GraphPad Prism, version 8.0.0).

2.3.3. Culturing of cells and management

2.3.3.1. Cell culture

PC3 (ATCC: CRL-1435) and LnCAP (ATCC: CRL-1740) cells were obtained from American Type Culture Collection (ATCC) and cultured at required density in T-25 cm^2 (Cat: 156367, Thermo Scientific™ Nunc™ Cell Culture Treated EasYFlasks™) in 6 ml RPMI 1640 (Table 2.2) supplemented with 10% foetal bovine serum and 2 mM L-glutamine (Table 2.2). The cells were incubated in 5% CO_2 at 37°C to grow. Media was replaced with new media twice weekly until the cells were reached to 80-90% confluency. Cells were passaged at approximately 80-90% confluency to prevent overcrowding. While passaging, cells were washed twice with 3 ml of PBS (Table 2.2) and incubated with 1 ml of 1x trypsin: versine at 37°C for 5-10 min to dislodge the cells from the flask surface. If the cells were not fully detached, gentle tapping was applied. Once cells were completely detached, 4 ml of growth media containing FBS was added into flask to neutralise the activities of trypsin. The cell suspension was centrifuged at 200x*g* for 2 min to get a cell pellet. Supernatant was carefully decanted without disturbing cell pellet which was then resuspended

in fresh medium at required dilution aseptically. Following counting, 5000 and 10000 cells were seeded into two T-25 cm^2 flasks with 6 ml of growth medium for further use.

2.3.3.2. Cell counting using haemocytometer

Haemocytometer was used to determine the cell number/ml in a cell suspension. Following resuspension of cell pellet in cell growth media, the cells were further diluted 1:5 into growth media from where 20 µl of diluted cell suspension was transferred into new fresh microcentrifuge tube in which 20 µl trypan blue (Table 2.2) was added (cell suspension: trypan blue = 1:1) and mixed using pipette tip. The cell mixture was then left for incubation for ~ 3 min. 10 µl of cell mixtures were loaded onto upper or lower chambers of the haemocytometer. The cells in the outer four large squares were counted and the cell density in cells/ml was calculated as follows: Cell count: (4 square/4) X Dilution factor X 10^4 X 1ml

2.3.3.3. Cryopreservation and thawing of cells

Cells were grown in T-25 cm^2 and aspirate the media and trypsinized as written in the cell culture. Once cells were detached, medium was added into the flask. Determination of cell viability was conducted using trypan blue by haemocytometer. 90% viable cells were considered to be healthy enough for freezing. Cells were centrifuged as same condition as described in cell culture section. The pellet was resuspended in freezing medium, which was made of 10% DMSO and 90% growth media/FBS, to prepare a cell suspension of $1x10^6$ cell/ml. 1 ml of cell suspension was aliquoted in each cryotube which was transferred into Mr. Frosty submerged in 100% isopropyl alcohol to start the steady freezing process by 1°C/min. Then cells were placed at -20°C for 1 h, followed by -80°C for overnight before permanent storage in liquid N_2. The cells were revived by removing the cryovial from liquid N_2 storage and placing immediately in 37°C water bath followed by quick gentle shaking for 80% thaw and pipetting into prewarm media. The cells were incubated at 37°C to grow and for further experiments.

2.3.3.4. Cell transfection

PC3 cells is AR independent, do not express (Ching et al., 1993). Investigation of AR translocation in PC3 cells was conducted by overexpressing AR in PC3 cells. AR inserted plasmid (Cat: RG215316, Origene) was obtained from Dr. Williamson Magalli, King's College London. Details of

the plasmid is described in appendix (Appx. 2.6). Qiagen transfecting reagent attractene (cat: 301005, Qiagen) was used. The attractene transfection reagent protocol (traditional version) was optimised to transfect cells in 10 mm dish. 10,000 PC3 cells were seeded in 5ml of RPMI 1640 culture media containing FBS and Pen-strep antibiotic (Cat:11074440001, Sigma-Aldrich) in 10mm dish. The cells were incubated under normal growth conditions (Sec. 2.3.3.1) to grow cells to reach 80-90% confluency to transfect. For transfection, 4 µg (dissolved in TE buffer) was mixed in medium without serum, proteins and antibiotic to a total volume of 300 µl. 15 µl of attractene transfection reagent was added to the DNA solution and was mixed by pipetting up and down and was briefly centrifuged. The sample was incubated for 15 min at RT to enable complex formation. Before adding the DNA complex solution, media was aspirated from the cells and 2ml of fresh media was added. Then transfection-complex was added to cells drop-wise and was gently swirl for uniform distribution of the transfection complexes. The cells were incubated under normal growth condition over-night and were check successful transfection observing GFP expression in transfected cells.

2.3.4. Western blotting (WB)

WB was conducted to investigate Wnt and AR signalling proteins in PC3 and LnCAP cells upon activation of those signal by treatment of their ligands such as Wnt3A, Wnt5A, Wnt9B and DHT

2.3.4.1. Treatment of LnCAP and PC3 cells with AR and Wnt signalling ligands

Two sets of experiments were designed in which each of the sets composed of a control cells (untreated or vehicle treated) and treated cells. The first set was conducted to compare the expression of AR and Wnt signalling target proteins in LnCAP cells in response to AR signalling ligands and Wnt signalling ligands treatment. The second set included the comparison of expression of AR and Wnt signalling target proteins in PC3 cells in response to AR and Wnt ligands LnCAP cells were grown in 2xT-25 cm^2 flask for each set of experiment and incubated for 48 h at 37°C. The cells were removed from the incubation at 90% confluency of cell growth. 5 ml of 6ml media was removed from the flask and, then 1 ml fresh medium was added into the flask and the cells were then treated with AR signalling ligand (e.g., DHT) and Wnt signalling ligands (e.g., Wnt3A, Wnt5A and Wnt9B) at the desired concentration (Table 2.3). The experiments were

carried out two more repeat independently using different passage and batch number of LnCAP cells. The control cells for each experiment were treated with PBH as a vehicle control. Similarly, PC3 cells were also treated with DHT, Wnt5A and Wnt9B to compare the expression of AR and Wnt signalling proteins in DHT and Wnt3A, Wnt5A and Wnt9B treated PC3 cell (Table 2.3).

2.3.4.2. Extraction of proteins from untreated and untreated whole cells

Cells were removed from incubator and placed on ice. The medium was aspirated followed by washing twice with ice cold PBS. Cells were scrapped with precooled scrapper and the cells transferred into 15 ml falcon tube before counting the cells with haemocytometer. The cells were centrifuged at 200x*g* for 2 min to get cell pellet. The pellet was transferred into 1.5 ml microcentrifuge tube in which lysis buffer (RIPA, 1x) (Cat:9806, Cell Signalling Technology) was added at 400µl/10^7 cells to the tube. Protease inhibitor (Complete, Cat. No. 11 836 170 001, Roche) and Phophatase inhibitor (PhosSTOP, Cat. No. 04 906 837 001, Roche) were added to the microcentrifuge tube according to manufacturer's instruction. The cells were then lysed by incubating at 4°C for 30 min with constant agitation before centrifugation at 16,000x*g* for 25 min. The centrifuge tube was gently removed and placed on ice and supernatant was transferred into a fresh tube. The cell lysate was used for protein assay and rest was stored at -80°C for further use.

2.3.4.3. Cell fractionations of PC3 and LnCAP cells

PC3 and LnCAP cells were used to extract proteins from their different fractions including membrane, cytoplasm and nucleus using Qproteome Cell Compartment Kit (Cat:37502, Qiagen). The cells were placed on ice and washed twice with ice-cold PBS buffer and were collected once cells were scrapped using an ice-cold scrapper. The cell suspension containing 5x10^6 cells was transferred to a 15 ml falcon tube and centrifuged at 500x*g* for 10 min at 4°C to achieve a pellet. Briefly 1 ml of CE1 buffer was added to 5x10^6 cells and 10 µl of protease inhibitor was also added to the cells followed by agitation end-over-end for 10 min at 4°C and centrifuged for 10 min at 1000x*g* at 4°C to separate cytosolic proteins. After collection of cytosolic protein, 1 ml of CE2 buffer was applied to the tube, followed by incubation for 30 min at 4°C with end-over-end shaking. Then centrifugation was performed at 6000x*g* for 10 min at 4°C. The total membrane

protein (e.g., proteins from plasma membrane as well as all organelle membranes except nuclear membrane, and proteins from the lumen of the ER and mitochondria) was transferred into a precooled microcentrifuge tube. 7 µl Benzonase and 13 µl distilled water were added to the pellet and incubated for 15 min on the bench at RT. 500 µl CE3 mixed with 5 µl protease inhibitor (100x) was added to the cells and incubated for 10 min at 4°C with end-over-end agitation followed by centrifugation at 6800x*g* for 10 min at 4°C and proteins was transferred into precooled microcentrifuge tube. This fraction contains soluble, and membrane bound nuclear proteins. The protein concentration was measured using the Thermo Scientific™ Pierce™ BCA protein assay kit (cat: 23225) assay.

2.3.4.4. Determination of protein concentration in cell lysate by BCA protein assay

Protein concentration in cell lysate was determined using the Thermo Scientific™ Pierce™ BCA protein assay kit (cat: 23225) assay which was invented in 1985 by Paul K. Smith at Pierce Chemical Company, a major distributor of this assay (Smith et al., 1985).

Preparation of standards and working reagent

A. Preparation of diluted albumin (BSA) standards

The BCA assay was conducted in Thermo Scientific™ Pierce™ 96-Well Plates. The protein standards BSA (Bovine Serum Albumin) was supplied with the kit as 1 ml ampule (2 mg/ml). A series of protein standard (BSA ranges 25-2000 µg/ml) was prepared from 2000 µg/ml stock diluted in homogenisation buffer. The following table shows the dilutions of BSA standards.

Table 2.9. The table is representing the steps of dilution procedure of BSA standardsh

Vial	Volume of diluent (µL)	Volume and source of BSA (µL)	Final BSA concentration (µg/mL)
A	0	300 of stock	2000
B	125	375 of stock	1500
C	325	325 of stock	1000
D	175	175 of vial B dilution	750
E	325	325 of vial C dilution	500
F	325	325 of vial E dilution	250
G	325	325 of vial F dilution	125
H	400	100 of vial G dilution	25
I	400	0	0 = Blank

Following preparation of series of different concentrations of BSA, the BCA working reagent was made.

B. Preparation of the BCA working reagent (WR)

15ml falcon tube was used to prepare the working WR using the following formula.

1. Volume of WR required was determined using the following formula:

Total Volume of WR: (# Standards + # unknown) x # replicates x# volume of WR of each sample

2. Preparation of working reagent

WR was prepared by mixing 50 parts of BCA reagent A (Sodium carbonate, sodium bicarbonate, bicinchoninic acid and sodium tartrate in 0.1M sodium hydroxide) with 1 part of BCA reagent B (4% cupric sulfate) (50:1, reagent A:B).

Protein was quantified using a microplate based procedure in which sample to WR ratio was = 1:8. 25 ul of each BSA standard (range 20 – 2000 µg/mL) and unknown protein samples with replicates were pipetted into a microplate well in 96-well plate. 200µL of the WR was added to each well of standard and unknown cell lysate and the plate was thoroughly shaken for 30 seconds. The plate was covered with aluminium foil and incubated at 37°C for 30 min. The plate was cooled at RT and the absorbance was measured at 562nm by Glomax Discover System (Promega). The average absorbance at 562 nm of blank standard and its replicate were subtracted from the average absorbance measurements of all other individual standard and unknow samples and their replicates. The absorbances of BSA standard and unknown protein were recorded to construct a standard curve from which protein concentrations of unknown cell lysate were measured.

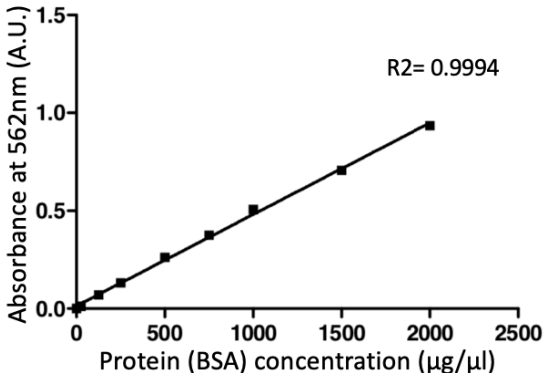

Figure 2.7. A typical example of standard curve for determination of protein concentration showing absorbance of BSA is increased with increase of its concentration. Linear regression line was used to calculate the concentration of cell lysate.

2.3.4.5. SDS-PAGE electrophoresis and staining of PVDF membrane

15 µg of protein of whole cell lysate or of each cell fractions of Wnt ligands e.g., (±)Wnt3A, (±) Wnt5A or PBS only and (±)Wnt9B or AR signalling ligands e.g.,(±)DHT treated LnCAP and PC3 were mixed with 5µl of loading buffer prepared by mixing Laemmli 4x sample buffer (Cat. 1610747, Bio-Rad) with β-mercaptoethanol at 9:1 dilution. Protein samples were boiled at 95°C for 8-10 min before loading into Precast protein gels (Bio-Rad) using Mini-PROTEAN Electrophoresis system (Cat. 17006570, Bio-RAD) for resolving the proteins. 6µl of Colour Pre-stained Protein Standard, broad range (NEB, Cat. No. P7719) was loaded onto gel as a protein molecular weight marker. During electrophoresis, 50 voltages current for 10 min was applied to run through stacking gel, then 120 voltages for 45 min was applied to run through resolving gel for separating the proteins. The resolved proteins were then transferred onto a PVDF (polyvinylidene difluoride) membrane using semi-dry Trans-Blot Turbo blotting system (Bio Rad). The PVDF membrane was blocked by incubating in 5% (v/v) non-fat dry milk, prepared in 0.1% Tween-20 TBST (Cat. J77500.K2, Alfa Aesar) for 2 h with constant shaking to mask all possible non-specific binding sites on the membrane. Following blocking, the PVDF membranes were washed with TBST (3x5') and cut into two strips of 250 to 57 kDa and 57 to 10 kDa. The membranes were probed with two different primary antibodies such as strip of 250-57 kDa was incubated with anti-β-catenin (Abcam: ab22656, predicted MW 85kDa) at 1:1,000 dilution in TBST and strip of 57 to 10kDa was incubated with the loading control anti-β-actin (Abcam: ab6276, predicted MW 42 kDa) at 1:5,000 dilution in TBST over night at 4°C. The membranes were then washed with TBST (3x5') to remove primary antibodies remain unattached with membrane and inner wall of the dish. The membranes were then incubated with appropriate HRP (horse radish peroxidase) conjugated secondary antibodies such as Peroxidase AffiniPure Donkey Anti-Mouse IgG (H+L) (JIL, cat: 715-035-151) at 1:4,000 dilution in TBST in 3.5-5% (v/v) non-fat dry milk for 2 h at RT. Following washing with TBST (3x5'), the HRP signal was detected by incubating 5 min in Bio Rad clarity Western enhanced chemiluminescence substrate (Cat: 1705061) followed by imaging using ChemiDoc imaging system (Bio Rad). The membrane bound

primary and secondary antibodies were stripped by incubating in Restore™ PLUS Western Blot Stripping Buffer (Cat. No. 46430, ThermoFisher Scientific) for 25 min at RT. Following washing twice with TBST, the membranes were blocked (described earlier) and washed. The membrane containing 250 to 57 kDa MW proteins was reprobed with nuclear protein marker antibody Anti-Lamin A (Cat. L1293; Sigma Aldrich, MW: 72 kDa) and the membrane with 57-10 kDa MW proteins was reprobed with Anti-GAPDH antibody (Table 2.10) as cytoplasmic and membrane protein marker. Subsequently the HRP signals were developed and imaged as described earlier. The protein bands were quantified using densitometry analysis using ImageJ. The value of protein bands was normalised to bands of β-actin. The following antibodies were used in protein expression analysis.

Table 2.10. The table represents a list of primary and secondary antibodies with their catalogue number, manufacturer's name and dilution rate used in the studies.

Primary antibody	Host Species type	Cat and Source	Dilution	Reason of using	References for antibodies
Anti-Androgen Receptor Antibody	Rabbit	Cat: 06-680, Merck Millipore	1:3000	AR target (Rubinfeld et al., 1993)	(Hay et al., 2014) and (Wu et al., 2014)
Anti-Androgen Receptor antibody	Rabbit	Cat: ab108341, ABCAM	1:3000	AR target	(Mutuku et al., 2019) and (Puca et al., 2018)
Anti-AR antibody (N-20)	Rabbit	Cat: Sc-816: Santa Cruz	1:250	Transactivator of AR (Simental et al., 1991)	(Sun et al., 2015) and
Anti-β Catenin antibody	Mouse	ab22656: ABCAM	1:3000	Wnt target (Rubinfeld et al., 1993)	(Hou et al., 2019)
Anti-Connexin-43 antibody	Rabbit	C6219: Sigma	1:3000	Wnt target in PC3 (Hou et al., 2019)	(Wang et al., 2017)
Anti-Cx31 antibody	Rabbit	36-5100: Invitrogen	1:1000	Connexin family (Plum et al., 2002)	(Wang et al., 2009)
Anti-PSA antibody	Rabbit	ab53774: ABCAM	1:1000	AR target (Lundwall and Lilja, 1987)	(Coleman et al., 2016)
Anti-Nkx3.1 antibody	Rabbit	Ab196020: ABCAM	1:2000	AR target (He et al., 1997)	(Leibold et al., 2020)
Anti-TMPRSS2 antibody	Rabbit	ab92323: ABCAM	1:2000	AR target (Cerveira et al., 2006)	(Ubuka et al., 2018)

Anti-c-Myc antibody		Rabbit	ab32072: ABCAM	1:1000	Wnt target in PC3 (Rennoll and Yochum, 2015)	(Han et al., 2021)
Anti-phospho-GSK-3β antibody		Rabbit	9331S: CST	1:1000	Wnt signalling protein (Amit et al., 2002)	(Wang et al., 2020)
Anti-Lamin A (C-terminal) antibody		Rabbit	L1293: Sigma	1:5000	Nuclear protein marker	(Toko et al., 2014)
Anti-β actin antibody		Mouse	Ab6276: ABCAM	1:5000	Loading control	(Yao et al., 2020)
Anti-GAPDH antibody		Rabbit	ab181602: ABCAM	1:3000	Loading control	(Ye et al., 2021)
Secondary antibody	Peroxidase AffiniPure Donkey Anti-Mouse IgG (H+L)	Donkey	715-035-151: Jackson Immunoresearch Laboratory (JIL)	1:5000	Secondary antibody Secondary antibody	(Hu et al., 2020)
	Peroxidase AffiniPure Donkey Anti-Rabbit IgG (H+L)	Donkey	711-035-152: Jackson Immunoresearch laboratory (JIL)	1:5000	Secondary antibody	(Molinari et al., 2021)

2.3.5. Co-Immunoprecipitation (Co-IP)

Co-IP was performed to isolate β-catenin complexed with AR using Thermo ScientificTM PierceTM Co-Immunoprecipitation (Co-IP) kit according to manufacturer's protocol. Resin was washed in a spin column, provided with Co-IP kit, with 1x coupling buffer prepared with 10 µg anti-β-catenin antibody (an affinity-purified antibody) added in 180 µl of ultrapure water and 10 µl of 20x coupling buffer. The flow-through was discarded. 200 µl of Quenching buffer was added to the column and was centrifuged and flow-through was discarded. 3 µl of sodium cyanoborohydride solution was added to the column and incubated for 15 min with gentle shake or end-over-end mixing. The spin column was then placed in a collection tube and centrifuged and flow through was discarded. The resin was washed with 1x coupling buffer followed by wash six times with 150 µl wash solution and kept for co-IP.

Cells were lysed using ice-cold 500 µl IP Lysis/Wash buffer by incubating on ice for 5 min with periodic mixing followed by centrifugation at ~13000x*g* for 10 min. The supernatant was

collected, and protein was quantified using the Thermo ScientificTM PierceTM BCA protein assay kit (cat: 23225) assay.

80 µl of the control agarose resin slurry was added to 1mg of lysate then added into a spin column followed by centrifugation to remove the storage buffer. 100 µl of 1x coupling buffer was added to the column and was centrifuged and flow-through was discarded. 1 mg of lysate containing resin was added to the column and incubated over night at 4°C with gentle end-over-end mixing. Then centrifugation was performed at 1000x*g* for 1 min and flow-through was collected. The antibody-couple resin was washed before adding the precleared lysate. Then precleared lysate was added to the column containing antibody-couple resin and the flow-through was discarded. The 50 µL of elution buffer was added to the column and was incubated for five min followed by centrifugation and collection of the flow-through which was used to run on SDS-PAGE.

2.3.6. Immunocytochemistry

Immunocytochemistry was conducted to investigate the subcellular migration of Wnt and AR signalling target proteins while activated with Wnt and AR signalling ligands.

2.3.6.1. Seeding, treatment and fixation of cells

PC3, AR transfected PC3 (Sec. 2.3.3.5) and LnCAP cells were grown in 8-well chamber slides (Lab Tek II, Nunc, ThermoFisher Scientific) at a density of 10,000 cells/well and incubated for approximately 3 days until the cells were reached 90% confluency. Prior treatment, old cell growth media was replaced with new fresh 500 µl of cell growth media. Cells were treated with Wnt ligands (e.g., Wnt5A and Wnt9B) and AR signalling ligand (e.g., DHT) at a working (final) concentration (Table 2.3.) and incubated for 3-4 h for PC3 and AR transfected PC3 cells) and overnight for LnCAP cells. The cells were fixed with PFA (4% Para formaldehyde). For this, cells were washed with PBS ($CaCl_2$ and $MgCl_2$ free, GIBCO) twice and incubated in 4% PFA for 15 min. Following fixation cells were washed with 3 times with ice-cold PBS. The chamber slides were wrapped with parafilm and stored at 4°C for staining.

2.3.6.2. Immunostaining of cells in ICC

Cells were washed with PBS prior to start permeabilization. The cells were permeabilized by incubation in permeabilization buffer, prepared with 0.4% Triton X-100 in PBS, for 10 min PC3 and AR transfected PC3 cells and 15 min for LnCAP cells at RT with gentle agitation. The cells were then washed with PBST wash buffer prepared with 0.01% Tween-20 in PBS. The cells were then blocked with 5% donkey serum prepared in PBST incubated for 1 hr. As the secondary antibodies were raised in donkey, donkey serum was used for blocking. Following washing with PBST, the cells were incubated with primary antibodies e.g., anti-β-catenin (Cat: ab22656, ABCAM, Dilution 1:250) for PC3 and AR transfected PC3 cells and anti-androgen receptor antibodies (Cat: 06-680, Merck Millipore, Dilution 1:250) for LnCAP cells (Table 2.10) over night at 4°C at 1:250 dilution in 1.5% donkey serum in PBST followed by washing with PBST wash buffer (3x5'). The cells were then incubated with secondary antibodies, such as Peroxidase AffiniPure Donkey Anti-Mouse IgG (H+L) (Table 2.10) was used against anti-β-catenin antibody and Peroxidase AffiniPure Donkey Anti-Rabbit IgG (H+L) was used against anti-androgen antibody. The cells were washed with PBST (3x5') in 1.5% donkey serum in PBST for 1 hr followed by washing with PBST (3x5'). The cells were incubated with tyramide Cy3 (Cat: NEL44001KT, PerkinElmer Life Science) for 10 min at room temperature. The cells were washed prior to nuclear counterstaining with DAPI. Following final wash with PBST, the chambers were removed, and cells were air dried and ProLong™ Gold Antifade Mountant (Cat. P10144, Thermo Fisher Scientific) was applied in slide before placing the cover slip on the slide. The slides were then sealed with nail polish to prevent air entry.

2.3.6.3. Confocal Imaging

The cells were imaged using a Leica SP8 laser scanning confocal microscope equipped with a 40x/1.3 NA oil objective. LAS X software was used for image acquisition in which three fields of the objects of each chamber were randomly selected based on DAPI staining. Each step size of Z-stacks for each image was 0.6 µm with 1.00 AU pinhole and 1.0 zoom. Images were captured using 10 x, 20 x, 40 x objectives and sometimes with combination of zoom function. The nuclear counterstain DAPI was excited at 405 nm and emission at 415-500 nm and the cyanine3 (Cy3) was excited at 615 nm and emission was at 575-650 nm. Sequential mode was applied for image

acquisition to avoid overlapping of channel spectra. Laser power and detector settings were kept similar across the chamber for comparison.

2.3.7. Quantitative PCR

qPCR was conducted to investigate expression of Wnt and AR signalling target proteins in PC3 and LnCAP cells upon activation with Wnt and AR signalling ligands.

2.3.7.1. Primer design

Primers for qPCR were designed using NCBI tool "Primer BLAST" (Ye et al., 2012) using the default settings against the RefSeq mRNA database for *Homo sapiens*. The Wnt target genes (e.g., *CTNNB1* and *GJA1*) *and* AR target genes (e.g., *Nkx3.1*, *TMPRSS2 and AR)* and housekeeping gene (e.g., *ACTB*) were targeted for AR and Wnt signalling study. The guidelines were followed while designing primer are summarised in the following table (Table 2.11). Primers were designed and ordered from Sigma-Aldrich and resuspended in ddH_2O to 100 µM stock solutions, which were kept at −20°C. Details of primers are in Tables 2.12 below.

Table 2.11. Representation of parameter of primer design

Primer template		
Accession, gi or FASTA sequence	Reference sequence of transcript for target gene retrieved from NCBI Genbank Nucleotide database, Selection of CDS	
Primer parameters		
PCR product size	PCR product sizes: 100-200bp	
Primer melting temperature (Tm)	Minimum: 56°C, Maximum 62	
Exon/intron selection		
Exon junction span	Primer must span an exon-exon junction	
To limit the amplification, one primer of primer pair has to span an exon-exon junction		

2.3.7.2. Primers used for qPCR

Table 2.12. The table representing genes and their corresponding primers used in qPCR

Name of the genes	Sequences
CTNNB1	Forward primer: 5'- TGCTCCGCTGACCTTAAAGA-3' Reverse primer: 5'- AGAAATGGTCGAAGTGCCCC-3'
Nkx3.1	Forward primer 5'- AGAAGCACTCCTCTTTGCCG-3' Reverse primer: 5'- CCCACGCAGTACAGGTATGG-3'

GJA1	Forward Primer: 5'-CCCACACTCTTGTACCTGGC-3' Reverse Primer:5'- CCCCCTCGCATTTTCACCTT-3'
ACTB	Forward Primer: 5'- GTACGTTGCTATCCAGGCTGT-3' Reverse primer: 5'-AGGTAGTCAGTCAGGTCCCG-3'
AR	Forward Primer: 5'- TGCTCCGCTGACCTTAAAGA-3' Reverse Primer: 5'- AGAAATGGTCGAAGTGCCCC-3'
TMPRSS2	Forward primer:5'-ACCATGGATACCAACCGGAA-3' Reverse primer: 5'-CTGTCCCGGATGGGGATTTG-3'

2.3.7.3. RNA extraction

RNA was extracted from PC3 and LnCAP cells (±)Wnt9B and (±)DHT. Cells were grown in 25 cm^2 flask. Once the cells were reached 90% confluency, the cells were treated with Wnt (e.g., Wnt9B) and AR signalling ligand (e.g., DHT) at working concentration (Table 2.3) and incubated for 4 h (PC3 cells) and overnight (LnCAP cells). For cell harvesting, 3 ml of versine were added in the flask and incubated at 37°C for 5 min to detach the cells from the surface. Once the cells were dislodged, 4 ml of cell growth media (RPMI 1640) was added into the flask to neutralize the activity of versine. The cells were collected in 15 ml falcon tube and centrifuge at 200x*g* for 2 min (Eppendorf benchtop 5424 centrifuge). The pellet was washed with ice cold PBS three times. Total RNA was purified with the RNeasy Plus kit (Cat. 74104 Qiagen) following the manufacturer's protocol; an additional step using gDNA eliminator column (Qiagen) was included to eliminate the genomic DNA impurities from the lysates. Total RNA was eluted in 30 µl of RNAse free water. The quality and concentration of the samples was measured using Nanodrop. RNA was stored at -20°C prior to convert into cDNA or place at -80°C for long term storage.

2.3.7.4. Reverse transcription

The total RNA was reverse transcribed to cDNA using QuantiTect® Reverse Transcription kit (Cat: 205311, Qiagen) following the manufacturer's protocol. The protocol included two steps.
1. Genomic DNA elimination reaction, 2. Reverse-transcription reaction.

1. Genomic DNA elimination reaction: The template RNA and gDNA wipeout buffer were thawed on ice. Genomic DNA elimination reaction was prepared on ice in 14 µl volume which composed of template RNA 1 µg, gDNA Wipeout buffer (7x) 2 µl with final concentration 1x and variable

amount of RNAse free water. The reaction mixture was incubated at 42°C for 2 min and then immediately placed on ice.

2. Reverse-transcription reaction: The reverse-transcription master mix was prepared in a RNAse free centrifuge tube in which 1 µl of Quantiscript reverse transcriptase, 4 µl of quantiscript RT buffer and 1 µl of RT primer mix and entire content (14 µl) genomic reaction sample were added. The entire mix was incubated for 15 min at 42°C followed by further incubation for 3 min at 95°C to inactivate quantiscript reverse transcriptase. The reverse transcription reaction mix was stored at -20°C for long term storage.

2.3.7.5. qPCR (Quantitative Polymerase Chain Reaction)

qPCR reactions were prepared in 384-well PCR plates (Bio-Rad, Cat. HSP- 3841) using the SYBR-Green PCR master mix (Applied Biosystems). For Wnt and AR signalling pathway investigation, each 10 µl reaction mixture consisted of: 5 µl SYBR-Green master mix, 1 µl of a 1:40 dilution of the cDNA in nuclease-free water, 1.25 µl of the primer pair (to a final concentration of 250 nM each), and 2.75 µl nuclease-free water; each sample was run in triplicate. The reaction was made of 5 µl SYBR-Green master mix, 2 µl of a 3:40 dilution of the cDNA in ddH_2O, 1.75 µl of the primer pair (to a final concentration of 350 nM each), and 1.25 µl ddH_2O; each sample was run in duplicate. qPCR was performed using a Bio-Rad CFX384 thermocycler; the RT-PCR thermal cycler parameters were the following: initial denaturation at 95°C for 1 min; 40×cycles of denaturation at 95°C for 15 s and annealing/extension at 60°C for 1 min; final extension at 65°C for 1 min; and 60 melting curve reads off, from 65 to 95°C (0.5°C per cycle). Expression levels of the genes of interest were normalised to *ACTB* using the $2^{-\Delta\Delta Cq}$ method (Livak and Schmittgen, 2001), and melting curves were analysed with Bio-Rad CFX Manager to verify products. Specific methods relating to results chapter are included in those chapters.

CHAPTER III

Analysis of in situ expression of Wnt, AR and Connexin signalling proteins in low- and high-grade human prostate cancer tissue

3.1. Introduction

3.1.1. Gleason Grading in Prostate cancer

This has been discussed in detail in Chapter I (Sec. 1.9). A brief reiteration is given here for contextualizing the results presented in this chapter.

Gleason grading is a useful predictor of prostate cancer prognosis (Gleason, 1992). The Gleason grading system utilizes the histological pattern of cells in H&E-stained sections of prostate tissue. The Gleason Score (GS) is the sum of the primary and secondary patterns with a range of 2 to 10. Aggressive disease is associated with higher Gleason sum scores. It has been reported that patients with GS $\geqq$ 7 are at risk for metastasis and biochemical recurrence; other studies have demonstrated that the prognosis of GS7 cancer varies considerably. Since its inception, GS was systematically changed to Gleason grading system based on needle biopsy (Epstein et al., 2005). Based on data obtained from 7869 patients (Epstein et al., 2005), that underwent radical prostatectomy at The Johns Hopkins Hospital, proposed a new grading system, by modification of Gleason score system; this new system is composed of 5 Grade groups. A study of 20,845 patients, distinct biochemical recurrence-free survival was observed between different grade groups (Epstein et al., 2005 and Epstein et al., 2016b). Based on radical prostatectomy, the 5 years biochemical risk-free survival for the 5 Grade Groups were 96%, 88%, 63%, 48% and 26%.

The 5 Grade Groups were also predictive for biopsy grade followed by radical prostatectomy or radiation therapy (Epstein et al., 2016b). Grade Group 1 (Gleason score 3+3=6) is homogenous and consists of individual discrete glands with an excellent prognosis. The tissue is supposed to be well differentiated and the cancer predicted to be less aggressive. A patient with Gleason score 6 does not, generally, show distant metastasis and prostate specific mortality and disease progression risk is very low (Hernandez et al., 2008). Grade Group 2 (Gleason score 3+4=7): The tissue sample is moderately differentiated and moderately aggressive. The patient has predominantly well-formed glands with lesser component of poorly formed/fused glands. Most of the cells appear similar to normal prostate cells and the cancer seems to grow slowly. Grade Group 3: This group includes the patients with Gleason score 4+3=7 with poorly

formed/fused/cribriform glands with a lesser component of well-formed glands (Epstein et al., 2016b and Amin et al., 2011). D'Amico and his colleagues showed Gleason score 7 within the intermediate risk category without recognizing the distinction between 3+4=7 and 4+3=7 (D'Amico et al., 1998). Grade Group 4 (Gleason score 4+4=8): The cells look abnormal and poorly differentiated or undifferentiated. The cancer may grow quickly and/or at moderate rate. Grade Group 5 (Gleason score 9 4+5 or 5+4=9 and 5+5=10): The cells look very abnormal, poorly differentiated or undifferentiated, highly aggressive and grow faster and spread to other organs (D'Amico et al., 1998).

3.1.2. Cellular localization of the Androgen Receptor (AR)

The eponymous AR signalling transducer, AR plays a key role in prostate development and continues to be expressed in secretory epithelia, which is thought to be transformed into prostate adenocarcinoma (De Marzo et al., 1998). AR is expressed in primary prostate cancer and can be observed through its progression (different Gleason grade) to hormone dependent PCa (Sadi et al., 1991 and Schatzl et al., 2002).

AR is nuclear receptor, localized in the cytoplasm and plays a central role in prostate cancer development and progression (Feldman and Feldman, 2001). AR is activated by androgens by binding to its ligand-binding domain (LBD) and moves into the nucleus where it accesses and regulates androgen-responsive genes (e.g., *KLK3* (PSA), *KLK2*, and *NKX3-1*) for growth and proliferation of prostate tissues (Georget et al., 1997 and Roy et al., 2001).

The expression of AR protein is higher in tumour than normal prostate and (Lekshmy and Prema, 2019) reported that AR expression shows nuclear immunoreactivity in benign and malignant epithelium. It has been noted that the AR positive cells are heterogeneously distributed within the tumour. Other studies reported similar findings (Sadi et al., 1991 and Takeda et al., 1991). Lekshmy and Prema also showed that AR expression has a negative correlation with Gleason score, indicating that with increasing Gleason scores, AR expression decreases (Lekshmy and Prema, 2019). Differentiated tumours were found to have a high percentage of AR stained cells and visually high staining intensity when compared with moderately and poorly differentiated tumours; similar results were reported by Miyamoto et al. and Takeda et al. (Miyamoto et al.,

1993 and Takeda et al., 1996). Husain et al. showed that the intensity of AR staining increased in well-differentiated tumours and was less in moderately to poorly differentiated tumours (Husain et al., 2016). These results were in agreement with the findings of (Theodoropoulos et al., 2005; Miyamoto et al., 1993 and Takeda et al., 1996). However, the opposite result was reported by e.g., Henshall et al. (Henshall et al., 2001). These studies reported that a higher AR expression was associated with high Gleason score. There thus appears to be controversy about AR expression in prostate cancer.

3.1.3. The Wnt signalling pathway

Another cell signalling pathway which is known to be important in prostate cancer, in addition to AR signalling activation, is the Wnt signalling network (Schaeffer et al., 2008). This has been discussed in detail in Chapter I.

β-catenin is a major transducer of Wnt signalling (Klaus and Birchmeier, 2008). Wnt/β-catenin signalling has been implicated in both normal prostate development and in PCa progression (Yu et al., 2009) , however, it also plays a major role in cellular adhesion (Bullions and Levine, 1998). The mechanism of Wnt signalling has been described in detail in Chap-I, Sec. 1.12 where β-catenin stabilization and its nuclear translocation is a major milestone in the signal transduction which involves numerous protein complexing (destruction complex) and phosphorylation events.

The pool of β-catenin at the plasma membrane is protected from degradation by its interaction with cadherins. Several investigations have reported that dysregulation of β-catenin is implicated in the pathogenesis of a number of human cancer (Bullions and Levine, 1998). In some cases, Wnt signalling plays a role in carcinogenesis through mutations in the CTNNB1 (β-catenin) gene itself (Morin et al., 1997). Thus, mutations in either APC or β-catenin interrupt β-catenin protein degradation, leading to abnormal, excessive, accumulation in the cytosol and nuclear translocation and gene transcription that includes proto-oncogenes (such as *c-MYC* and *FRA1* amongst others).

In the nucleus, β-catenin interacts with the member of T-cell transcription factors to express downstream target genes which are crucial for neoplastic transformation (Fearon, 1997). A number of investigations have demonstrated that abnormal levels of β-catenin is expressed in

23% of the tumour samples obtained from radical prostatectomy and correlated with high Gleason score and in early-stage cancers (Chesire et al., 2000). Other studies have shown that β-catenin expression is higher in prostate cancer patients with high Gleason score sum (8 or 9) than patients with Gleason score sum 7 or less. No significant difference in β-catenin expression between cases with ≥7 and <7 (Arslan et al., 2020).

3.1.4. Wnt signalling related proteins

The multifunctional membrane and cytosolic protein, β-catenin is associated with cytoplasmic domain of E-cadherin for the functioning of intercellular adhesion complexes (Davies et al., 2001). β-catenin expression and localization are thought to become nuclear during prostate cancer progression (Hayashida et al., 2005). TCF-1 isoform supresses Wnt target gene expression by interacting with Groucho/transducin like enhancer of split (Gro/TLE) corepressor (Cavallo et al., 1998). But accumulation of β-catenin in nucleus promote interaction with TCF/LEF to activate transcription of Wnt signalling target genes.

The expression of FRA-1, target of Wnt mediated gene transcription, is known to be upregulated in animal cancer (Arthurs et al., 2020 and Arya et al., 2015) but little information on the *in situ* expression of FRA1 exists in human cancers, particularly, in prostate cancer.

Another Wnt signalling related protein is Pygopus (Pygo) which was discovered as component of Wnt signalling that is essential for the transcriptional activity of Armadillo (of which β-catenin is a human orthologue) during Drosophila development (Kramps et al., 2002). In vertebrates two Pygo orthologues are found, which contribute to efficient β-catenin-mediated transcription during development (Belenkaya et al., 2002 and Li et al., 2007) and in cancer cell lines with high Wnt pathway activity (Kramps et al., 2002). *PYGOPUS2* (PYGO2) (an isoform of the *PYGOPUS* gene) is expressed in nucleus and remain an important component of Wnt/β-catenin transcriptional complexes and is closely related to genes active during development. The expression of PYGO2 was found to be higher in CRPC than hormone naïve PCa (Taylor et al., 2010 and Abeshouse et al., 2015) but its prognostic expression in different Gleason grade prostate cancer is yet to be determined.

3.1.5. Connexin 43 (Cx43) in PCa

Connexin 43 (Cx43) is a member of a family of transmembrane proteins to form cell-to-cell channels in gap junctions. Connexins provide direct intercellular pathway to promote signalling molecule exchange (<1kDa) and communication of adjacent cells, which plays a vital role in regulation of cell proliferation, differentiation and homoeostasis (Vinken et al., 2006). A list of members of connexin family is reviewed (Söhl and Willecke, 2004). Of particular interest here is Cx31.

Cx43 is predominantly found in undifferentiated and mature basal cells of the prostate epithelium (Habermann et al., 2001) and may act as a tumour suppressor gene (Fukushima et al., 2007). The role of Cx43 in different carcinomas (e.g., Li et al., 2008) and in prostate cancer has also been investigated (Fukushima et al., 2007). Cx43 expression in prostate cancer may decrease that may correlate to unfavourable prognosis (Benko et al., 2011). A comparative analysis of Cx43 expression assessed its role in association with clinicopathological features and biochemical recurrence of prostate cancer after radical prostatectomy. The authors concluded that: 1. expression of Cx43 was significantly reduced in prostate cancer compared to that in BPH tissues, 2. Cx43 expression was reduced with high Gleason score after radical prostatectomy (Xu et al., 2016). It was suggested that Cx43 could repress migration and invasion of tumour cell (Alexander and Goldberg, 2003). Habermann and his colleagues also suggested that Cx43 expression in prostate cancer was downregulated compared to BPH, which contributed to the de-differentiation and progression of the tumours (Habermann et al., 2001). Recently, a novel function of Cx43 was found to be related to its translocation into the nucleus with a key transducer of Wnt signalling β-catenin by (Hou et al., 2019). This raises the question whether other members of the Connexin family may be involved in intracellular Wnt signal transduction?

3.1.6. Rationale and aims for experiments in this chapter

It is clear that both AR and Wnt signalling plays a key role prostate cancer. Unfortunately, most of the studies have been conducted in cell lines and human tissue studies described above used non-quantitative methods of protein expression and small number of samples to investigate the role of Wnt signalling in prostate cancer. This is also the case, particularly for the expression of

Wnt signalling related proteins in low and high grade prostate cancer. Furthermore, there is a lack of studies that have simultaneously measured Wnt and AR signalling pathway proteins in the same set of samples using a quantitative approach. This is essential to identify the interactions between these two key carcinogenic pathways.

There is very little information on the interaction of AR and Wnt signalling in prostate cancer, particularly in human tissue. A previous study showed some interaction of AR and Wnt signalling proteins in cell lines such as PC3 (Verras et al., 2004), CWR22- Rv1 (Chesire et al., 2002), DU145 (Chesire et al., 2002) and in LnCAP cell (Sharma et al., 2013). Cx43 expression is reduced or absent in prostate cancer tissues which is vastly related to disease progression and poor prognosis (Benko et al., 2011).

Protein expression, unlike gene expression analysis, is a better indicator of change in function. I therefore rationalized that it is important to assess the expression of AR and Wnt signalling proteins in prostate tissue diagnosed for low to high Gleason grades. Based on the introduction above, I choose a combination of AR and Wnt related proteins β-catenin, FRA-1, PYGO2, TCF-1 and Cx43 to test in lower grade to higher Gleason grade PCa *in-situ*.

I have investigated and quantified the expression of AR and Wnt signalling related proteins in prostate cancer samples of: Gleason grade 3 (Gleason score 6: 3+3), Gleason grade 4 (Gleason score 7: 3+4 or 4+3) and Gleason grade 5 (Gleason score 9: 4+5 or 5+4) using tissue arrays for standardization of staining and comparison; each cancer tissue core was flanked with a cancer adjacent normal prostate tissue, identified by an expert pathologist. I have used quantitative immunohistochemistry (DAB chromogenic staining) to measure the expression of: 1. β-catenin, TCF-1, PYGO2, FRA-1 related to Wnt signalling and 2. Androgen receptor protein as a paradigm for AR signalling; I have also included 3. Cx43 which was recently found to be associated with Wnt signalling.

3.2. Aims

The overall aim was to assess the expression of AR and Wnt signalling proteins in tissue arrays comprising of normal, Gleason grade 3, 4 and 5. I, therefore, aimed to employ the unbiased, quantitative immunohistochemical approach to measure and quantify the expression of:

(i) Androgen receptor protein

(ii) β-catenin, FRA-1, PYGO2, and TCF-1 proteins

(iii) the newly discovered Wnt signalling related protein Cx43

A further aim, as a proof of concept, was to assess the utility of the expression of the above proteins as biomarkers of different grades of cancer

3.3. Methods

3.3.1. Tissue collection and designing of Tissue Array (TA)

Thirty samples (individual patients) of 15 normal prostate tissues (NPT) and 15 prostate cancer tissues of Grade 3+3 (5 samples), Grade 4+4 (5 samples) and Grade 4+5/5+4 (5 samples) were collected from Rui Henrique (Guest Professor, Department of Pathology and Molecular Immunology Abel Salazar Institute of Biomedical Sciences University of Porto). These were arrayed on different blocks termed RH16, RH17, RH18 & RHC1, for high grade and normal prostate tissue. Ideally, more samples for high grade prostate cancer would have had been used, however, at the time of these experiments these were not available. Following H&E staining, the region of interests (ROIs) was identified by the Pathologist (Chap-II, Sec. 2.3.1.3). Details of patients and sample have been provided in appendix (Appx. 2). The tissue cores on the slide were designed in a manner where cancer tissue and normal tissues samples were cored side by side on three individual TA blocks. A detailed layout of the TA is given in appendix (Appx. 2). Each of the block contained 30 cores, composed of 15 normal NPT, 5 Grade 3+3, 5 Grade 4+4 and 5 Grade 4+5/5+4. Each of cancer tissue cores on the slide was flanked by NPT.

3.3.2. Tissue array (TA) construction

Details of the TA construction have been discussed previously (Chap-II, Sec. 2.3.1.3.). Briefly, the recipient wax block was placed on the block holder and punched. Identical circular indents were made by the small (recipient) and large (donor) 3 mm deep punches. The large punch *stylate* was

used to inject the tissue core (the term 'core' is used interchangeably for tissue core) into the indented hole created by smaller punch. The diameter of core was 1mm and distance between two adjacent cores was 2.5 mm. Following construction, TA was incubated at 37°C for 30 min by applying light and even pressure to the surface of block to level the height of the cores.

3.3.3. Tissue dewaxing and antigen retrieval

The tissues were sectioned with microtome with 6 μm thickness. Details of procedure of tissue dewaxing and antigen retrieval are described in chapter 2 (Sec. 2.3.1.4. and Sec. 2.3.1.5)

3.3.4. Blocking of non-specific binding site

The tissue sections were blocked by incubating in 3% H_2O_2 menthol solution for 30 mins for endogenous peroxidase activity. Non-specific binding was blocked by incubation with 10% normal serum and 1% BSA. Details are discussed in chapter 2 (Sec. 2.3.1.6.).

3.3.5. Immunostaining of tissue arrays

AR target proteins (e.g., AR) and Wnt target proteins (e.g., FRA-1, β-catenin, PYGO2, TCF-1 and c-MYC) were investigated in NPT, Grade 3+3, Grade 4+4 and Grade 4+4. A total of 30 cores, consist of 15 cores from NPT (n=15), 5 cores from Grade 3+3 (n=5), 5 cores from Grade 4+4 (n=5) and 5 cores from Grade 4+5/5+4 (n=5) were distributed on a slide termed RH16. Two repeat slides with distinct layout were also constructed (RH17 and RH18). Layout of cores on the slide is discussed in appendix (Appx. 2). The tissue cores were stained using automated Bond immunohistochemical system (Leica Biosystem), conducted by Mike Millar, The Queens Medical Research Institute, University of Edinburgh for staining with automated Bond immunohistochemical system (Leica Biosystem). Six antibodies (Table 3.1) were used in the staining procedure. Name of the antibody, dilution rate and manufacturer names are given the following table (Table 3.1). The experiments were conducted in a double blind manner and neither the experimenter nor the analyser were aware of the identity of the antibodies nor the tissue type until all the quantitative analysis was completed.

Table 3.1. A list of six antibodies, their hosts and dilution used in chromogenic technique

Primary antibody		Host	Catalogue no. and Manufacturer	Dilution	Cores on the slide were Stained
Anti-β-Catenin antibody		Mouse	Ab22656, ABCAM	1: 200	RH16, RH17, RH18 & RHC1
Anti-FRA-1 antibody		Rabbit	ab252421, ABCAM	1:1000	RH16, RH17, RH18 & RHC1
Anti-TCF-1 antibody		Rabbit	2203S, Cell signalling technology	1:100	RH16, RH17, RH18 & RHC1
Anti-PYGO2 antibody		Rabbit	ab99274, ABCAM	1:200	RH16, RH17, RH18 & RHC1
Anti-AR antibody		Rabbit	Ab133273, ABCAM	1:400	RH16, RH17, RH18 & RHC1
Ani-Cx43 antibody		Rabbit	C6219: Sigma	1:1000	RH16, RH17, RH18 & RHC1
Secondary antibody	Peroxidase AffiniPure Donkey Anti-Mouse IgG (H+L)	Donkey	715-035-151, Jackson Immunoresearch Laboratory (JIL)	1:500	Used against Ant-mouse primary antibody
	Peroxidase AffiniPure Donkey Anti-Rabbit IgG (H+L)	Donkey	711-035-152, Jackson Immunoresearch laboratory (JIL)	1:500	Used against Anti-rabbit primary antibodies

Anti-β-catenin, -FRA-1, -TCF-1, -PYGO2, -AR and -Cx43 antibodies (Table 3.1) were used for DAB staining using Bond automated systems according to manufacturer's protocol. Briefly, following xylene deparaffinisation and EtOH incubation, the tissues were hydrated with water. The tissue cores were incubated in 0.6% H_2O_2 in methanol for 15 min followed by washing with PBS. The tissues were blocked with primary antibodies (Table 3.1) at the corresponding dilution. The TA slides were washed with PBS and incubated in secondary antibodies (Table 3.1). Following washing with PBS, the TA slide was incubated in chromogenic buffer (DAB) and co-inter-stained with haematoxylin. The tissue sections were dried and rehydrated with a serial dilution of EtOH and water respectively. Slides were left in xylene until they were cover slipped. The slides were mounted, and coverslips were remained until harden.

3.3.6. Imaging and signal quantitation and statistical analysis

The tissue cores were scanned with NanoZoomer-RS Scanner (Type: C10730-02) with resolution 0.23µm/pixel (40x high resolution mode) using. The images were opened using NDP.view 2.3 software.

Anti-β-Catenin, -FRA-1, -TCF-1, -PYGO2, -AR and -Cx43 antibody-labelled DAB-stained cores were scanned using using NanoZoomer-RS Scanner (Type: C10730-02) with resolution 0.23µm/pixel

(40x high resolution mode) (Hamamatsu Photonics UK Ltd, Welwyn Garden City, UK) and the image of an individual core was segregated and compiled and indexed according to the configuration of TA (Appx. 2). A semi-automated and unbiased quantitative method, ImageJ software (Schneider et al., 2012) where an algorithm developed in our lab was incorporated (Arya et al., 2015 and Symes et al., 2013). DAB stain (brown) on the tissue core was segmented on hue, saturation and brightness. Area containing tissue were identified on the duplicate image by conversion to 8-bit and application of a threshold. Only measure pixel that are not the same intensity as the background. Thresholds were optimised on a practical set of images before being. Applied to the whole image set for standardization of quantitation. A macro was compiled for an unbiased quantitation to measure both the amount of DAB signal and the amount of tissue. Area of folded tissue was fitted to a probit regression (AFperAMT).

3.3.7. Statistical analysis

Further statistical analysis was performed of median of observations using Mann Whitney U test (* $P<0.05$, ** $P<0.01$, *** $P<0.001$) to calculate the significance of difference of expression of AR, β-catenin, FRA-1, PYGO, TCF-1 and Cx43 in Grade 3+3, Grade 4+4 and Grade 4+5/5+4 compared to NPT. GraphPad Prism, version 8.0.0 (GraphPad Software, San Diego, California. USA) was used to construct box and mountain plot and for AUC calculation for ROC.

3.4. Results

3.4.1. Characterisation of normal, Grade 3+3, Grade 4+4 and Grade 4+5/5+5 PCa tissue cores

Two sets of pathological analysis were conducted. Firstly, whole tissue blocks were marked by a pathologist prior to coring and adding these on the TA block; secondly, the H&E image of TA was re-analysed by the pathologist for confirmation of diagnosis of each core. Following staining with H&E, the TA slides were imaged using NanoZoomer-RS Scanner (Type: C10730-02) with resolution 0.23µm/pixel 40x high resolution mode (Fig. 3.1). The normal prostate tissue (NPT) cores were identified with the help of the pathologist observing morphologically distinct, well organised epithelial layer containing luminal cells and basal cells (Szczyrba et al., 2017). The Grade 3+3 was characterised with developed well-differentiated glands, which are separated by stroma. The glands appear close to each other with minimum amount of intervening stroma

(Roehrborn, 2008). The glands are lined by columnar neoplastic cells, but lacking a layer of basal cells. The Grade 4+4 was identified by observing abnormal and poorly differentiated or undifferentiated. The cancer may grow quickly and/or at moderate rate. Grade 4+5/5+4 group includes the patients with Gleason score 9 (4+5 or 5+4=9) and 10 (5+5). The cells look very abnormal, poorly differentiated or undifferentiated, highly aggressive and grow faster and spread to others organ (D'Amico et al., 1998).

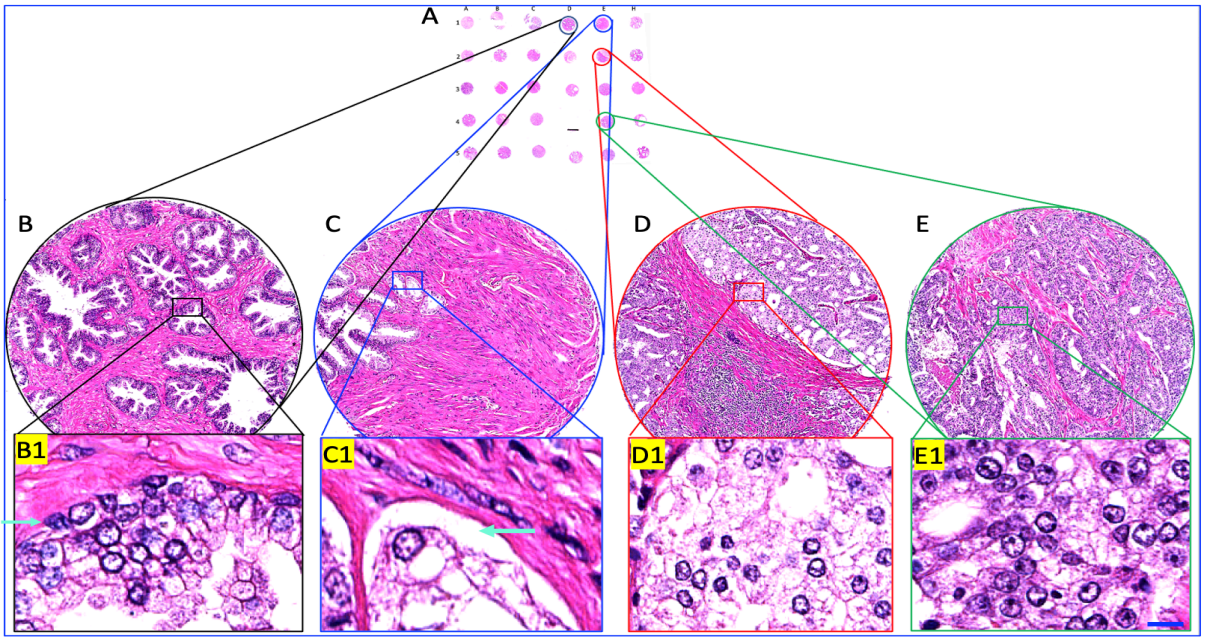

Figure 3.1 Representative images of H&E stained prostate tissue cores of normal, Grade 3+3, Grade 4+4 and Grade 4+5/5+4 PCa tissues. (A) A scanned image of a tissue array on slide composed of normal prostate tissue PCa tissues of Grade 3+3, Grade 4+4 and Grade 4+5/5+4. The 20x zoomed image of individual tissue core B, C, D and E displays prognosis of carcinoma of normal prostate tissue, Grade 3+3, Grade 4+4 and Grade 4+5/5+4 PCa tissue core respectively. 40x zoomed (cropped) image B1, C1, D1 and E1 at the bottom row displaying stratification of epithelial layer of gland. Scale bar: 10µm.

3.4.2. Expression analysis of AR, β-catenin, FRA-1, PYGO2, TCF-1 and Cx43 in Grade 3+3, Grade 4+4 and Grade 4+5/5+4 compared to normal prostate tissue (NPT)

NPT, Grade 3+3, Grade 4+4 and Grade 4+5/5+4 PCa tissues cores on slide RH16 RH17 and RH18 stained with six different antibodies, individually, (Table 3.1) for the analysis of AR, β-catenin, FRA-1, PYGO2, TCF-1 and Cx43 protein expression. For expression analysis of each protein, the antibody-stained core image was cropped out (segregated) representative images are shown in Fig. 3.2 and Fig.3.3. The representative core for AR expression in Fig. 3.2.A (A1: 20X magnification)

indicated higher expression in epithelial layer of glandular in NPT than in Grade 3+3, Grade 4+4 and Grade 4+5/5+4 showed in Fig. 3.2.B-D (B1-D1: 20x magnification) respectively. Staining for β-catenin expression in Grade 4+5/5+4 (Fig. 3.2.H; H2: 20x magnification) was observed darker than in NPT (Fig. 3.2.E; E1:20x magnification), Grade 3+3 (Fig. 3.2.F; F1: 20x magnification), Grade 4+4 (Fig. 3.2.G; G1:20x magnification). Staining of FRA-1 showed higher expression in Grade 3+3 (Fig. 3.2.J; J1: 20x magnification), Grade 4+4 (Fig. 3.2.K; K1: 20x magnification), Grade 4+4/5+4 (Fig. 3.2.L; L1: 20x magnification) than in NPT (Fig. 3.2.I; I1: 20x magnification). Staining with PYGO2 antibody indicated higher expression of PYGO2 in Grade 4+5/5+4 (Fig. 3.3.D; D2: 20x magnification) than in NPT (Fig. 3.3.A; A2:20x magnification), in Grade 3+3 (Fig. 3.3.B; B2: 20x magnification), in Garde 4+4 (Fig. 3.3.C; C2: 20x magnification). TCF-1 showed higher expression in Grade 4+5/5+4 (Fig. 3.3.H; H: 20x magnification) than in NPT, Grade 3+3 and Grade 4+4 showed in (Fig. 3.3.A-C; E1-G1: 20x magnification). Antibody staining for Cx43 showed darker staining in NPT. Expression of Cx43 showed higher expression in NPT (Fig. 3.3.I; I:20x magnification) than in Grade 3+3, Grade 4+4 and Grade 4+5/5+4 showed in Fig. 3.3.J-L; J1-L1:20x magnification.

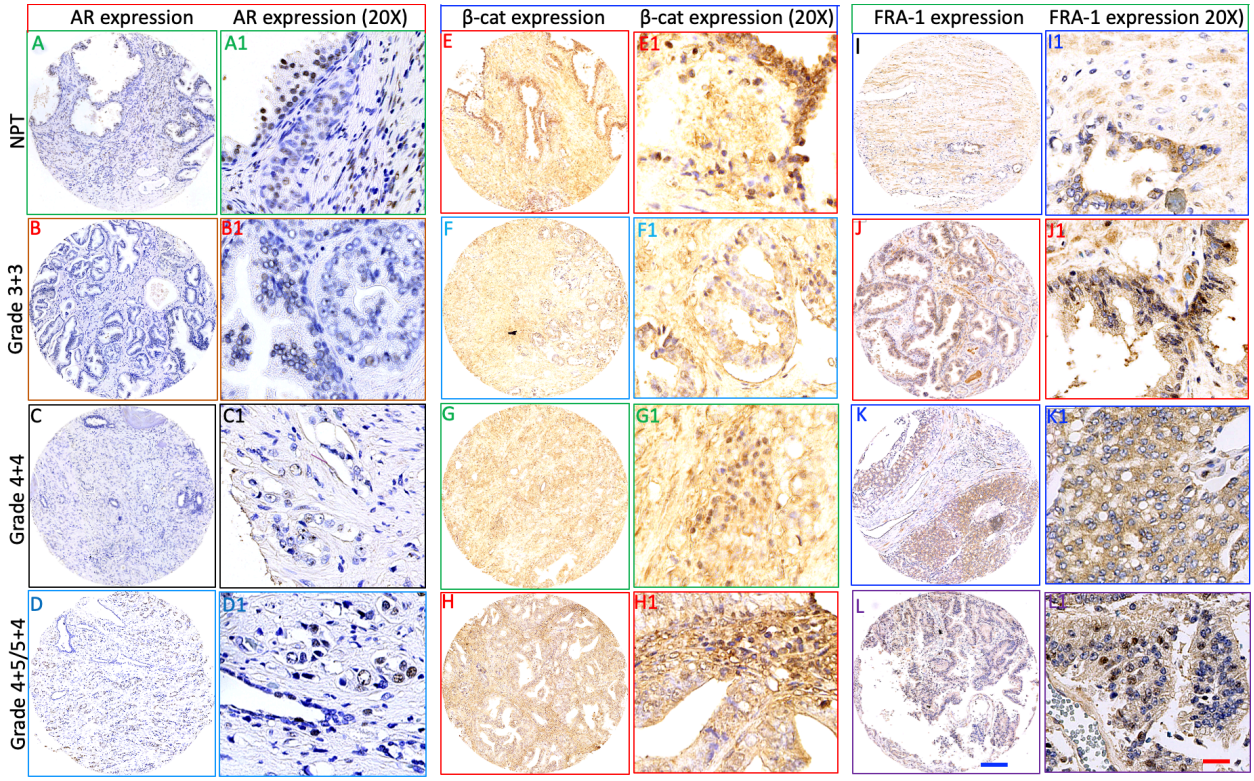

Figure 3.2. Representation of anti-AR, -β-catenin and -FRA-1 antibody-stained NPT, Grade 3+3, Grade 4+4 and Grade 4+5/5+4 PCa tissue core with magnified images. A-D representing AR expression in NPT, Grade 3+3, Grade 4+4 and Grade 4+5/5+4, and their corresponding magnified images indicated with A1-D1 respectively. E-H representing β-

catenin expression in NPT, Grade 3+3, Grade 4+4 and Grade 4+5/5+4, and their corresponding magnified images indicated with E1-H1 respectively; in high grade cancer the nuclear AR and β-catenin staining is also visible (G1 and H1). I-L representing FRA-1 expression in NPT, Grade 3+3, Grade 4+4 and Grade 4+5/5+4, and their corresponding magnified images indicated with I1-L1 respectively.

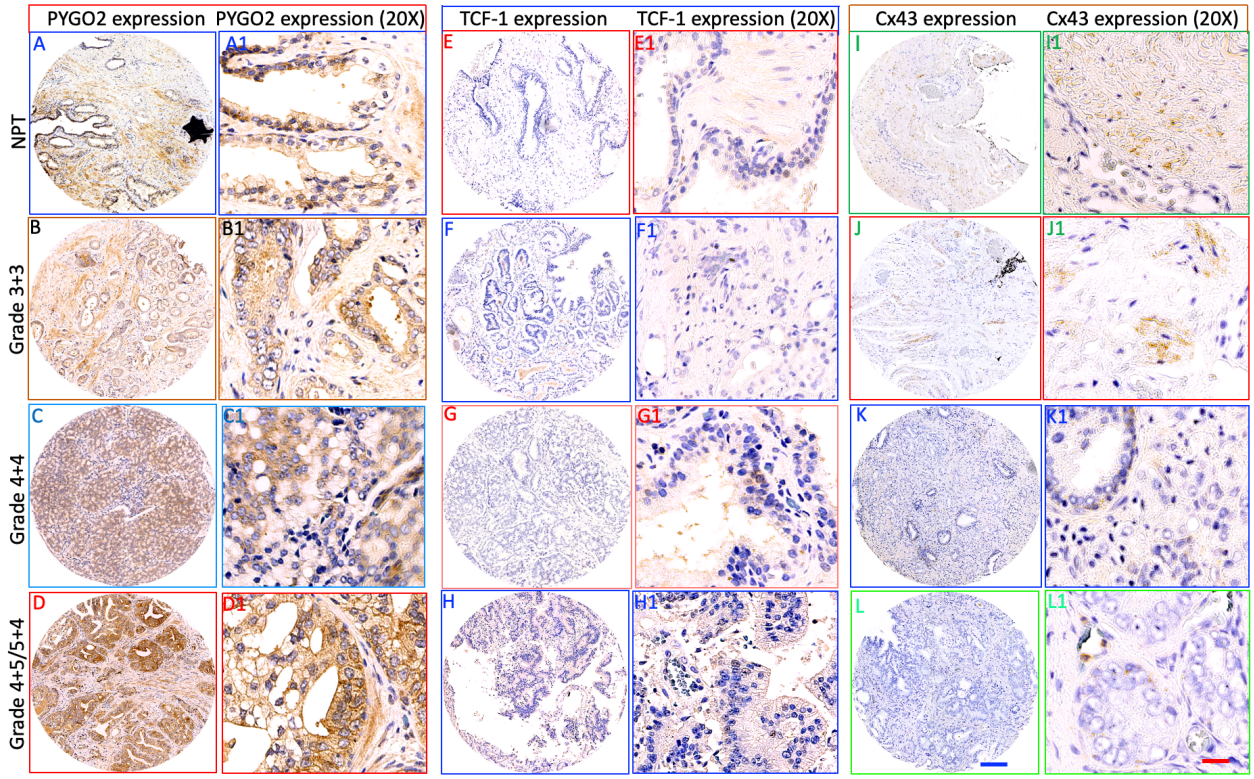

Figure 3.3. Representation of anti-PYGO2, -TCF-1 and -Cx43 antibody-stained NPT, Grade 3+3, Grade 4+4 and Grade 4+5/5+4 PCa tissue core with magnified images. A-D representing PYGO2 expression in NPT, Grade 3+3, Grade 4+4 and Grade 4+5/5+4, and their corresponding magnified images indicated with A1-D1 respectively. E-H representing TCF-1 expression in NPT, Grade 3+3, Grade 4+4 and Grade 4+5/5+4, and their corresponding magnified images indicated with E1-H1 respectively. I-L representing Cx43 expression in NPT, Grade 3+3, Grade 4+4 and Grade 4+5/5+4, and their corresponding magnified images indicated with I1-L1 respectively. Nuclear expression of the transcription factor PYGO2 and TCF1 is also visible in D1 and H1.

The images of each antibody for NPT, Grade 3+3, Grade 4+4 and Grade 4+5/5+4 were used to analyse the expression of AR, β-catenin, FRA-1, PYGO2, TCF-1 and Cx43 using ImageJ (Chap-II, Sec. 2.3.1.8.1) followed by calculation of significance of differences using Mann Whitney U test. The next six sections showed the analysis of these proteins.

3.4.3. Analysis of expression of AR, Wnt and Connexin target proteins in NPT, Grade 3+3, Grade 4+4, Grade 4+5/5+4 PCa tissue

The tissue cores were probed with antibodies against AR, β-catenin, FRA-1, PYGO2, TCF-1 and Cx43 and stained with DAB-HRP in normal prostate tissue (NPT), Grade 3+3, Grade 4+4 and Grade 4+5/5+4. A total 30 samples of NPT (n=15), Grade 3+3 (n=5), Grade 4+4 (n=5) and Grade 4+5/5+4 (n=5) distrbuted on three slides (Appx. 2) were used on each TA slide. Layout of the cores on the slide is given in appendix (Appx. 2)

Anti-AR, -β-Catenin, -FRA-1, -PYGO2, -TCF-1 and -Cx43 antibody-labelled DAB-stained cores were scanned using NanoZoomer-RS Scanner Hamamatsu Photonics UK Ltd, Welwyn Garden City, UK) as described above, and the images of individual cores were segregated and compiled and indexed according to the configuration of TA (Appx. 2). Details of the quantitative analysis have been described above and in an earlier chapter (Chap II, Sec. 2.3.1.8.1).

To investigate the utility of these proteins as putative biomarkers for prostate cancer, the true positive rate (sensitivity) and false positive rate (1-specificity) were calculated from the data used for the ROC curve (Fig. 3.10 and Fig. 3.11). The AF/AT data were converted into probit and fitted to a Gaussian function. The AUC values of 1.0 for an ROC imply high selectivity and sensitivity, on the contrary, if the values for AUC for an ROC curve fall at or below 0.5, suggests that the tested marker does not distinguish between groups normal and different cancer Grades (NPT vs Grade 3+3, NPT vs Grade 4+4, NPT vs Grade 4+5/5+4). Positive likelihood ratio (LR+) for each biomarker was calculated to find if each of the protein is correlated with the presence of disease. A LR+ ratios over 1.0 suggest that the result for which protein is associated with the presence of disease (Altman and Deeks, 2004). LR+ values for each protein were found at AUC value.

3.4.3.1. Expression of AR in NPT, Grade 3+3, Grade 4+4 and Grade 4+5/5+4 PCa tissues

This is the first time that lower to high grade prostate cancer tissues were used to measure AR expression using a semiautomated and reproducible technique. For this investigation, anti-AR antibody (ab22656, ABCAM) was used to stain the tissues using DAB-HRP chromogenic technique (For detail: Chapter 2, Sec. 2.3.1.8.1). Following quantitation, the data were used to create

mountain plot and ROC curve by GraphPad prism and calculation of significance of difference performed by Mann-Whitney U test.

A representative image for the expression of AR in normal and PCa tissue is shown in Fig. 3.4. The results show there were expression of AR in NPT (Fig. 3.4.A); but expression was decreased in Grade 4+4 and Grade 4+5/5+4 PCa (Fig. 3.4.C and D).

The corresponding masked images for ImageJ analysis are shown in Fig. 3.4. A2-D2 . These images were used to quantify the pixel intensity for the DAB signal for AR expression. The converted images (Fig. 3.4.A2-D2) show the pixel intensity quantified to construct the mountain plots (Fig. 3.4. B3 to D3). The tabulated data of NPT v Gleason grades is also presented in Table 3.2 and 3.3. The result showed that expression of AR in Grade 3+3 was decreased (-1.30± 0.84) but not significantly different (ns) (Table 3.2) (Fig. 3.4.B3). The AUC value for ROC was found as 0.70 (ns) (Fig. 3.10). The results of fold changes showed as mean±SEM. AR expression was decreased (-1.23 ±0.46-fold) in Grade 4+4 (**P<0.01) (Fig. 3.4.C3) and AUC for ROC was 0.84 (**P<0.01) (Fig. 3.10). AR expression was also significantly decreased (-1.53 ± 0.46-fold) in Grade 4+5/5+4 (*P<0.05) (Fig. 3.4.D3). The AUC value was 0.76 (*<0.05) (Table 3.3) (Fig. 3.10). LR+ was found as 4.2, 10, 10 in Grade 3+3, Grade 4+4 and Grade 4+5/5+4. Therefore, AR presence indicate a disease state and could be considered as a putative biomarker for Grade 4+4, Grade 4+5/5+4 PCa, as has been shown using, largely, qualitative approaches, previously (Husain et al., 2016).

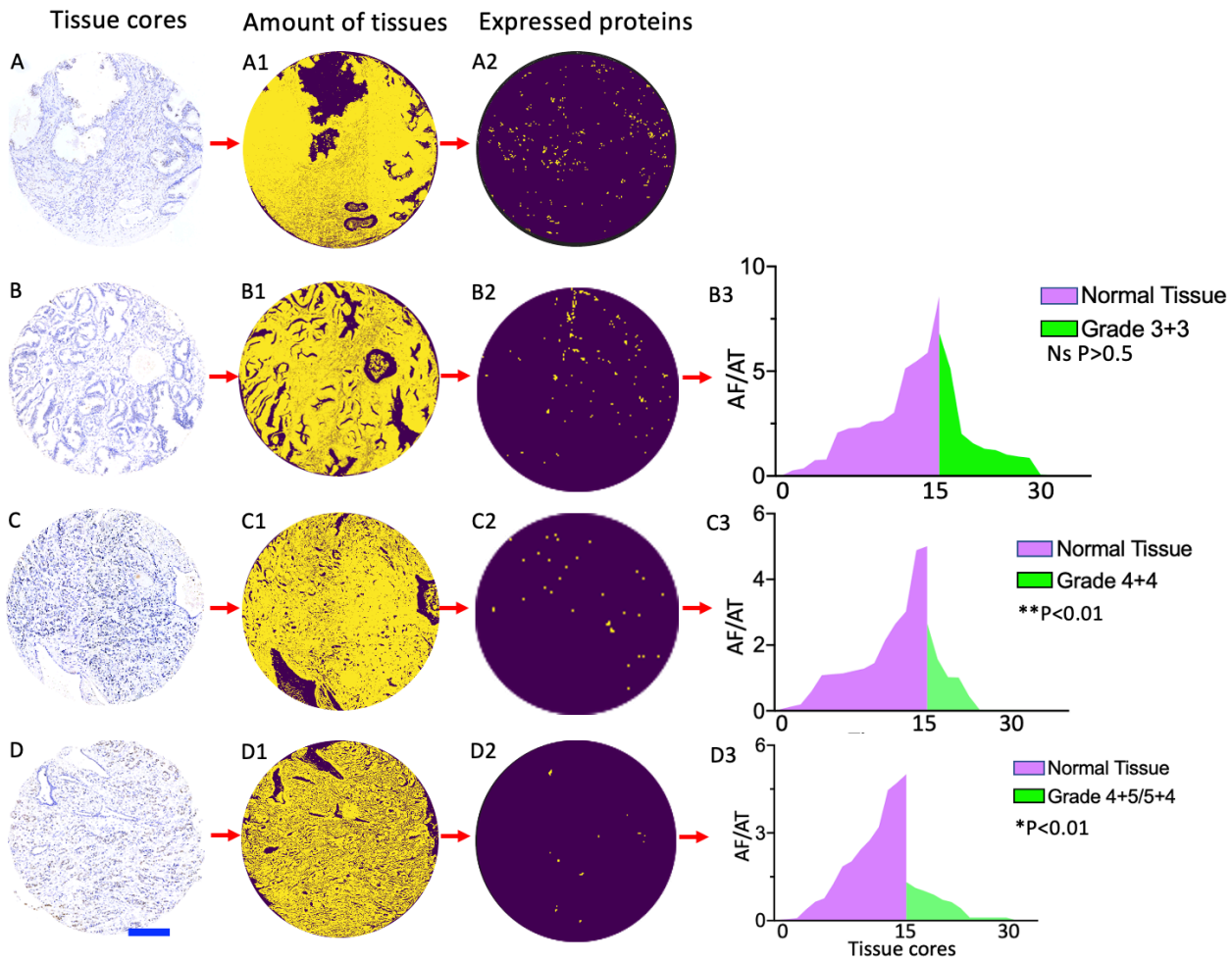

Figure 3.4. Representative images for the staining and quantitation of DAB signal for AR in normal prostate tissue, Grade 3+3, Grade 4+4 and Grade 4+5/5+4 PCa tissues. A, B, C and D representing the stained tissue cores of normal prostate tissue, Grade 3+3, Grade 4+4 and Grade 4+5/5+4 respectively. Following staining of the tissue with DAB-HRP for AR, the tissue arrays were imaged with NanoZoomer-RS Scanner (Type: C10730-02) with resolution 0.23µm/pixel (40x high resolution mode) and each of the image of cores was undertaken to measure expression of AR. An unbiased ImageJ was used to quantify protein expression (Sec. 3.3.6). The RGB coloured images A1, B1, C1 and D1 representing the amount of tissues (yellow colour) in core of A, B, C and D respectively. The coloured images were masked to obtain AR protein expression indicated in A2, B2, C2 and D2 in NPT, Grade 3+3, Grade 4+4 and Grade 4+5/5+4. The quantified data were obtained as AF per AT which were used to construct mountain plot indicated as A3, B3, C3, D3 of A2, B2, C2 and D2 respectively. Each bin is the data for an individual, normal prostate tissue (n=15) and Grade 3+3, Grade (4+4) (n=15) and Grade 4+5/5+4 (n=15) PCa tissue. Statistical analysis was performed using Mann–Whitney U test to calculate the significance of difference of AR expression in Grade 3+3 vs NPT, Grade 4+4 vs NPT, Grade 4+5/5+4 vs NPT. The analysis showed expression of AR in Grade 3+3 was remained same as in NPT. But the expression was significantly reduced in Grade 4+4 and expression was further decreased in Grade 4+4/5+4. (*P<0.05; **P<0.01). (AF: Area Fraction, AT: Amount of Tissue). Scale bar:100µm

3.4.3.2. Expression of β-catenin in NPT, Grade 3+3, Grade 4+4 and Grade 4+5/5+4 PCa tissues

β-catenin is an intracellular transducer of Wnt signalling; the expression of β-catenin was measured using anti-β-catenin antibody (ab22656, ABCAM) with DAB-HRP staining procedure in NPT, Grade 3+3, Grade 4+4, Grade 4+5/5+4. Representative images of tissue cores in Fig. 3.5., NPT (Fig. 3.5.A), Grade 3+3 (Fig. 3.5.B), Grade 4+4 (Fig. 3.5.C) and Grade 4+5/5+4 (Fig. 3.5.D) are shown. The images were used to quantify DAB signal for β-catenin expression using ImageJ are shown in Fig. 3.5. A2 -D2. The quantified data is shown in Table 3.2 and in Fig. 3.5. B3-D3. The results of fold changes showed as mean±SEM. These data show there was no significant increase in the overall expression of β-catenin expression in Grade 3+3 compared to NPT (-0.046 ± 0.33-fold) with AUC calculated from the receiver operating curve (ROC) 0.52 (ns) compared to NPT (Table 3.3). β-catenin expression was not also significantly changed in Grade 4+4 PCa (Fig.3.5.C3), with an AUC value from the ROC 0.52 (ns) compared to NPT. The expression of β-catenin in highest Grade (4+5/5+4) PCa was significantly increased (*P<0.05) with AUC value from the ROC 0.75 (*P<0.05) (Table 3.3). LR+ was: 0.92 for Grade 3+3 and 1 for Grade 4+4 and Grade 4+5/5+4. These results suggest that Wnt/β-catenin signalling may play a key role in progression of PCa as its expression, compared to NPT is increased in highest grade cancer. This is a first report of quantitative, *in situ* expression of β-catenin in human PCa tissue of different grades.

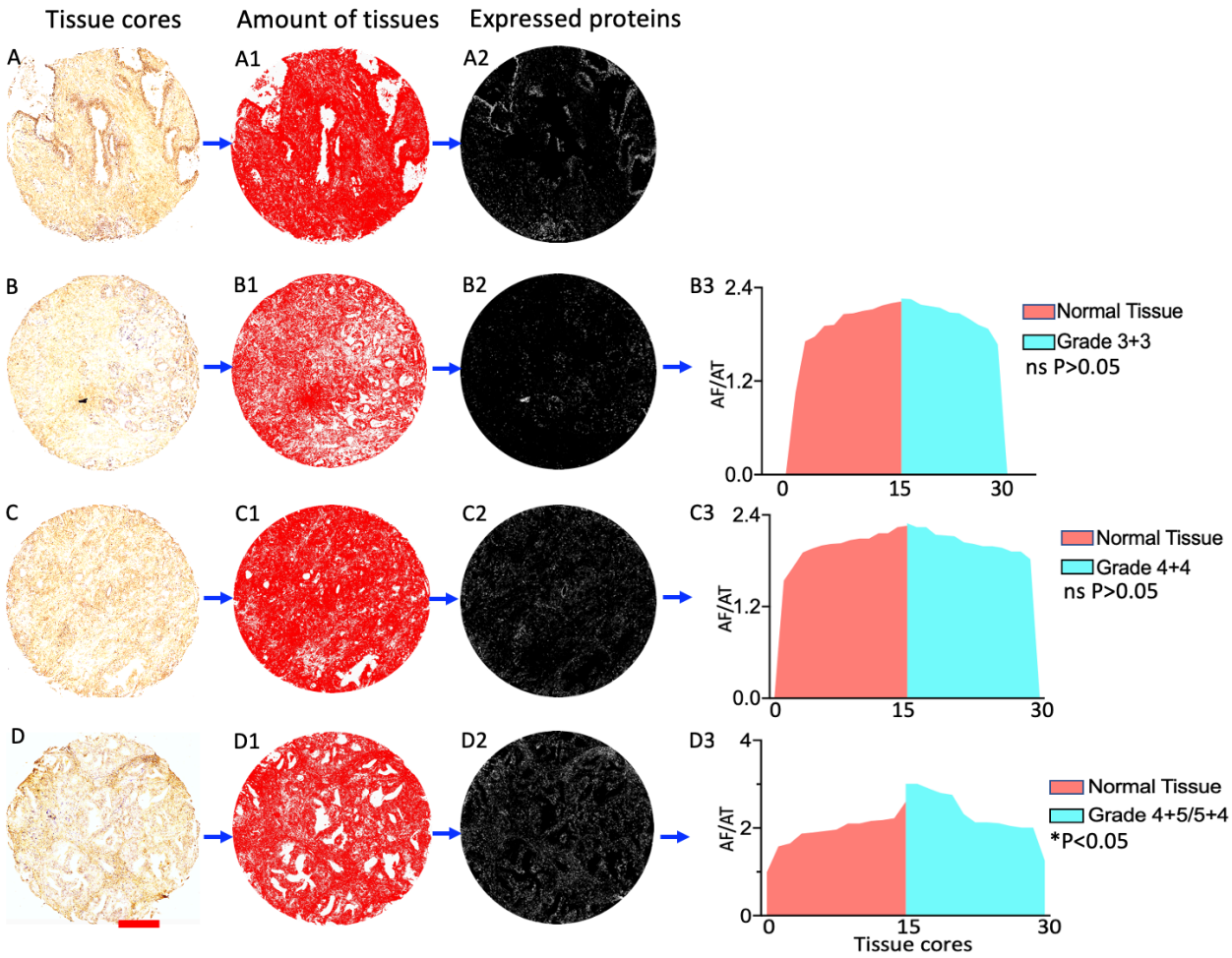

Figure 3.5. Representative images for the staining and quantitation of DAB signal for β-catenin in normal prostate tissue, Grade 3+3, Grade 4+4 and Grade 4+5/5+4 PCa tissues. A, B, C and D representing the stained tissue cores of normal prostate tissue, Grade 3+3, Grade 4+4 and Grade 4+5/5+4 respectively. Following staining of the tissue with DAB-HRP for β-catenin, the tissue arrays were imaged with NanoZoomer-RS Scanner (Type: C10730-02) with resolution 0.23µm/pixel (40x high resolution mode) and the each of the image of cores was undertaken to measure expression of β-catenin. An unbiased ImageJ was used to quantify protein expression (Sec. 3.3.6). The RGB coloured images A1, B1, C1 and D1 representing the amount of tissues (red colour) in core of A, B, C and D respectively. The coloured images were masked to obtain β-catenin protein expression indicated in A2, B2, C2 and D2 in NPT, Grade 3+3, Grade 4+4 and Grade 4+5/5+4. The quantified data were obtained as AF per AT which were used to construct mountain plot indicated as A3, B3, C3, D3 of A2, B2, C2 and D2 respectively. Each bin is the data for an individual, normal prostate tissue (n=15) and Grade 3+3, Grade (4+4) (n=15) and Grade 4+5/5+4 (n=15) PCa tissue. Statistical analysis was performed using Mann–Whitney U test to calculate the significance of difference of β-catenin expression in Grade 3+3 vs NPT, Grade 4+4 vs NPT, Grade 4+5/5+4 vs NPT. The analysis showed expression of β-catenin in Grade 3+3 and Grade 4+4 was remained same as in NPT. But the expression was significantly increased in Grade 4+5/5+4. NS: not significant: *P<0.05. (AF: Area Fraction, AT: Amount of Tissue). Scale bar: 100 µm.

3.4.3.3. Expression of FRA-1 in NPT, Grade 3+3, Grade 4+4 and Grade 4+5/5+4 PCa tissues

FRA-1 is a Wnt signalling target gene for transcription. The expression of FRA1 was investigated using anti-FRA-1 antibody (ab252421: ABCAM).x Representative tissue cores for each condition (Normal and different Gleason grade cancer) are shown in Fig. 3.6: NPT (Fig. 3.6.A) which was compared to FRA-1 expression in Grade 3+3 (Fig. 3.6.B), Grade 4+4 (Fig. 3.6.C) and Grade 4+5/5+4 (Fig. 3.6.D). A visual analysis suggests an increase in the expression of FRA-1 in acinar cell in glandular in all three grades compared to NPT. The visual observation is confirmed by the quantitative analysis shown in Fig. 3.6.A2-D2 quantified using ImageJ. The data from this analysis is given in Tables 3.2 and 3.3. The results of fold changes showed as mean±SEM. The analysis indicates that the expression of FRA-1 was significantly increased by 1.19± 0.55-fold (*P<0.05) in Grade 3+3 compared to NPT (Table 3.2) (Fig. 3.6.B3); the AUC values for ROC curve was 0.73 (*P<0.05) (Fig. 3.10; Table 3.3). The expression was also significantly increased in Grade 4+4 (0.96±0.36-fold) (*P<0.05; Fig. 3.6.C3) with AUC value of ROC curve was 0.73 (*P<0.05) (Fig. 3.10). In Grade 4+5/5+4, FRA-1 expression was also increased (0.95±0.45-fold) significantly (*P<0.05; Fig. 3.6.D3; Table 3.2) with AUC value of ROC was 0.74 (*P<0.05) (Fig. 3.10; Table 3.3) compared to NPT. LR+ was found at AUC was 1 for Grade 3+3, Grade 4+4 and Grade 4+5/5+4. FRA-1 could be considered as a biomarker for prostate cancer. The result overall indicates a progressive increase in FRA-1 expression in prostate carcinogenesis. This is a first investigation of a key Wnt target protein and a transcription factor that could be an important protein in PCa.

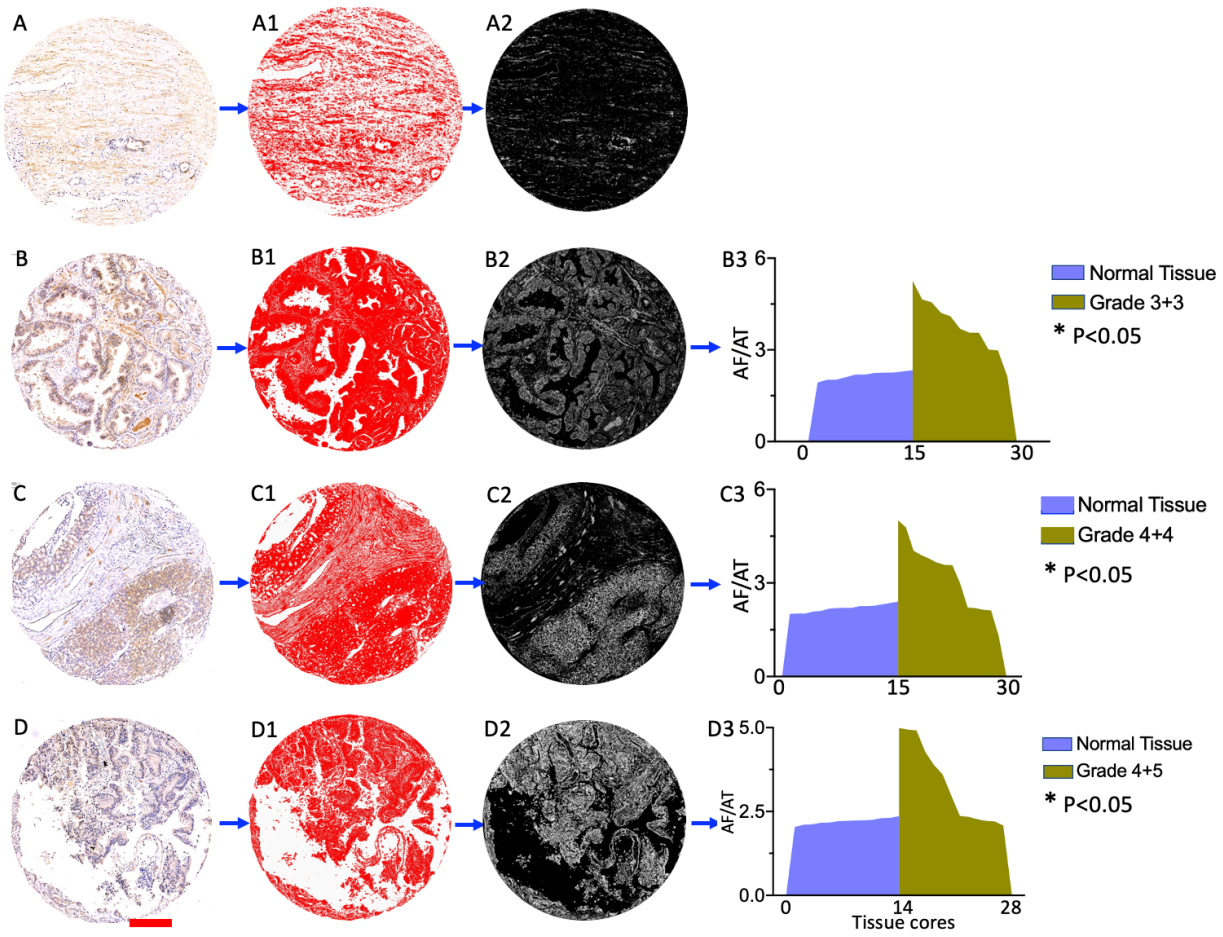

Figure 3.6. Representative images for the staining and quantitation of DAB signal for FRA-1 in normal prostate tissue, Grade 3+3, Grade 4+4 and Grade 4+5/5+4 PCa tissues. A, B, C and D representing the stained tissue cores of normal prostate tissue, Grade 3+3, Grade 4+4 and Grade 4+5/5+4 respectively. Following staining of the tissue with DAB-HRP for FRA-1, the tissue arrays were imaged with NanoZoomer-RS Scanner (Type: C10730-02) with resolution 0.23µm/pixel (40x high resolution mode) and the each of the image of cores was undertaken to measure expression of FRA-1. An unbiased ImageJ was used to quantify protein expression (Sec. 3.3.6). The RGB coloured images A1, B1, C1 and D1 representing the amount of tissues (red colour) in core of A, B, C and D respectively. The coloured images were masked to obtain FRA-1 protein expression indicated in A2, B2, C2 and D2 in NPT, Grade 3+3, Grade 4+4 and Grade 4+5/5+4. The quantified data were obtained as AF per AT which were used to construct mountain plot indicated as A3, B3, C3, D3 of A2, B2, C2 and D2 respectively. Each bin is the data for an individual, normal prostate tissue (n=15) and Grade 3+3, Grade (4+4) (n=15) and Grade 4+5/5+4 (n=15) PCa tissue. Statistical analysis was performed using Mann–Whitney U test to calculate the significance of difference of FRA-1 expression in Grade 3+3 vs NPT, Grade 4+4 vs NPT, Grade 4+5/5+4 vs NPT. The analysis showed expression of FRA-1 was increased significantly in Grade 3+3 and Grade 4+4 and Grade 4+5/5+4. ns: not significant: *P<0.05. (AF: Area Fraction, AT: Amount of Tissue). Scale bar: 100 µm.

3.4.3.4. Expression of PYGO2 in NPT, Grade 3+3, Grade 4+4 and Grade 4+5/5+4 PCa tissues

It has been suggested that PYGO2, a mammalian orthologue of Armadillo gene, that forms the transcription complex with β-catenin, may provide the nuclear localization signal for β-catenin that it lacks. PYGO2 is also a target gene for Wnt/β-catenin mediated transcription. The expression of PYGO2 in NPT, Grade 3+3, Grade 4+4 and Grade 4+5/5+4 was measured using an anti-PYGO2 antibody (ab99274, ABCAM) stained with DAB-HRP showed in Fig. 3.7.A-D which, through visual inspection, indicates the higher intensity for PYGO2 expression in Grade 4+5/5+5 than NPT, Grade 3+3, Grade 4+4. This expression was reflected in image obtained from ImageJ algorithm (Fig. 3.7.A2-D2) The expression was quantitated and the analysis of the results showed PYGO2 expression did not significantly change in Grade 3+3 (Fig. 3.7.B3) and Grade 4+4 (Fig. 3.7.C3; Table 3.2) with AUC value for ROC was 0.50 (ns) and 0.63 (ns), respectively (Fig. 3.11; Table 3.3) compared to NPT. The results of fold changes showed as mean±SEM. But the expression was significantly increased (0.57±0.26-fold) in Grade 4+5/5+4 (*P<0.05) (Fig. 3.7.D3; Table 3.2) compared to NPT. The AUC value for ROC was calculated as 0.76 (*P<0.05) (Fig. 3.11, Table 3.3). In case PYGO2, LR+ was found at AUC was 0.78 for Grade 3+3 and 1 for Grade 4+4 and Grade 4+5/5+4. PYGO2 could be used as biomarker for only Grade 4+5/5+4 PCa.

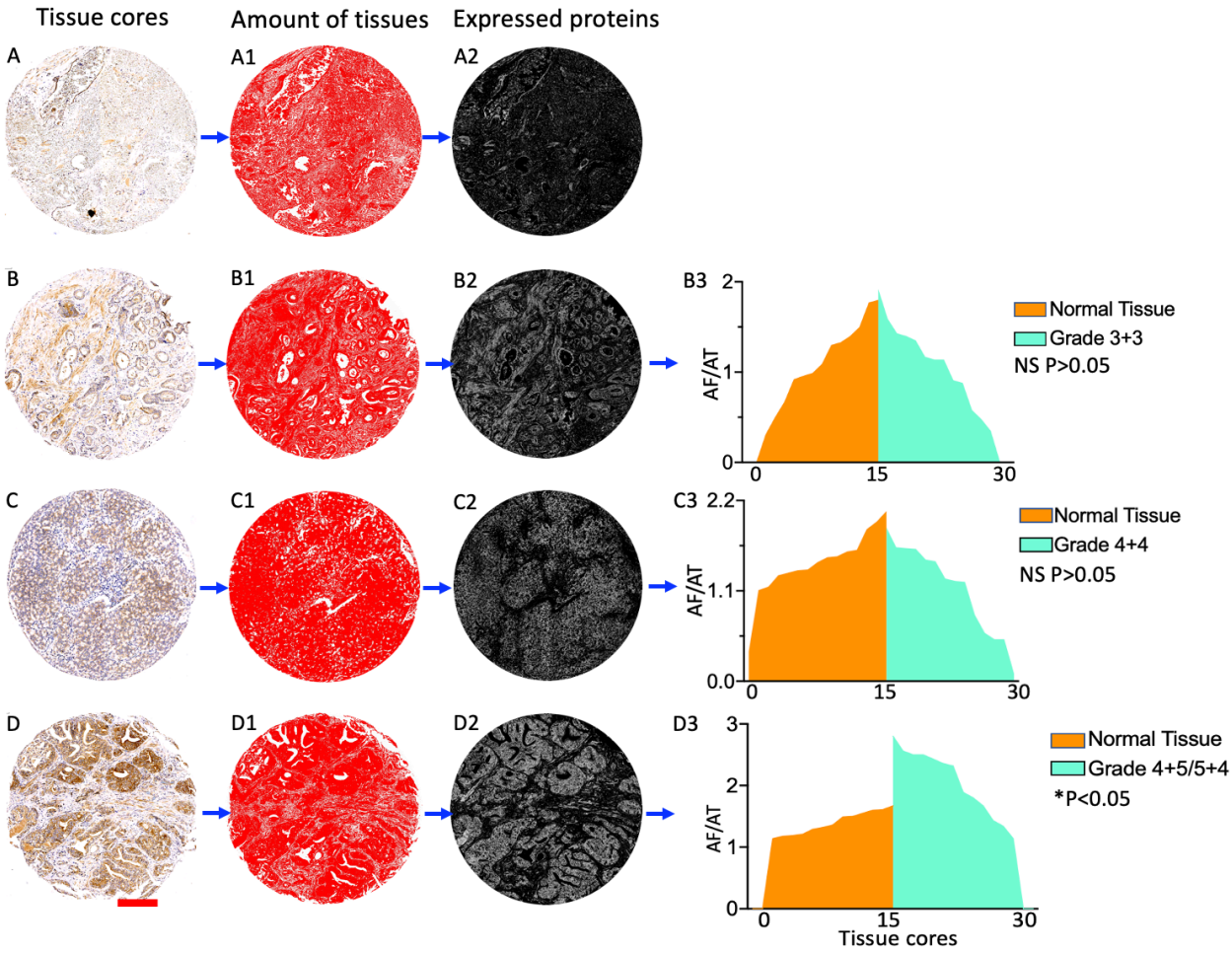

Figure 3.7. Representative images for the staining and quantitation of DAB signal for PYGO2 in normal prostate tissue, Grade 3+3, Grade 4+4 and Grade 4+5/5+4 PCa tissues. A, B, C and D representing the stained tissue cores of normal prostate tissue, Grade 3+3, Grade 4+4 and Grade 4+5/5+4 respectively. Following staining of the tissue with DAB-HRP for PYGO2, the tissue arrays were imaged with NanoZoomer-RS Scanner (Type: C10730-02) with resolution 0.23µm/pixel (40x high resolution mode) and the each of the image of cores was undertaken to measure expression of PYGO2. An unbiased ImageJ was used to quantify protein expression (Sec. 3.3.6). The RGB coloured images A1, B1, C1 and D1 representing the amount of tissues (red colour) in core of A, B, C and D respectively. The coloured images were masked to obtain PYGO2 protein expression indicated in A2, B2, C2 and D2 in NPT, Grade 3+3, Grade 4+4 and Grade 4+5/5+4. The quantified data were obtained as AF per AT which were used to construct mountain plot indicated as A3, B3, C3, D3 of A2, B2, C2 and D2 respectively. Each bin is the data for an individual, normal prostate tissue (n=15) and Grade 3+3, Grade (4+4) (n=15) and Grade 4+5/5+4 (n=15) PCa tissue. Statistical analysis was performed using Mann–Whitney U test to calculate the significance of difference of PYGO2 expression in Grade 3+3 vs NPT, Grade 4+4 vs NPT, Grade 4+5/5+4 vs NPT. The analysis showed expression of PYGO2 was remained unchanged in Grade 3+3 and Grade 4+4 butt increased significantly in Grade 4+5/5+4. ns: not significant: *P<0.05. (AF: Area Fraction, AT: Amount of Tissue). Scale bar: 100µm.

3.4.3.5. Expression of TCF-1 in NPT, Grade 3+3, Grade 4+4 and Grade 4+5/5+4 PCa tissues

TCF-1 is another vital protein in the Wnt signalling pathway and also part of the β-catenin transcription complex. Its expression in NPT, Grade 3+3, Grade 4+4 and Grade 4+5/5 was investigated using anti-TCF-1 antibody (2203s, CST) stained with DAB-HRP protocol (Fig. 3.8.A-D). Visual inspection indicated the higher expression of TCF-1 in Grade 4+5/5+4 compared to that of NPT, Grade 3+3 and Grade 4+4. This inspection was also reflected in the masked images obtained from ImageJ (Fig. 3.8. A2-D2). The results of fold changes showed as mean±SEM. Analysis of data showed no significant increase of TCF-1 expression in Grade 3+3 (Fig. 3.8.B3) and Grade 4+4 (Fig. 3.8.C3) where the AUC value for ROC was 0.53 (ns) and 0.66 (ns) respectively (Fig. 3.11; Table 3.3) compared to NPT, whereas expression of TCF-1 was increased (0.61 ± 0.28-fold) significantly (*P<0.05) (Table 3.2) in Grade 4+4/5+4 (Fig. 3.8.D3) with AUC value for ROC was 0.74 (*P<0.05) (Fig. 3.11; Table 3.3). Considering the AUC value, TCF-1 could be considered as a biomarker for Grade 4+5/5+4 only.

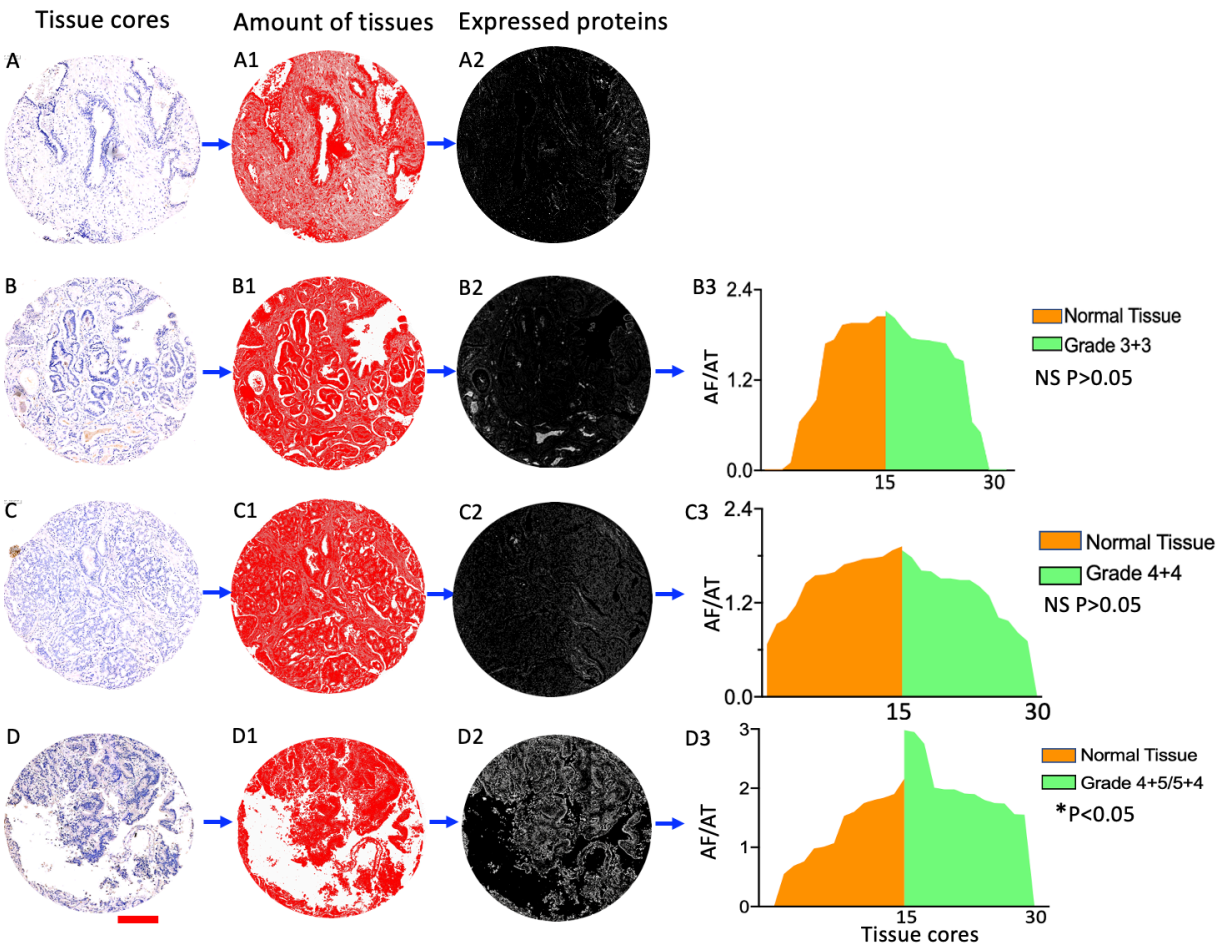

Figure 3.8. Representative images for the staining and quantitation of DAB signal for TCF-1 in normal prostate tissue, Grade 3+3, Grade 4+4 and Grade 4+5/5+4 PCa tissues. A, B, C and D representing the stained tissue cores of normal prostate tissue, Grade 3+3, Grade 4+4 and Grade 4+5/5+4 respectively. Following staining of the tissue with DAB-HRP for TCF-1, the tissue arrays were imaged with NanoZoomer-RS Scanner (Type: C10730-02) with resolution 0.23µm/pixel (40x high resolution mode) and the each of the image of cores was undertaken to measure expression of TCF-1. An unbiased ImageJ algorithm was used to quantify protein expression (Sec. 3.3.6). The RGB coloured images A1, B1, C1 and D1 representing the amount of tissues (red colour) in core of A, B, C and D respectively. The coloured images were masked to obtain TCF-1 protein expression indicated in A2, B2, C2 and D2 in NPT, Grade 3+3, Grade 4+4 and Grade 4+5/5+4. The quantified data were obtained as AF per AT which were used to construct mountain plot indicated as A3, B3, C3, D3 of A2, B2, C2 and D2 respectively. Each bin is the data for an individual, normal prostate tissue (n=15) and Grade 3+3, Grade (4+4) (n=15) and Grade 4+5/5+4 (n=15) PCa tissue. Statistical analysis was performed using Mann–Whitney U test to calculate the significance of difference of TCF-1 expression in Grade 3+3 vs NPT, Grade 4+4 vs NPT, Grade 4+5/5+4 vs NPT. The analysis showed expression of TCF-1 was remained unchanged in Grade 3+3 and Grade 4+4 but increased significantly in Grade 4+5/5+4. ns: not significant: *P<0.05. (AF: Area Fraction, AT: Amount of Tissue). Scale bar: 100µm.

3.4.3.6. Expression of Cx43 in NPT, Grade 3+3, Grade 4+4 and Grade 4+5/5+4 PCa tissues

A further Wnt related protein, not part of the known transcription complex, Cx43 was investigated to assess its expression in NPT, Grade 3+3, Grade 4+4 and Grade 4+5/5+4 using anti-Cx43 antibody (2203s, CST) stained with DAB-HRP protocol. The representative images of NPT, Grade 3+3, Grade 4+4 and Grade 4+5/5+4 images in Fig. 3.9. A, B, C and D were analysed using ImageJ algorithm and showed in Fig. 3.9. A2, B2, C2 and D2 respectively. The results of fold changes showed as mean±SEM. The quantified analysis showed the expression of Cx43 was not significantly changed in Grade 3+3 PCa tissue compared to NPT. But the expression of Cx43 was decreased significantly in Grade 4+4 (-3.04±1.07-fold; **P<0.01) (Fig. 3.9.C3) compared to NPT. Expression of Cx43 was further reduced in Grade 4+5/5+4 (-2.61±0.54-fold; ****P<0.0001) (Fig. 3.9.D3; Table 3.2) compared to NPT. AUC value of ROC for Grade 3+3, Grade 4+4 and Grade 4+5/5+4 was 0.70 (ns), 0.81 (*P<0.05) and 0.93 (****P<0.0001) respectively (Fig. 3.11; Table 3.3). LR+ for CX43 was obtained as 10 for Grade 3+3, Grade 4+4 and Grade 4+5/5+4. Presence of Cx43 indicates a disease condition and could be considered as a biomarker for Grade 4+4 and Grade 4+5/5+4.

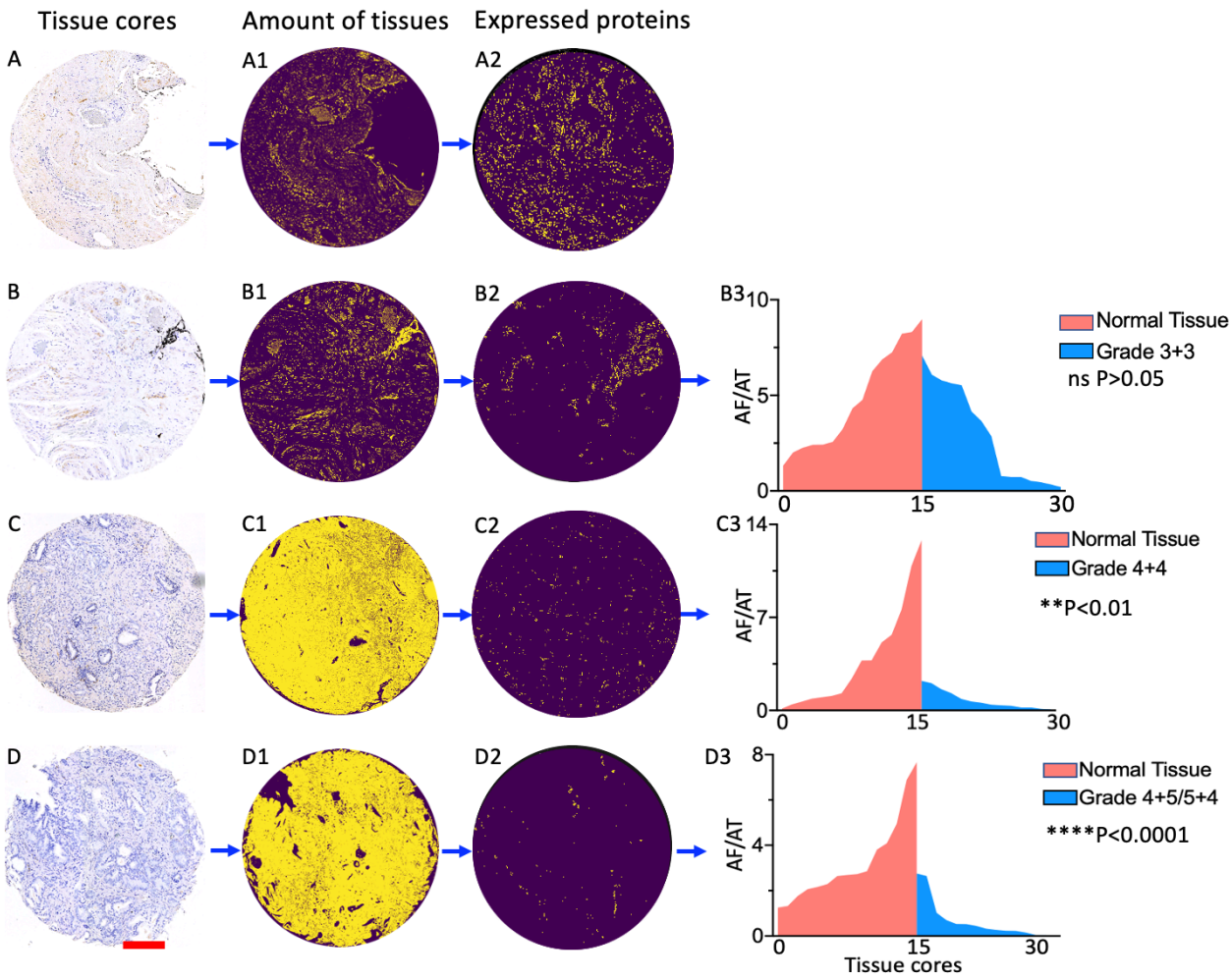

Figure 3.9. Representative images for the staining and quantitation of DAB signal for Cx43 in normal prostate tissue, Grade 3+3, Grade 4+4 and Grade 4+5/5+4 PCa tissues. A, B, C and D representing the stained tissue cores of normal prostate tissue, Grade 3+3, Grade 4+4 and Grade 4+5/5+4 respectively. Following staining of the tissue with DAB-HRP for Cx43, the tissue arrays were imaged with NanoZoomer-RS Scanner (Type: C10730-02) with resolution 0.23µm/pixel (40x high resolution mode) and the each of the image of cores was undertaken to measure expression of Cx43. An unbiased ImageJ algorithm was used to quantify protein expression (Sec. 3.3.6). The RGB coloured images A1, B1, C1 and D1 representing the amount of tissues (yellow colour) in core of A, B, C and D respectively. The coloured images were masked to obtain Cx43 protein expression indicated in A2, B2, C2 and D2 in NPT, Grade 3+3, Grade 4+4 and Grade 4+5/5+4. The quantified data were obtained as AF per AT which were used to construct mountain plot indicated as A3, B3, C3, D3 of A2, B2, C2 and D2 respectively. Each bin is the data for an individual, normal prostate tissue (n=15) and Grade 3+3, Grade (4+4) (n=15) and Grade 4+5/5+4 (n=15) PCa tissue. Statistical analysis was performed using Mann–Whitney U test to calculate the significance of difference of Cx43 expression in Grade 3+3 vs NPT, Grade 4+4 vs NPT, Grade 4+5/5+4 vs NPT. The analysis showed expression of Cx43 was significantly decreased in in Grade 3+3 (*P<0.05) and was further decreased in Grade 4+4 (**P<0.01) and in Grade 4+5/5+4 (****P<0.0001). (AF: Area Fraction, AT: Amount of Tissue). Scale bar: 100 µm.

Table 3.2. Quantitative analysis of protein expression in Grade 3+3, Grade 4+4 and Grade 4+5/5+4 PCa tissues arrays. The results showed as mean ± SEM compared to NPT.

Protein	PCa Grade 3+3		PCa Grade 4+4		PCa Grade 4+5/5+4	
	Fold change of Probit in Grade 3+3	Significance (<P)	Fold change of Probit in Grade 4+4	Significance (<P)	Fold change of Probit in Grade 4+5	Significance (<P)
AR	-1.30± 0.84	ns	-1.23 ± 0.46	**P<0.01	-1.53 ± 0.46	*P<0.05
β-catenin	-0.046 ± 0.33	ns	0.03 ± 0.20	ns	0.40± 0.17	*P<0.05
FRA-1	1.19 ± 0.55	*P<0.05	0.96± 0.36	*P<0.05	0.95 ± 0.45	*P<0.05
PYGO2	-0.01 ± 0.21	ns	-0.29 ± 0.17	ns	0.57 ± 0.26	*P<0.05
TCF-1	0.06 ± 0.29	ns	-0.22± 0.16	ns	0.61 ± 0.28	*P<0.05
Cx43	-1.77 ± 0.95	ns	-3.04 ± 1.07	** P<0.01	-2.61 ± 0.54	****P<0.0001

The expression of DAB-HRP labelled proteins such as AR, β-catenin, FRA-1, PYGO2, TCF-1 and Cx43 were quantified in an unbiased manner by using a reproducible, semi-automated particle analysis protocol (Sec. 3.3.6) using a written script adapted to ImageJ. Fold increase/decrease is relative to normal for each protein (e.g., Grade 3+3 vs NPT, Grade 4+4 vs NPT and Grade 4+5/5+4 vs NPT and significance of difference was calculated using Mann Whitney U test.

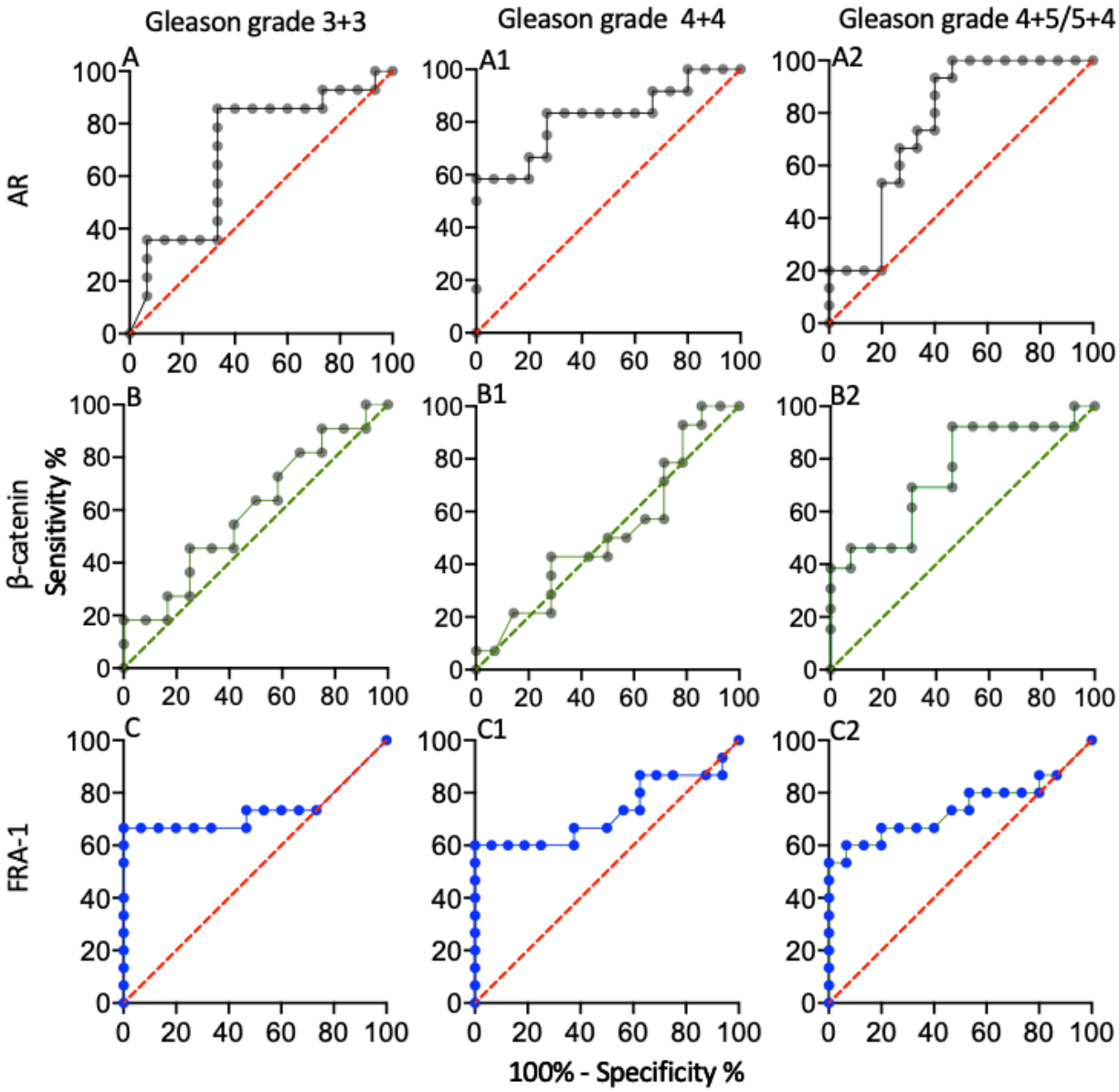

Figure 3.10. ROC of the AR, β-catenin, FRA-1 in Grade 3+3, Grade 4+4 and Grade 4+5/5+4 PCa tissues. ROC curve displays the discriminating performance of the AR, β-catenin and FRA-1 expression in the differentiation between NPT vs Grade 3+3, NPT vs Grade 4+4 and NPT vs Grade 4+5/5+4 PCa tissue cores using probit (AF/AT) data for AR, β-catenin and FRA-1. The dotted line represents the ROC area of 0.5.

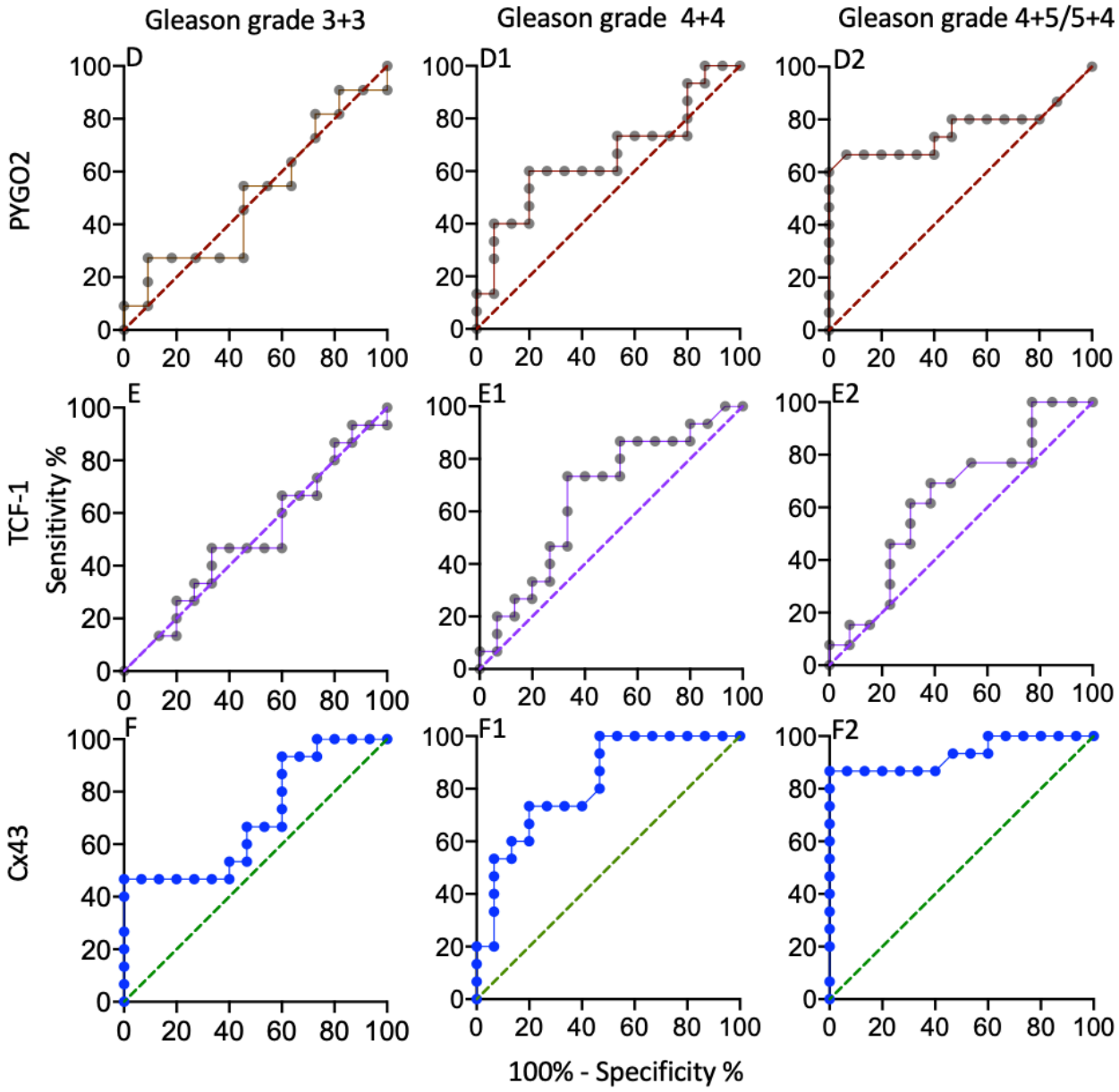

Figure 3.11. ROC of the PYGO2, TCF-1, Cx43 in Grade 3+3, Grade 4+4 and Grade 4+5/5+4 PCa tissues. ROC curve displays the discriminating performance of the PYGO2, TCF-1 and Cx43 expression in the differentiation between Grade 3+3, Grade 4+4 and Grade 4+5/5+4 PCa tissue cores using probit (AF/AT) data for PYGO2, TCF-1 and Cx43. The dotted line represents the ROC area of 0.5.

Table 3.3. AUC value and significance of difference of AR, β-catenin, FRA-1, PYGO2, TCF-1, Cx43 expression in Grade 3+3, Grade 4+4 and Grade 4+5 compared to normal prostate.

Protein	PCa Grade 3+3			PCa Grade 4+4			PCa Grade 4+5/5+4		
	AUC	Significance (<P)	LR(+)	AUC	Significance (<P)	LR(+)	AUC	Significance (<P)	LR(+)
AR	0.70	ns	4.2	0.84	**P<0.01	10	0.76	*P<0.05	10
β -catenin	0.52	ns	0.92	0.52	ns	1	0.75	*P<0.05	1
FRA-1	0.73	*P<0.05	1	0.73	*P<0.05	1	0.74	*P<0.05	1
PYGO2	0.50	ns	0.78	0.63	ns	1	0.76	*<0.05	1
TCF-1	0.53	ns	1	0.66	ns	2.5	0.74	*P<0.05	1
Cx43	0.70	ns	10	0.81	*P<0.05	10	0.93	****P<0.0001	10

When a comparison of protein expression for the antibodies tested was conducted between different grades of prostate cancer a preliminary but interesting picture appears to emerge regarding the interaction between AR and Wnt signalling (Fig. 3.12).

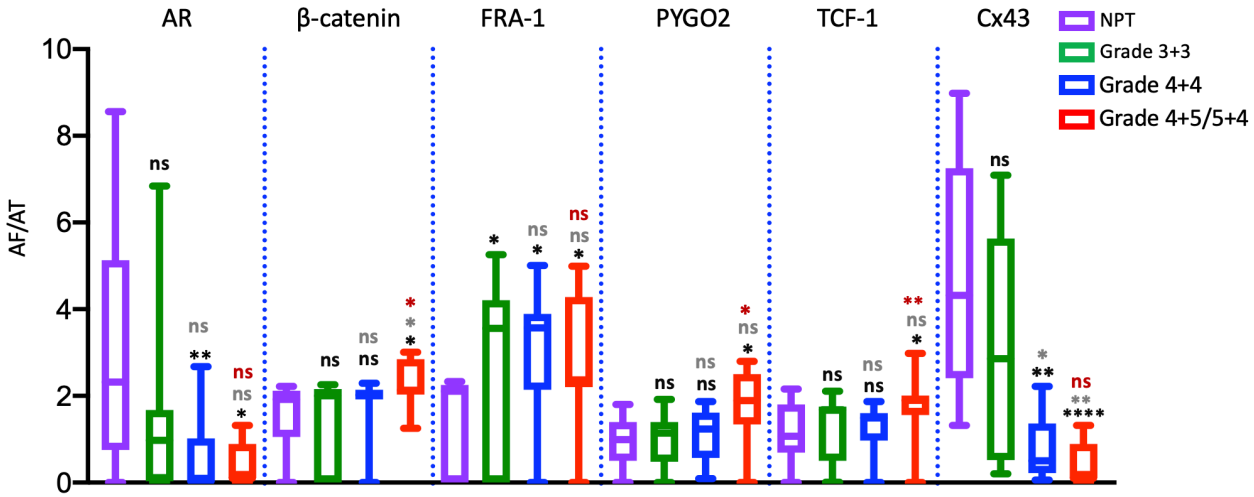

Figure 3.12. A box plot calculated for the expression of AR and Wnt related proteins (β-catenin, FRA-1, PYGO2, TCF-1 and Cx43) in NPT, Grade 3+3, Grade 4+4, Grade 4+5/5+4 prostate tissue. AF/AT of each protein was used to construct the box plot using GraphPad prism. The data are presented for individual protein elsewhere. Significance of difference between each condition (NPT v Grade 3+3, NPT v 4+4, NPT v 4+5/5+4 (black asterisks or ns); 3+3 v 4+4 (grey asterisks or ns); 4+4 v 4+5/5+4 (red asterisks or ns); *P<0.05; ** P<0.01; ****P<0.0001) is shown. ns means no significant difference (with the same colour scheme as for NPT v different grades). NB: These data are extracted form NPT v all cancers (all grades combined) as represented in mountain plots above.

There is no significant change in expression of AR protein with increasing Gleason grade, although there appears to be a trend towards a gradual decrease correlated to Gleason grade increase. Conversely, β-catenin expression is increased in Grade 4+5/5+4 compared to Grade 4+4, as is the expression of key β-catenin transcription complexing proteins TCF-1 and PYGO2. The expression

of Cx43, similar to AR, is not significantly different but shows a decreasing trend as Gleason grades increase. These results raise the notion that there may be a yin/yang, co-ordinated transcriptional relationship between AR and β-catenin gene transcriptional programs. However, this requires further investigations with appropriate sample sizes.

3.4.3.7. Logistic regression model – does combining the expression of more than one protein yields better AUC?

A combination of different permutations analysis of AR, β-catenin, FRA-1, PYGO2, TCF-1 and Cx43 protein via binary regression model was conducted to identify marker to improve diagnostic ability. The table 3.4 is showing the combination of AR with β-catenin, FRA-1, PYGO2, TCF-1 and Cx43 and β-catenin with FRA-1, PYGO2, TCF-1 and Cx43 in Grade 3+3 vs Grade 4+4, Grade 3+3 vs Grade 4+5/5+4 and Grade 4+4 vs Grade 4+5/5+4. The other combinations are showed in appendix (Appx. 3.7).

Table 3.4. Logistic regression model to identify combination of markers that may improve diagnostic power

PCa Grade 3+3 vs Grade 4+4				
Protein combination	% cases correctly classified*	AUC	Std Error	95% CI
AR and β-catenin	95	0.95	0.04	0.7 to 0.9
AR and FRA-1	95	0.95	0.05	0.8 to 0.9
AR and PYGO2	95	0.95	0.04	0.7 to 0.9
AR and TCF-1	100	1	0	0.8 to 1
AR and Cx43	87	0.87	0.08	0.7 to 0.9
β-catenin and FRA-1	100	1	0	0.8 to 1
β-catenin and PYGO2	92	0.92	0.05	0.7 to 0.9
β-catenin and TCF-1	96	0.96	0.04	0.8 to 0.9
β-catenin and Cx43	84	0.85	0.07	0.6 to 0.9
Grade 3+3 vs Grade 4+5/5+4				
AR and β-catenin	95	0.95	0.04	0.7 to 0.9
AR and FRA-1	95	0.95	0.04	0.7 to 0.9
AR and PYGO2	96	0.96	0.04	0.8 to 0.9
AR and TCF-1	96	0.96	0.04	0.8 to 0.9
AR and Cx43	88	0.9	0.06	0.7 to 0.9
Grade 3+3 vs Grade 4+5/5+4				

β-catenin and FRA-1	100	1	0	0.8 to 1
β-catenin and PYGO2	91	0.92	0.06	0.7 to 0.9
β-catenin and TCF-1	91	0.92	0.06	0.7 to 0.9
β-catenin and Cx43	83	0.84	0.08	0.6 to 0.9
Grade 4+4 vs Grade 4+5/5+4				
AR and β-catenin	92	0.93	0.05	0.7 to 0.9
AR and FRA-1	93	0.93	0.05	0.7 to 0.9
AR and PYGO2	92	0.93	0.05	0.7 to 0.9
AR and TCF-1	100	1	0	0.8 to 1
AR and Cx43	100	1	0	0.8 to 1
β-catenin and FRA-1	100	1	0	0.8 to 1
β-catenin and PYGO2	100	1	0	0.8 to 1
β-catenin and TCF-1	100	1	0	0.8 to 1
β-catenin and Cx43	100	1	0	0.8 to 1

MedCalc software was used to employ a logistic regression model for analysing the relationship between one dichotomous dependent variable (Grade 3+3 v Grade 4+4 etc) and one or more independent variables (two proteins). The outcome (percentage of cases correctly identified) suggests that within the cohort of samples used in this study, the diagnostic power to identify differences within Gleason Grades is increased, significantly ($P<0.001$) with the combination of multiple protein expression in two different Grades of PCa. It must be noted that sample size was small (24-27) for this analysis, however, the proof of concept that combining protein expression data for two proteins increases the power of difference. Other permutations are shown in appendix (Appx. 3.7).

A perfect biomarker should have a zero false positive and false negative rate. In biology such biomarkers rarely exist. A quick glance at Fig. 3.10 and 3.11 and Table 3.3 show that other than Cx43 in Gleason grade 4+5, none of the protein expression shows a very low false positivity and negativity rates. Even the Cx43 AUC analysis reaches only 0.93 (Table 3.3). Logistic regression of combined expression of two proteins can enhance the utility of protein expression data to increase the percentage case identification within a cohort. In our laboratory we have applied logistic regression to protein expression data (e.g., (Symes et al., 2013)) to enhance the utility of expression to act as reliable biomarkers. The results are presented here (Table 3.4) show that combining multiple markers (e.g., AR/β-catenin, FRA-1, PYGO2, TCF-1 and Cx43 etc) increases the power of detection between different Gleason Grades.

3.5. Discussion

PCa is the most prevalent malignancy among men (Siegel et al., 2016). The heterogeneity of PCa histology was initially described by Donald Gleason in the 1960s and has improved over the years (Sec. 3.1.1). Despite significant advances, prostate cancer remains a major medical problem for men who have it, with an urgent need to improve the efficacy of current therapies for metastatic disease and minimise unnecessary overtreatment of more benign disease. Study of disease stratification by Gleason grading is an important way to diagnose the disease appropriately. Immunohistochemical approach is a powerful tool in the diagnostic confirmation of the disease which has been gaining acceptance.

It is known that prostate tumorigenesis and carcinogenesis are driven through input, interaction and dysregulation of multiple signalling pathways. AR signalling plays a crucial role in development and prostate carcinogenesis. Additionally, Wnt signalling pathway has active roles in prostate cancer development. I aimed to investigate these two signalling pathways in this chapter using *in situ*, quantitative techniques.

These experiments were conducted to investigate the hypothesis that Wnt and AR signalling pathways interact in carcinogenesis of PCa and to investigate their utility as putative biomarkers of PCa and disease stratification. To my knowledge this is the first time a comparative, *in situ*, analysis of AR and Wnt related protein expression is conducted in human prostate tissue. I have included AR as a principal component of AR signalling pathway and five other proteins, four of which β-catenin, PYGO2, TCF-1 and possibly Cx43 are related to Wnt/β-catenin transcription complex; FRA-1 is a putative transcriptional target of the Wnt signalling pathways.

3.5.1. AR expression in Grade 3+3, Grade 4+4 and Grade 4+5/5+4 PCa and putative utility as a biomarker

AR is nuclear receptor and AR signalling pathway is activated by binding with its ligand testosterone or dihydrotestosterone (Sec. 1.11). Binding of testosterone/DHT induces a conformational change in the AR resulting of releasing the HSP (when bound with AR) and is dimerized before translocating into the nucleus where it activates the transcription of target genes and maintain prostate homeostasis (Zhou et al., 2015) during normal development. During

postnatal development, stromal (mesenchymal) and epithelial compartment interact reciprocally. The stromal cells are believed to release peptide growth factors (andromedins, see section 1.5.2.) in response to androgen signalling through AR in these cells.

Even though there is considerable evidence that PCa is caused by prostate epithelial cells, there is disagreement over whether the tumours are caused by basal cells or luminal epithelial cells (Lawson et al., 2010). Multiple tumour foci as well as prostatic intraepithelial neoplasia (PIN) lesions, the suspected precursor to PCa, are common in the prostate.

Tumours become less structured as they grow, with smaller ductal structures, and eventually lose these structures totally. The tumours infect surrounding tissues and spread to the lymph nodes, bladder, and bone as they grow (Miller et al., 2003). To my knowledge, there has not been comparative studies conducted to measure the level of AR expression in Grade 3+3, Grade 4+4 and Grade 4+5/5+4 compared to normal prostate tissues (NPT). Therefore, the current study was designed to measure the AR expression levels in Grade 3+3, Grade 4+4 and Grade 4+5/5+4 to investigate its quantitative expression in different Gleason grades of PCa and as a prelude to evaluating its potential functional role of AR and Wnt signalling (Chap-V).

I discovered that expression of AR in Grade 3+3 (-1.30±0.84-fold, mean±SEM, ns $P>0.05$) was not changed significantly (Fig. 3.4). The expression of AR changed significantly in Grade 4+4 (-1.23±0.46-fold, mean±SEM; **$P<0.01$), also observed significant change in Grade 4+5/5+4 (-1.53±0.46-fold, mean±SEM; *<0.05). The fold change was indicated AR expression was decreased in Grade 4+4 and Grade 4+5/5+4 significantly (Table 3.2).

In low grade prostate cancer, Grade 3+3, the histological changes are minimum compared to NPT tissues. AR is expressed in basal and luminal cells in well differentiated glands which is also present in Grade 3+3 where glands are well-differentiated which are separated by stroma (Roehrborn, 2008). As a minimum level of histological change in Grade 3+3, no significant change in the expression of AR in Grade 3+3 compared to NPT was therefore expected.

As the disease progresses, in Grade 4+4 PCa tissues, AR expression was observed to be significantly reduced. A similar observation was also reported by (Miyamoto et al., 1993), for validating this approach. Chodak and his colleagues revealed that AR content in well

differentiated prostatic epithelium cells was significantly higher compared to moderately and poorly differentiated adenocarcinoma (Chodak et al., 1992), was supported by Masai et al. and Takeda et al. (Masai et al., 1990 and Takeda et al., 1996). Husain et al. demonstrated that prostate cancer with moderate AR immunostaining had a Gleason score of >8. But the intensity of AR staining was high in well differentiated tumour and low in moderately to poorly differentiated tumours (Husain et al., 2016) . This result was concordance with the studies carried out by Theodoropoulos et al. and Miyamoto et al. (Theodoropoulos et al., 2005 and Miyamoto et al., 1993). Conversely, Henshall et al. reported that AR expression is associated with high grade prostate cancer (Henshall et al., 2001). This discrepancy could be due to heterogenous expression of AR in prostate carcinoma. Sadi et al. suggested that cancerous prostate tumours contain both androgen-dependent and androgen independent cells suggesting that AR expression may depend upon the presence of the type of cells that are numerous within the tumours (Sadi et al., 1991). Incidentally, expression of AR in Grade 4+4 and Grade 4+5/5+4 PCa was reduced significantly when compared with NPT (Fig. 3.4). There was no significant change observed in Grade 3+3 PCa. These results indicate that AR signalling may itself be reduced during prostate cancer progression. This is most likely to be manifested by decrease in AR mediated gene transcription targets that include for example KLK2, KLK3, NKX3, TMPRSS2, SGK, IQGAP2, FN1 (Jin et al., 2013). It would be expected that when AR expression decreases that the target genes are also decreased. However, this may not necessarily be the case because the gene transcription is a highly complicated process and gene transcription is under the control of multiple inputs (Arya et al., 2015 and Marino et al., 2006).

Another way of looking at this would be to investigate common Wnt and AR gene transcription targets in low and high grade cancer. Jin and colleagues analysed the gene expression data and indicated that in multiple studies, NDRG1 appears as a target for AR mediated gene transcription (Jin et al., 2013). Interestingly, Symes et al. showed that NDRG1 expression is increased in prostate cancer; neither of these studies investigated the change in expression in different grades of prostate cancer (Symes et al., 2013). An interesting experiment that was designed to specifically investigate the expression of common targets such as NDRG1, unfortunately could not be completed due to Covid 19 restrictions in 2020. This would have involved isolating RNA

from the FFPE samples, which is now possible but a technically demanding procedure, requiring considerable optimization. This is something that could be done in the future, either using fresh frozen sample (ideal sample for good quality RNA isolation) or from an FFPE cohort where RNA degradation is likely to occur.

Although this has been postulated before, my results also suggests that AR could be considered as a prognostic marker for Grade 4+4 and Grade 4+5/5+4 PCa (Table 3.2). I found AUC value for ROC (Fig. 3.10) for Grade 3+3, Grade 4+4 and grade 4+5/5+4 was 0.70 (ns $P>0.05$), 0.84 (**$P<0.01$) and 0.76 (*$P<0.05$), respectively. This also indicates that AR could be considered as a prognostic marker for Grade 4+4 and Grade 4+5/5+4 PCa (Table 3.3). Likelihood ratio (LR)(+) was found to be 4.2, 10, 10 for Grade 3+3, Grade 4+4 and Grade 4+5/5+4 respectively. It is to be noted that a likelihood ratio of greater than 1 indicates that the result is associated with the presence of disease. However, the AUC curve values do not make AR out to be a very good biomarker of disease stratification, at least in this study. 1-sensitivity and specificity values of 1 indicate a 'perfect' marker that can distinguish between two comparisons (e.g., 3+3 and 4+4 grade prostate cancers). The 'best' ROC value was for AR expression as a biomarker for Grade 4+4 (0.84 with $p<0.05$). However, this is well below what might be useful in clinic where minimal false negative rates are necessary for correct stratification.

Another method of increasing the 1-sensitivity and specificity would be to combine biomarker expression analysis using logistic regression as described by by Symes et al. who used n values of over 400 (Symes et al., 2013). This could be performed by analysing the relationship between one dichotomous dependent variable (e.g., non-malignant v malignant or Gleason grade 3+3 v 4+4) and one or more independent variables (two biomarkers). A proof of concept for the smaller cohort available to me is given in Table 3.4. However, for this analysis a large sample size is necessary which was not available for high grade cohort. Nonetheless, this study sets a template through which large scale analysis can be performed.

3.5.2. β-catenin expression in normal and low and high Gleason Grade PCa

β-catenin is a multifunctional protein that plays a critical role in mediating cell adhesion and signal transduction (Wnt signalling) (Bullions and Levine, 1998). Upon binding of Wnt ligand with

Fzd, Wnt signalling is activated and β-catenin is released from the destruction complex composed of numerous proteins including CK1, Axin, APC and GSK-3β, a process termed as 'stabilization' (Chap-I, Sec. 1.12.6). The stabilization of β-catenin in cytoplasm facilitates its translocation in nucleus where it complexes with the DNA-binding protein T-cell factor (Molenaar et al., 1996) and lymphoid enhancer factor, LEF, (Huber et al., 1996) to activate the expression of number of downstream target proto-genes including *c-MYC*, and *cyclin D1* and also its own transcription complex proteins such as TCF-1 and FRA1 for example (Chap-I, Sec. 1.12.6).

Wnt/β-catenin signalling has been implicated in both normal prostate development and in PCa progression (Symes et al., 2013). Primary evidence of the involvement of β-catenin and Wnt signalling in cancer comes from colon cancer where nearly 60% of colon cancers contain a mutation in the adenomatous polyposis coli (APC), a tumour suppressor gene. The mutations in the APC occur early during tumour development (Kinzler and Vogelstein, 1996). The dysregulation of Wnt signalling in cancer may also occur as a direct result of mutations in the β-catenin (CTNNB1) gene itself (Morin et al., 1997). Several studies revealed that abnormal β-catenin signalling might have role in prostatic tumorigenesis. Specifically, about 5% of prostatic adenocarcinomas have been observed with β-catenin mutations (Chesire et al., 2000). The frequency of APC mutations in prostatic adenocarcinomas varies to up to 14% (Gerstein et al., 2002).

In this investigation, I observed that β-catenin expression was not significantly changed in Grade 3+3 (0.046±0.33-fold, mean±SEM; ns) and Grade 4+4 (0.03±0.20-fold, mean±SEM; ns) compared to NPT. But in highest ascribed pathology grade, Grade 4+5/5+4 (0.40±0.17-fold, mean±SEM; *P<0.05) of prostate cancer, expression of β-catenin was significantly increased (Table 3.2) (Fig. 3.5). More interestingly, nuclear expression of β-catenin was visible in high grade PCa (Fig. 3.2). This would be expected if Wnt/β-catenin transcription contributed towards increase in carcinogenesis. Similar results regarding the expression level of β-catenin in Grade 3+3 and Grade 4+4 were observed by Said and colleagues ((Said et al., 2017). On the other hand, opposite observation was found by Bismar and colleagues who showed loss of β-catenin was associated with high tumour grade (Bismar et al., 2004). This discrepancy between my result for Grade 3+3 and Grade 4+4 might be associated with methodological difference, patient sampling, fixation

and the protocol used for immunohistochemical techniques but most likely to be their lack of quantitative, objective, unbiased approach used here. In addition, their explanation was that β-catenin is part of E-cadherin that act as cell-cell adhesion. During carcinogenesis, cell-cell adhesion is reduced, resulting in the loss of cell polarity and altered in histological structure, that is the morphologic hallmark of malignant tumours (Hirohashi and Kanai, 2003). Furthermore, in their (Bismar et al., 2004) summary they focus only upon β-catenin's role as a cell adhesion molecule rather than a signal transduction. This may have also contributed to anomalies, a drawback of conducting only visual analysis.

In my study, I observed that β-catenin expression was significantly increased in Grade 4+5/5+4 compared to NPT (Fig. 3.5). A similar result was found in other studies (e.g., (Chen et al., 2004b)). Advance prostate cancers have higher nuclear localization of β-catenin than malignancies in the early stage (Chesire et al., 2002 and Chen et al., 2004b) . As stated earlier, when in the nucleus, β-catenin act as transcription co-activator for proto-oncogenes that increase malignancy activating the transcription of proto-oncogenes.

A further study by Said and colleagues (Said et al., 2017) revealed abnormal β-catenin gene expression, found in 23% of tumour samples tested (212 patients) from radical prostatectomy that correlates with high Gleason score (de la Taille et al., 2003). Results from this study were also supported by Chen et al. (Chen et al., 2004b), who demonstrated that β-catenin protein expression was associated with high Gleason score tumours. Although there are numerous investigations of gene and protein expression of β-catenin, the function of β-catenin in human prostate cancer in unclear (Kypta and Waxman, 2012). I have attempted to elucidate the mechanisms of Wnt/β-catenin (and also its interaction with AR signalling) signalling in a later chapter (Chap-V).

One explanation for the increased expression of β-catenin in Grade 4+5/5+4 might be associated with the loss of *PTEN* which is frequently altered in prostate cancer, with mutations and/or deletions found in 30% primary cancers and 63% of metastatic prostate cancer. PTEN is a phosphatase that negatively regulates the phosphatidylinositol-3-kinase/Akt (PI3K/ Akt) pathway (Song et al., 2012). Loss of PTEN accelerates phosphorylation of Akt through PI3K, which then target GSK3b for phosphorylation – a critical step in the stabilization of β-catenin in the so-called

destruction complex. The activated pathway then increases cell proliferation, cell survival, and protein synthesis (Song et al., 2012). It has been shown that β-catenin interacts with the PI3K/Akt pathway following PTEN loss, through the inactivation of GSK-3b and stabilization of β-catenin. PTEN null prostate cancer cells have enhanced nuclear β-catenin expression, TCF promoter activity and expression of the β-catenin regulated gene Cyclin D1 and other proto-oncogene, which are suppressed upon re-expression of wild type PTEN (Persad et al., 2001). This may be one possible explanation for the higher expression of β-catenin in Grade 4+5/5+4. Therefore, β-catenin can be used as a prognostic marker for higher grade PCa (e.g., Grade 4+5/5+4). Another novel explanation derived from my results would be the brake that AR presence may employ on Wnt/β-catenin transcription, as discussed earlier.

Additionally, I found that AUC value for ROC curve (Fig. 3.10) was 0.52 (ns $P>0.05$), 0.52 (ns $P>0.5$) and 0.75 (*$P<0.05$) for Grade 3+3, Grade 4+4 and Grade 4+5/5+4 respectively. Therefore, β-catenin could be used as a putative biomarker for Grade 4+5/5+4 (Table 3.3), albeit with the same arguments and limitations proposed for AR, above. As with AR, a logistic regression, with the sample size caveat stated above, shows an improvement when expression of β-catenin is combined with other proteins for an evaluation as a putative disease stratification biomarker.

3.5.3. Expression of FRA-1 in normal, Grade 3+3, Grade 4+4 and Grade 4+5/5+4 PCa

The *FOSL1* (locus: 11q13) gene encoded FRA-1 (FOS-related antigen-1) protein localizes to the cytoplasm and nucleus and is modified by post-translational phosphorylation. FRA-1 along with c-FOS, FOSB, FOSB2 and FRA-2 constitutes the FOS group AP-1 transcription factors (Cohen et al., 1989). AP-1 functions through dimerization with Jun-group (e.g., c-JUN, JUNB, JUND), FOS, ATF (ATF1-4, ATF-6, b-ATF, ATFx) and MAF (c-MAF, MAFA, MAFB, MAFG/F/K, and NRL) proteins (Eferl and Wagner, 2003). The formation of AP-1 dimer is dependent on the basic leucine zipper (bZIP) domain on JUN and FOS, which also binds to DNA, while AP-1 can control target genes through this bZIP domain by binding to the TRE (TPA (Tetradecanoylphorbol-13-acetate) responsive element: TGAC/GTCA), a specific DNA sequence on the promoter or enhancer of target genes, thereby influencing proliferation, differentiation, invasion and apoptosis of tumour cells; FRA-1 has been linked to multiple cancers, including breast, bladder, colon, oesophagus cancers and HNSCC (Xiao et al., 2014). FRA1 expression is also upregulated in epithelial cancers in other

animals (Arthurs et al., 2020). In prostate cancer, FRA-1 stimulates cell metastasis by increasing N-cadherin and SNAIL and decreasing E-cadherin (Luo et al., 2018).

In my study, I investigated the expression of FRA-1 in NPT, Grade 3+3, Grade 4+4 and Grade 4+5/5+4 prostate cancer to investigate its expression in prostate cancer and also to evaluate its potential use as a risk stratification biomarker for different grades of PCa (Fig. 3.6). The result obtained from the investigation are promising. FRA-1 expression was found significantly increased in Grade 3+3 (1.19 ± 0.55-fold, mean±SEM; *P<0.05). Similar expression result was observed in Grade 4+4 and Grade 4+5/5+4. The expression was increased significantly in Grade 4+4 (0.96± 0.36-fold, mean±SEM; *P<0.05) and was also observed significant increase in Grade 4+5/5+4 (0.95±0.45-fold, mean±SEM; *P<0.05) (Table 3.2). These results show that there is a general increase in the expression of FRA1 in all grades of prostate cancer compared to normal. These results suggest that FRA1 could be a useful marker for stratification of prostate cancer. To the best of my knowledge this is the first detailed investigation of the expression of FRA1 in prostate cancer, although, as stated earlier, our laboratory has investigated the protein expression of FRA1 in other animal epithelial cancers (Giuliano et al., 2016). The following putative mechanism may explain the reason of increase the metastasis and expression of FRA-1 in different grade PCa sample. It is likely that FRA-1 expression was increased as it is Wnt/β-catenin signalling target gene. Additionally, I found AUC value for ROC curve (Fig. 3.10) 0.73 (*P<0.05), 0.73 (*P<0.05) and 0.74 (*P<0.05) for Grade 3+3, Grade 4+4 and Grade 4+5/5+4 respectively. This indicates FRA-1 could be used as a putative biomarker for different grade of PCa (Table 3.3).

3.5.4. PYGO2 expression in normal, Grade 3+3, Grade 4+4 and Grade 4+5/5+4 PCa

Pygopus (Pygo) gene was first identified in Drosophila melanogaster and Pygo proteins act as transcription co-factor of β-catenin in Wnt signalling pathway during Drosophila development (Kramps et al., 2002). In the cell nucleus Pygo associates with Armadillo/β-catenin via adapter protein Legless (or BCL9), although their molecular function with regard to TCF-dependent transcription remain unclear. Once PYGO is recruited to Drosophila TCF (dTCF) target genes via Legless-Armadillo adaptor chain (Städeli et al., 2006), and then stimulates Wnt-induced transcription by recruiting an unknown transcriptional co-activator (Kramps et al., 2002) and

(Hoffmans et al., 2005). Unlike flies, which have one *PYGOPUS* gene, mammals have two PYGOPUS homologs namely *PYGOPUS1* (*PYGO1*) and *PYGOPUS2* (*PYGO2*) (Belenkaya et al., 2002).

PYGO2 is an important component of Wnt/β-catenin transcription complex engaged in gene function during development (Chen et al., 2007) but has a broader role in chromatin modelling in cancer. Chromatin modelling is influenced by the specific interaction of PYGO2 proteins with Wnt/β-catenin. This plays a pivotal role in tissue development through gene activation (Jessen et al., 2008). PYGO2 proteins have two distinct conserved domains, an N-terminal homology domain (NHD) and a C-terminal PHD (plant homology domain) zinc finger motif (Belenkaya et al., 2002) and (Kramps et al., 2002). This domain shares many proteins those play key roles in chromatin remodelling and transcription co-activation. The PHD finger of PYGO2 is crucial for its function, as a point mutation in the PHD finger disrupts Wnt signalling (Belenkaya et al., 2002). It has also N-terminal homology domain (NHD) (Belenkaya et al., 2002 and Kramps et al., 2002). PYGO2 plays a pivotal role in multiple cancers including breast cancer (Zhang et al., 2016) and intestinal tumours (Talla and Brembeck, 2016).

Elevated *PYGO2* gene expression depends on direct repression of Retinoblastoma (Rb) tumour suppressor function and is activated by the ETS-related transcription factor, Elf-1 (Andrews et al., 2008). This observation is especially relevant as Rb loss is associated with metastatic and castrate resistant PCa (Kramps et al., 2002).

The expression of PYGO2 was only significantly increased in highest grade (Fig. 3.7) prostate cancer samples tested, implying that expression of PYGO2 is increased only when cancer has progressed a significant threshold (Table 3.2). PYGO2 expression was also visible in the nuclei that fits with the pattern of the activation of Wnt/β-catenin transcription, perhaps to maintain carcinogenesis and move towards metastases. This is the first time that the expression of PYGO2 protein is investigated in different grade of prostate cancer. An *in vivo* experiment (mouse model), conducted by Tzenov et al. showed PYGO2 upregulation related with high Gleason score and metastasis to lymph nodes and bone, PYGO2 silencing obstructed tumour progression. PYGO2 is also thought to be an important factor to stimulate the transcriptional activation in response to ligand-induced Wnt/β-catenin signalling (Tzenov et al., 2013).

PYGO2 is also active in human brain glioma, Wang and colleagues reported that PYGO2 expression was increased in human primary glioma tissue (Wang et al., 2016). PYGO2 was not expressed in normal brain tissue, but low expression was noticed in grade II glioma tissue and high expression was found in grade IV glioma tissue. This suggests that PYGO2 could be active in the same manner in high grade PCa. PYGO2 expression was also increased in breast (Popadiuk et al., 2006) and epithelial ovarian cancers (Wang et al., 2016). These two studies imply that PYGO2 is an important component for the proliferation of breast and epithelial ovarian cancer cells. A potential target that the PHD finger in PYGO2 may bind to di- and tri-methylated lysine 4 of histone H3 (H3k4me2/3). As a result, a molecule inhibitor blocking the PHD finger that may serve as beneficial compound for PYGO2-overexpressed lethal PCa. I also observed AUC value for ROC curve (Fig. 3.11) was 0.5 (ns $P>0.05$), 0.63 (ns $P>0.05$) and 0.76 (*$P<0.05$). It indicates PYGO2 can be used as a putative biomarker for Grade 4+5/5+4.

3.5.5. TCF-1 expression in normal, Grade 3+3, Grade 4+4 and Grade 4+5/5+4 PCa

TCF-1 is T-lymphocyte-specific transcription factor-1 (Oosterwegel et al., 1991) was identified by its capability to bind to the specific sequence motif "AACAAAG" in the CD3E enhancer. TCF-1 belongs to a family of proteins that utilize a region with the homology to high-mobility group (HMG) I proteins for sequence-specific DNA binding. This region was termed HMG box which binds with high affinity to sequence motifs in other T-cell enhancers, i.e., TCR-α, TCR-β, TCR-δ (Oosterwegel et al., 1991). The enhancer sequence in TCR-α is LEF1 that is also a cloned B lymphocyte (Travis et al., 1991). The HMG boxes of TCF-1 and LEF-1 are virtually identical and likely display indistinguishable DNA binding specificities (Clevers et al., 1993).

During Wnt/β-catenin signalling activation, nuclear β-catenin forms a complex with T cell factor/lymphoid enhancer factor (TCF/LEF) family transcription factors and activates the transcription of target genes (Cadigan, 2008). TCF/LEF is a principal element in the manifestation of the Wnt/β-catenin signalling pathway through gene transcription and acts as a key factor for tumorigenesis (e.g., gastrointestinal tumours, lymphoid hematopoietic tumour, etc) (Cadigan, 2008). Until my investigation, TCF-1 expression had not been measured in prostate adenocarcinoma or in different grade of prostate cancer.

In this study, I used TCF-1 (Fig. 3.8) to measure its expression in normal prostate tissue, Grade 3+3, Grade 4+4 and Grade 4+5/5+5 to assess its potential to be used as a risk stratification biomarker for the different grade of PCa. The result showed that the expression of TCF-1 was not changed in Grade 3+3 and Grade 4+4. But TCF-1 expression was significantly increased in Grade 4+5/5+4 (0.61±0.28-fold, mean±SEM; *P<0.05). This indicate this could be used as putative bio marker for Grade 4+5/5+4 PCa. Again, nuclear expression was also visible (Fig. 3.3) indicating a putative complexing with β-catenin, essential for Wnt/β-catenin transcriptional activity.

The mechanism involved in TCF-1 role in prostate cancer could be speculated from the results described above. Wnt signalling pathway is a crucial pathway in carcinogenesis. Any genetic defection in this pathway may lead to development of prostate and other cancers (Chap-I, Sec. 1.14). Furthermore, mutations, such as that in the APC gene (see above) leads to stabilization of β-catenin which in turn mediates in appropriate gene activation (Polakis, 2000). Increased β-catenin in advance malignant prostate cancer increases the expression of TCF-1, as some of the genes involved in Wnt signal transduction are also targets of Wnt/β-catenin transcription.

The SOX18 (Sex determining region Y (SRY)-box 18 (SOX18)) gene encodes transcription factors that have been recently discovered to be overexpressed in various human types of cancer and maintain behaviour of cancer cells (Wünnemann et al., 2016). Transcription factor SOX18 is overexpressed in PCa, the expression of SOX18 is notable correlated with both the clinical characteristics of patients and the malignant biological behaviour of PCa cells. SOX18 may promote PCa progression via the upregulation of various transcription factor including TCF-1 (Yin et al., 2017).

3.5.6. Cx43 expression in normal, Grade 3+3, Grade 4+4 and Grade 4+5/5+4 PCa

Cx43 is an archetypal member of the gap junction protein family. Gap junction proteins complex to form transmembrane protein channels between two adjacent cells to allow the exchange of intracellular content (small molecules and ions) and communication for regulation of cell proliferation, differentiation and homeostasis (Alexander and Goldberg, 2003). Generally, Cx43 is expressed in the cell membrane of mesenchymal and epithelial cells to form a gap junction to communicate with adjacent cells. Gap junctions are known to be involved in PCa development

and progression (Czyż et al., 2012). In the prostatic epithelial cells, Cx43 shows specific expression pattern and is expressed in undifferentiated progenitor and basal epithelial cells (Habermann et al., 2001). The nature of interaction between cancer epithelial cells and tumour microenvironment (TME, the surrounding stromal compartment in which cancer cells resides), is complex (Krušlin et al., 2015). TME also contains different types of non-malignant cells such as activated fibroblasts, infiltrating macrophage and other immune cells and endothelial cells (Mueller and Fusenig, 2004). Gap junction communication may also regulate the cancer cell interaction with the TME.

I believe this is the first systematic investigation of the expression of Cx43 in normal, low grade and high grade prostate cancer to investigate Cx43 expression. It was particularly important to investigate the expression of Cx43 in PCa tissue as our laboratory recently identified it as a protein that complexes with β-catenin and is critical for Wnt signalling in prostate cancer cells (Hou et al., 2019). The objective therefore was to characterize the expression of Cx43 in PCa tissue to gain insights into its putative function in PCa. The results are described in section 3.4.3.6 and could be summarized to suggest that for the first time that Cx43 expression, specifically, is inversely co-related with the progression of high Gleason score in prostate cancer (Fig. 3.9).

There are some previous investigations that show anomalous Cx43 expression and loss of GJIC function is connected to the progression of urological tumours (Czyż et al., 2012). Different connexin levels were negatively correlated to tumour malignancy while increased connexin expression or restoration of GJIC function obstructed the tumour growth and overturned malignant tumour or malignant phenotypes (Xing et al., 2007). Cx43 could also repress tumour cell migration and invasion (Alexander and Goldberg, 2003). Habernmann and colleagues revealed that Cx43 was reduced in prostate cancer compared to that of BPH, which contributed to de-differentiation and progression (Habermann et al., 2001). Another study revealed that Cx43 expression showed a negative co-relation with established pathological features indicative of worse prognosis such as follow up time and preoperative PSA (Benko et al., 2011). In that study, univariate and multivariate analyses indicated that a decreased in Cx43 expression was found to be significant predictor of biochemical recurrence free-survival (BFS) (Benko et al., 2011). Furthermore, a significant reduction or loss of Cx43 expression in PCa tissues was related with

advanced clinic-pathological features and poor BFS or patients after radical prostatectomy (Xu et al., 2016).

Cx43 may play a suppressive role in tumorigenesis via GJIC or C-terminal tail-mediated signalling. The following mechanism could be postulated to explain the reduced expression of Cx43 with the progression of malignancy.

Firstly, Cx43-GJIC was found to facilitate the transmission of cAMP, leading to increased p27 levels and reduced tumour growth. Secondly, Cx43 is co-localized with β-catenin at the contact areas of adjacent cells. The binding of cell surface Cx43, free β-catenin amount is reduced for Wnt signalling, leading to regulation of cyclin D1 and anti-apoptotic Bcl-2 and reduced cell proliferation (Ai et al., 2000). Wang and colleagues also demonstrated that gap junction not only operate as a cell communication bridge but also affects permeability of cytotoxic medicine (Wang et al., 2007b). It has also been shown that the restoration of Cx43 expression triggered TNF-β receptor signalling to induce apoptosis of prostate cancer cells.

It could be postulated that Cx43 may protect against progression of prostate cancer. However, the underlying mechanism can be explained for the loss of Cx43 expression and the closure of the gap junction, leading to altered immune surveillance and in turn to the spread of the tumour cells. Majority of the neoplastic cells contain fewer gap junctions and GJIC has been obstructed compared with non-neoplastic cells. These findings could indicate that reduced Cx43 expression led to reduced GJIC, which could promote to unregulated epithelial development. Therefore, the result obtained from my studies support the suitability of Cx43 to be used as prognostic marker for Grade 4+4, Grade 4+5/5+4. Additionally, I observed the AUC value for ROC curve (Fig. 3.11) was found as 0.70 (ns $P>0.05$), 0.81 (*$P<0.05$) and 0.93 (****$P<0.0001$). This indicates that Cx43 could be proposed as a biomarker for risk stratification of PCa diagnosis (Table 3.3).

3.5.7. A possible explanation of malignancy in PCa based on the results described in this chapter

The results described in sections 3.4.3.2, 3.4.3.4 -3.4.3.6 investigated proteins that are part of the β-catenin transcription complex (Bian et al., 2020) and also AR protein critical for AR signalling which is known to play a role in normal prostate development and PCa. These results suggest a

consistent increase in the expression in Wnt/β-catenin transcription complex, by far the first comprehensive analysis of β-catenin transcription complex in PCa. An interesting observation is a putative antagonistic interaction between the increase in β-catenin transcription proteins compared to a decrease in the AR in high grade PCa. Of the various implications of these results could be that the progression of PCa is largely a function of which Wnt/β-catenin signalling plays a critical role. AR may act as a brake on Wnt/β-catenin and a progressive decrease in AR protein in increasing grade of PCa allows Wnt/β-catenin transcription. If this were the case an increase in Wnt/β-catenin gene transcription targets will be expected in higher grade PCa. This hypothesis could be tested by performing targeted or whole genome sequencing of low to high grade PCa.

In addition to direct activation of gene transcription, e.g., those of proto-oncogenes, a further mechanism of Wnt/β-catenin signal activation may be via changes in the expression of MicroRNAs (miRs). miRs play a pivotal role in regulating Wnt/β-catenin signalling pathway (Siemens et al., 2013). miRs change the expression of canonical Wnt signalling protein by binding mRNA to downstream 3'UTR region of the target mRNA. This normally leads to translational repression or mRNA degradation that affects both early development of embryo, tumorigenesis and metastasis (Timms and Hofkamp, 2011). For instance, the silencing of miR-34a and subsequent up-regulation of its target, β-catenin, was linked with liver metastasis of colon cancer (Siemens et al., 2013). For prostate cancer tumorigenesis, the miR-34 has demonstrated anti-proliferative and apoptotic function. But it has been observed that miR-34 is not active in malignant prostate cancer (Cheng et al., 2014).

3.5.8. Implications of the results presented in this chapter on PCa therapy

Our laboratory also focuses upon targeting Wnt signalling for prostate cancer therapy, as novel functional aspects of Wnt signalling have been identified (e.g., (Thrasivoulou et al., 2013 and Ashmore et al., 2019)) and it has been proposed that membrane potential regulating compounds, small molecules, already in clinical use to treat diseases other than cancer could be used to treat cancer. The results here will provide useful input in determining the different grades of cancer where this therapy could be most effective.

3.6. Summary

I believe that I have provided the first detailed analysis of the expression of Wnt related proteins, particularly Wnt/β-catenin transcription complex proteins such as PYGO2 and TCF-1 in different grades of prostate cancer. A further value is the investigation of AR in conjunction with Wnt signalling related proteins and also the expression analysis of Cx43, considered to enter the nucleus upon the activation of Wnt signalling as shown in the study by Hou et al. and may act as part of the TCF/LEF transcription complex. That a number of proteins involved in Wnt/β-catenin gene transcription process is dysregulated in higher grade prostate cancer, indicates a clear involvement of this key signalling pathway in prostate cancer.

The results in this chapter also showed the expression of AR and Wnt proteins in various grades of prostate cancer and how these signalling pathways may be simultaneously dysregulated in prostate cancer in general and in different grades of prostate cancer. A key discovery is the antagonizing feature of Wnt related and AR proteins, that suggest, for the first time that AR may be acting as a brake on Wnt transcriptional activity during the development of carcinogenesis. Future studies could include measurement of co-localization of all the nuclear protein to identify whether these form complexes or act independently at different sites on the genome.

3.7. Limitations

A limitation is the availability of number of tissue samples for different grades of cancer. This is a common problem when working with human tissue although a putative offsetting factor is the use of unbiased quantitative measurement of protein expression in this study. Another limitation that needs to be kept in mind is regarding the initial categorization of the pathology which is visual assessment and has its own limitations. This could also be addressed by incorporating within the sample size calculation. Another improvement could be introduced by validating the results by using an independent method such as measurement of gene transcription for the proteins investigated in this chapter. I aimed to improve this by implementing the RNAscope technique in the castrate resistant prostate cancer experiments described in the next chapter. Neither of these could be performed due to interruption because of Covid19 pandemic when the laboratory was shut down for nearly 8 months. Another way of doing this is to isolate RNA and

perform large scale or targeted gene expression analysis. This technique is difficult to implement in FFPE tissue samples where RNA is generally degraded. However, these experiments are now being conducted in our laboratory and future experiments may address this deficiency.

A key limitation however could be the limited sample size, particularly for high grade cancer. Our technical sample size calculation based on a large number of studies indicate that for a normal vs cancer categorization at least 18 normal and 25-30 samples are necessary (Arthurs et al., 2020; Symes et al., 2013; Arya et al., 2015 and Giuliano et al., 2016). The sample size used here was limited due to availability of tissue samples from the same hospital, within a limited span, with different grades for age and cohort matching. Ideally, this study should have been conducted with a larger sample size. This could be done in the future and the data from this study could be incorporated to increase the sample size. I would also have liked to analyse the survival data, but it was not available. Future studies could also investigate specific nuclear expression of these transcription factors, a limitation of the current study.

CHAPTER IV

Expression analysis of Wnt, AR and Connexin signalling proteins in human Castration Resistant Prostate Cancer (CRPC) *in situ*

4.1. Introduction

4.1.1. Role of androgen and androgen receptor (AR) signalling in prostate cancer

Prostate cancer (PCa) development depends on androgen signalling (Huggins and Hodges, 1972). Following Androgen Deprivation Therapy (ADT), PCa regresses temporarily, but generally recurs after 4-5 years of ADT and termed CRPC; these cancers then generally metastasize. Detailed mechanisms of CRPC development from hormone naïve PCa have been discussed in Chapter-I (Sec. 1.11.7).

PCa growth depends on the ratio of cells proliferating to those dying. There are several pathways via which CRPC development may occur. Androgens and AR signalling are a major, and one of the most studied, regulatory components for prostate growth, survival and apoptosis. Because of this ADT is primary treatment for PCa. The principal androgen in males is testosterone, produced mostly (~90%) by the Leydig cells in the testes and remainder in adrenal cortex, it then enters the blood stream, through binding with albumin and also with sex-hormone-binding globulin (SHBG). Testosterone is diffused into cytoplasm and converted by 5α-reductase to Dihydrotestosterone (DHT) a metabolite with enhanced binding affinity to the LBD of AR (Feldman and Feldman, 2001). DHT binds to the AR by replacing HSP (Brinkmann et al., 1999) followed by dimer complex formation which enters into nucleus and binds to androgen responsive elements (ARE – a sequence of nucleotides) in the promoter region of target genes followed by recruiting of co-activator which allow AR complex to interact with the general transcription apparatus (GTA) to stimulate or inhibit the target gene transcription (Shah et al., 2004 and Huggins, 1967).

ADT is the primary treatment procedure for metastatic and locally advanced disease by either medicinal or surgical castration in which source of testosterone supply is eliminated through the removal of the testes or applying hormonal treatment as antagonist (Crawford and Hou, 2009). ADT is still the most widely used treatment for patients with progressed PCa. Indeed, it has been reported that androgen deprivation lowers androgen receptor (AR) expression, apoptosis and the volume of tumour cell, but most of PCas eventually attain the ability to grow with little androgen availability (e.g., CRPC) (Kyprianou and Isaacs, 1988 and Kim et al., 2002). The

mechanisms leading to CRPC are categorised into three general classes, which mainly relate to AR signalling, namely (i) AR amplification, (ii) AR mutation and (iii) AR splice isoform overexpression. Another mechanism for increasing AR activity is the endogenous expression of androgen synthesizing enzymes in tumour tissues leading to *de novo* androgen synthesis and conversion of existing low amount of adrenal androgens into testosterone and DHT (Titus et al., 2005 and Locke et al., 2008). An increase in mRNA and protein for AR was shown in ~80% of CRPC (Linja et al., 2001; Haapala et al., 2007 and Taylor et al., 2010). AR signalling is activated by binding to its specific ligand, DHT and testosterone to LBD but mutations in LBD may broaden its stringent specificity. As a consequence, cancerous cells continue to proliferate and resist apoptosis through their use of other circulating steroid hormones if androgens level become minimal.

In LnCAP cells, generally used as an AR positive *in vitro* model cell line, the first AR mutation was discovered by Veldscholte and colleagues (Veldscholte et al., 1992). The presence of mutation in AR facilitates androgen antagonist e.g., flutamide and androgen agonist steroid hormone such as progestins, oestrogens and anti-androgens to bind to its LBD to activate AR signalling for PCa growth (Taplin et al., 1999). Certain growth factors such as insulin-like growth-factor-1 (IGF-1), keratinocyte growth factor (KGF) and epidermal growth factor (EGF) can activate the AR signalling by creating an 'outlaw' receptor and thereby induce AR target genes in the absence of androgen (Culig et al., 1994). IGF-1, the most efficient of the factors studied, induced a five-fold increase of PSA secretion in LNCaP cell (Culig et al., 1994).

AR activation promotes a proliferation of androgen-dependent cancer cells and a depletion in androgens results in the inhibition of apoptosis. A successful bypass of the cascade for AR signalling will lead to proliferation and inhibition of apoptosis, even without androgen and AR. The *BCL2* gene is an apparent candidate gene for bypass that can inhibits apoptosis. In the secretory epithelial cells, *BCL2* is not generally expressed except in Prostatic Intraepithelial Neoplasia (PIN) or CRPC (Colombel et al., 1993). Furthermore, by selecting for growth of prostate cancer xenograft in castrated mice, Liu et al. (1996) found the expression of *BCL2* in tumours that did not initially express *BCL2*. A blockage of *BCL2* in LnCAP xenograft model with anti-sense oligonucleotides was shown to delay the development of CRPC (Gleave et al., 1999).

4.1.2. Role of Wnt signalling in cancer and cross talk between different signalling pathways

Cell signalling is a complex and interactive process and although aberrant AR signalling pathway is recognised to be the most crucial pathway in CRPC, other pathways are also likely to be involved. It has been shown that exposure to androgen regulates the genes previously known to be involved in prostate carcinogenesis in PCa (Schaeffer et al., 2008 and Zhang et al., 2006). Some of these genes encode for proteins that are engaged in other developmental and carcinogenic pathways, for instance Wnt signalling regulated angiogenesis, apoptosis, migration and proliferation. A general narrative with regards to cell signalling pathways suggests that intracellular signalling pathways are always interconnected and there is considerable 'cross-talk' between different pathways.

It has been postulated that aberrant activation of Wnt/β catenin pathways, on its own, contributes to human cancer development (Davies et al., 2001). Wnt signalling was discovered to be associated in development of most colorectal cancer where mutation of APC is prevalent (Groden et al., 1991). Mutations in a number of genes in the Wnt signalling pathway (such as, Axin loss of function and constitutively activating *CTNNB1* mutations) are associated with different type of tumours (Herr et al., 2012) e.g., human breast cancer (Shulewitz et al., 2006); Triple Negative Breast Cancer (TNBC) also exhibits hyperactive Wnt signalling (Polakis, 2012). The subtype of TNBC including, ER (oestrogen receptor), PR (progesterone receptor) and HER2 (Human Epidermal Growth Factor Receptor 2) constitutes 15-20% of newly diagnosed breast cancer cases, is linked to higher grade, stem cell-like characteristics, increased aggression, unique pattern of metastasis and poor survival of patient (Lehmann et al., 2011). In the invasive TNBC subgroup, Wnt/β-catenin signal activation was selectively detected in conjunction with poor prognosis as identified by nuclear β-catenin and over expression of Wnt target Cyclin D1 (Khramtsov et al., 2010). Furthermore, it was found that canonical Wnt signalling pathway seems to contribute to the development of malignant melanoma, but their mechanism still remain unclear (Lim and Nusse, 2013). A number of trials have demonstrated an increased overall rate of patients with high nuclear β-catenin melanoma (Bachmann et al., 2005 and Chien et al., 2009).

Wnt signalling is also involved in leukaemia in which this signal is increased in haematopoiesis and leukaemia (Lento et al., 2013).

In addition, deregulation in Wnt signalling leads to imbalance of the process resulting in malignancies in intestine, liver (Guan et al., 2012 and Davies et al., 2001). Prostate morphogenesis is regulated by Wnt and AR signalling pathways (Logan and Nusse, 2004). Various studies have shown a close and functional interaction between AR and the Wnt signalling pathway that stimulate development of prostate tumours via over-expression of AR (Schweizer et al., 2008a), indicating a role for Wnt signalling in hormone refractory prostate cancer (recurrence of cancer after androgen deprivation therapy).

The main transducer of Wnt signalling pathway is β-catenin which is thought to interact with AR signalling pathway by binding with AR (Schweizer et al., 2008a and Yokoyama et al., 2014). Truica et al. showed that β-catenin directly binds to AR to stimulate its transcriptional activity by androgen, androstenedione and oestradiol in LnCAP cells (Truica et al., 2000). Some studies identified that β-catenin localisation in nucleus of autopsy samples collected from CRPC patients (de la Taille et al., 2003). Experiments were conducted to investigate the presence of β-catenin in CRPC. But the level or the location of expression for β-catenin was not undertaken into this investigation. Wnt signalling target proteins have not been investigated to determine their expression or location in CRPC. The mechanisms of AR and β-catenin interaction and how the activation of signalling that may lead to protein-protein interaction, however, remain largely unexamined. A functionally reciprocal and protein-protein interaction between AR and β-catenin may explain biological significance of β-catenin in PCa cells.

4.1.3. Role of Connexin 43 in Wnt signalling and cancer

Connexin 43, a widely expressed transmembrane protein which are known to form gap junction channels intercellularly in associated with other member of GAP junction proteins (Kotini and Mayor, 2015) (Discussed in Chap-III, Sec. 3.1.5). As stated previously, Cx43 was recently discovered in our lab as a target protein of Wnt signalling pathway (Hou et al., 2019). The expression of Cx43 was previously suggested to be involved in pathological progression of PCa (Benko et al., 2011). These authors showed that the expression of Cx43 is significantly altered in the aggressive prostate cancer cells and the expression level is negatively correlated with

pathological grading (Benko et al., 2011). A quantitative analysis of this is presented in the previous chapter confirms Benko et al's qualitative analysis. However, whether Cx43 is over-expressed in CRPC is not known and neither is its pattern of distribution in human prostate tissue, particularly in relation to Wnt and AR target proteins.

I believe that understanding the nature of expression and co-localization of AR, Wnt and Cx43 may enhance our understanding of putative interaction between these signalling pathways, particularly in CRPC. It is also to be noted, that most previous protein expression in PCa did not quantify protein expression (only visual, semi-quantitative analysis of scoring was performed). By using quantitative immunohistochemical techniques developed in our laboratory e.g., (Symes et al., 2013), I have aimed also to quantify the expression of AR, Wnt and Cx43 related proteins in CRPC.

I show for the first time that in addition to AR expression in CRPC, Wnt signalling targets β-catenin, other Wnt target proteins such as FRA-1, c-MYC and Cx43 are also expressed in CRPC. I have also analysed the co-localisation of AR and Wnt signalling target proteins in CRPC tissues to shed further light on the interaction between these critical cell signalling pathways.

4.2. Aims

In CRPC and non-CRPC tissue:

(i) Analyse the expression of AR protein

(ii) Quantify and compare the expression of Wnt target proteins including β-catenin, FRA-1 and TCF-1

(iii) Identify if Cx43, a new target of Wnt signalling, is expressed

(iv) Analyse co-localisation of AR and Wnt signalling protein including β-catenin, FRA-1, and c-MYC

(v) A further aim was to investigate the *in situ* RNA expression for Wnt signalling related genes in normal, low and high grade and CRPC

4.3. Methods

4.3.1. Immunohistochemical staining

4.3.1.1. Tissue collection and designing of Tissue Array (TA)

Human prostate tissue samples (a total of 56) were obtained from Guest Professor (Pathologist), Department of Pathology and Molecular Immunology Abel Salazar Institute of Biomedical Sciences University of Porto Professor, Portugal). The samples were 21 normal prostate tissue (NPT), 10 benign prostatic hyperplasia (BPH), 5 Grade 3+3 and 20 CRPC used to construct two slides named: RH19 and RH20_CRPC). RH19 slide composed of 36 samples (41 individual tissue cores): 21 NPT (21 cores), 5 Grade 3+3 (5 cores + 5 repeat cores), 10 BPH. RH20_CRPC slide made of 20 samples (40 cores): CRPC samples (20 CRPC cores +20 CRPC repeat cores). Prior to TA construction, H&E staining was performed (Chap-II, Sec. 2.3.1.1) to identify the region of interests by Pathologist (Sec. 2.3.1.2). Details of patients and sample are provided in appendix (Appx. 2).

4.3.1.2. Tissue array construction

Details of the tissue array construction were described earlier in Chap-II (Sec. 2.3.1.3). Briefly, the recipient block was placed on the block holder. The identical circular indents were made by the small (recipient) and large (donor) punches. Each of the punch was 3mm deep into a paraffin block. The large punch *stylate* was used to inject the tissue core into the hole created by smaller punch. The diameter of core was 1mm and distance between two adjacent cores was 2.5mm. Following construction, TA was incubated at 37°C for 30 min by applying light and even pressure to the surface of block to level the height of the cores.

4.3.1.3. Tissue dewaxing and antigen retrieval

The tissues were sectioned with microtome with 6 µm thickness. Details of procedure of tissue dewaxing and antigen retrieval were described in Chap-II (Secs. 2.3.1.4. and 2.3.1.5).

4.3.1.4. Blocking of non-specific binding site

The tissue sections were blocked by incubating in 3% H_2O_2 menthol solution for 30 min for endogenous peroxidase activity. Non-specific binding was blocked by incubation with 10% normal serum and 1% BSA. Details were discussed in Chap-II (Sec. 2.3.1.6).

4.3.1.5. Determination of specificities of antibodies

A negative control (omission of primary antibody) experiment was performed to assess whether the secondary antibodies generate any non-specific band (Chap-II, Sec. 2.3.1.7).

4.3.1.6. Immunostaining of Prostate and PCa tissues

Wnt, AR and Connexin signalling proteins were investigated to measure their expression in NPT, BPH, Grade 3+3 PCa and CRPC tissue using two methods: 1. Chromogenic (DAB:3,3'-Diaminobenzidine) and 2. Immunofluorescence staining methods. Staining of slides was conducted by Mike Millar (University of Edinburgh) (Chap-II, Sec. 2.3.1.8). The latter was an improvement on only the single label (DAB) analysis presented in the previous chapter. Multi-label immunofluorescence also provides a further layer of analysis as co-localization of multiple proteins can also be measured (Symes et al., 2013 and Arthurs et al., 2017).

4.3.1.6.1. Immunostaining of prostate and PCa tissues using single label chromogenic staining method

Chromogenic (DAB: 3,3'-Diaminobenzidine) staining was described in detail previously (Chap-II, Sec. 2.3.1.8.1). The DAB staining was aimed to determine the sole expression of a protein of Wnt and AR signalling pathways in non-CRPC and CRPC tissues.

The TAs were termed RH19 and RH20_CRPC; 56 samples, of which 36 on RH19 (41 cores: 21 NPT + 10 BPH + 10 Grade 3+3) and 20 RH20_CRPC (40 cores: 20 cores + 20 cores repeat) were used for the DAB staining. Anti-AR and anti-Cx43 antibodies (Table 4.1) were used to measure the expression of AR and Cx43 in NPT, BPH, Grade 3+3 and CRPC tissues.

Table 4.1. Details of antibodies used in chromogenic staining. The table is representing the antibodies and their corresponding host, catalogue, manufacturer and dilution used in the experiment

Primary antibody		Host	Cat. and Manufacturer	Dilution	Cores on the slide were Stained
Anti-AR antibody		Rabbit	Ab133273, ABCAM	1:400	RH19: 41 cores, RH20_CRPC: 40 cores
Anti-Cx43 antibody		Rabbit	C6219: Sigma	1:1000	RH19: 41 cores, RH20_CRPC: 40 cores
Secondary antibody	Peroxidase AffiniPure Donkey Anti-Rabbit IgG (H+L)	Donkey	711-035-152, Jackson Immunoresearch laboratory (JIL)	1:500	Used against Anti-rabbit primary antibodies

The tissue sections were stained with anti-AR and -Cx43 antibodies (Table 4.1) using Bond Max automated staining system (Leica Biosystems, Milton Keynes, UK) according to manufacturer's protocol (Chap-II, Sec. 2.3.1.8.1).

4.3.1.6.2. Imaging and signal quantitation

AR and Cx43 Ab-labelled DAB-stained cores were scanned using NanoZoomer-RS Scanner. Following segregation of images, an unbiased and semiautomated method was used to the DAB signal for anti-AR and anti-Cx43 antibodies. For quantitation, ImageJ software using an algorithm was used. The data were generated as AFperAMT which were fitted to probit regression (Chap-II, Sec. 2.3.1.8.1A) for AR and Cx43.

4.3.1.6.3. Statistical analysis

Mountain plot and Box plots were constructed using GraphPad Prism, version 8.0.0 (GraphPad Software, San Diego, California USA. Median selection and statistical test (significance of differences) were performed using Mann-Whitney U test (ns $P>0.05$; *$P<0.05$; P**<0.01; ***$P<0.001$; ****$P<0.0001$).

4.3.1.6.4. Immunostaining of prostate and PCa tissues using fluorescence staining method

Multi-label immunofluorescence staining was conducted using similar techniques as that for chromogenic label, except a Tyramide based system (Toth and Mezey, 2007) refined by our laboratory was used (Symes et al., 2013; Arya et al., 2015; Giuliano et al., 2016; Arthurs et al., 2017 and Arthurs et al., 2020). Wnt and AR signalling protein proteins were investigated to

measure the expression and co-localization in non-CRPC (normal prostate tissue (NPT), benign prostatic hyperplasia, Grade 3+3) and CRPC tissues. 56 samples of which 36 on RH19 (41 cores: 21 NPT + 10 BPH + 10 Grade 3+3) and 20 RH20_CRPC (40 cores: 20 cores + 20 cores repeat) used for the fluorescence staining.

4.3.1.6.4.1. Immunostaining of non-CRPC and CRPC tissues

A multilabel fluorescence staining experiments was carried out to measure the expression and co-localisation of AR, β-catenin, FRA-1and c-MYC.

Table 4.2. List of antibodies for immunofluorescence staining. The table is representing the antibodies and their corresponding host, catalogue, manufacturer and dilution used in the experiment.

Primary antibody	Fluorophores (Laser/excitation-emission (nm)	Host	Cat and Source	Dilution
Anti-Fra-1 antibody	Tyr-Alexa 405 (405/415-480)	Rabbit	ab252421: ABCAM	1:200
Anti-β-Catenin antibody	Tyr-FITC (488/500-550)	Mouse	Ab22656, ABCAM	1:200
Anti-AR antibody	Tyr-Cy3 (559/575-620)	Rabbit	Ab133273, ABCAM	1:250
Anti-c-MYC antibody	Tyr-Cy5 (635/645-740)	Rabbit	C3956, Sigma	1:200
Secondary antibody	Peroxidase AffiniPure Donkey Anti-Mouse IgG (H+L)	Donkey	715-035-151: Jackson Immunoresearch Laboratory (JIL)	1:500
	Peroxidase AffiniPure Donkey Anti-Rabbit IgG (H+L)	Donkey	711-035-152: Jackson Immunoresearch laboratory (JIL)	1:500

Immunofluorescence staining was conducted using an automated bond system using a protocol adapted from (Toth and Mezey, 2007). The staining protocol is described elsewhere (e.g., (Arya et al., 2015)).

4.3.1.6.4.2. Fluorescence imaging of antibodies FRA-1, β-catenin, AR and c-MYC signal

Image of each core of RH19 and RH20 were obtained using Zeiss Axioscan Z.1 slide scanner (Carl Zeiss) at 20x magnification (Arya et al., 2015). The fluorescent signals were optimised prior to conducting Axioscan to avoid oversaturation of signal faint for each antibody. For a standardized comparison, the power of Calibri.2 LED lights and integration times of the Hamamatsu ORCA Flash4 camera (Hamamatsu Photonics) were kept constants for all samples. The imaging of the

slides was carried out at the same time sequentially with identical image acquisition settings. Montages of each core were automatically generated and accumulated from multiple 2048x2048 pixel with 16-bit gray level which were compiled locally on the acquisition computer.

4.3.1.6.4.3. Quantitation of the expression of Wnt and AR signalling proteins

The experimental design was double blind, as described in previous chapter. To quantify the expression of each protein, an unbiased, reproducible and automated analysis was employed to quantify the intensity of each fluorophore used in the tissue array to measure the amount of expression of each antibody in prostate normal and malignant tissues (Symes et al., 2013). A plugin adapted to ImageJ was scripted to semi-automatically discriminate the whole TA, largely based on a threshold segmentation routine, was used. Lower and upper threshold parameters was standardised prior to include the median to maximum gray value of a range of samples across the whole sample set. These values were then used to perform a batch analysis of the entire sample set, where the mean gray values per TMA core was calculated (Symes et al., 2013).

4.3.1.6.4.4. Quantitative co-localization of Wnt and AR target proteins using High resolution confocal microscopy

Eighty cores of control and malignant tissues were used in which 3 ROIs in each core were selected and imaged with confocal Microscope Leica TCS SP8 using oil emersion 63X 1NA objectives with zoom 6x (Chap-II, Sec. 2.3.1.8.2). The images were saved as a lif file which were imported to Huygens Professional Software for deconvolution. The deconvolved images were saved as Huygens specific (HDF5) files for each channel (excitation/emission nm). The antibodies (Table 4.2) were fluorescently labelled with Tyr-Alexa 405 (405/415-480: Blue), Tyr-FITC (488/500-550: Green), Tyr-Cy3 (559/575-620: Orange), Tyr-Cy5 (635/645-740: Red) and the HDF5 files were used to calculate Pearson coefficient for co-localisation using a written script adapted to Huygens pro (Arya et al., 2015).

4.3.2. RNAscope for single molecule RNA analysis

Single molecule RNA detection combined with protein expression for the products of the same RNA molecules could provide a powerful correlation and a clear picture of transcriptional and translational changes that may occur during different stages of a disease. The ultimate objective

is to conduct both single molecule RNA and protein expression on the same slide; to establish this technique and work towards the longer-term aim, however, I have conducted these experiments to be conducted on different tissue array slides.

4.3.2.1. Application of positive and negative control to verify RNA quality and specificity

Peptidylprolyl Isomerase B (PPIB) and RNA Polymerase II Subunit A (POLR2A) were used to assess the quality of RNA expression of PPIB and POLR2A in each core of the slides. A universal negative control with probes targeting the Dap B (Diaminopimelate B) gene, encodes dihydrodipicolinate reductase, from the soil born bacterium*, Bacillus subtilis* strain SMY was used to observe the background staining (Chap-II, Sec. 2.3.2.1).

4.3.2.2. RNAscope: in situ single molecule RNA analysis in normal, low, high grade and castration resistant prostate cancer tissue

Four Wnt signalling related proteins including β-catenin, PYGO2, FRA-1 and TCF-1 were used to determine their RNA expression based on the contribution in PCa development. Tissue cores of normal prostate, BPH, Grade 3+3, Grade 4+4, Grade 4+5/5+4 and CRPC distributed over slides RH16, RH17, RH18, RH19 and RH20_CRPC (Appx. 2) were undertaken into the experiment. RNA probes were designed to hybridize the target RNA molecules of Wnt targets including β-catenin, PYGO, FRA-1 and TCF. Details staining described in Chap-II (Sec. 2.3.2.2).

4.3.2.3. Detection of signal of RNAscope probes

Detail protocol for detection of signal of RNAscope probe has been described in Chap-II (Sec. 2.3.2).

4.3.2.4. Imaging and statistical analysis

RNAscope slides were scanned using Axioscan (Carl Zeiss) with 40x, 20x and 10x objectives. The stained cores were also scanned using NanoZoomer-RS Scanner (Type: C10730-02) with resolution 0.23µm/pixel (40x high resolution mode) (Hamamatsu Photonics UK Ltd, Welwyn Garden City, UK). Python software with Jupyter notebook (batch analysis) was used to quantitate the expression of β-catenin RNA (red punctate dot). RNA expression (green punctate dot) for FRA-1, PYGO2 and TCF-1 expression was counted manually. Prior to quantitation, threshold was

applied for each image using hue, saturation and brightness. Each of the punctate dot indicate a single molecule of each RNA molecule. The quantified number was used to construct box to measure the expression of each single RNA molecule. Statistical analysis was performed (Sec. 4.3.1.6.3).

4. 4. Results

To elucidate the role of Wnt and AR pathways in PCa, it was also important to determine the level of expressions and interactions of Wnt and AR signalling protein and RNA *in-situ*. This is the first-time multi-fluorophore labelled, quantitative immunofluorescence technique, in combination with high throughput and confocal imaging and unbiased fluorophore signal quantification are being applied to investigate the expression and co-localization of Wnt and AR signalling targets in PCa (and normal and BPH) tissue *in-situ*.

Our laboratory has developed and refined unbiased, quantitative immunohistochemistry to identify and characterize various biomarkers and proteins in PCa and other cancers (Symes et al., 2013 and Arthurs et al., 2017). RNA levels, particularly, are highly dynamic and integrate both genetic and epigenetic mechanisms of gene regulation, serving as an excellent molecular phenotypic readout of the functional state of cells and tissues.

4.4.1. Histological characterisation of non-CRPC cores (e.g., normal, BPH and Grade 3+3 tissue) and CRPC tissue cores

The tissue cores were histologically analysed to characterise the NPT, BPH, grade 3+3 and CRPC by using magnified images of the tissue cores obtained from AxioScan (e.g., Fig. 4.8). The cores were magnified into 40x to identify histological feature of the tissues. The normal prostate tissues were recognised by observing the morphologically distinct well organised epithelial layer containing luminal cells and basal cells (Szczyrba et al., 2017). The benign prostatic hyperplasia (BPH) was predominantly characterised by an increased number of epithelial and stromal cells in perineural area of the prostate and nodules in stroma and gland (Roehrborn, 2008) and Grade 3+3 is characterized with developed well-differentiated glands, which are separated by stroma. The glands are arisen close to each other with minimum amount of intervening stroma. The

glands are lined by columnar neoplastic cells but lacking a layer of basal cells (Kweldam et al., 2019).

4.4.2. Analysis of the expression of Wnt and AR target proteins through chromogenic immunostaining in non-CRPC (e. g. normal prostate, BPH and lower Gleason grade 3+3) and CRPC tissues

In the previous chapter (Chap-III, Sec. 3.4), I analysed the expression of AR and Wnt signalling proteins (e.g., AR, β-catenin, FRA-1, PYGO2, TCF-1 and Cx43) in NPT and prostate cancer tissue of different grades (Grade 3+3, Grade 4+4 and Grade 4+5/5+4). Here, I have analysed and quantified the expression of AR (e.g., AR) and Wnt (e.g., Cx43) signalling proteins in CRPC and also will show the expression in NPT, BPH and Grade 3+3 PCa tissue. 41 non-CRPC and 40 CRPC cores were used in this staining. Negative staining (omitting primary antibody) experiment were also conducted to check quality of the antibodies against target proteins.

4.4.3. Quantitative analysis of AR and Wnt signalling related protein expression in non-CRPC and CRPC tissue

The non-CRPC (n=41) and CRPC (n=40) were stained with DAB-HRP using anti-AR and Anti-Cx43 antibodies. Following staining, the cores on the slide were scanned using a Nanozoomer slide scanner at 40x magnification (0.23μm/pixel resolution). Following segregation of images, an unbiased and semiautomated method was used to measure the DAB signal for anti-AR and anti-Cx43 antibodies. For quantitation, ImageJ software using an algorithm was used. The data were generated as AFperAMT (area fraction/amount of tissue on the core) which were fitted to probit regression (Chap-II, Sec. 2.3.1.8.1.). Significance of difference between NPT vs BBPH, NPT vs Grade 3+3 and NPT vs CRPC was calculated using Mann-Whitney U test (* $P<0.05$, ** $P<0.01$, *** $P<0.001$).

Prior to staining with primary antibodies against AR and Wnt related proteins, a negative staining control for these antibodies was performed in both non-CRPC and CRPC tissue cores. Figure 4.1 shows that there was virtually no background signal or autofluorescence when only secondary antibodies were used as negative controls.

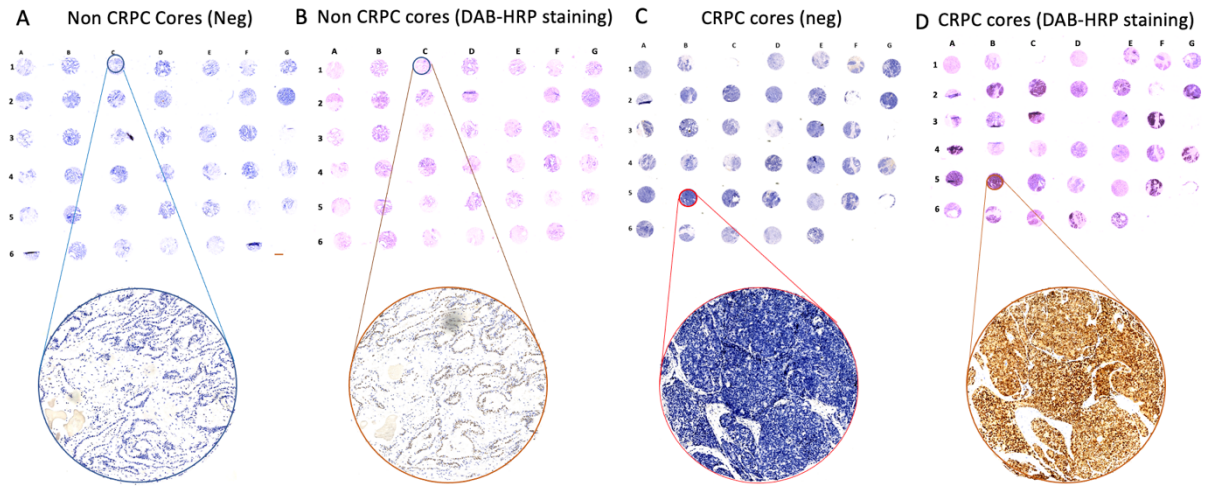

Figure 4.1. Representative images for the negative staining of non-CRPC and CRPC cores. A. Negative staining of non-CRPC cores. B. Anti-AR antibody with DAB-HRP staining of non-CRPC cores. C. Negative staining of CRPC cores. D. Anti-AR antibody with DAB-HRP staining of CRPC cores.

4.4.3.1. Expression analysis of AR in NPT, BPH, Grade 3+3 and CRPC tissues

AR protein was expressed in normal prostate tissues (NPT), BPH, Grade 3+3 and CRPC tissue samples (Fig. 4.2). The Fig. 4.2.B shows increased expression of AR in BPH compared to AR expression in NPT (Fig. 4.2.A). The probit value (AF/AT) (Chap-II, Sec. 2.3.1.8.1.) was used for statistical analysis (e.g., Mann-Whitney U test) and to construct mountain plot to calculate the level of protein expression (Fig. 4.2.B2-D3). Fig. 4.2 shows that AR expression was significantly increased in BPH (11.46±0.64-fold, mean±SEM; *P<0.05) compared to NPT. This indicates AR receptor may play an important role in BPH development. A decreased AR expression was observed in Grade 3+3 tissue (Fig. 4.2.C1, a magnified image of tissue core 4.2.C) compared to AR expression in NPT. The result (Fig. 4.2.C2) indicated AR expression was significantly reduced in Grade 3+3 PCa tissue (-0.81 ± 0.39-fold, mean±SEM; *P<0.05) when compared to NPT. This result reflects the result observed in Chap-III where AR expression was reduced in Grade 3+3 PCa (Chap-III, Sec. 3.4.2.1). This confirms that AR expression is reduced with moderately differentiated cells in PCa tissue (Chap-III, Sec. 3.1). The result (Fig. 4.2.D) showed higher intensity of DAB signal for AR expression than AR signal in NPT, Grade 3+3 PCa (Fig. 4.2.A and C). The analysis showed AR expression was significantly increased in CRPC (9.07 ± 2.67-fold, mean±SEM; **P<0.01) and (8.94 ± 1.91-fold; mean±SEM; ***P<0.01) and compared to AR expression in NPT (Fig. 4.2. D2) and non-CRPC tissue (NPT, BPH and Grade 3+3 were included) (Fig. 4.2.D3)

respectively. This result confirms overexpression of AR in CRPC tissue which was found by Grasso et al. (Grasso et al., 2012).

I also investigated the usefulness of AR protein as biomarkers for prostate cancer by calculating the true positive rate (sensitivity) and false positive rate (1-specificity) by ROC curve (Fig. 4.4). An area under the curve (AUC) of 1.0 for an ROC curve suggests a high selectivity and sensitivity; a value of 0.5 indicates the marker cannot distinguish between condition A and condition B. AR analysis yielded an AUC value for ROC curve 0.76 (Table 4.4).

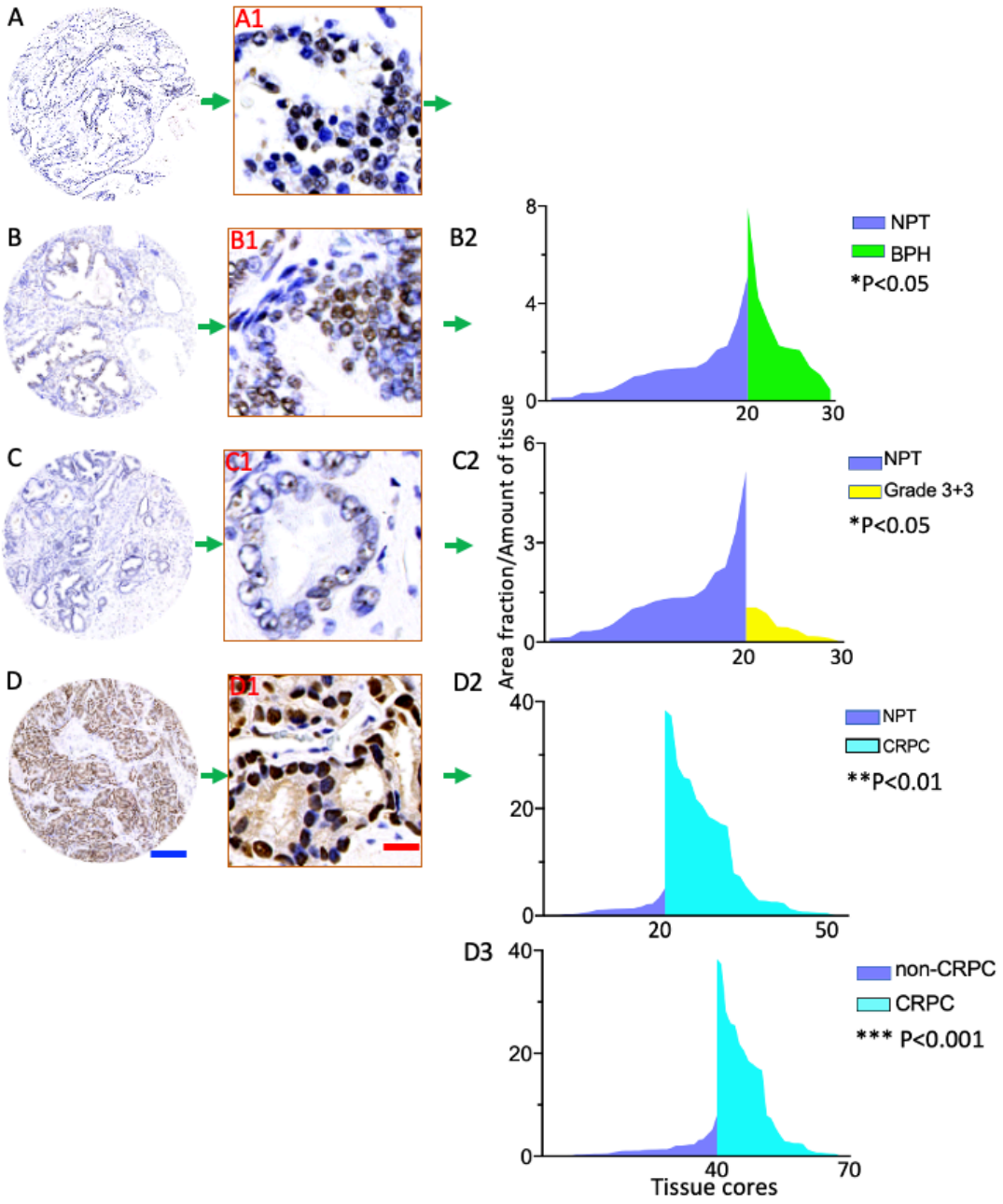

Figure 4.2. Representative images for the staining and quantification of DAB signal for AR in NPT, BPH, Grade 3+3 and CRPC. The A, B, C and D representing AR antibody with DAB-HRP staining cores of NPT (n=21), BPH (n=10), Grade 3+3 (n=10) and CRPC (n=40), respectively. A1, B1, C1 and D1 are the 40x magnification of A, B, C and D respectively to illustrate the expression. The tissue cores were scanned with NanoZoomer-RS Scanner (Type: C10730-02) with resolution 0.23µm/pixel (40x high resolution mode). Each of the image of cores was undertaken to measure expression of AR. An unbiased ImageJ was used to quantify protein expression (Sec. 4.3.1.6.2). Following quantitation, the data were generated as area fraction (AF)/amount of tissue (AMT) which were used to construct mountain plot. B2, C2 and D2 representing the expression of AR in BPH vs NPT, Grade 3+3 vs NPT and CRPC vs NPT of B, C and D respectively. D3 representing AR expression in CRPC compared to non-CRPC (combine of AR expression in NPT, BPH and Grade 3+3). The expression of AR vs BPH showed significant higher expression (* P<0.05) in BPH whereas expression of AR was decreased significantly (* p<0.05) in Grade 3+3 and but was increased in CRPC vs non-CRPC (*** P<0.001). (AF: Area Fraction; AT: Amount of Tissue). Scale bar: 100 µm (for full core image) and 10 µm (Fragmented image)

Table 4.3. Quantitative analysis of protein expression in BPH, Grade 3+3 and CRPC tissue arrays. The table shows the fold increase of expression and significance of differences for AR and Cx43 proteins in BPH, Grade 3+3 and CRPC compared to NPT. The results represent as mean±SEM of values of AF/AT (probit).

Protein	BPH		PCa Grade 3+3		CRPC	
	Fold change	Significance (<P)	Fold change	Significance (<P)	Fold change to non-CRPC	Significance (<P)
AR	1.46 ± 0.64	*P<0.05	-0.82 ± 0.40	*P<0.05	8.94 ± 1.92	***P<0.001
Cx43	4.82 ± 1.99	*P<0.05	-3.13 ± 1.45	*P<0.05	-3.00 ± 1.00	**P<0.01

4.4.3.2. Expression analysis of Cx43 in NPT, BPH, Grade 3+3 and and CRPC tissues

This is the first systematic analysis of the expression of Cx43 in large number of human prostate tissue samples. Cx43 was expressed in NPT, but its expression was increased significantly in BPH (4.82 ± 1.99-fold, mean±SEM; *P<0.05) compared to Cx43 expression in NPT (Fig. 4.2.B2). The expression of Cx43 was significantly reduced in Grade 3+3 (-3.13±1.4-fold, mean±SEM; P<0.05) compared to Cx43 expression in NPT (Fig. 4.2.C2). Its expression was further reduced in CRPC (-3.008 ± 1.002-fold, mean±SEM; **P<0.01) (Fig. 4.2.D2). The AUC value for ROC curve was 0.77, 74 and 71 for Cx43 expression in BPH, Grade 3+3 and CRPC respectively, that indicates its suitability to be used as potential biomarker (Table 4.4). Although at first sight it appears counterintuitive that a protein involved in Wnt signalling may show a reduced expression. However, the role of Cx43 has been proposed as a chaperon protein, possibly involved in the destruction complex – a protein complex that sequesters β-catenin, a transcription factor co-activator and a key transducer of Wnt signalling (Clevers, 2006). Interestingly, (Hou et al., 2019) showed that knockdown of Cx43 in prostate cancer cells desequesters (allows it to become free

in the cytosol) β-catenin which will increase its availability in the cytosol and increased probability of β-catenin entry into the nucleus. This in turn may result in increased Wnt/β-catenin mediated gene transcription which includes many proto-oncogenes and transcription factors. Conversely, an increase in the expression of Cx43 in BPH, in the specific context of Wnt signalling, may indicate that there is a reduced role of Wnt/β-catenin transcription in BPH. However, another function of Cx43 is its function as intercellular gap-junctions (Söhl and Willecke, 2003). Indeed, (Habermann et al. found similar observations in frozen human prostate BPH section, although no quantitation was performed (Habermann et al., 2001).

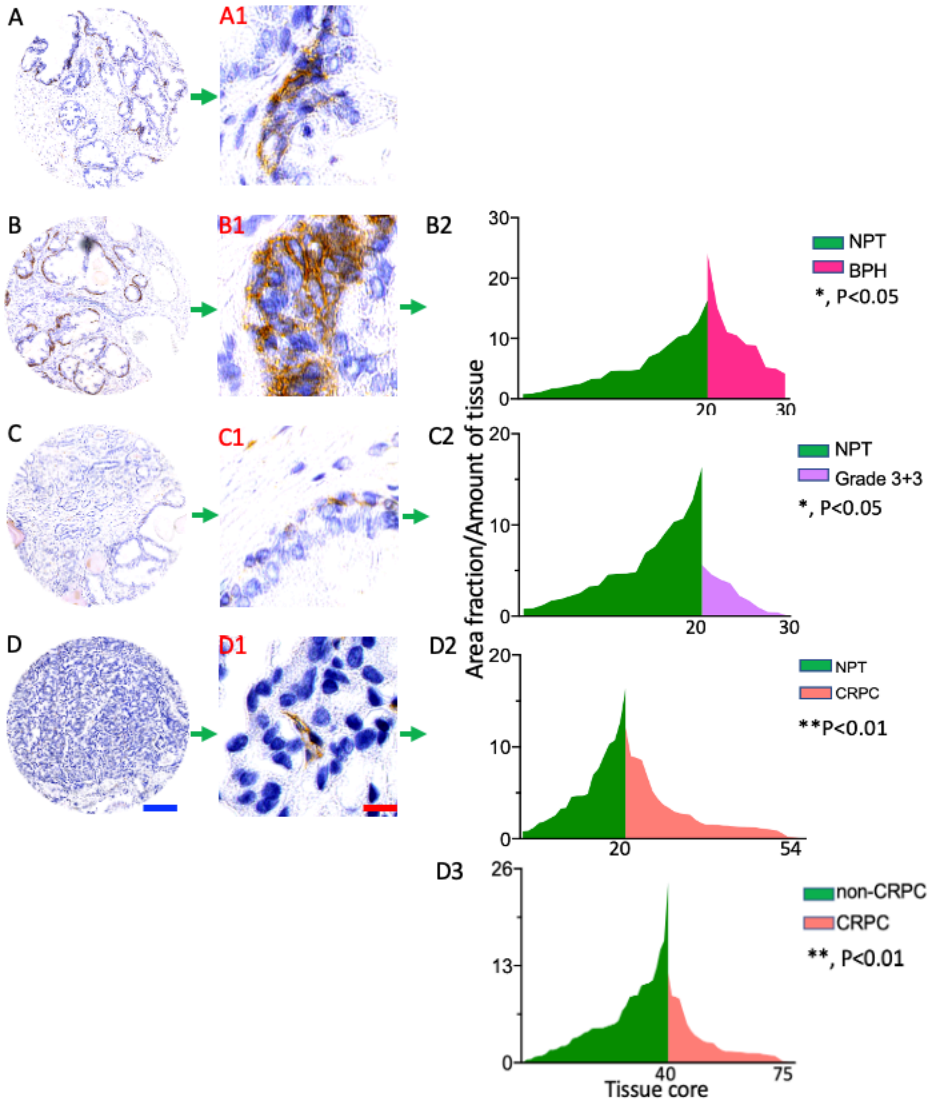

Figure 4.3. Representative images for the staining and quantification of DAB signal of Cx43 in NPT, BPH, Grade 3+3 and CRPC. The A, B, C and D representing staining of AR antibody with DAB-HRP staining cores of NPT, BPH, Grade 3+3 and CRPC respectively. A1, B1, C1 and D1 are the 40x magnification of A, B, C and D respectively to illustrate the

expression. The tissue cores were scanned with NanoZoomer-RS Scanner (Type: C10730-02) with resolution 0.23µm/pixel (40x high resolution mode). Each of the image of cores was undertaken to measure expression of AR. An unbiased ImageJ was used to quantify protein expression (Sec. 4.3.1.6.2). Following quantitation, the data were generated as area fraction (AF)/amount of tissue (AMT) which were used to construct mountain plot. B2, C2 and D2 representing the expression of AR in BPH vs NPT, Grade 3+3 vs NPT and CRPC vs NPT of B, C and D respectively. D3 representing Cx43 expression in CRPC compared to non-CRPC (combining of Cx43 expression in NPT, BPH and Grade 3+3). The expression of Cx43 in BPH showed significant higher expression (*P<0.05) whereas expression of Cx43 was decreased significantly (* p<0.05) in Grade 3+3 and was reduced further in CRPC vs non-CRPC (**P<0.01). (AF: Area Fraction; AT: Amount of Tissue). Scale bar: 100 µm (for full core image) and 10 µm (Fragmented image).

ROC curve was constructed to calculate true positive rate (sensitivity) and false positive rate (1-specicity) to establish whether AR and Cx43 could be the potential candidate to be used as biomarkers for prostate cancer diagnosis. AUC values of 1 for an ROC curve of each protein implies high selectivity and sensitivity (see above).

Table 4.4. AUC for the protein expression of AR and Cx43 BPH, Grade 3+3 and CRPC. The table is representing AUC value, likelihood ration and significance of differences of AR and Cx43.

Protein	BPH			PCa Grade 3+3			CRPC		
	AUC	Significance (<P)	LR(+)	AUC	Significance (<P)	LR(+)	AUC	Significance (<P)	LR(+)
AR	0.76	*P<0.05	1+	0.75	*P<0.05	1+	0.74	***P<0.001	1+
Cx43	0.77	*P<0.05	1+	0.74	*P<0.05	-	0.71	**P<0.01	-

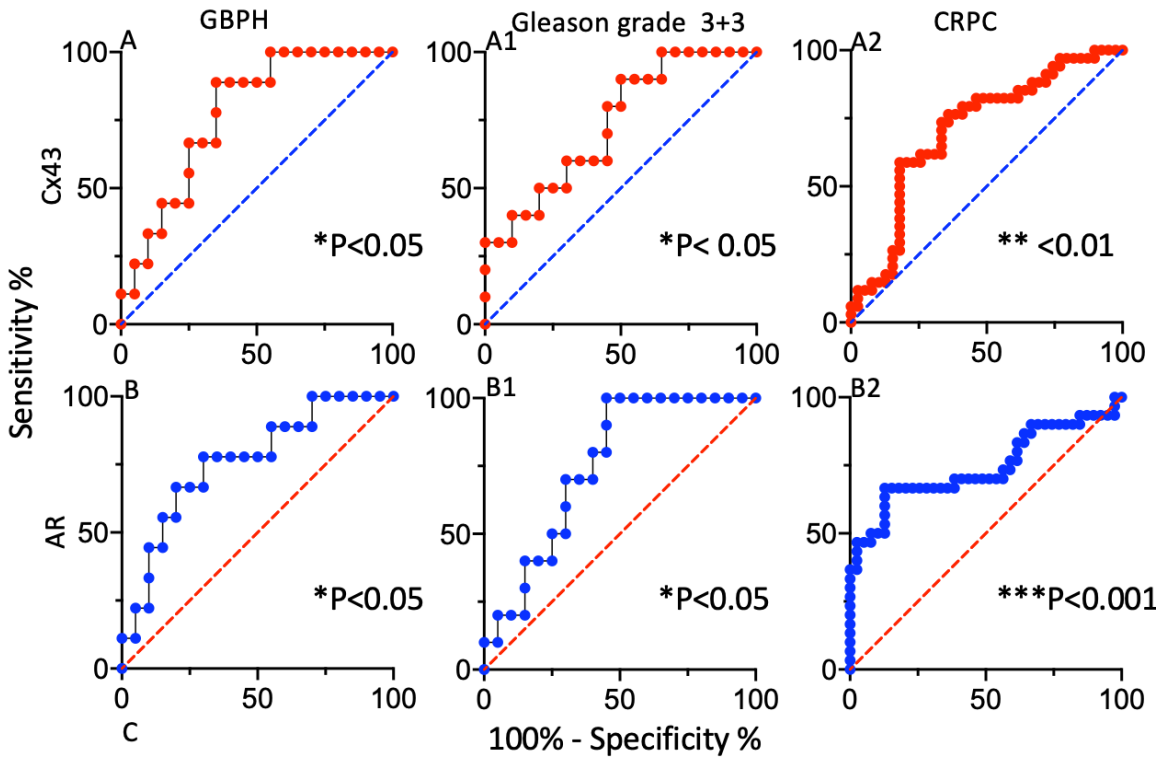

Figure 4.4. ROC of the AR and Cx43 in BPH, Grade 3+3 and CRPC tissues. ROC curve displaying the discriminating performance of the AR and Cx43 expression in the differentiation between NPT vs BPH, NPT vs Grade 3+3 and non-CRPC vs CRPC tissues using AF/AT data for AR and Cx43. The dotted line represents the ROC area of 0.5.

4.4.4. Analysis of expression of Wnt and AR target proteins using multilabel immunofluorescence staining in Non-CRPC and CRPC tissues

4.4.4.1. Staining and imaging of tissue arrays

The TA slides were probed with four antibodies, anti-FRA-1, anti-β-catenin, anti-AR and anti-c-MYC antibodies (Table 4.2) followed by staining with four fluorophores namely, Alexa Fluor-405, FITC, Cy3 and Cy5 (Table 4.2) sequentially. Imaging of each tissue core from TA RH19 and RH20 was performed using Zeiss Axioscan Z.1 slide scanner (Carl Zeiss) at 10x magnification to locate the core. Once the cores have been located were scanned with 20x magnification as described in materials and methods (Sec. 4.3.1.6.4.3).

All four fluorescent label signals were optimized at the start of study to avoid oversaturation of the fluorescence signal for each antibody. For a standardized comparison, the power settings for Calibri.2 LED lights and integration times of the Hamamatsu ORCA Flash4 camera (Hamamatsu Photonics) were kept constants for all samples. The imaging was performed on both slides (RH19

and RH20_CRPC) on the same day with identical image acquisition settings. Montages of the individual TA cores were automatically constructed from multiple 2048 x 2048 pixel 16 bit gray level images and stored locally on the acquisition computer. Composite images of whole tissue array used in this study are given in Fig. 4.5 and 4.6. I used the Axioscan acquired images to set up an imaging protocol.

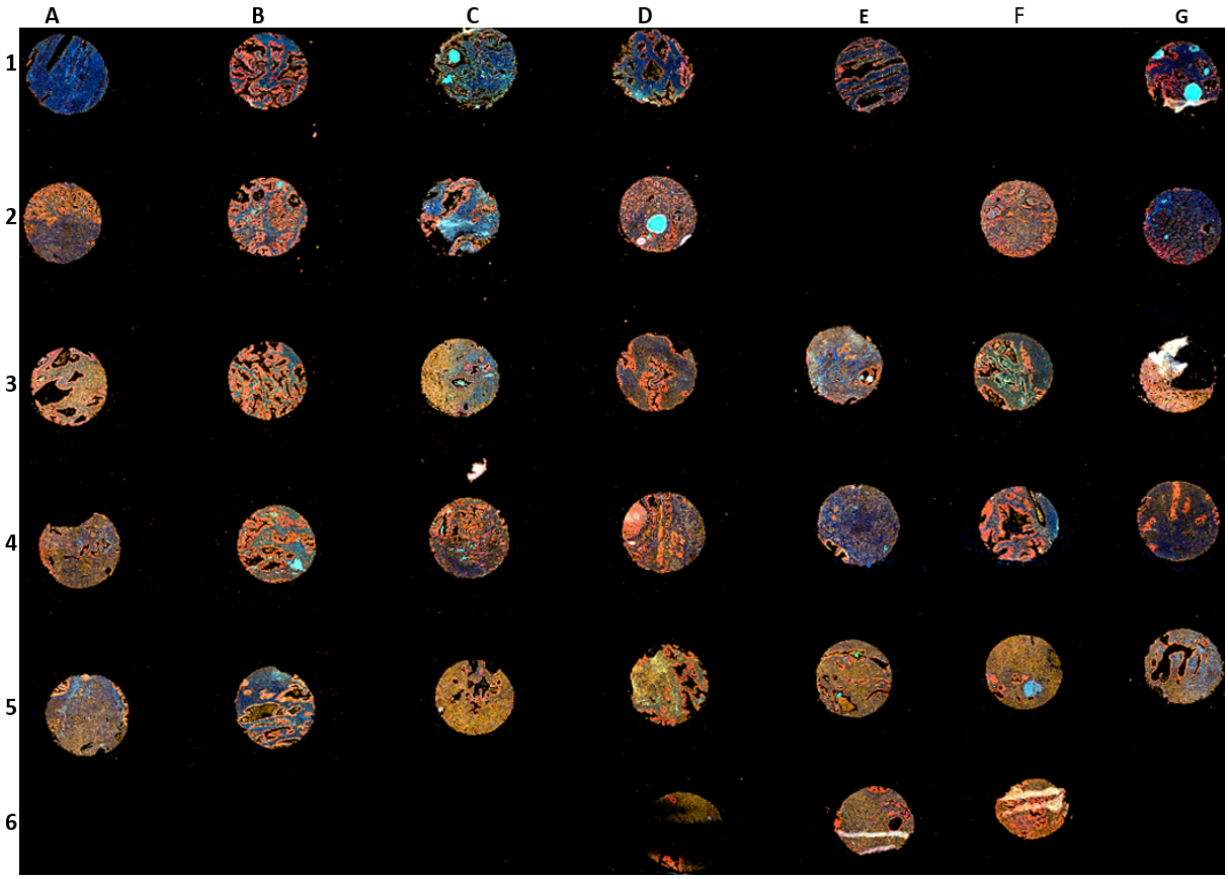

Figure 4.5. AxioScan image of whole non-CRPC tissue arrays. The tissue cores on the RH19 slide were stained with four fluorophores namely, Tyr-Alexa-405, -FITC, -Cy3, and -Cy5 for FRA-1, β-catenin, AR and c-MYC respectively and imaged using Zeiss AxioScan Z1 slide scanner. Displayed images of cores are composite (overlay of four fluorophores). The tissue array contains 41 non-CRPC tissues cores which includes normal prostate tissues (21 cores), BPH (10 cores) and Grade 3+3 (10 cores).

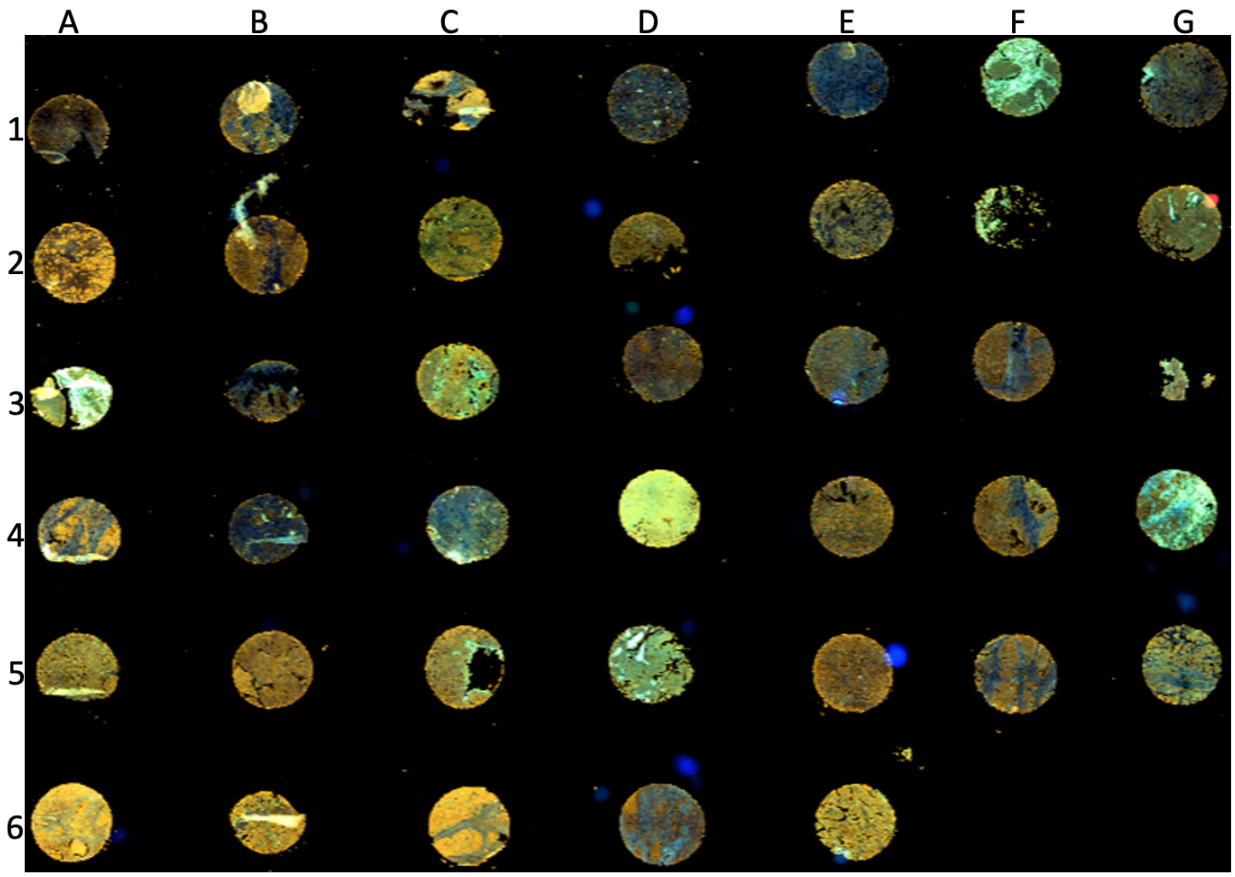

Figure 4.6. AxioScan image of CRPC tissue arrays on slide RH20_CRPC used in this study. The tissue cores were stainedwith four fluorophores namely Tyr-Alexa-405, -FITC, -Cy3, -Cy5 for FRA-1, β-catenin, AR and c-MYC respectively and imaged using Zeiss AxioScan Z1 slide scanner. Displayed image of cores are composite (overlay of four fluorophores). The TA contains 40 CRPC cores.

It is clear, even by visual analysis, that the expression of the four proteins tested, FRA1, β-catenin, AR and c-MYC are different. For example, the overall color representation appears dominant for red/brown stain in Fig. 4.5, compared to the predominant hue of green in Fig. 4.6. The macro level, visual analysis shows that the expression of Wnt targets in non-CRPC compared to CRPC tissue is likely to be different.

Two further types of analysis were therefore conducted: 1. Basic histological analysis 2. Quantitation of expression of the four proteins and analysis of their colocalization (Symes et al., 2013). The results for these are presented below. Four representative cores were selected from each category of normal prostate tissue (NPT) and PCa sample from AxioScan image for further histological assessment.

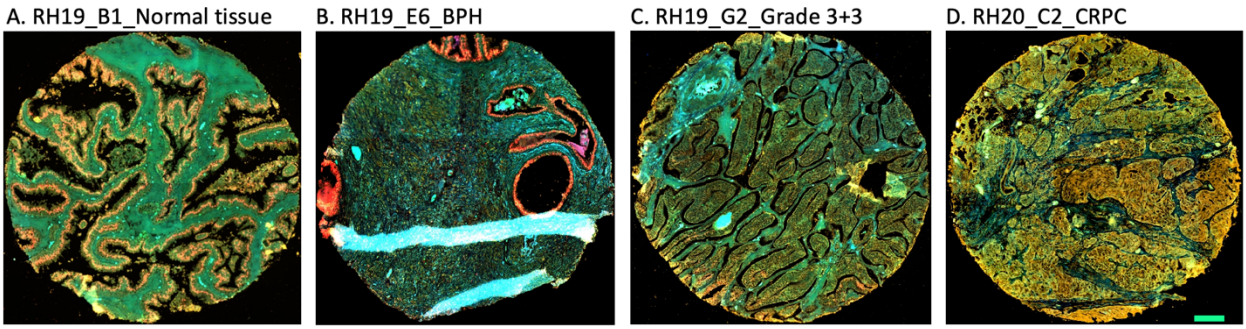

Figure 4.7. Representative images of 4 cores from each category (NPT) and PCa samples showing staining for FRA-1 with Tyr-Alexa-405, β-catenin -FITC, AR -Cy3 and c-MYC -Cy5. A. A normal prostate tissue cores of four fluorescent labelled obtained from the AxioScan image of RH19 where the core is located at B1 position. B. C. D. representing BPH, Grade 3+3 and CRPC cores, respectively, located at E6 on RH19, G2 on RH19 and C2 on RH20_CRPC. Scale bar: 100µm. There is an imaging/staining artefact is visible at the bottom of image B. These cores show distinct, representative morphology, as expected for each condition. It is to be noted that morphology was also assessed by an expert pathologist on similar cores stained with H&E, prior to the construction of tissue array (see methods). (The core B, RH19_E6_BPH shows a staining artefact of turquoise streak at the bottom; a similar staining and or imaging artefact can be seen in C. These artefacts are excluded from quantitative analysis, as presented below).

4.4.4.2. Histological characterisation of non-CRPC and CRPC tissue

4.4.4.2.1. Histological characterisation of non-CRPC cores (e.g., normal, BPH and Grade 3+3 tissue)

The tissue cores were histologically analysed to characterise the NPT, BPH, Grade 3+3 and CRPC by using magnified images of the tissue cores obtained from AxioScan (e.g., Figure 4.8). The cores were magnified to 40x to identify histological feature of the tissues. The normal prostate tissues were recognised by observing the morphologically distinct well organised epithelial layer containing luminal cells and basal cells (Szczyrba et al., 2017). BPH was predominantly characterised by an increased number of epithelial and stromal cells in perineural area of the prostate and nodules in stroma and gland (Roehrborn, 2008) and Grade 3+3 is characterized with developed well-differentiated glands, which are separated by stroma. The glands are arisen close to each other with minimum amount of intervening stroma. The glands are lined by columnar neoplastic cells but lacking a layer of basal cells (Kweldam et al., 2019).

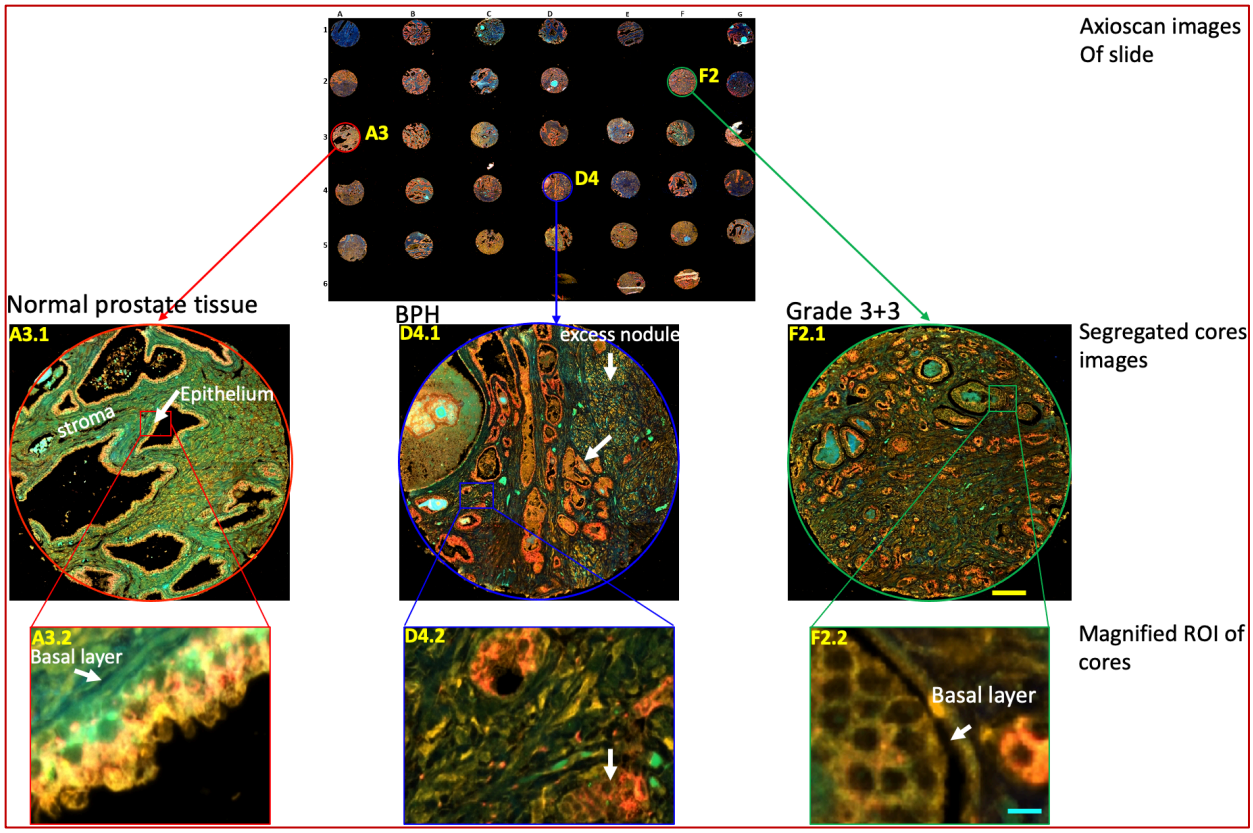

Figure 4.8. Representative images of histological features of non-CRPC cores such as NPT, BPH and Grade 3+3 PCa tissues in an axioScan image of slide RH19. The cores NPT (A3), BPH (D4) and Grade 3+3 (F2) were 20x zoomed and segregated as a separate core shown in middle row such as, NPT (A3.1), BPH (D4.1) and Grade 3+3 (F2.1). A3.2, D4.2 and F2.2 are higher magnified (40x) cores of A3.1, D4.1 and F2.1 respectively. A3.2 displaying the distinctly arranged epithelial layer of basal and luminal cells. D4.1 showing the stroma with hyperplastic growth of cells and multiple nodule formation and Grade 3+3 at F2.2 characterised by the absence of basal layer and the glandular are distinctly separated by stroma. Scale bar: 100µm (core image, middle row), 10 µm (magnified image). Also see Appendix 4.3.2.

4.4.4.2.2. Histological characterisation of CRPC tissue cores

The CRPC tissue cores were also extracted from AxioScan image of slide RH20_CRPC and stored (Fig. 4.9). Three cores were randomly selected for 40x magnification to conduct histological characterisation. The cores were characterised with prominent periacinar retraction clefting. The glands seem to float freely within locunar space. The CRPC tissue also possesses large amount of connective tissue and smooth muscle bundles. The malignant cells were arranged in clusters, rows or as single cells or arranged into small groups located in the prostate stroma with prominent fibrils of collagen (Korček et al., 2020).

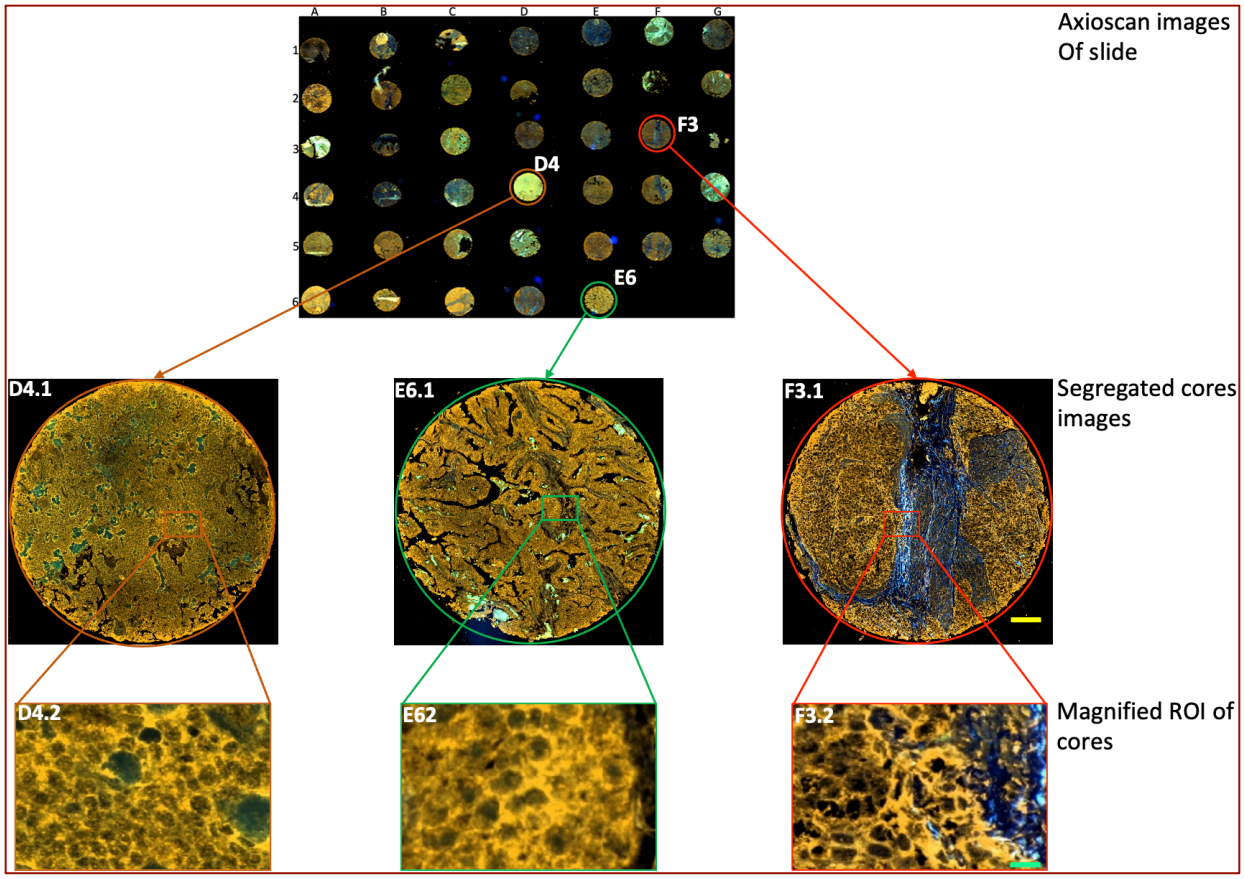

Figure 4.9. Representative images for the of histological features of three CRPC tissue cores. The AxioScan image of the slide RH20_CRPC is on top. Three cores D4, E6 and F3 were randomly selected and stored as 20x image which of D4.1, E6.1 and F3.1 respectively (showed in the middle row). D4.2, E6.2 and F3.2 are the 40x magnified image of D4.2, E6.2 and F3.2, respectively. The malignant single cells are distinctly visible in all three cores where epithelial layer is disappeared in the glands. Scale bar: 100 µm (core image), 10 µm (magnified image).

4.4.4.3. Quantitative analysis of Wnt and AR signalling related proteins expressed in PCa

The tissue cores on slides RH19 and RH20_CRPC were investigated with 4 antibodies namely, anti-FRA-1, anti-β-catenin, anti-AR and anti-c-MYC antibodies (FRA-1 with Tyr-Alexa-405, β-catenin -FITC, AR -Cy3 and c-MYC -Cy5, Table 4.2). I next used these images to quantify the amount (in pixels) of each the fluorophore labels representing expression of Wnt and AR signalling proteins FRA-1, β-catenin, AR and c-MYC. This IHC quantitative analysis has been developed in our laboratory and described in detail in section 2.3.1.8.1A. Expression of four fluorophore labelled proteins was quantified with an unbiased manner using technique described by Symes et al. (Symes et al., 2013). Expression of proteins in each core was quantified with a script written for automated analysis using ImageJ software. Image of each core, composite of

four channel of normal prostate tissue, BPH, Grade 3+3 and CRPC are displayed with their individual channels.

4.4.4.4. Expression analysis of AR and Wnt target proteins FRA-1, β-catenin, AR and c-MYC signalling target in prostate cancer tissue

An analysis was performed to measure the expression of Wnt signalling proteins (e.g., β-catenin, FRA-1, c-MYC) and AR signalling protein (e.g., AR) in normal prostate tissue. A core, E1 (Fig. 4.10.A), of normal NPT selected from RH19 slide (showed in AxioScan core image) is shown as an example of the analysis. Fig. 4.10.B shows a higher magnification Axioscan image of core E1, which was used for ImageJ analysis and expression was quantified using a written scripts adapted to ImageJ software followed by construction of bar graph using GraphPad Prism, version 8.0.0 (GraphPad Software, San Diego, California. USA). The ImageJ script separates the four fluorescence labels (Figs. 4.10.C and D-G) into 4 channels for analysis of the individual label intensity analysis as shown in Fig. 4.10.H.

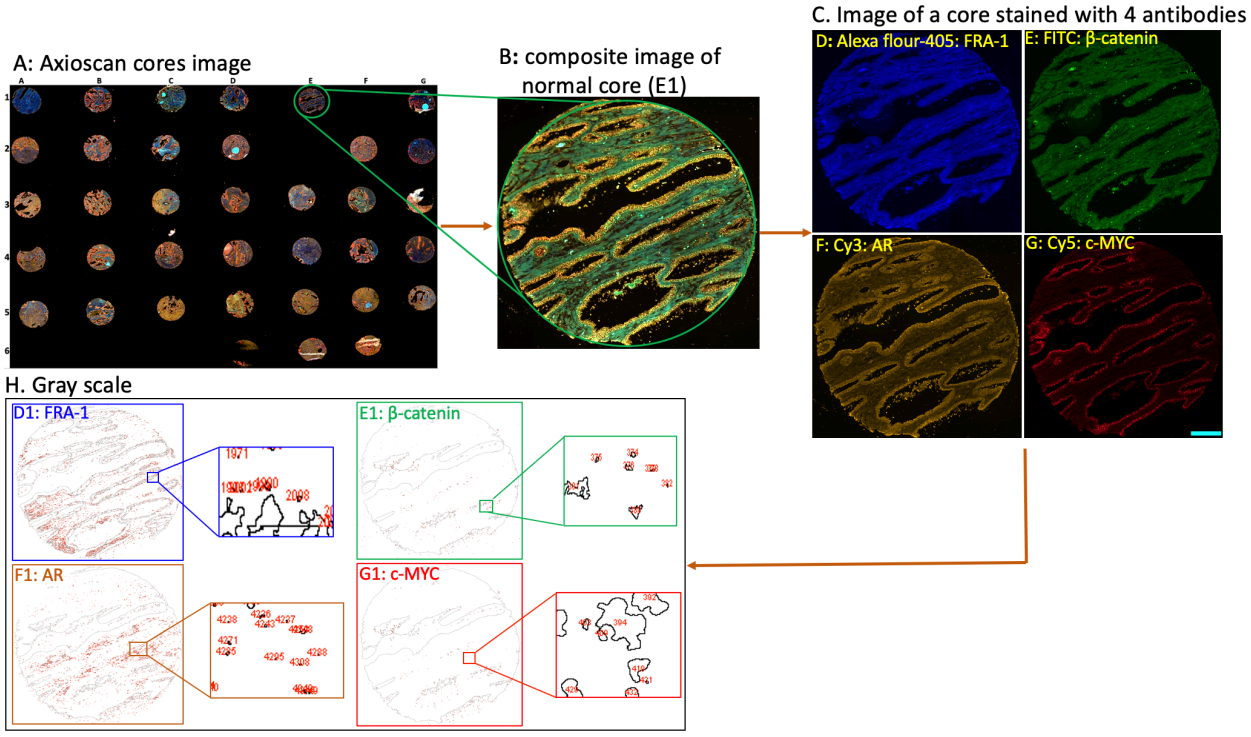

Figure 4.10. Representative images of individual core captured from Zeiss AxioScan Z1 slide scanner. A. displaying the AxioScan image of slide RH19 (41 cores: 21 NPT, 10 BPH and 10 Grade 3+3). B. A randomly selected 20x magnified composite image of NPT core. C. The composite image composed of four fluorophores namely, Alexa fluor-405 (blue: 405/415-480nm), FITC (green: 488/500-550nm), Cy3 (orange: 559/575-620nm) and Cy5 (red: 635/645-740) for anti-FRA-1, anti-β- catenin, anti- AR and anti-c-MYC antibodies respectively, to determine the expression of FRA-1, β-

catenin, AR and c-MYC proteins in NPT. H. Expression of each protein showed as red dot in each image of each fluorophore channel indicated as D1 for FRA-1, E1 for β- catenin, F1 for AR and G1 for c-MYC proteins. H. The red dots in each individual core were quantified. Scale bar: 100µm.

4.4.4.5. Quantitative analysis of Wnt and AR signalling proteins in non-CRPC and CRPC tissue

Wnt signalling proteins (e.g., FRA-1, β-catenin, c-MYC) and AR signalling protein (e.g.AR) were used to investigate their expression. The quantitative expression of FRA-1, β-catenin, AR and c-MYC proteins in NPT, BPH, Grade 3+3 and CRPC tissue are given in Fig 4.11 and shows that there is no significant difference in the expression of the four proteins tested in NPT tissue.

FRA-1 displays an increased expression in prostate cancer tissue (Fig. 3.12), c-MYC is proto-oncogene expressed in nucleus (Bostwick et al., 1996), β-catenin is expressed in epithelium and act as a prognostic factor of PCa and AR shows an increased expression in epithelium in prostate and promote metastatic prostate cancer (Augello et al., 2014). Expression of FRA-1, c-MYC, β-catenin and AR in NPT, BPH, Grade 3+3 and CRPC were quantified for each category of samples (Sec. 4.4.4.4). This section will analyse the expression of each protein in non-CRPC including NPT, BPH, Grade 3+3 and CRPC tissue. 81 tissue cores (non-CRPC: 21 NPT, 10 BPH, 10 Grade 3+3 and 41 CRPC) were stained with 4 antibodies (Table 4.2) visualized with four fluorophores (Table: 4.2) to observe the expression FRA-1, β-catenin, AR and c-MYC. The quantitation was carried out on the non-enhanced, original gray images for which all settings were identical for all tissue cores in an unbiased procedure using technique described in section 4.3.1.6.4.3.

4.4.4.5.1. Quantitative analysis of FRA-1 in non-CRPC and CRPC tissue

Expression of FRA-1 in non-CRPC and CRPC tissue cores was analysed using the AxioScan image on slide RH19 and RH20_CRPC. Calculations of intensity and integrated gray value per core of non-CRPC and CRPC tissue cores of FRA-1 fluorophore are shown in Fig. 4.11. Mean gray values were used to construct box plot and Mann–Whitney U test was performed to calculate the level of intensity of each protein in non-CRPC and CRPC tissue. A comparative plot with all different disease conditions (BPH, Grade 3+3 and CRPC) compared to NPT is shown in Fig. 4.11. FRA-1 expression in individual condition compared to NPT is also shown in Fig. 4.11.B-D for clarity.

FRA-1 expression was significantly increased in Grade 3+3 (*P<0.05) (Fig. 4.11.C) and CRPC (*P<0.05) (Fig. 4.11.D), compared to NPT. There is no statistically significant difference in FRA-1 expression in BPH when compared to NPT (Fig. 4.11.B). This implies, FRA-1 expression is upregulated in cancerous tumours (Grade 3+3) and CRPC. Therefore, FRA-1 could be used as a biomarker in lower grade PCa (Grade 3+3) and CRPC.

Figure 4.11: Expression of FRA-1 in Normal, BPH, 3+3, CRPC tissue

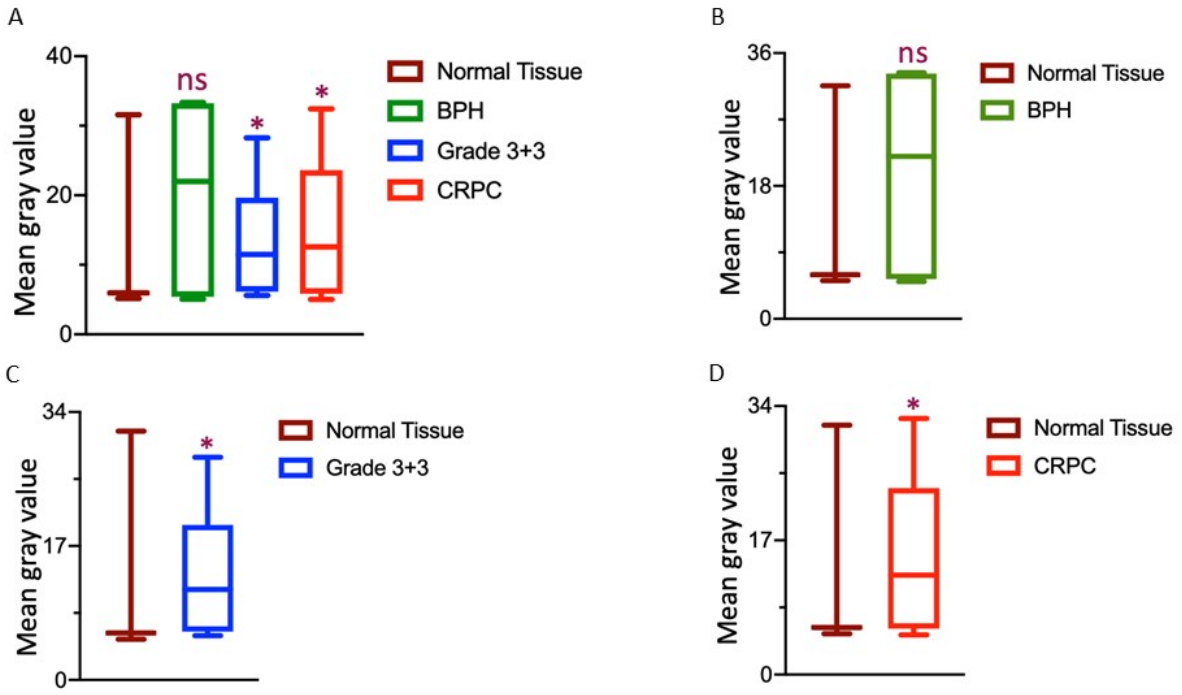

Figure 4.11. Box plot displaying the quantitation of expression of FRA-1 in NPT (n=21), BPH (n=10), Grade 3+3 (n=10) and CRPC (n=40). A. Mean gray value of fluorophore for the expression of FRA-1 in NPT, BPH, Grade 3+3 and CRPC were used to construct box plot which indicates the distribution of median of mean gray values. The graphs for individual protein expression in different disease conditions is also provided for clarity (B-D). B. Box plot displaying variation of expression of FRA-1 in BPH. C. Box plot displaying the significance of the difference of expression of FRA-1 in Grade 3+3 compared to NPT. Expression of FRA-1 is consistent in Grade 3+3 tissue. D. Box plot suggesting expression of FRA-1 in CRPC compared to NPT.

4.4.4.5.2. Quantitative analysis of β-catenin in non-CRPC and CRPC tissue

Expression of β-catenin in non-CRPC (NPT, Grade 3+3 and CRPC) and CRPC tissue cores was analysed using the AxioScan image of the tissue cores on slide RH19 and RH20_CRPC. The fluorescence (fluorophore labelled protein) of the image was converted into gray scale using written script adapted to ImageJ software. The mean gray values were used to construct box plot

and Mann–Whitney U test was performed to calculate the level of intensity of each protein in non-CRPC and CRPC tissue. A similar template to present the figures as described for FRA-1 is used for β-catenin expression here. All diseases comparison to NPT are shown in Fig. 4.12.A. β-catenin expression fluorophore showed that the protein expression was significantly increased in CRPC (*P<0.05) (Fig. 4.12.D). In case of BPH and Grade 3+3 the expression of β-catenin was not significantly different (Figs. 4.12.B and 4.12.C).

Figure 4.12: Expression of β-catenin in Normal, BPH, 3+3, CRPC tissue

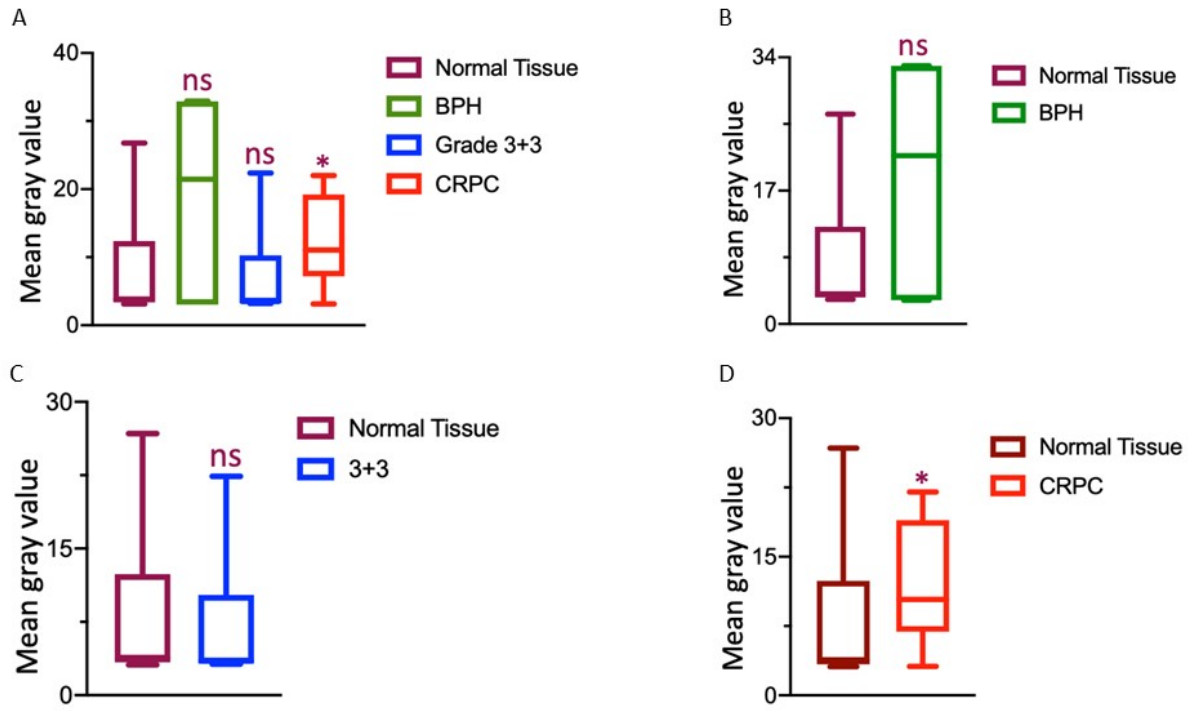

Figure 4.12. Box plot displaying the quantitation of expression of β-catenin in NPT, BPH, Grade 3+3 and CRPC. A. Mean gray value of the intensity of the expression of β-catenin in NPT (n=21), BPH (n=10), Grade 3+3 (n=10) and CRPC (n=40) were used to construct box plot, indicating the distribution of median of mean gray value. The graph was then segregated into three graphs tissue wise to display expression of the protein. B. Box plot displaying nonsignificant expression of β-catenin in BPH. C. Box plot displaying the non-significant difference of expression of β-catenin in Grade 3+3 compared to NPT. D. Box suggesting expression of β-catenin in CRPC is significantly higher in CRPC.

4.4.4.5.3. Quantitative analysis of AR in non-CRPC and CRPC tissue

Fig. 4.13.A. shows all disease vs NPT comparison for the expression of AR. AR expression was significantly increased in all conditions except when compared to Grade 3+3 (Fig. 4.13.B-D).

Figure 4.13: Expression AR in Normal, BPH, 3+3, CRPC tissue

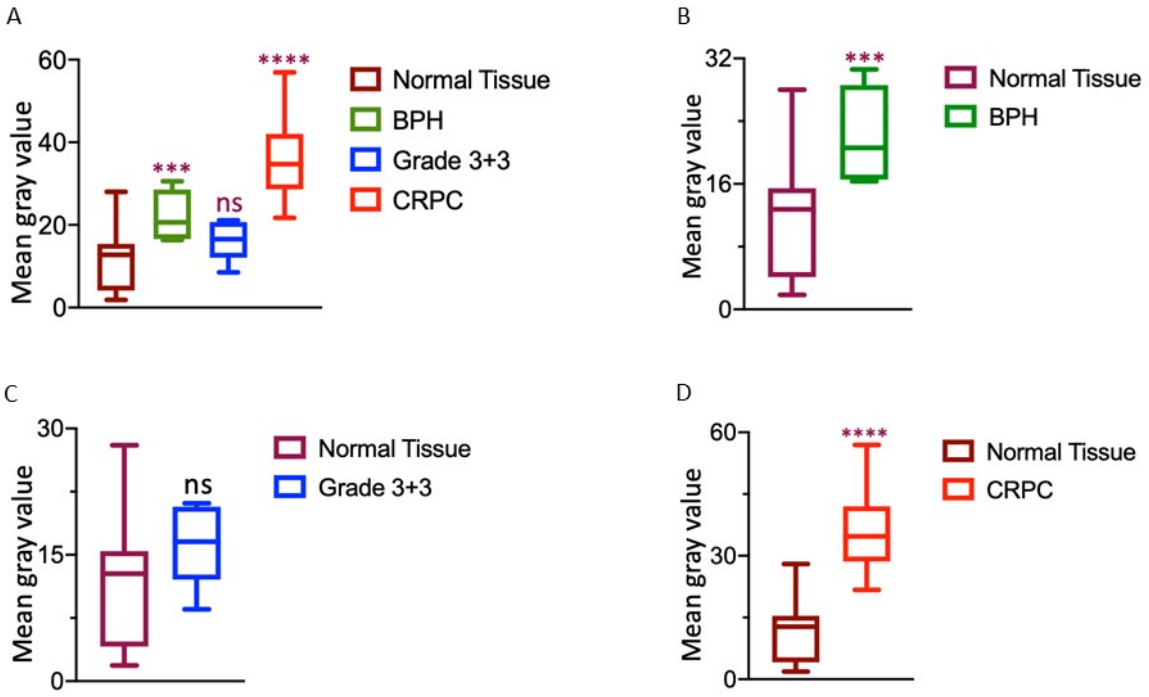

Figure 4.13. Box plot for the quantitation of expression of AR in NPT (n=21), BPH (n=10), Grade 3+3 (n=10) and CRPC (n=40). A. Mean gray value of the intensity of the expression of β-catenin in NPT, BPH, Grade 3+3 and CRPC were used to construct box plot which indicates the distribution of median of mean gray value in the box. The graph was then segregated into three graphs tissue wise to display expression of the protein. B. Box plot displaying the significance increase in expression of AR in BPH. C. Box plot displaying the non-significant difference of expression of AR in Grade 3+3 compared to NPT. D. Box plot suggesting expression of AR in CRPC is significantly higher in CRPC. (*** P<0.001; **** P<0.0001).

4.4.4.5.4. Quantitative analysis of c-MYC in non-CRPC and CRPC tissue

For c-MYC, there was no statistically significant difference of expression in BPH compared to NPT prostate tissue (Fig. 4.14.B). Unfortunately, due to an unknown technical difficulty the antibody for c-MYC did not show any signal in CRPC tissue. Due to limited tissue availability and also because of Covid19, these experiments could not be redone for c-MYC expression on another TA slide. However, c-MYC only showed a significant difference in the expression in Grade 3+3 when compared to NPT.

Figure 4.14: Expression c-MYC in Normal, BPH, 3+3, CRPC tissue

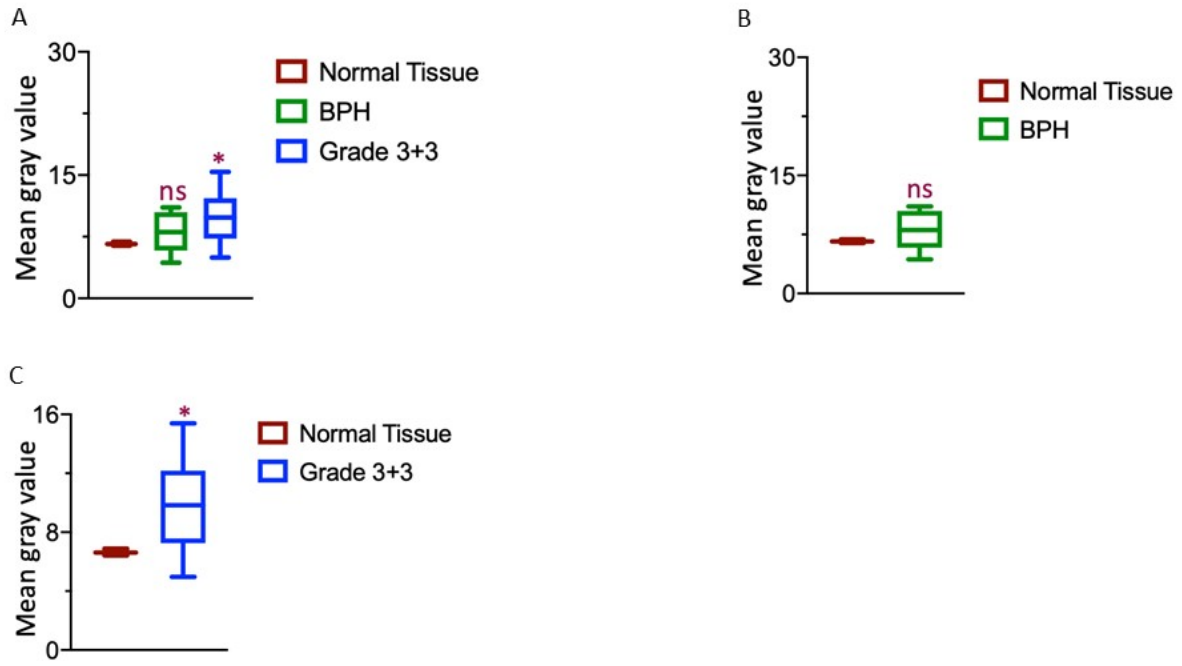

Figure 4.14. Box plot for the quantitation of expression of c-MYC in NPT (n=21), BPH (n=10), grade 3+3(n=10) and CRPC (n=40). A. Mean gray values of the intensity of the expression of c-MYC in NPT, BPH, Grade 3+3 and CRPC were used to construct box plot which indicate the distribution of median of mean gray value. The graph was then segregated into three graphs tissue wise to display expression of c-MYC. B. Box plot displaying the non-significant increase in expression of c-MYC in BPH. C. Box plot displaying the significant increase of expression of c-MYC in Grade 3+3 compared to NPT.

The expression of Wnt and AR signalling proteins in NPT and BPH, Grade 3+3 and CRPC was compiled and summarised in single graph (Fig. 4.15). The Wnt signalling protein, FRA-1 expression was significantly increased in Grade 3+3 and CRPC tissue. But significant increase of expression of β-catenin was found in CRPC and not in lower grade cancer tissue, Grade 3+3 (confirming the results from single label staining experiments in the previous chapter). But there was no significant difference of FRA-1 and β-catenin expression in BPH. It can be concluded that FRA-1 and β-catenin can be used as biomarker for metastatic prostate cancer. FRA-1 expression was also increased in Grade 3+3 PCa which was similar to c-MYC which also showed significant increase in expression in Grade 3+3 PCa. So, I can conclude that FRA-1 and c-MYC could be a biomarker for lower Grade 3+3 PCa. The CRPC cores did not show any signal for c-MYC due to technical issues. β-catenin expression remained unchanged in Grade 3+3 and BPH compared to NPT. By proxy it appears that β-catenin may not be involved in PCa progression, but Wnt

signalling may become activated after it progresses to highest Gleason grade. Expression of AR was increased significantly in BPH whereas remained unchanged in Grade 3+3 confirming that AR may play a role in the development of BPH. In lower grade prostate cancer (Grade 3+3), there was no significant difference observed in the expression of AR compared to NPT. As expected, the expression of AR was highest in CRPC tissue samples in relation to all other comparators (Fig. 4.15).

Figure 4.15:Expression of FRA-1, β-catenin, AR and c-MYC

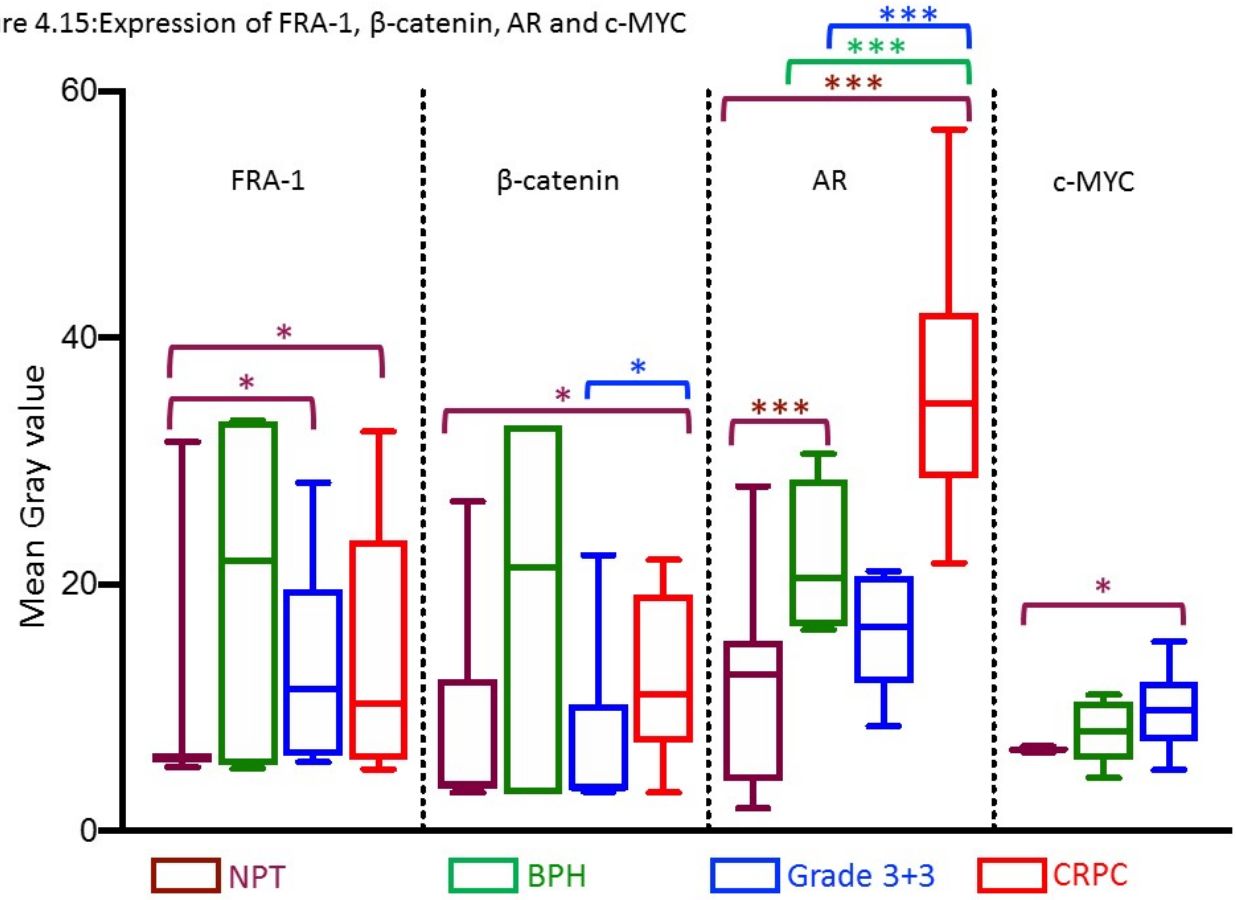

Figure 4.15. Expression of FRA-1, β-catenin, AR and c-MYC in NPT (n=21), BPH (n=10), Grade 3+3 (n=10) and CRPC (n=40) using Box plot. The box plot was constructed using the mean gray value per core for each protein obtained from normal prostate tissue (NPT) (dark red), BPH (green), Gleason grade 3+3 (blue) and CRPC (red). Mann-Whitney U test was performed for statistical analysis to determine the level of expression of the proteins. The analysis of expression of each protein was demonstrated in non-CRPC and CRPC tissue showed previously (Sec. 4.4.2.5). (* P<0.05; ***P<0.001; ****P<0.0001).

4.4.4.6. Deconvolution for quantitative co-localization of FRA-1, β-catenin, AR and c-MYC

In addition to the intensity of protein expression (as measured above), localization of proteins can also serve as an indicator of change of function in disease (Symes et al., 2013). It is to be noted that alterations in co-localization of two proteins may occur without any change in the expression in two sets of tissue samples (e.g., NPT v BPH).

High magnification immunofluorescence of each core was obtained to investigate whether the localization of two proteins was altered in diseased tissue samples when compared to NPT. A protocol similar to that developed in our laboratory (Symes et al., 2013) was used to examine whether co-localization of a combination of two proteins could be used as putative biomarkers for diagnosis or for prognostic stratification of the disease. (A1=RH19A3, B1=RH19G4, C1=20C2).

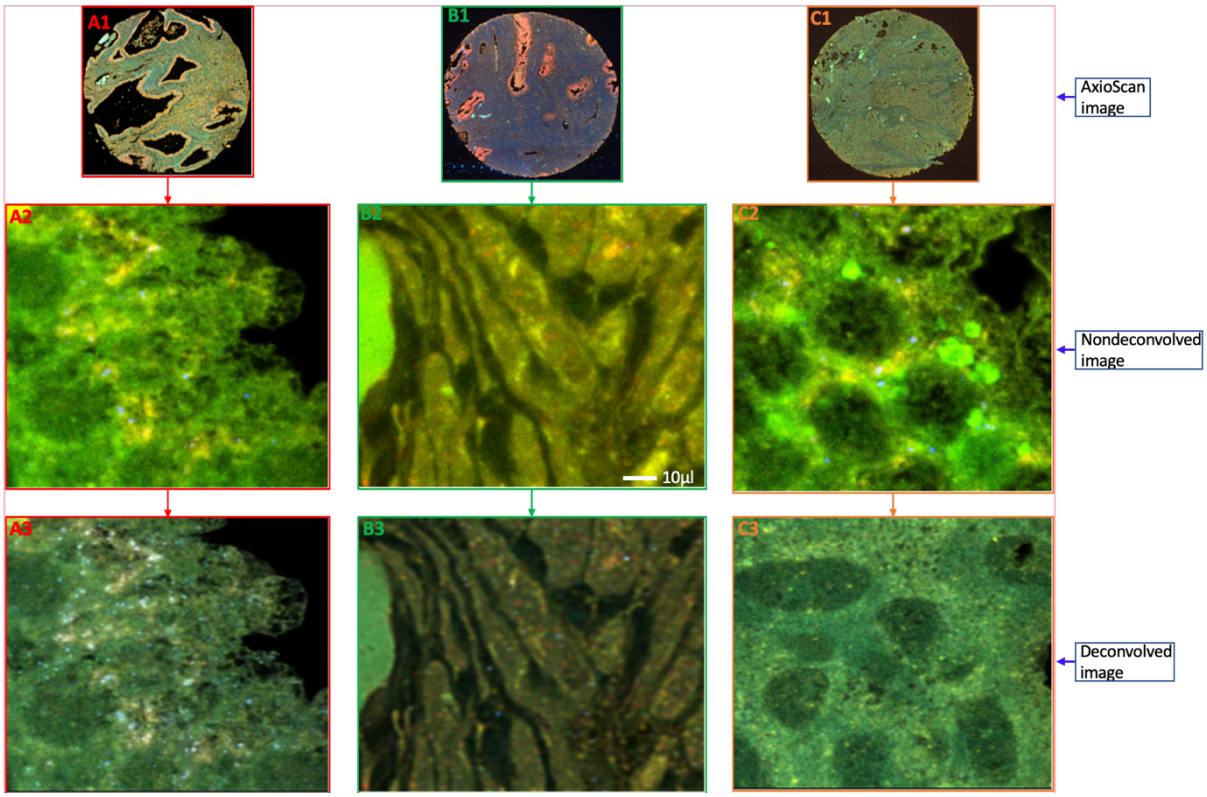

Figure 4.16. Representative images of high magnification of deconvolved images for FRA-1, β-catenin, AR and c-MYC co-expression in normal, BPH and CRPC tissue cores: Highly magnified deconvolved images displaying co-expression of FRA-1 (Alexa-405: blue), β-catenin (FITC: green), AR (Cy3: orange) and c-MYC (Cy5 red) in normal, BPH. Following deconvolution, the represented composite micrographs of immunofluorescence stained normal and malignant tissue cores were used to quantify co-localization of four proteins. 81 tissue cores (Normal: 21, BHP: 5, BPH replicate: 5, Grade (3+3): 5, repeat of Grade (3+3): 5, CRPC: 20 and CRPC repeat: 20) obtained from 56 patients were imaged using confocal Microscope Leica TCS SP8. Prior to perform deconvolution with Huygens Professional software, a high magnification imaging (at 1024x1024) was carried out. The high magnification images were used to reduce noise

during deconvolution and converted to 16 bit and generated Huygens specific files (HDF5) for each fluorophore (Alexa Fluor-405, FITC, Cy3 and Cy5) which were then imported into Huygens deconvolution software and pseudo coloured (Alexa Fluor-405: blue, FITC: green, Cy3: orange and Cy5: red). 25-30 slices of image of Z-projections for each ROIs of each tissue cores were deconvolved and the generated highly magnified images were used to measure quantitative co-localization.

4.4.4.7. Quantitative Co-localization of FRA-1, β-catenin and AR

Comparative co-localisation analysis was conducted using images obtained at high magnification (63x) which were imported into Huygens Professional software for deconvolution. The deconvolved images were stored as Huygens specific (HDF5) files which were imported into Huygens co-localization script to calculate Pearson coefficient for co-localisation of the proteins. The Pearson co-localization coefficient refers the measurement of the spatial overlap of two proteins in different types of tissue samples (NPT, BPH, Grade 3+3 and CRPC tissue). The Pearson coefficient (r_p) were compared for 3 permutations (in sets of co-localisation of 2 proteins at a time) such as FRA-1/β-catenin, FRA-1/AR, β-catenin/AR. Each of the permutations was compared in 6 conditions such as NPT vs BPH, NPT vs Grade 3+3, NPT vs CRPC, BPH vs Grade 3+3, BPH vs CRPC, Grade 3+3 vs CRPC using Mann–Whitney U test.

4.4.4.7.1. Co-localization of FRA-1/β-catenin in NPT, BPH, Grade 3+3 and CRPC

There was no significant difference in the colocalization of FRA-1/β-catenin in NPT when compared to BPH or when BPH was compared to Grade 3+3. Significant difference in the co-localization of FRA-1/β-catenin was found in NPT vs Grade 3+3 (*P<0.05) and NPT vs CRPC (****P<0.0001), BPH vs CRPC (*P<0.05) and Grade 3+3 vs CRPC (*P<0.05).

Figure 4.17: Colocalization - FRA-1/β-catenin

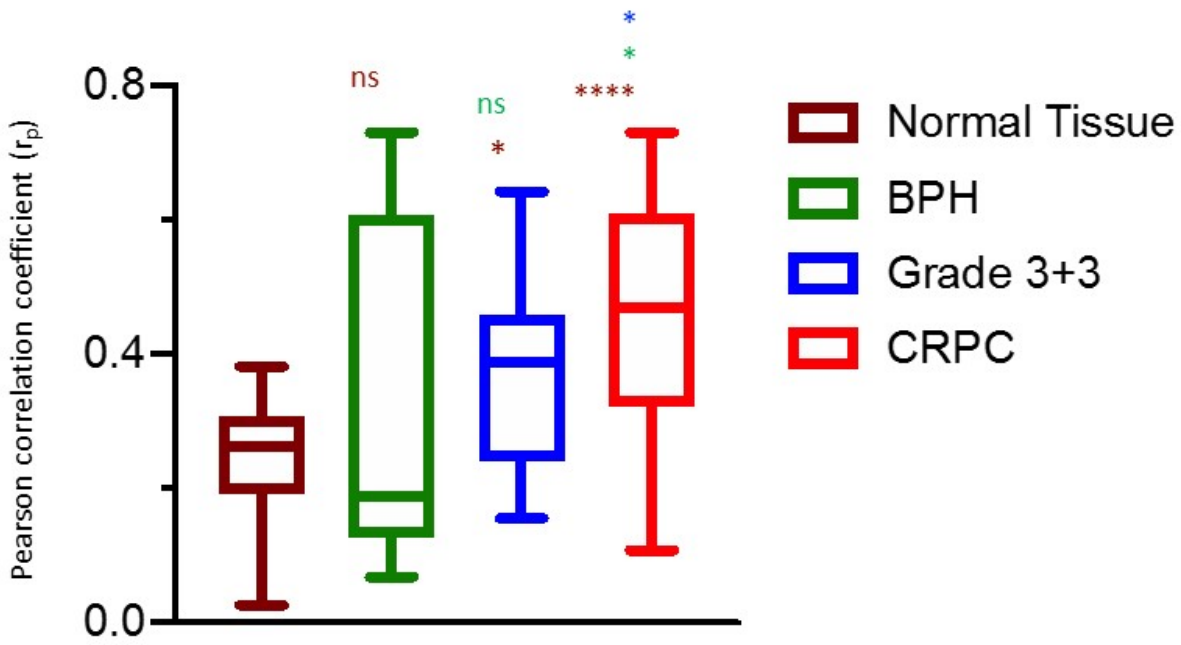

Figure 4.17. Co-localization of Wnt signalling proteins in NPT, BPH, Grade 3+3 and CRPC. Pearson correlation coefficient (rP) was calculated for FRA-1/β-catenin permutation of FRA-1/β-catenin from the deconvolved, high magnification immunofluorescence image obtained from Huygens software. Statistical analysis was conducted using Mann-Whitney U test to calculate any significance of differences in rp values to distinguish NPT vs BPH, NPT vs Grade 3+3 and NPT vs CRPC as shown in green above the respective boxes, BPH vs Grade 3+3 and BPH vs CRPC as shown in red and Grade 3+3 vs CRPC as shown in blue above the CRPC box (* P< 0.05; *** P<0.001 and ns= not significant; NPT=Normal prostate tissue).

4.4.4.7.2. Co-localization of FRA-1/AR in NPT, BPH, Grade 3+3 and CRPC

There was significant difference in the co-localization of FRA-1/AR in NPT vs BPH (*P<0.05), NPT vs Grade 3+3 (**P<0.01), NPT vs CRPC (****P<0.0001), BPH vs CRPC (**P<0.01) and Grade 3+3 vs CRPC (***P<0.001) but this permutation did not show any significant difference of co-localization in BPH vs Grade 3+3. This combination is an interesting example of the value of measuring colocalization in addition to intensity of expression. For example, there is no significant difference in the expression of FRA1 in BPH compared to NPT (Figs. 4.11 and 4.15), whereas there is a difference within BPH and NPT for the expression of AR (Figs. 4.13 and 4.15). However, there is a change in the colocalization of these two proteins that can serve as an enhanced biomarker. There was an increase in AR expression in BPH and CRPC, compared to NPT (Figs. 4.13 and 4.15); there was no change in β-catenin expression except in CRPC when

compared with normal prostate (Figs. 4.12 and 4.15). A key hypothesis in this thesis is that there may be close interaction between AR and Wnt signalling pathway. These *in situ* results suggest that these pathways may co-operate both antagonistically and co-operatively in different stages of PCa progression. For example, in moderate Grade (4+4) disease downregulation of AR signalling and upregulation of Wnt signalling may be the dominant signalling pathway and castration resistance either activates or is co-regulated by Wnt signalling pathway.

Figure 4.18.: Colocalization - FRA-1/AR

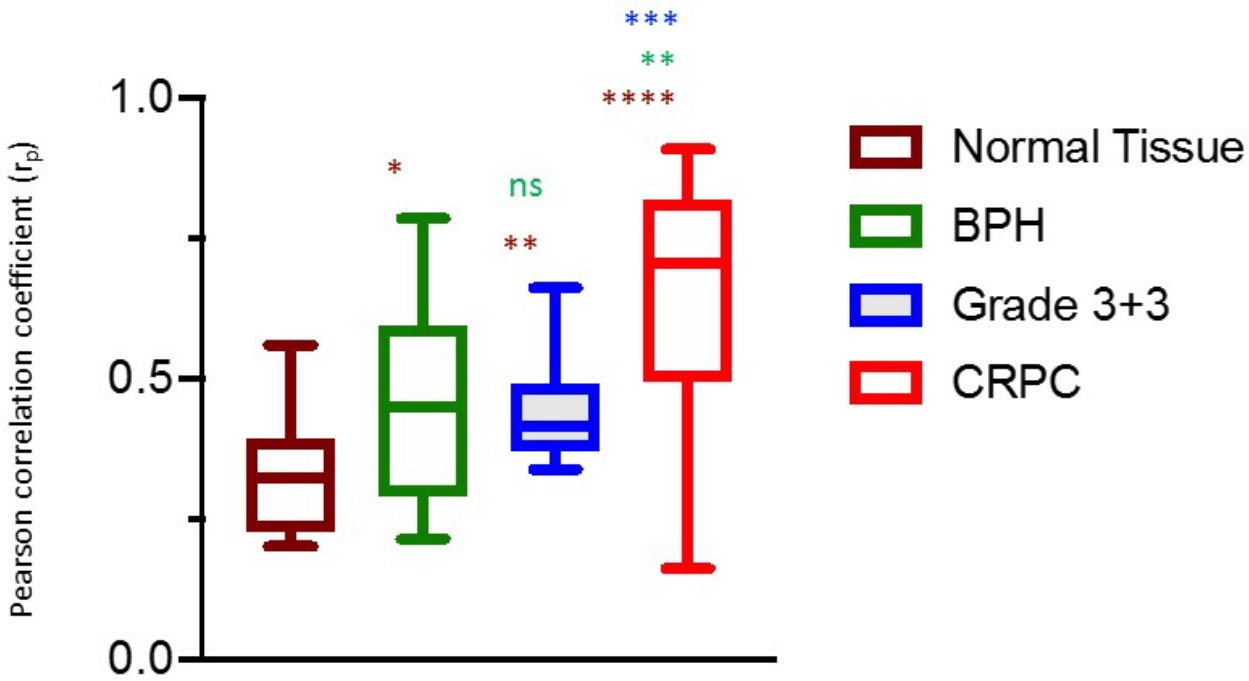

Figure 4.18. Co-localization of AR and Wnt signalling proteins in NPT, BPH, Grade 3+3 and CRPC. Pearson correlation coefficient (r_P) was calculated for FRA-1/AR permutation of FRA-1 and AR from the deconvolved, high magnification immunofluorescence images obtained from Huygens software. Statistical analysis was conducted using Mann-Whitney U test to calculate any significant nonsignificant different in r_p value to distinguish NPT vs BPH, NPT vs Grade 3+3 and NPT vs CRPC as shown in green above the respective boxes, BPH vs Grade 3+3 and BPH vs CRPC as shown in red and Grade 3+3 vs CRPC as shown in blue above the CRPC box. (** P<0.01, **** P<0.0001 and ns= not significant).

4.4.4.7.3. Colocalization of β-catenin/AR in NPT, BPH, Grade 3+3 and CRPC

Significant difference in the co-localisation of β-catenin/AR combination was found between NPT vs BPH (**P<0.01), NPT vs CRPC (****P<0.0001), BPH vs CRPC (*P<0.05), Grade 3+3 vs CRPC

(***P<0.001). Other permutations, including NPT vs Grade 3+3, BPH vs Grade 3+3 did not show any significant difference for the colocalization of β-catenin/AR.

Figure 4.19.: Colocalization - β-catenin/AR

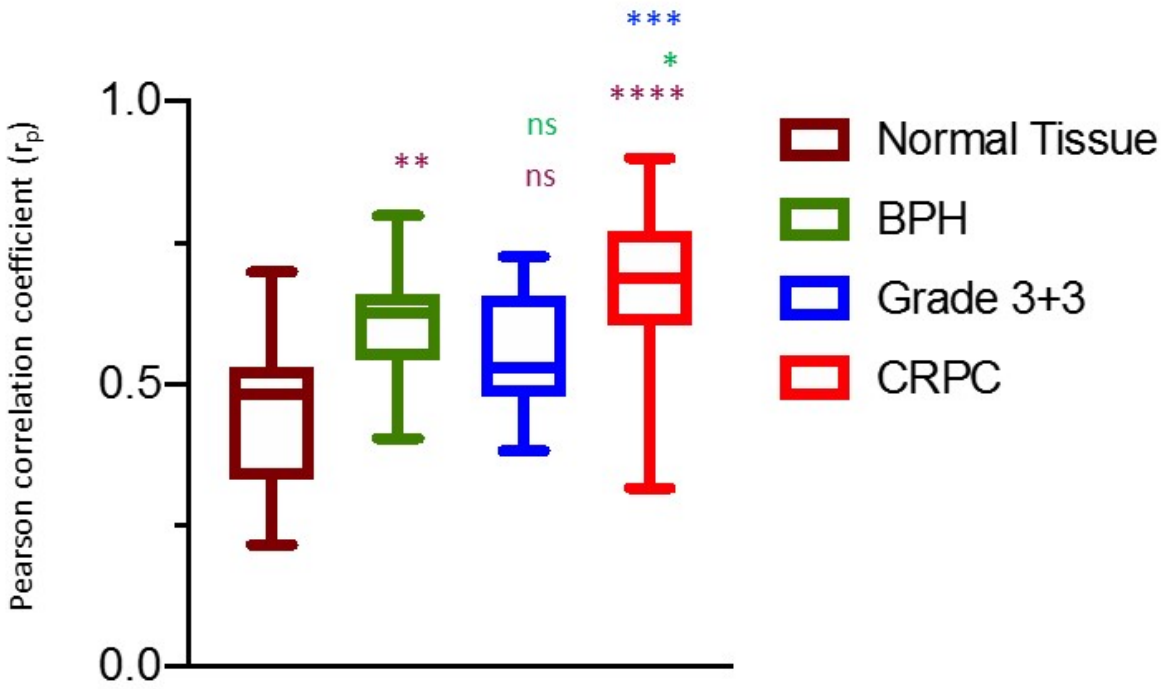

Figure 4.19. Co-localization of AR and β-catenin in NPT, BPH, Grade 3+3 and CRPC. Pearson correlation coefficient (r_P) was calculated for β-catenin/AR permutation of β-catenin and AR from the deconvolved, high magnification immunofluorescence images obtained from Huygens software. Statistical analysis was conducted using Mann-Whitney U test to calculate any significant difference in r_p value to distinguish NPT vs BPH, NPT vs Grade 3+3 and NPT vs CRPC as shown in green above the respective boxes, BPH vs Grade 3+3 and BPH vs CRPC as shown in red and Grade 3+3 vs CRPC as shown in blue above the CRPC box (*P<0.05; **P<0.01; ***P<0.001; ****P<0.0001 and ns= not significant).

Other combination such as colocalization of FRA-1 with β-catenin and AR were also investigated. For FRA1 and β-catenin (panel 1, Fig. 4.20), there was no difference in the co-localization between normal and BPH tissue. There was a significant change in the co-localization of FRA-1 and AR in BPH compared to normal; indeed, this was the case for all other permutations except for BPH and Grade 3+3. In this case, a lack of any change may be because Grade 3+3 is the lowest grade of prostate cancer and there is no significant interaction between AR and Wnt pathways at this early stage cancer. However, in comparison with normal, BPH or Grade 3+3 and CRPC, there was a significant difference in the colocalization for all protein combinations. Increased colocalization

of the co-transcription factor, β-catenin, and the transcription factor may mean an increase in Wnt/β-catenin mediated gene transcription in CRPC suggesting an increased role of Wnt and AR signalling in this type of advanced prostate cancer.

Figure 4.20.: Summary - Colocalization of all proteins

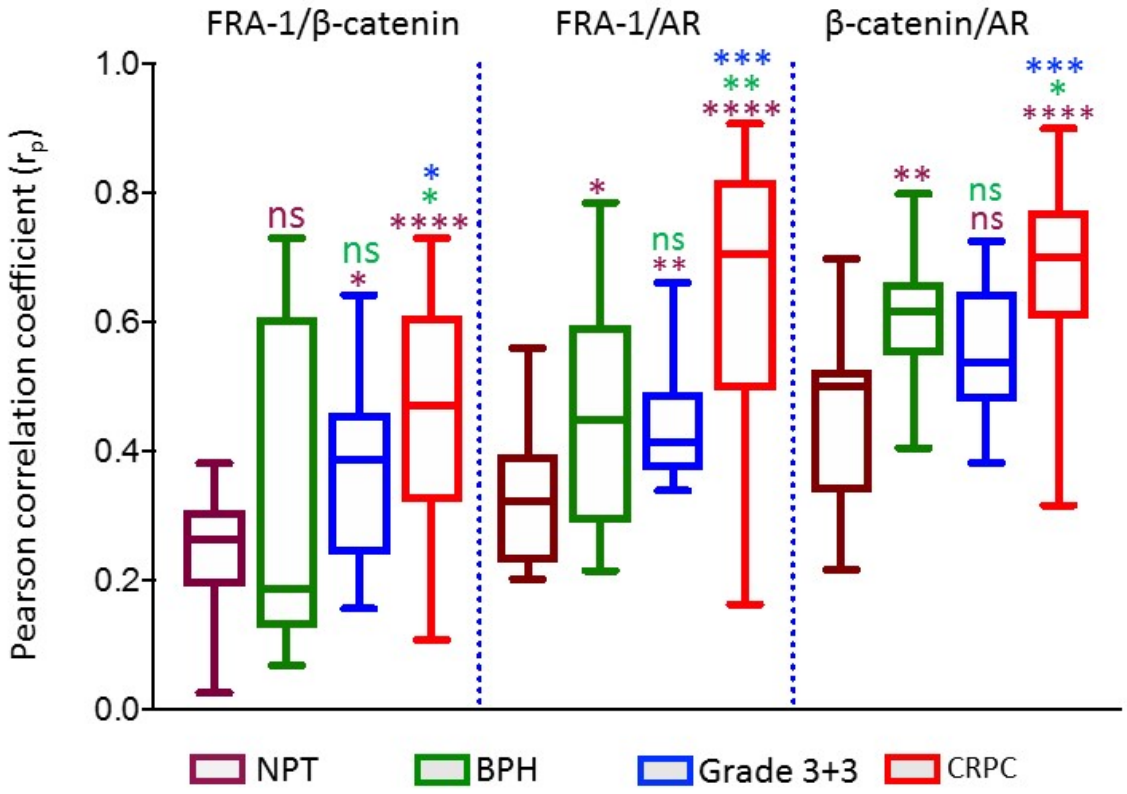

Figure 4.20. Combined graphs for co-localization analysis of AR and Wnt signalling proteins in NPT, BPH, Grade 3+3 and CRPC. Pearson correlation coefficient (r_P) was calculated for FRA-1/β-catenin, FRA-1/AR and β-catenin/AR permutation of three fluorophores of individual proteins from the deconvolved, high magnification immunofluorescence images obtained from Huygens software. Statistical analysis was conducted using Mann-Whitney U test to calculate any significant or nonsignificant different in r_p value to distinguish NPT vs BPH, NPT vs Grade 3+3 and NPT vs CRPC as shown in green above the respective boxes, BPH vs Grade 3+3 and BPH vs CRPC as shown in red and Grade 3+3 vs CRPC as shown in blue above the CRPC box (ns P>0.05; *P<0.05; **P<0.01, *** P<0.001; ****P<0.0001 and ns= not significant). The ß-catenin and AR combination is the same data as presented that in Fig. 4.23. It is re-presented in this figure for comparative reasons.

4.4.5. Expression of mRNA for Wnt target genes

Wnt signalling proteins are associated with tumour progression and carcinogenesis and could be used as prognostic marker in various epithelial cancers, including prostate cancer (Symes et al., 2013; Arya et al., 2015 and Arthurs et al., 2020). Measurement of RNA expression of Wnt target

genes could validate its potentiality to be used as risk stratification biomarker for lower grade to high grade prostate cancer. RNAscope (automated) duplex was used to detect two RNA single molecule RNA. RNA probes were obtained from ACD (Advance cell diagnostics) and this was involved two channels. Chanel 1 (C1) refers to green and channel 2 (C2) refers to fast red.

The layout of the TA slide used for single molecule RNA expression using RNAscope is given in Appx. 2. Four RNA probes, targets of Wnt signalling were used: β-catenin, FRA-1, PYGO2 and TCF-1 all purchased from ACD Bioscience (UK).

Staining of the tissue cores were performed by Automated Bond Biosystem according to the protocol described previously (Chap-II, Sec. 2.3.1.8.2). Following staining, the stained cores were scanned using Zeiss AxioScan Z1 slide scanner to observe the quality of staining. Each of the mRNA molecules was observed as a punctate dot which were quantitated using an algorithm, written in our lab, incorporated into Jupyter notebook (Python software). mRNA punctate dots for β-catenin were quantified using the above software and for FRA-1, PYGO2 and TCF-1 were counted manually.

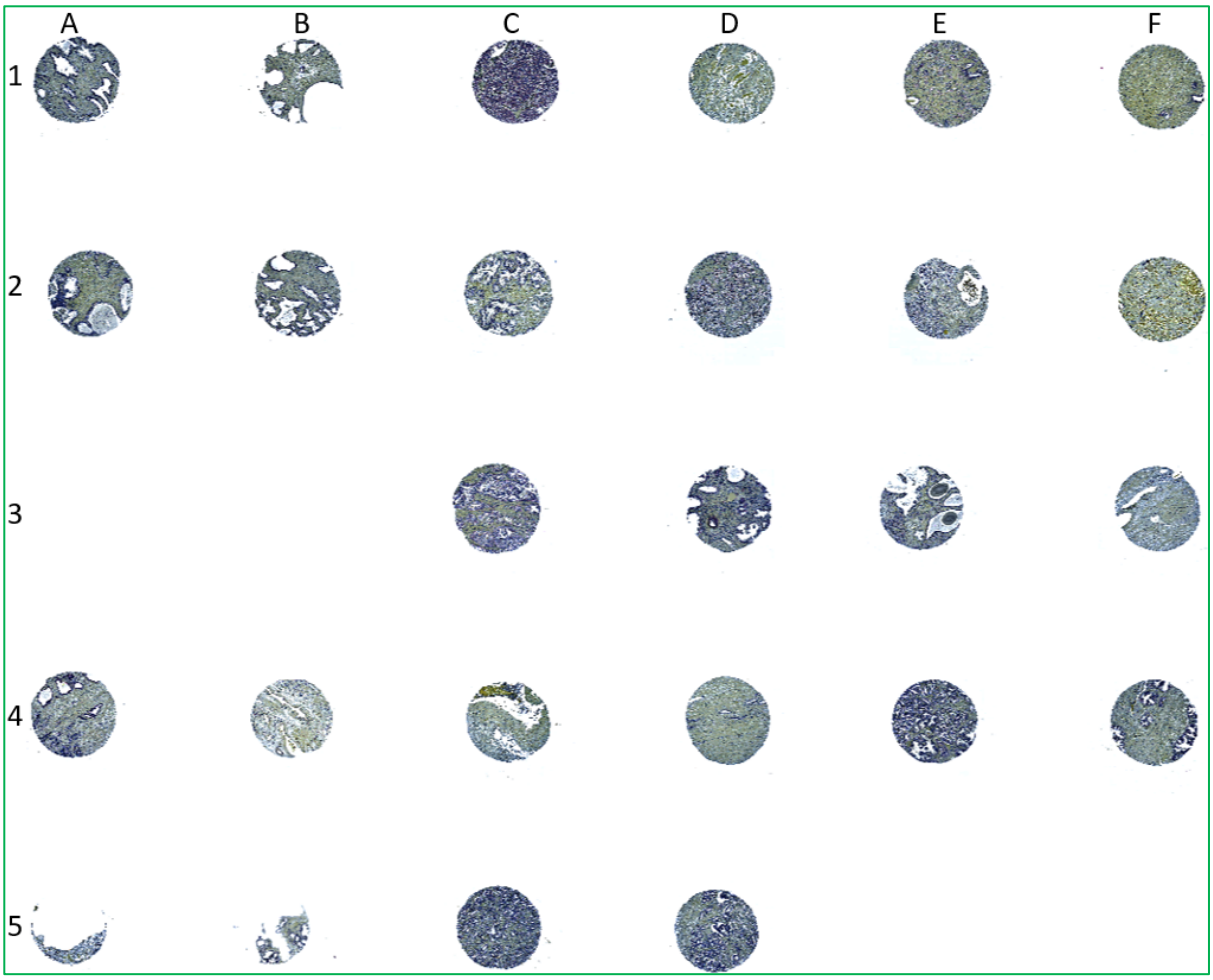

Figure 4.21. Representative images for the of AxioScan mage of RNAscope stained tissue arrays (slide RH17: composed of 30 cores cores). The slide contains 30 cores of 15 NPT, 5 Grade 3+3, 5 Grade 4+4 and 5 Grade 4+5/5+4. Layout of slide has been given in appendix (Appx. 2).

4.4.5.1. Expression of POLR2A and PPIB for assessment of quality of mRNA

Two control probes POLR2A and PPIB were used as a positive control experiment (Fig. 4.22) to observe the quality of RNA in the tissue. Duplex (2 plex) was used to detect two RNA single molecule RNA. Chanel 1 (C1) refers to green and channel 2 (C2) refers to fast red. Each punctate dot (Red/Green) indicates expression of each single molecule mRNA of β-catenin, PYGO2, FRA-1 and TCF-1 (Fig. 4.22). RNA expression of PPIB in each core of NPT, Grade 3+3, Grade 4+4 and Grade 4+5/5+4 was calculated as mean±SE; 145±0.88, 69±2.06, 116±1.46 and 62±0.05 for NPT, Grade 3+3, Grade 4+4 and Grade 4+5/5+4 respectively. These indicate quality of RNA was good enough to conduct further analysis of RNA. DapB was used as negative control; there was virtually

no expression of DapB in human prostate tissue (personal communication with Mike Millar, Queen's Medical Research Institute, University of Edinburgh).

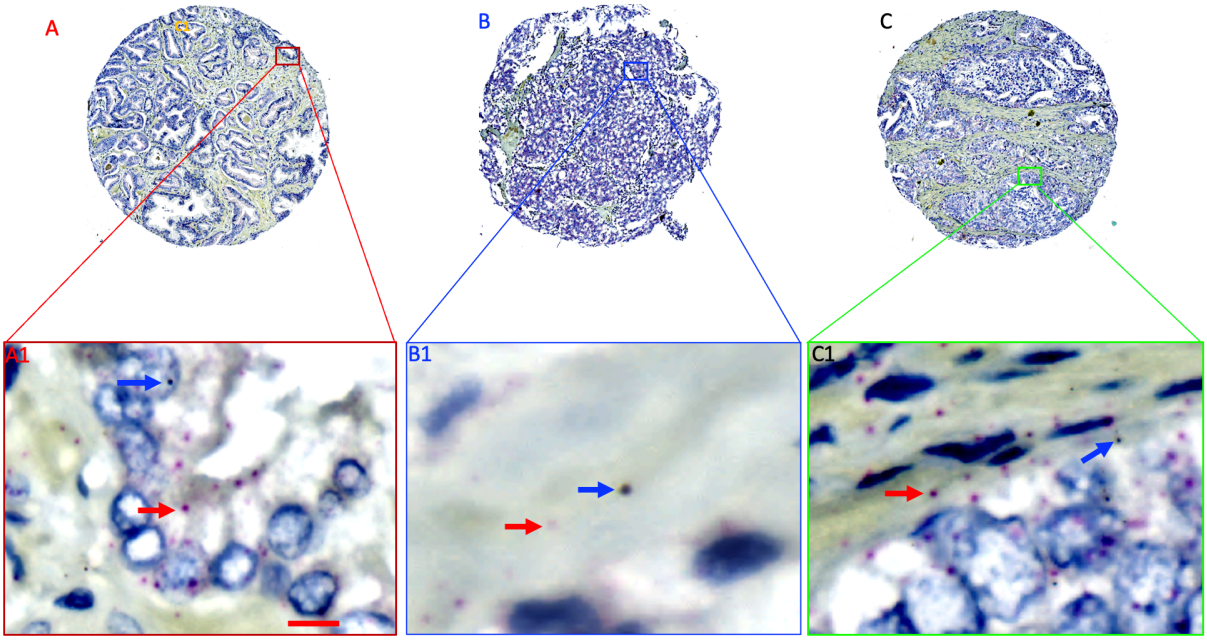

Figure 4.22. Representative images for the of high magnification of an AxioScan image displaying RNA expression of POLR2A and PPIB. Image A1, B1 and C1 is cropped of higher magnification of A, B and C of AxioScan image of stained tissue cores. Green punctate dot (pointed by blue arrow) indicates the expression of single molecule RNA of PPIB and Red punctate dot indicate the expression of single molecule RNA of POLR2A. Scale bar: 10 µm.

4.4.5.2. Analysis of mRNA of β-catenin, FRA-1, PYGO2 and TCF-1 RNA in NPT, Grade 3+3, Grade 4+4, Grade 4+5/5+4 and CRPC

Following staining, the stained tissue cores were scanned using Nanozoomer slide scanner (Hammamatsu Photonics UK Ltd, Welwyn Garden City, UK) at 40x magnification (0.23µm/pixel resolution). Prior to executing the quantitation algorithm, threshold of each image was optimised, and hue, saturation and brightness were customised. The results indicate the number of mRNA molecules of β-catenin were expressed in the tissue. A 2-plex staining approach was applied in each staining procedure; representative figures for individual tissue cores are shown in Fig. 4.22. Red channel (Chap-II, Sec. 2.3.2.2) was used for β-catenin while staining for FRA-1, PYGO2 and FRA-1 where green channel, such as β-catenin (red) vs FRA-1 (green), β-catenin (red) vs PYGO2 (green), β-catenin (red) vs TCF-1 (green). All the counts were acquired and plotted a box and whisker plot. Significance of difference were calculated using Mann-Whitney U test (ns P>0.05; *P<0.05; **P<0.01; ***P<0.001; ****<0.0001).

4.4.5.2.1. Analysis of mRNA of β-catenin in NPT, Grade 3+3, Grade 4+4, Grade 4+5/5+4 and CRPC

There was no increase in the mRNA expression for β-catenin in BPH compared to normal tissue. The level of expression for β-catenin mRNA in Grade 3+3 PCa was similar to that in NPT. The β-catenin mRNA expression corelates to those found for protein expression for β-catenin. However, the box plot (Fig. 4.23) indicates its median of expression of mRNA for β-catenin was slightly increased in Grade 3+3. Expression was further and significantly increased in Grade 4+4 (116.45 ± 31.29-fold, mean±SEM; **P<0.01) vs NPT. β-catenin mRNA expression was even further increased in Grade 4+5/5+4 (120.00 ± 19.43-fold, mean±SEM; ****P<0.0001) when compared to NPT. In CRPC tissue (59.38 ± 19.37-fold, mean±SEM; ***P<0.001), β-catenin mRNA expression was detected at significantly higher levels than that observed in NPT (Fig. 4.23).

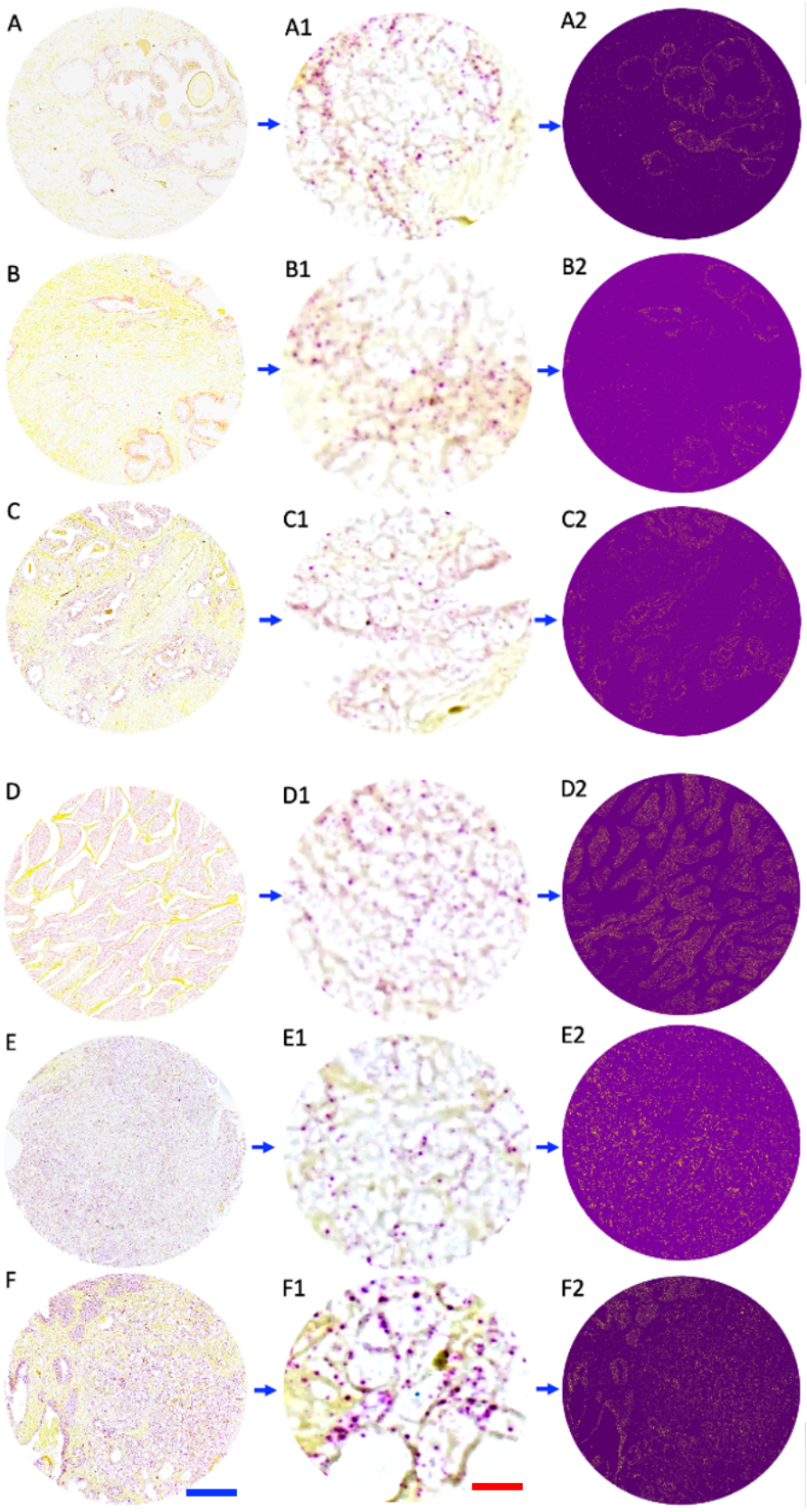
A
A1
A2
B
B1
B2
C
C1
C2
D
D1
D2
E
E1
E2
F
F1
F2

G. Box and Whisker Plot

Figure 4.23: RNAscope - β-catenin

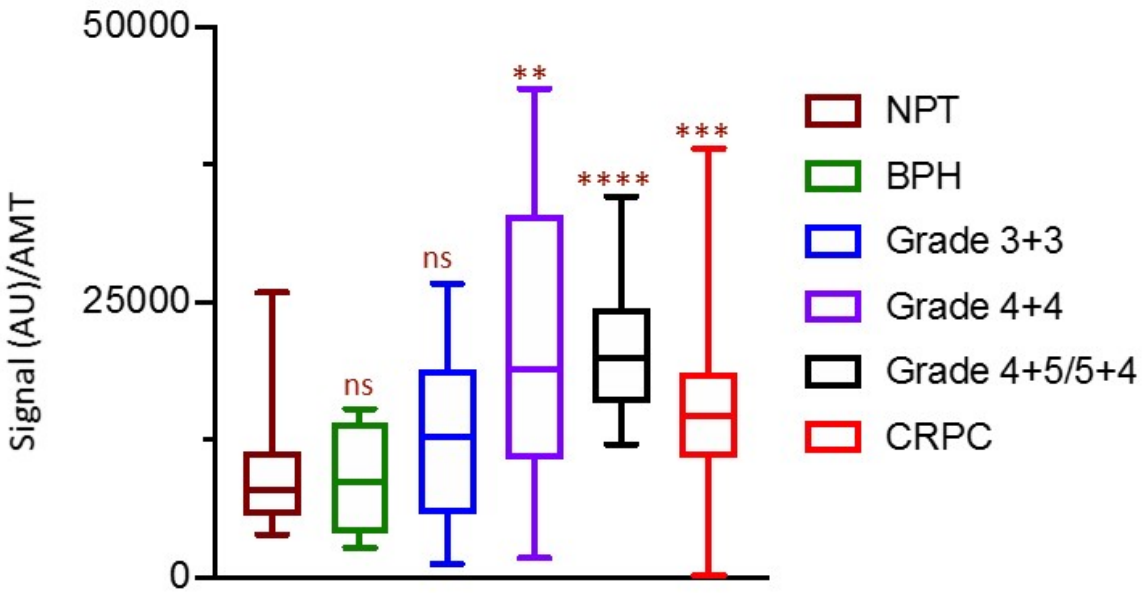

Figure 4.23. Micrographs are representative figures showing mRNA expression of β-catenin in normal (NPT), Grade 3+3, Grade 4+4, Grade 4+5/5+4 prostate tissue. A, B, C, D, E and F represent a core of NPT (n=36), BPH (n=10), Grade 3+3 (n=25), Grade 4+4 (n=15), Grade 4+5/5+4 (n=15) and CRPC (n=40). A, B, C1, D1, E1, and F1 are the magnified cropped images of A, B, C, D, E and F respectively. Following application of image analytical technique, a digital image of the objective was produced indicated as A2, B2, C2 D2, E2 and F2 of A, B, C, D, E and F respectively. Each dot on the image represents the expression of single mole mRNA of β-catenin. All the single counts were quantitated and acquired and plotted into Box and Whisker Plot (G). Significance of difference was calculated using Mann-Whitney U test (ns P>0.05; **P<0.01; ***P<0.001; ****P<0.0001). All the comparison were made against NPT. Scale bar: Blue for 100 µm and red for 10 µm.

4.4.5.2.2. Analysis of the expression of mRNA for FRA-1 in NPT, Grade 3+3, Grade 4+4, Grade 4+5/5+4 and CRPC

The analysis showed there was no change in the expression of mRNA for FRA-1 in BPH compared to NPT. All fold changes represent as mean±SEM. Significant increase was observed in Grade 3+3 (58.43 ± 22.26-fold, **P<0.01). mRNA expression of FRA-1 was also increased significantly in Grade 4+4 (30.05 ± 9.73-fold, mean±SEM; **P<0.01) and Grade 4+5/5+4 (35.43 ± 11.30-fold, mean±SEM; **P<0.01) and in CRPC (28.39 ± 13.31-fold, mean±SEM; *P<0.05). This was also observed for other combinations and types of tissue (Fig. 4.24). These results are correlated to those observed for proteins, above (Chap-III, Sec 3.4.2.3).

Figure 4.24: RNAscope - FRA-1

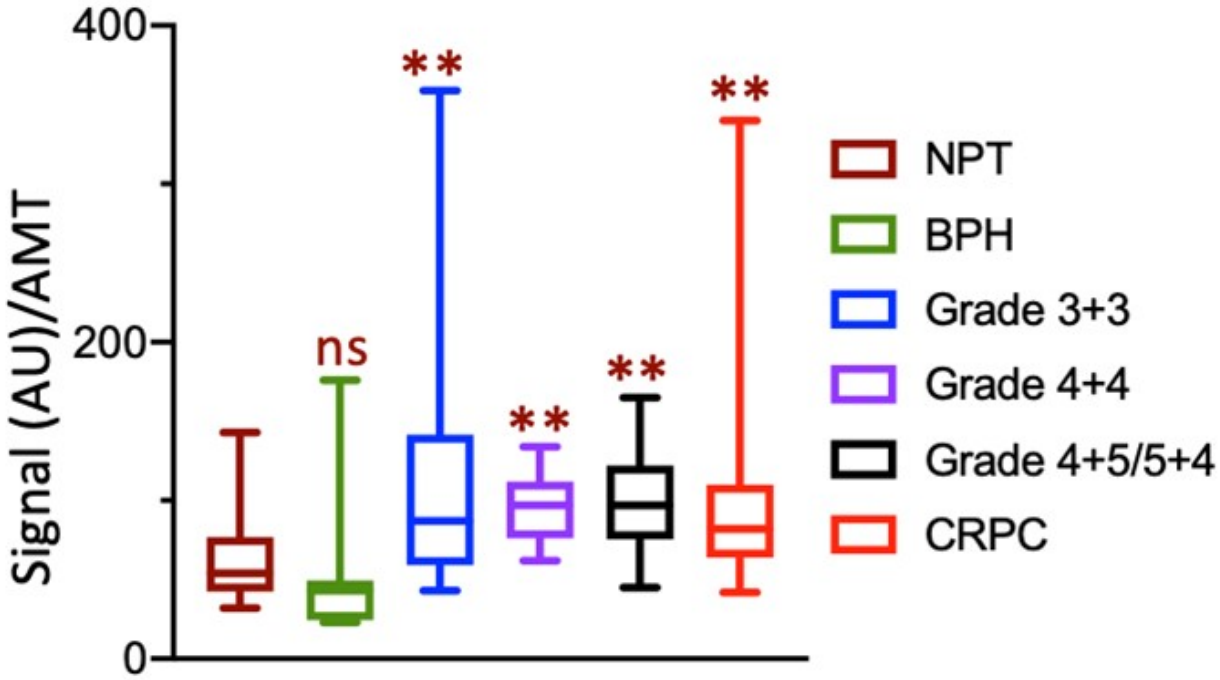

Figure 4.24. Box and Whisker Plot displaying expression of FRA-1 mRNA expression in NPT (n=36), BPH (n=10), Grade 3+3 (n=25), Grade 4+4 (n=15), Grade 4+5/5+4 (n=15) and CRPC (n=40). All the punctate dots were acquired, and significance of difference was calculated using Mann-Whitney U test (ns P>0.05; **P<0.01).

4.4.5.2.3. Analysis of mRNA expression for PYGO2 in NPT, Grade 3+3, Grade 4+4, Grade 4+5/5+4 and CRPC

Expression levels of PYGO2 mRNA did not change in BPH and Grade 3+3 compared to NPT. But expression was increased dramatically in Grade 4+4 (89.07 ± 28.90-fold, mean±SEM; **P<0.01) compared to NPT. Its expression further increased in Grade 4+5/5+4 (196.70±49.49-fold, mean±SEM; ****P<0.0001) compared to NPT. But its expression was not much increased in CRPC (17.17 ± 16.94-fold, *P<0.05) compared to NPT.

Figure 4.25. RNAscope - PYGO2

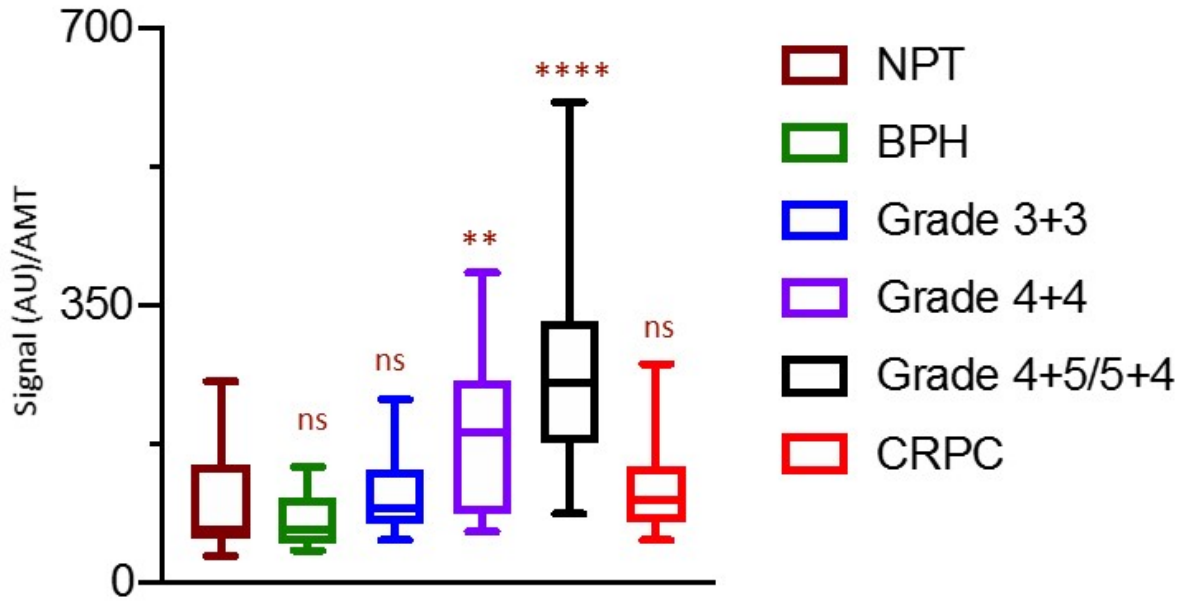

Figure 4.25. Box and Whisker Plot displaying expression of PYGO2 mRNA expression in NPT (n=36), BPH (n=10), Grade 3+3 (n=25), Grade 4+4 (n=15), Grade 4+5/5+4 (n=15) and CRPC (n=40). All the punctate dots were acquired, and significance of difference was calculated using Mann-Whitney U test (ns P>0.05; *P<0.05; **P<0.01; ****P<0.0001).

4.4.5.2.4. Analysis of mRNA of TCF-1 in NPT, Grade 3+3, Grade 4+4, Grade 4+5/5+4 and CRPC

No significant change in expression of TCF-1 in BPH and Grade 3+3 compared to NPT was observed (Fig. 26). All fold changes represent as mean±SEM. A significant increase in expression was observed in Grade 4+4 (35.62 ± 10.30-fold, *P<0.05) and also in Grade 4+5/5+4 (71.81 ± 14.82-fold, ****P<0.0001) vs NPT. There was also a significant increase in expression of TCF-1 in CRPC (40.64 ± 13.90-fold, ***P<0.001) vs NPT.

Figure 4.26: RNAscope - TCF-1

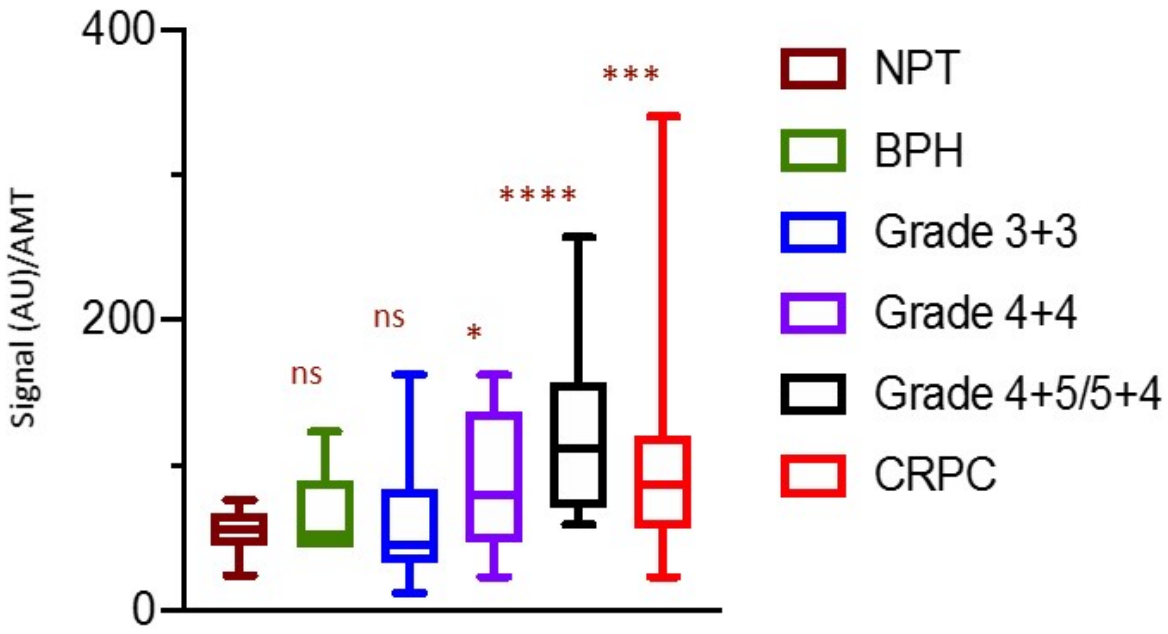

Figure 4.26. Box and Whisker Plot displaying expression of TCF-1 mRNA expression in NPT(n=36), BPH (n=10), Grade 3+3 (n=25), Grade 4+4 (n=15), Grade 4+5/5+4 (n=15) and CRPC (n=40). All the punctate dots were acquired, and significance of difference was calculated using Mann-Whitney U test (ns P>0.05; **P<0.01; ****P<0.0001).

4.5. Discussion

4.5.1. An assessment of expression of AR protein in normal and cancerous prostate including CRPC

4.5.1.1. Expression of AR protein in prostate

AR is a member of the nuclear steroid receptor superfamily of transcription factors and is classified as NR3C4 (nuclear receptor sub-family 3, group C, member 4) (Lu et al., 2006). AR plays a pivotal role in prostate development and carcinogenesis. Binding of DHT with AR triggers dissociation of HSP followed by dimerization of DHT-AR complex and translocate into the nucleus where it binds to DNA and interacts with a series of transcriptional coregulators to regulate target gene expression (Koochekpour, 2010).

4.5.1.1.1. The role of AR in normal prostate

AR is expressed in outer layer of urogenital mesenchyme (UGM). AR regulates gene expression which is crucial to normal prostate development and function (Heinlein and Chang, 2002). Stromal AR resides in the UGM and UGM controls ductal morphogenesis using paracrine signalling to initiate prostate development. Stromal AR is the principal modulator of epithelial cell differentiation in the normal developing prostate (Cunha et al., 2004) whereas epithelial AR appears to have the main role to play in the production of secreted prostate proteins.

4.5.1.1.2. The role of AR in BPH

Of the three zones of the human prostate (Fig. 1.4, section 1.3), (central, peripheral and transition zones), BPH develops from the transition of the prostate. BPH mostly consist of stromal cells (88.4%) with only 9% epithelial cells (Svindland et al., 1996); this indicates that stromal cells may contribute mostly towards the development of BPH, even though both stromal and epithelial compartments are involved in development of BPH. The modification of different growth factors by stromal AR signals may promote the initiation and progression of BPH in a paracrine and/or autocrine manner (Thomson, 2008). For instance, some variables related in change of cell proliferation/differentiation, or stem cell population as well as factors involved in the EMT (Alonso-Magdalena et al., 2009) or inflammation/immune tolerance (Kramer et al., 2007) and (Fibbi et al., 2010), have been suggested to be directly or indirectly linked to the AR. Therefore, the targeting of AR signals may play an important role in combating BPH progression (Svindland et al., 1996).

4.5.1.1.3. The role of AR in CRPC development

Tumorigenesis of PCa is androgen dependent and following ADT, the cancer tumour responds initially, but become refractory to treatment afterword. There is no cure for castration resistant prostate cancer (CRPC), which is ADT resistant but AR dependent. Details of CRPC development have been described in Chap-I (Sec. 1.11.7). Briefly, AR signal become reactivated, and tumours over-expressing AR accelerate to regrow than normal tumour (Chen et al., 2004a). Numerous mechanisms have been implicated in aberrant AR reactivation. These include increases of AR

expression, AR point mutation that alters AR activity, changes in cell signalling pathways that modulate AR function, changes in coregulatory proteins, and changes in steroid metabolism within tumours cells (Agoulnik and Weigel, 2006 and Chen et al., 2008).

4.5.1.1.4. AR expression as putative biomarker

In this study, I aimed to measure the expression of AR protein in BPH, Grade 3+3 and CRPC compared to NPT in single level staining (DAB staining) and multilabel fluorescence staining. Just to summarize: DAB staining analysis showed that AR expression was increased significantly in BPH (1.46±0.64-fold, mean±SEM; *P<0.05), but its expression decreased in Grade 3+3 PCa (-0.82±0.40-fold, mean±SEM; *P<0.05). AR expression increased significantly in CRPC (8.94±1.92-fold, mean±SEM; ***P<0.001) (Fig. 4.2). CRPC could be histologically identified, and the expression of AR expression correlates with the histological analysis. Fluorescence staining showed AR expression was also increased significantly in BPH (***P<0.001) (Fig. 4.13), but there was no change in expression in Grade 3+3, whereas its expression dramatically increased in CRPC (****P<0.0001) (Fig. 4.13).

As discussed elsewhere, tissue arrays provide a useful tool for expression analysis for RNA and proteins, particularly for tissue samples that are difficult to obtain or for rare diseases (Johal et al., 2021). A technique commonly used in our laboratory is to maximize the use of precious tissue samples by using multiple antibodies on the same TA slide (Arya et al., 2015; Giuliano et al., 2016) and Johal et al., 2021). In experiments conducted for other projects in our laboratory, particularly when both single label (DAB) stain and multilabel (fluorescence) staining have been conducted for the same antibody, the results are generally within ranged for both single and multilabel analysis e.g., (Symes et al., 2013); Ms Bushra Kanwal (personal communication). However, it is not unusual that there could be some differences in a comparative analysis between these two approaches. An obvious reason is that there is no technical interference due to sequential staining (Materials and Methods) for multilabel staining with multiple antibodies, nor signal interference from multiple fluorophores which causes ‘bleed-through’ (Kim et al., 2013) . In this study I used multi fluorophore labelling using four fluorophores listed in Table 2.8, it may be

possible that the small discrepancy between single label (Figs. 3.12 and 4.15) and multilabel results for AR staining in Grade 3+3 could be due to this reason.

The distribution and expression of AR in BPH was investigated in other studies, previously, but the conclusions were inconsistent. Some studies found that AR was abundantly expressed in nuclei of epithelial and stroma using IHC (Alonso-Magdalena et al., 2009). Nicholson et al. revealed that using of multilabel IHC in which he noticed that an increased percentage of AR positive cells and increased AR intensity in both epithelial and stromal cells on BPH compared to NPT (Nicholson et al., 2013).

AR activity linked to BPH development has been documented. Peters and Barrack showed that AR is expressed exclusively in the epithelial cell nuclei, little in the stromal cells (Peters and Walsh, 1987). However, another study revealed that AR was expressed in both epithelial and stromal cells of hyperplastic nodule with higher expression in BPH epithelial cells (Kyprianou and Davies, 1986). Objective, unbiased, quantitation as used here, with single label staining, showed that AR in epithelial cells and stromal cells in BPH was increased compared to normal prostate tissue and the size of the nucleus in epithelial and stromal cells in BPH was smaller than that of normal prostate tissue. These findings show that BPH cells are more sensitive to androgens even as exposure to androgens decreases with ageing (Nicholson and Ricke, 2011). AR and ER Gene expression level is higher in patient with larger prostate. Hetzl et al. however, showed that the AR immunoreactivity in BPH was similar to that in normal prostate (Hetzl et al., 2012).

In CRPC, expression of AR protein was significantly increased both in DAB and fluorescence-stained tissue. This suggests, in relation to the discussion above regarding the discrepancy between single and multi-label AR expression, that for larger range changes both techniques yield similar outcomes. Linja et al. have reported that an increase in the amplification of the AR gene during androgen deprivation therapy and concluded that the proliferation of cancer cells in an environment with a low concentration of androgens may involve the overexpression of the AR (Linja et al., 2001). Several studies reported that advancement to CRPC is linked to AR overexpression, and that reduced AR represses tumour growth in PCa, even in CRPC (Chen et al., 2004b).

Additionally, AR expression is increased in majority of CRPCs, of which only 10–20% showed amplification of the AR gene (Linja et al., 2001), implying that increased AR expression in CRPC may result from other factors other than gene amplification. Even though expression of proteins, such as the AR protein, is governed by several steps (transcription, translation, and post-translational regulation such as protein stability), the transcriptional step could be important in maintenance of protein expression.

A recent clinical trial with abiraterone, 17-(3-Pyridinyl)androsta-5,16-dien-3β-ol acetate, a hormone therapy drug, on the other hand, demonstrated that CRPC is still androgen dependent (Attard et al., 2008). Numerous enzymes engaged in steroidogenesis are thought to be upregulated in CRPC cells, suggesting cancer cells may produce androgens during androgen withdrawal (Holzbeierlein et al., 2004 and Locke et al., 2008). Furthermore, experimental models for CRPC have revealed that many androgen-regulated genes are elevated in CRPC (Gregory et al., 1998).

This is a first investigation of AR expression in an unbiased, quantitative manner. The results presented here have been conducted in relatively large sample set and also across different types of prostate tissue samples (normal, different grades and CRPC), standardizing the staining. The weight of evidence from this study and some of the previous studies suggest that in early stages of prostate carcinogenesis there is a decrease in the expression of AR.

The increased expression of AR in BPH has been suggested previously (Izumi et al., 2013), although its role in the development of BPH remains unclear. It has been proposed that increase in AR activity may activate epithelial to mesenchyme transition. It is also known that Wnt signalling may also play a role in epithelial to mesenchyme transition (Kalluri and Weinberg, 2009). However, in this study, there was no significant change in the expression of β-catenin or other Wnt related markers in BPH compared to normal samples. Conversely, the expression of AR and all Wnt target genes and proteins tested was significantly increased in high grade prostate cancer and CRPC (Fig. 4.12, 4.14 and 4.15). The expression of AR was seen to be significantly increased in CRPC, confirming previous observations (Robinson et al., 2015) and validating the tissue set used in this study. These results indicate a different role in the interaction of AR and Wnt signalling pathways in two different proliferative diseases. This direct comparison in the

same tissue set using quantitative immunohistochemistry is the first detailed report to arrive at this conclusion.

4.5.1.2. *In situ* expression of Cx43 in prostate

Cx43 plays a key role in cell-cell communication, signal transduction (Cronier et al., 2009). Cx43 is known to be dysregulated in multiple types of cancers and engaged in tumour progression including gastric, cervical, colorectal and prostate cancer. Expression and localisation of Cx43 is associated with pathological progression of the PCa (Tsivian et al., 2009).

The role of Cx43 has also been investigated in mouse models of cancer, previously. For instance, crossing of null mutant Cx43 mouse line with erythroblastic leukaemia viral oncogene homologue overexpressing mice (Plante et al., 2011) delayed onset and fewer and smaller primary breast tumours than in wild type mice but increase metastasis to the lung (Plante et al., 2011). On the other hand, in human, Cx43 overexpression in highly metastatic lung cancer cells reversed the metastatic tumour phenotype but reduced Cx43 gene expression produced breast cancer cells (MDA-MB-231) with increased metastatic potential (Shao et al., 2005).

Cx43 is one of the most studied connexin isotype in cancer and has been reported to play suppressive role in tumorigenesis. In Chapter III (Sec. 3.4.3.6), I investigated the expression of Cx43 in high grade cancer and the results suggest that Cx43 expression was significantly reduced in higher grade PCa. In this chapter, I measured the expression of Cx43 in BPH, Grade 3+3 prostate and CRPC (Fig. 4.3). To my knowledge there has been no previous studies to measure the expression of Cx43 in different stages of PCa. The result showed expression of Cx43 was significantly increased in BPH (4.82±1.99 -fold, mean±SEM; *P<0.05) compared to NPT, but its expression was significantly reduced in Grade 3+3 compared to NPT (-0.82±0.40-fold, mean±SEM; *<0.05) and its expression was further decreased in CRPC (-3.00±1.00-fold, mean±SEM; **P<0.01) (Fig. 4.3). When considered in conjunction with the Hou et al. (2019) data, this may suggest a putative tumour suppression role in regulating Wnt/β-catenin transcription supporting the notion by others that Cx43 may act as a tumour suppressor gene (Fukushima et al., 2007).

It was previously shown that Cx43-GJIC facilitates cAMP transmission, leading to higher levels of p27 and lowered tumour growth (Zhang et al., 2001). Another study showed that the expression of Cx43 was increased in metastatic lesions (Tang et al., 2011). Its impaired expression is associated with cancer progression (Benko et al., 2011).

Habermann et al. showed that expression of Cx43 in BPH was significantly higher and expression was lost in malignant tissue (Habermann et al., 2001), which was supported by (Tsai et al., 1996). Their result showed strong intensity of Cx43 expression in stromal cells. This appears plausible as BPH mostly consist of stromal cells (88.4%) and only 9% epithelial cells (Svindland et al., 1996). BPH is a benign proliferative condition of prostate gland and Cx43 expression may be increased accordingly, whereas prostate cancer is a malignant disease and loss of Cx43 expression may be responsible to alter cell growth and differentiation via different mechanisms; it is also plausible that Cx43 expression was decreased due to poorly differentiation of cancer cells. These could involve GJIC related functions or Wnt related mechanisms involving Cx43 (Hou et al., 2019) or both. In CRPC, Cx43 expression was reduced significantly. This may suggest decreased gap junction communication between cells. Cx43 activates TNF-β receptor signalling to induce apoptosis of prostate cancer cells (Wang et al., 2007a).

4.5.1.2.1. The following mechanism may help explain the reduction of expression of Cx43 in higher grade cancer

An interesting corollary of my novel observation that Cx43 expression decreases with increasing Gleason grading of PCa is the comparison of mechanistic data showed from our laboratory in prostate cancer cells (Hou et al., 2019) where it was shown that Cx43 is a regulatory partner of Wnt/β-catenin signalling. In that report, Hou et al. showed that the effect of Cx43 and β-catenin in the absence of Wnt signal activation is to act as a brake on the stabilization and nuclear translocation of each protein. When Wnt signal is active they move into the nucleus, together (Hou et al., 2019). When Cx43 or β-catenin is knocked down from PC3 cells, the other protein becomes stabilized (freely available) in the cytosol and is also found in the nucleus. I have shown that there is a decrease in Cx43 expression with increasing Gleason grading and a corresponding increase in β-catenin expression (Sec. 4.4.3.2; Fig. 4.3 and Sec. 4.4.5.2; Fig. 4.12).

Furthermore, most neoplastic cells have fewer gap junctions and the gap junctional intercellular communication compared with non-neoplastic cells. These findings might suggest that reduced Cx43 expression leads to lower GJIC which could cause aberrant and uncontrolled development of the epithelium (Benko et al., 2011). Interestingly, the reduction in GJIC could be due to activation of Wnt signalling that removes Cx43 from the membrane fraction into the nucleus (Fig. 2 in (Hou et al., 2019)). It appears that the *in vitro* mechanistic results are aptly supported by *in situ* quantitative immunohistochemical analysis in human PCa tissue.

microRNAs that regulate metastatic behaviours of cancer cells via targeting Cx43

Cx43 expression in breast cancer cells is known to be regulated by multiple microRNAs including miR-200a, miR-206 and miR-381. Cx43 in MDA-MB-231 cells was also observed to be targeting miR-200a, that was reduced in metastatic breast cancer tissue (Ming et al., 2015).

miRNAs are also closely associated with prostate cancer. The miR-34c, miR-205, miiR-34a and miR-15a-miR-16-1 clusters function as tumour suppressor genes in prostate cancer, are down regulated in PCa and (Hagman et al., 2010). On the contrary, miR-21, miR-let7c, miR-100 and miR-218 are upregulated in prostate cancer (Leite et al., 2011). Newly discovered, miR-20 expression is higher in prostate cancer tissue than normal prostate tissue. It has been observed that overexpression of Cx43, significantly, inhibited prostate cancer cell proliferation compared with that of Cx43 containing a miR-20a binding site. Because the endogenous miR-20a cannot bind the mutant 3'UTR of Mut Cx43, the expression of Cx43 in cells transfected with Mut Cx43 was higher and cell viability and proliferation were inhibited more than that of wild type Cx43 transfection (Benko et al., 2011). In addition, CX43 expression has been revealed to be strongly linked with characteristics that indicate a poorer prognosis and decreased Cx43 expression has been a significant predictor of free survival of bio-chemical recurrence in PCa (Benko et al., 2011).

4.5.1.3. c-MYC in PCa

c-MYC is a member of MYC oncogene family which consists of three members including *C-MYC*, *MYCN* and *MYCL*, that encode c-MYC, N-MYC and L-MYC genes, respectively (Dang, 2012). c-MYC contains the basic-region/helix-loop-helix/leucine-zipper (BR/HLH/LZ) motif at the C terminus and three highly conserved elements, known as MYC boxes 1–3 at the N terminus (Meyer and

Penn, 2008). c-MYC is also known as “super-transcription factor” that regulates a variety of downstream cellular process such as cell growth and proliferation, cell-cycle progression, transcription, transcription, differentiation, apoptosis and cellular motility (Knoepfler, 2007). The over expression of c-MYC linked to wide variety of cancers such as 80% of breast cancers, 70% of the colon cancer, 90% of the gynaecological cancers, 50% of hepatocellular carcinomas and a variety of haematological tumours (Knoepfler, 2007). Overexpression of c-MYC in PCa has been known since 1986 (Fleming et al., 1986). There are however, few systematic, standardized investigations that have employed unbiased quantitation to measure the expression of c-MYC in different grades of PCa.

In this study, I investigated the expression of c-MYC in NPT, BPH, Grade 3+3 PCa and CRPC. The result showed the expression was not changed in BPH compared to NPT, but its expression was significantly increased in Grade 3+3 (*$P<0.05$) compared to NPT (Fig. 4.14). There was no signal found while staining CRPC tissue cores. This was most likely due to unexplained technical issues as there was expression in TAs other than CRPC TA.

Gurel et al. (2008) reported that c-MYC is frequently overexpressed in prostate intraepithelial lesions (PINs) with an incremental increase from normal tissue to low-grade PIN to high-grade PIN (Gurel et al., 2008). Various studies using mouse models have demonstrated that c-MYC overexpression in prostate luminal cells can lead to hyperplasia and PIN lesions but not invasive carcinoma. c-MYC mRNA expression in cancer tumour was reported to be significantly higher than in benign tissue (Hawksworth et al., 2010).

It is likely that activation of Wnt signalling with increasing expression of β-catenin with increasing Gleason grading may also be responsible for over-expression of c-MYC, as it is a target gene for Wnt/β-catenin transcription. There might also be an alternative mechanism associated for the c-MYC overexpression (Gurel et al., 2008). Over-expression of c-MYC protein may also begin with amplification of *c-MYC* locus on the chromosome. However, (Hawksworth et al., 2010) could not find any correlation with 8q24 locus amplification. A recent report suggests that TMPRSS2-ERG fusion (Chap-I, Sec. 1.10.2.2) activates c-MYC and disrupt prostate epithelial differentiation, indicating a potential mechanism for the early c-MYC overexpression in a subset of PCa (Sun et al., 2010).

4.5.1.4. β-catenin in CRPC

β-catenin is a component of the adherent junction complex and principal transducer in Wnt/β-catenin that remains sequestered in cytoplasm in the absence of Wnt signal activation at the cell membrane. Increasing of β-catenin in cytoplasm facilitates its nuclear entry, where β-catenin interacts with lymphoid-enhancing factor-1 (LEF1) and activates the transcription of genes containing LEF1/TCF binding sites, including the *LEF1* gene (Kypta and Waxman, 2012). Importantly, β-catenin can cause ligand-independent activation of AR in prostate cells (Wang et al., 2008).

There is an ongoing debate whether β-catenin has an impact on CRPC development? Some studies documented that the excessive amount of β-catenin results in an increase of progressing PCa stage (Chesire et al., 2000), whereas others documented the inverse relationship (Whitaker et al., 2008). Previous studies were limited by use of visual methods of immunohistochemistry (IHC) quantitation, together with the known alternative impacts of variations in IHC and fixation protocol (Whitaker et al., 2008).

The result presented here show that the expression of β-catenin in BPH was not significantly different, though there may be a slightly higher β-catenin expression in BPH (Fig. 4.12). Similar result found for Grade 3+3, where expression did not change significantly when compared to NPT. However, the expression was significantly increased in CRPC (*$P<0.05$) (Fig. 4.12). This indicates β-catenin may contribute towards progression to advanced disease.

There was no sign of dysregulation in Wnt signalling components in BPH (Fig. 4.12). Very few studies have been conducted to evaluate β-catenin expression in BPH. Although Olson and colleagues showed an increased cytoplasmic and nuclear β-catenin expression (Olson et al., 2019). Another study reported loss of expression for e-, n- and p cadherin and α- and β catenin in BPH compared to normal prostate tissue (Arenas et al., 2000). Incidentally, AR expression was significantly higher in BPH (Fig. 4.13). These results in conjunction with those showing an antagonistic relationship between AR and Wnt signalling pathways (e.g., Chap III and IV) suggest that both these pathways may be crucial not only development of normal prostate but also in proliferative diseases of the prostate.

My analysis also showed β-catenin expression was not significantly changed in lower grade prostate cancer. In lower grade prostate cancer, Grade 3+3, a fraction is changed histologically in epithelial layer (Fig. 4.8 and Chap-I, Sec. 1.9). This is not likely to impact protein expression analysis when compared to AR expression in whole cores where little histological changes occur (Fig. 4.8). Miyamoto et al. revealed other proto oncogenic proteins such as c-MYC might be expressed higher in Grade 3+3 and initiate cancer progression (Miyamoto et al., 2009). Indeed, FRA-1 was found significant higher expression in Grade 3+3 (Chap-III, Sec. 3.4.3.3) and may be added to the list of transcription factors that may activate transcription of oncogenes.

My result further showed β-catenin expression was significantly increased in CRPC (Fig. 4.12). Multiple lines of evidence suggest that dysregulation of Wnt/β-catenin associated in PCa development (Yokoyama et al., 2014 and Kypta and Waxman, 2012). Stability of β-catenin is tightly regulated by APC which directs β-catenin for phosphorylation, ubiquitylation and degradation. Accumulation of β-catenin in cytoplasm indicates dysregulation in Wnt signalling pathway. Also, β-catenin pool at the plasma membrane is protected from degradation by its interaction with cadherins. A number of PCa tumours contain increased level of β-catenin in the cytoplasm and/or nucleus because of gene mutation or more nongenomic changes in the expression of inhibitors and activators of Wnt signalling (Kypta and Waxman, 2012).

Mutation in gene *CTNNB1* (encode β-catenin) and A*XIN1* (encode APC) increases the signal of Wnt/β-catenin signalling pathway in colorectal cancer, but is sporadic in prostate cancer (Yokoyama et al., 2014 and Kypta and Waxman, 2012). But genetic changes are found more frequently in CRPC than in hormone naïve prostate cancer. A study showed 12% samples of CRPC contained mutation in *CTNNB1* whereas 22% samples were found to have mutation in *APC* (Grasso et al., 2012).

Interestingly, human AR gene itself is a target gene for Wnt induced gene transcription. Stimulation of Wnt/β-catenin by Wnt can increase AR expression via TCF/LEF-1 binding site on the AR promoter, leading to upregulation of AR target genes including β-catenin. This proposition is supported by the data presented in this thesis. I have shown that β-catenin expression increases with increasing Gleason grading of PCa (Chap-III, Sec. 3.4.3.2.and Fig. 3.5) and in CRPC samples (Fig. 4.12); the opposite is observed for AR expression (Chap-III, Sec. 3.4.3.1 and Fig. 3.4)

except AR expression in CRPC. There is also an increase in β-catenin RNA expression with increasing Gleason grading diagnosis, although, there is a significant increase in β-catenin RNA in CRPC (Fig. 4.23). Furthermore, in CRPC tissue samples, there is increased co-localization of AR and β-catenin (Figs. 4.12 and 4.13). These data appear to suggest that an inverse expression relationship between AR and β-catenin expression in low to high grade cancer, whereas this shifts after PCa becomes castration resistant. In CRPC, the relationship between AR and Wnt signalling appears to be complementary as there is concomitant increase in the expression of both AR and β-catenin proteins, indicating that perhaps there is amplification of gene expression targets of both AR and Wnt signalling.

4.5.1.5. FRA-1 in PCa and CRPC

FRA-1 (Fos-like antigen 1) is an important member of FOS which is a vital component of activating protein-1 (AP-1) transcription factors, which are involved in promoting carcinogenesis (Vogt, 2002). The FOS family includes c-FOS, FOSB, FOS-associated antigen 1 (FOSL1 or FRA-1) and FOS-associated antigen 2 (FOSL2 or FRA-2). The FOS family contain highly homologous bZIP domain (Chap-III, Sec. 3.5.33), but compared to c-FOS and FOSB, FRA-1 and FRA-2 do not have C-terminal transactivation domain. Therefore, FRA-1 and FRA-2 are considered to be less potent factors for transcriptional activation (Wisdon and Verma, 1993). FRA-1 can inhibit the expression of c-FOS by binding with its promoter and also hinder c-FOS mediated transcriptional activation and is recognised as a suppressor of AP-1 transcriptional activity (Ito et al., 1990 and Yoshioka et al., 1995). Conversely, other members of AP-1 can also increase transcriptional activity by binding to its promoter. FRA-1 is phosphorylated by ERK kinase after interaction with extracellular compound, thus controlling downstream signalling component (Galvagni et al., 2013).

4.5.1.5.1. Regulation of FRA-1

FRA-1 is an unstable protein with short half-life and the instability is caused by a single destabilising sequence located within 30-40 amino acid residues at the C-terminus (Basbous et al., 2008). The regulation of FRA-1 is multifaceted, among those its post-translational phosphorylation is vital and occurs at serine and threonine residues and thus neutralize its degradation and promotes protein stabilization (Basbous et al., 2008). FRA-1 is also

phosphorylated by kinases such as mitogen-activated protein kinase (MAPK), protein kinase C (PKC), cAMP-dependent kinase (PKA), and cyclin-dependent kinase 1-cdc2 (CDC2) (Gruda et al., 1994).

Endogenous microRNAs with 22 nucleotides have regulatory roles in cells. Many of those have been shown to obstruct tumorigenesis by downregulation of FRA-1 expression. These include but not limited to the miR-19a/b in breast cancer and cervical cancer, miR-138 in squamous cell carcinoma, miR-497 in colorectal cancer, miR-130a in breast cancer, miR-195 in prostate cancer, miR-34 in breast cancer and colon cancer (Jiang et al., 2020).

FRA-1 was previously thought to be associated with embryonic development and bone formation (Jiang et al., 2020). Now numerous cancers have been associated with over-expression of FRA-1, namely, breast cancer, lung cancer, colorectal cancer, ovarian cancer, Thyroid cancer, Skin cancer, Gastric cancer (Jiang et al., 2020).

FRA-1 expression has not been investigated in different pathological grades of prostate cancer, previously. To establish its status as prognostic biomarker I used NPT, Grade 3+3 and CRPC tissue stained with fluorescent labelled FRA-1 antibody to measure its expression. The result showed the expression of FRA-1 was not increased in BPH, but significant increase was observed in Grade 3+3 (*P<0.05) and CRPC (*P<0.05 (Fig. 4.11). This indicates during cancer progression its expression was changed and has a significant effect on carcinogenesis and metastasis.

FRA-1 expression was significantly higher in Grade 3+3 (*P<0.05) and CRPC (*P<0.05) compared to NPT (Fig. 4.11). In my previous result I found the expression of β-catenin was not significantly increased in Grade 3+3 but the results indicate that the trend for β-catenin expression was still higher (Fig. 4.12.B). This may suggest that β-catenin is responsible for FRA-1 gene transcription and ultimately protein over-expression or it regulated through another gene transcription control pathway. A further explanation would be an increase in the life-span of FRA-1 protein due to increased stability due to protein stabilization and regulation mechanisms discussed above.

β-catenin expression was found significantly higher in CRPC tissue (Fig. 4.12) and may be the cause of increased FRA-1 transcription and subsequently increased expression of FRA-1 protein in CRPC tissue. Another possibility could be that E-cadherin and α-catenin are shown to

antagonize the Wnt signal (Fagotto et al., 1998). The loss of the proteins during progression of cancer may increase the β-catenin signal further in neoplastic cells and subsequently increase FRA-1 transcription (Mann et al., 1999).

Another further mechanism for a higher expression of FRA-1 in CRPC tissue could involve miRNAs. Numerous genetic mutations, aberrant gene expression and miRNA dysregulation are involved in carcinogenesis and progression (Zhu et al., 2007). miRNAs with 22 nucleotides are widespread in mammalian cells and affect numerous cellular processes including differentiation, proliferation, cell cycle control and apoptosis, migration and invasion (Calin and Croce, 2006). miRNA regulates the target mRNAs by binding to partially complementary sequence in the 3'-untranslated region (3'-UTR) of the target mRNAs in a sequence specific manner. Evidence shows that there are numerous miRNAs which regulate various oncogenes and tumour suppressor (Bartel, 2009). Among them, miRNA-195 was found to be associated with FRA-1 regulation. miRNA is FRA-1 specific and suppresses the expression of FRA-1. But in CRPC and advance prostate tissue miRNA-195 was found to be deregulated (Wu et al., 2015).

4.5.2. Colocalization of Wnt related proteins in non-CRPC vs CRPC

Colocalization analysis of 6 permutations (e.g., NPT vs BPH, NPT vs Grade 3+3, NPT vs CRPC, BPH vs Grade 3+3, BPH vs CRPC, Grade 3+3 vs CRPC) of 3 proteins in NPT, BPH, Grade 3+3 and CRPC depicted in multiple graphs (Figs. 4.17, 4.18 and 4.19) are compiled and presented in single graph (Fig. 4.20) to illustrate the quantitative result for their colocalizations.

Symes et al. suggested that in addition to alterations in protein expression, co-localization coefficients of two proteins may also serve as biomarker for PCa (Symes et al., 2013). Further studies in a variety of cancers in both man and animals (Arya et al., 2015; Giuliano et al., 2016 and Arthurs et al., 2017) demonstrated the utility of co-localization analysis as a disease biomarker. This has been particularly useful for Wnt signalling related proteins not just in cancer (Arya et al., 2015 and Giuliano et al., 2016), but also in other urological disorders such as Posterior urethral valves (Johal et al., 2021).

The comparison of NPT and BPH revealed significant co-localisation for FRA-1/AR, β-catenin/AR, there was increase in NPT vs CRPC for FRA-1/AR, β-catenin/AR can be used a biomarker for NPT,

Grade 3+3 and CRPC. For BPH vs Grade 3+3, there was no change for any combination. For Grade 3+3 vs CRPC, FRA-1/β-catenin, FRA-1/AR and β-catenin/AR, there was a significant change from NPT vs CRPC. FRA-1/β-catenin, FRA-1/AR and β-catenin/AR combination can be used as prostate biomarker. This combination could be used as a marker for CRPC to distinguish from non-CRPC tissue. The results presented in Fig. 4.20 indicate that multiple combinations of co-localization biomarkers may be developed, with further research, into clinically useful markers of disease diagnosis and prognostication.

4.5.3. Single molecule mRNA analysis in PCa tissue samples usefulness as biomarkers

Biomarker discovery is important for diagnosing clinical diseases and to develop therapy. Diagnosis in early stage of the diseases trigger to measure appropriate therapeutic application to cure the disease. mRNAs, like proteins that these encode, can be used as a biomarker to explore cancer pathogenesis (Rapisuwon et al., 2016).

Recently, RNA has been suggested to be an ideal predictor of diverse genetic expression in cell. The use of traditional *in situ* (ISH) method to map RNA expression to single cell is useful, but low performance and high technical complexity of these methods has impeded its use (Cassidy and Jones, 2014). The RNAscope$^{(R)}$ procedure provides significant advance on RNA ISH technology and offers a spatial and morphological framework for single-cell resolution in addition to precise quantitation (Wang et al., 2012). RNAscope$^{(R)}$ features a distinct signal amplification step to visualise the target RNAs as a punctate dot (Anderson et al., 2016). I used four Wnt signalling targets namely, β-catenin, PYGO2, TCF-1 and FRA-1 to measure their mRNA expression in NPT, BPH, Grade 3+3, Grade 4+4, Grade 4+5/5+4 and CRPC to be used as a potential biomarker for the respective category of tissue.

4.5.3.1. β-catenin single molecule mRNA expression

The result showed mRNA expression of β-catenin in BPH or Grade 3+3 PCa did not change significantly. But the expression was significantly increased in Grade 4+4 (**P<0.01), Grade 4+5/5+5 (**** P<0.0001) and CRPC (***P<0.001) (Fig. 4.23).

The results indicate transcription of β-catenin begun to increase at Grade 4+4 and the phenomenon continues in Grade 4+5/5+4. There has been no previous investigation of single molecule RNA analysis for Wnt signalling targets in PCa.

An interesting question is how is β-catenin mRNA expression increased in high Grade PCa?

There is various possible explanation that also highlight the integration of transcription processes and the complexity through which a transcription factor A can activate the expression of transcription factor B and that transcription factor B in turn regulates the expression of transcription factor A. An example of such a mechanism is hypothesized below: In my study (Chap-III, Sec. 3.4.3.3), I found the expression of FRA-1 was significantly increased in Grade 3+3 and Grade 4+4. FRA-1 could be used as a transcription factor for β-catenin to increase the transcription induced by β-catenin-TCF-LEF complex (Akiyama, 2000), and subsequently upregulate β-catenin mRNA expression.

Just as protein stability for FRA-1 could result in its over-expression (Sec. 4.5.1.5.1.), increased stability of RNA may result in the expressed gene stability. (Ebert et al., 2002) conducted SSCP analysis of exon 3 where mutations are known in β-catenin gene and found that mutation in that exon inhibit the degradation of RNA and subsequently β-catenin was stabilised. They found possible association between mutational changes of the genes and enhanced β-catenin gene transcription (Ebert et al., 2002). The molecular mechanisms underlying this possible association, however, remain largely unknown.

Nevertheless, elevation of β-catenin mRNA may also result from activation of Wnt signalling pathway or mutations in either the APC or β-catenin gene, which leads to the β-catenin protein accumulation (sequencing of the samples used can answer this question, see limitations). Apart from this, the rise of β-catenin mRNA can also be assumed to be independent of the Wnt pathway. There was, however, a decrease in β-catenin mRNA in CRPC tissue compared to high grade PCa samples (Fig. 4.23). This is an interesting observation and may suggest that the increase in the protein expression in CRPC may be gene transcription independent. This suggests that other mechanism such as increase in protein stability may be responsible for the increased expression of β-catenin protein in CRPC (Ebert et al., 2002). Although a majority of mutations in

genes are thought to be destabilizing for protein expression, stabilizing mutations may also occur; this may offer one possibility of an increase in protein expression for β-catenin in CRPC with a corresponding decrease in single molecule mRNA expression. In CRPC, increased AR, FRA-1, PYGO2 may act as transcriptional activators for β-catenin to initiate transcription of β-catenin and subsequently β-catenin mRNA expression may be increased through this transcriptional regulation.

4.5.3.2. FRA-1 – single molecule mRNA expression

Analysis of mRNA expression showed (Fig. 4.24) that its expression was not changed in BPH but significantly increased in Grade 3+3 (**P<0.01), Grade 4+4 (**P<0.01) and CRPC (**P<0.01). This result reflects my earlier observations (Chap-III, Sec. 3.4.3.3) which showed FRA-1 protein expression was increased significantly in Grade 3+3 (*P<0.05), Grade 4+4 (*P<0.05), Grade 4+5/5+4 (*P<0.05). A consequence of increase in FRA-1 on increased transcription of β-catenin is discussed above (Sec. 4.5.3.1).

4.5.3.3. PYGO2 single molecule mRNA expression

Very little information exists regarding PYGO2 in PCa. PYGO2 is considered the most downstream component of the Wnt signalling transcriptional complex. Wnt activation occurs by nuclear translocation of β-catenin. The armadillo (Arm) repeats in β-catenin binds to TCF (Städeli et al., 2006). The adaptor protein legless (Lgl/Bcl-9) relates ARM repeat to Pygopus2. The transcription of Pygopus2 is accomplished through by interaction of the N-terminal homology domain (NHD) and Med12 and Med13 (Carrera et al., 2008). Analysis of mRNA expression of PYGO2 showed that expression was not significantly changed in BPH and Grade 3+3. But expression was significantly increased Grade 4+4 (**P<0.01), Grade 4+5/5+4 (****P<0.0001) and CRPC (*P<0.05) (Fig. 4.25).

Expression of mRNA of PYGO2 echoed protein expression of PYGO2 in Grade 3+3 and Grade 4+5/5+4. PYGO2 protein expression change was not significantly increased in Grade 4+4 (ns P>0.05), but mRNA expression in Grade 4+4 (**P<0.01) was significantly increased (Fig. 4.25). This is an interesting observation and if true, this suggests a complex relationship between transcription and translation and require more detailed investigation. miR-516-3P was still

present at initial stage of prostate cancer. It could be speculated that protein stability may be a regulatory factor in Gleason grade 4+4 disease.

4.5.3.4. TCF-1 single molecule mRNA expression in PCa

TCF-1 mRNA expression was not significantly changed in BPH and Grade 3+3, but its expression was significantly increased in Grade 4+4 (*P<0.05) (Fig. 4.26). The expression was further increased in Grade 4+5/5+4 (****P<0.0001) and CRPC (***P<0.001) (Fig. 4.26). Analysis of protein showed that protein was not significantly increased in Grade 4+4, but mRNA expression was significantly increased in Grade 4+4. It is important to note that both TCF-1 and PYGO2 may form transcriptional complex with β-catenin to activate Wnt mediated gene transcription. The lack of increase in protein expression for both these transcription partners may have some significance for the disease and consequences for Wnt/β-catenin transcription.

4.6. Summary

In this study, *in situ* expression of AR, β-catenin, FRA-1, c-MYC and Cx43 was investigated in NPT, BPH, Grade 3+3 and CRPC using IHC methods. The results showed AR may contribute to BPH development due to increase AR signalling in BPH by increasing its significant expression in BPH and highlight the correlation between AR and Wnt signalling in proliferative diseases of the prostate. There was also an increase in the expression of AR and β-catenin in CRPC tissue. The pathological consequences of AR in initiating CRPC development and progression may be via interacting with β-catenin. β-catenin may be a dominant oncogenic pathway associated with advance PCa development. The increased expression of β-catenin may activate expression FRA-1 and c-MYC gene because the proteins encoded by these genes also showed higher expression in Grade 4+5/5+4 and CRPC PCa. *In situ* mRNA expression showed a result broadly correlated protein expression data, although there are notable exceptions (e.g., Grade 4+4 disease). Expression of mRNA of β-catenin was observed significantly increased in higher grade PCa and CRPC tissue which is increased the expression of mRNA of FRA-1 and TCF-1, but PYGO2 showed increased expression in higher grade PCa and not in CRPC tissue.

4.7. Limitations

Ideally, I would have liked to align the RNAscope probes and antibodies, i.e., same targets for RNAscope probes and antibodies. This would have had allowed a direct comparative analysis of gene and protein expression and perhaps refined the biomarker analysis. This is not always possible as sometimes there are RNAscope probes available and not the antibodies and vice versa. The situation is improving with increasing availability for off the shelf single molecule RNA probes (which costs less than custom designed probes) but still problematic.

A further improvement would have been to conduct a thorough gene expression analysis in different grades of PCa and in CRPC to investigate the expression of AR and Wnt gene targets. This would have allowed a comprehensive analysis of all known Wnt and AR targets in the corresponding cohort and enhanced the power of the single molecule mRNA and protein analysis. This is challenging as all the samples I have used were FFPE and there are issues of the quality of RNA isolation for gene expression analysis from FFPE samples.

CRPC tissue samples were obtained from the Institute of Portuguese Oncology Porto (IPOPORTO) through Professor Rui Henrique. The treatment pathway for patients with CRRPC has been described in Chap-II (Sec. 2.3.1, Page-143). The treatment strategy for each patient was not supplied to the pathologist and it was impossible for him to access the full clinical history of individual patients. Therefore, it was not possible to determine homogeneity of patients based on their treatment perspectives. However, the goal of treatment was generally to obstruct or reduce testosterone production or to construct a barrier between testosterone and AR, to hinder the AR signalling pathways. Subsequently, AR expression was increased in CRPC tissue that reflects the treatment pathway.

CHAPTER V

Functional interaction of Wnt, Androgen Receptor and Connexin signalling in PCa cells

5.1. Introduction

Androgen receptor and Wnt signalling pathways are the two critical signalling pathways which play a vital role in development of many cancers including in PCa (Kyprianou and Isaacs, 1988). A detailed description of AR and Wnt signalling pathways and the role of Cx43 in Wnt signalling is given in Chapter I. Some important points are reiterated here as a rejoinder.

5.1.1. AR signalling

AR signalling is essential not only for the normal development of prostate gland (Tan et al., 2015), but also plays a key role in the initiation and progression and transition of PCa to castration resistant prostate cancer (CRPC) state (Tan et al., 2015) (Chapter 1, Sec. 1.16). AR signalling is activated by binding of testosterone or dihydrotestosterone (DHT) to the ligand binding domain (LBD) of AR in the cell cytoplasm. Subsequent to the binding of DHT to LBD, AR dissociates from heat shock proteins (HSPs) followed by dimerization of the AR-DHT complex exposing the nuclear localization signal site as a prelude to nuclear translocation (Debes and Tindall, 2002). Following translocation into the nucleus, the dimerized complex binds androgen responsive elements (AREs) and interacts with several co-regulatory proteins composed of co-activators and chromatin remodelling complexes that ultimately lead to transcription of target genes (Di Zazzo et al., 2016).

5.1.2. Castrate resistant prostate cancer (CRPC)

ADT therapy restricts the progression of androgen-dependent prostate cancer by altering the AR signalling pathway (e.g., (Hearn et al., 2016)). However, after a period of time the cancer reappears and its reappearance is correlated with increased expression of PSA (*KLK3*) (Prensner et al., 2012). This indicates that adaptive androgen signalling is activated in the tumour; this state is termed as castrate resistant prostate cancer (CRPC) (Feldman and Feldman, 2001) and is characterized by (i) an increased expression and stability of AR protein, and (ii) activating mutations in this receptor that alters its ligand specificity and changes in the expression of transcriptional co-regulators of the AR (Kypta and Waxman, 2012).

5.1.3. Wnt signalling and the role of Connexin proteins

Wnt signalling is an important regulator of cell function with free intracellular $[Ca^{2+}]_i$ and β-catenin as intracellular transducers. β-catenin is a 92 kDa protein that acts as transcription factor co-activator upon activation by the Wnt signal. Wnt signalling plays a key role in various fundamental processes such as cell proliferation, stem cell maintenance and differentiation, cell fate determination and motility (Logan and Nusse, 2004 and Lien and Fuchs, 2014).

Wnt signal activation results in stabilization of β-catenin in the cytoplasm and subsequent translocation in the nucleus where it can activate a gene transcriptional program that includes a number of proto-oncogenes, and also its own transcription activators such as FRA-1 (see above section 4.5.1.5.1), hence its critical role in a number of cancers including colorectal, breast, liver, skin and prostate (Sherwood and Leigh, 2016 and Shulewitz et al., 2006).

Connexins are a large family (20 members) of proteins that are involved in the formation of gap junctions for intercellular communication. Very recently, our laboratory has shown that upon activation of Wnt signalling, Cx43, a gap junction hemichannel forming protein also translocates into the nucleus with β-catenin. This indicates a close, functional and mechanistic interaction between Wnt and Connexin signalling in mammalian cells and also suggests that Cx43 may be part of the so-called destruction complex (Hou et al., 2019). Cx43 is also related to pathological progression of PCa (Benko et al., 2011). Cx43 expression is significantly altered in the late/high grade aggressive prostate cancer cells and the expression level was negatively correlated with pathological grading. Chen and his colleagues showed expression of Cx43 is decreases while AR signalling is activated (Chen et al., 2015a). Structurally, connexin proteins are conserved and show a high level of sequence identity. For example, Cx43 (NCBI accession number NP000156.1) and Cx31 (NCBI accession number 076872.1) show significant overlap in their sequences. It is therefore possible that other connexin proteins may also be involved in Wnt signalling.

Connexin 31 (Cx31) another member of the Connexin family forms aqueous channels for intercellular communication. Mutation in Cx31 gene, Gap junction beta-3 (GJB3), is linked to skin disorder erythrokeratodermia variabilis (Richard et al., 2000) and deafness (Rabionet et al., 2002). The associated member of Cx31 is Cx43 which has been studied in PCa development. Little

information exists regarding Cx31 expression in PCa. However, LnCAP cells neither express Cx43 protein nor Cx32 (another member of Connexin family). As I showed later in this chapter, Cx31 is expressed in LnCAP cells. Structurally, connexin proteins are conserved and show a high level of sequence identity. For example, Cx43 (NCBI accession number NP000156.1) and Cx31 (NCBI accession number 076872.1) show significant overlap in their sequences. It is therefore possible that other connexin proteins may also be involved in Wnt signalling.

The focus of this chapter is the interaction between Wnt/β-catenin/Connexin and AR signalling pathways.

5.1.4. Interaction between AR and Wnt signalling

Interactions between AR and Wnt signalling have been suggested in that deregulation of both pathways leads to diseases such as cancer (Davies et al., 2001). Canonical Wnt signalling (Wnt/β-Catenin) is reported to interact with AR signalling in CRPC (Schweizer et al., 2008a) where β-Catenin could bind to AR to stimulate its transcriptional cascade triggered by androgen, androstenedione or oestradiol in LnCAP cell (Truica et al., 2000). Binding of β-Catenin to ligand bound AR is also thought to facilitates the migration of β-catenin into nucleus (Mulholland et al., 2002). Furthermore, Wnt/β-Catenin signalling may enhance AR gene expression via TCF/LEF-1 by binding to promoter of AR (Li et al., 2009). In active state, the noncanonical Wnt signalling pathway (Wnt/Ca^{2+}) releases intracellular $[Ca^{2+}]_i$ and increases CaMKII in PCa cells line (Wang et al., 2010a). The Wnt/β-Catenin and Wnt/Ca^{2+} were considered independent from each other. Thrasivoulou et al. demonstrated that activation of Wnt/Ca^{2+} signalling release free $[Ca^{2+}]_i$ in mammalian cytoplasm that depolarizes the nuclear membrane that facilitates β-Catenin entry into cell nucleus (Thrasivoulou et al., 2013). However, in hormone naïve PCa cells, Wnt/β-Catenin signalling may trigger transcription of AR target genes, whereas, AR signalling inhibits the transcription of Wnt/β-Catenin target genes (Lee et al., 2015).

In a previous chapter (Chapter III), using *in situ* staining for Wnt and AR related proteins in low and high grade cancer, I showed that there may be a correlation between AR and β-catenin related protein expression. In Chapter IV, using the same quantitative IHC, I showed that there is an increase in AR expression and also that of β-catenin in CRPC prostate tissue. This raises the

possibility that in CRPCs, the AR and Wnt/β-Catenin signalling pathways may promote each other to activate a distinct pool of target genes for stimulating androgen-independent growth and progression of PCa cells.

AR expression was also increased in benign prostatic hyperplastic tissue, but β-catenin expression remained unchanged (Chap-IV, Sec. 4.4.4.5.2) compared to NPT. In Grade 3+3 PCa tissue, AR expression was decreased (Chap-IV, Sec. 4.4.3.1) but β-catenin expression was not changed. AR and β-catenin expression were both increased in CRPC tissue (Chap-IV, Secs. 4.4.3.1; 4.4.4.5.2 and 4.4.4.5.3), indicating synergistic interaction between these two critical signalling pathways.

However, molecular mechanisms of the nature of the interaction between AR and Wnt signalling remains unclear. As suggested above, it is known that AR and Wnt signalling pathways may interact to exacerbate progression of prostate cancer. Furthermore, our discovery that Wnt can stabilize and translocate proteins other than β-catenin, i.e., Cx43, give rise to the notion that other transducers may also be activated by Wnt signalling. I hypothesized that AR receptor and Wnt signalling pathways interact at a functional level with reciprocal activation of transducers by ligands for Wnt and AR signalling.

The following questions are addressed in this chapter:

1. Does ligand activation by Wnts e.g., Wnts 5A, 9B and 3A (paradigm ligands of the previously ascribed non-canonical and canonical Wnt pathways) directly activate AR signal activation?
2. Does ligand activation by DHT increases β-catenin stabilization and its translocation in the nucleus in model cell lines of metastasized prostate cancer?
3. Does the putative reciprocal Wnt and AR signal activation involves Connexin proteins, a newly discovered component of Wnt/β-catenin signalling pathway?

Addressing the above questions would enhance our understanding of the interaction of AR and Wnt signalling pathways in prostate cancer and may further elucidate fundamental mechanism of Wnt and AR signalling pathways.

5.2. Aims

In this study I used heterologous expression in PC3 and LnCAP cells (AR negative wild type PC3 cells, AR positive LnCAP cells and, wild type PC3 cells transfected with AR termed $PC3^{(AR+)}$) combined with cellular, immunochemical and gene transcriptional analysis to understand the interaction of AR, Wnt and Connexins in cells with activation of Wnt and AR signalling pathways. The overall aim was to investigate the interaction between Wnt and AR signalling pathways by:

(i) elucidating the mechanisms of interaction and translocation of AR and β-Catenin into the nucleus of PCa cells treated with Wnt and AR signalling ligands (e.g., Wnt 3A, Wnt 5A, Wnt 9B and DHT) using WB and co-immunoprecipitation.

(ii) validating the mechanisms of translocation AR and β-Catenin into nucleus in PC3 cells transfected with AR inserted plasmids ($PC3^{(AR+)}$).

(iii) confirming the WB results by measuring expression of Wnt and AR signalling proteins in prostate cancer cell lines and the translocation of AR and β-Catenin into nucleus of PCa cells treated with Wnt and AR ligands using immunocytochemistry.

(iv) quantifying the expression of Wnt and AR target protein in PCa cells treated with Wnt and AR ligands using qPCR.

5.3. Methods

5.3.1. Cell culture of PCa cells for WB

PC3 and LnCAP cells were obtained from American Type Culture Collection (ATCC) and cultured at required density in T-25 cm^2 (Cat: 156367, Thermo Scientific™ Nunc™ Cell Culture Treated EasYFlasks™) in 6 ml RPMI 1640 (Chap-II, Table 2.2) supplemented with 10% foetal bovine serum and 2 mM L-glutamine (Chap-II, Table 2.2). The details of cell culture are described in Chap-II (Sec. 2.3.3.1).

5.3.2. Western blotting (WB)

WB in conjunction with cell fractionation was a major technique used here to investigate expression and interaction of Wnt and AR signalling proteins in PC3 and LnCAP cells. WB, subsequent to cell fractionation allows probing for multiple antibodies on the same sample and unlike immunocytochemistry provides a quantitative analysis of proteins in different cellular

fractions (e.g., total membrane, cytosol, nucleus). Wnt signalling pathway was activated by treating the cells with ligands such as Wnt3A, Wnt5A, Wnt9B (Chap-I, Sec. 1.12.4) and AR signalling pathway was activated with DHT.

5.3.2.1. Treatment of LnCAP and PC3 cells with AR and Wnt signalling ligands

LnCAP cells were grown in 2xT-25 cm^2 flask for each set of experiments and incubated for 48hrs at 37°C (Chap-II, Sec. 2.3.4.1). The cells were removed from the incubation at 90% confluency of cell growth. 5ml of 6ml media was removed and 1ml fresh medium was added into the flask and the cells were then treated with AR signalling ligand (e.g., DHT, 15 nM) and Wnt signalling ligands (e.g., Wnt3A, 10 nM; Wnt5A, 10 nM and Wnt9B, 10 nM) (Table 5.1). Two more repeat experiments were carried out independently using different passage and batch number of LnCAP and PC3 cells. The control cells for each experiment were treated with PBH as a vehicle control.

Similarly, PC3 cells were also treated with DHT, Wnt5A and Wnt9B to compare the expression and interaction of AR in AR signalling pathway in PC3 cells.

Table 5.1. The table representing the AR and Wnt signalling ligands with the working concentrations

Name of the ligands	Catalog and Source	Stock concentration	Working concentration
Wnt-3A	Cat: CSB-EP026136HU1, CUSABIO	1 µg/µl	10 nM
Wnt-5A	Cat: 645-WN-010, R&D systems	0.1 µg/µl	10 nM
Wnt-9B	Cat: 3669-WN-025, R&D system)	0.1 µg/µl	10 nM
DHT	Cat: D-073, Sigma-Aldrich	1 mg/ml	15 nM

5.3.2.2. Extraction of proteins as a whole cell lysate from untreated and treated cells

The cells were scrapped with precooled cell-scrapper. Details are given in Chap-II (Sec. 2.3.4.2). Briefly, the cells were centrifuged at 200x*g* for 2 min to get cell pellet. The pellet was transferred into 1.5 ml microcentrifuge tube in which lysis buffer (RIPA, 1x) (Cat:9806, Cell Signalling Technology) was added at 400 µl/10^7 cells to the tube. Protease inhibitor (Complete, Cat. No. 11 836 170 001, Roche) and Phosphatase inhibitor (PhosSTOP, Cat. No. 04 906 837 001, Roche) were added to the microcentrifuge tube according to manufacturer instruction. The cells were then lysed by incubating at 4°C for 30 min with constant agitation before centrifugation at 16,000x*g* for 25 min. The centrifuge tube was gently removed and placed on ice and supernatant was

transferred into a fresh tube. The cell lysate was used for protein assay and rest was stored at -80°C for further use.

5.3.2.3. Cell fractionations of PC3 and LnCAP cells

Qproteome Cell Compartment Kit (Cat:37502, Qiagen) was used to extraction proteins from Wnt and AR signalling ligands (Table 5.1) treated and untreated LnCAP and PC3 cells. A detailed protocol is given in Chap-II (Sec. 2.3.4.3). Briefly, 1 ml of CE1 buffer was added to $5x10^6$ cells and 10 µl of protease inhibitor was also added to the cells followed by agitation end-over-end for 10 min at 4°C and centrifuged for 10 min at 1000x*g* at 4°C to separate cytosolic proteins. After collection of cytosolic protein, 1 ml of CE2 buffer was applied to tube followed by incubation for 30 min at 4°C with end-over-end shaking. Then centrifugation was performed at 6000x*g* for 10 min at 4°C. The total membrane protein (e.g., proteins from plasma membrane as well as all organelle membranes except nuclear membrane and proteins from the lumen of the ER and mitochondria) was transferred into a precooled microcentrifuge tube. 7 µl Benzonase and 13 µl distilled water were added to the pellet and incubated for 15 mins on the bench at RT. 500 µl CE3 mixed with 5 µl protease inhibitor (100x) was added to the cells and incubated for 10 min at 4°C with end-over-end agitation followed by centrifugation at 6800x*g* for 10 min at 4°C and proteins was transferred into precooled microcentrifuge tube. This fraction contains soluble, and membrane bound nuclear proteins. The protein concentration was measured using the Thermo Scientific™ Pierce™ BCA protein assay kit (cat: 23225) assay, Details provided elsewhere (Chap-II, Sec. 2.3.4.4).

5.3.2.4. SDS-PAGE electrophoresis

Protein (15 µg) from whole cell lysate or each compartmental fraction from LnCAP and PC3 treated with (±)Wnt3A, (±)Wnt5A, (±)Wnt9B and AR signalling ligand (±)DHT. Prior to loading, the cell lysates were mixed with 5µl of loading buffer prepared by mixing laemmli 4x sample buffer (Cat. 1610747, Bio-Rad) with β-mercaptoethanol at 9:1 dilution. Protein samples were boiled at 95^{o}C for 8-10 min before loading into Precast protein gels (Bio-Rad) using Mini-PROTEAN Electrophoresis system (Bio-RAD) for resolving the proteins. SDS PAGE gels consists of two portions, stacking and resolving gels, these differ in their composition by 4% of

polyacrylamide in stacking gel and 12% of polyacrylamide in resolving gel. 6µl of Colour Pre-stained Protein Standard was loaded onto precast SDS PAGE gels. During electrophoresis, 50V were applied for 10 min for initial electrophoresis through the stacking gel, then 120V were applied for 45 min through resolving gel. The resolved proteins were then transferred onto a polyvinylidene difluoride (PVDF) membrane using semi-dry Trans-Blot Turbo blotting system (Cat. 17006570, Bio Rad). The PVDF membrane was blocked by incubating in 5% (v/v) non-fat dry milk (NFDM), prepared in 0.1% Tween-20 TBST (Cat. J77500.K2, Alfa Aesar) for 2 h with constant shaking to mask all possible non-specific binding sites on the membrane. Following blocking with NFDM, the PVDF membranes were washed with TBST (3x5') and cut into two strips of 250 to 57 kDa and 57 to 10 kDa to be probed and reprobed for multiple proteins in different cell compartments, simultaneously.

5.3.2.4.1. Probing, stripping and reprobing the blotted proteins with different antibodies

The of 250-57 kDa strip was incubated with anti-β-catenin (Abcam: ab22656, predicted MW 85kDa) at 1:1,000 dilution in TBST and the 57 to 10 kDa strip was incubated with the loading control anti-β-actin (Abcam: ab6276, predicted MW 42 kDa) at 1:5,000 dilution in TBST over night at 4°C. The membranes were then washed with TBST (3x5') and incubated with appropriate HRP (horse radish peroxidase) conjugated secondary antibodies such as Peroxidase AffiniPure Donkey Anti-Mouse IgG (H+L) (JIL, cat: 715-035-151) at 1:4,000 dilution in TBST in 3.5-5% (v/v) NFDM for 2 h at RT. Following washing with TBST (3x5'), the HRP signal was detected by incubating 5 min in Bio Rad clarity Western enhanced chemiluminescence substrate (Cat: 1705061, Bio Rad) followed by imaging using ChemiDoc imaging system (Bio-Rad, 2012) .

After recording the signals for β-catenin and β-actin, the membranes were reprobed with other antibodies (e.g., anti-Lamin A antibody to identify enrichment of the nuclear fraction). For reprobing with other antibodies, a so-called 'stripping' of PVDF membranes was employed; 'stripping' membranes, already probed for an antibody, is an established technique for 'reprobing' with other antibodies that may resolve at the same molecular weight (anti-AR antibody for AR with 110 kDa and anti-AR (N-ter) antibody for AR (N-ter) with 110 kDa). The membrane bound primary and secondary antibodies were 'stripped' off by incubating in Restore™ PLUS Western Blot Stripping Buffer (Cat. 46430, ThermoFisher Scientific) for 25 min at

RT. Following washing twice with TBST, the membranes were blocked (Sec. 5.3.2.4) and washed. The membrane of 250 to 57 kDa was reprobed with nuclear protein marker antibody Anti-Lamin A (Cat. No. L1293; Sigma Aldrich, MW: 72 kDa) and the membrane of 57-10 kDa was reprobed with Anti-GAPDH antibody (Table 5.2) as cytoplasmic and membrane protein marker. Subsequent procedures were followed before incubating with Peroxidase AffiniPure Donkey Anti-Rabbit IgG (H+L) (Cat. 711-035-152, JIL) 1:4,000 dilution in 5% non-fat dried milk in TBST. Following this, the HRP signals were developed and imaged as described earlier. The bands were quantified using densitometry analysis using ImageJ. The value of bands was normalised to bands of β-actin. The following antibodies were used in protein expression analysis.

Table 5.2. The table representing a list of primary and secondary antibodies with their catalogue number, manufacturer's name and dilution rate used in the studies

Primary antibody	Host Species	Cat and Source	Dilution	Reason of using	References for antibodies
Anti-Androgen Receptor Antibody	Rabbit	Cat: 06-680, Merck Millipore	1:3000	AR target (Rubinfeld et al., 1993)	(Hay et al., 2014) and (Wu et al., 2014)
Anti-Androgen Receptor antibody	Rabbit	Cat: ab108341, ABCAM	1:3000	AR target	(Mutuku et al., 2019) and (Puca et al., 2018)
Anti-AR antibody (N-20)	Rabbit	Cat: Sc-816: Santa Cruz	1:250	Transactivator of AR (Simental et al., 1991)	(Sun et al., 2015) and
Anti-β Catenin antibody	Mouse	ab22656: ABCAM	1:3000	Wnt target (Rubinfeld et al., 1993)	(Hou et al., 2019)
Anti-Connexin-43 antibody	Rabbit	C6219: Sigma	1:3000	Wnt target in PC3 (Hou et al., 2019)	(Wang et al., 2017)
Anti-Cx31 antibody	Rabbit	36-5100: Invitrogen	1:1000	Connexin family (Plum et al., 2002)	(Wang et al., 2009)
Anti-PSA antibody	Rabbit	ab53774: ABCAM	1:1000	AR target (Lundwall and Lilja, 1987)	(Coleman et al., 2016)
Anti-Nkx3.1 antibody	Rabbit	Ab196020: ABCAM	1:2000	`AR target (He et al., 1997)	(Leibold et al., 2020)
Anti-TMPRSS2 antibody	Rabbit	ab92323: ABCAM	1:2000	AR target (Cerveira et al., 2006)	(Ubuka et al., 2018)

Anti-c-Myc antibody		Rabbit	ab32072: ABCAM	1:1000	Wnt target in PC3 (Rennoll and Yochum, 2015)	(Han et al., 2021)
Anti-phospho-GSK-3β antibody		Rabbit	9331S: CST	1:1000	Wnt signalling protein (Amit et al., 2002)	(Wang et al., 2020)
Anti-Lamin A (C-terminal) antibody		Rabbit	L1293: Sigma	1:5000	Nuclear protein marker	(Toko et al., 2014)
Anti-β actin antibody		Mouse	Ab6276: ABCAM	1:5000	Loading control	(Yao et al., 2020)
Anti-GAPDH antibody		Rabbit	ab181602: ABCAM	1:3000	Loading control	(Ye et al., 2021)
Secondary antibody	Peroxidase AffiniPure Donkey Anti-Mouse IgG (H+L)	Donkey	715-035-151: Jackson Immunoresearch Laboratory (JIL)	1:5000	Secondary antibody Secondary antibody	(Hu et al., 2020)
	Peroxidase AffiniPure Donkey Anti-Rabbit IgG (H+L)	Donkey	711-035-152: Jackson Immunoresearch laboratory (JIL)	1:5000	Secondary antibody	(Molinari et al., 2021)

Anti-Androgen Receptor Antibody (Cat: 06-680, Merck Millipore) was used throughout the study to observe the redistribution of AR signalling target protein, e.g., AR across the cytosol, membrane and nucleus. Another anti-AR antibody from ABCAM (Cat: ab108341) was used to check any variability from the anti-AR antibody from Merck Millipore. Similar redistribution was observed in WB experiments. Anti-AR (N-ter) antibody (Table 5.4) was used to observe its translocation into nucleus due to its transactivation function. The N terminal of AR (NTD) plays a key role in transactivation and function of the AR. The effective activation of AR requires first 30 amino acids of the NTD for amino-carboxyl terminal (N/C) interaction. Intracellular trafficking is a pivotal mechanism in the regulation of transcription factors including. Therefore, its translocation into nucleus indicates the increase of transcription of target genes, subsequently increase the expression of AR target proteins.

5.3.3. Co-Immunoprecipitation (Co-IP)

Co-IP was performed to investigate the interaction between AR and β Catenin. Details have been described in Chap-II (Sec. 2.3.5).

5.3.4. Immunocytochemistry (ICC)

Immunocytochemistry was conducted to investigate the subcellular migration of Wnt and AR signalling target proteins while activated with Wnt and AR signalling ligands.

5.3.4.1. Seeding, treatment and fixation of cells

PC3, AR transfected PC3 (Chap-II, Sec. 2.3.3.4) and LnCAP cells were grown in 8-well chamber slides (Lab Tek II, Nunc, ThermoFisher Scientific) at a density of 10,000 cells/well and incubated for approximately 72 h until the cells were reached 90% confluency. Cells were treated with Wnt ligands (e.g., Wnt5A or Wnt9B) and AR signalling ligand (e.g., DHT) at a working (final) concentration (Table 5.1) and incubated for 3-4 h for PC3 and AR transfected PC3 cells) and overnight for LnCAP cells. The cells were fixed with PFA (4% Para formaldehyde) (Sec. 2.3.6.1).

5.3.4.2. Immunostaining of cells using ICC

Cells were washed with PBS prior to start permeabilization. The cells were permeabilized by incubation in permeabilization buffer, prepared with 0.4% Triton X-100 in PBS, for 10 mins PC3 and AR transfected PC3 cells and 15 min for LnCAP cells at RT with gentle agitation. The cells were then washed with PBST wash buffer prepared with 0.01% Tween-20 in PBS. The cells were then blocked with 5% donkey serum prepared in PBST incubated for 1 h. Following washing with PBST, the cells were incubated with primary antibodies e.g., anti-β-catenin (Cat: ab22656, ABCAM, Dilution 1:250) for PC3 and AR transfected PC3 cells and anti-androgen receptor antibodies (Cat: 06-680, Merck Millipore, Dilution 1:250) for LnCAP cells (Table 5.2) over night at 4°C at 1:250 dilution in 1.5% donkey serum in PBST followed by washing with PBST wash buffer (3x5'). The cells were then incubated with secondary antibodies, such as Peroxidase AffiniPure Donkey Anti-Mouse IgG (H+L) (Table 5.2) was used against anti-β-catenin antibody and Peroxidase AffiniPure Donkey Anti-Rabbit IgG (H+L) was used against anti-androgen antibody. The cells were washed with PBST (3x5') in 1.5% donkey serum in PBST for 1 h followed by washing with PBST (3x5'). The cells were incubated with tyramide Cy3 (Cat: NEL44001KT, PerkinElmer Life Science) for 10 min at room temperature. The cells were washed prior to nuclear counterstaining with DAPI. Following final wash with PBST, the chambers were removed, and cells were air dried and ProLong™ Gold Antifade Mountant (Cat. P10144, Thermo Fisher Scientific) was applied in slide before placing the cover slip on the slide. The slides were then sealed with nail polish to prevent air entry and oxidation.

5.3.4.3. Confocal Imaging

The cells were imaged using a Leica SP8 laser scanning confocal microscope equipped with a 40x/1.3 NA oil objective. LAS X software was used for image acquisition in which three fields of the objects of each chamber were randomly selected based on DAPI staining. Each step size of of Z-stacks for each image was 0.6 µm with 1.00 AU pinhole and 1.0 zoom (Chap-II, Sec. 2.3.6.3).

5.3.5. Quantitative PCR

qPCR was performed to investigate expression of Wnt and AR signalling target proteins in PC3 and LnCAP cells upon activation with Wnt and AR signalling ligands.

5.3.5.1. Primers used for qPCR

Primers for qPCR were designed using NCBI "Primer BLAST" tool using the default settings against the RefSeq mRNA database for Homo sapiens. The Wnt target genes (e.g., *CTNNB1* and *GJA1*) and AR target genes (e.g., *Nkx3.1*, *ERG*, *AR*) and housekeeping gene (e.g., *ACTB*) were targeted for AR and Wnt signalling study. Primer design has been described in Chap-II (Sec. 2.3.7.1.) The guidelines for primer design are summarised in the following table (Table 5.3). Primers were designed and ordered from Sigma-Aldrich and resuspended in ddH2O to 100 µM stock solutions, which were kept at −20°C. Details of primers are in Tables 5.3 below.

Table 5.3. The table representing gene and their corresponding primer used in qPCR

Gene name	Sequence
CTNNB1	Forward primer: 5'- TGCTCCGCTGACCTTAAAGA-3' Reverse primer: 5'- AGAAATGGTCGAAGTGCCCC-3'
Nkx3.1	Forward primer 5'- AGAAGCACTCCTCTTTGCCG-3' Reverse primer: 5'- CCCACGCAGTACAGGTATGG-3'
Cx43	Forward Primer: 5'-CCCACACTCTTGTACCTGGC-3' Reverse Primer:5'- CCCCCTCGCATTTTCACCTT-3'
ACTB	Forward Primer: 5'- GTACGTTGCTATCCAGGCTGT-3' Reverse primer: 5'-AGGTAGTCAGTCAGGTCCCG-3'
AR	Forward Primer: 5'- TGCTCCGCTGACCTTAAAGA-3' Reverse Primer: 5'- AGAAATGGTCGAAGTGCCCC-3'
TMPRSS2	Forward primer:5'-ACCATGGATACCAACCGGAA-3' Reverse primer: 5'-CTGTCCCGGATGGGGATTTG-3'

5.3.5.2. RNA extraction

RNA was extracted from PC3 and LnCAP cells treated with (±)Wnt9B and (±)DHT using RNeasy Plus kit (Cat. 74104 Qiagen) according to the manufacturer's protocol (Chap-II, Sec. 2.3.7.3).

5.3.5.3. Reverse transcription

The total RNA was reverse transcribed to cDNA using QuantiTect® Reverse Transcription kit (Cat: 205311, Qiagen) following the manufacturer's protocol. The protocol included two steps. 1. Genomic DNA elimination reaction, 2. Reverse-transcription reaction (Chap-II, Sec. 2.3.7.4).

5.3.5.4. qPCR

qPCR reactions were prepared in 384-well PCR plates (Bio-Rad, Cat. HSP- 3841) using the SYBR-Green PCR master mix (Applied Biosystems). For the Wnt and AR signalling pathway study, each 10 µl reaction mixture consist of: 5 µl SYBR-Green master mix, 1 µl of a 1:40 dilution of the cDNA in nuclease-free water, 1.25 µl of the primer pair (to a final concentration of 250 nM each), and 2.75 µl nuclease-free water; each sample was run in triplicate. The reaction was made of: 5 µl SYBR-Green master mix, 2 µl of a 3:40 dilution of the cDNA in ddH_2O, 1.75 µl of the primer pair (to a final concentration of 350 nM each), and 1.25 µl ddH_2O; each sample was run in duplicate. qPCR was performed using a Bio-Rad CFX384 thermocycler; the RT-PCR thermal cycler parameters were the following: initial denaturation at 95 °C for 1 min; 40× cycles of denaturation at 95°C for 15 s and annealing/extension at 60°C for 1 min; final extension at 65°C for 1 min; and 60 melting curve reads off, from 65 to 95 °C (0.5°C per cycle). Expression levels of the genes of interest were normalised to *ACTB* using the $2^{-\Delta\Delta Cq}$ method (Livak and Schmittgen, 2001), and melting curves were analysed with Bio-Rad CFX Manager to verify products.

5.4. Results

Proteins have been recognised for their capabilities to shuttle in and out from the nucleus as crucial to numerous essential cellular processes such as cell cycle progression. Also, particular tissue or cells require orchestrated nuclear presence of certain cytosolic proteins (Nigg, 1997 and Görlich, 1998). β-catenin is an oncogenic transcriptional factor co-activator and a Wnt signal intracellular transducer protein which is translocated into nucleus in PC3 cells after Wnt signal

activation (Thrasivoulou et al., 2013). Our laboratory has also demonstrated that Wnt signalling activation trigger cytosolic migration of Cx43 in PC3 cells (Hou et al., 2019), indicating that Connexins may also be co-translocated in response to Wnt signal activation. They proposed that Cx43 may be an integral protein in Wnt signal intracellular transduction. To investigate the interaction between the Wnt and AR signalling pathways, here I tested the hypothesis that translocation of β-catenin, Connexins and AR occurs in an orchestrated manner in response to the activation of Wnt and AR signalling.

5.4.1. Analysis of the expression and translocation of AR and Wnt signalling proteins

5.4.1.1. Assessment of background signal by the secondary antibody

WB analysis was used to investigate intracellular Wnt and AR target protein expression and their translocation between different cellular compartments (e.g., similar to the techniques in (Hou et al., 2019)). The target proteins were investigated using the antibodies (Table 5.2). Prior to conducting these experiments, the specificity of primary and secondary antibodies was checked. A negative control (without primary antibody) experiment was performed where only secondary antibody was used. The secondary antibody did not generate any visible band, indicating an absence of background, non-specific signal (Fig. 5.1).

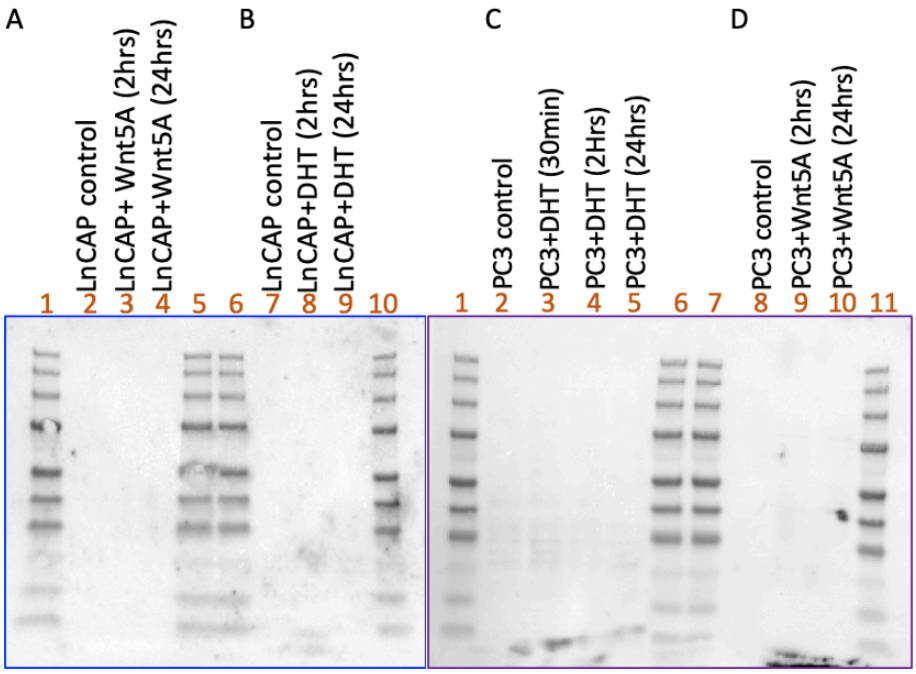

Figure 5.1. A Representative WB image of a negative control experiment. 15 µg of proteins of LnCAP and PC3 cells treated with Wnt5A and DHT were loaded into each well of the gel A (L-2, 3, 4), B (L-7, 8, 9), C (L-2, 3, 4, 5) and D (L-8, 9, 10). 5µl of prestain protein standard ladder (cat: P7719, NEB) was loaded in A (L-1, 5), B (L-6, 10), C (L-1, 6), D (L-7, 11). Following the elimination of primary antibody incubation, proteins in membrane A and B were stained with Donkey anti-mouse (Table 5.2) and proteins in the membrane C and D were stained with Donkey anti-rabbit (Table 5.2). Peroxidase AffiniPure Donkey Anti-Mouse IgG (H+L) and Peroxidase AffiniPure Donkey Anti-Rabbit IgG (H+L) secondary antibodies did not show any non-specific binding.

5.4.1.2. Optimization of concentration of internal loading controls (ILC)

Anti-β actin antibody and anti-GAPDH antibody (Table 5.2) were used as internal loading control. The band intensity of anti-β actin was proportionally increased with the increasing of concentration of target proteins.

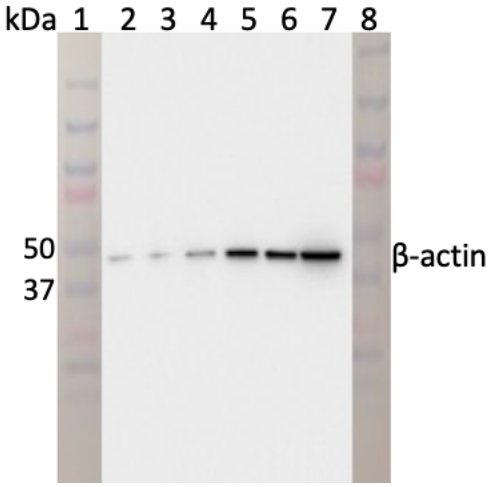

Figure 5.2. A Representative WB image showing concentration dependant β-actin expression as ILC (Internal Loading control). 1, 3, 6, 8, 10, 15 µg of protein from LnCAP cells was loaded into L-2, 3, 4, 5, 6 and 7. 5 µl of protein standard (Cat: 161-0374, BioRad) was loaded into L-1 and 8. The membrane was probed with anti β-actin antibody with recommended dilution (Table 5.2) followed by probing with secondary antibody. The detected signal intensity of β-actin appeared to be increased with the increasing amount of protein. 15 µg of protein was selected for the rest of experiments.

5.4.1.3. Concentration dependent protein expression

A similar experiment, as above (Sec. 5.4.2.2) was conducted with increasing amount of protein probed with AR antibody (Fig. 5.3). It was observed that 10-15 µg of loaded protein produced distinctly visible band when probed with an anti-AR antibody at 1:3000 dilution (Fig. 5.3).

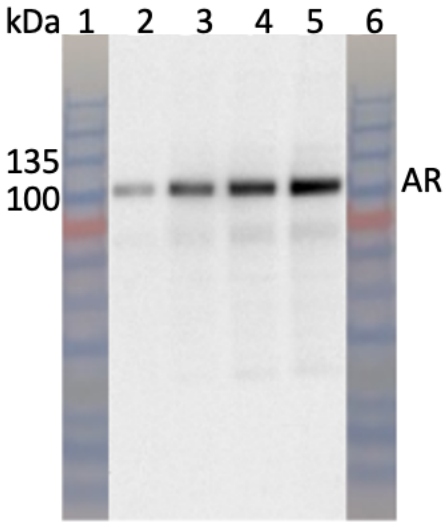

Figure 5.3. A Representative WB of protein concentration dependence for the signal for AR in whole cell lysates using WB. 3, 7, 10 and 15µg of protein from LnCAP cells were loaded into L-2, 3, 4, 5, 6 and 7. 5 µl of protein standard (cat: 161-0374, BioRad) was loaded into L-1 and 6. The membrane was probed with anti-AR antibody (Cat: 06-680,

Merck Millipore) at 1:3000 dilution (Table 5.2) followed by staining with secondary antibody. The detected signal intensity increases with the increasing amount of protein. 10-15 μg of protein was selected for further experiments.

5.4.1.4. Translocation of AR and Wnt signalling proteins in DHT treated LnCAP cells

AR signalling in LnCAP cell was activated with DHT. The activated AR signalling affected the basal distribution of AR across the cytosol, membrane and nucleus (Fig. 5.4 – A-E, where A is a representative WB and B-E are quantitation for the signal for each antibody used). Average of 3 independent experiments (Appx. 5.1 and the original PVDF membrane in Appx.5.1.1) showed membrane expression of AR (full length) was increased (Fig. 5.4.F.1) but its expression was sharply increased in the nucleus. At least three independent experiments were performed to test reproducibility, different batch of cells and ligands were used to establish if the WB results were consistent. The pattern of distribution of AR (N-ter) was found to be similar as AR (full length) in cytosol, membrane and nucleus. AR (N-ter) was found higher in nucleus compared to nucleus in untreated LnCAP cells (Figs. 5.4.C and 5.4.F.2). The AR (N-ter) antibody was used to observe its translocation into nucleus due to its transactivation function. The N terminal of AR (NTD) plays a key role in transactivation and function of the AR. In addition, it was observed that activated AR signalling triggered β-catenin to be detected in cytosol and nucleus (Figs. 5.4.D and Fig. 5.4.F.3). The analysis indicates β-catenin is displaced from the cell membrane to cytosol and then translocates into nucleus (Fig. 5.4.F.3). It is to be noted that there is no Cx43 expression in LnCaP cells. As there is a high sequence identity (see above) between Cx31 and Cx43 proteins (Au et al., 2020), and Cx31 is expressed in LnCAP cells, I decided to investigate the Cx31 expression redistribution in response to Wnt and AR ligands as a substitute for the known Cx43. Cx31 was found to be translocated into nucleus when AR signalling was activated with DHT. These results suggest a close interaction of AR, Wnt and connexin signalling pathways in LnCAP cell. β-actin expression was also quantified (Appx. 5.12.1) to check homogenous loading of proteins.

A. Western blot images

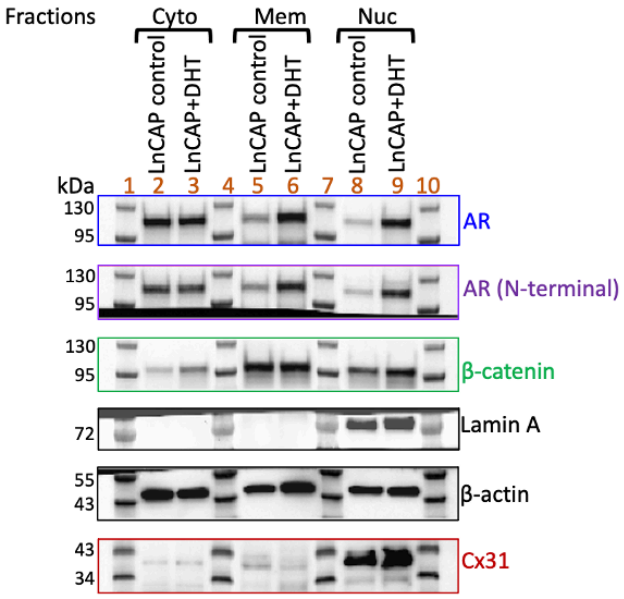

B. AR expression

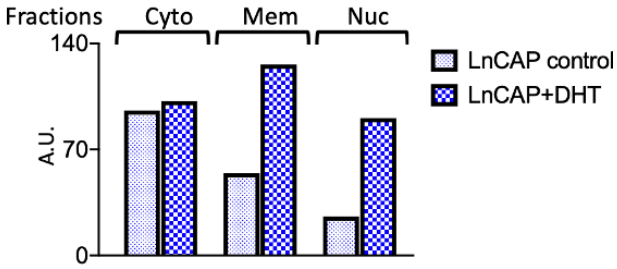

C. AR (N-ter) expression

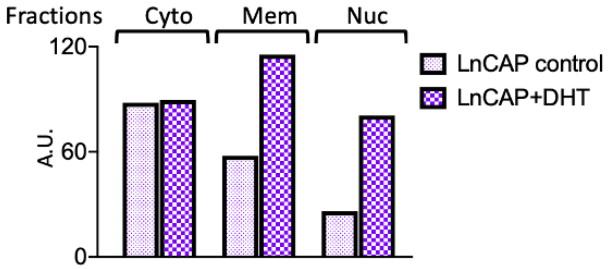

D. β-catenin expression

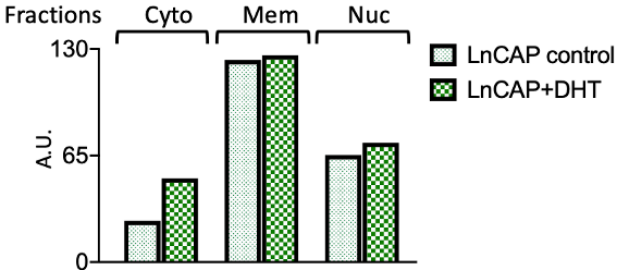

E. Cx31 expression

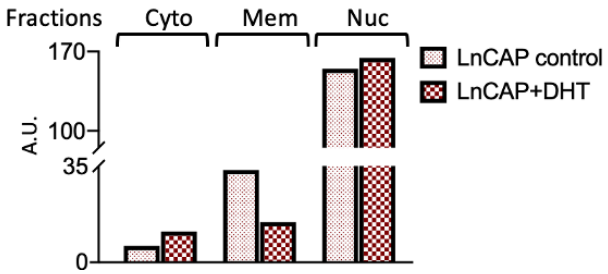

F. Average expression of proteins of three independent experiments

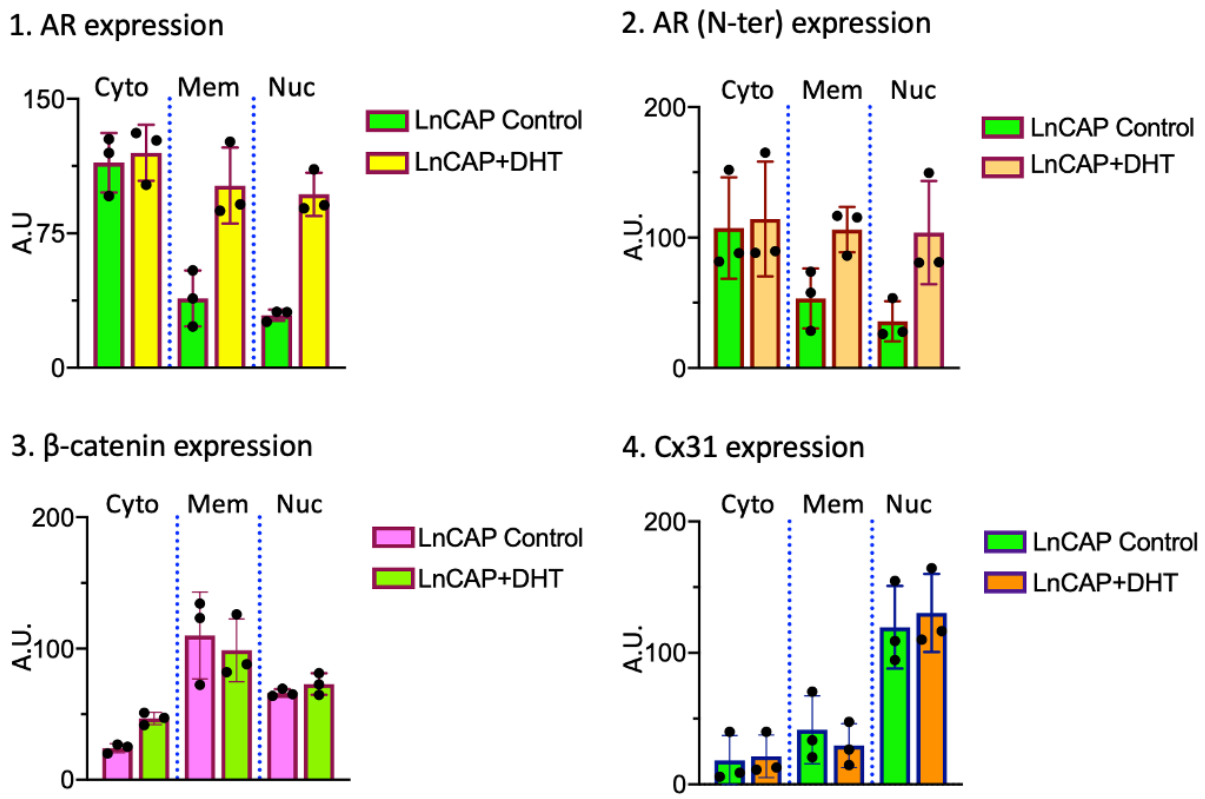

Figure 5.4. A representative WB image for the expression of AR and Wnt signalling proteins in different fractions of LnCAP cells (±DHT). A. 15µg of fractionated protein of LnCAP cells (±DHT) was loaded onto gel in the following order; cytosolic protein loaded into lane 2 and 3, membrane protein into lane 5 and 6 and nuclear protein into lane 8 and 9. 6µl of Colour Prestained Protein standard, Broad Range (Cat: P7719, NEB) was loaded into lane 1, 4, 7 and 10. The PVDF membrane was cut into two strips of 250 to 57 kDa and 57 to 10kDa and incubated with anti-Lamin A and anti-β actin antibody. Following image capture with GelDoc system (BioRad), the membranes were stripped off with "Restore™ PLUS Western Blot Stripping buffer (Cat: 46430, Thermo Scientific). The membranes were reprobed with anti-AR, anti-AR (N-ter) and anti-β-catenin and anti-Cx31 antibodies sequentially. Cx31 was used as a paradigm member of the Cxn signalling proteins and transactivation function. The intensity of bands for each antibody was observed and quantified with ImageJ. B, C, D and E displaying the comparative expression of AR, AR (N-ter), β-catenin and Cx31 respectively, in cytosol, membrane and nucleus in LnCAP cell (±DHT). F.1, F.2, F.3 and F.4 show bar charts representing the mean (mean±SEM) of n = 3 independent experiments (Appx. 5.1) of AR, AR (N-ter), β-catenin and Cx31 expression respectively.

5.4.1.5. Nuclear translocation of AR and Wnt signalling proteins in Wnt3A treated LnCAP cells

To test the hypothesis that Wnt activation increases the translocation of AR and Wnt signalling proteins, LnCAP cells were treated with Wnt 3A protein, LnCAP cells were initially treated with Wnt3A at lower concentration (5nM which did not give consistent results (Appx. 5.2.1). At 10nM Wnt3A, there was an optimal response. The PVDF membrane was probed sequentially with

multiple antibodies namely, anti-AR, anti-AR (N-ter), anti-Cx31, anti-β-catenin. Anti-β-actin and Lamin A were used as loading control and nuclear protein marker respectively. AR expression was increased in nucleus in Wnt3A treated LnCAP cells compared to untreated cells (Figs. 5.5.A and B). Two replicates (Appx. 5.2.3 and 5.2.4) were also performed. Figs. 5.5 C, D, E show expression pattern for AR (N-ter), β-catenin and Cx31. Fig. 5.5.F shows graphical representation of the expression intensity analysis conducted using ImageJ (see methods). This graph also indicated AR expression was slightly reduced in cytoplasm but increased in membrane. These results suggest that after Wnt3A treatment, AR expression was redistributed in cytoplasm, membrane and nucleus where cytoplasmic expression was slightly reduced but increased in membrane and nucleus. These results also indicate that both membrane and cytoplasm sequester AR and it is most likely that AR translocates into the nucleus from these cellular compartments. Similar pattern of distribution of AR (N-ter) expression was found in Wnt3A treated LnCAP cells where AR (N-ter) expression was reduced slightly in cytoplasm but increased in membrane and nucleus, indicating the translocation of AR (N-ter) into nucleus in Wnt3A treated LnCAP cells when compared with untreated LnCAP cells. β-catenin expression was increased in cytoplasm, membrane and nucleus after addition of Wnt3A (Fig. 5.5.F.2). These results suggest that treatment with Wnt3A activated the Wnt signalling pathways that released β-catenin in cytoplasm. Increased β-catenin in the cytoplasm results in an increase in β-catenin availability in membrane and nuclear compartment and subsequently increased expression in nucleus (Fig. 5.5.F.3). Wnt3A treatment reduced the expression of Cx31 in cytoplasm but increased in membrane and nucleus. This indicates that the translocation of Cx31 into nucleus in LnCAP cells treated with Wnt3A ligands (Fig. 5.5.F.4). β-actin expression was also quantified (Appx. 5.12.2) to check homogenous loading of proteins.

A. Western blot images

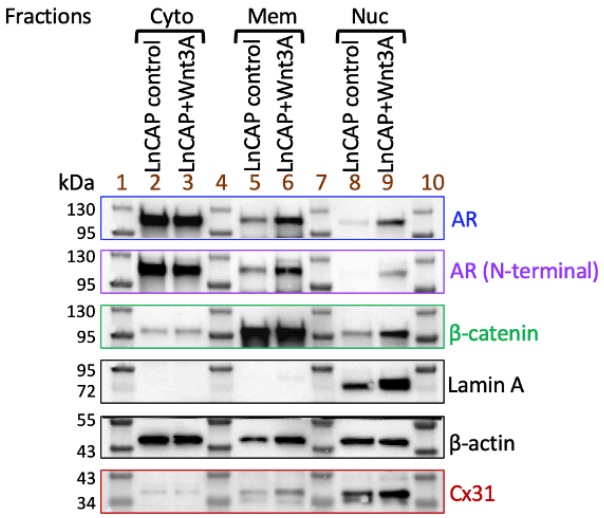

B. AR expression

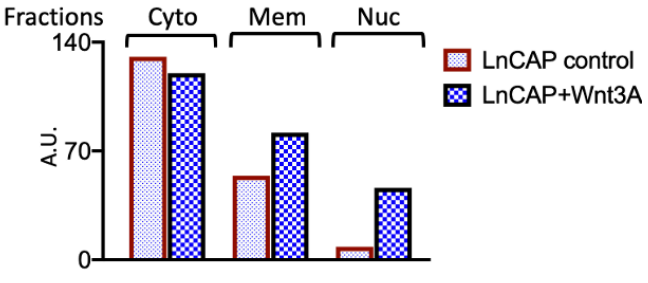

C. AR (N-ter) expression

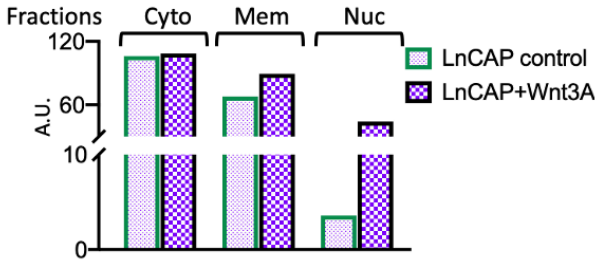

D. β-catenin expression

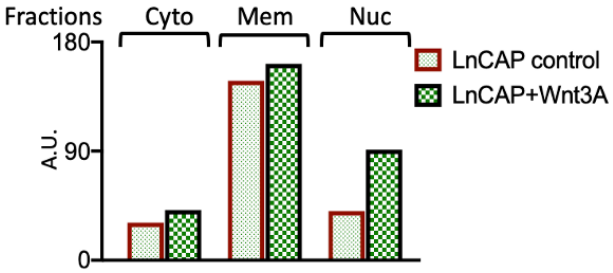

E. Cx31 expression

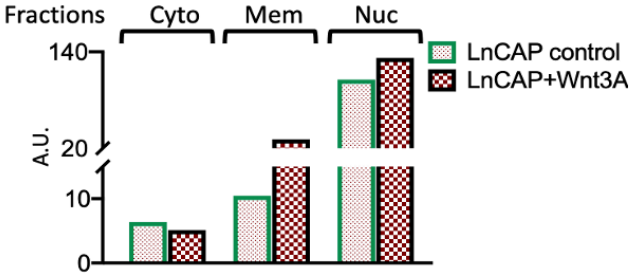

F. Average expression of proteins of three independent experiments

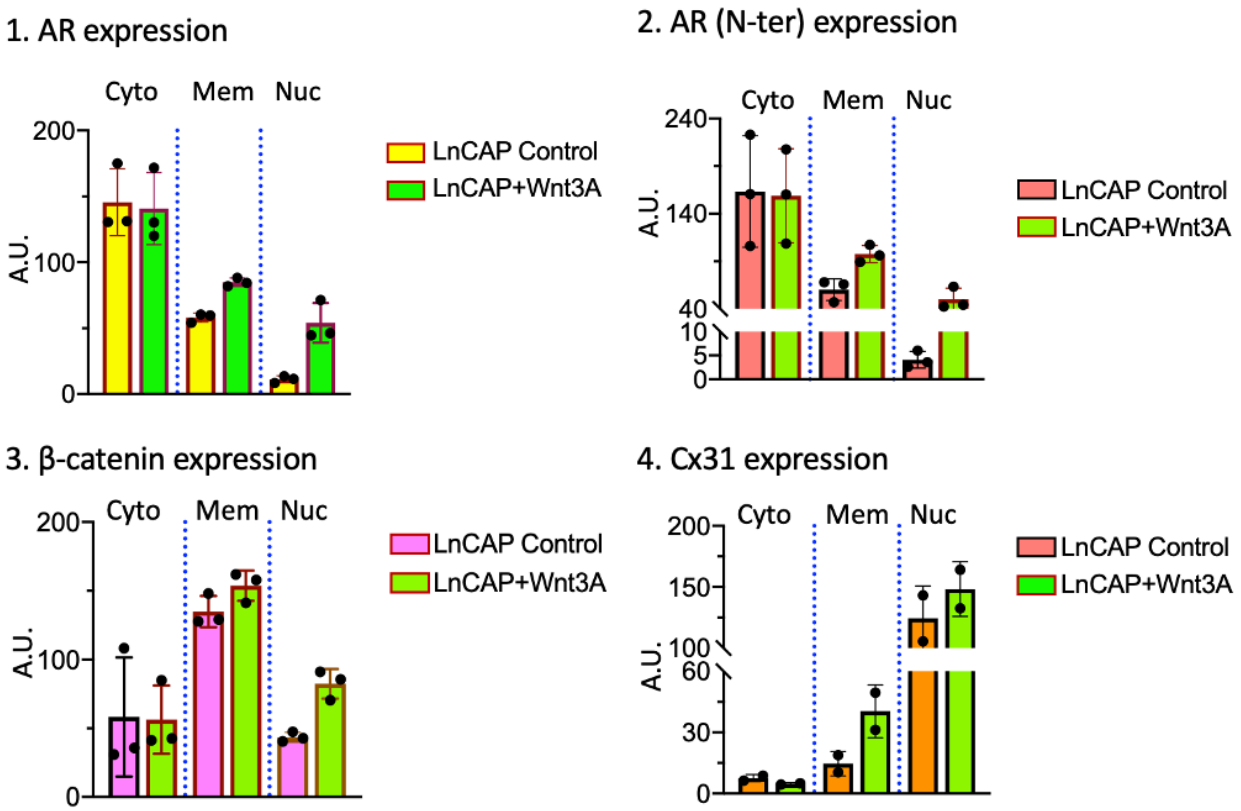

Figure 5.5. A representative WB image for the expression of AR and Wnt signalling proteins in different fractions of LnCAP cells (±Wnt3A). 15 µg of fractionated protein of LnCAP cells (±Wnt3A) was loaded onto gels in the following order; cytosolic protein loaded into lane 2 and 3, membrane protein into lane 5 and 6 and nuclear protein into lane 8 and 9. 6 µl of Colour Prestained Protein standard, Broad Range (Cat: P7719, NEB) was loaded into lane 1, 4, 7 and 10. The PVDF membrane was cut into two strips of 250 to 55 kDa and 55 to 10kDa and incubated with anti-Lamin A (expected size ~70 kDa), a marker for the nuclear fraction, and anti-β actin antibody (expected size ~ 42 kDa). Following capturing image with GelDoc system (BioRad), the membranes were stripped off with "Restore™ PLUS Western Blot Stripping buffer (Cat: 46430, Thermo Scientific). The membranes were reprobed with anti-AR, anti-AR (N-ter) (expected size ~110 kDa) and anti-β-catenin (~ expected size 90 kDa) and anti-Cx31 (~ expected size 31 kDa) antibodies sequentially. The intensity of bands for each antibody was observed and quantified with ImageJ. B, C, D and E displaying the comparative expression of AR, AR (N-ter), β-catenin and Cx31 respectively, in cytosol, membrane and nucleus in Wnt3A (±) treated LnCAP cell. F.1, F.2, F.3 and F.4 show bar charts representing the mean (mean±SEM) of n = 3 independent experiments of AR, AR (N-ter), β-catenin and Cx31 expression respectively.

5.4.1.6. Analysis of translocation AR and Wnt signalling proteins in Wnt5A treated LnCAP cells

Activation of Wnt signalling with Wnt5A ligand altered the cellular location of AR and Wnt signalling target proteins. Following activation, it was also observed that AR expression was slightly reduced in cytosol and membrane but increased in nucleus (Fig. 5.5.B). The primary (pre-stripping) images of PVDF membranes (all raw data) are deposited in appendix (Appx. 5.3.2). Analysis of three independent experiments (Appx. 5.3.3 and 5.3.4) showed, AR expression slightly reduced in cytosol but increased in membrane and nucleus (Fig. 5.6.F.1). AR (N-ter) expression was reduced slightly in cytosol (Fig. 5.6.C) which was also appeared in repeat experiments showed through mean analysis (Fig. 5.6.F.2). Membrane localization of AR (N-ter) was also decreased in membrane (Fig. 5.6.C), but its expression was increased in nucleus (Figs. 5.6.C and 5.5.F.2). It indicates the translocation occurs continuously as soon as the protein is available in the cytosol. The expression of β-catenin was also seen to change in cytosol, membrane and nucleus. Activation Wnt signalling released β-catenin in cytosol (Figs. 5.6.D and 5.6.F.3) and then translocated into nucleus (Figs. 5.6.D and 5.6.F.3). Similar result was found for Cx31 the surrogate for Cx43 in LnCAP cells. After the treatment with Wnt5A, Cx31 was reduced in cytosol and membrane and but increased dramatically in nucleus. This implies the translocation of Cx31 into nucleus. This is the first report showing that members of the gap junction family, other than Cx43, are also under the regulatory control of Wnt signalling. β-actin expression was also quantified (Appx. 5.12.3) to check homogenous loading of proteins.

A. Western blot images

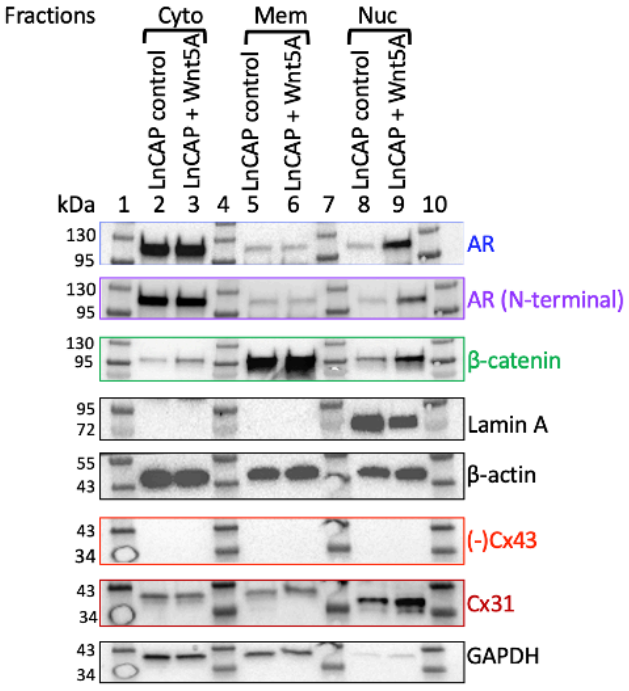

B. AR expression

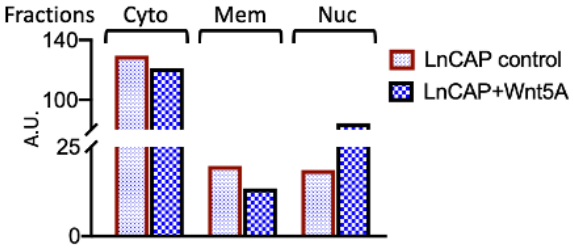

C. AR (N-ter) expression

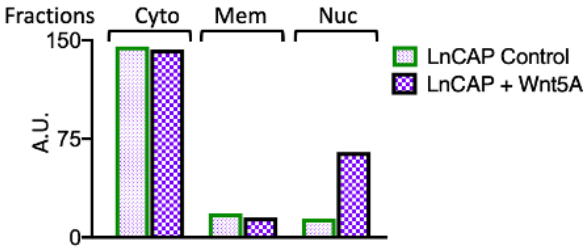

D. β-catenin expression

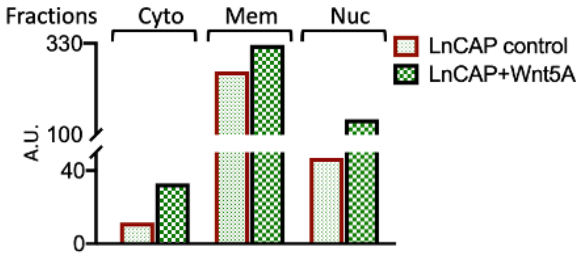

E. Cx31 expression

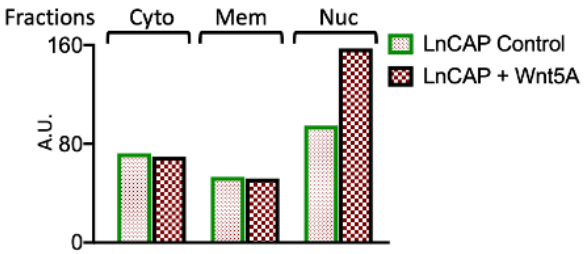

F. Average of expression of three independent experiments

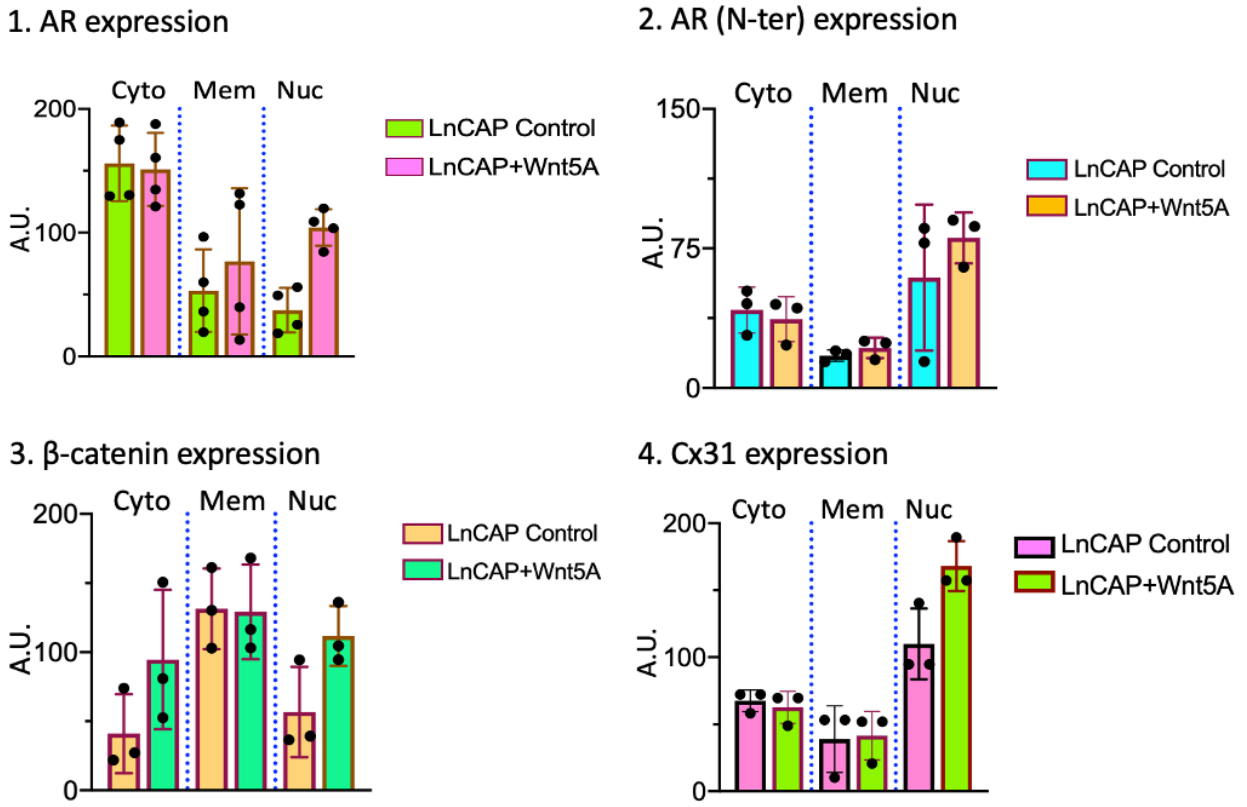

Figure 5.6. A representative WB image for the expression of AR and Wnt signalling proteins in different fractions of LnCAP cells (±Wnt5A). 15 µg of fractionated protein of LnCAP cells (±Wnt5A) was loaded onto gels in the following order cytosolic protein loaded into lane 2 and 3, membrane protein into lane 5 and 6 and nuclear protein into lane 8 and 9. 6µl of Colour Prestained Protein standard, Broad Range (Cat: P7719, NEB) was loaded into lane 1, 4, 7 and 10. The PVDF membrane was cut into two strips of 250 to 57 kDa and 57 to 10 kDa and incubated with anti-Lamin A (expected size ~70 kDa) and anti-β actin antibody (expected size ~ 42 kDa). Following capturing image with GelDoc system (BioRad), the membranes were stripped off with "Restore™ PLUS Western Blot Stripping buffer (Cat: 46430, Thermo Scientific). The membranes were reprobed with anti-AR, anti-AR (N-ter) (expected size ~110 kDa) and anti-β-catenin (~ expected size 90 kDa) and anti-Cx31 (~ expected size 31 kDa) antibodies sequentially. The intensity of bands for each antibody was observed in WB images and quantified with ImageJ. B, C, D and E displaying the comparative expression of AR, AR (N-ter), β-catenin and Cx31 respectively, in cytosol, membrane and nucleus in Wnt5A (±) treated LnCAP cell. F.1, F.2, F.3 and F.4 show bar charts representing the mean (mean±SEM) of n = 3 independent experiments of AR, AR (N-ter), β-catenin and Cx31 expression respectively.

5.4.1.7. Analysis of translocation AR and Wnt signalling proteins in Wnt9B treated LnCAP cells

Prior to treatment with Wnt9B, an optimization experiment was performed (Appx. 5.4.1) with lower concentration of Wnt9B (5 nM), This showed translocation of AR but β-catenin was not translocated into nucleus. Treatment of Wnt9B (10nM) activated the Wnt signalling which trigger the translocation of AR in LnCAP. Wnt9B treatment increased expression of AR in membrane and

its expression was also increased in the nucleus (Figs. 5.7.B and 5.7.F.1). The original PVDF membrane (also termed the non-stripped or primary probed membrane) are shown in appendix (Appx. 5.4.2). There was no difference observed for AR (N-ter) distribution when cells were treated with different Wnt ligands (Wnt3A, Wnt5A and Wnt9B), AR (N-ter) followed the same mechanism of AR for subcellular localization in response to Wnt activation. Wnt signalling activated with Wnt 9B increased β-catenin expression in the nucleus, a result identical to that for Wnt3A (Fig. 5.5.D) and Wnt5A (Fig. 5.6.D) activation in LnCAP cells. This indicates Wnt signalling activation released β-catenin in cytosol and β-catenin was stabilized and subsequently translocated into nucleus (Figs. 5.7.C and 5.7.F.3). Cx31 was also found to be translocated into the nucleus when LnCAP cells were exposed with Wnt9B, similar to that of Wnt3A and Wnt5A treatment of LnCAP cells. Results of replicate experiments are provided in the appendix (Appx. 5.4.3 and 5.4.3). These results confirm those obtained with other Wnt ligands (3A and 5A) and show that both AR and β-catenin are stabilized intracellularly upon activation of Wnt signalling. β-actin expression was also quantified (Appx. 5.12.4) to check homogenous loading of proteins.

A. Western blot images

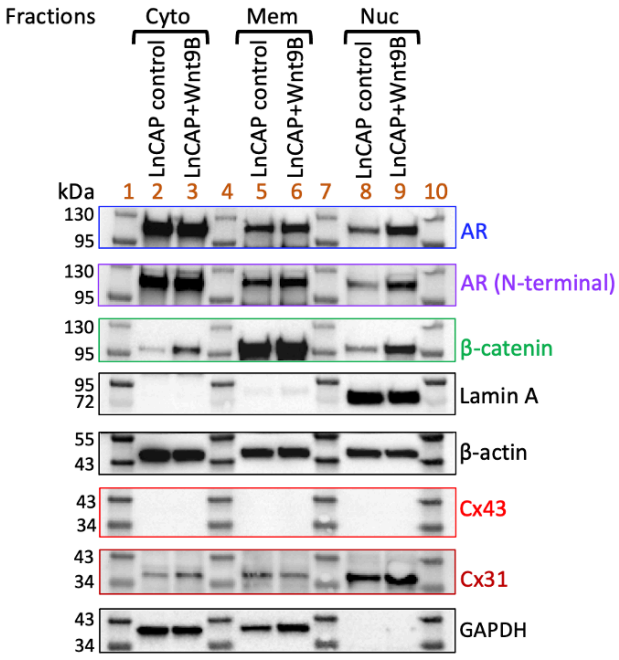

B. AR expression

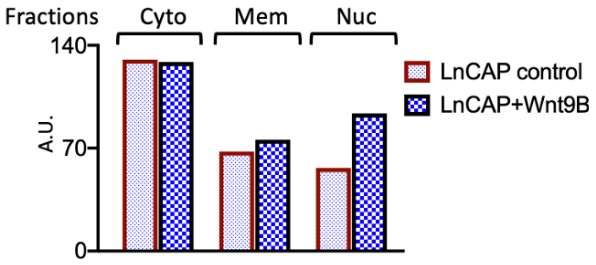

C. AR (N-ter) expression

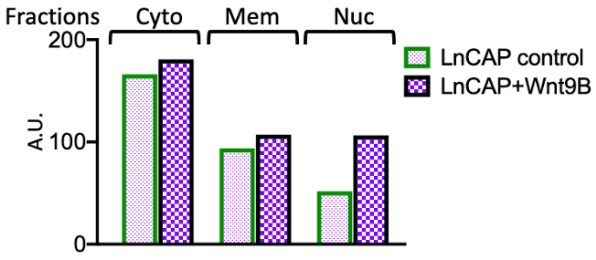

D. β-catenin expression

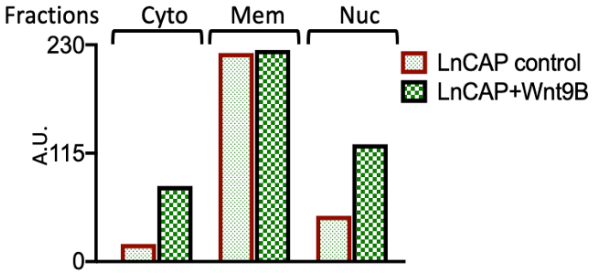

E. Cx31 expression

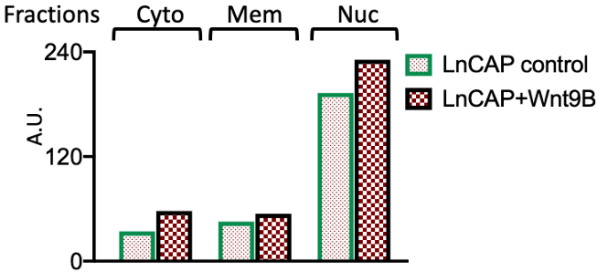

F. Average expression of proteins of three independent experiments

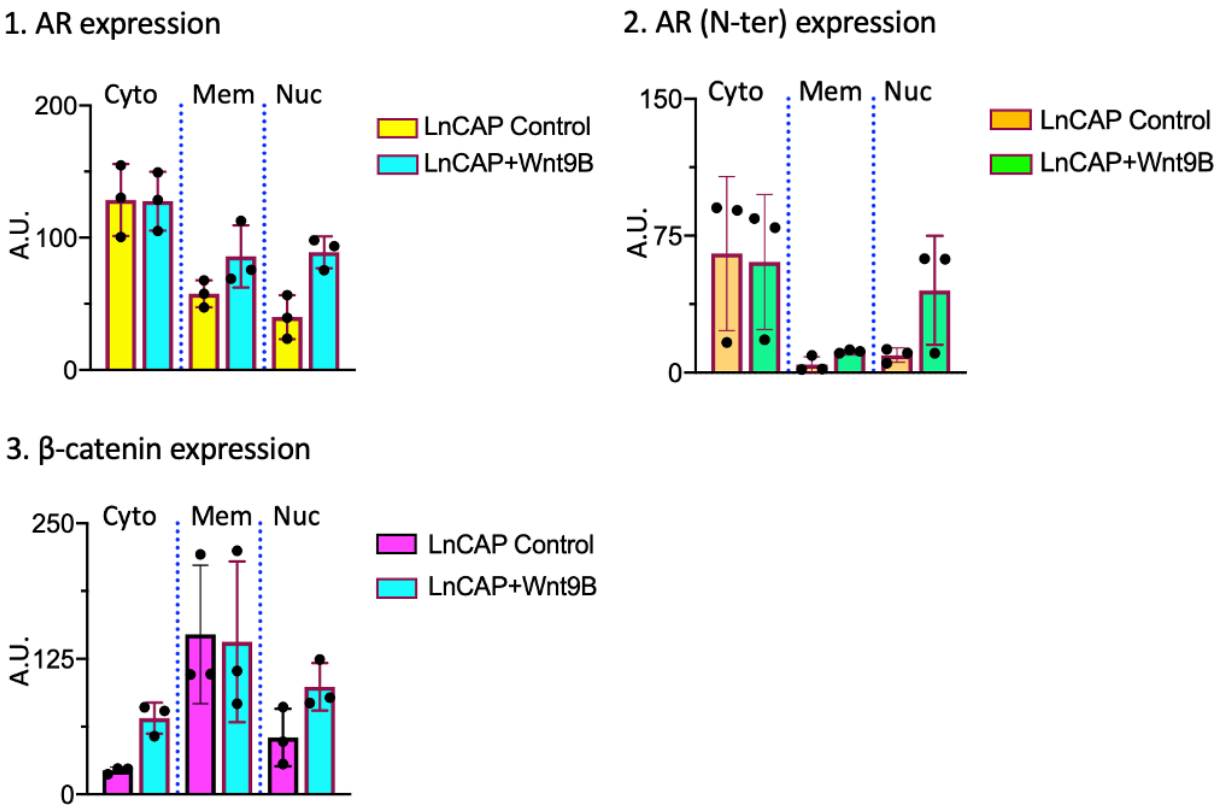

Figure 5.7. A representative WB image for the expression of AR and Wnt signalling proteins in different fractions of LnCAP cells (±Wnt9B). A. 15 µg of fractionated protein of LnCAP cells (± Wnt9B) was loaded onto gels in the following order; cytosolic protein loaded into lane 2 and 3, membrane protein into lane 5 and 6 and nuclear protein into lane 8 and 9. 6µl of Colour Prestained Protein standard, Broad Range (Cat: P7719, NEB) was loaded into lane 1, 4, 7 and 10. The PVDF membrane was cut into two strips of 250 to 57 kDa and 57 to 10kDa and incubated with anti-Lamin A and anti-β actin antibody. Following capturing image with GelDoc system (BioRad), the membranes were stripped off with "Restore™ PLUS Western Blot Stripping buffer (Cat: 46430, Thermo Scientific). The membranes were reprobed with anti-AR, anti-AR (N-ter) and anti-β-catenin and anti-Cx31 antibodies sequentially. The intensity of bands for each antibody was observed in WB images (Fig. 5.7.A) and quantified with ImageJ. B, C, D and E displaying the relative expression of AR, AR (N-ter), β-catenin and Cx31 respectively, in cytosol, membrane and nucleus in (±)Wnt9B treated LnCAP cell. F.1, F.2 and F.3 show bar charts representing the mean (mean±SEM) of n = 3 independent experiments of AR, AR (N-ter). and β-catenin expression respectively.

5.4.1.8. Analysis of translocation Wnt signalling proteins in Wnt9B treated PC3 cells

In previous sections, I have shown that reciprocal activation of Wnt and AR signalling pathways in LnCAP cells with AR and Wnt signalling ligands (Wnt 3A, 5A and 9B and DHT), indicating cross-talk and interaction between these two critical carcinogenic pathways. This reciprocal activation triggered a redistribution of AR and Wnt target proteins across the cytosol, membrane and nucleus. For example, treatment of LnCAP cells with AR and Wnt ligands released β-catenin into

cytosol (Figs. 5.4.F.3; 5.5.F.3; 5.6.F.3 and 5.7.F.3) probably from membrane as membrane β-catenin was reduced during activation and subsequently translocated into nucleus where it interacts with transcriptional co-regulatory compounds to enhance transcription of target genes including AR in LnCAP cells. Cx31, an orthologue of Cx43, the former is expressed in LnCAP whilst the latter is not, was found also translocated into nucleus in LnCAP cells. Wnt activation increased AR and AR (N-ter) expression in cytosol and nucleus but slightly decreased in membrane in LnCAP cells (Figs. 5.4.F.1; 5.4.F.2; 5.5.F.1; 5.5.F.2.; 5.6.F.1 and 5.6.F.2). Conversely, DHT treatment increases not only cytosolic and nuclear AR but also membrane AR expression (Figs. 5.4.F.1 and 5.4.F.2). This may be because of either an increased transcription of AR or post-translational modification that allows availability of AR in these compartments.

Also, research in our laboratory previously showed β-catenin and Cx43 translocation into the nucleus in PC3 cells, that do not express AR, treated Wnt5A and Wnt9B using ICC, immunoelectron microscopy and WB (Hou et al., 2019 and Thrasivoulou et al., 2013). I wanted to confirm these results in my hand. I therefore conducted WB analysis to re-confirm the expression and nuclear translocation of β-catenin and Cx43 in PC3 cells when Wnt signal was activated. The results (Fig. 5.8) confirm the observations by Thrasivoulou et al. and Hou et al. that Wnt signal activation in PC3 cells increases β-catenin and Cx43 expression in the nucleus suggesting nuclear translocation. The original PVDF membranes from which these images are extracted are shown in appendix (Appx. 5.5).

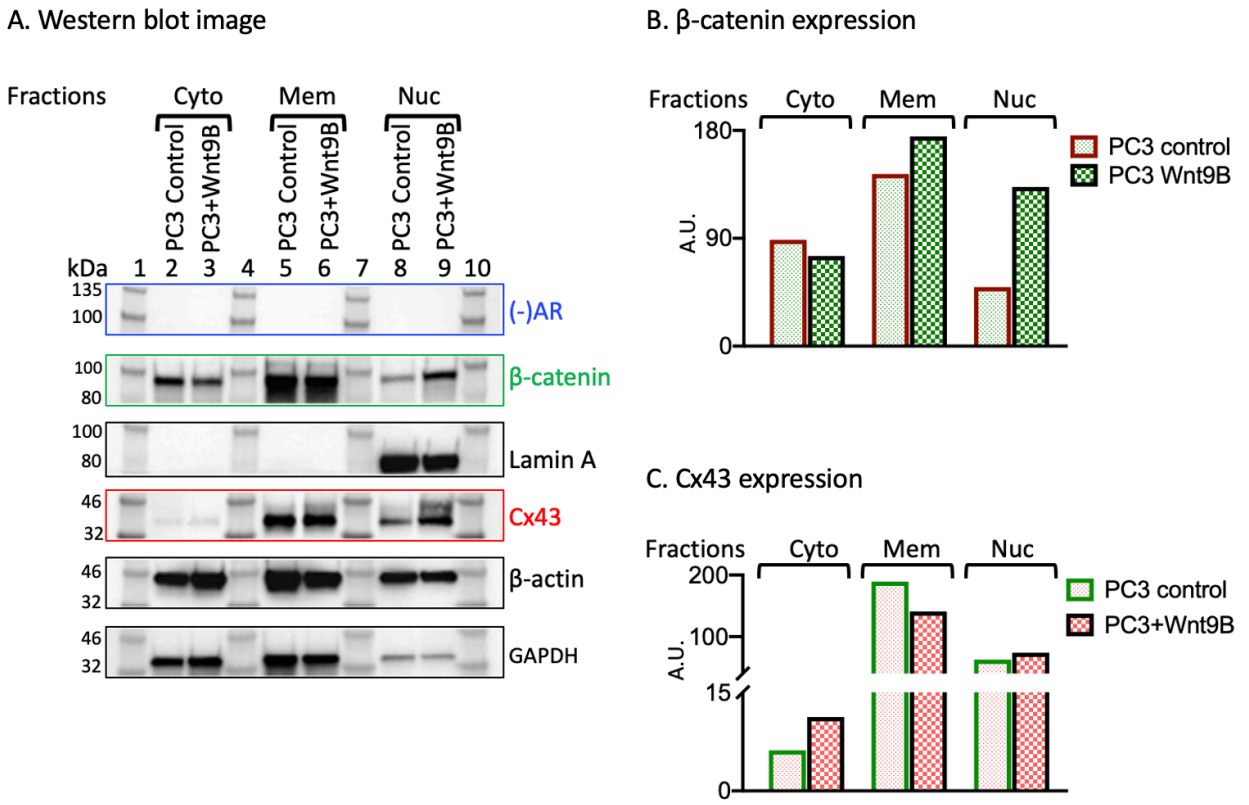

Figure 5.8. A representative WB image of expression of AR and Wnt signalling proteins in different fractions of PC3 cells (±Wnt9B). 15 µg of fractionated protein of PC3 cells (±Wnt9B) was loaded onto gels in the following order; cytosolic protein loaded into lane 2 and 3, membrane protein into lane 5 and 6 and nuclear protein into lane 8 and 9. 6µl of Colour Prestained Protein standard, Broad Range (Cat: P7719, NEB) was loaded into lane 1, 4, 7 and 10. The PVDF membrane was cut into two strips of 250 to 57 kDa and 57 to 10kDa and incubated with anti-Lamin A (expected size ~70 kDa) and anti-β actin antibody (expected size ~ 42 kDa). Following capturing image with GelDoc system (BioRad), the membranes were stripped off with "Restore™ PLUS Western Blot Stripping buffer (Cat: 46430, Thermo Scientific). The membranes were reprobed with anti-AR and β-catenin (~ expected size 90 kDa) and anti-Cx43 (~ expected size 43 kDa) antibodies sequentially. The intensity of bands for each antibody was observed and quantified with ImageJ. B and C displaying the comparative expression of β-catenin and Cx43 in cytosol, membrane and nucleus in PC3 cell (±Wnt9B) respectively.

5.4.1.9. Validation of Wnt induced translocation of AR and DHT induced translocation of β-catenin in a cell line other than LnCAP

The novel mechanism of the reciprocal activation of Wnt and AR signalling by the ligands of either signalling pathway in LnCAP cells could be important in understanding the process of carcinogenesis and metastasis of prostate and other cancers. To eliminate the question that this could be specific only to LnCAP cells, I aimed to validate this in another cell line. To do this, I chose PC3 cells.

PC3 cells, like LnCAP cells are derived from a metastasized prostate cancer, differ from LnCAP in two key respects: (i) PC3 cells do not express AR receptor either at gene or protein level (Tilley et al., 1990), (ii) PC3 cells do not express Cx31 but express Cx43. I rationalized that by transfecting AR into PC3 cells and taking advantage of the endogenous expression of Cx43, I could validate the reciprocal activation of both Wnt, Connexin and AR signalling pathways. However, before conducting these experiments, I measured if there were any effects of DHT treatment on β-catenin and Cx43 in wild type PC3 cells that do not express AR. These are described below.

The initial experiments showed peculiar observations when wild type PC3 cells (that do not express AR) were incubated with DHT for only 30 min: there was a lower expression of β-catenin and Cx43 proteins in nucleus (Appx. 5.6.2). This was curious because this was opposite to the observation of PC3 cells treated with Wnt ligand where both β-catenin and Cx43 proteins. To investigate if this process was time dependent I incubated PC3 cells with DHT for 30 min and 2 h. The WB result showed β-catenin and Cx43 expression in nucleus decreased with increasing of incubation time (Fig. 5.9). Interestingly, membrane β-catenin and Cx43 expression was increased after 30 min incubation. After 2 h incubation membrane expression was not changed. These results indicate that DHT treatment inhibit the basal (without additional Wnt treatment) level translocation of β-catenin and Cx43 into nucleus. Probing with anti-AR antibody did not produce any protein band (Fig. 5.9), as would be expected for PC3 cells as these do not express AR protein (Tilley et al., 1990). This, incidentally, also serves as a specificity control for the AR antibody. The original PVDF membranes and repeat experiments are given in appendix (Appx. 5.6.1 and Appx. 5.6.2). This is an interesting observation as PC3 cells do not express the AR and suggests that DHT may be inducing its effects on β-catenin and Cx43 via an unknown mechanism that remains to be elucidated.

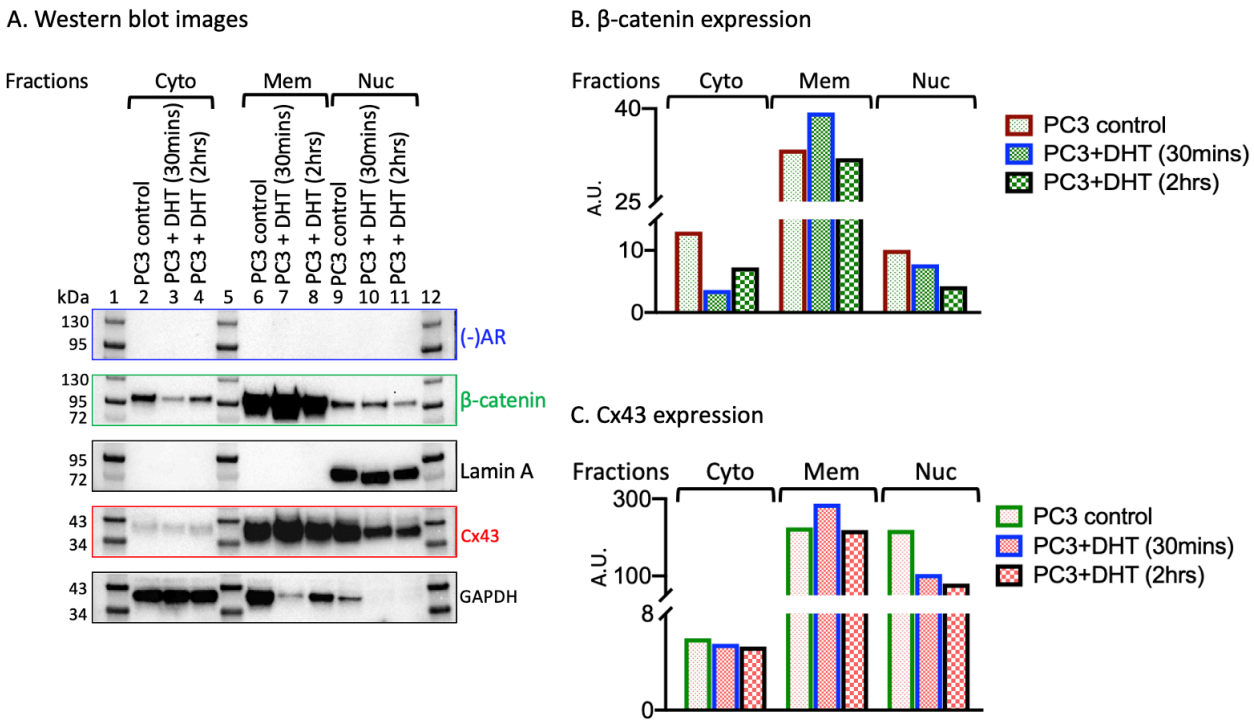

Figure 5.9. A representative WB image for the expression of AR and Wnt signalling proteins in different fractions of PC3 cells (±DHT). A. 15 µg of fractionated protein of PC3 cells (±DHT) was loaded onto gels in the following order; cytosolic protein loaded into lane 2, 3 and 4, membrane protein into lane 6, 7 and 8, and nuclear protein into lane 8, 10 and 11. 6µl of Colour Prestained Protein standard, Broad Range (Cat: P7719, NEB) was loaded into lane 1, 5 and 12. The PVDF membrane was cut into two strips of 250 to 57 kDa and 57 to 10kDa and incubated with anti-Lamin A and anti-β actin antibody. Following capturing image with GelDoc system (BioRad), the membranes were stripped off with "Restore™ PLUS Western Blot Stripping buffer (Cat: 46430, Thermo Scientific). The membranes were reprobed with anti-AR (not expected) and β-catenin and anti-Cx43 antibodies sequentially. The intensity of bands for each antibody was observed and quantified with ImageJ. B and C displaying the comparative expression of β-catenin and Cx43 in cytosol, membrane and nucleus in PC3 cell (±DHT) respectively.

5.4.1.10. Analysis of translocation Wnt signalling proteins in PC3 cells treated with DHT and Wnt9B

As DHT treatment inhibited the translocation of β-catenin and Cx43 in a time dependent manner, I wanted to answer the following question: Does Wnt signal activate stabilization and nuclear translocation of β-catenin and Cx43 when cells are treated with both DHT and Wnts? To investigate whether the effect of DHT remained same in the presence of Wnt signal activation by Wnt ligands, I performed another experiment with PC3 cells treated with both DHT and Wnt9B.

A comparative investigation showed that treatment of PC3 cells with DHT reduced the translocation of β-catenin and Cx43, but their expression was increased in nucleus when treated with Wnt9B (Fig. 5.10). This suggests that Wnt signal activation over-rode the unknown

mechanism by which DHT influenced β-catenin nuclear translocation in the wild type PC3 cells. The original PVDF membranes and repeat experiments are shown in appendix (Appx. 5.7.1 and Appx. 5.7.2).

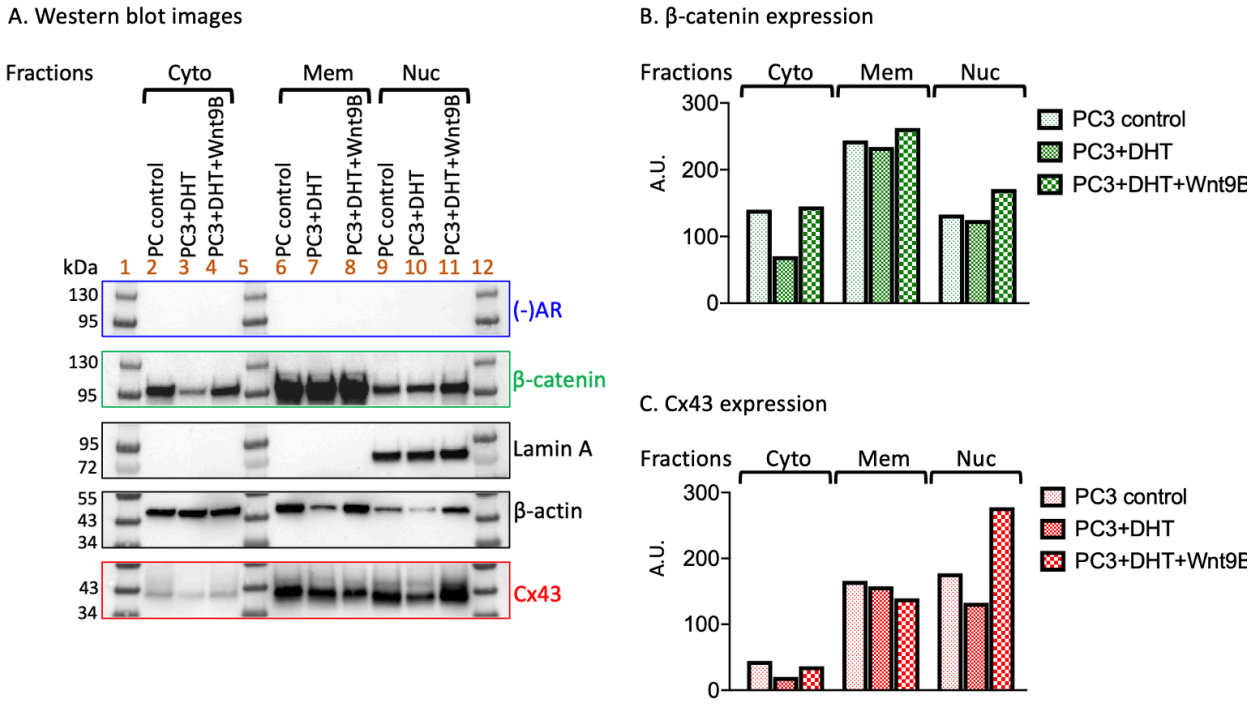

Figure 5.10. A representative WB image for the expression of AR and Wnt signalling proteins in different fractions of PC3 cells (untreated, +DHT, +DHT+Wnt9B). 15 µg of fractionated protein of PC3 cells (±DHT, +DHT+Wnt9B) was loaded onto gels in the following order; cytosolic protein loaded into lane 2, 3 and 4, membrane protein into lane 6, 7 and 8, and nuclear protein into lane 8, 10 and 11. 6µl of Colour Prestained Protein standard, Broad Range (Cat: P7719, NEB) was loaded in lane 1, 5 and 12. The PVDF membrane was cut into two strips of 250 to 57 kDa and 57 to 10kDa and incubated with anti-Lamin A and anti-β actin antibody. Following capturing image with GelDoc system (BioRad), the membranes were stripped off with "Restore™ PLUS Western Blot Stripping buffer (Cat: 46430, Thermo Scientific). The membranes were reprobed with anti-AR (not expected) and β-catenin and anti-Cx43 antibodies sequentially. The intensity of bands for each antibody was observed and quantified with ImageJ. B and C displaying the comparative expression of β-catenin and Cx43 in cytosol, membrane and nucleus in PC3 cell (±DHT), respectively.

After establishing the baseline ±Wnt and ±DHT, I wanted to validate the observations seen in LnCAP regarding the reciprocal activation of Wnt and AR signalling pathways. To do this I transfected wild type, non-AR expressing, PC3 cells with pCMV6-AC-GFP (Appx. 2.6) which contains AR genes and GFP reporter gene and has been shown to express and stabilize AR protein (Ramos et al., 2018), (Chap-II, Sec. 2.3.3.4). The results of transfection and confirmation of the expression of AR are shown in Fig. 5.11.

5.4.1.11. AR expression in non-AR expressing PC3 cells

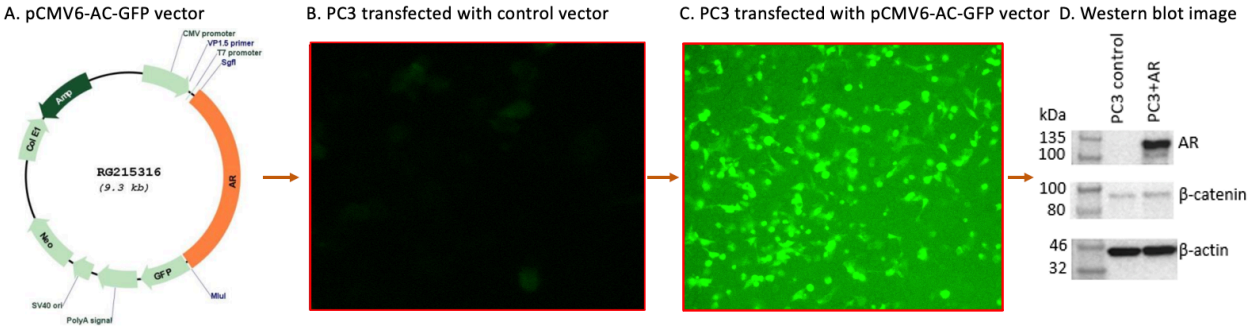

Figure 5.11. Transfection of PC3 cells with pCMV6-AC-GFP. A. pCMV6-AC-GFP, a mammalian vector with C-terminal tGFP tag with Androgen Receptor (AR) (NM_000044) Human Tagged ORF clone. B. PC3 cells transfected with empty vector (AR-) viewed under Leica fluorescence Microscope with 10x objectives. C. PC3 cells transfected with pCMV6-AC-GFP with stable expression of GFP reporter gene. The transfected PC3 was designated as $PC3^{(AR+)}$ cells for downstream use. D. WB image shows the expression of AR in $PC3^{(AR+)}$ (transfected with AR inserted plasmid) cells but $PC3^{(AR-)}$ (transfected with empty plasmid) did not show any sign of AR expression.

5.4.1.12. Translocation of Wnt signalling proteins in PC3(AR+) cells treated with DHT

AR transfected PC3 cells ($PC3^{(AR+)}$) showed increased AR expression in nucleus after treatment with DHT (Fig. 5.12). Interestingly, there was noticeable increase in the expression of β-catenin and Cx43 in the membrane fraction in PC3 $^{(AR+)}$ (Fig. 5.12). β-catenin and Cx43 expression was, however, reduced in nucleus in PC3 $^{(AR+)}$ cells compared to untransfected PC3 (wild type or control control) cells, in a similar manner as (Prelich, 2012). There is a known concept that heterologous over-expression of a protein can inhibits another protein expression. For example, over-expression of the mammalian ubiquitin E3 ligase MKRN1 results in the degradation of the hTERT telomerase subunit (Kim et al., 2005). Treatment of PC3 $^{(AR+)}$ cells with DHT (Fig. 5.12) increased the translocation of β-catenin and Cx43 in nucleus (Fig 5.12). This indicates that downstream Wnt signalling may have been activated by DHT (Fig. 5.12). It further appears that there is a concomitant depletion of β-catenin and Cx43 from the membrane fraction in PC3 $^{(AR+)}$ cells after treatment with DHT and it is this fraction that ends up in the nucleus. The stained main PVDF membranes are shown in appendix (Appx. 5.8).

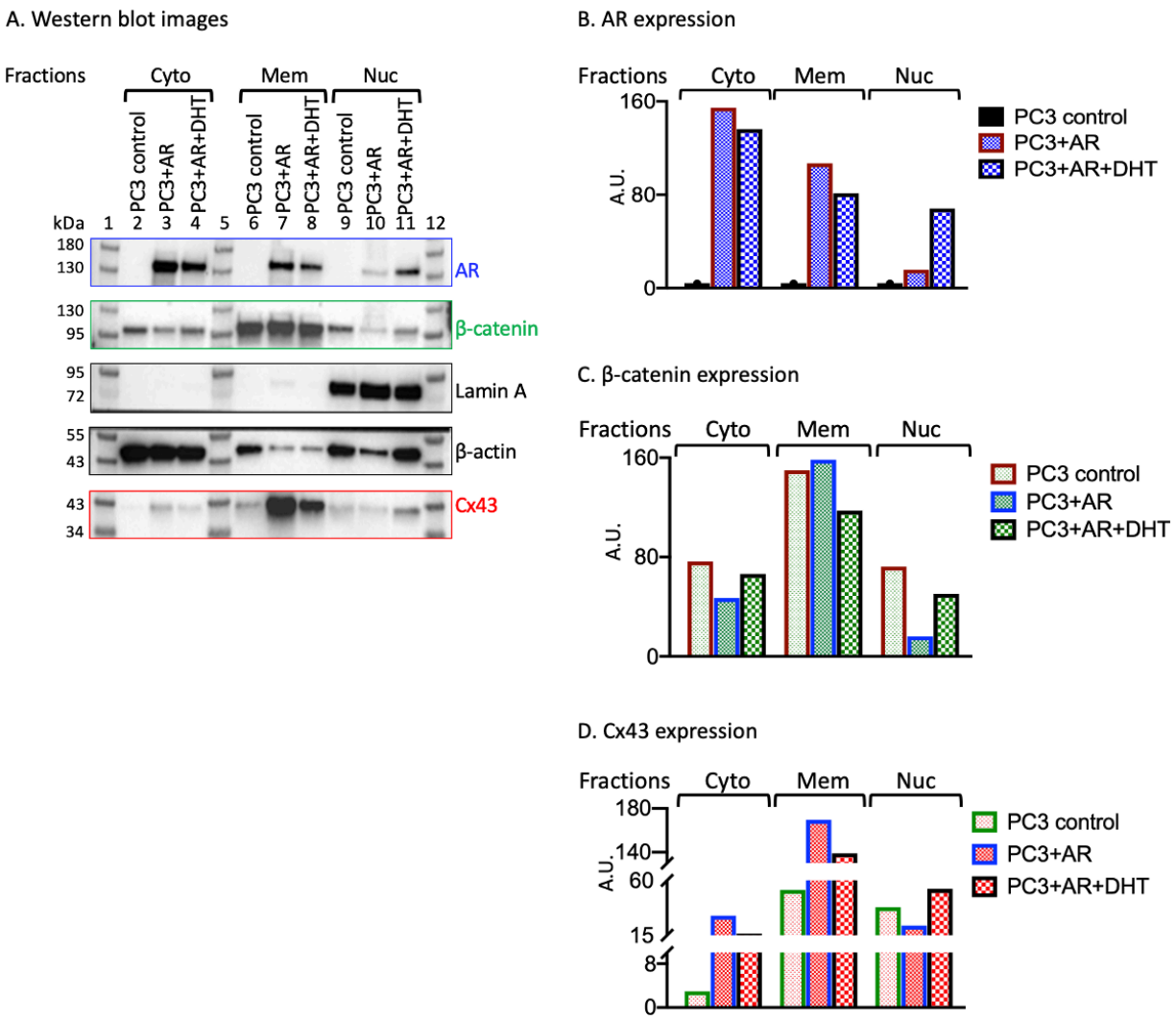

Figure 5.12. A representative WB image for the expression of AR and Wnt signalling proteins in different fractions of PC3, PC3$^{(AR+)}$, PC3$^{(AR+)}$+DHT cells. A. 15 µg of fractionated protein of PC3, PC3$^{(AR+)}$, PC3$^{(AR+)}$+DHT cells was loaded onto gels in the following order; cytosolic protein loaded into lane 2, 3 and 4, membrane protein into lane 6, 7 and 8, and nuclear protein into lane 8, 10 and 11. 6 µl of Colour Prestained Protein standard, Broad Range (Cat: P7719, NEB) was loaded into lane 1, 5 and 12. The PVDF membrane was cut into two strips of 250 to 57 kDa and 57 to 10kDa and incubated with anti-Lamin A (expected size ~70 kDa) and anti-β actin antibody (expected size ~ 42 kDa). Following capturing image with GelDoc system (BioRad), the membranes were stripped off with "Restore™ PLUS Western Blot Stripping buffer (Cat: 46430, Thermo Scientific). The membranes were reprobed with anti-AR (expected) and β-catenin (~ expected size 90 kDa) and anti-Cx43 (~ expected size 43 kDa) antibodies sequentially. The intensity of bands for each antibody was observed and quantified with ImageJ. B and C displaying the comparative expression of AR, β-catenin and Cx43 in cytosol, membrane and nucleus in PC3 and PC3$^{(AR+)}$ cell respectively.

5.4.1.13. Translocation Wnt signalling proteins in PC3(AR+) cells treated with Wnt9B

When PC3$^{(AR+)}$ cells were exposed to Wnt 9B (10 nM), it resulted in the activation of Wnt signalling, as expected, with an increase in the expression of β-catenin and AR compared to

control PC3$^{(AR+)}$ cell. These results and those presented in section 5.4.1.12 suggest that β-catenin and AR translocate into the nucleus together, and perhaps AR might act as chaperon protein in CRPC. Cx43 expression was also increased in the nucleus in PC3$^{(AR+)}$ cell treated with Wnt9B compared to control PC3 $^{(AR+)}$ cell. It was observed that Cx43 expression was higher in cytosol and membrane in PC3$^{(AR+)}$ cells. Treatment with Wnt9B reduced cytosolic and membrane Cx43 expression but nuclear expression was increased. That indicates Cx43 was translocated from membrane or cytosol (Fig. 5.13). The stained main PVDF membranes are located in appendix (Appx. 5.9.1; 5.9.2 and 5.9.3).

A. Western blot images

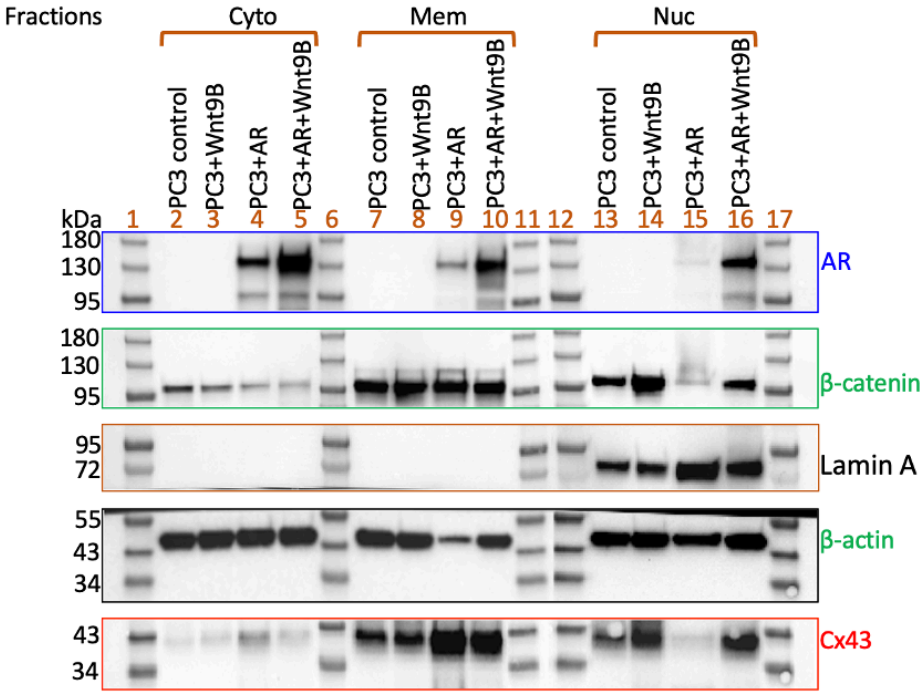

B. AR expression

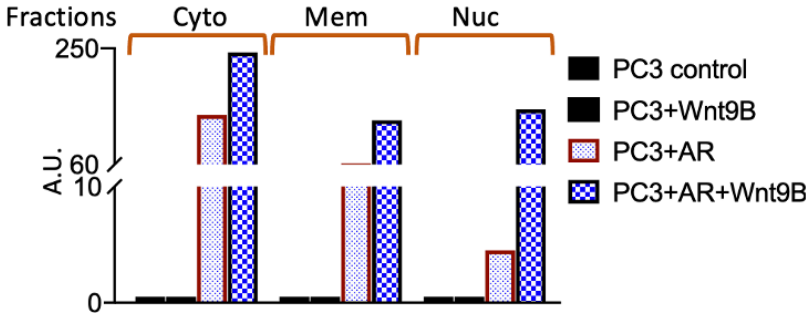

C. β-catenin expression

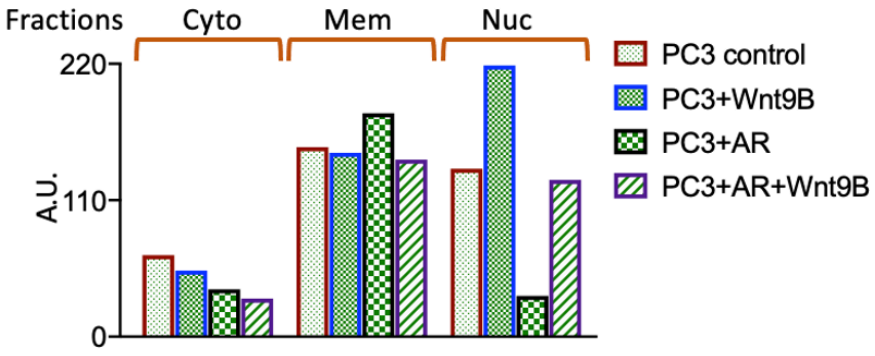

D. Cx43 expression

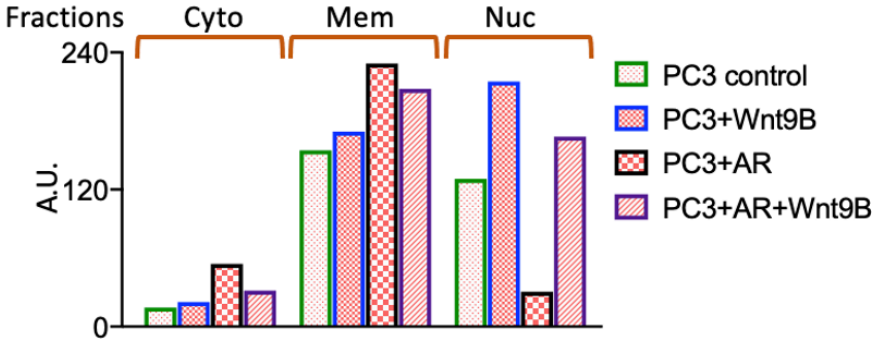

Figure 5.13. A representative WB image for the expression of AR and Wnt signalling proteins in different fractions of PC3, PC3+Wnt9B, PC3$^{(AR+)}$ cell, PC3$^{(AR+)}$ + Wnt9B cells. A. 15 µg of fractionated protein of PC3, PC3+Wnt9B, PC3$^{(AR+)}$ cell, PC3$^{(AR+)}$ + Wnt9B cells was loaded onto gels in the following order; cytosolic protein loaded into lane 2, 3, 4 and 5, membrane protein into lane 7, 8, 9 and 10, nuclear protein into lane 13, 14, 15 and 16. 6µl of Colour Prestained Protein standard, Broad Range (Cat: P7719, NEB) was loaded into lane 1, 6, 11, 12 and 17. The PVDF membrane was cut into two strips of 250 to 57 kDa and 57 to 10kDa and incubated with anti-Lamin A (expected size ~70 kDa) and anti-β actin antibody (expected size ~ 42 kDa). Following capturing image with GelDoc system (BioRad), the membranes were stripped off with "Restore^{TM} PLUS Western Blot Stripping buffer (Cat: 46430, Thermo Scientific). The membranes were reprobed with anti-AR (expected) and β-catenin (~ expected size 90 kDa) and anti-Cx43 (~ expected size 43 kDa) antibodies sequentially. The intensity of bands for each antibody was observed and quantified with ImageJ. B, C and D displaying the comparative expression of AR, β-catenin and Cx43 in cytosol, membrane and nucleus in cell respectively.

5.4.2. Physical interaction between AR and β-catenin assessed using Co-IP

Protein-protein interactions are critical for cell function and result due to physical proximity between two proteins. Co-immunoprecipitation (Co-IP) is a commonly used approach to identify such interactions between two physiologically relevant proteins by using target protein specific antibodies that bind to this target protein. The reciprocal activation of Wnt and AR pathways

raised the question whether there was any physical interaction between the intracellular transducers of these signalling pathways? I aimed to address this question by measuring the physical interaction between AR and β-catenin by Co-IP. Prior to conducting Co-IP, LnCAP cells were treated with DHT and Wnt5A and Co-IP was performed using anti-AR antibody. The results (Fig. 5.14) indicate a clear physical interaction between AR and β-catenin. IP with AR antibody in lane 3, 5, 7 showing dark band at ~110kDa when probed with AR. When the same blot is reprobed with anti- β-catenin antibody, subsequent to stripping (see Methods), it also gave bands at ~95kDa, indicating β-catenin protein was precipitated with AR antibody (Fig. 5.14); this occurred for both ±Wnt and ±DHT. These results indicate for the first time that reciprocal activation of AR and Wnt signalling by specific ligands activates downstream signal for both these pathways and that it results in physical interaction between AR and β-catenin proteins.

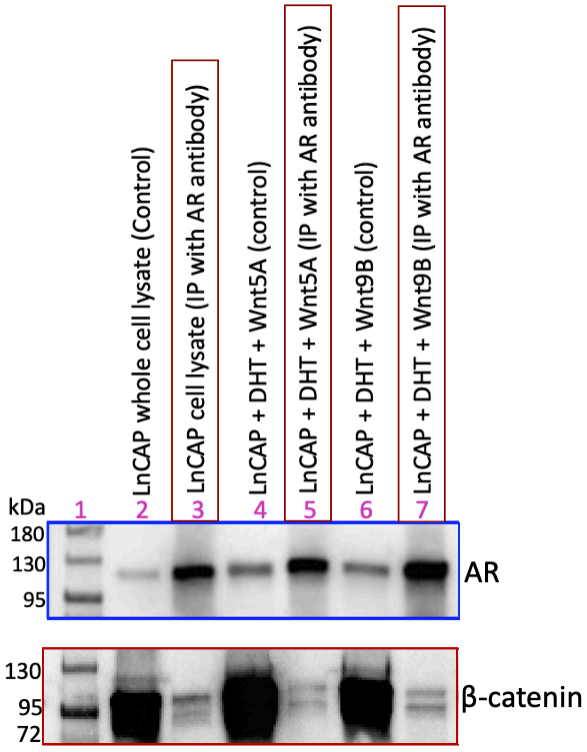

Figure 5.14. Image of Co-IP for interaction of AR and β-catenin. Immunoblot/coimmunoprecipitation (Co-IP) analysis of whole-cell LnCAP lysate treated with Wnt5A and Wnt9B using the ant-AR antibody. Molecular weight marker was loaded into lane-1. AR and β-catenin were detected from LnCAP cells. Anti-AR and Anti-β-catenin antibodies were used for Western blot to detect AR and β-catenin proteins. Anti-Rabbit and Anti-mouse secondary antibodies were used for anti-AR and anti-β-catenin primary antibodies respectively.

5.4.3. Immunocytochemical analysis of translocation of AR and Wnt signalling proteins in LnCAP cells

The WB technique is a useful tool and its use in the experiments described above resulted in the novel discovery of a reciprocal activation of Wnt and AR signalling pathways in PC3 and synergistic and a physical interaction between AR and β-catenin proteins in LnCAP cells. Although WB provides advantage such as enriched protein fractions and ability to investigate physical interactions, one drawback of WB is that it requires fractionation of cells to isolate cellular compartments and does not relate to *in situ* localization of the proteins of interest in the cell. To do this and also to validate the results obtained with WB, I used the traditional ICC where protein expression could be investigated with intact cellular morphology.

Based on previous experiments that showed translocation of AR and Wnt signalling proteins in LnCAP and PC3 cells upon treatment with AR (e.g., DHT) and Wnt (Wnt3A, Wnt5A and Wnt9B) signalling ligands, I designed an immunocytochemical study to validate the WB results (Sec. 5.4.1). Translocation of β-catenin into nucleus, after signal activation with Wnt ligands, has already been shown in PC3 cells (Thrasivoulou et al., 2013) using ICC and also using electron microscopy (Hou et al., 2019). The experiments in PC3 cells were also reproduced contemporaneously by Marta Reyes-Corral with my help (Reyes-Corral, PhD thesis, 2020). Therefore, staining for β-catenin translocation in PC3 cells was not included in this study.

I evaluated the expression and translocation of AR in LnCAP cells upon treatment with AR and Wnt signalling ligands. LnCAP cells were treated with DHT (15 nM) and Wnt9B (10 nM) and incubated overnight at 37^{o}C. The expression was examined by colocalization of AR and nuclear (e.g., DAPI) staining in cells. Control experiments included untreated LnCAP cells, to observe the basal expression of β-catenin in the cells, and to compare the translocation of AR into the nucleus.

Following staining, the cells were imaged using SP8 confocal microscopy to observe the expression and localization of AR in LnCAP cells treated with AR ligand (e.g., DHT) Wnt ligands (e.g., Wnt9B for canonical and Wnt5A for noncanonical) to activate expression and potential

translocation of AR using ICC, Western blotting. Signal of AR expression was amplified using TSA (Tyramide Signal Amplification) tagged with Cy3 (red) fluorophore.

There is little expression of AR in control, vehicle treated, LnCAP cells (Fig. 5.15), showing AR (A, Cy3), DAPI nuclear counterstain (A1) whereas micrograph A2 shows a composite image of Cy3 and DAPI staining. Treatment with vehicle (Fig. 5.15.A) or DHT (Fig. 5.15.B), Wnt9B (Fig. 5.15.C) and Wnt5A (Fig. 5.18.D) demonstrate translocation of AR in the nucleus compared to LnCAP vehicle treated controls. Nuclear region is pointed with arrows. The results show translocation of AR into the nucleus indicated by bright red staining which could be observed to be nuclear staining in response to DHT, Wnt5A and Wnt9B (Figs. 5.15 B2, C2 and D2). These results concur with those obtained using WB.

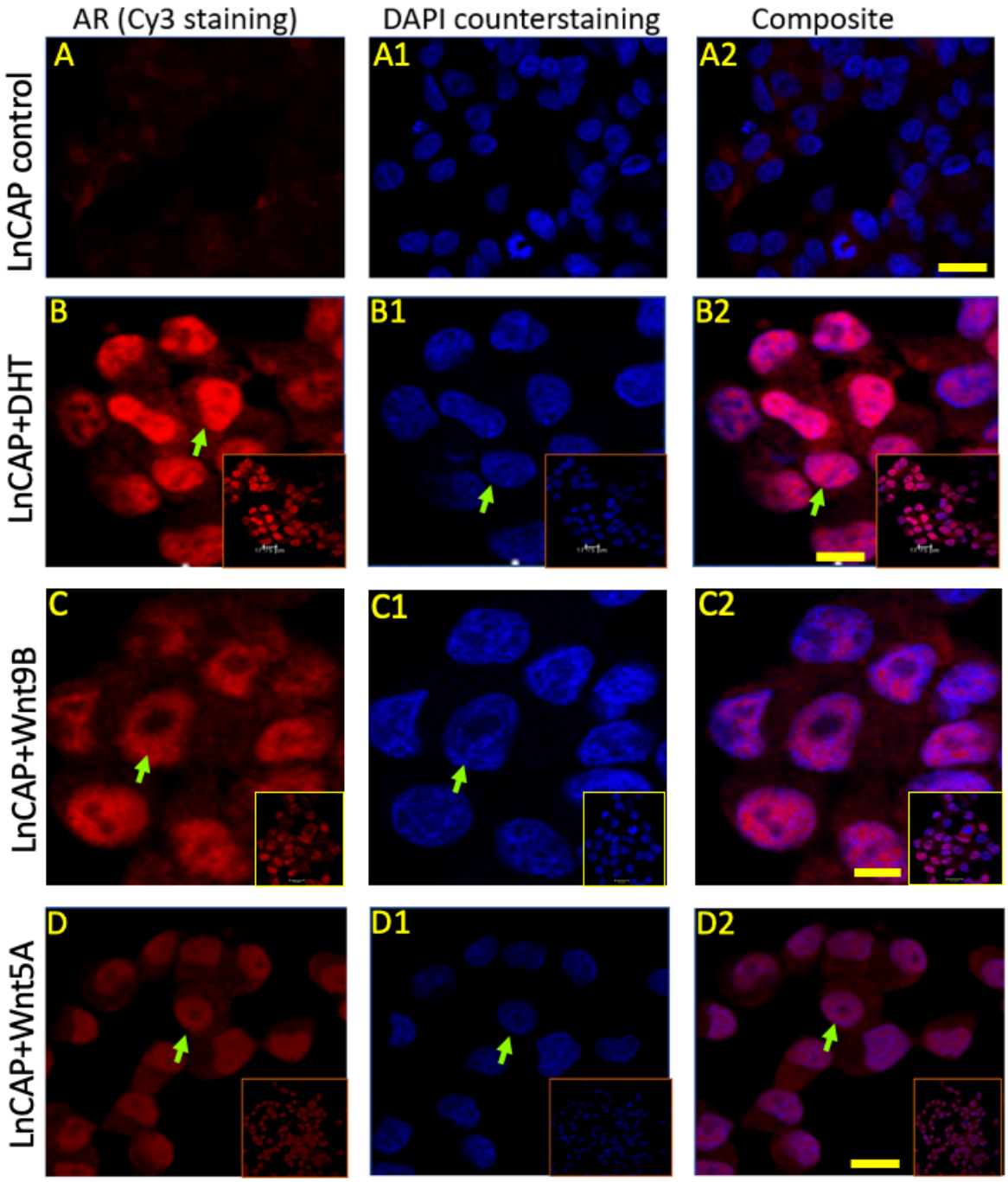

Figure 5.15. Nuclear translocation of AR in LnCAP cells treated with Wnt and AR ligands. LnCAP cells were grown on 8-well glass chamber slides and treated with AR ligand (DHT, 15 nM) and Wnt ligands (Wnt9B, 15 nM and Wnt5A, 10 nM). Control experiment was run parallel. Following fixation, cells were incubated with anti-AR antibody followed by staining with Cy3 (red) and the signal was amplified with TSA. DAPI (blue) was used as nuclear counterstaining. The stained cells on slides were imaged using Leica SP8 confocal microscope equipped with a 40x1.3NA oil objectives and z-stacks acquired using 0.6µm step size. Representative maximum intensity projections from ~5.5µm z-stack from n=3-4 experiments for: A-A2: LnCAP cells (untreated, control); B-B2: LnCAP cells treated with DHT; C-C2: LnCAP cells treated with Wnt9B; D-D2: LnCAP cells treated with Wnt5A. Representative images of three independent experiments are shown. Arrow indicates the nuclear region. Scale bar, 10µm.

β-catenin was originally identified as Cadherin Associated Protein-β. Cadherins are a family of proteins that allow physical contact between cells and are expressed in cell membrane (Willert and Nusse, 1998). The expression and location of β-catenin has not been well investigated in LnCAP cells, and neither the translocation in response to AR or Wnt signal activation using ICC. In LnCAP cells treated with DHT, β-catenin appear to be stabilized and translocated into the nucleus (as seen in Fig. 5.15). It is useful to note that the β-catenin resides mostly in the membrane (Fig. 5.16) in LnCAP cells (control). The β-catenin in LnCAP cells (DHT treated) translocates into the nucleus indicated with bright red staining at the centre of cells (indicated with arrows, Fig. 5.16). These results are also in concordance with those obtained using WB.

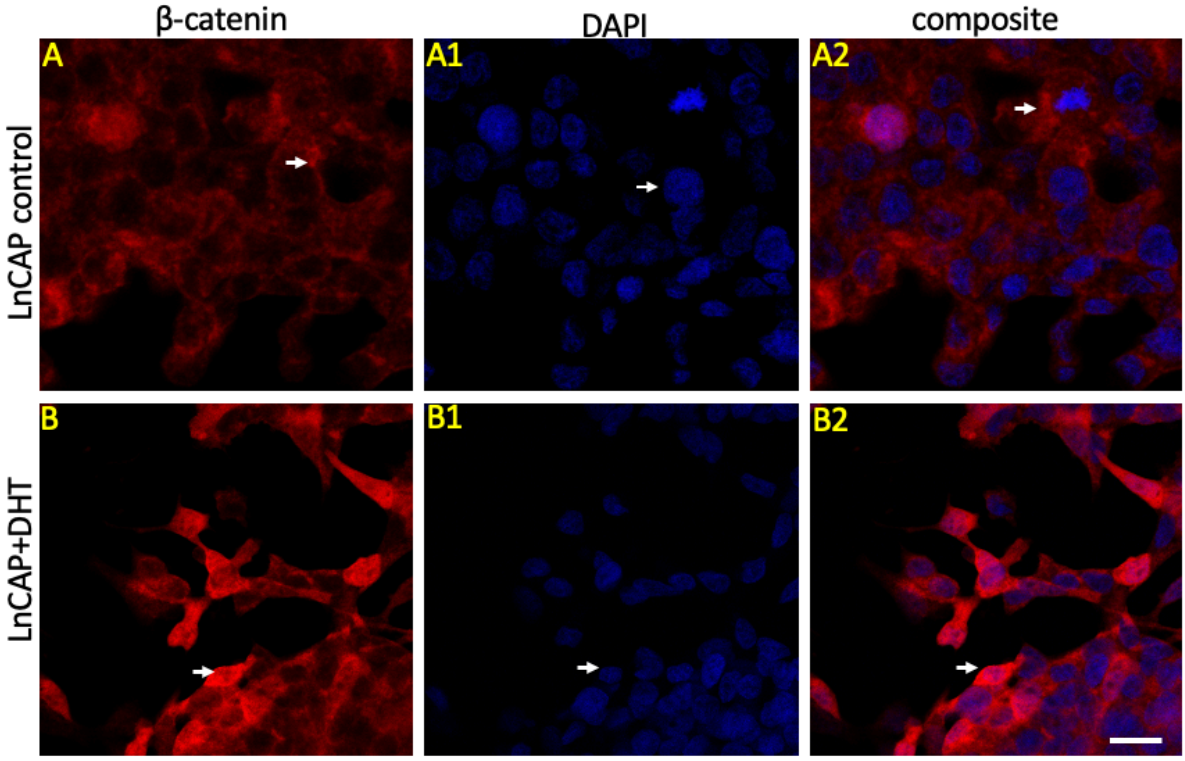

Figure 5.16. Nuclear translocation of β-catenin in LnCAP cells treated with AR signalling ligand. LnCAP cells were treated with AR ligand (DHT, 15 nM). Same procedure was followed as described for Fig.5.15. Anti-β-catenin antibody was used for staining. A-A2: LnCAP cells (untreated, control); B-B2: LnCAP cells treated with DHT. Representative images of three independent experiments are shown. Arrow indicates the nuclear region. Scale bar, 10µm.

As stated above, PC3 cells do not express AR. AR translocation into nucleus in PC3$^{(AR+)}$ cells was shown earlier (Sec. 5.4.1.12). To further establish this observation, ICC was performed in PC3$^{(AR+)}$ cells. PC3 cells were transfected with AR inserted plasmid vector pCMV6-AC-GHP (Appx. 2.6).

Once AR expression in PC3 cells had been stabilised, the cells were treated with DHT, Wnt9B or Wnt5A and stained with an anti-AR antibody (Table 5.2). The control PC3 cells did not show a signal for AR expression, indicating absence of AR in PC3 (Fig. 5.17.A). AR expression was found in $PC3^{(AR+)}$ cell, residing mostly outside of nucleus (Fig. 5.17.B), though a small fraction of AR was detected in nucleus of control $PC3^{(AR+)}$ cells in WB experiment (Fig. 5.13B). Treatment with DHT (Fig. 5.17.C), Wnt9B (Fig. 5.17.D) and Wnt5A (Fig. 5.17.E) increased the expression of AR in the nucleus in $PC3^{(AR+)}$ cells indicating DHT and Wnt mediated nuclear translocation. These results confirm the observations made using WB. A clear implication of these results is that both AR and Wnt signalling pathway can act in synergy and therefore amplify the oncogenic pathways in prostate cancer. A clear consequence will be increased in gene transcription of the targets of AR and β-catenin transcription, a number of which are proto-oncogenes. This could be one way in which reciprocal activation of Wnt and AR signalling could increase carcinogenesis and metastasis of prostate cancers.

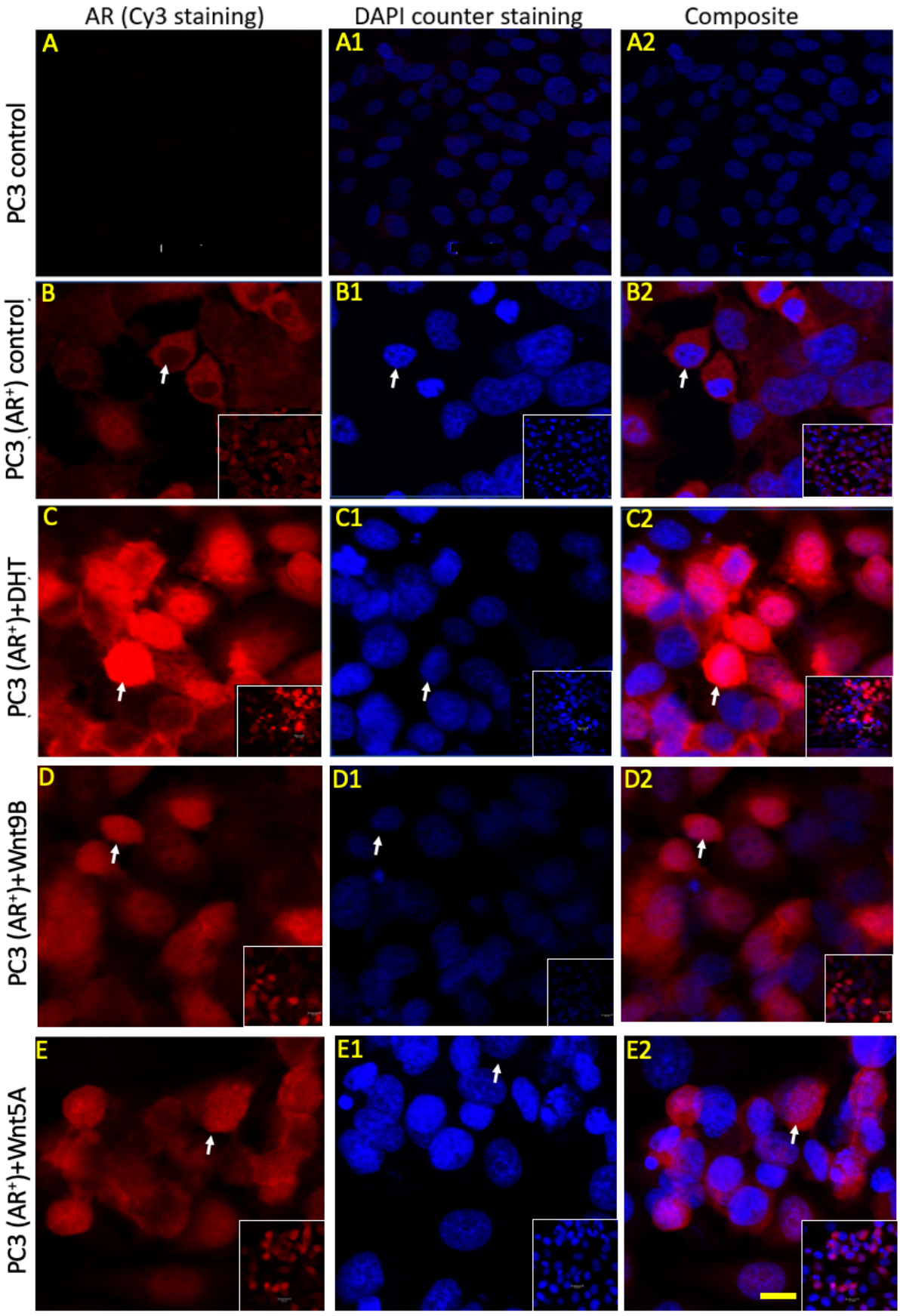
AR (Cy3 staining)
DAPI counter staining
Composite
A
A1
A2
PC3 control
B
B1
B2
PC3 (AR+) control
C
C1
C2
PC3 (AR+)+DHT
D
D1
D2
PC3 (AR+)+Wnt9B
E
E1
E2
PC3 (AR+)+Wnt5A

Figure 5.17. Nuclear translocation of AR in PC3(AR+) cells treated with AR and Wnt signalling ligands. $PC3^{(AR+)}$ cells were treated with AR ligand (e.g., DHT) and Wnt signalling ligands (e.g., Wnt9B and Wnt5A, 500ng/ml. Same procedure was followed as described for Fig. 5.18. Anti-AR antibody was used for staining. A-A2: PC3 cell (control); B-B2: $PC3^{(AR+)}$ cells (Control); C-C2: $PC3^{(AR+)}$ cells treated with DHT; D-D2: $PC3^{(AR+)}$ treated with Wnt9B; E-E2: $PC3^{(AR+)}$ cell treated with Wnt5A.Representative images of three independent experiments are shown. Arrow indicates nuclear region. Scale bar, 10μm.

Conversely, β-catenin was translocated into nucleus when treated with Wnt3A, Wnt5A and Wnt9B showed in WB (Figs. 5.5., 5.6 and 5.7). I already observed in my previous study that Wnt5A and Wnt9B treatment trigger translocation of β-catenin and Cx43 into nucleus.

Using WB, I showed that DHT treatment to PC3 cells inhibited β-catenin and Cx43 translocation (Fig. 5.9). This appears to be confirmed when ICC was used as well (Fig. 5.18). The image in Fig. 5.18 shows the expression of Cx43 in nucleus as well as membrane in control conditions. When PC3 cells were treated with DHT, Cx43 appears to move out from the nucleus and towards membrane. Interestingly, the effect of DHT and Wnt treatment seems to cause an opposite effect on its translocation into the nucleus. The ICC, although not complete (e.g., lack of determination of β-catenin expression treated with DHT in conjunction with Wnt in $PC3^{(AR+)}$ cells), the ICC data generally agrees with the results observed in WB. An interesting observation is the effect of DHT in PC3 cells that do not express AR.

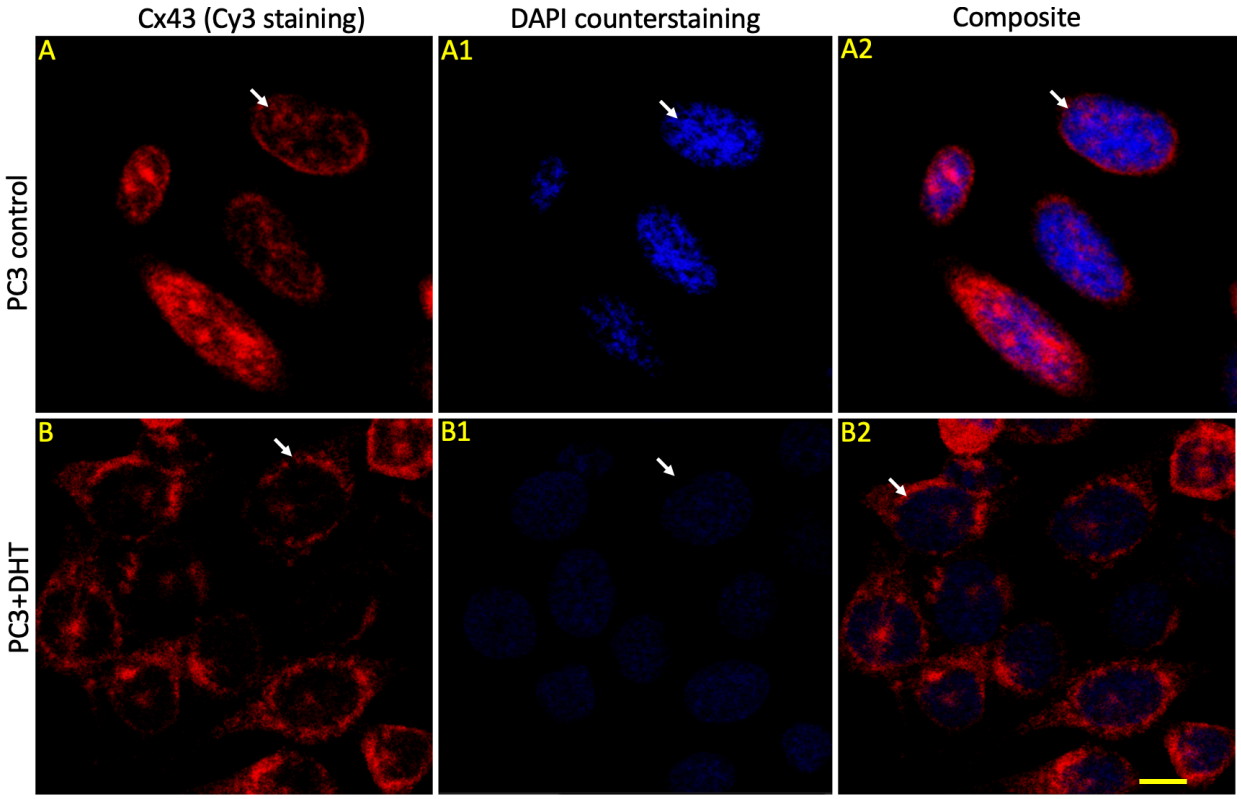

Figure 5.18. Redistribution of Cx43 in PC3 cells treated with AR signalling ligand (DHT). PC3 cells were treated with DHT (15 nM) followed by staining with anti-Cx43 antibody. Same procedure was followed as described for Fig. 5.18. A-A2: PC3 cell (control); B-B2: PC3 cells treated with DHT. Arrow pointing the location of Cx43. Scale bar, 10 µm.

5.4.4. Expression analysis of AR and Wnt signalling proteins in PCa cells

Table 5.2 provides a list of putative proteins (targets) of AR and Wnt signalling pathways. As both these signalling pathways are involved in gene transcription, protein synthesis and stabilization, I wanted to investigate if there was a short-term impact of signal activation by AR and Wnt signalling on the amount of protein (either through increase in gene transcription) or via increase in protein availability or stabilization (Acebron et al., 2014). The role of Wnt signalling in gene transcription is well established (Nusse and Clevers, 2017), its role in protein synthesis and stabilization has also been investigated in relation to GSK-3β activity and stability of its components e.g., β-catenin via eukaryotic initiation factor 6 (Ji et al., 2008) and promotion of protein stability in general (Acebron et al., 2014). Similarly, AR is also known as a regulator of protein synthesis and stability (Liu et al., 2019). AR is thought to negatively regulates protein synthesis and low AR abundance increases translation. This suggests a rather complicated picture of interaction of these two key cell regulatory signalling pathways in protein stability.

Untangling these complicated, inter-related mechanisms was not within the scope of my study. However, I wanted to begin to investigate whether there was any alteration in Wnt and AR related proteins when either of the signalling pathways was activated on its key transducers, namely AR and β-catenin, and also on some downstream targets such as AR related proteins TMPRSS2, PSA and Nkx3.1 and β-catenin for Wnt signalling. These experiments were performed using short time scale minutes to hours in cultured cells and therefore do not represent long term changes induced by these signalling pathways or their influence on cell function. I also used, in a limited fashion, qPCR to investigate AR and Wnt related gene expression and the results are presented in the next two sections.

5.4.4.1. Effect of DHT application on the expression of Wnt and AR signalling proteins in LnCAP cells

LnCAP cells were treated with DHT and incubated for 2 or 24 h and whole cell lysate was isolated using the protocol described in Chap-2 (Sec. 2.3.4.2). WB analysis was normalised with β-actin (Fig. 5.19.B) which was used as a protein loading control. As expected, in whole cell lysates, cells treated with DHT showed an increase in AR expression (Fig. 5.19). An average of three independent experiments of cells ±DHT is shown in (Appx. 5.10.1; 5.10.2 and 5.10.3). Other AR signalling proteins including TMPRSS2, PSA, Nkx3.1 also showed an increase in expression. Average of three independent experiment showed that β-catenin, TMPRSS2, PSA and Nkx3.1 expressions were upregulated while activated AR signalling pathway with DHT treatment. DHT treatment also increased β-catenin and GSK-3β which are related to Wnt signalling (Table 5.2). The stained complete PVDF membranes are given in appendix (Appx. 5.10.1).

There was a general increase in the expression of all proteins tested subsequent to DHT treatment (Fig. 5.19.A). The data for protein expression was quantified and normalized to β-actin expression (Fig. 5.19.B). The expression of all proteins tested remained similar after 2 and 24 h treatment with DHT (Fig. 5.19. D-I) with the exception of AR whose expression was greater at 2 h and then declined after 24 h treatment (Fig. 5.19.C). These results indicate that there is an increase in the expression of both AR and Wnt target proteins after DHT treatment. An increase after 2 h may indicate increase in protein availability and stability, as the time required for protein synthesis would be expected to be greater (Aymoz et al., 2016).

A. Western blot images

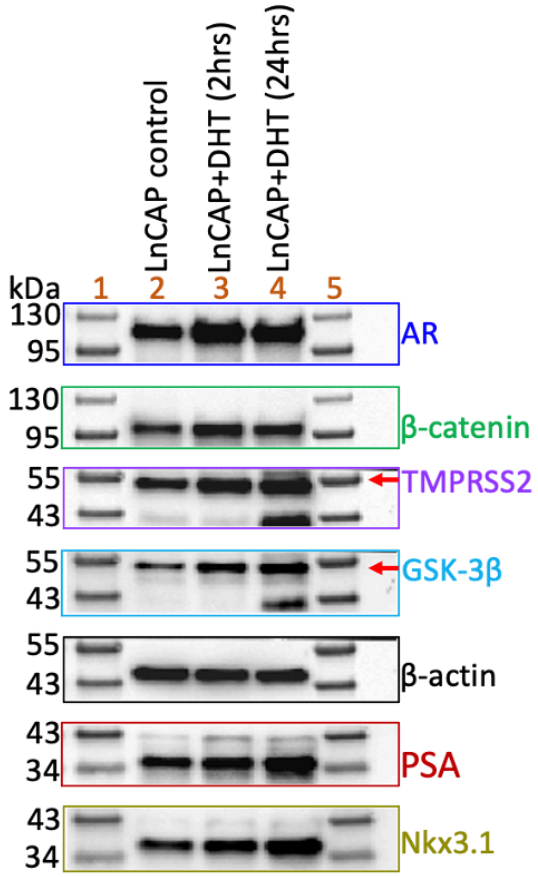

B. β-actin expression

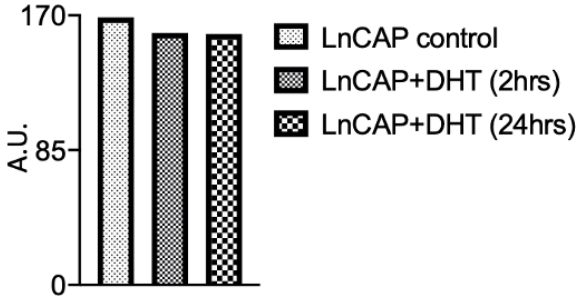

C. AR expression

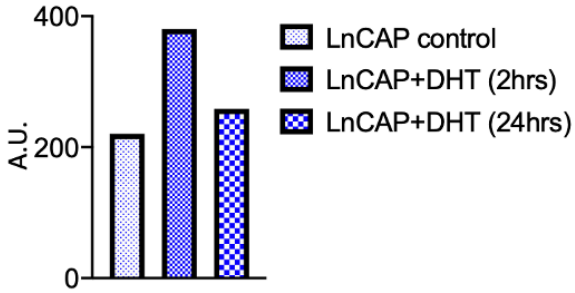

D. β-catenin expression

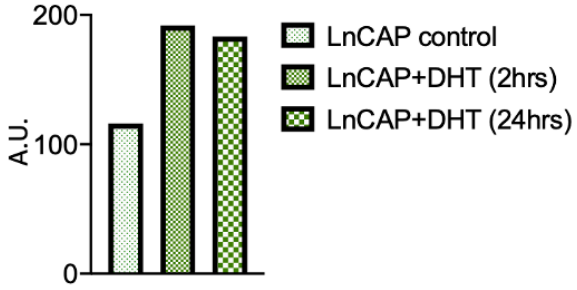

E. Nkx3.1 expression

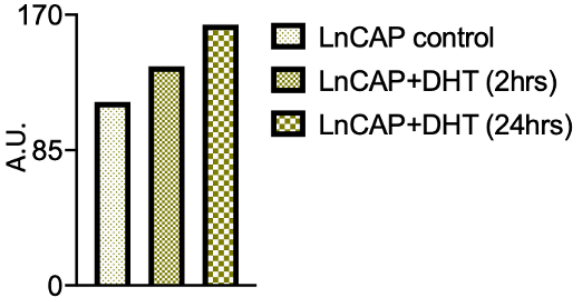

F. TMPRSS2 expression

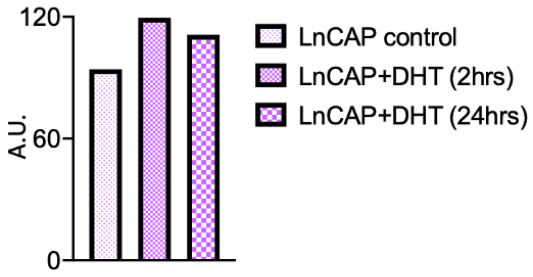

G. GSK-3β expression

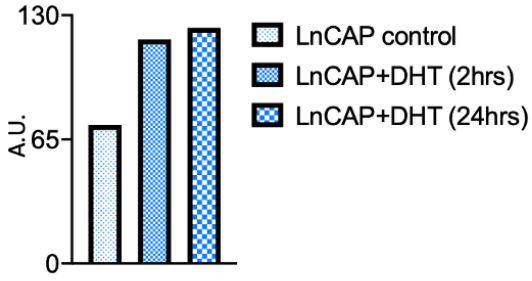

H. PSA expression

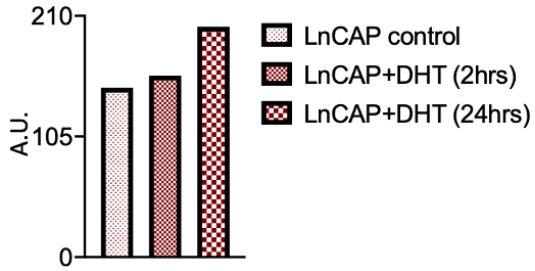

I. Average expression of three independent experiments

1. β- actin expression

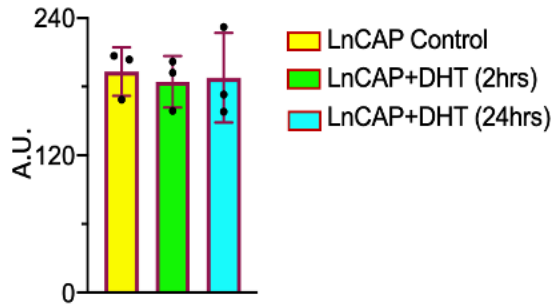

2. AR expression

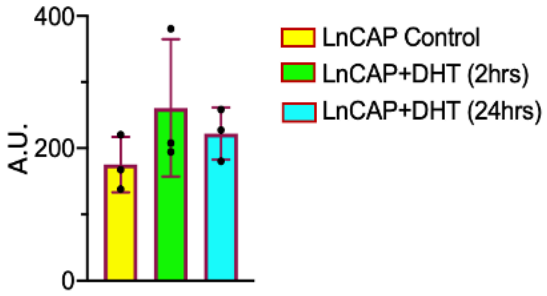

3. β-catenin expression

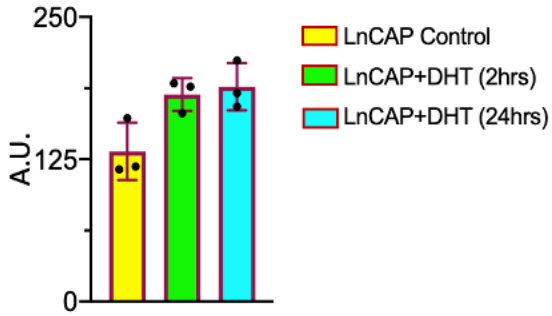

4. Nkx3.1 expression

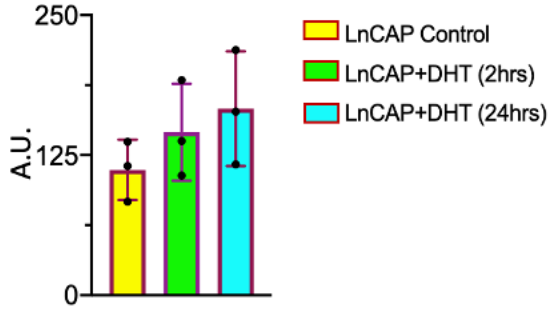

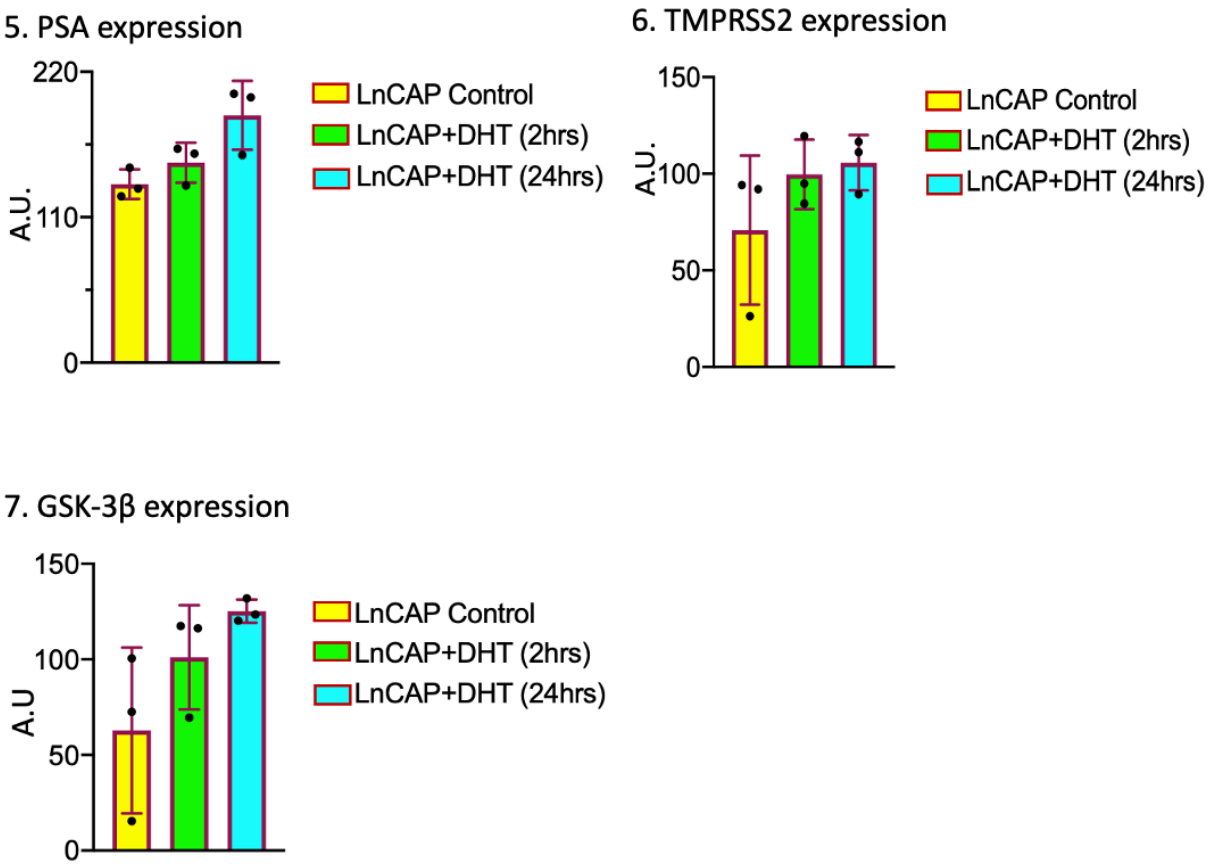

Figure 5.19. A representative WB image for the expression of AR and Wnt target proteins in LnCAP±DHT cells. A. 15 µg protein of whole cell lysate of LnCAP cells (untreated, +DHT (2 h), +DHT (24 h)) was loaded into lane 2, 3 and 4 respectively. 5 µl of colour prestained protein standard (cat: P7719, NEB) was loaded into L-1 and L-5. Following blocking, the PVDF membrane was cut into two strips of 250 to 57 kDa and 57 to 10 kDa and probed with anti-AR antibody (cat: 06-680, Merck Millipore) and anti-β actin antibody (cat: Ab6276, ABCAM) respectively. Following capturing image with GelDoc system (BioRad), the membranes were stripped off with "Restore™ PLUS Western Blot Stripping buffer (Cat: 46430, Thermo Scientific). The membranes were reprobed with anti-β catenin, anti-TMPRSS2, anti-GSK-3β, anti-PSA and anti-Nkx3.1. Each of primary antibody incubation was followed by appropriate secondary antibody incubation and image capturing and stripping off the membrane. B, C, D, E, F, G and H display the expression of β-actin, AR, β-catenin, Nkx3.1, TMPRSS2, GSK-3β and PSA, respectively. The mean (n=3) of their expression indicates the increased expression of AR and Wnt signalling proteins indicated as I.1, I.2, I.3, I.4, I.5, I.6 and I.7 for β actin, AR, β catenin, Nkx3.1, PSA, TMPRSS2 and GSK-3β.

5.4.4.2. Effect of Wnt5A application on the expression of Wnt and AR signalling proteins in LnCAP cells

I also assessed AR and β-catenin protein expression after with Wnt 5A treatment for 2 and 24 h in LnCAP cells. After Wnt5A incubation whole cell lysates (not fractionated cell lysates as used earlier) were isolated and probed for expression of AR and β-catenin antibodies. There was an increase in the AR protein in cell lysates, however, there was no change in the expression of β-

catenin (Fig. 5.20). The latter is not an unusual observation and has been reported previously (Wang et al., 2010c). It should be noted that unlike the results presented for β-catenin translocation in different compartments of cells (Sec. 5.4.1.6), these results are from whole cell lysates, meaning, it is stabilization and translocation to nucleus which is a key property of Wnt/β-catenin signalling.

A. Western blot image

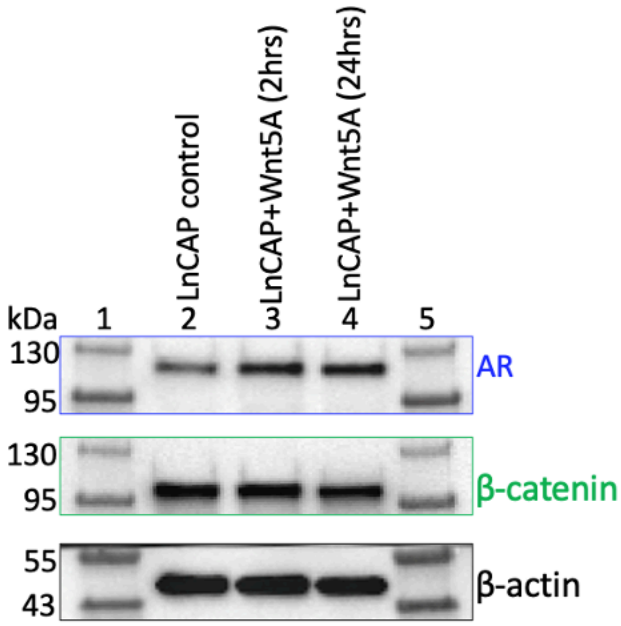

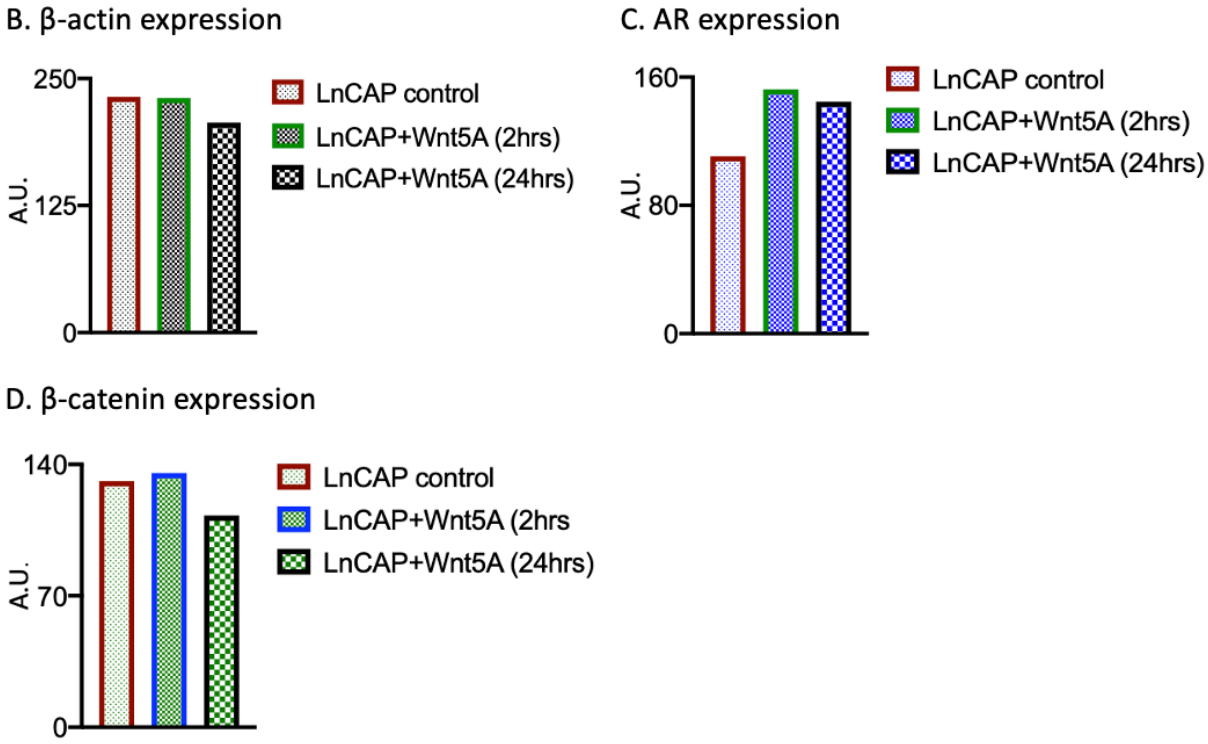

Figure 5.20. A representative WB image for the expression of AR and Wnt target proteins in LnCAP cells. A. 15µg protein of whole cell lysate of LnCAP cells (untreated, +Wnt5A (2 h), +Wnt5A (24 h)) was loaded into lane 2, 3 and 4 respectively. 5 µl of colour prestained protein standard (cat: P7719, NEB) was loaded into lane 1 and 5. Following blocking, the PVDF membrane was cut into two strips of 250 to 57 kDa and 57 to 10 kDa and probed with anti-AR antibody and anti-β actin antibody respectively. Following capturing image with GelDoc system (BioRad), the membranes were stripped off with Restore™ PLUS Western Blot Stripping buffer (Cat: 46430, Thermo Scientific). The membranes were reprobed with anti-β catenin. Each of the primary antibody incubation was followed by appropriate secondary antibody incubation and image capturing and stripping off the membrane. B, C and D show the expression of β-actin, AR and β-catenin respectively.

5.4.4.3. Effect of Wnt9B on the expression of Wnt related proteins in PC3 cells

The previous two sections utilized LnCAP cells. I further investigated the expression of Wnt related proteins in PC3 cells treated with Wnt 9B. Wnt signalling has been well characterized in PC3 cells at a functional level in our laboratory (e.g., (Thrasivoulou et al., 2013; Hou et al., 2019 and Ashmore et al., 2019) where experiments are conducted in short (ms to min) time scale. Here I chose also a shorter time point, because protein stability changes can manifest in much shorter time than protein synthesis. Expression analysis showed that β-catenin expression was increased in PC3 cells with increasing of incubation time, 30 min to 2 h, with Wnt9B. Similar result was found for TMPRSS2 whose expression also increased with the increasing of incubation time. Expression of Cx43 and c-MYC (Appx. Figs. 5.30. and 5.31) did not change after exposure to

Wnt9B. The stained PVDF membranes (raw data) are shown in appendix (Appx. 5.11.1). These results indicate a general phenomenon of an increase in protein expression either via increase in protein availability or protein stability; long term effects on gene transcription and subsequent translation are certainly possible. These are preliminary data upon which future studies can be designed to probe, for example, the mechanisms (e.g., via eukaryotic initiation factors) by which AR and Wnt signalling may increase protein expression, particularly in cancer.

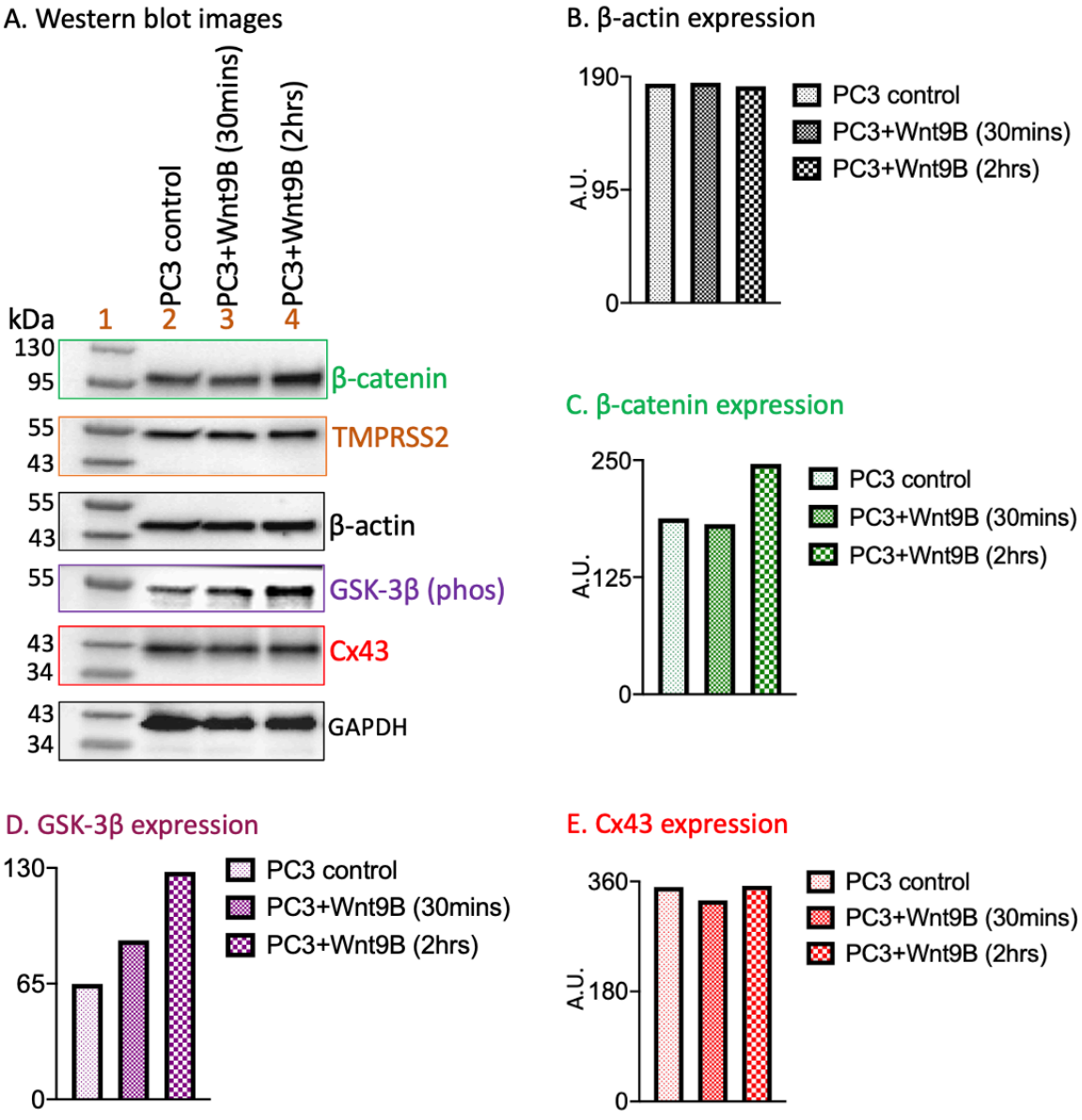

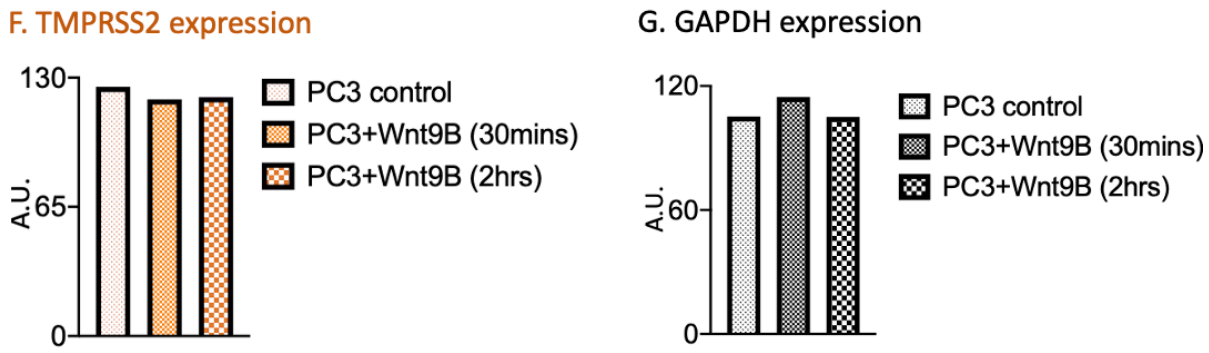

H. Average expression of three independent experiments

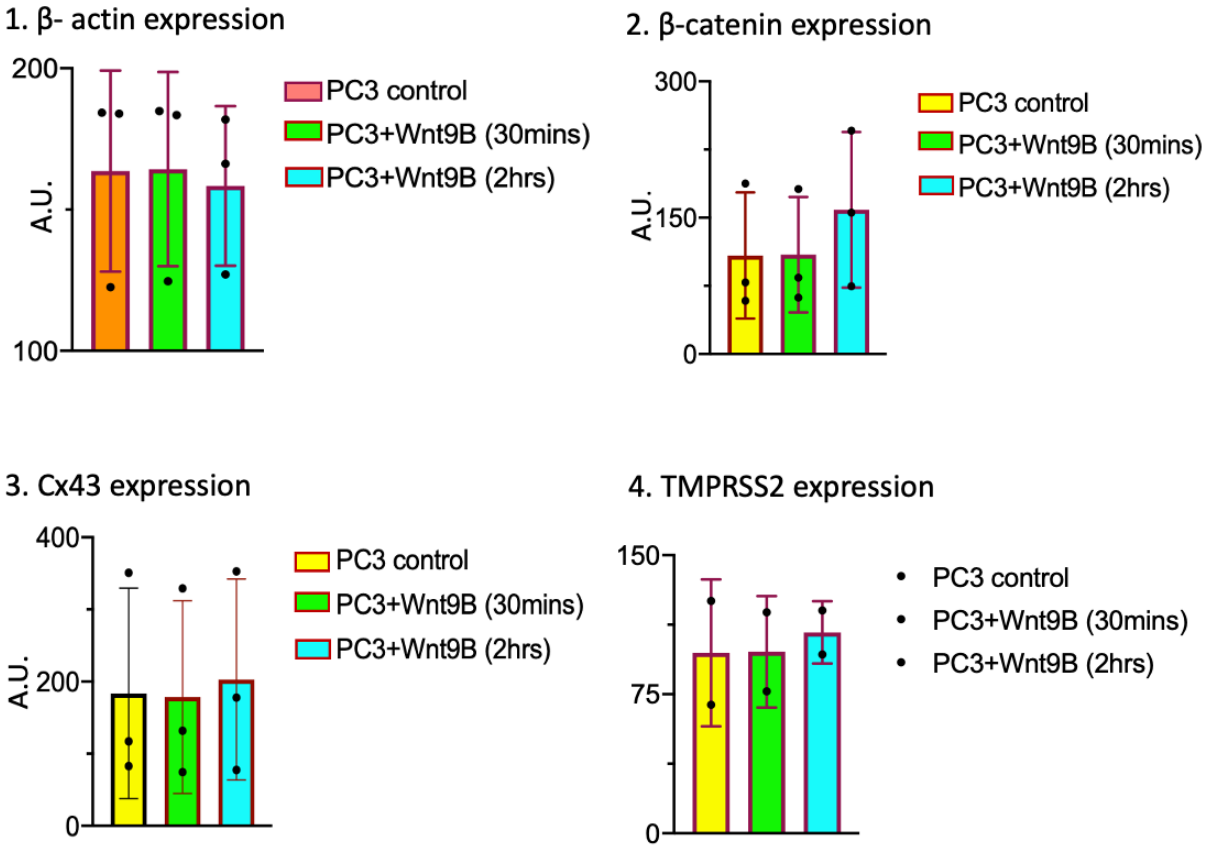

Figure 5.21. A representative WB image for the expression of AR and Wnt target proteins in PC3 cells (untreated, +Wnt9B (30 min), +Wnt9B (2 h)). A. 15 µg protein of whole cell lysate of PC3 cells (untreated, +Wnt9B (30 min), +Wnt9B (2 h)) was loaded into lane 2, 3 and 4 respectively. 5 µl of colour prestained protein standard (cat: P7719, NEB) was loaded into L 1 and 5. Following blocking, the PVDF membrane was cut into two strips of 250 to 57 kDa and 57 to 10 kDa and probed with anti- β-catenin and anti-β actin antibodies respectively. Following capturing image with GelDoc system (BioRad), the membranes were stripped off with Restore™ PLUS Western Blot Stripping buffer (Cat: 46430, Thermo Scientific). The membranes were reprobed with anti-Cx43 and anti-TMPRSS2 antibodies. Each of the primary antibody incubation was followed by appropriate secondary antibody incubation and image capturing

and stripping off the membrane. B, C, D, E, F and G show the expression of β-actin, β-catenin, GSK-3β, Cx43, TMPRSS2 and GAPDH respectively. F shows the average expression of three independent experiments (n=3) of F.1, F.2, F.3 and F.4 for β-actin, β-catenin Cx43 and TMPRSS2 respectively.

5.4.5. Expression analysis of Wnt and AR target proteins using qPCR

I also investigated gene transcription related changes due to the activation of Wnt and AR signalling in LnCAP and PC3 cells. The PC3 and LnCAP cells were treated with Wnt signalling ligand Wnt9B (5nM) and AR signalling ligand DHT (15 nM) and incubated for 2 h for PC3 cells and overnight for LnCAP cells. In WB experiment, I observed treatment with Wnt5A (supposed non-canonical) (Sec. 5.4) and Wnt9B (supposed canonical ligand – please note that in mammalian cells both canonical and non-canonical Wnt ligands activate both intracellular calcium and β-catenin stabilization (Thrasivoulou et al., 2013 and Hou et al., 2019) and had a similar effect on Wnt target proteins. Two Wnt target genes namely, β-catenin and Gap Junction Alpha-1 (*GJA1*) and four AR target genes, AR, *KLK3*, *TMPRSS2* and *Nkx3.1* were selected to investigate their expression while relevant signalling pathway is activated.

The expression of the six genes is shown in Fig. 5.22. DHT treatment to LnCAP cells enhanced transcription of AR target genes whereas Wnt9B activated Wnt signalling for target gene transcription. AR RNA and proteins are regulated by androgens. DHT treatment could upregulate (Kerr et al., 1995) and down regulate AR mRNA (Trapman et al., 1990).

Statistical analysis was conducted using unpaired t-test showed there was no expression of AR in PC3 cells, as would be expected (Fig. 5.8, above, shows no protein expression) (Ching et al., 1993). The results represent as mean±SEM (n=3). There was a nominal increase in Wnt 9B treated LnCAP cells (0.84 ± 0.51-fold; ns), but DHT treated LnCAP cells, AR expression (Fig. 5.22) decreased significantly (-7.68 ± 1.09-fold; **P<0.01).

There was no significant change in the expression of other AR target genes, namely, *KLK3* (Fig. 5.22.B), *TMPRSS2* (Fig. 5.22.C) and *Nkx3.1* (Fig. 5.22.D) in LnCAP cells treated Wnt9B, but significant change was found for *KLK3* (11.33 ± 1.2-fold; **P<0.01, green), *TMPRSS2* (9.34 ± 1.72-old; **P<0.01, green) and *Nkx3.1* (7.03 ± 1.38-fold; **P<0.01, green) in DHT treated LnCAP cells. *CTNNB1* was not changed in Wnt 9B treated PC3 cells (-0.19 ± 0.50-fold, ns) (Fig. 5.22.E). *CTNNB1*

expression was not changed in Wnt9B treated LnCAP cells (0.22 ± 0.26-fold; ns) but significant change occurred in DHT treated LnCAP cells (3.26 ± 0.27-fold; ***P<0.001; green).

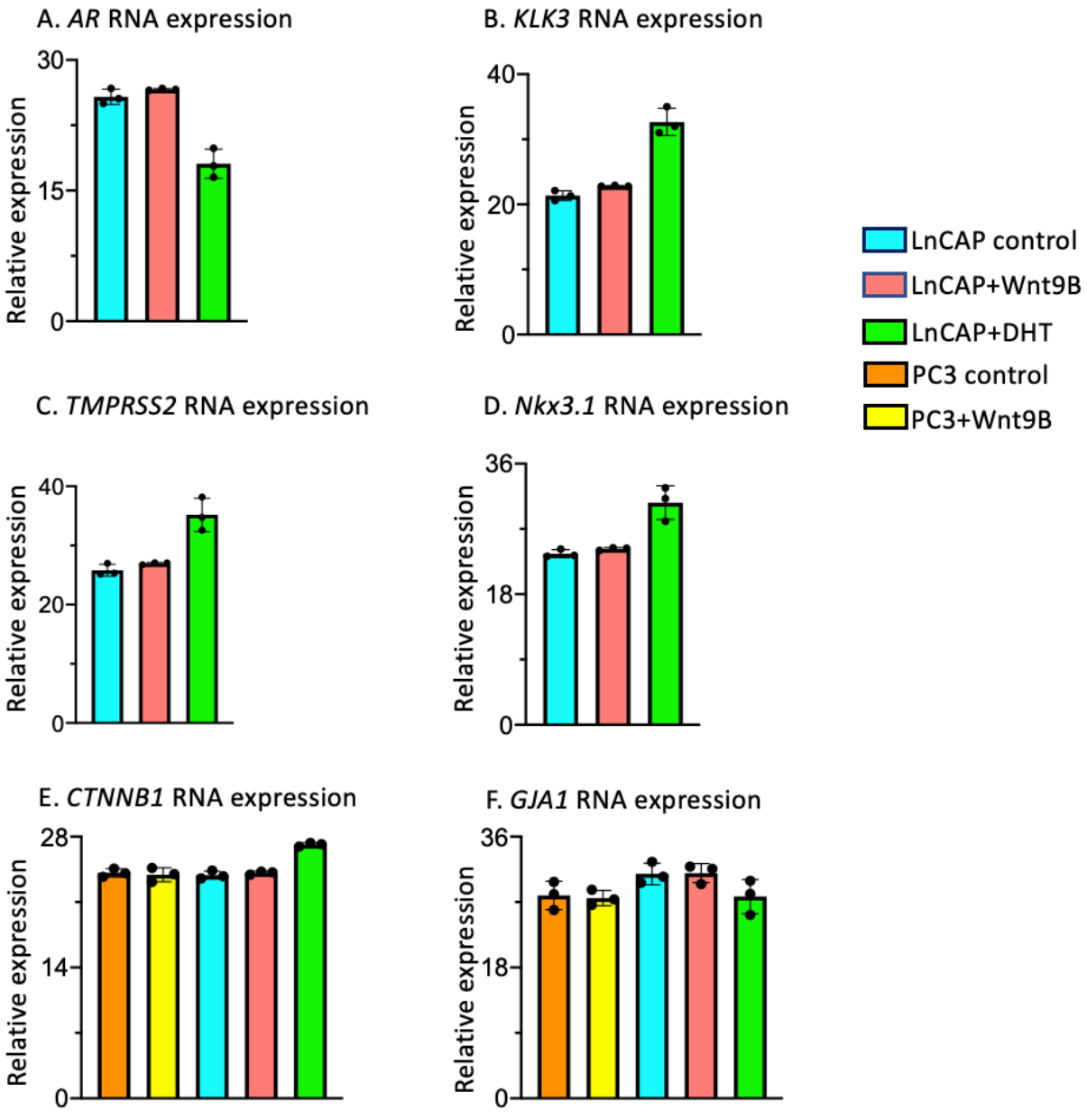

Figure 5.22. RNA expression of Wnt and AR target genes in PC3 and LnCAP cells. A. *AR*; B. *KLK3*; C. *TMPRSS2*; D. *Nkx3.1*; E. *CTNNB1* and F. *GJA1* in untreated LnCAP (cyan), Wnt9B treated LnCAP (pink colour), DHT treated LnCAP (green), untreated PC3 (orange) and Wnt9B treated PC3 (yellow). The expression level of these genes was normalized to *ACTB* gene and compared to untreated cells using the 2 −ΔΔCq method. The results represent the mean±SEM of n=3 experiments with technical replicates.

RNA expression of *GJA1* was not changed in Wnt9B treated PC3 (Fig. 5.22.F) (-0.35 ± 1.27-fold; ns) compared to the expression of untreated PC3. *GJA1* gene expression was visible in LnCAP cells and remain unchanged while treated Wnt9B (.09 ± 1.14-fold) and DHT (-3.13 ± 1.60-fold).

However, expression of GJA1 was not expected in LnCAP cells as its encoded protein was not expressed in LnCAP (Fig. 5.8). DHT treatment decreased AR RNA expression (Fig. 5.22) but increased the expression of AR protein (Fig. 5.19). These results support the suggestions proposed in section 5.4.4 above, suggesting that short term changes are most likely due to increase in protein availability and stability rather than via an increase in gene transcription. A further explanation could be the threshold amount of β-catenin that may be necessary for gene transcription activation. I believe, these results set a path for future experimental design, particularly for gene transcriptional analysis.

5.5. Discussion

Androgen receptor (AR), β-catenin and Cx43 are the crucial components of AR (Kim et al., 2002), Wnt (Logan and Nusse, 2004) and Connexin signalling pathways (Steger et al., 1999), respectively, and are regulated by androgens (e.g. Testosterone, Dihydrotestosterone) and Wnt ligands (canonical: Wnt1, Wnt3A, Wnt8, Wnt9B and Wnt10A and noncanonicl: Wnt4, Wnt5A, Wnt5B, Wnt6, Wnt7A, and Wnt11) (Siar et al., 2012). In this study, I discovered these three signalling pathways interact with each other and regulate the subcellular localization of the AR, β-catenin and Cx43 across the cytosol, membrane and nucleus in PCa cells (e.g., LnCAP and PC3 cells). This discovery has important implications for the mechanisms of intracellular signalling and also for proliferative diseases such as cancer. A better understanding of these interactions may result in better future therapies.

The known mechanisms of Wnt and AR signalling pathways have been described in Chap-I. To reiterate briefly, the canonical (also known as Wnt/β-catenin) and the noncanonical (major noncanonical: Wnt/Ca^{2+}) are the two major signalling pathways with β-catenin, a transcription factor co-activator, and $[Ca^{2+}]_i$ as major intracellular transducers. The other noncanonical signalling pathway included PCP (Planar cell polarity) (Gubb and García-Bellido, 1982) and cGMP/phosphodiesterase pathway (Ahumada et al., 2002). This categorization was initially

tagged as distinct and independent, but the recent evidence scrutinized the mechanisms and discovered their interaction (Van Amerongen, 2012 and Thrasivoulou et al., 2013). β-catenin remains sequestered as part of E-cadherin but the released β-catenin is continuously degraded in the proteasome directed predominantly by a multi-protein destruction complex which is dephosphorylated by the activation of Wnt/β-catenin signalling pathway, resulting in accumulation of β-catenin in cytoplasm. Activation of Wnt pathway releases free intra cellular $[Ca^{2+}]_i$ which depolarizes the nuclear envelope (NE) which in turn facilitates β-catenin to enter the nucleus where it interacts with LEF/Tcf family member to mediate transcriptional induction of Wnt signalling target (Reya and Clevers, 2005).

Translocation of β-catenin into nucleus in PC3 cells has been studied only by using ICC (immunocytochemistry) and immune electron microscopy. β-catenin is not only an interactive compound between the two Wnt signalling pathways (Thrasivoulou et al., 2013), β-catenin is thought to be in cross talk with another receptor important in prostate cancer, namely, androgen receptor (AR) (Schweizer et al., 2008a).

AR is a member of the nuclear receptor group. Canonical nuclear receptor composed of N-terminal domain (NTD), possessing a ligand independent transcription activation function 1 (AF1) and DBD and the carboxyl-terminal site contain LBD and activation function 2 (AF-2) and flexible hinge region that separate DBD and LBD (Robinson-Rechavi et al., 2003) (Chap-I, Sec. 1.11.2). Following diffusion to the cell, DHT binds to AR and dimerized and translocates into nucleus where it binds to AR-binding sequences such as ARE (androgen response element), ARR (androgen regulatory region) or HRE (hormone response element) (McEwan, 2004) along with binding sites for housekeeping (Sp1, CCAAT and NF-1), inducible (NF-kB, ETs and AP-1) and tissue-specific transcription factors (McEwan, 2004) and directs the transcription of androgen-regulated genes by recruiting coactivators (Schaufele et al., 2005).

Connexins are critical in gap junction formation for inter-cellular contact (See. 5.1.3), however, my interest in Connexin family was in the context of its members (e.g., Cx43) joining a signal transduction mechanism to facilitate Wnt signalling, as shown by Hou et al. (Hou et al., 2019).

Although there have been suggestions that Wnt and AR pathways interact to ultimately control gene transcription (Yang et al., 2002), what has not been investigated is the direct intracellular impact of Wnt and AR ligands activation on the reciprocal intracellular transducers β-catenin, Cxns and AR. In this chapter I have aimed to investigate this direct functional activation by analyzing Wnt and AR mediated (i) translocation of their previously known intracellular transducers, (ii) interactions between β-catenin, AR, Cx31 and 43 (iii) mechanism of action on downstream target expression.

5.5.1. Wnt and DHT induced translocation of β-catenin and AR: implications on mechanisms of Wnt and AR signalling

5.5.1.1 An initial target for both Wnt and DHT-TRPM8

In this study, LnCAP cells treated with DHT (AR signalling ligand), Wnt3A (previously thought to belong to canonical Wnt pathway), Wnt9B (canonical and noncanonical), Wnt5A (noncanonical) and fractionated into cytosolic, membrane and nuclear fractions and observed redistribution of AR and β-catenin across the cytosol, membrane and nucleus (Fig.5.4). Basal expression of AR in LnCAP showed highest expression in cytosol and least expression was observed in nucleus (Fig. 5.4.B). Treatment of LnCAP cells with DHT showed increased expression of AR in nucleus compared to untreated AR nuclear expression. Following application of DHT to LnCAP cell media, DHT entered the cytoplasm by diffusion and bound to AR by replacing HS (heat shock protein) and subsequently translocated into nucleus following normal cellular mechanism and directed transcription of target genes; N-terminal AR was also increased in nucleus. (Figs. 5.4.B; 5.4.C; 5.4.F1. and 5.4.F2). The translocation of AR receptor occurs not only through activation of AR signalling with DHT treatment, activation of TRPM8 (transient receptor potential melastatin family member 8) channel might also involve the AR translocation process (Grolez et al., 2019 and Asuthkar et al., 2015). Incidentally, TRPM8 was recently proposed to be a target for Wnt ligands in their control of cell membrane potential (Ashmore et al., 2019).

TRPM8 is the main receptor for a broad range of cold temperature in the peripheral nervous system and is thought to be associated with PCa development (Zhang and Barritt, 2006). Compound such as menthol, icilin, eucalyptol, geraniol and linalool are agonists for TRPM8

(McKemy, 2007). TRPM8 expression is known to be regulated by androgens. Once activated AR binds to the ARE (androgen response element) located upstream of the TRPM8 promoter gene (Grolez et al., 2019). AR might affect the TRPM8 in a non-genomic manner, Gkika and colleagues showed AR and TRPM8 are translocated into nucleus. I observed that lower concentrations of DHT did not translocate AR or β-catenin into nucleus in LnCAP cells (Gkika et al., 2020). But with increasing of DHT concentration (15 nM) enhanced translocation of AR, β-catenin and Cx31 into nucleus in LnCAP cells was observed (Fig. 5.4.F1-5.4.F.4; Fig. 5.5.F.1-5.5.F.4; Fig. 5.6.F.1-5.6.F.4 and Fig. 5.7.F1-5.7.F.4).

Although I did not directly measure TRPM8 (its role in Wnt signalling was only identified late in my PhD studies), my results concur with Gkika et al's observations and may provide a mechanism for these observations (Gkika et al., 2020). The possible impact of my results on those of previous and recent observations regarding Wnt and AR signalling, particularly the role of cell membrane receptors and a key role for intracellular $[Ca^{2+}]_i$ are discussed below.

5.5.1.2. Translocation of large proteins like β-catenin and AR into the nucleus – problems and explanation

β-catenin is, a 92 kDa, negatively charged protein and enters into the nucleus through the nuclear envelope (NE). This is an important issue, as the nucleus, composed of a double layer of membrane, called the nuclear envelope, imposes a limit to passive diffusion of molecules across the nuclear pore complex (NPC)-suggested to be <10 kDa (Mazzanti et al., 2001). Also, β-catenin protein does not contain a nuclear localization signal (NLS) motif (see below) or Ran-GTPase activity, both necessary for proteins to traverse the NE. (Thrasivoulou et al., 2013) also stated that "The NE is also an ion-selective membrane with a dynamic trans-NE electrical potential that is responsive to changes in Ca^{2+} and K^+ concentrations". Furthermore, (Mazzanti et al., 2001) proposed that intranuclear space acts as a negatively charged sink, because of the presence with DNA molecules with PO_4- groups. These physico-chemical features would make β-catenin entry into the nucleus, after being desequestered from the destruction complex in response to Wnt signal activation at the cell membrane, very difficult. (Thrasivoulou et al., 2013) proposed that release of intracellular $[Ca^{2+}]_i$ in response to both canonical and non-canonical ligands facilitate entry of a 92 kDa protein into the nucleus including by depolarizing the NE. My results suggest a

further mechanism for β-catenin entry into the nucleus, at least in cells where AR signalling is active.

AR, like β-catenin is a large 110 kDa protein, there should be an active transporting factor for AR through nuclear pore complex (NPC) to enter and leave the nucleus. AR resides in the cytoplasm in the absence of ligand (e.g., DHT) and translocate into nucleus in the presence of ligand (Roy et al., 2001). Similarly, AR ligand is removed while leaving nucleus for cytoplasm (Tyagi et al., 2000). AR, unlike β-catenin, has both a NLS and a Nuclear Export Signal (NES) and that their operations are either directly or indirectly governed by androgens. AR contains a defined bipartite NLS, composed of two cluster of basic amino (underlined) acids separated by 10 amino acid residues RKCYEAGMTLGARKLKK in the DBD and hinge region at amino acids 617-633 (Zhou et al., 1994). Importin-α interacts with the AR hinge region that determines AR nuclear localization. The strong association between the AR NLS and importin-α which provide binding site for NLS of AR and importin-β accounts for the subsequent interactions with the NPC that leads to translocate into nucleus (Görlich, 1998). The translocation of the trimeric NLS/importin α/β complex into nucleus through NPC requires energy which is obtained from GTP hydrolysis by RAN (Melchior et al., 1993).

My data shows that there is a physical interaction between AR and β-catenin (Sec. 5.4.2) and suggests that β-catenin may utilize binding with other proteins to lend itself with appropriate protein machinery to enter the nucleus. Indeed, a similar role was proposed for Cx43 by Hou et. al. (Hou et al., 2019). In this way, in addition to putative gene transcriptional impact, β-catenin and AR interaction may provide a functional role for Wnt signalling due to their physical interaction.

Conversely, Wnt signal activation may also have a useful functional role for AR signalling, particularly its translocation into the nucleus. I showed that addition of Wnt ligands to LnCAP cells induces AR translocation into nucleus. This was done by treating LnCAP cells with Wnt3A (Fig. 5.5.A), Wnt5A (Fig. 5.6.A), Wnt9B (Fig. 5.7.A); all these ligands have previously been shown to activate (i) free intracellular Ca^{2+} and (ii) β-catenin translocation into the nucleus. Results shown in Figs 5.5. and 5.6. clearly demonstrate that Wnt signal activation by Wnt3A, Wnt5A and Wnt9B induces translocation of AR into the nucleus. This was confirmed by using at least two

different antibodies (AR and AR N-terminal). If Thrasivolou et al's (2013) proposal that Wnt induced $[Ca^{2+}]_i$ facilitates β-catenin translocation into the nucleus, it would follow that $[Ca^{2+}]_i$ may be acting as a general facilitator of large protein entry into the nucleus. There is a evidence that translocation of AR in nucleus in Wnt ligand treated LnCAP cells may deploy a similar mechanism as β-catenin entry into the nucleus with the help of free intracellular $[Ca^{2+}]_i$. Application of DHT to LnCAP cells induce TRPM8 to bind to AR receptor and release $[Ca^{2+}]_i$ in cytosol, an identical feature of Wnt signalling in various cell lines as shown previously (Ashmore et al., 2019 and Thrasivoulou et al., 2013). Ashmore et al. also suggested that Wnt can have direct interaction with TRP membrane channels proteins putatively with TRPM4 and/or TRPM8 which is a signal for free intracellular $[Ca^{2+}]_i$ release activation, thus making it a potential target for therapy in diseases where Wnt (and AR) signalling are active (Zholos, 2010 and Ashmore et al., 2019). Based on the evidence above, I propose that TRPM8 may be a common target for Wnt ligands (e.g., Wnt3A, Wnt9B and Wnt5A) and AR ligands such as DHT. This could, therefore, be a critical step in the initiation of both Wnt and AR signalling.

5.5.1.3. Other mechanisms of entry of large proteins into the nucleus

I have touched upon the hypothetical impediments to β-catenin translocation into nucleus, due to its size and the overall negative charge (Thrasivoulou et al., 2013). I have also proposed putative novel mechanisms between AR and β-catenin that could be co-operative (NLS in AR and Wnt induced $[Ca^{2+}]_i$ being two). This proposal is supported by previous suggestions that β-catenin has to enter the nucleus by binding to NLS-containing LEF/TCF transcription factors in the cytoplasm (Huber et al., 1996). Another proposal was published as an alternative concept in which β-catenin is able to enter the nucleus independently of LEF/TCF interaction (Fagotto et al., 1998). This concept was developed based on research of nuclear localization of recombinant β-catenin in digitonin-permeabilized cells where β-catenin enter the nucleus on its own, without the need for exogenous extract (Fagotto et al., 1998). The conclusion of this study was that β-catenin translocation was independent of importin/karyopherins as well as any LEF/TCF protein. The absence of β-catenin import activity in the presence of normal cytosol implies that its import may be control by an upstream function in the Wnt signalling pathway (Fagotto et al., 1998). Nevertheless, NE (Nuclear Envelope) macromolecular mobility consists of diverse array of

biochemical and electro chemical process which are independent and interdependent (Mazzanti et al., 2001). This may include a nuclear localization signal binding of the proteins for the nucleus with other cytosolic proteins that facilitate the entry necessitating energy dependent process or phosphorylation of specific proteins (Moroianu et al., 1995).

Though β-catenin lacks NLS, but an interaction may occur to recognise β-catenin between arm domain of β-catenin and NPC component proteins. Once β-catenin is in a close proximity to NE due to activation of Wnt signalling, it encounters a considerable obstacle to enter the nucleoplasm as β-catenin is of 92 kDa and negatively charged. As mentioned above, $[Ca^{2+}]_i$ ions also play important role in the trans-NE transport of macromolecules (Mazzanti et al., 2001). Reduction of intracellular $[Ca^{2+}]_i$ can obstruct macromolecular transport of particularly intermediate size (70k Da) but also small (<10 kDa) macromolecules across NE (Stehno-Bittel et al., 1995). The main purpose of Wnt/β-catenin signalling pathway is to transverse β-catenin (92 kDa, transcription factor) from cytosol to nucleus through NE. Activation of Wnt/β-catenin signal with Wnt3A and Wnt9B release β-catenin in cytosol. Wnt5A activated Wnt/Ca^{2+} signalling pathway increase intracellular $[Ca^{2+}]_i$ which depolarises the NE. This facilitates the β-catenin to transverse the NE to enter nucleus where it interacts with LEF/TCF for transcription of target genes (Thrasivoulou et al., 2013).

5.5.2. Possible explanation of increased expression of AR in DHT treated LnCAP cell

There was an increased expression observed in cytosol and membrane in DHT treated LnCAP cell compared to untreated LnCAP cells. It could be due to excessive transcription of AR which results in higher protein expression in cytosol and membrane. DHT treatment can regulate androgen-regulated gene expression which involves a coordinated interactions of the receptor protein and other transcription factors. The AR gene could be autoregulated by androgens and thus regulate AR gene expression in cytosol. An interesting point to note is that the AR do not contain TATA box, androgen response element (ARE) or Androgen regulatory region) (ARR) over 2kb downstream of the start codon site (Grad et al., 1999). TATA box, ARE and ARR are the androgen binding sites on target genes. This would indicate that increased AR expression in cytoplasm could be associated secondary messenger which relates a potential cAMP response element located 5' promoter region of the AR genes (Lindzey et al., 1994). Thus, AR gene expression in

LnCAP involve AR interactions with cAMP rather than more proximal upstream AREs (Stubbs et al., 1996).

5.5.3. Translocation of AR and Wnt signalling target proteins into nucleus: possible importance in gene transcription and cell function particularly in cancer

PC3 cells do not express AR gene and although AR protein is not expressed in PC3, does not indicate absence of AR gene. To understand AR signalling and its impact on Wnt signalling pathway, PC3 cells were transfected with AR inserted plasmid and empty plasmid (Fig. 5.11). Once AR expression in PC3 (designated as $PC3^{(AR+)}$) was stable and the $PC3^{(AR+)}$ cell was treated with DHT (Fig. 5.12). The untransfected PC3 cells did not show any AR expression. The least expression of AR was found in nucleus in untreated $PC3^{(AR+)}$ cells; AR expression was found decreased in cytosol and membrane but increased abruptly in nucleus in DHT treated $PC3^{(AR+)}$ cells compared to cytosol, membrane and nucleus in control $PC3^{(AR+)}$ cells. This indicates translocation of AR into nucleus from membrane and probably from cytosol as well.

It should however be noted that there has been some controversy regarding the expression of AR in PC3 cells. Alimirah et al. showed presence of AR mRNA and protein in PC3 cells, albeit at a much lower level than LnCAP cells and also reported nuclear translocation of AR protein in response to DHT (Alimirah et al., 2006). The data presented here, demonstrating the close interaction and reciprocal activation of both Wnt and AR signalling pathways by the ligands for either, offers another explanation for the translocation of AR in PC3 cells: in the basal state Wnt signalling activation might be responsible for the translocation of AR into nucleus in PC3 cells used by (Alimirah et al., 2006).

In my experiments, the results from Wnt treatment of $PC3^{(AR+)}$ showed similar levels of AR translocation into the nucleus as it's known activator, namely, DHT. This close interaction has important implications both for Wnt and AR induced gene expression analysis and also for functional regulation, as I have also shown that there is a physical interaction between AR and β-catenin. For example, it is known that β-catenin mediated transcription could be cell context dependent (Masuda and Ishitani, 2017). This means that some genes are activated by β-catenin transcriptional activity during embryogenesis and may not be transcribed during organogenesis

or during normal compared to disease. For example, β-catenin transcriptional activity transcribes the expression of cell cycle-related genes and consequent cell proliferation in neural progenitor cells, whereas it activates the expression of neural differentiation-related genes in differentiating neurons (Masuda and Ishitani, 2017). My results showing close cross-talk and close interaction between Wnt and AR pathways suggests that this could be one mechanism of differential, context dependent gene transcription. This proposition also opens up the possibility of AR and β-catenin interacting with other transcription factors and further differences in gene transcriptional activity by activation of one signalling pathway.

Ideally, I would have liked to have conducted whole genome sequencing and expression analysis to identify the common transcriptional targets of both Wnt and AR signalling, however, this plan was derailed due to intervention of Covid19. This would have allowed to dissect the complex transcriptional activity, with and without AR or β-catenin transcription, for example in Wnt ligand or DHT treated PC3$^{(AR-)}$ and PC3$^{(AR+)}$ cells and also PC3$^{(\beta\text{-}catenin\text{-})}$ cells (we have previously used a β-catenin knockdown cells to measure its interaction with Cx43). Another interesting path would be to investigate if Connexins, which I have also shown to be closely related to both Wnt and AR signalling, play role in this context dependent transcription.

5.5.4. Inhibition of translocation β-catenin in PC3 cell treated with DHT

In PC3 cells, the majority of β-catenin is located in membrane where it directly links the E-cadherin, which is in turn bound to the actin-based cytoskeleton, forming an adhesion complex (Weis and Nelson, 2006). The unbound cytoplasmic β-catenin is kept at low level by degradation of destruction complex made of GSK-3β, Axin, Casein Kinase1α (CK1α) and APC (Adenomatous polyposis coli protein) (Chen et al., 2013). Wnt signalling pathway controls the degradation and stability of cytoplasmic β-catenin which is responsible for the balance between cytoplasmic and nuclear β-catenin during development (van Leeuwen et al., 1994). Activation of Wnt signalling with Wnt ligands desequesters β-catenin which accumulates in the cytoplasm and subsequently transverse the NE and inter nucleus.

I mentioned above that PC3 do not express AR protein, although there is at least one dissent by (Alimirah et al., 2006) in this regard. It was, however, clear that the PC3 cells used in this project

did not express AR (e.g., Fig. 5.9). When these PC3, AR receptor negative, cells were treated with DHT, an AR ligand, there was observed, decrease in the expression of β-catenin in nucleus (Fig. 5.9). It is to be noted that a minimal amount of β-catenin is found in the nucleus in most cells as they express low level of endogenously secreted Wnt glycoproteins (Blauwkamp et al., 2012). The DHT effect was time dependent as increasing the time of incubation, progressively reduced nuclear β-catenin expression (Fig. 5.9). As there is no AR expression in these PC3 cells, this signal cannot be transduced via the conventional DHT receptor, i.e., AR. This raises the possibility that DHT may be binding to another unknown receptor. This is something that needs to be further investigated. It is important to note that the treatment of PC3 cells with DHT does not release any excess β-catenin in cytoplasm, rather it may enhance proteasomal degradation of cytoplasmic β-catenin. This is unlikely to be via DHT action of other key elements of Wnt/β-catenin signalling such as GSK-3β. This is because Schutz and colleagues have suggested that DHT promotes inhibition of GSK-3β and is therefore more likely to desequester β-catenin from the destruction complex and increase nuclear availability of β-catenin (Schütz et al., 2010)

Following treatment of DHT treated PC3 cells with Wnt9B, it was observed that nuclear β-catenin translocation was reversed (Fig. 5.10), indicating that Wnt signal activation over-rides the non-AR dependent DHT function in AR negative PC3 cells. The mechanism of how DHT may reduce nuclear β-catenin expression requires further studies.

5.5.5. Translocation of β-catenin into nucleus in PC3$^{(AR+)}$ treated with DHT and Wnt9B

An investigation was carried out by transient expression of AR in PC3 to establish AR signalling pathway in PC3 to observe pattern of interaction between AR and Wnt signalling pathway. PC3 cells were transfected with both control plasmid (empty plasmid) and AR inserted plasmid containing GFP reporter gene (Fig. 5.11). The PC3$^{(AR+)}$ was treated with DHT to explore whether DHT affects the Wnt signalling pathways? The WB image (Fig. 5.12) showed slightly lower nuclear expression of β-catenin compared to control, vehicle treated, PC3 cells. These results indicate that transient expression of AR in PC3 cell initially inhibited expression of β-catenin as similar manner as described by others (e.g., (Kim et al., 2005 and Du et al., 2011)). Treatment of PC3$^{(AR+)}$ with DHT increased the translocation of β-catenin in nucleus (Fig. 5.12), as observed in endogenously AR+ LnCAP cells. Conversely, treatment of PC3$^{(AR+)}$ with Wnt9B activated the

Wnt/β-catenin and Wnt/Ca^{2+} which redistributed β-catenin across the cytosol, membrane and nucleus (Fig. 5.13). This showed membrane expression of β-catenin was decreased but nuclear expression was increased compared to PC3 and $PC3^{(AR+)}$. This indicates membrane bound β-catenin may have translocated into the nucleus.

5.5.6. Colocalization of AR and β-catenin into nucleus in LnCAP and PC3(AR+) Cells: implications for castration resistant prostate cancer

A critical role of AR signalling pathway is well studied in CRPC (Chen et al., 2004a). Recent findings also demonstrated that advanced prostate cancer is implicated with the Wnt/β-catenin signalling pathway (Chesire and Isaacs, 2003).

There is a crosstalk between AR and Wnt signalling pathway that Wnt ligands can transactivate the AR (Verras et al., 2004). β-catenin interacts with the AR to elevate its transcriptional activity (Truica et al., 2000 and Yang et al., 2002), a phenomenon whose mechanisms I have attempted to elucidate in this chapter. Previous studies have not examined the interaction of AR and Wnt signalling pathways while both are activated with their corresponding ligands. The result showed AR and β-catenin were translocated in nucleus in LnCAP when treated with ligands of either signalling pathway.

New questions about AR and β-catenin colocalization in the nucleus?

I have examined the mutual advantages that interaction of Wnt and AR pathways may confer on each other's function, above. Exploration of colocalization of AR and β-catenin in LnCAP cells may give insight into interaction of the AR and Wnt signalling pathways. AR contains NLS that directs translocation of AR into nucleus. β-catenin structure lacks NLS, its translocation into nucleus is independent of the importin/karyopherin and Ran pathways (Yang et al., 2002 and Chesire et al., 2002). A previous study showed APC (adenomatous polyposis coli, a tumour suppressor protein) can shuttle β-catenin for nuclear localization (Henderson, 2000). Co-expression of TCF protein stimulate β-catenin to enter nucleus (Huber et al., 1996). These findings indicate that auxiliary proteins are needed to chaperone β-catenin to translocate into nucleus and I have made the argument, based upon my new observations, that AR may perform such a function for β-catenin to facilitate its entry into the nucleus.

This supports the notion that ligand bound AR may act chaperone for β-catenin translocation in nucleus in LnCAP cells. The mechanism appears to be used for β-catenin translocation associated with direct protein-protein interaction, so no secondary signalling might involve. Hou et al. showed that Cx43 may be a chaperone protein for β-catenin. The implication of these observation is that β-catenin may be an opportunistic hijacker of proteins that may facilitate its entry into the nucleus (Hou et al., 2019). As Wnt signalling is critical in so many cellular processes and its dysregulation cause of serious diseases, it makes evolutionary sense to limit its ability to enter the nucleus except under tightly regulated context with strict regulatory control. Additionally, my study (and other studies) demonstrated that ligand bound AR, but not GR (Glucocorticoid receptor), progesterone receptor (PR), oestrogen receptor α (ERα) translocated β-catenin into nucleus (Pawlowski et al., 2002a).

In addition, Co-IP result (Fig. 5.14) showed AR and β-catenin are interacted which is taken place between LBD of AR and armadillo repeat β-catenin. Binding of β-catenin to LBD region, dissociate the heat shock protein (Pawlowski et al., 2002a and Song et al., 2003). Armadillo repeats and $AR_{DBD/LBD}$ sequence is sufficient for ligand-dependent nuclear translocation of AR and transcription activation (Mulholland et al., 2002). AR does not require to be dimerized to bind β-catenin as it is already in a heterodimeric state (Schweizer et al., 2008a) and able to enter the nucleus. AR/β-catenin complex can then directly bind to an AR regulated promoter (Mulholland et al., 2002). However, the inference is that binding of β-catenin to LBD of AR dissociate HSP and its NLS is exposed to importin and translocate into nucleus and bind to promoter of target gene.

5.5.7. Translocation of Cx43 into nucleus in PC3 treated with Wnt ligand

In this chapter, I also investigated a newly discovered partner of β-catenin, namely, Cx43 (Cx31 in LnCAP cells) to elucidate its role in the interaction of Wnt and AR signalling pathways.

Cx43 is a member of Gap Junction intercellular communication (GJIC) which plays a key role in tissue homoeostasis and regulation of cell growth and differentiation (Aasen et al., 2019). Cx43 is most widely studied member among 21 members of connexin family (Aasen et al., 2019) and expressed in different cell types (Willecke et al., 2002). The crucial part of Cx43 is its carboxyl terminal domain (CTD), that plays a significant role in multiple proteomic interactions. Cx43

functions as a tumour suppressor (Li et al., 2012), its dysregulation is involved in multiple types of cancer including PCa. Cx43 is expressed in PC3 and DU145, but not detectable expression in LnCAP cells (Zhang et al., 2015). Cx31, isomer of Cx43 was detected in LnCAP. A study from our laboratory was based on translocation of Cx43 into nucleus in PC3 cells treated with Wnt5A and Wnt9B (Hou et al., 2019). The study demonstrated, in addition of β-catenin, Cx43 is also a Wnt target protein. Cx43 was also included in this study to explore any relationship with AR signalling pathway.

Until the work reported here, there was no previous study conducted on Cx31 in PCa.

The figure 5.8. shows increased expression of Cx43 in nucleus in PC3 cell treated with Wnt9B compared to that of control PC3 cell. The treated PC3 showed expression of Cx43 was found higher in nucleus and membrane as it was expected whereas basal expression of Cx43 in nucleus was expected. As Cx43 possesses a nuclear targeting sequence in its COOH-domain (Zhou and Jiang, 2014) and this is true for both, the whole, or partial (COOH terminus), acetylated or phosphorylated Cx43 protein (Chen et al., 2016 and Gago-Fuentes et al., 2015). There is another reason for Cx43 expression commonly observed in the nucleus, for instance, analysis of immunoprecipitation and mass spectrometric recommends that Cx43 binds to two components of the nuclear translocation system: the GTP-binding nuclear protein Ran (RAN) and importin (KPNB1) (Gago-Fuentes et al., 2015). In addition, using the NLS map, the Cx43 COOH-terminal tail has been demonstrated to carry two conceivably nuclear localization signals identified by the importin complex that ship proteins to the nucleus through the RAN-GTP cycle (Gago-Fuentes et al., 2015). This implies that Cx43 or its COOH terminal tail may influence chromatin organization, nuclear activity, rRNA transcription, and termination (Gago-Fuentes et al., 2015). Cx43 translocates into the nucleus through A-kinase anchoring protein 95 (AKAP95) at the late G1 phase throughout the cell cycle advancement of cell lines of A549 lung cancers. In the nucleus, the Cx43-AKAP95 protein complex concurrently binds DNA and this colocalization indicates the Cx43 governs DNA expression or participates in DNA aggregation and condensation (Chen et al., 1995). Again, the utility of Connexins co-translocating with β-catenin could be their nuclear targeting capability to allow β-catenin entry into the nucleus.

5.5.8. Inhibition of Cx43 translocation into nucleus in PC3 cells treated with DHT

As Cx43 is integral to Wnt signalling in PC3 cells (Hou et al., 2019), I also investigated the interaction between AR and Cx43. DHT treatment to PC3 altered the distribution of Cx43 in PC3 (Fig. 5.9). PC3 was treated with DHT and incubated for 2 h and showed decreased nuclear expression of Cx43 (Appx. 5.6.2). A time dependent experiment was conducted to observe the pattern of distribution of Cx43 expression in the cytosol, membrane and nucleus. The result showed (WB image; Fig. 5.9) Cx43 expression in cytosol was gradually reduced with increasing of time but a concurrent increase in its membrane expression was observed. Expression was also decreased in nucleus with increasing time. This indicates DHT treatment inhibited translocation of Cx43. There is a reciprocal relationship between DHT and nuclear translocation of Cx43. This result is supported by (Chen et al., 2015a), who reported that testosterone addition decreased the Cx43 expression.

DHT treatment displayed expression of Cx43 in cytoplasm was decreased compared to untreated PC3 cells, which might affect the translocation of Cx43 in nucleus (Fig. 5.9). However, it also indicated that Cx43 appeared to be degraded in cytoplasm due to addition of DHT in PC3 cell. The mechanism of degradation of Cx43 could be similar as Cx32 (Kumar and Gilula, 1996), another member of the Connexin family of proteins. As previously shown Cx32 and Cx43 were degraded by the proteasomal and lysosomal pathways in several cell culture model systems (Musil et al., 2000 and VanSlyke and Musil, 2005). This result is, indirectly, supported by other study in which activation of AR pathway repress the Cx43, and inhibition of AR pathway increased Cx43 expression (Chen et al., 2015a).

5.5.9. Suppression of DHT function in PC3 cells with Wnt9B

PC3 cells do not have AR signalling pathway. DHT treatment to PC3 inhibit translocation of Wnt signalling target proteins (Fig. 5.9). But the activity of DHT in PC3 cells might be neutralized or suppressed with Wnt signalling activation. Induction of Wnt signalling suppress the activity of DHT in PC3 cells or became dominant over DHT activity. Wnt9B was added to PC3+DHT cells, result showed expression of Cx43 was increased in nucleus (Fig. 5.10). Treatment of DHT treated

PC3 cells with Wnt9B might inhibit Cx43 degradation and subsequently increase Cx43 in cytosol and translocated into nucleus.

5.5.10. Expression analysis of AR and Wnt target proteins

AR and Wnt signalling pathways function separately in different individual cell under normal conditions. But their interaction initiates PCa initiation and progression. A series of findings have documented the physical, functional and genetic interaction between AR and Wnt signalling targets (Li et al., 2009). I believe, this study further enhances our understanding and molecular mechanisms of this interaction which can be critical association in the progression of prostate cancer. It is very likely that the manifestation of the effects of this interaction between AR and Wnt signalling is through activation of gene transcription and protein synthesis and stabilization (discussed above section 5.5.3).

In this study, AR and Wnt signalling protein such as AR, Nkx3.1, TMPRSS2, PSA, β-catenin, Cx43 and Cx31, GSK-3β were analysed for their expression in LnCAP and PC3 cells treated with AR (e.g., DHT) and Wnt ligand (e.g., Wnt9B) (Fig. 5.19).

The oncogenic effect of Connexins and β-catenin has been discussed above. TMPRSS2 is the transmembrane serine protease 2 (TMPRSS2) and an androgen-regulated member of the type two transmembrane protease (TTSP) family (Chen et al., 2010). TMPRSS2 expression was increased by the incubation of LnCAP cells with both Wnt and AR ligands. TMPRSS2 expression is increased in high grade prostate cancer (Lucas et al., 2008).

NKx3.1 encodes a prostate specific homeobox protein which is involved in the development of normal prostate (Bieberich et al., 1996). This protein is believed to be a tumour suppressor (Mogal et al., 2007). Androgen-sensitive LNCaP prostate cancer cells, which retain Nkx3.1 expression, this gene still has a function which might differ from its role in prostate development and carcinogenesis (Possner et al., 2008). Further investigation is required to understand these mechanisms in prostate carcinogenesis.

GSK-3β (Glycogen Synthase kinase-3β) is one of the prominent members of β-catenin destruction complex which plays an important role in degradation of β-catenin to maintain the level of β-catenin in cytosol (Stamos and Weis, 2013). In the absence of Wnt, APC directs β-catenin to the

destruction complex (Salic et al., 2000). Following being phosphorylated by GSK-3β or CK1, the phosphorylated APC recruits unphosphorylated β-catenin to the destruction complex. After being dephosphorylated by protein phosphatase 2A (PP2A), APC hands β-catenin to Axin to undergo phosphorylation and ubiquitination (Kennell and Cadigan, 2009). Following priming of phosphorylation of β-catenin at Ser45 by CK1α, β-catenin is phosphorylated by GSK-3β at Ser33, Ser37 and Thr41 and this present the phosphorylated β-catenin to E3 ligases (Amit et al., 2002). In the presence of Wnt, phosphorylated LRP5/6 produce a binding site for Axin and GSK-3β through the PPPsPxS motifs which disassembles the destruction complex and increase GSK-3β and β-catenin in cytosol (Zeng et al., 2008).

My results from *in situ* investigation of prostate cancer tissue (Chap III and IV) show that both AR and Wnt signalling related proteins are over-expressed in high grade and CRPC. My results from *in vitro* experiments indicate that one mechanism of this increase in multiple targets of both AR and Wnt signalling targets could be due to the amplification effect due to co-operative interaction between Wnt and AR signalling pathways.

5.5.11. Expression of AR and Wnt target RNA

AR and Wnt target protein expression was analysed in LnCAP and PC3 cells treated with AR and Wnt signalling ligands. It is also important to observe the RNA expression of AR and Wnt signalling target whether to see what changes may occur at gene and protein expression. The mechanism of increased expression of AR in LnCAP cell have been described previously (Sec. 5.5.1). For KLK3, Wnt9B treatment did not change the RNA expression in LnCAP cells and DHT treatment increased the KLK3 RNA expression (Fig. 5.22.B). Similar results for RNA expression were found for TMPRSS2 (Fig. 5.22.C) and Nkx3.1 (Fig. 5.22.D) with Wnt9B treatment to LnCAP cells. DHT treatment increased their RNA expression. In PC3 cells, CTNNB1 and GJA1 were not changed in PC3 and LnCAP cells treated with Wnt9B (Fig. 5.22.E) but CTNNB1 RNA expression was increased while LnCAP treated with DHT but GJA1 RNA expression was decreased while treated with DHT (Fig. 5.22.F). Cx43 for GJA1 do not express in LnCAP cells. Its reduced RNA expression was observed in LnCAP cells.

A limited analysis of selected gene transcription targets using qPCR was conducted in this study. LnCAP and PC3 cells were treated with Wnt and AR signalling ligands. RNA expression of *AR*, *KLK3*, *TMPRSS2*, *Nkx3.1*, *CTNNB1* and *GJA1* genes were analysis (Fig. 5.22). AR RNA expression was slightly increased when treated the cells with Wnt9B. But the gene expression changes were more pronounced when treated with DHT. Treatment of LnCAP cells with DHT reduced AR RNA expression. On the other hand, upregulation of AR RNA by androgens has been observed in other cell types including human hepato cellular carcinoma and osteoblastic cell lines (Wiren et al., 1997). The 5' and 3' untranslated region (UTR) plays a key role in maintaining AR RNA level at post transcriptional level. The human AR RNA has relatively long 5'-UTR of about 1100nt (Dang, 2012). Yeap *et al*. (1999) showed DHT/testosterone decreases AR RNA levels but increase the AR protein level in both prostate cancer LnCAP and breast cancer MDA453 cell (Yeap et al., 1999). The AR is autoregulated by androgen, which reduces AR RNA in both rat tissue and LNCaP cells (Quarmby et al., 1990 and Krongrad et al., 1991). However, the AR 5' upstream promoter location does not have a typical TATA box, but contains Sp1-binding sites at -46bp (Takane and McPhaul, 1996); (Ren et al., 2000). The TATA box is binding site for general transcription factor IID (TFIID)/TFIID binding protein and is required for directing accurate transcription initiation sites (Roeder, 1996).

5.6. Summary

I believe the following new key information has been described in the results in this chapter:

1. Results from *in vitro*, functional and mechanistic studies, indicated AR, Wnt and Connexin signalling interact closely in PC3 and LnCAP cells. These results complement the results from *in situ* protein expression analysis in human prostate cancer tissue presented in previous chapters.

2. DHT ligand activates AR signalling as well as Wnt signalling pathway. Ligand dependent activation of AR signalling translocate AR and Wnt target protein β-catenin into nucleus. The translocation of AR into nucleus stimulates transcription of AR signalling target genes and proteins. This was confirmed by the translocation of AR (N-ter) which acts as a transactivation agent. This suggests that increasing testosterone level in blood may increase the expression of AR signalling and Wnt signalling proteins enhance prostate cancer progression. DHT treatment

to PC3 cells, where AR signalling is absent, inhibit the translocation of Wnt signalling proteins e.g., β-catenin and Cx43. It was observed β-catenin and Cx43 was moved towards cell membrane. I propose that DHT treatment to PC3 cells decrease the transcription of β-catenin target genes and increase the cell adhesion and GAP junction communication between two adjacent cells to establish well communication and thus limiting the progression of cancer.

3. Wnt ligands (e.g., Wnt3A, Wnt5A, Wnt9B) can functionally activate AR signalling, reciprocally, in addition to Connexin signalling. Activation of Wnt signalling in AR dependent cells can stimulate transcription of AR target genes by translocating AR in nucleus. It is highly likely that cells in the CRPC tissue could be highly proliferative not only for the presence of AR signalling, Wnt signalling activation could be another major factor.

4. Activation of AR and Wnt signalling translocate both AR and β-catenin into nucleus. My result indicated the translocation of AR and β-catenin occurs together amplifying the carcinogenic potential via AR and β-catenin induced transcription.

5.7. Limitations

A major limitation is the *in vitro* nature of the work and limitations of the interpretation of the data to *in vivo* conditions. A mitigation for this in this project is that I have used human prostate cancer tissue to investigate AR and Wnt related proteins and the overall mechanism seem to be similar between *in situ* and in vitro experiments. It is to be noted that dissecting signalling mechanisms can only be done *in vitro*. Some experiments can be replicated in mouse models, although these have limitations to human condition. This is particularly true for prostate cancer for which very few useful mouse models are available.

A further limitation is the identification of target genes that transcribed when AR and Wnt signalling is activated by ligands of either signalling pathways. An interesting experiment would be to conduct gene expression analysis in cells treated with AR or Wnt ligands and also both together.

CHAPTER VI

Conclusions and future perspectives

6.1. An overall summary of findings

Interactions between AR and Wnt signalling pathways, in PCa tissue in situ and cell line models in vitro, were investigated in this thesis. The expression of AR for AR signalling and β-catenin, FRA-1, PYGO2, TCF-1 and Cx43 proteins for Wnt signalling pathways was investigated in normal prostate tissue (NPT), benign prostatic hyperplasia (BPH), Grade 3+3, Grade 4+4, Grade 4+5/5+4 and castration resistant prostate cancer (CRPC) PCa tissue (Chaps. III and IV). AR expressing (LnCAP), non-expressing (PC3) cells, and additionally, AR transfected PC3 cells (PC3AR+) were used to investigate functional and structural changes (signal activation and protein-protein interaction) of AR, AR (N-ter), β-catenin, Cx43 and Cx31 (surrogate for Cx43 in LnCaP cells) in response to signal activation by DHT,for AR signalling and Wn3A, Wnt5A and Wnt9B, for the Wnt signalling pathway.

Quantitative IHC showed AR expression was decreased in high grade prostate cancer tissue and increased in BPH and CRPC tissue compared to NPT. β-catenin expression was increased in Grade 4+5/5+4 and CRPC but remained unchanged in BPH, compared to NPT. FRA-1 expression was increased in Grade 3+3, Grade 4+4 and Grade 4+5/5+4 compared to NPT (Chap-III, Sec. 3.4.3.3). PYGO2 and TCF-1 expression was increased in Grade 4+5/5+4 compared to NPT (Chap-III, Sec. 3.4.3.4; 3.4.3.5). Cx43 expression was decreased in Grade 4+4 and Grade 4+5/5+4 (Chap-III, Sec 3.4.3.6), CRPC (Chap-IV, Sec. 4.4.3.2) but increased in BPH compared to NPT (Chap-IV, Sec 4.4.3.2). PYGO2 expression was significantly increased in Grade 4+5/5+4 PCa tissue compared to NPT and TCF1 expression was also significantly increased in Grade 4+5/5+4 PCa tissue compared to NPT. I also demonstrated, for the first time, a combinatorial approach of using single molecule RNA measurement (Chap IV) in different types of PCa and protein expression in large sample sets. This combined, automated approach, in conjunction with unbiased quantitative analysis, as employed here, could prove useful for biomarker discovery for diagnosis and prognostication of PCa.

A key mechanistic discovery in this project was the reciprocal functional activation of AR signalling with Wnt ligands and Wnt signalling with AR (Chap-V). The results show that activation

of AR signalling with DHT resulted in the translocation of AR (detected with both full length AR and N-terminal AR antibodies), β-catenin, Cx43 and Cx31 into cell nucleus (Chap-V, Sec. 5.4.1.4). Reciprocally, exposure of LnCAP cells to Wnt3A, Wnt5A and Wnt9B also resulted in the translocation of AR, β-catenin, Cx43 and Cx31 into nucleus (Chap-V, Secs. 5.4.1.5; 5.4.1.6; 5.4.1.7). An obvious implication of these novel observations is that prostate carcinogenesis may be a result of activation and co-operativity between AR and Wnt signalling mechanisms resulting in an eventual amplification of gene expression to initiate proliferative and anti-apoptotic programs. These data support the proposed hypothesis (Chap-IV and V) regarding interaction between AR and Wnt signalling pathways acting as an amplifier of carcinogenesis in the prostate.

DHT treatment of PC3 cells, without AR expression, inhibited nuclear translocation of β-catenin and Cx43, interestingly, these proteins were redirected towards cell membranes (Chap-V, Fig. 5.9). However, in PC3(AR+) cells (PC3 cells transfected with AR as PC3 cells do not express AR), DHT behaved as it does in AR expressing cells, i.e., facilitating the translocation of AR and as discovered here, β catenin into cell nucleus. This indicates that without AR expression androgens may act as a brake on Wnt signal mediated β-catenin and Cx43 translocation into the nucleus and inhibit Wnt/β-catenin induced carcinogenic gene expression programs. Close interaction between AR and Wnt signalling pathways is also confirmed by a physical interaction between AR and β-catenin (Chap-V, Fig 5.14). The gene expression induced by AR and Wnt signalling was demonstrated in a limited manner here: cells treated with AR and Wnt ligands increased the translocation of AR and β-catenin into the nucleus (Chap-V, Fig. 5.4-5.7) and increased the transcription of the AR and Wnt signalling related targets such as TMPRSS2, KLK3, Nkx3.1 (Chap-V, Fig. 5.19). A gene expression analysis should be conducted in the future to confirm the PCR data as it will allow a global view of the gene transcriptional effects of AR and Wnt signalling activation by AR.

Thus, in addition to reciprocal AR and Wnt signal activation by ligands for either signalling pathway, there appears to be further antagonistic interaction between AR ligands and Wnt signalling. This new mechanism of AR and Wnt signalling requires further studies. These new findings indicate that activation of AR signalling alone is not the only factor in the progression of

CRPC, interaction of AR signalling and Wnt signalling may also be a contributing factor for CRPC development.

6.2. AR expression in higher grade and castration resistant prostate cancer (CRPC)

A functional AR, activated by testosterone and dihydrotestosterone, is required for the growth and development of the prostate and for the development, growth and progression of PCa. AR expression is observed in primary prostate cancer and detected throughout in both hormone sensitive and hormone refractory PCa (Sadi et al., 1991 and Chodak et al., 1992). The mechanisms associated in initiation and progression of prostatic carcinogenesis and the development of CRPC are not well known and it is generally considered that AR is thought to play an important role in these changes to the prostatic cell phenotype. Evaluation of AR expression in normal, lower to high grade PCa and CRPC has been a major focus to understand the mechanisms responsible for malignant transformation and CRPC.

In a study with biopsy tissue, the expression intensity of AR was found to be significantly higher in cancer tissue with a low Gleason score than those with higher Gleason scores (Takeda et al., 1996). The intensity of AR staining in prostate cancer significantly reduces as the Gleason grade of the tumour increases. In addition, other studies showed AR expression was inversely proportional to histological grade (Chodak et al., 1992 and Masai et al., 1990). Segawa and colleagues found a decrease in AR expression in poorly-differentiated carcinomas as well as metastatic carcinomas (Segawa et al., 2001) but another study described decreased AR expression in moderately differentiated carcinomas (G2) and an increase in poorly differentiated carcinomas (Qiu et al., 2008). In this thesis I observed that there was a progressive decrease of AR expression in lower to higher grade PCa. Epigenetic silencing of AR expression by methylation may occur and has been observed in 8% of primary prostate cancers (Sasaki et al., 2002). Another possibility for the loss of AR expression in tumour cells is a decrease in AR protein stability that reduces the AR protein level to one difficult to detect immunohistochemically. AR is also degraded by ubiquitin targeting to the proteasome (Lin et al., 2002).). Ubiquitination of AR is promoted by Akt kinase-mediated phosphorylation of the receptor, suggesting that cells with increased Akt activation may have a reduced AR protein level). Ubiquitination of AR is promoted

by Akt kinase-mediated phosphorylation of the receptor, suggesting that cells with increased Akt activation may have a reduced AR protein level (Lin et al., 2002).

PCa progression could activate PI3K/Akt pathway as prostate cancer progresses toward a resistant and metastatic disease. Signalling of this pathway activates numerous survival, growth, metabolic, and metastatic characteristics of aggressive cancer. Biomarkers of this pathway have correlated activation of this pathway to high grade disease and higher risk of disease progression (Toren and Zoubeidi, 2014).

However, this variation in study results may be due to heterogeneous expression of AR in prostate carcinoma, differences in the antibodies used to detect AR receptor in various studies and differences in quantitation of AR immune reactivity. Although a cutting-edge multiplex staining methodology and standard AR immunoreactivity counting system were used, further are recommended with a greater number of normal and PCa samples to demonstrate molecular markers of prostate carcinoma.

The androgen/AR signalling pathway continues to be an important predictor of cell proliferation in CRPC, in spite of decreased amounts of androgens after ADT (Litvinov et al., 2003). AR hypersensitivity, local intracrine production of androgen, promiscuous activation of AR by adrenal androgens, non-androgenic steroids and even anti-antiandrogen, as well as activation of the AR by growth factors and cytokines have all been implicated in the recurrence and upregulation of androgen/AR signalling pathway in CRPC (Debes and Tindall, 2004).

6.3. Wnt signalling in high grade PCa and CRPC tissue

The Wnt signalling pathway has been revealed to be dysregulated in a variety of cancers, with few substantial modifications discovered in PCa (Kypta and Waxman, 2012).

In my study, expression of Wnt signalling proteins, including β-catenin, FRA-1, PYGO2, TCF-1, Cx43 and c-MYC, was investigated to measure their expression in low to high grade PCa and CRPC tissues. The result showed β-catenin, PYGO2 and FRA-1 expression was significantly increased in higher grade PCa only, but FRA-1 showed significant increase in low grade as well as higher grade PCa.

In my study, expression of Wnt signalling proteins, including β-catenin, FRA-1, PYGO2, TCF-1, Cx43 and c-MYC, was investigated to measure their expression in low to high grade PCa and CRPC tissues. The result showed β-catenin, PYGO2 and FRA-1 expression was significantly increased in higher grade PCa only, but FRA-1 showed significant increase in low grade as well as higher grade PCa.

A hallmark of canonical Wnt signalling is the stabilization and nuclear translocation of β-catenin which acts as a transcription factor co-activator of target genes. The function of β-catenin in human prostate cancer is unclear (Kypta and Waxman, 2012), but unlike colon cancer it is unlikely to be due to gene structure changes in CCTNNB1 (e.g. shown in only 5% or prostate cancers (Murillo-Garzón and Kypta, 2017)). However, it is most likely to play a role at the protein and functional levels through release of intracellular calcium (Thrasivoulou et al., 2013) or through ß-catenin-mediated gene transcriptional programs, consistent with previous observations of β-catenin stabilization and translocation as prostate cancer progresses (Chen et al., 2004b). Mouse models have demonstrated that activation of β-catenin, through generation of a non-degradable form of this protein, leads to prostate neoplasia and squamous trans-differentiation. Yu and his colleagues demonstrated β-catenin contributed to prostate cancer progression and increased in high grade prostate cancer (Yu et al., 2009).

6.4. AR and Wnt signalling in high grade PCa and CRPC

AR signal activation was significantly reduced but Wnt signalling activation was significantly increased in high grade PCa (Chap-III). This indicates AR signalling act as a brake of Wnt signalling activation. As the cancer progresses, cells started to turn from a moderately to a poorly differentiated state, that possibly explains why reduction of AR expression occurs. In CRPC Wnt signalling, β-catenin acts as a co-factor with AR, suggesting it has a role in CRPC. Nuclear localization of β-catenin may result in increased complexation between AR and β-catenin in prostate cancer cells, deleteriously altering target gene activation (Mulholland et al., 2003). In my study, the result showed a significant increase of Wnt and AR signalling activation in CRPC tissue.

TCF-LEF family members are the key transcription factors for Wnt/β-catenin-dependent transcription, but other transcription factors, such as FRA-1 and PYGO2 also interact with β-catenin in specific cell types and tissues. I have shown that AR is an important, functional and physical, interacting partner of β-catenin in prostate cancer. Given the influence of AR in prostate cancer, the importance of this interaction has been speculated in review papers (Terry et al., 2006 and Wang et al., 2008). The correlation between higher malignancy related to CRPC and β-catenin implies Wnt/β-catenin signalling pathway upregulation in CRPC, as has also been previously suggested (Lombardi et al., 2013). The data presented in this thesis further supports the notion that co-expression of AR and β-catenin in CRPC tissues is likely to be correlated with disease progression.

The results obtained from this study were analysed using statistical analyses described in Chap-III, Sec 3.3.7. The expression of each protein in normal, lower and higher grade PCa and CRPC tissues was compared using nonparametric tests, Mann–Whitney U tests, with data expressed as medians and interquartiles, and so independent of the number of data samples in each independent group of tissues. During image analysis colour threshold was determine using hue, saturation and brightness from 0 to 255 and the data were not normally distributed.

6.5. Further research

The work presented here could be progressed to develop a better understanding of both fundamental scientific mechanisms and to develop clinically useful biomarkers and therapies. I believe the research presented here provides a firm foundation for further research to enhance our knowledge of the mechanisms of interaction between AR and Wnt signalling. My research also provides molecular evidence for co-operativity between AR and Wnt, the two key cellular signalling pathways in cancer. I believe the following further research could prove useful:

6.5.1. To identify new targets of AR and Wnt signalling and validate the proteins tested here as biomarkers for diagnosis and prognosis of prostate cancer. As a first step, gene expression with and without DHT and Wnts, in vitro, and in different grade prostate cancer tissue, in situ, needs to be investigated. This may also shed light on (i) whether transcriptional or translational mechanisms are dominant during carcinogenesis and (ii) how AR and Wnt signalling are involved

in prostate cancer becoming resistant to ADT and what role the balance of activation between these two signalling pathways may play? This could be performed by isolating RNA from frozen or FFPE prostate tissue from different types of PCa and subjecting these samples to RNA sequencing; expression analysis of AR+ and AR- cells ±DHT ±Wnt ligands followed by RNA sequencing to measure gene expression to identify the network of genes that are under the control of transcription of AR and Wnt signalling. Such an approach would also 'reverse-validate' the single molecule RNA and protein expression in situ. Indeed, this was my plan but was disrupted due to the Covid 19 pandemic.

My results also hint towards a number of RNAs and protein targets that could be used a biomarker for diagnosis and perhaps a molecular stratification of PCa. To convert this proof of concept into clinically useful, validated predictive biomarkers, gene, RNA and protein expression analysis in an unbiased, quantitative manner with appropriate sample size should be conducted.

6.5.2. Translocation of AR, AR (N-ter), β-catenin, Cx31 was demonstrated in LnCAP and $PC3^{(AR+)}$ cells using DHT, Wnt3A, Wnt5A, Wnt9B. To confirm the reciprocal activation of each ligand, knockdown and over-expression experiments for each key element in the signalling pathways (AR, β-catenin, Cx43 would be desirable. For instance, (i) AR signalling could be deactivated by treating LnCAP cells with flutamide, which inhibits binding of AR receptor to its ligands, testosterone or DHT. This could be followed by treatment of cells with Wnt ligands, to activate Wnt signalling pathways, to observe translocation of β-catenin and AR into translocation, individually or together. (ii) AR expression could be silenced by using siRNA/shRNA AR to observe the translocation of β-catenin into the nucleus. (iii) AR/β-catenin gene knockout using Cas9/CRISPR strategy. This kind of knockdown/knockout/over-expression will validate the role and importance of each component in a signalling pathway. This is also important to identify the key steps that could be targeted for therapeutic purposes.

6.6. Future perspective

A clinical implication of the in situ and in vitro results shows Wnt signalling contributing to high grade malignancy and CRPC progression and development. Therefore, blocking Wnt signalling may be implemented to impair the disease progression. Together with the cooperativity between

AR and Wnt signalling, this could interfere with both signalling mechanisms, hence, perhaps providing greater inhibition of prostate carcinogenesis.

6.6.1. Treatment by Membrane Potential Regulatory Compounds (MPRCs) – a discovery from our laboratory

Recent research in our laboratory has identified a novel mechanism of Wnt signalling showing that Wnt ligands activate ion channels (e.g. TRPM8) on the cell membrane followed by releasing] of intracellular $[Ca^{2+}]_i$; the same mechanism for Wnt signal activation occurs in both AR+ (LnCAP) and AR-(PC3) cell lines. It has been further suggested that membrane potential regulating compounds (MPRC) could be used to inhibit Wnt/Ca2+ and Wnt/β-catenin signalling (Ahmed, A, International Patent Application PCT/GB2014/053138; British patent application No. 1318659.8; USPTO 2016/0271157A1), thus providing a new anti-cancer, therapeutic target. The development of Wnt signalling inhibitors has had limited success (Polakis, 2012 and Kahn, 2014) and few Wnt modulators have been approved for clinical use (Harb et al., 2019) (also see below). Indeed among MRPCs (e.g. propranolol, a repurposed drug) could be used to intervene Wnt signalling pathway and may present several advantages: (i) this could target one of the earlier steps in Wnt pathway (e.g., Wnt signalling receptor), (ii) this could exert its effect at the cell membrane level, as MPRCs act on cell surface and do not need to enter the cell, (iii) its dose, adverse effects and contraindications are already established. These imply that this candidate, which inhibits Wnt signalling, could readily be applied to clinical practice: a more time and cost effective alternative than drug development of new anti-cancer agents (Ashburn and Thor, 2004 and Bhattarai et al., 2016).

Given the reciprocity of Wnt and AR signalling and that DHT also activates release of intracellular $[Ca^{2+}]_i$ and β-catenin translocation into the nucleus, it could be hypothesized that AR signalling may also require upstream activation of ion channels. This hypothesis could be tested in LnCAP cells by measuring ion channel and release of intracellular $[Ca^{2+}]i$ with ±DHT ±Wnt ±membrane potential regulating compounds. This will answer the question whether membrane potential regulating compounds could be used to inhibit AR signalling? If true, this could open another avenue to counteract prostate cancer becoming androgen resistant. If successful, the membrane

potential regulating compounds could be used adjuvant to ADT which initially works well to inhibit prostate carcinogenesis.

6.6.2. Treatment to inhibit Wnt signalling in PCa cells and CRPC

In situ analysis showed an increased expression of β-catenin and AR in CRPC. Wnt and AR signalling pathways are reciprocally activated at ligand binding and translocate β-catenin and AR for transcription activities in PCa cells. These results suggest both signalling pathways are activated in CRPC and PCa cells. To treat the disease, it would be logical to inhibit translocation of β-catenin and AR into nucleus or to deactivate the Wnt and AR signalling pathways in CRPC. To treat the CRPC patient, the Food and Drug Administration (FDA) approved Olaparib (Lynparza, an inhibitor of PARP enzymes), darolutamide (Nubeqa), Enzalutamide (an androgen-receptor inhibitor), apalutamide (Erleada, an androgen-receptor inhibitor) and docetaxel (testosterone blocking). It is possible that these drugs may also block the Wnt pathway and this should be investigated.

As described above, deregulation of the Wnt/β-catenin pathway is closely associated in initiation and progression of various types of cancers (Gajos-Michniewicz and Czyz, 2020 and He and Tang, 2020). Several strategies targeting Wnt signalling as therapies have been proposed and discussed briefly, below.

6.6.2.1. Porcupine inhibitors

Porcupine (PORCN), a family member of membrane-bound O-acyltransferases (MBOT), is the key enzyme for the secretion of Wnt ligands (Torres et al., 2019). Several inhibitors that target PORCN prevent palmitoylation of Wnt proteins in the endoplasmic reticulum, which subsequently prevents their secretion (Krishnamurthy and Kurzrock, 2018). Blocking the acylation of Wnt with a PORCN inhibitor to abolish Wnt secretion becomes an effective treatment strategy. Wnt974 (LGK974) is an orally accessible small molecule inhibitor that reduces the viability of epithelial ovarian cancer (EOC) in vitro and supresses tumour growth in vivo. Wnt974 exhibits increased anti-tumour activity in EOC preclinical mouse models when combined with paclitaxel(Doo et al., 2020). Patients with pancreatic cancer, triple-negative breast cancer, cervical squamous cell

carcinoma are currently being studied in a phase I clinical trial using Wnt974 monotherapy (NCT01351103).

Table 6.1. Wnt/β-catenin signalling inhibitors in current and past clinical trials. Adapted from (Jung and Park, 2020)

Drug	Mechanism of action	Cancer type	Phase	Identifier
*WNT974 (with LGX818 and Cetuximab)	PORCN inhibitor	Metastatic CRC	Phase 1	NCT02278133
WNT974	PORCN inhibitor	Squamous cell cancer Head&Neck	Phase 2	NCT02649530
WNT974	PORCN inhibitor	Pancreatic cancer BRAF mutant CRC Melanoma TNBC H&N Squamous cell cancer (cervical, esophageal, lung)	Phase 1	NCT01351103
ETC-1922159	PORCN inhibitor	Solid tumor	Phase 1	NCT02521844
RXC004	PORCN inhibitor	Solid tumor	Phase 1	NCT03447470
CGX1321	PORCN inhibitor	Colorectal adenocarcinoma Gastric adenocarcinoma Pancreatic adenocarcinoma Bile duct carcinoma HCC Esophageal carcinoma Gastrointestinal cancer	Phase 1	NCT03507998
*CGX1321 (with Pembrolizumab)	PORCN inhibitor	Solid tumors GI cancer	Phase 1	NCT02675946
OTSA101-DTPA-90Y	FZD10 antagonist	Sarcoma, Synovial	Phase 1	NCT01469975
*OMP-18R5 (with Docetaxel)	Monoclonal antibody against FZD receptors	Solid tumors	Phase 1	NCT01957007
OMP-18R5	Monoclonal antibody against FZD receptors	Metastatic breast cancer	Phase 1	NCT01973309
OMP-18R5	Monoclonal antibody against FZD receptors	Solid tumors	Phase 1	NCT01345201
*OMP-18R5 (with Nab-Paclitaxel and Gemcitabine)	Monoclonal antibody against FZD receptors	Pancreatic cancer Stage IV pancreatic cancer	Phase 1	NCT02005315
*OMP-54F28 (with Sorafenib)	FZD8 decoy receptor	Hepatocellular cancer Liver cancer	Phase 1	NCT02069145
*OMP-54F28 (with Paclitaxel & Carboplatin)	FZD8 decoy receptor	Ovarian cancer	Phase 1	NCT02092363
*OMP-54F28 (with Nab-Paclitaxel and Gemcitabine)	FZD8 decoy receptor	Pancreatic cancer Stage IV pancreatic cancer	Phase 1	NCT02050178
OMP-54F28	FZD8 decoy receptor	Solid tumors	Phase 1	NCT01608867
PRI-724	CBP/β-catenin antagonist	Advanced pancreatic cancer Metastatic pancreatic cancer Pancreatic adenocarcinoma	Phase 1	NCT01764477
PRI-724	CBP/β-catenin antagonist	Advanced solid tumors	Phase 1	NCT01302405
PRI-724	CBP/β-catenin antagonist	Acute myeloid leukemia Chronic myeloid leukemia	Phase 2	NCT01606579
*PRI-724 (with Leucovorin Calcium, Oxaliplatin, or Fluorouracil)	CBP/β-catenin antagonist	Acute myeloid leukemia Chronic myeloid leukemia	Phase 2	NCT02413853
SM08502	β-catenin-controlled gene expression inhibitor	Solid tumors	Phase 1	NCT03355066

6.6.2.2. Wnt/Fzd antagonists

The canonical Wnt signalling pathway can be inhibited by antagonising Wnt ligands and Fzd receptors. Ipafricept (OMP54F28; IPA) is a recombinant fusion protein, including the cysteinerich domain of Fzd8 fused to a human IgG1 Fc fragment This molecule may easily bind to Wnt signalling ligands, compete with the Fzd8 receptor for Wnt binding, thereby suppressing Wnt regulated activities (Moore et al., 2019). Fischer et al showed, using a patient-derived ovarian

cancer xenograft mice model, that ipafricept decreased the population of stem cells, suppressed tumour formation and promoted differentiation. Furthermore, when taken two to three days ahead of chemotherapy, ipafricept showed synergistic anti-tumour effects when paired with texanes in preclinical tests, with 82% of patients attained a partial or complete response (Fischer et al., 2017).

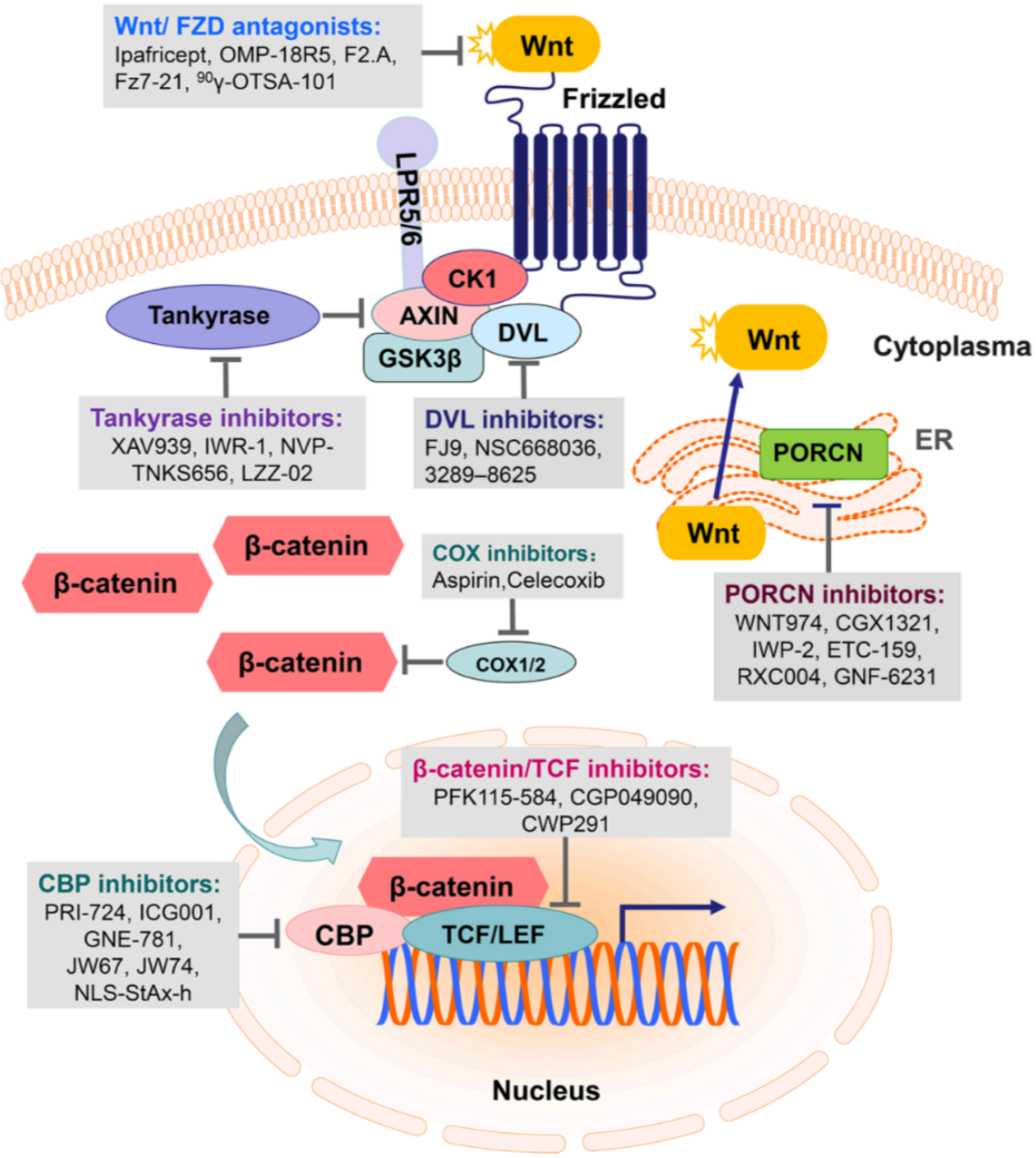

Figure 6.1. Schematic overview of Wnt/β-catenin signalling pathway targeted interventions in cancer studies. Promising therapeutics targeting Wnt ligand/receptor interface, β-catenin destruction complex and TCF/β-catenin transcription complex is investigated in preclinical and clinical evaluations. Adapted from (Zhang and Wang, 2020).

6.6.2.3. LRP5/6 inhibitors

The phosphorylation of LRP5/6, a Wnt co-receptor, increases the activation of the Wnt/β-catenin signalling pathway. The Wnt-Fzd-LRP5/6-DVL molecular complex generates a structural site for Axin to bind which prevents β-catenin degradation. Utilizing pharmacophore-based virtual screening and in vitro testing, BMD4503-2, a quinoxaline moiety, was found as a novel small molecule inhibitor of the LRP5/6 sclerostin interaction. The compound, BMD4503-2 has the potential to restore the Wnt/β-catenin signalling activity through competitively binding to the LRP5/6-sclerostin complex (Choi et al., 2018).

6.6.2.4. DVL inhibitors

DVL is a vital element in the Wnt signalling pathway by engaging components of the β-catenin destruction complex to the cell membrane. PDZ domain of DVL binds to the cytoplasmic carboxyl terminal end of Fzd proteins (Wong et al., 2003). NSC668036, FJ9, and 3289–8625 are some of the compounds that inhibit the signal transduction pathway by blocking the DVL-PDZ interaction (Grandy et al., 2009).

6.6.2.5. Tankyrase inhibitors

Given that the β-catenin protein destruction complex plays a key role in negatively regulating Wnt signalling, restoring this protein destruction complex could effectively suppress Wnt/β-catenin signalling. Tankyrase interacts with Axin and uses ubiquitin-mediated proteosomal degradation to degrade it. Inhibitors of tankyrase have been produced. β-catenin stabilization is decreased by tankyrase inhibitors. Tankyrase inhibitors including XAV939, JW-55, RK-287107, and G007-LK, stabilized AXIN by inhibiting the poly-ADP-ribosylating enzyme Tankyrase (Morrone et al., 2012). However, currently, no clinical trials are being conducted with Tankyrase inhibitors.

6.6.2.6. CK1 agonists

Accumulation of β-catenin destruction complex in the cytoplasm prevents β-catenin entering the nucleus, rendering it a promising therapeutic target. Pyrvinium is an anti-helminthic medication that has been approved by the FDA. Pyrinium binds to members of the CK1 family in vitro, elevating CK1 activity (Thorne et al., 2010).

6.6.2.7. Inhibitors of β-catenin transcriptional activity

β-catenin act as a transcription factor co-activator of target genes such as CCND1, CD44, Axin2 and MYC97-100 which contribute to tumorigenesis. Thus, approaches that inhibit either β-catenin transcriptional activity or β-catenin target genes have been developed as potential therapeutic candidates for Wnt signalling-associated malignancies. β-Catenin/CBP (CREB-binding protein) binds to WRE (Wnt-responsive element; 5'-CTTTGA/TA/T-3') and activates target gene transcription (Yu et al., 2017). PRI-724 (ICG-001; NIH clinical trial numbers: NCT01302405, NCT02413853, NCT01764477, and NCT01606579) inhibits the interaction between CBP and β-catenin and prevents transcription of Wnt target genes (Takemaru and Moon, 2000 and Jung and Park, 2020).

Whether any of these modulators will reach the clinic remains to be seen. It is therefore important to discover alternatives to inhibit the Wnt pathway, for example, as proposed through MPRC inhibition of Wnt signalling. This, as indicated, has the advantage of cell surface interactivity and detailed, known and minimal side-effects.

Implementation of novel strategies are also imperative to improve the prognosis of cancer patients. With the advancement in understanding of molecular mechanisms and continuous endeavour for the improvement, preclinical research and clinical trials have been performed on Wnt/β-catenin signalling targeted therapies in malignancies. Wnt/β-catenin signalling targeted therapies have been shown to be viable options for customised cancer therapy approaches. These strategies have not been implemented for PCa treatment as identification of association of Wnt signalling in PCa and CRPC development has not been investigated and discovered prior to these studies (Chap-III, IV and V). Nevertheless, obstructing the Wnt signalling may impairs tissue homeostasis and regeneration. Therefore, further investigations are required to the safety, efficacy, patient stratification and drug delivery of innovative Wnt/β-catenin targeted therapies in PCa.

References

Aaron, L., Franco, O. E. & Hayward, S. W. 2016. Review of prostate anatomy and embryology and the etiology of benign prostatic hyperplasia. *Urologic Clinics,* 43**,** 279-288.

Aasen, T., Leithe, E., Graham, S. V., Kameritsch, P., Mayán, M. D., Mesnil, M., Pogoda, K. & Tabernero, A. 2019. Connexins in cancer: bridging the gap to the clinic. *Oncogene,* 38**,** 4429-4451.

Abeshouse, A., Ahn, J., Akbani, R., Ally, A., Amin, S., Andry, C. D., Annala, M., Aprikian, A., Armenia, J. & Arora, A. 2015. The molecular taxonomy of primary prostate cancer. *Cell,* 163**,** 1011-1025.

Acebron, S. P., Karaulanov, E., Berger, B. S., Huang, Y.-L. & Niehrs, C. 2014. Mitotic wnt signaling promotes protein stabilization and regulates cell size. *Molecular cell,* 54**,** 663-674.

Adaimy, L., Chouery, E., Mégarbané, H., Mroueh, S., Delague, V., Nicolas, E., Belguith, H., De Mazancourt, P. & Mégarbané, A. 2007. Mutation in WNT10A is associated with an autosomal recessive ectodermal dysplasia: the odonto-onycho-dermal dysplasia. *The American Journal of Human Genetics,* 81**,** 821-828.

Adami, H.-O., Mclaughlin, J. K., Hsing, A. W., Wolk, A., Ekbom, A., Holmberg, L. & Persson, I. 1992. Alcoholism and cancer risk: a population-based cohort study. *Cancer Causes & Control,* 3**,** 419-425.

Agoulnik, I. U. & Weigel, N. L. 2006. Androgen receptor action in hormone-dependent and recurrent prostate cancer. *Journal of cellular biochemistry,* 99**,** 362-372.

Ahrens-Fath, I., Politz, O., Geserick, C. & Haendler, B. 2005. Androgen receptor function is modulated by the tissue-specific AR45 variant. *The FEBS journal,* 272**,** 74-84.

Ahumada, A., Slusarski, D. C., Liu, X., Moon, R. T., Malbon, C. C. & Wang, H.-Y. 2002. Signaling of rat Frizzled-2 through phosphodiesterase and cyclic GMP. *Science,* 298**,** 2006-2010.

Ai, Z., Fischer, A., Spray, D. C., Brown, A. M. & Fishman, G. I. 2000. Wnt-1 regulation of connexin43 in cardiac myocytes. *The Journal of clinical investigation,* 105**,** 161-171.

Akiyama, T. 2000. Wnt/β-catenin signaling. *Cytokine & growth factor reviews,* 11**,** 273-282.

Al-Agha, O. M. & Axiotis, C. A. 2007. An in-depth look at Leydig cell tumor of the testis. *Archives of pathology & laboratory medicine,* 131**,** 311-317.

Alahmar, A. T. 2019. Role of Oxidative Stress in Male Infertility: An Updated Review. *J Hum Reprod Sci,* 12**,** 4-18.

Albadine, R., Latour, M., Toubaji, A., Haffner, M., Isaacs, W. B., Platz, E. A., Meeker, A. K., Demarzo, A. M., Epstein, J. I. & Netto, G. J. 2009. TMPRSS2–ERG gene fusion status in minute (minimal) prostatic adenocarcinoma. *Modern Pathology,* 22**,** 1415-1422.

Alexander, D. B. & Goldberg, G. S. 2003. Transfer of biologically important molecules between cells through gap junction channels. *Current medicinal chemistry,* 10**,** 2045-2058.

Alexander, D. D., Mink, P. J., Cushing, C. A. & Sceurman, B. 2010. A review and meta-analysis of prospective studies of red and processed meat intake and prostate cancer. *Nutrition journal,* 9**,** 50.

Ali, T., Epstein, J., Bieberich, C. & De Marzo, A. NKX3. 1 as a new tissue marker of prostatic adenocarcinoma. Laboratory Investigation, 2006. NATURE PUBLISHING GROUP 75 VARICK ST, 9TH FLR, NEW YORK, NY 10013-1917 USA, 128A-128A.

Alimirah, F., Chen, J., Basrawala, Z., Xin, H. & Choubey, D. 2006. DU-145 and PC-3 human prostate cancer cell lines express androgen receptor: implications for the androgen receptor functions and regulation. *FEBS letters,* 580**,** 2294-2300.

Alonso-Magdalena, P., Brössner, C., Reiner, A., Cheng, G., Sugiyama, N., Warner, M. & Gustafsson, J.-Å. 2009. A role for epithelial-mesenchymal transition in the etiology of benign prostatic hyperplasia. *Proceedings of the National Academy of Sciences,* 106**,** 2859-2863.

Altman, D. & Deeks, J. 2004. Diagnostic tests 4: likelihood ratios. *BMJ,* 329**,** 168-9.

Alvarez-Cubero, M., Entrala, C., Fernandez-Rosado, F., Martinez-Gonzalez, L., Alvarez, J., Suarez, A., Lorente, J. & Cozar, J. 2012. Predictive value in the analysis of RNASEL genotypes in relation to prostate cancer. *Prostate cancer and prostatic diseases,* 15**,** 144-149.

Ambros, V. 2004. The functions of animal microRNAs. *Nature,* 431**,** 350-355.

Amin, A., Partin, A. & Epstein, J. I. 2011. Gleason score 7 prostate cancer on needle biopsy: relation of primary pattern 3 or 4 to pathological stage and progression after radical prostatectomy. *The Journal of urology,* 186**,** 1286-1290.

Amit, S., Hatzubai, A., Birman, Y., Andersen, J. S., Ben-Shushan, E., Mann, M., Ben-Neriah, Y. & Alkalay, I. 2002. Axin-mediated CKI phosphorylation of β-catenin at Ser 45: a molecular switch for the Wnt pathway. *Genes & development,* 16**,** 1066-1076.

Anderson, C. M., Zhang, B., Miller, M., Butko, E., Wu, X., Laver, T., Kernag, C., Kim, J., Luo, Y. & Lamparski, H. 2016. Fully automated RNAscope in situ hybridization assays for formalin-fixed paraffin-embedded cells and tissues. *Journal of cellular biochemistry,* 117**,** 2201-2208.

Andrews, P. G., Kennedy, M. W., Popadiuk, C. M. & Kao, K. R. 2008. Oncogenic activation of the human Pygopus2 promoter by E74-like factor-1. *Molecular Cancer Research,* 6**,** 259-266.

Andriole, G., Bruchovsky, N., Chung, L. W., Matsumoto, A. M., Rittmaster, R., Roehrborn, C., Russell, D. & Tindall, D. 2004. Dihydrotestosterone and the prostate: the scientific rationale for 5α-reductase inhibitors in the treatment of benign prostatic hyperplasia. *The Journal of urology,* 172**,** 1399-1403.

Arenas, M. I., Romo, E., Royuela, M., Fraile, B. & Paniagua, R. 2000. E-, N-and P-cadherin, and α-, β-and γ-catenin protein expression in normal, hyperplastic and carcinomatous human prostate. *The Histochemical Journal,* 32**,** 659-667.

Arora, R., Koch, M. O., Eble, J. N., Ulbright, T. M., Li, L. & Cheng, L. 2004. Heterogeneity of Gleason grade in multifocal adenocarcinoma of the prostate. *Cancer: Interdisciplinary International Journal of the American Cancer Society,* 100**,** 2362-2366.

Arslan, A. I., Karabag, S., Akgul, M. & Yildirim, I. 2020. Immunohistochemical expression of E-Cadherin and β-catenin in prostate adenocarcinoma and benign prostate hyperplasia. *Medicine,* 9**,** 530-4.

Arthurs, C., Murtaza, B. N., Thomson, C., Dickens, K., Henrique, R., Patel, H. R., Beltran, M., Millar, M., Thrasivoulou, C. & Ahmed, A. 2017. Expression of ribosomal proteins in normal and cancerous human prostate tissue. *PloS one,* 12**,** e0186047.

Arthurs, C., Suarez-Bonnet, A., Willis, C., Xie, B., Machulla, N., Mair, T. S., Cao, K., Millar, M., Thrasivoulou, C. & Priestnall, S. L. 2020. Equine penile squamous cell carcinoma: Expression of biomarker proteins and EcPV2. *Scientific reports,* 10**,** 1-13.

Arya, M., Thrasivoulou, C., Henrique, R., Millar, M., Hamblin, R., Davda, R., Aare, K., Masters, J. R., Thomson, C. & Muneer, A. 2015. Targets of wnt/ß-catenin transcription in penile carcinoma. *PLoS One,* 10**,** e0124395.

Ashburn, T. T. & Thor, K. B. 2004. Drug repositioning: identifying and developing new uses for existing drugs. *Nature reviews Drug discovery,* 3**,** 673-683.

Ashmore, J., Olsen, H., Sørensen, N., Thrasivoulou, C. & Ahmed, A. 2019. Wnts control membrane potential in mammalian cancer cells. *The Journal of physiology,* 597**,** 5899-5914.

Asuthkar, S., Velpula, K. K., Elustondo, P. A., Demirkhanyan, L. & Zakharian, E. 2015. TRPM8 channel as a novel molecular target in androgen-regulated prostate cancer cells. *Oncotarget,* 6**,** 17221.

Attard, G., Clark, J., Ambroisine, L., Mills, I., Fisher, G., Flohr, P., Reid, A., Edwards, S., Kovacs, G. & Berney, D. 2008. Heterogeneity and clinical significance of ETV1 translocations in human prostate cancer. *British journal of cancer,* 99**,** 314-320.

Augello, M. A., Den, R. B. & Knudsen, K. E. 2014. AR function in promoting metastatic prostate cancer. *Cancer and Metastasis Reviews,* 33**,** 399-411.

Ayala, A. G. & Ro, J. Y. 2007. Prostatic intraepithelial neoplasia: recent advances. *Archives of pathology & laboratory medicine,* 131**,** 1257-1266.

Aymoz, D., Wosika, V., Durandau, E. & Pelet, S. 2016. Real-time quantification of protein expression at the single-cell level via dynamic protein synthesis translocation reporters. *Nature communications,* 7**,** 1-12.

Bachmann, I. M., Straume, O., Puntervoll, H. E., Kalvenes, M. B. & Akslen, L. A. 2005. Importance of P-cadherin, β-catenin, and Wnt5a/frizzled for progression of melanocytic tumors and prognosis in cutaneous melanoma. *Clinical Cancer Research,* 11**,** 8606-8614.

Baillie, A. 1964. Further observations on the growth and histochemistry of the Leydig tissue in the postnatal prepubertal mouse testis. *Journal of anatomy,* 98**,** 403.

Bänziger, C., Soldini, D., Schütt, C., Zipperlen, P., Hausmann, G. & Basler, K. 2006. Wntless, a conserved membrane protein dedicated to the secretion of Wnt proteins from signaling cells. *Cell,* 125**,** 509-522.

Barker, N. 2014. Adult intestinal stem cells: critical drivers of epithelial homeostasis and regeneration. *Nat Rev Mol Cell Biol,* 15**,** 19-33.

Bartel, D. P. 2009. MicroRNAs: target recognition and regulatory functions. *cell,* 136**,** 215-233.

Bartscherer, K., Pelte, N., Ingelfinger, D. & Boutros, M. 2006. Secretion of Wnt ligands requires Evi, a conserved transmembrane protein. *Cell,* 125**,** 523-533.

Basbous, J., Jariel-Encontre, I., Gomard, T., Bossis, G. & Piechaczyk, M. 2008. Ubiquitin-independent-versus ubiquitin-dependent proteasomal degradation of the c-Fos and Fra-1 transcription factors: is there a unique answer? *Biochimie,* 90**,** 296-305.

Bass, B. P., Engel, K. B., Greytak, S. R. & Moore, H. M. 2014. A review of preanalytical factors affecting molecular, protein, and morphological analysis of formalin-fixed, paraffin-embedded (FFPE) tissue: how well do you know your FFPE specimen? *Archives of pathology and laboratory medicine,* 138**,** 1520-1530.

Bass, J. J., Wilkinson, D. J., Rankin, D., Phillips, B. E., Szewczyk, N. J., Smith, K. & Atherton, P. J. 2017. An overview of technical considerations for Western blotting applications to physiological research. *Scandinavian journal of medicine & science in sports,* 27**,** 4-25.

Basuyaux, J. P., Ferreira, E., Stéhelin, D. & Butticè, G. 1997. The Ets transcription factors interact with each other and with the c-Fos/c-Jun complex via distinct protein domains in a DNA-dependent and-independent manner. *Journal of Biological Chemistry,* 272**,** 26188-26195.

Baylin, S. B. 2005. DNA methylation and gene silencing in cancer. *Nature clinical practice Oncology,* 2**,** S4-S11.

Belenkaya, T. Y., Han, C., Standley, H. J., Lin, X., Houston, D. W., Heasman, J. & Lin, X. 2002. pygopus Encodes a nuclear protein essential for wingless/Wnt signaling.

Beltran, H., Yelensky, R., Frampton, G. M., Park, K., Downing, S. R., Macdonald, T. Y., Jarosz, M., Lipson, D., Tagawa, S. T. & Nanus, D. M. 2013. Targeted next-generation sequencing of advanced prostate cancer identifies potential therapeutic targets and disease heterogeneity. *European urology,* 63**,** 920-926.

Ben-Shlomo, Y., Evans, S., Ibrahim, F., Patel, B., Anson, K., Chinegwundoh, F., Corbishley, C., Dorling, D., Thomas, B. & Gillatt, D. 2008. The risk of prostate cancer amongst black men in the United Kingdom: the PROCESS cohort study. *European urology,* 53**,** 99-105.

Benko, G., Spajić, B., Demirović, A., Štimac, G., Kruslin, B. & Tomas, D. 2011. Prognostic value of connexin43 expression in patients with clinically localized prostate cancer. *Prostate cancer and prostatic diseases,* 14**,** 90-95.

Berman, D. M., Tian, H. & Russell, D. W. 1995. Expression and regulation of steroid 5 alpha-reductase in the urogenital tract of the fetal rat. *Molecular Endocrinology,* 9**,** 1561-1570.

Bhattarai, D., Singh, S., Jang, Y., Hyeon Han, S., Lee, K. & Choi, Y. 2016. An insight into drug repositioning for the development of novel anti-cancer drugs. *Current topics in medicinal chemistry,* 16**,** 2156-2168.

Bian, J., Dannappel, M., Wan, C. & Firestein, R. 2020. Transcriptional regulation of Wnt/β-catenin pathway in colorectal cancer. *Cells,* 9**,** 2125.

Bieberich, C. J., Fujita, K., He, W.-W. & Jay, G. 1996. Prostate-specific and androgen-dependent expression of a novel homeobox gene. *Journal of Biological Chemistry,* 271**,** 31779-31782.

Bio-Rad, L. 2012. A Guide to Polyacrylamide Gel Electrophoresis and Detection. *Laboratories Bio-Rad.*

Bismar, T. A., Humphrey, P. A., Grignon, D. J. & Wang, H. L. 2004. Expression of β-catenin in prostatic adenocarcinomas: a comparison with colorectal adenocarcinomas. *American journal of clinical pathology,* 121**,** 557-563.

Bisson, I. & Prowse, D. M. 2009. WNT signaling regulates self-renewal and differentiation of prostate cancer cells with stem cell characteristics. *Cell research,* 19**,** 683-697.

Blauwkamp, T. A., Nigam, S., Ardehali, R., Weissman, I. L. & Nusse, R. 2012. Endogenous Wnt signalling in human embryonic stem cells generates an equilibrium of distinct lineage-specified progenitors. *Nature communications,* 3**,** 1-10.

Bobrow, M. N., Harris, T. D., Shaughnessy, K. J. & Litt, G. J. 1989. Catalyzed reporter deposition, a novel method of signal amplification application to immunoassays. *Journal of immunological methods,* 125**,** 279-285.

Bornholdt, D., Oeffner, F., König, A., Happle, R., Alanay, Y., Ascherman, J., Benke, P. J., Del Carmen Boente, M., Van Der Burgt, I. & Chassaing, N. 2009. PORCN mutations in focal dermal hypoplasia: coping with lethality. *Human mutation,* 30**,** E618-E628.

Bostwick, D. 1989a. Prostatic intraepithelial neoplasia (PIN). *Urology (Suppl),* 34**,** 16-22.

Bostwick, D. G. 1989b. The pathology of early prostate cancer. *CA: a cancer journal for clinicians,* 39**,** 376-393.

Bostwick, D. G. & Brawer, M. K. 1987. Prostatic intra-epithelial neoplasia and early invasion in prostate cancer. *Cancer,* 59**,** 788-794.

Bostwick, D. G., Burke, H. B., Djakiew, D., Euling, S., Ho, S. M., Landolph, J., Morrison, H., Sonawane, B., Shifflett, T. & Waters, D. J. 2004a. Human prostate cancer risk factors. *Cancer: Interdisciplinary International Journal of the American Cancer Society,* 101**,** 2371-2490.

Bostwick, D. G., Burke, H. B., Djakiew, D., Euling, S., Ho, S. M., Landolph, J., Morrison, H., Sonawane, B., Shifflett, T., Waters, D. J. & Timms, B. 2004b. Human prostate cancer risk factors. *Cancer,* 101**,** 2371-490.

Bostwick, D. G. & Cheng, L. 2008. *Urologic surgical pathology*, Elsevier Health Sciences.

Bostwick, D. G., Pacelli, A. & Lopez-Beltran, A. 1996. Molecular biology of prostatic intraepithelial neoplasia. *The Prostate,* 29**,** 117-134.

Bostwick, D. G. & Qian, J. 2004. High-grade prostatic intraepithelial neoplasia. *Modern pathology,* 17**,** 360-379.

Bovolenta, P., Esteve, P., Ruiz, J. M., Cisneros, E. & Lopez-Rios, J. 2008. Beyond Wnt inhibition: new functions of secreted Frizzled-related proteins in development and disease. *Journal of cell science,* 121**,** 737-746.

Bowen, C., Bubendorf, L., Voeller, H. J., Slack, R., Willi, N., Sauter, G., Gasser, T. C., Koivisto, P., Lack, E. E. & Kononen, J. 2000. Loss of NKX3. 1 expression in human prostate cancers correlates with tumor progression1, 2. *Cancer research,* 60**,** 6111-6115.

Bratt, O. 2002. Hereditary prostate cancer: clinical aspects. *The Journal of urology,* 168**,** 906-913.

Bray, F., Ferlay, J., Soerjomataram, I., Siegel, R. L., Torre, L. A. & Jemal, A. 2018. Global cancer statistics 2018: GLOBOCAN estimates of incidence and mortality worldwide for 36 cancers in 185 countries. *CA: a cancer journal for clinicians,* 68**,** 394-424.

Brinkmann, A., Blok, L., De Ruiter, P., Doesburg, P., Steketee, K., Berrevoets, C. & Trapman, J. 1999. Mechanisms of androgen receptor activation and function. *The Journal of steroid biochemistry and molecular biology,* 69**,** 307-313.

Bui, T., Zhang, L., Rees, M., Bicknell, R. & Harris, A. 1997. Expression and hormone regulation of Wnt2, 3, 4, 5a, 7a, 7b and 10b in normal human endometrium and endometrial carcinoma. *British journal of cancer,* 75**,** 1131-1136.

Bullions, L. C. & Levine, A. J. 1998. The role of beta-catenin in cell adhesion, signal transduction, and cancer. *Current opinion in oncology,* 10**,** 81-87.

Burdova, A., Bouchal, J., Tavandzis, S. & Kolar, Z. 2014. TMPRSS2-ERG gene fusion in prostate cancer. *Biomedical Papers of the Medical Faculty of Palacky University in Olomouc,* 158.

Burnette, W. N. 1981. "Western blotting": electrophoretic transfer of proteins from sodium dodecyl sulfate-polyacrylamide gels to unmodified nitrocellulose and radiographic detection with antibody and radioiodinated protein A. *Analytical biochemistry,* 112**,** 195-203.

Burrus, L. W. & Mcmahon, A. P. 1995. Biochemical analysis of murine Wnt proteins reveals both shared and distinct properties. *Experimental cell research,* 220**,** 363-373.

Cadigan, K. M. 2008. Wnt–β-catenin signaling. *Current Biology,* 18**,** R943-R947.

Cai, X., Hagedorn, C. H. & Cullen, B. R. 2004. Human microRNAs are processed from capped, polyadenylated transcripts that can also function as mRNAs. *Rna,* 10**,** 1957-1966.

Calin, G. A. & Croce, C. M. 2006. MicroRNA-cancer connection: the beginning of a new tale. *Cancer research,* 66**,** 7390-7394.

Camp, N. J. & Tavtigian, S. V. 2002. Meta-analysis of associations of the Ser217Leu and Ala541Thr variants in ELAC2 (HPC2) and prostate cancer. *The American Journal of Human Genetics,* 71**,** 1475-1478.

Cancer, I. a. F. R. O. 2003. *World cancer report: World Health Organization*, IARC Press.

Cancilla, B., Jarred, R. A., Wang, H., Mellor, S. L., Cunha, G. R. & Risbridger, G. P. 2001. Regulation of prostate branching morphogenesis by activin A and follistatin. *Dev Biol,* 237**,** 145-58.

Cao, K., Arthurs, C., Atta-Ul, A., Millar, M., Beltran, M., Neuhaus, J., Horn, L.-C., Henrique, R., Ahmed, A. & Thrasivoulou, C. 2018. Quantitative analysis of seven new prostate cancer biomarkers and the potential future of the 'biomarker laboratory'. *Diagnostics,* 8**,** 49.

Cao, S., Zhan, Y. & Dong, Y. 2016. Emerging data on androgen receptor splice variants in prostate cancer. *Endocrine-related cancer,* 23**,** T199.

Capasso, L. L. 2005. Antiquity of cancer. *International journal of cancer,* 113**,** 2-13.

Carpten, J., Nupponen, N., Isaacs, S., Sood, R., Robbins, C., Xu, J., Faruque, M., Moses, T., Ewing, C. & Gillanders, E. 2002. Germline mutations in the ribonuclease L gene in families showing linkage with HPC1. *Nature genetics,* 30**,** 181-184.

Carrera, I., Janody, F., Leeds, N., Duveau, F. & Treisman, J. E. 2008. Pygopus activates Wingless target gene transcription through the mediator complex subunits Med12 and Med13. *Proceedings of the National Academy of Sciences,* 105**,** 6644-6649.

Carroll, A. G., Voeller, H. J., Sugars, L. & Gelmann, E. P. 1993. p53 oncogene mutations in three human prostate cancer cell lines. *The Prostate,* 23**,** 123-134.

Carter, B. S., Beaty, T. H., Steinberg, G. D., Childs, B. & Walsh, P. C. 1992. Mendelian inheritance of familial prostate cancer. *Proceedings of the National Academy of Sciences,* 89**,** 3367-3371.

Cavallo, R. A., Cox, R. T., Moline, M. M., Roose, J., Polevoy, G. A., Clevers, H., Peifer, M. & Bejsovec, A. 1998. Drosophila Tcf and Groucho interact to repress Wingless signalling activity. *Nature,* 395**,** 604-608.

Cerveira, N., Ribeiro, F. R., Peixoto, A., Costa, V., Henrique, R., Jerönimo, C. & Teixeira, M. R. 2006. TMPRSS2-ERG gene fusion causing ERG overexpression precedes chromosome copy number changes in prostate carcinomas, paired HGPIN lesions. *Neoplasia,* 8**,** 826-832.

Chae, W.-J. & Bothwell, A. L. 2018. Canonical and non-canonical Wnt signaling in immune cells. *Trends in immunology,* 39**,** 830-847.

Chan, J. K. 2014. The wonderful colors of the hematoxylin–eosin stain in diagnostic surgical pathology. *International journal of surgical pathology,* 22**,** 12-32.

Chan, S. C., Li, Y. & Dehm, S. M. 2012. Androgen receptor splice variants activate androgen receptor target genes and support aberrant prostate cancer cell growth independent of canonical androgen receptor nuclear localization signal. *Journal of Biological Chemistry,* 287**,** 19736-19749.

Chapman, A., Durand, J., Ouadi, L. & Bourdeau, I. 2011. Identification of genetic alterations of AXIN2 gene in adrenocortical tumors. *The Journal of Clinical Endocrinology & Metabolism,* 96**,** E1477-E1481.

Chen, C. D., Welsbie, D. S., Tran, C., Baek, S. H., Chen, R., Vessella, R., Rosenfeld, M. G. & Sawyers, C. L. 2004a. Molecular determinants of resistance to antiandrogen therapy. *Nature medicine,* 10**,** 33-39.

Chen, G., Shukeir, N., Potti, A., Sircar, K., Aprikian, A., Goltzman, D. & Rabbani, S. A. 2004b. Up-regulation of Wnt-1 and β-catenin production in patients with advanced metastatic prostate carcinoma: Potential pathogenetic and prognostic implications. *Cancer: Interdisciplinary International Journal of the American Cancer Society,* 101**,** 1345-1356.

Chen, H., Griffin, A., Wu, Y., Tomsho, L., Zuhlke, K., Lange, E., Gruber, S. & Cooney, K. 2003. RNASEL mutations in hereditary prostate cancer. *Journal of medical genetics,* 40**,** e21-e21.

Chen, Q., Takada, R. & Takada, S. 2012. Loss of Porcupine impairs convergent extension during gastrulation in zebrafish. *Journal of cell science,* 125**,** 2224-2234.

Chen, R., Luan, Y., Liu, Z., Song, W., Wu, L., Li, M., Yang, J., Liu, X., Wang, T. & Liu, J. 2015a. AR pathway is involved in the regulation of CX43 in prostate cancer. *BioMed research international,* 2015.

Chen, S.-C., Pelletier, D. B., Ao, P. & Boynton, A. L. 1995. Connexin43 reverses the phenotype of transformed cells and alters their expression of cyclin/cyclin-dependent kinases. *Cell growth & differentiation: the molecular biology journal of the American Association for Cancer Research,* 6**,** 681-690.

Chen, W.-Y., Liu, S.-Y., Chang, Y.-S., Yin, J. J., Yeh, H.-L., Mouhieddine, T. H., Hadadeh, O., Abou-Kheir, W. & Liu, Y.-N. 2015b. MicroRNA-34a regulates WNT/TCF7 signaling and inhibits bone metastasis in Ras-activated prostate cancer. *Oncotarget,* 6**,** 441.

Chen, X., Kong, X., Zhuang, W., Teng, B., Yu, X., Hua, S., Wang, S., Liang, F., Ma, D. & Zhang, S. 2016. Dynamic changes in protein interaction between AKAP95 and Cx43 during cell cycle progression of A549 cells. *Scientific reports,* 6**,** 1-13.

Chen, Y., Whetstone, H. C., Lin, A. C., Nadesan, P., Wei, Q., Poon, R. & Alman, B. A. 2007. Beta-catenin signaling plays a disparate role in different phases of fracture repair: implications for therapy to improve bone healing. *PLoS Med,* 4**,** e249.

Chen, Y.-W., Lee, M.-S., Lucht, A., Chou, F.-P., Huang, W., Havighurst, T. C., Kim, K., Wang, J.-K., Antalis, T. M. & Johnson, M. D. 2010. TMPRSS2, a serine protease expressed in the prostate on the apical surface of luminal epithelial cells and released into semen in prostasomes, is misregulated in prostate cancer cells. *The American journal of pathology,* 176**,** 2986-2996.

Chen, Y. C., Page, J. H., Chen, R. & Giovannucci, E. 2008. Family history of prostate and breast cancer and the risk of prostate cancer in the PSA era. *The Prostate,* 68**,** 1582-1591.

Chen, Z., He, X., Jia, M., Liu, Y., Qu, D., Wu, D., Wu, P., Ni, C., Zhang, Z. & Ye, J. 2013. β-catenin overexpression in the nucleus predicts progress disease and unfavourable survival in colorectal cancer: a meta-analysis. *PLoS One,* 8**,** e63854.

Cheng, C.-Y., Hwang, C.-I., Corney, D. C., Flesken-Nikitin, A., Jiang, L., Öner, G. M., Munroe, R. J., Schimenti, J. C., Hermeking, H. & Nikitin, A. Y. 2014. miR-34 cooperates with p53 in suppression of prostate cancer by joint regulation of stem cell compartment. *Cell reports,* 6**,** 1000-1007.

Cheng, L., Paterson, R. F., Beck, S. D. & Parks, J. 2004. Prostatic intraepithelial neoplasia: an update. *Clinical prostate cancer,* 3**,** 26-30.

Chesire, D. & Isaacs, W. 2003. Beta-catenin signaling in prostate cancer: an early perspective. *Endocrine-related cancer,* 10**,** 537-560.

Chesire, D. R., Ewing, C. M., Gage, W. R. & Isaacs, W. B. 2002. In vitro evidence for complex modes of nuclear β-catenin signaling during prostate growth and tumorigenesis. *Oncogene,* 21**,** 2679-2694.

Chesire, D. R., Ewing, C. M., Sauvageot, J., Bova, G. S. & Isaacs, W. B. 2000. Detection and analysis of β-catenin mutations in prostate cancer. *The Prostate,* 45**,** 323-334.

Cheville, J. C., Lloyd, R. V., Sebo, T. J., Cheng, L., Erickson, L., Bostwick, D. G., Lohse, C. M. & Wollan, P. 1998. Expression of p27kip1 in prostatic adenocarcinoma. *Modern pathology: an official journal of the United States and Canadian Academy of Pathology, Inc,* 11**,** 324-328.

Chien, A. J., Moore, E. C., Lonsdorf, A. S., Kulikauskas, R. M., Rothberg, B. G., Berger, A. J., Major, M. B., Hwang, S. T., Rimm, D. L. & Moon, R. T. 2009. Activated Wnt/ß-catenin signaling in melanoma is associated with decreased proliferation in patient tumors and a murine melanoma model. *Proceedings of the National Academy of Sciences,* 106**,** 1193-1198.

Ching, K. Z., Ramsey, E., Pettigrew, N., D'cunha, R., Jason, M. & Dodd, J. G. 1993. Expression of mRNA for epidermal growth factor, transforming growth factor-alpha and their receptor in human prostate tissue and cell lines. *Molecular and cellular biochemistry,* 126**,** 151-158.

Chodak, G. W., Kranc, D. M., Puy, L. A., Takeda, H., Johnson, K. & Chang, C. 1992. Nuclear localization of androgen receptor in heterogeneous samples of normal, hyperplastic and neoplastic human prostate. *The Journal of urology,* 147**,** 798-803.

Choi, J., Lee, K., Kang, M., Lim, S.-K. & No, K. T. 2018. In silico discovery of quinoxaline derivatives as novel LRP5/6-sclerostin interaction inhibitors. *Bioorganic & Medicinal Chemistry Letters,* 28**,** 1116-1121.

Chrambach, A. 1985. *practice of quantitative gel electrophoresis*, VCH.

Christie, M., Jorissen, R., Mouradov, D., Sakthianandeswaren, A., Li, S., Day, F., Tsui, C., Lipton, L., Desai, J. & Jones, I. 2013. Different APC genotypes in proximal and distal sporadic colorectal cancers suggest distinct WNT/β-catenin signalling thresholds for tumourigenesis. *Oncogene,* 32**,** 4675-4682.

Chuang, A.-Y., Demarzo, A. M., Veltri, R. W., Sharma, R. B., Bieberich, C. J. & Epstein, J. I. 2007. Immunohistochemical differentiation of high-grade prostate carcinoma from urothelial carcinoma. *The American journal of surgical pathology,* 31**,** 1246-1255.

Clark, C. C., Cohen, I., Eichstetter, I., Cannizzaro, L. A., Mcpherson, J. D., Wasmuth, J. J. & Iozzo, R. V. 1993. Molecular cloning of the human proto-oncogene Wnt-5A and mapping of the gene (WNT5A) to chromosome 3p14-p21. *Genomics,* 18**,** 249-260.

Clark, J., Merson, S., Jhavar, S., Flohr, P., Edwards, S., Foster, C., Eeles, R., Martin, F. L., Phillips, D. & Crundwell, M. 2007. Diversity of TMPRSS2-ERG fusion transcripts in the human prostate. *Oncogene,* 26**,** 2667-2673.

Clevers, H. 2006. Wnt/β-catenin signaling in development and disease. *Cell,* 127**,** 469-480.

Clevers, H. C., Oosterwegel, M. A. & Georgopoulos, K. 1993. Transcription factors in early T-cell development. *Immunology today,* 14**,** 591-596.

Clinckemalie, L., Vanderschueren, D., Boonen, S. & Claessens, F. 2012. The hinge region in androgen receptor control. *Molecular and cellular endocrinology,* 358**,** 1-8.

Cohen, D. R., Ferreira, P., Gentz, R., Franza, B. & Curran, T. 1989. The product of a fos-related gene, fra-1, binds cooperatively to the AP-1 site with Jun: transcription factor AP-1 is comprised of multiple protein complexes. *Genes & development,* 3**,** 173-184.

Coleman, D. J., Van Hook, K., King, C. J., Schwartzman, J., Lisac, R., Urrutia, J., Sehrawat, A., Woodward, J., Wang, N. J. & Gulati, R. 2016. Cellular androgen content influences enzalutamide agonism of F877L mutant androgen receptor. *Oncotarget,* 7**,** 40690.

Colombel, M., Symmans, F., Gil, S., O'toole, K. M., Chopin, D., Benson, M., Olsson, C. A., Korsmeyer, S. & Buttyan, R. 1993. Detection of the apoptosis-suppressing oncoprotein bc1-2 in hormone-refractory human prostate cancers. *The American journal of pathology,* 143**,** 390.

Coombs, G. S., Yu, J., Canning, C. A., Veltri, C. A., Covey, T. M., Cheong, J. K., Utomo, V., Banerjee, N., Zhang, Z. H. & Jadulco, R. C. 2010. WLS-dependent secretion of WNT3A requires Ser209 acylation and vacuolar acidification. *Journal of cell science,* 123**,** 3357-3367.

Coons, A. H., Creech, H. J., Jones, R. N. & Berliner, E. 1942. The demonstration of pneumococcal antigen in tissues by the use of fluorescent antibody. *The Journal of Immunology,* 45**,** 159-170.

Coons, A. H., Leduc, E. H. & Connolly, J. M. 1955. Studies on antibody production: I. A method for the histochemical demonstration of specific antibody and its application to a study of the hyperimmune rabbit. *The Journal of experimental medicine,* 102**,** 49-60.

Crawford, E. D. & Hou, A. H. 2009. The role of LHRH antagonists in the treatment of prostate cancer. *Oncology,* 23**,** 626.

Cronier, L., Crespin, S., Strale, P.-O., Defamie, N. & Mesnil, M. 2009. Gap junctions and cancer: new functions for an old story. *Antioxidants & redox signaling,* 11**,** 323-338.

Culig, Z., Hobisch, A., Cronauer, M. V., Radmayr, C., Trapman, J., Hittmair, A., Bartsch, G. & Klocker, H. 1994. Androgen receptor activation in prostatic tumor cell lines by insulin-like growth factor-I, keratinocyte growth factor, and epidermal growth factor. *Cancer research,* 54**,** 5474-5478.

Culig, Z., Steiner, H., Bartsch, G. & Hobisch, A. 2005. Interleukin-6 regulation of prostate cancer cell growth. *Journal of cellular biochemistry,* 95**,** 497-505.

Cunha, G. R., Ricke, W., Thomson, A., Marker, P. C., Risbridger, G., Hayward, S. W., Wang, Y., Donjacour, A. A. & Kurita, T. 2004. Hormonal, cellular, and molecular regulation of normal and neoplastic prostatic development. *The Journal of steroid biochemistry and molecular biology,* 92**,** 221-236.

Cunha, G. R., Vezina, C. M., Isaacson, D., Ricke, W. A., Timms, B. G., Cao, M., Franco, O. & Baskin, L. S. 2018. Development of the human prostate. *Differentiation,* 103**,** 24-45.

Czyż, J., Szpak, K. & Madeja, Z. 2012. The role of connexins in prostate cancer promotion and progression. *Nature Reviews Urology,* 9**,** 274-282.

D'amico, A. V., Whittington, R., Malkowicz, S. B., Schultz, D., Blank, K., Broderick, G. A., Tomaszewski, J. E., Renshaw, A. A., Kaplan, I. & Beard, C. J. 1998. Biochemical outcome after radical prostatectomy, external beam radiation therapy, or interstitial radiation therapy for clinically localized prostate cancer. *Jama,* 280**,** 969-974.

Dagnelie, P., Schuurman, A., Goldbohm, R. & Van Den Brandt, P. 2004. Diet, anthropometric measures and prostate cancer risk: a review of prospective cohort and intervention studies. *BJU international,* 93**,** 1139-1150.

Dang, C. V. 2012. MYC on the path to cancer. *Cell,* 149**,** 22-35.

Dauge, M., Delmas, V. & Mandarim De Lacerda, C. 1986. Contribution à l'étude du développement de la prostate humaine aux premiers stades de la période fœtale. Etude morphométrique. *Bulletin de l'Association des anatomistes,* 70**,** 5-11.

Davidson, G., Wu, W., Shen, J., Bilic, J., Fenger, U., Stannek, P., Glinka, A. & Niehrs, C. 2005. Casein kinase 1 γ couples Wnt receptor activation to cytoplasmic signal transduction. *Nature,* 438**,** 867-872.

Davies, G., Jiang, W. G. & Mason, M. D. 2001. The interaction between β-catenin, GSK3β and APC after motogen induced cell-cell dissociation, and their involvement in signal transduction pathways in prostate cancer. *International journal of oncology,* 18**,** 843-847.

De Angelis, R., Sant, M., Coleman, M. P., Francisci, S., Baili, P., Pierannunzio, D., Trama, A., Visser, O., Brenner, H. & Ardanaz, E. 2014. Cancer survival in Europe 1999–2007 by country and age: results of EUROCARE-5—a population-based study. *The lancet oncology,* 15**,** 23-34.

De Ferrari, G., Chacon, M., Barria, M., Garrido, J., Godoy, J., Olivares, G., Reyes, A., Alvarez, A., Bronfman, M. & Inestrosa, N. 2003. Activation of Wnt signaling rescues neurodegeneration and behavioral impairments induced by β-amyloid fibrils. *Molecular psychiatry,* 8**,** 195-208.

De La Taille, A., Rubin, M. A., Chen, M.-W., Vacherot, F., De Medina, S. G.-D., Burchardt, M., Buttyan, R. & Chopin, D. 2003. β-Catenin-related anomalies in apoptosis-resistant and hormone-refractory prostate cancer cells. *Clinical Cancer Research,* 9**,** 1801-1807.

De Marzo, A. M., Haffner, M. C., Lotan, T. L., Yegnasubramanian, S. & Nelson, W. G. 2016. Premalignancy in prostate cancer: rethinking what we know. *Cancer Prevention Research,* 9**,** 648-656.

De Marzo, A. M., Meeker, A. K., Epstein, J. I. & Coffey, D. S. 1998. Prostate stem cell compartments: expression of the cell cycle inhibitor p27Kip1 in normal, hyperplastic, and neoplastic cells. *The American journal of pathology,* 153**,** 911-919.

Debes, J. D. & Tindall, D. J. 2002. The role of androgens and the androgen receptor in prostate cancer. *Cancer letters,* 187**,** 1-7.

Debes, J. D. & Tindall, D. J. 2004. Mechanisms of androgen-refractory prostate cancer. *New England Journal of Medicine,* 351**,** 1488-1490.

Dehm, S. M., Schmidt, L. J., Heemers, H. V., Vessella, R. L. & Tindall, D. J. 2008. Splicing of a novel androgen receptor exon generates a constitutively active androgen receptor that mediates prostate cancer therapy resistance. *Cancer research,* 68**,** 5469-5477.

Demarzo, A. M., Nelson, W. G., Isaacs, W. B. & Epstein, J. I. 2003. Pathological and molecular aspects of prostate cancer. *The Lancet,* 361**,** 955-964.

Denmeade, S. R., Lin, X. S. & Isaacs, J. T. 1996. Role of programmed (apoptotic) cell death during the progression and therapy for prostate cancer. *The Prostate,* 28**,** 251-265.

Desjardins, P., Hansen, J. B. & Allen, M. 2009. Microvolume protein concentration determination using the NanoDrop 2000c spectrophotometer. *JoVE (Journal of Visualized Experiments)***,** e1610.

Di Cristofano, A., De Acetis, M., Koff, A., Cordon-Cardo, C. & Pandolfi, P. P. 2001. Pten and p27 KIP1 cooperate in prostate cancer tumor suppression in the mouse. *Nature genetics,* 27**,** 222-224.

Di Leva, G., Garofalo, M. & Croce, C. M. 2014. MicroRNAs in cancer. *Annual Review of Pathology: Mechanisms of Disease,* 9**,** 287-314.

Di Zazzo, E., Galasso, G., Giovannelli, P., Di Donato, M., Di Santi, A., Cernera, G., Rossi, V., Abbondanza, C., Moncharmont, B. & Sinisi, A. A. 2016. Prostate cancer stem cells: the role of androgen and estrogen receptors. *Oncotarget,* 7**,** 193.

Discacciati, A., Orsini, N. & Wolk, A. 2012. Body mass index and incidence of localized and advanced prostate cancer—a dose–response meta-analysis of prospective studies. *Annals of oncology,* 23**,** 1665-1671.

Doles, J., Cook, C., Shi, X., Valosky, J., Lipinski, R. & Bushman, W. 2006. Functional compensation in Hedgehog signaling during mouse prostate development. *Developmental biology,* 295**,** 13-25.

Donahue, H. J., Qu, R. W. & Genetos, D. C. 2018. Joint diseases: from connexins to gap junctions. *Nature Reviews Rheumatology,* 14**,** 42-51.

Dong, B., Kim, S., Hong, S., Gupta, J. D., Malathi, K., Klein, E. A., Ganem, D., Derisi, J. L., Chow, S. A. & Silverman, R. H. 2007. An infectious retrovirus susceptible to an IFN antiviral pathway from human prostate tumors. *Proceedings of the National Academy of Sciences,* 104**,** 1655-1660.

Dong, J.-T. 2001. Chromosomal deletions and tumor suppressor genes in prostate cancer. *Cancer and Metastasis Reviews,* 20**,** 173-193.

Doo, D. W., Meza-Perez, S., Londoño, A. I., Goldsberry, W. N., Katre, A. A., Boone, J. D., Moore, D. J., Hudson, C. T., Betella, I. & Mccaw, T. R. 2020. Inhibition of the Wnt/β-catenin pathway enhances antitumor immunity in ovarian cancer. *Therapeutic advances in medical oncology,* 12**,** 1758835920913798.

Du, J. X., Hagos, E. G., Nandan, M. O., Bialkowska, A. B., Yu, B. & Yang, V. W. 2011. The E3 ubiquitin ligase SMAD ubiquitination regulatory factor 2 negatively regulates Krüppel-like factor 5 protein. *Journal of Biological Chemistry,* 286**,** 40354-40364.

Duchartre, Y., Kim, Y.-M. & Kahn, M. 2016. The Wnt signaling pathway in cancer. *Critical reviews in oncology/hematology,* 99**,** 141-149.

Dufau, M. L. 1998. The luteinizing hormone receptor. *Annual review of physiology,* 60**,** 461-496.

Ebert, M. P., Fei, G., Kahmann, S., Müller, O., Yu, J., Sung, J. J. & Malfertheiner, P. 2002. Increased β-catenin mRNA levels and mutational alterations of the APC and β-catenin gene are present in intestinal-type gastric cancer. *Carcinogenesis,* 23**,** 87-91.

Eeles, R. A., Kote-Jarai, Z., Giles, G. G., Al Olama, A. A., Guy, M., Jugurnauth, S. K., Mulholland, S., Leongamornlert, D. A., Edwards, S. M. & Morrison, J. 2008. Multiple newly identified loci associated with prostate cancer susceptibility. *Nature genetics,* 40**,** 316.

Eferl, R. & Wagner, E. F. 2003. AP-1: a double-edged sword in tumorigenesis. *Nature Reviews Cancer,* 3**,** 859-868.

Eiberger, J., Degen, J., Romualdi, A., Deutsch, U., Willecke, K. & Söhl, G. 2001. Connexin genes in the mouse and human genome. *Cell communication & adhesion,* 8**,** 163-165.

Elçioglu, N. & Hall, C. M. 1998. Temporal aspects in craniometaphyseal dysplasia: autosomal recessive type. *American journal of medical genetics,* 76**,** 245-251.

Eleftheriou, A., Yoshida, M. & Henderson, B. R. 2001. Nuclear export of human β-catenin can occur independent of CRM1 and the adenomatous polyposis coli tumor suppressor. *Journal of Biological Chemistry,* 276**,** 25883-25888.

Emmert-Buck, M. R., Vocke, C. D., Pozzatti, R. O., Duray, P. H., Jennings, S. B., Florence, C. D., Zhuang, Z., Bostwick, D. G., Liotta, L. A. & Linehan, W. M. 1995. Allelic loss on chromosome 8p12–21 in microdissected prostatic intraepithelial neoplasia. *Cancer research,* 55**,** 2959-2962.

Epstein, J. I., Allsbrook Jr, W. C., Amin, M. B., Egevad, L. L. & Committee, I. G. 2005. The 2005 International Society of Urological Pathology (ISUP) consensus conference on Gleason grading of prostatic carcinoma. *The American journal of surgical pathology,* 29**,** 1228-1242.

Epstein, J. I., Egevad, L., Amin, M. B., Delahunt, B., Srigley, J. R. & Humphrey, P. A. 2016a. The 2014 International Society of Urological Pathology (ISUP) consensus conference on Gleason grading of prostatic carcinoma. *The American journal of surgical pathology,* 40**,** 244-252.

Epstein, J. I., Zelefsky, M. J., Sjoberg, D. D., Nelson, J. B., Egevad, L., Magi-Galluzzi, C., Vickers, A. J., Parwani, A. V., Reuter, V. E. & Fine, S. W. 2016b. A contemporary prostate cancer grading system: a validated alternative to the Gleason score. *European urology,* 69**,** 428-435.

Evatt, E. J. 1909. A Contribution to the Development of the Prostate in Man. *Journal of anatomy and physiology,* 43**,** 314.

Ewing, L. L. & Eik-Nes, K. B. 1966. On the formation of testosterone by the perfused rabbit testis. *Canadian journal of biochemistry,* 44**,** 1327-1344.

Fagotto, F., Glück, U. & Gumbiner, B. M. 1998. Nuclear localization signal-independent and importin/karyopherin-independent nuclear import of β-catenin. *Current Biology,* 8**,** 181-190.

Fearon, E. R. 1997. Human cancer syndromes: clues to the origin and nature of cancer. *Science,* 278**,** 1043-1050.

Feldman, B. J. & Feldman, D. 2001. The development of androgen-independent prostate cancer. *Nature Reviews Cancer,* 1**,** 34-45.

Ferlay, J., Ervik, M., Lam, F., Colombet, M., Mery, L., Piñeros, M., Znaor, A., Soerjomataram, I. & Bray, F. 2018a. Global cancer observatory: cancer today. *Lyon, France: international agency for research on cancer***,** 1-6.

Ferlay, J., Ervik, M., Lam, F., Colombet, M., Mery, L., Piñeros, M., Znaor, A., Soerjomataram, I. & Bray, F. 2018b. Global cancer observatory: cancer today. *Lyon, France: International Agency for Research on Cancer*.

Ferlay, J., Ervik, M., Lam, F., Colombet, M., Mery, L., Piñeros, M., Znaor, A., Soerjomataram, I. & Bray, F. 2018c. Global cancer Observatory: cancer today. Lyon, France: international agency for research on cancer. *Cancer Today*.

Ferlay, J., Ervik, M., Lam, F., Colombet, M., Mery, L., Piñeros, M., Znaor, A., Soerjomataram, I. & Bray, F. 2019. Global Cancer Observatory: Cancer Tomorrow. Lyon, France: International Agency for Research on Cancer, 2018.

Ferraldeschi, R., Welti, J., Luo, J., Attard, G. & De Bono, J. 2015. Targeting the androgen receptor pathway in castration-resistant prostate cancer: progresses and prospects. *Oncogene,* 34**,** 1745-1757.

Fibbi, B., Penna, G., Morelli, A., Adorini, L. & Maggi, M. 2010. Chronic inflammation in the pathogenesis of benign prostatic hyperplasia. *International journal of andrology,* 33**,** 475-488.

Fischer, M. M., Cancilla, B., Yeung, V. P., Cattaruzza, F., Chartier, C., Murriel, C. L., Cain, J., Tam, R., Cheng, C.-Y. & Evans, J. W. 2017. WNT antagonists exhibit unique combinatorial antitumor activity with taxanes by potentiating mitotic cell death. *Science advances,* 3**,** e1700090.

Fleming, W. H., Hamel, A., Macdonald, R., Ramsey, E., Pettigrew, N. M., Johnston, B., Dodd, J. G. & Matusik, R. J. 1986. Expression of the c-myc protooncogene in human prostatic carcinoma and benign prostatic hyperplasia. *Cancer research,* 46**,** 1535-1538.

Fodde, R. 2002. The APC gene in colorectal cancer. *European journal of cancer,* 38**,** 867-871.

Foulkes, W. 1995. A tale of four syndromes: familial adenomatous polyposis, Gardner syndrome, attenuated APC and Turcot syndrome. *QJM: An International Journal of Medicine,* 88**,** 853-863.

Fowler, C. B., Man, Y.-G., Zhang, S., O'leary, T. J., Mason, J. T. & Cunningham, R. E. 2011. Tissue microarrays: construction and uses. *Formalin-Fixed Paraffin-Embedded Tissues.* Springer.

Fraenkel-Conrat, H. & Olcott, H. S. 1948. The reaction of formaldehyde with proteins. V. Cross-linking between amino and primary amide or guanidyl groups. *Journal of the American Chemical Society,* 70**,** 2673-2684.

Francis, J. C., Thomsen, M. K., Taketo, M. M. & Swain, A. 2013. β-catenin is required for prostate development and cooperates with Pten loss to drive invasive carcinoma. *PLoS Genet,* 9**,** e1003180.

Francis, R., Xu, X., Park, H., Wei, C.-J., Chang, S., Chatterjee, B. & Lo, C. 2011. Connexin43 modulates cell polarity and directional cell migration by regulating microtubule dynamics. *PloS one,* 6**,** e26379.

Franks, L. 1954. Benign Nodular Hyperplasia of the Prostate: Erasmus Wilson Demonstration delivered at the Royal College of Surgeons of England on 24th November 1953. *Annals of the Royal College of Surgeons of England,* 14**,** 92.

Freedland, S. J., Isaacs, W. B., Platz, E. A., Terris, M. K., Aronson, W. J., Amling, C. L., Presti Jr, J. C. & Kane, C. J. 2005. Prostate size and risk of high-grade, advanced prostate cancer and biochemical

progression after radical prostatectomy: a search database study. *Journal of clinical oncology,* 23**,** 7546-7554.

Fukushima, M., Hattori, Y., Yoshizawa, T. & Maitani, Y. 2007. Combination of non-viral connexin 43 gene therapy and docetaxel inhibits the growth of human prostate cancer in mice. *International journal of oncology,* 30**,** 225-231.

Gago-Fuentes, R., Fernández-Puente, P., Megias, D., Carpintero-Fernández, P., Mateos, J., Acea, B., Fonseca, E., Blanco, F. J. & Mayan, M. D. 2015. Proteomic analysis of connexin 43 reveals novel interactors related to osteoarthritis. *Molecular & Cellular Proteomics,* 14**,** 1831-1845.

Gai, Z., Wang, Y., Tian, L., Gong, G. & Zhao, J. 2021. Whole Genome Level Analysis of the Wnt and DIX Gene Families in Mice and Their Coordination Relationship in Regulating Cardiac Hypertrophy. *Frontiers in Genetics,* 12.

Gajos-Michniewicz, A. & Czyz, M. 2020. WNT signaling in melanoma. *International Journal of Molecular Sciences,* 21**,** 4852.

Galluzzi, L., Spranger, S., Fuchs, E. & López-Soto, A. 2019. WNT signaling in cancer immunosurveillance. *Trends in cell biology,* 29**,** 44-65.

Galvagni, F., Orlandini, M. & Oliviero, S. 2013. Role of the AP-1 transcription factor FOSL1 in endothelial cells adhesion and migration. *Cell adhesion & migration,* 7**,** 408-411.

Garcia, C. F. & Swerdlow, S. H. 2009. Best practices in contemporary diagnostic immunohistochemistry: panel approach to hematolymphoid proliferations. *Archives of pathology & laboratory medicine,* 133**,** 756-765.

Gassmann, M., Grenacher, B., Rohde, B. & Vogel, J. 2009. Quantifying Western blots: pitfalls of densitometry. *Electrophoresis,* 30**,** 1845-1855.

Gaudin, P. B., Sesterhenn, I. A., Wojno, K. J., Mostofi, F. & Epstein, J. I. 1997. Incidence and clinical significance of high-grade prostatic intraepithelial neoplasia in TURP specimens. *Urology,* 49**,** 558-563.

Georget, V., Lobaccaro, J., Terouanne, B., Mangeat, P., Nicolas, J.-C. & Sultan, C. 1997. Trafficking of the androgen receptor in living cells with fused green fluorescent protein–androgen receptor. *Molecular and cellular endocrinology,* 129**,** 17-26.

Gerstein, A. V., Almeida, T. A., Zhao, G., Chess, E., Shih, I. M., Buhler, K., Pienta, K., Rubin, M. A., Vessella, R. & Papadopoulos, N. 2002. APC/CTNNB1 (β-catenin) pathway alterations in human prostate cancers. *Genes, Chromosomes and Cancer,* 34**,** 9-16.

Giannakis, M., Hodis, E., Mu, X. J., Yamauchi, M., Rosenbluh, J., Cibulskis, K., Saksena, G., Lawrence, M. S., Qian, Z. R. & Nishihara, R. 2014. RNF43 is frequently mutated in colorectal and endometrial cancers. *Nature genetics,* 46**,** 1264-1266.

Gioeli, D., Ficarro, S. B., Kwiek, J. J., Aaronson, D., Hancock, M., Catling, A. D., White, F. M., Christian, R. E., Settlage, R. E. & Shabanowitz, J. 2002. Androgen receptor phosphorylation Regulation and identification of the phosphorylation sites. *Journal of Biological Chemistry,* 277**,** 29304-29314.

Giuliano, A., Swift, R., Arthurs, C., Marote, G., Abramo, F., Mckay, J., Thomson, C., Beltran, M., Millar, M. & Priestnall, S. 2016. Quantitative expression and co-localization of Wnt signalling related proteins in feline squamous cell carcinoma. *PLoS One,* 11**,** e0161103.

Gkika, D., Lolignier, S., Grolez, G. P., Bavencoffe, A., Shapovalov, G., Gordienko, D., Kondratskyi, A., Meleine, M., Prival, L. & Chapuy, E. 2020. Testosterone-androgen receptor: The steroid link inhibiting TRPM8-mediated cold sensitivity. *The FASEB Journal,* 34**,** 7483-7499.

Gleason, D. F. 1966. Classification of prostatic carcinomas. *Cancer Chemother. Rep.,* 50**,** 125-128.

Gleason, D. F. 1992. Histologic grading of prostate cancer: a perspective. *Human pathology,* 23**,** 273-279.

Gleave, M., Tolcher, A., Miyake, H., Nelson, C., Brown, B., Beraldi, E. & Goldie, J. 1999. Progression to androgen independence is delayed by adjuvant treatment with antisense Bcl-2 oligodeoxynucleotides after castration in the LNCaP prostate tumor model. *Clinical Cancer Research,* 5**,** 2891-2898.

Goodenough, D. A., Goliger, J. A. & Paul, D. L. 1996. Connexins, connexons, and intercellular communication. *Annual review of biochemistry,* 65**,** 475-502.

Goodman, R. M., Thombre, S., Firtina, Z., Gray, D., Betts, D., Roebuck, J., Spana, E. P. & Selva, E. M. 2006. Sprinter: a novel transmembrane protein required for Wg secretion and signaling. *Development,* 133**,** 4901-4911.

Gordon, M. D. & Nusse, R. 2006. Wnt signaling: multiple pathways, multiple receptors, and multiple transcription factors. *Journal of Biological Chemistry,* 281**,** 22429-22433.

Görlich, D. 1998. Transport into and out of the cell nucleus. *The EMBO journal,* 17**,** 2721-2727.

Grad, J. M., Le Dai, J., Wu, S. & Burnstein, K. L. 1999. Multiple androgen response elements and a Myc consensus site in the androgen receptor (AR) coding region are involved in androgen-mediated up-regulation of AR messenger RNA. *Molecular endocrinology,* 13**,** 1896-1911.

Grandy, D., Shan, J., Zhang, X., Rao, S., Akunuru, S., Li, H., Zhang, Y., Alpatov, I., Zhang, X. A. & Lang, R. A. 2009. Discovery and characterization of a small molecule inhibitor of the PDZ domain of dishevelled. *Journal of Biological Chemistry,* 284**,** 16256-16263.

Grant, W. B. & Peiris, A. N. 2012. Differences in vitamin D status may account for unexplained disparities in cancer survival rates between African and white Americans. *Dermato-endocrinology,* 4**,** 85-94.

Grasso, C. S., Wu, Y.-M., Robinson, D. R., Cao, X., Dhanasekaran, S. M., Khan, A. P., Quist, M. J., Jing, X., Lonigro, R. J. & Brenner, J. C. 2012. The mutational landscape of lethal castration-resistant prostate cancer. *Nature,* 487**,** 239-243.

Gregory, C. W., Hamil, K. G., Kim, D., Hall, S. H., Pretlow, T. G., Mohler, J. L. & French, F. S. 1998. Androgen receptor expression in androgen-independent prostate cancer is associated with increased expression of androgen-regulated genes. *Cancer research,* 58**,** 5718-5724.

Gregory, C. W., Johnson, R. T., Mohler, J. L., French, F. S. & Wilson, E. M. 2001. Androgen receptor stabilization in recurrent prostate cancer is associated with hypersensitivity to low androgen. *Cancer research,* 61**,** 2892-2898.

Groden, J., Thliveris, A., Samowitz, W., Carlson, M., Gelbert, L., Albertsen, H., Joslyn, G., Stevens, J., Spirio, L. & Robertson, M. 1991. Identification and characterization of the familial adenomatous polyposis coli gene. *Cell,* 66**,** 589-600.

Grolez, G. P., Gordiendko, D. V., Clarisse, M., Hammadi, M., Desruelles, E., Fromont, G., Prevarskaya, N., Slomianny, C. & Gkika, D. 2019. TRPM8-androgen receptor association within lipid rafts promotes prostate cancer cell migration. *Cell death & disease,* 10**,** 1-17.

Gruda, M. C., Kovary, K., Metz, R. & Bravo, R. 1994. Regulation of Fra-1 and Fra-2 phosphorylation differs during the cell cycle of fibroblasts and phosphorylation in vitro by MAP kinase affects DNA binding activity. *Oncogene,* 9**,** 2537-2547.

Guan, C.-N., Chen, X.-M., Lou, H.-Q., Liao, X.-H., Chen, B.-Y. & Zhang, P.-W. 2012. Clinical significance of axin and β-catenin protein expression in primary hepatocellular carcinomas. *Asian Pacific Journal of Cancer Prevention,* 13**,** 677-681.

Gubb, D. & García-Bellido, A. 1982. A genetic analysis of the determination of cuticular polarity during development in Drosophila melanogaster.

Gudjonsson, J. E., Johnston, A., Stoll, S. W., Riblett, M. B., Xing, X., Kochkodan, J. J., Ding, J., Nair, R. P., Aphale, A. & Voorhees, J. J. 2010. Evidence for altered Wnt signaling in psoriatic skin. *Journal of Investigative Dermatology,* 130**,** 1849-1859.

Guh, D. P., Zhang, W., Bansback, N., Amarsi, Z., Birmingham, C. L. & Anis, A. H. 2009. The incidence of co-morbidities related to obesity and overweight: a systematic review and meta-analysis. *BMC public health,* 9**,** 88.

Gupta, S. 2007. Prostate cancer chemoprevention: current status and future prospects. *Toxicology and applied pharmacology,* 224**,** 369-376.

Gurel, B., Iwata, T., Koh, C. M., Jenkins, R. B., Lan, F., Van Dang, C., Hicks, J. L., Morgan, J., Cornish, T. C. & Sutcliffe, S. 2008. Nuclear MYC protein overexpression is an early alteration in human prostate carcinogenesis. *Modern pathology,* 21**,** 1156-1167.

Guthrie, S. C. & Gilula, N. B. 1989. Gap junctional communication and development. *Trends in neurosciences,* 12**,** 12-16.

Haapala, K., Kuukasjärvi, T., Hyytinen, E., Rantala, I., Helin, H. J. & Koivisto, P. A. 2007. Androgen receptor amplification is associated with increased cell proliferation in prostate cancer. *Human pathology,* 38**,** 474-478.

Habas, R., Kato, Y. & He, X. 2001. Wnt/Frizzled activation of Rho regulates vertebrate gastrulation and requires a novel Formin homology protein Daam1. *Cell,* 107**,** 843-854.

Habermann, H., Ray, V., Habermann, W. & Prins, G. S. 2001. Alterations in gap junction protein expression in human benign prostatic hyperplasia and prostate cancer. *The Journal of urology,* 166**,** 2267-2272.

Haggman, M. J., Macoska, J. A., Wojno, K. J. & Oesterling, J. E. 1997. The relationship between prostatic intraepithelial neoplasia and prostate cancer: critical issues. *The Journal of urology,* 158**,** 12-22.

Hagman, Z., Larne, O., Edsjö, A., Bjartell, A., Ehrnström, R. A., Ulmert, D., Lilja, H. & Ceder, Y. 2010. miR-34c is downregulated in prostate cancer and exerts tumor suppressive functions. *International journal of cancer,* 127**,** 2768-2776.

Hall, P., Irby, D. & Kretser, D. D. 1969. Conversion of cholesterol to androgens by rat testes: comparison of interstitial cells and seminiferous tubules. *Endocrinology,* 84**,** 488-496.

Han, J., Zhang, Y., Xu, J., Zhang, T., Wang, H., Wang, Z., Jiang, Y., Zhou, L., Yang, M. & Hua, Y. 2021. Her4 promotes cancer metabolic reprogramming via the c-Myc-dependent signaling axis. *Cancer Letters,* 496**,** 57-71.

Hansson, V., Skålhegg, B. S. & Taskén, K. 1999. Cyclic-AMP-dependent protein kinase (PKA) in testicular cells. Cell specific expression, differential regulation and targeting of subunits of PKA. *The Journal of steroid biochemistry and molecular biology,* 69**,** 367-378.

Harb, J., Lin, P.-J. & Hao, J. 2019. Recent development of Wnt signaling pathway inhibitors for cancer therapeutics. *Current oncology reports,* 21**,** 1-9.

Harman, S. M., Metter, E. J., Tobin, J. D., Pearson, J., Blackman, M. R. & Baltimore Longitudinal Study Of, A. 2001. Longitudinal effects of aging on serum total and free testosterone levels in healthy men. Baltimore Longitudinal Study of Aging. *J Clin Endocrinol Metab,* 86**,** 724-31.

Hart, M., Concordet, J., Lassot, I., Albert, I., Del Los Santos, R., Durand, H., Perret, C., Rubinfeld, B., Margottin, F. & Benarous, R. 1999. The F-box protein β-TrCP associates with phosphorylated β-catenin and regulates its activity in the cell. *Current biology,* 9**,** 207-211.

Hauet, T., Yao, Z.-X., Bose, H. S., Wall, C. T., Han, Z., Li, W., Hales, D. B., Miller, W. L., Culty, M. & Papadopoulos, V. 2005. Peripheral-type benzodiazepine receptor-mediated action of

steroidogenic acute regulatory protein on cholesterol entry into leydig cell mitochondria. *Molecular Endocrinology,* 19**,** 540-554.

Hawksworth, D., Ravindranath, L., Chen, Y., Furusato, B., Sesterhenn, I., Mcleod, D., Srivastava, S. & Petrovics, G. 2010. Overexpression of C-MYC oncogene in prostate cancer predicts biochemical recurrence. *Prostate cancer and prostatic diseases,* 13**,** 311-315.

Hay, C. W., Watt, K., Hunter, I., Lavery, D. N., Mackenzie, A. & Mcewan, I. J. 2014. Negative regulation of the androgen receptor gene through a primate-specific androgen response element present in the 5′ UTR. *Hormones and Cancer,* 5**,** 299-311.

Hayashida, Y., Honda, K., Idogawa, M., Ino, Y., Ono, M., Tsuchida, A., Aoki, T., Hirohashi, S. & Yamada, T. 2005. E-cadherin regulates the association between β-catenin and actinin-4. *Cancer research,* 65**,** 8836-8845.

Hayward, S., Baskin, L., Haughney, P., Cunha, A., Foster, B., Dahiya, R., Prins, G. & Cunha, G. 1996. Epithelial development in the rat ventral prostate, anterior prostate and seminal vesicle. *Cells Tissues Organs,* 155**,** 81-93.

Hayward, S. W., Haughney, P. C., Rosen, M. A., Greulich, K. M., Weier, H. U. G., Dahiya, R. & Cunha, G. R. 1998. Interactions between adult human prostatic epithelium and rat urogenital sinus mesenchyme in a tissue recombination model. *Differentiation,* 63**,** 131-140.

He, S. & Tang, S. 2020. WNT/β-catenin signaling in the development of liver cancers. *Biomedicine & Pharmacotherapy,* 132**,** 110851.

He, T.-C., Sparks, A. B., Rago, C., Hermeking, H., Zawel, L., Da Costa, L. T., Morin, P. J., Vogelstein, B. & Kinzler, K. W. 1998. Identification of c-MYC as a target of the APC pathway. *Science,* 281**,** 1509-1512.

He, W. W., Sciavolino, P. J., Wing, J., Augustus, M., Hudson, P., Meissner, P. S., Curtis, R. T., Shell, B. K., Bostwick, D. G. & Tindall, D. J. 1997. A novel human prostate-specific, androgen-regulated homeobox gene (NKX3. 1) that maps to 8p21, a region frequently deleted in prostate cancer. *Genomics,* 43**,** 69-77.

He, X., Semenov, M., Tamai, K. & Zeng, X. 2004. LDL receptor-related proteins 5 and 6 in Wnt/β-catenin signaling: arrows point the way. *Development,* 131**,** 1663-1677.

Hearn, J. W., Abuali, G., Reichard, C. A., Reddy, C. A., Magi-Galluzzi, C., Chang, K.-H., Carlson, R., Rangel, L., Reagan, K. & Davis, B. J. 2016. HSD3B1 and resistance to androgen-deprivation therapy in prostate cancer: a retrospective, multicohort study. *The Lancet Oncology,* 17**,** 1435-1444.

Heinlein, C. A. & Chang, C. 2002. Androgen receptor (AR) coregulators: an overview. *Endocrine reviews,* 23**,** 175-200.

Heinlein, C. A. & Chang, C. 2004. Androgen receptor in prostate cancer. *Endocrine reviews,* 25**,** 276-308.

Helgeson, B. E., Tomlins, S. A., Shah, N., Laxman, B., Cao, Q., Prensner, J. R., Cao, X., Singla, N., Montie, J. E. & Varambally, S. 2008. Characterization of TMPRSS2: ETV5 and SLC45A3: ETV5 gene fusions in prostate cancer. *Cancer research,* 68**,** 73-80.

Hemminki, K. & Chen, B. 2005. Familial association of prostate cancer with other cancers in the Swedish Family-Cancer Database. *The Prostate,* 65**,** 188-194.

Hemminki, K. & Czene, K. 2002. Age specific and attributable risks of familial prostate carcinoma from the family-cancer database. *Cancer,* 95**,** 1346-1353.

Henderson, B. R. 2000. Nuclear-cytoplasmic shuttling of APC regulates β-catenin subcellular localization and turnover. *Nature cell biology,* 2**,** 653-660.

Henshall, S. M., Quinn, D. I., Lee, C. S., Head, D. R., Golovsky, D., Brenner, P. C., Delprado, W., Stricker, P. D., Grygiel, J. J. & Sutherland, R. L. 2001. Altered expression of androgen receptor in the malignant epithelium and adjacent stroma is associated with early relapse in prostate cancer. *Cancer research,* 61**,** 423-427.

Henzler, C., Li, Y., Yang, R., Mcbride, T., Ho, Y., Sprenger, C., Liu, G., Coleman, I., Lakely, B. & Li, R. 2016. Truncation and constitutive activation of the androgen receptor by diverse genomic rearrangements in prostate cancer. *Nature communications,* 7**,** 1-12.

Hernandez, D. J., Nielsen, M. E., Han, M., Trock, B. J., Partin, A. W., Walsh, P. C. & Epstein, J. I. 2008. Natural history of pathologically organ-confined (pT2), Gleason score 6 or less, prostate cancer after radical prostatectomy. *Urology,* 72**,** 172-176.

Herr, P., Hausmann, G. & Basler, K. 2012. WNT secretion and signalling in human disease. *Trends in molecular medicine,* 18**,** 483-493.

Hetzl, A., Favaro, W., Billis, A., Ferreira, U. & Cagnon, V. 2012. Steroid hormone receptors, matrix metalloproteinases, insulin-like growth factor, and dystroglycans interactions in prostatic diseases in the elderly men. *Microscopy research and technique,* 75**,** 1197-1205.

Hiatt, R. A., Armstrong, M. A., Klatsky, A. L. & Sidney, S. 1994. Alcohol consumption, smoking, and other risk factors and prostate cancer in a large health plan cohort in California (United States). *Cancer Causes & Control,* 5**,** 66-72.

Hirohashi, S. & Kanai, Y. 2003. Cell adhesion system and human cancer morphogenesis. *Cancer science,* 94**,** 575-581.

Hoffmans, R., Städeli, R. & Basler, K. 2005. Pygopus and legless provide essential transcriptional coactivator functions to armadillo/β-catenin. *Current Biology,* 15**,** 1207-1211.

Holzbeierlein, J., Lal, P., Latulippe, E., Smith, A., Satagopan, J., Zhang, L., Ryan, C., Smith, S., Scher, H. & Scardino, P. 2004. Gene expression analysis of human prostate carcinoma during hormonal therapy identifies androgen-responsive genes and mechanisms of therapy resistance. *The American journal of pathology,* 164**,** 217-227.

Homma, Y., Gotoh, M., Yokoyama, O., Masumori, N., Kawauchi, A., Yamanishi, T., Ishizuka, O., Seki, N., Kamoto, T. & Nagai, A. 2011. Outline of JUA clinical guidelines for benign prostatic hyperplasia. *International Journal of Urology,* 18**,** 741-756.

Hoosein, N. M., Boyd, D. D., Hollas, W. J., Mazar, A., Henkin, J. & Chung, L. W. 1991. Involvement of urokinase and its receptor in the invasiveness of human prostatic carcinoma cell lines. *Cancer communications,* 3**,** 255-264.

Hörnberg, E., Ylitalo, E. B., Crnalic, S., Antti, H., Stattin, P., Widmark, A., Bergh, A. & Wikström, P. 2011. Expression of androgen receptor splice variants in prostate cancer bone metastases is associated with castration-resistance and short survival. *PloS one,* 6.

Horoszewicz, J. 1980. The LNCaP cell line-a new model for studies on human prostatic carcinoma. *Prog Clin Biol Res,* 37**,** 115-132.

Horoszewicz, J. S., Leong, S. S., Kawinski, E., Karr, J. P., Rosenthal, H., Chu, T. M., Mirand, E. A. & Murphy, G. P. 1983. LNCaP model of human prostatic carcinoma. *Cancer research,* 43**,** 1809-1818.

Horvath, L. G., Henshall, S. M., Lee, C.-S., Head, D. R., Quinn, D. I., Makela, S., Delprado, W., Golovsky, D., Brenner, P. C. & O'neill, G. 2001. Frequent loss of estrogen receptor-β expression in prostate cancer. *Cancer research,* 61**,** 5331-5335.

Hosain, G. M., Sanderson, M., Du, X. L., Chan, W. & Strom, S. S. 2011. Racial/ethnic differences in predictors of PSA screening in a tri-ethnic population. *Central European journal of public health,* 19**,** 30.

Hou, X., Khan, M. R., Turmaine, M., Thrasivoulou, C., Becker, D. L. & Ahmed, A. 2019. Wnt signaling regulates cytosolic translocation of connexin 43. *American Journal of Physiology-Regulatory, Integrative and Comparative Physiology,* 317**,** R248-R261.

Howlader, N., Noone, A., Krapcho, M., Garshell, J., Neyman, N., Altekruse, S., Kosary, C., Yu, M., Ruhl, J. & Tatalovich, Z. 2013. SEER cancer statistics review, 1975–2010. *Bethesda, MD: National Cancer Institute,* 21**,** 12.

Howlader, N., Noone, A., Krapcho, M., Miller, D., Bishop, K., Altekruse, S., Kosary, C., Yu, M., Ruhl, J. & Tatalovich, Z. 2016a. SEER Cancer Statistics Review, 1975-2013, National Cancer Institute. Bethesda, MD.

Howlader, N., Noone, A., Krapcho, M., Miller, D., Bishop, K., Altekruse, S., Kosary, C., Yu, M., Ruhl, J. & Tatalovich, Z. 2016b. SEER cancer statistics review, 1975–2013. *Bethesda, MD: National Cancer Institute,* 19.

Hruz, T., Wyss, M., Docquier, M., Pfaffl, M. W., Masanetz, S., Borghi, L., Verbrugghe, P., Kalaydjieva, L., Bleuler, S. & Laule, O. 2011. RefGenes: identification of reliable and condition specific reference genes for RT-qPCR data normalization. *BMC genomics,* 12**,** 1-14.

Hsu, S.-M. & Soban, E. 1982. Color modification of diaminobenzidine (DAB) precipitation by metallic ions and its application for double immunohistochemistry. *Journal of Histochemistry & Cytochemistry,* 30**,** 1079-1082.

Hu, B. R., Fairey, A. S., Madhav, A., Yang, D., Li, M., Groshen, S., Stephens, C., Kim, P. H., Virk, N. & Wang, L. 2016. AXIN2 expression predicts prostate cancer recurrence and regulates invasion and tumor growth. *The Prostate,* 76**,** 597-608.

Hu, R., Isaacs, W. B. & Luo, J. 2011. A snapshot of the expression signature of androgen receptor splicing variants and their distinctive transcriptional activities. *The Prostate,* 71**,** 1656-1667.

Hu, R., Lu, C., Mostaghel, E. A., Yegnasubramanian, S., Gurel, M., Tannahill, C., Edwards, J., Isaacs, W. B., Nelson, P. S. & Bluemn, E. 2012. Distinct transcriptional programs mediated by the ligand-dependent full-length androgen receptor and its splice variants in castration-resistant prostate cancer. *Cancer research,* 72**,** 3457-3462.

Hu, X. & Lazar, M. A. 2000. Transcriptional repression by nuclear hormone receptors. *Trends in Endocrinology & Metabolism,* 11**,** 6-10.

Hu, Y., Chen, I.-P., De Almeida, S., Tiziani, V., Do Amaral, C. M. R., Gowrishankar, K., Passos-Bueno, M. R. & Reichenberger, E. J. 2013. A novel autosomal recessive GJA1 missense mutation linked to Craniometaphyseal dysplasia. *PloS one,* 8**,** e73576.

Hu, Y., Zhang, X., Gong, C. & Li, J. 2020. Aberrant expression of miR-4728 in patients with non-small cell lung cancer and its regulatory effects on tumor progression in tumor cells. *Experimental and Therapeutic Medicine,* 20**,** 1-1.

Huang, S.-P., Ting, W.-C., Chen, L.-M., Huang, L.-C., Liu, C.-C., Chen, C.-W., Hsieh, C.-J., Yang, W.-H., Chang, T.-Y. & Lee, H.-Z. 2010. Association analysis of Wnt pathway genes on prostate-specific antigen recurrence after radical prostatectomy. *Annals of surgical oncology,* 17**,** 312-322.

Huber, O., Korn, R., Mclaughlin, J., Ohsugi, M., Herrmann, B. G. & Kemler, R. 1996. Nuclear localization of β-catenin by interaction with transcription factor LEF-1. *Mechanisms of development,* 59**,** 3-10.

Huggins, C. 1967. Endocrine-induced regression of cancers. *Science,* 156**,** 1050-1054.

Huggins, C. & Clark, P. J. 1940. Quantitative studies of prostatic secretion: II. The effect of castration and of estrogen injection on the normal and on the hyperplastic prostate glands of dogs. *The Journal of experimental medicine,* 72**,** 747-762.

Huggins, C. & Hodges, C. V. 1972. Studies on prostatic cancer: I. The effect of castration, of estrogen and of androgen injection on serum phosphatases in metastatic carcinoma of the prostate. *CA: a cancer journal for clinicians,* 22**,** 232-240.

Huggins, C., Scott, W. W. & Hodges, C. V. 1941. Studies on prostatic cancer. III. The effects of fever, of desoxycorticosterone and of estrogen on clinical patients with metastatic carcinoma of the prostate. *The Journal of Urology,* 46**,** 997-1006.

Husain, I., Shukla, S., Soni, P. & Husain, N. 2016. Role of androgen receptor in prostatic neoplasia versus hyperplasia. *Journal of cancer research and therapeutics,* 12**,** 112.

Isaacs, J. T. 1997. Molecular markers for prostate cancer metastasis. Developing diagnostic methods for predicting the aggressiveness of prostate cancer. *The American journal of pathology,* 150**,** 1511.

Isaacs, W. B., Carter, B. S. & Ewing, C. M. 1991. Wild-type p53 suppresses growth of human prostate cancer cells containing mutant p53 alleles. *Cancer research,* 51**,** 4716-4720.

Ishitani, T., Kishida, S., Hyodo-Miura, J., Ueno, N., Yasuda, J., Waterman, M., Shibuya, H., Moon, R. T., Ninomiya-Tsuji, J. & Matsumoto, K. 2003. The TAK1-NLK mitogen-activated protein kinase cascade functions in the Wnt-5a/Ca2+ pathway to antagonize Wnt/β-catenin signaling. *Molecular and cellular biology,* 23**,** 131-139.

Ito, E., Sweterlitsch, L., Tran, P., Rauscher 3rd, F. & Narayanan, R. 1990. Inhibition of PC-12 cell differentiation by the immediate early gene fra-1. *Oncogene,* 5**,** 1755-1760.

Ito, M., Yang, Z., Andl, T., Cui, C., Kim, N., Millar, S. E. & Cotsarelis, G. 2007. Wnt-dependent de novo hair follicle regeneration in adult mouse skin after wounding. *Nature,* 447**,** 316-320.

Izumi, K., Mizokami, A., Lin, W.-J., Lai, K.-P. & Chang, C. 2013. Androgen receptor roles in the development of benign prostate hyperplasia. *The American journal of pathology,* 182**,** 1942-1949.

Jagla, M., FèVe, M., Kessler, P., Lapouge, G., Erdmann, E., Serra, S., Bergerat, J.-P. & Céraline, J. 2007. A splicing variant of the androgen receptor detected in a metastatic prostate cancer exhibits exclusively cytoplasmic actions. *Endocrinology,* 148**,** 4334-4343.

Janda, C. Y., Waghray, D., Levin, A. M., Thomas, C. & Garcia, K. C. 2012. Structural basis of Wnt recognition by Frizzled. *Science,* 337**,** 59-64.

Ji, Y., Shah, S., Soanes, K., Islam, M., Hoxter, B., Biffo, S., Heslip, T. & Byers, S. 2008. Eukaryotic initiation factor 6 selectively regulates Wnt signaling and β-catenin protein synthesis. *Oncogene,* 27**,** 755-762.

Jiang, X., Xie, H., Dou, Y., Yuan, J., Zeng, D. & Xiao, S. 2020. Expression and function of FRA1 protein in tumors. *Molecular biology reports,* 47**,** 737-752.

Jin, H.-J., Kim, J. & Yu, J. 2013. Androgen receptor genomic regulation. *Translational andrology and urology,* 2**,** 158.

Johal, N., Cao, K., Arthurs, C., Millar, M., Thrasivoulou, C., Ahmed, A., Jabr, R. I., Wood, D., Cuckow, P. & Fry, C. H. 2021. Contractile function of detrusor smooth muscle from children with posterior urethral valves–The role of fibrosis. *Journal of Pediatric Urology,* 17**,** 100. e1-100. e10.

Johns, L. & Houlston, R. 2003. A systematic review and meta-analysis of familial prostate cancer risk. *BJU international,* 91**,** 789-794.

Jung, Y.-S. & Park, J.-I. 2020. Wnt signaling in cancer: therapeutic targeting of Wnt signaling beyond β-catenin and the destruction complex. *Experimental & Molecular Medicine,* 52**,** 183-191.

Kaaks, R. & Stattin, P. 2010. Obesity, endogenous hormone metabolism, and prostate cancer risk: a conundrum of “highs” and “lows”. *Cancer Prevention Research,* 3**,** 259-262.

Kahn, M. 2014. Can we safely target the WNT pathway? *Nature reviews Drug discovery,* 13**,** 513-532.

Kalantari, N., Bayani, M. & Ghaffari, T. 2016. Deparaffinization of formalin-fixed paraffin-embedded tissue blocks using hot water instead of xylene. *Analytical biochemistry,* 507**,** 71-73.

Kallio, H. M., Hieta, R., Latonen, L., Brofeldt, A., Annala, M., Kivinummi, K., Tammela, T. L., Nykter, M., Isaacs, W. B. & Lilja, H. G. 2018. Constitutively active androgen receptor splice variants AR-V3, AR-V7 and AR-V9 are co-expressed in castration-resistant prostate cancer metastases. *British journal of cancer,* 119**,** 347-356.

Kalluri, R. & Weinberg, R. A. 2009. The basics of epithelial-mesenchymal transition. *The Journal of clinical investigation,* 119**,** 1420-1428.

Karaca, M., Liu, Y., Zhang, Z., De Silva, D., Parker, J. S., Earp, H. S. & Whang, Y. E. 2015. Mutation of androgen receptor N-terminal phosphorylation site Tyr-267 leads to inhibition of nuclear translocation and DNA binding. *PloS one,* 10**,** e0126270.

Keer, H. N., Gaylis, F. D., Kozlowski, J. M., Kwaan, H. C., Bauer, K. D., Sinha, A. A. & Wilson, M. J. 1991. Heterogeneity in plasminogen activator (PA) levels in human prostate cancer cell lines: increased PA activity correlates with biologically aggressive behavior. *The Prostate,* 18**,** 201-214.

Kennell, J. & Cadigan, K. M. 2009. APC and β-catenin degradation. *APC Proteins***,** 1-12.

Keogh, J. W. & Macleod, R. D. 2012. Body composition, physical fitness, functional performance, quality of life, and fatigue benefits of exercise for prostate cancer patients: a systematic review. *Journal of pain and symptom management,* 43**,** 96-110.

Kerr, J. E., Allore, R. J., Beck, S. G. & Handa, R. J. 1995. Distribution and hormonal regulation of androgen receptor (AR) and AR messenger ribonucleic acid in the rat hippocampus. *Endocrinology,* 136**,** 3213-3221.

Khramtsov, A. I., Khramtsova, G. F., Tretiakova, M., Huo, D., Olopade, O. I. & Goss, K. H. 2010. Wnt/β-catenin pathway activation is enriched in basal-like breast cancers and predicts poor outcome. *The American journal of pathology,* 176**,** 2911-2920.

Kiciński, M., Vangronsveld, J. & Nawrot, T. S. 2011. An epidemiological reappraisal of the familial aggregation of prostate cancer: a meta-analysis. *PloS one,* 6.

Kim, D., Curthoys, N. M., Parent, M. T. & Hess, S. T. 2013. Bleed-through correction for rendering and correlation analysis in multi-colour localization microscopy. *Journal of optics,* 15**,** 094011.

Kim, D., Gregory, C. W., French, F. S., Smith, G. J. & Mohler, J. L. 2002. Androgen receptor expression and cellular proliferation during transition from androgen-dependent to recurrent growth after castration in the CWR22 prostate cancer xenograft. *The American journal of pathology,* 160**,** 219-226.

Kim, J. H., Park, S.-M., Kang, M. R., Oh, S.-Y., Lee, T. H., Muller, M. T. & Chung, I. K. 2005. Ubiquitin ligase MKRN1 modulates telomere length homeostasis through a proteolysis of hTERT. *Genes & development,* 19**,** 776-781.

Kim, S. H., Shin, Y. K., Lee, K. M., Lee, J. S., Yun, J. H. & Lee, S. M. 2003. An improved protocol of biotinylated tyramine-based immunohistochemistry minimizing nonspecific background staining. *Journal of Histochemistry & Cytochemistry,* 51**,** 129-132.

Kinzler, K. W. & Vogelstein, B. 1996. Lessons from hereditary colorectal cancer. *Cell,* 87**,** 159-170.

Kirby, R., Christmas, T. & Brawer, M. 1999. Prostate Cancer, 2nd International Consultation on Prostate Cancer. *Paris, Mosby***,** 263-326.

Kirikoshi, H., Sekihara, H. & Katoh, M. 2001. Molecular cloning and characterization of WNT14B, a novel member of the WNT gene family. *International journal of oncology,* 19**,** 947-952.

Klarmann, G. J., Decker, A. & Farrar, W. L. 2008. Epigenetic gene silencing in the Wnt pathway in breast cancer. *Epigenetics,* 3**,** 59-63.

Klaus, A. & Birchmeier, W. 2008. Wnt signalling and its impact on development and cancer. *Nature Reviews Cancer,* 8**,** 387-398.

Knoepfler, P. S. 2007. Myc goes global: new tricks for an old oncogene. *Cancer research,* 67**,** 5061-5063.

Koeneman, K. S., Pan, C.-X., Jin, J.-K., Pyle, J. M., Flanigan, R. C., Shankey, T. V. & Diaz, M. O. 1998. Telomerase activity, telomere length, and DNA ploidy in prostatic intraepithelial neoplasia (PIN). *The Journal of urology,* 160**,** 1533-1539.

Köhler, G. & Milstein, C. 1975. Continuous cultures of fused cells secreting antibody of predefined specificity. *nature,* 256**,** 495-497.

Kohn, A. D. & Moon, R. T. 2005. Wnt and calcium signaling: β-catenin-independent pathways. *Cell calcium,* 38**,** 439-446.

Koivisto, P., Kononen, J., Palmberg, C., Tammela, T., Hyytinen, E., Isola, J., Trapman, J., Cleutjens, K., Noordzij, A. & Visakorpi, T. 1997. Androgen receptor gene amplification: a possible molecular mechanism for androgen deprivation therapy failure in prostate cancer. *Cancer research,* 57**,** 314-319.

Kolonel, L. N., Altshuler, D. & Henderson, B. E. 2004. The multiethnic cohort study: exploring genes, lifestyle and cancer risk. *Nature Reviews Cancer,* 4**,** 519-527.

Komiya, Y. & Habas, R. 2008. Wnt signal transduction pathways. *Organogenesis,* 4**,** 68-75.

Kong, J., Bell, N. A. & Keyser, U. F. 2016. Quantifying nanomolar protein concentrations using designed DNA carriers and solid-state nanopores. *Nano letters,* 16**,** 3557-3562.

Kononen, J., Bubendorf, L., Kallionimeni, A., Bärlund, M., Schraml, P., Leighton, S., Torhorst, J., Mihatsch, M. J., Sauter, G. & Kallionimeni, O.-P. 1998. Tissue microarrays for high-throughput molecular profiling of tumor specimens. *Nature medicine,* 4**,** 844-847.

Koochekpour, S. 2010. Androgen receptor signaling and mutations in prostate cancer. *Asian journal of andrology,* 12**,** 639.

Koochekpour, S., Maresh, G. A., Katner, A., Parker-Johnson, K., Lee, T. J., Hebert, F. E., Kao, Y. S., Skinner, J. & Rayford, W. 2004. Establishment and characterization of a primary androgen-responsive African-American prostate cancer cell line, E006AA. *The Prostate,* 60**,** 141-152.

Korček, M., Sekerešová, M., Makarevich, A. V., Gavurová, H., Olexíková, L., Pivko, J. & Barreto, L. 2020. Morphological and functional alterations of the prostate tissue during clinical progression in hormonally-naïve, hormonally-treated and castration-resistant patients with metastatic prostate cancer. *Oncology Letters,* 20**,** 1-1.

Korver, W., Guevara, C., Chen, Y., Neuteboom, S., Bookstein, R., Tavtigian, S. & Lees, E. 2003. The product of the candidate prostate cancer susceptibility gene ELAC2 interacts with the γ-tubulin complex. *International journal of cancer,* 104**,** 283-288.

Kotini, M. & Mayor, R. 2015. Connexins in migration during development and cancer. *Developmental biology,* 401**,** 143-151.

Kozlowski, J. M., Fidler, I. J., Campbell, D., Xu, Z.-L., Kaighn, M. E. & Hart, I. R. 1984. Metastatic behavior of human tumor cell lines grown in the nude mouse. *Cancer research,* 44**,** 3522-3529.

Kral, M., Rosinska, V., Student, V., Grepl, M., Hrabec, M. & Bouchal, J. 2011. Genetic determinants of prostate cancer: a review. *Biomedical Papers of the Medical Faculty of Palacky University in Olomouc,* 155.

Kramer, G., Mitteregger, D. & Marberger, M. 2007. Is benign prostatic hyperplasia (BPH) an immune inflammatory disease? *European urology,* 51**,** 1202-1216.

Kramps, T., Peter, O., Brunner, E., Nellen, D., Froesch, B., Chatterjee, S., Murone, M., Züllig, S. & Basler, K. 2002. Wnt/wingless signaling requires BCL9/legless-mediated recruitment of pygopus to the nuclear β-catenin-TCF complex. *Cell,* 109**,** 47-60.

Krieger, J., Ross, S. & Riley, D. 2002. Chronic prostatitis: epidemiology and role of infection. *Urology,* 60**,** 8-12.

Krieger, J. N., Nyberg Jr, L. & Nickel, J. C. 1999. NIH consensus definition and classification of prostatitis. *Jama,* 282**,** 236-237.

Krishnamurthy, N. & Kurzrock, R. 2018. Targeting the Wnt/beta-catenin pathway in cancer: Update on effectors and inhibitors. *Cancer treatment reviews,* 62**,** 50-60.

Krongrad, A., Wilson, C. M., Wilson, J. D., Allman, D. R. & Mcphaul, M. J. 1991. Androgen increases androgen receptor protein while decreasing receptor mRNA in LNCaP cells. *Molecular and cellular endocrinology,* 76**,** 79-88.

Krušlin, B., Ulamec, M. & Tomas, D. 2015. Prostate cancer stroma: an important factor in cancer growth and progression. *Bosnian journal of basic medical sciences,* 15**,** 1.

Kühl, M., Geis, K., Sheldahl, L. C., Pukrop, T., Moon, R. T. & Wedlich, D. 2001. Antagonistic regulation of convergent extension movements in Xenopus by Wnt/β-catenin and Wnt/Ca2+ signaling. *Mechanisms of development,* 106**,** 61-76.

Kuiper, G., Faber, P., Van Rooij, H., Van Der Korput, J., Ris-Stalpers, C., Klaassen, P., Trapman, J. & Brinkmann, A. 1989. Structural organization of the human androgen receptor gene. *Journal of molecular endocrinology,* 2**,** R1-R4.

Kumar, N. M. & Gilula, N. B. 1996. The gap junction communication channel. *Cell,* 84**,** 381-388.

Kurien, B. T. & Scofield, R. H. 2006. Western blotting. *Methods,* 38**,** 283-293.

Kurien, B. T. & Scofield, R. H. 2015. Western blotting: an introduction. *Western Blotting***,** 17-30.

Kweldam, C., Van Leenders, G. & Van Der Kwast, T. 2019. Grading of prostate cancer: a work in progress. *Histopathology,* 74**,** 146-160.

Kyle, C., Ewing, T., Wu, X., Mercante, D., Lifsey, D., Meunier, C., Jefferson, L., Sartor, O. & Rayford, W. 2004. Statewide analysis of serum prostate specific antigen levels in Louisiana men without prostate cancer. *The Journal of the Louisiana State Medical Society: official organ of the Louisiana State Medical Society,* 156**,** 319-323.

Kyprianou, N. & Davies, P. 1986. Association states of androgen receptors in nuclei of human benign hypertrophic prostate. *The Prostate,* 8**,** 363-380.

Kyprianou, N. & Isaacs, J. T. 1988. Activation of programmed cell death in the rat ventral prostate after castration. *Endocrinology,* 122**,** 552-562.

Kyprianou, N. & Isaacs, J. T. 1989. "Thymineless" death in androgen-independent prostatic cancer cells. *Biochemical and biophysical research communications,* 165**,** 73-81.

Kypta, R. M. & Waxman, J. 2012. Wnt/β-catenin signalling in prostate cancer. *Nature Reviews Urology,* 9**,** 418.

Laemmli, U. K. 1970. Cleavage of structural proteins during the assembly of the head of bacteriophage T4. *nature,* 227**,** 680-685.

Lawson, D. A., Zong, Y., Memarzadeh, S., Xin, L., Huang, J. & Witte, O. N. 2010. Basal epithelial stem cells are efficient targets for prostate cancer initiation. *Proceedings of the National Academy of Sciences,* 107**,** 2610-2615.

Lawson, J. S., Tran, D. & Rawlinson, W. D. 2001. From Bittner to Barr: a viral, diet and hormone breast cancer aetiology hypothesis. *Breast Cancer Research,* 3**,** 1-5.

Le, P. N., Mcdermott, J. D. & Jimeno, A. 2015. Targeting the Wnt pathway in human cancers: therapeutic targeting with a focus on OMP-54F28. *Pharmacology & therapeutics,* 146**,** 1-11.

Lee, D. K. & Chang, C. 2003. Molecular communication between androgen receptor and general transcription machinery. *The Journal of steroid biochemistry and molecular biology,* 84**,** 41-49.

Lee, E., Ha, S. & Logan, S. K. 2015. Divergent androgen receptor and beta-catenin signaling in prostate cancer cells. *PloS one,* 10**,** e0141589.

Legendre, N. 1990. Immobilon-P transfer membrane: applications and utility in protein biochemical analysis. *BioTechniques,* 9**,** 788-805.

Lehmann, B. D., Bauer, J. A., Chen, X., Sanders, M. E., Chakravarthy, A. B., Shyr, Y. & Pietenpol, J. A. 2011. Identification of human triple-negative breast cancer subtypes and preclinical models for selection of targeted therapies. *The Journal of clinical investigation,* 121**,** 2750-2767.

Leibold, J., Ruscetti, M., Cao, Z., Ho, Y.-J., Baslan, T., Zou, M., Abida, W., Feucht, J., Han, T. & Barriga, F. M. 2020. Somatic tissue engineering in mouse models reveals an actionable role for WNT pathway alterations in prostate cancer metastasis. *Cancer discovery,* 10**,** 1038-1057.

Leissner, K. H. & Tisell, L. E. 1979. The weight of the human prostate. *Scand J Urol Nephrol,* 13**,** 137-42.

Leite, K. R., Sousa-Canavez, J. M., Reis, S. T., Tomiyama, A. H., Camara-Lopes, L. H., Sañudo, A., Antunes, A. A. & Srougi, M. Change in expression of miR-let7c, miR-100, and miR-218 from high grade localized prostate cancer to metastasis. Urologic Oncology: Seminars and Original Investigations, 2011. Elsevier, 265-269.

Lejeune, S., Huguet, E. L., Hamby, A., Poulsom, R. & Harris, A. L. 1995. Wnt5a cloning, expression, and up-regulation in human primary breast cancers. *Clinical Cancer Research,* 1**,** 215-222.

Lekshmy, K. & Prema, N. 2019. Study of Various Prognostic Factors in Prostate Cancer and its Correlation with Androgen Receptor Expression. *Journal of Evolution of Medical and Dental Sciences,* 8**,** 2687-2694.

Lento, W., Congdon, K., Voermans, C., Kritzik, M. & Reya, T. 2013. Wnt signaling in normal and malignant hematopoiesis. *Cold Spring Harbor perspectives in biology,* 5**,** a008011.

Leong, A. Y. & Wright, J. 1987. The contribution of immunohistochemical staining in tumour diagnosis. *Histopathology,* 11**,** 1295-1305.

Leydig, F. 1850. Zur Anatomie der männlichen Geschlechtsorgane und Analdrüsen der Säugethiere. *Z Wiss Zool,* 2**,** 1-57.

Li, B., Rhéaume, C., Teng, A., Bilanchone, V., Munguia, J. E., Hu, M., Jessen, S., Piccolo, S., Waterman, M. L. & Dai, X. 2007. Developmental phenotypes and reduced Wnt signaling in mice deficient for pygopus 2. *genesis,* 45**,** 318-325.

Li, H., Wang, Z., Xiao, W., Yan, L., Guan, W., Hu, Z., Wu, L., Huang, Q., Wang, J. & Xu, H. 2018. Androgen-receptor splice variant-7-positive prostate cancer: a novel molecular subtype with markedly worse androgen-deprivation therapy outcomes in newly diagnosed patients. *Modern Pathology,* 31**,** 198-208.

Li, L.-C., Carroll, P. R. & Dahiya, R. 2005. Epigenetic changes in prostate cancer: implication for diagnosis and treatment. *Journal of the National Cancer Institute,* 97**,** 103-115.

Li, L.-C., Okino, S. T. & Dahiya, R. 2004. DNA methylation in prostate cancer. *Biochimica et Biophysica Acta (BBA)-Reviews on Cancer,* 1704**,** 87-102.

Li, X., Pan, J.-H., Song, B., Xiong, E.-Q., Chen, Z.-W., Zhou, Z.-S. & Su, Y.-P. 2012. Suppression of CX43 expression by miR-20a in the progression of human prostate cancer. *Cancer biology & therapy,* 13**,** 890-898.

Li, Y., Alsagabi, M., Fan, D., Bova, G. S., Tewfik, A. H. & Dehm, S. M. 2011. Intragenic rearrangement and altered RNA splicing of the androgen receptor in a cell-based model of prostate cancer progression. *Cancer research,* 71**,** 2108-2117.

Li, Y., Chan, S. C., Brand, L. J., Hwang, T. H., Silverstein, K. A. & Dehm, S. M. 2013. Androgen receptor splice variants mediate enzalutamide resistance in castration-resistant prostate cancer cell lines. *Cancer research,* 73**,** 483-489.

Li, Y., Wang, L., Zhang, M., Melamed, J., Liu, X., Reiter, R., Wei, J., Peng, Y., Zou, X. & Pellicer, A. 2009. LEF1 in androgen-independent prostate cancer: regulation of androgen receptor expression, prostate cancer growth, and invasion. *Cancer research,* 69**,** 3332-3338.

Li, Z. G., Mathew, P., Yang, J., Starbuck, M. W., Zurita, A. J., Liu, J., Sikes, C., Multani, A. S., Efstathiou, E. & Lopez, A. 2008. Androgen receptor–negative human prostate cancer cells induce osteogenesis in mice through FGF9-mediated mechanisms. *The Journal of clinical investigation,* 118**,** 2697-2710.

Lickert, H., Kispert, A., Kutsch, S. & Kemler, R. 2001. Expression patterns of Wnt genes in mouse gut development. *Mechanisms of development,* 105**,** 181-184.

Lien, W.-H. & Fuchs, E. 2014. Wnt some lose some: transcriptional governance of stem cells by Wnt/β-catenin signaling. *Genes & development,* 28**,** 1517-1532.

Lim, X. & Nusse, R. 2013. Wnt signaling in skin development, homeostasis, and disease. *Cold Spring Harbor perspectives in biology,* 5**,** a008029.

Lin, H.-K., Wang, L., Hu, Y.-C., Altuwaijri, S. & Chang, C. 2002. Phosphorylation-dependent ubiquitylation and degradation of androgen receptor by Akt require Mdm2 E3 ligase. *The EMBO journal,* 21**,** 4037-4048.

Lin, S.-Y., Xia, W., Wang, J. C., Kwong, K. Y., Spohn, B., Wen, Y., Pestell, R. G. & Hung, M.-C. 2000. β-catenin, a novel prognostic marker for breast cancer: its roles in cyclin D1 expression and cancer progression. *Proceedings of the National Academy of Sciences,* 97**,** 4262-4266.

Lindzey, J., Kumar, M. V., Grossman, M., Young, C. & Tindall, D. J. 1994. Molecular mechanisms of androgen action. *Vitamins and hormones,* 49**,** 383-432.

Linja, M. J., Savinainen, K. J., Saramäki, O. R., Tammela, T. L., Vessella, R. L. & Visakorpi, T. 2001. Amplification and overexpression of androgen receptor gene in hormone-refractory prostate cancer. *Cancer research,* 61**,** 3550-3555.

Lintern, K. B., Guidato, S., Rowe, A., Saldanha, J. W. & Itasaki, N. 2009. Characterization of wise protein and its molecular mechanism to interact with both Wnt and BMP signals. *Journal of Biological Chemistry,* 284**,** 23159-23168.

Litvinov, I. V., De Marzo, A. M. & Isaacs, J. T. 2003. Is the Achilles' heel for prostate cancer therapy a gain of function in androgen receptor signaling? *The Journal of Clinical Endocrinology & Metabolism,* 88**,** 2972-2982.

Liu, L., Xie, N., Sun, S., Plymate, S., Mostaghel, E. & Dong, X. 2014. Mechanisms of the androgen receptor splicing in prostate cancer cells. *Oncogene,* 33**,** 3140-3150.

Liu, Y., Horn, J. L., Banda, K., Goodman, A. Z., Lim, Y., Jana, S., Arora, S., Germanos, A. A., Wen, L. & Hardin, W. R. 2019. The androgen receptor regulates a druggable translational regulon in advanced prostate cancer. *Science translational medicine,* 11.

Livak, K. J. & Schmittgen, T. D. 2001. Analysis of relative gene expression data using real-time quantitative PCR and the 2− ΔΔCT method. *methods,* 25**,** 402-408.

Locke, J. A., Guns, E. S., Lubik, A. A., Adomat, H. H., Hendy, S. C., Wood, C. A., Ettinger, S. L., Gleave, M. E. & Nelson, C. C. 2008. Androgen levels increase by intratumoral de novo steroidogenesis during progression of castration-resistant prostate cancer. *Cancer research,* 68**,** 6407-6415.

Logan, C. Y. & Nusse, R. 2004. The Wnt signaling pathway in development and disease. *Annu. Rev. Cell Dev. Biol.,* 20**,** 781-810.

Lombardi, A. P. G., Royer, C., Pisolato, R., Cavalcanti, F. N., Lucas, T. F., Lazari, M. F. M. & Porto, C. S. 2013. Physiopathological aspects of the Wnt/β-catenin signaling pathway in the male reproductive system. *Spermatogenesis,* 3**,** e23181.

Lorenzo, P. I., Arnoldussen, Y. J. & Saatcioglu, F. 2007. Molecular mechanisms of apoptosis in prostate cancer. *Critical Reviews™ in Oncogenesis,* 13.

Lowry, O. H., Rosebrough, N. J., Farr, A. L. & Randall, R. J. 1951. Protein measurement with the Folin phenol reagent. *Journal of biological chemistry,* 193**,** 265-275.

Lowsley, O. S. 1912. The development of the human prostate gland with reference to the development of other structures at the neck of the urinary bladder. *American journal of Anatomy,* 13**,** 299-349.

Lu, N. Z., Wardell, S. E., Burnstein, K. L., Defranco, D., Fuller, P. J., Giguere, V., Hochberg, R. B., Mckay, L., Renoir, J.-M. & Weigel, N. L. 2006. International Union of Pharmacology. LXV. The pharmacology and classification of the nuclear receptor superfamily: glucocorticoid, mineralocorticoid, progesterone, and androgen receptors. *Pharmacological reviews,* 58**,** 782-797.

Lubahn, D. B., Brown, T. R., Simental, J. A., Higgs, H. N., Migeon, C. J., Wilson, E. M. & French, F. S. 1989. Sequence of the intron/exon junctions of the coding region of the human androgen

receptor gene and identification of a point mutation in a family with complete androgen insensitivity. *Proceedings of the National Academy of Sciences,* 86**,** 9534-9538.

Lubahn, D. B., Joseph, D. R., Sullivan, P. M., Willard, H. F., French, F. S. & Wilson, E. M. 1988. Cloning of human androgen receptor complementary DNA and localization to the X chromosome. *Science,* 240**,** 327-330.

Lucas, J., True, L., Hawley, S., Matsumura, M., Morrissey, C., Vessella, R. & Nelson, P. 2008. The androgen-regulated type II serine protease TMPRSS2 is differentially expressed and mislocalized in prostate adenocarcinoma. *The Journal of Pathology: A Journal of the Pathological Society of Great Britain and Ireland,* 215**,** 118-125.

Lucocq, J. 1985. Colloidal gold and colloidal silver-metallic markers for light microscopic histochemistry. *Techniques in Immunohistochemistry,* 3**,** 203-236.

Luger, K., Mäder, A. W., Richmond, R. K., Sargent, D. F. & Richmond, T. J. 1997. Crystal structure of the nucleosome core particle at 2.8 Å resolution. *Nature,* 389**,** 251-260.

Lundwall, Å. & Lilja, H. 1987. Molecular cloning of human prostate specific antigen cDNA. *FEBS letters,* 214**,** 317-322.

Luo, Y., He, P. & Qiu, M. 2018. FOSL1 enhances growth and metastasis of human prostate cancer cells through epithelial mesenchymal transition pathway. *Eur Rev Med Pharmacol Sci,* 22**,** 8609-8615.

Maclean, H. E., Warne, G. L. & Zajac, J. D. 1997. Localization of functional domains in the androgen receptor. *The Journal of steroid biochemistry and molecular biology,* 62**,** 233-242.

Macphee, D. J. 2010. Methodological considerations for improving Western blot analysis. *Journal of pharmacological and toxicological methods,* 61**,** 171-177.

Maehama, T. & Dixon, J. E. 1998. The tumor suppressor, PTEN/MMAC1, dephosphorylates the lipid second messenger, phosphatidylinositol 3, 4, 5-trisphosphate. *Journal of Biological Chemistry,* 273**,** 13375-13378.

Makridakis, N., Ross, R. K., Pike, M. C., Chang, L., Stanczyk, F. Z., Kolonel, L. N., Shi, C.-Y., Mimi, C. Y., Henderson, B. E. & Reichardt, J. K. 1997. A prevalent missense substitution that modulates activity of prostatic steroid 5α-reductase. *Cancer research,* 57**,** 1020-1022.

Malathi, K., Dong, B., Gale, M. & Silverman, R. H. 2007. Small self-RNA generated by RNase L amplifies antiviral innate immunity. *Nature,* 448**,** 816-819.

Mani, R.-S., Tomlins, S. A., Callahan, K., Ghosh, A., Nyati, M. K., Varambally, S., Palanisamy, N. & Chinnaiyan, A. M. 2009. Induced chromosomal proximity and gene fusions in prostate cancer. *Science,* 326**,** 1230-1230.

Mann, B., Gelos, M., Siedow, A., Hanski, M., Gratchev, A., Ilyas, M., Bodmer, W., Moyer, M., Riecken, E. & Buhr, H. 1999. Target genes of β-catenin–T cell-factor/lymphoid-enhancer-factor signaling in human colorectal carcinomas. *Proceedings of the National Academy of Sciences,* 96**,** 1603-1608.

Mao, S.-Y., Javois, L. C. & Kent, U. M. 1999. Overview of antibody use in immunocytochemistry. *Immunocytochemical Methods and Protocols.* Springer.

Marchiani, S., Tamburrino, L., Nesi, G., Paglierani, M., Gelmini, S., Orlando, C., Maggi, M., Forti, G. & Baldi, E. 2010. Androgen-responsive and-unresponsive prostate cancer cell lines respond differently to stimuli inducing neuroendocrine differentiation. *International journal of andrology,* 33**,** 784-793.

Marcus, A. & Oransky, I. 2012. Can we trust western blots. *Lab Times,* 2**,** 41.

Marino, M., Galluzzo, P. & Ascenzi, P. 2006. Estrogen signaling multiple pathways to impact gene transcription. *Current genomics,* 7**,** 497-508.

Masai, M., Sumiya, H., Akimoto, S., Yatani, R., Chang, C., Liao, S. & Shimazaki, J. 1990. Immunohistochemical study of androgen receptor in benign hyperplastic and cancerous human prostates. *The Prostate,* 17**,** 293-300.

Mason, D. & Sammons, R. 1978. Alkaline phosphatase and peroxidase for double immunoenzymatic labelling of cellular constituents. *Journal of clinical pathology,* 31**,** 454-460.

Masters, J. R. 2002. HeLa cells 50 years on: the good, the bad and the ugly. *Nature Reviews Cancer,* 2**,** 315-319.

Masuda, T. & Ishitani, T. 2017. Context-dependent regulation of the β-catenin transcriptional complex supports diverse functions of Wnt/β-catenin signaling. *The Journal of Biochemistry,* 161**,** 9-17.

Matsumoto, A., Naito, M., Itakura, H., Ikemoto, S., Asaoka, H., Hayakawa, I., Kanamori, H., Aburatani, H., Takaku, F. & Suzuki, H. 1990. Human macrophage scavenger receptors: primary structure, expression, and localization in atherosclerotic lesions. *Proceedings of the National Academy of Sciences,* 87**,** 9133-9137.

Mazzanti, M., Bustamante, J. O. & Oberleithner, H. 2001. Electrical dimension of the nuclear envelope. *Physiological Reviews,* 81**,** 1-19.

Mcbride, R. B. 2012. *Obesity and aggressive prostate cancer bias and biomarkers*, Columbia University.

Mcconnell, J. 1995. Prostatic growth: new insights into hormonal regulation. *British journal of urology (Print),* 76**,** 5-10.

Mcdermott, U., Sharma, S. V., Dowell, L., Greninger, P., Montagut, C., Lamb, J., Archibald, H., Raudales, R., Tam, A. & Lee, D. 2007. Identification of genotype-correlated sensitivity to selective kinase inhibitors by using high-throughput tumor cell line profiling. *Proceedings of the National Academy of Sciences,* 104**,** 19936-19941.

Mcewan, I. J. 2004. Molecular mechanisms of androgen receptor-mediated gene regulation: structure-function analysis of the AF-1 domain. *Endocrine-related cancer,* 11**,** 281-293.

Mcewen, D. G. & Peifer, M. 2000. Wnt signaling: Moving in a new direction. *Current Biology,* 10**,** R562-R564.

Mckemy, D. D. 2007. TRPM8: the cold and menthol receptor. *TRP ion channel function in sensory transduction and cellular signaling cascades*.

Mcneal, J. E. 1988a. Normal histology of the prostate. *The American journal of surgical pathology,* 12**,** 619-633.

Mcneal, J. E. 1988b. The prostate gland: morphology and pathobiology. *Monogr. Urol.,* 9**,** 36-54.

Mcneal, J. E. & Bostwick, D. G. 1986. Intraductal dysplasia: a premalignant lesion of the prostate. *Human pathology,* 17**,** 64-71.

Meeker, A. K., Hicks, J. L., Platz, E. A., March, G. E., Bennett, C. J., Delannoy, M. J. & De Marzo, A. M. 2002. Telomere shortening is an early somatic DNA alteration in human prostate tumorigenesis. *Cancer research,* 62**,** 6405-6409.

Melchior, F., Paschal, B., Evans, J. & Gerace, L. 1993. Inhibition of nuclear protein import by nonhydrolyzable analogues of GTP and identification of the small GTPase Ran/TC4 as an essential transport factor. *The Journal of cell biology,* 123**,** 1649-1659.

Merrimen, J. L., Evans, A. J. & Srigley, J. R. 2013. Preneoplasia in the prostate gland with emphasis on high grade prostatic intraepithelial neoplasia. *Pathology,* 45**,** 251-263.

Meyer, N. & Penn, L. Z. 2008. Reflecting on 25 years with MYC. *Nature Reviews Cancer,* 8**,** 976-990.

Mickey, D. D., Stone, K. R., Wunderli, H., Mickey, G. H., Vollmer, R. T. & Paulson, D. F. 1977. Heterotransplantation of a human prostatic adenocarcinoma cell line in nude mice. *Cancer Research,* 37**,** 4049-4058.

Mii, Y. & Taira, M. 2011. Secreted Wnt “inhibitors” are not just inhibitors: Regulation of extracellular Wnt by secreted Frizzled-related proteins. *Development, growth & differentiation,* 53**,** 911-923.

Milde, P., Merke, J., Ritz, E., Haussler, M. R. & Rauterberg, E. W. 1989. Immunohistochemical detection of 1, 25-dihydroxyvitamin D3 receptors and estrogen receptors by monoclonal

antibodies: comparison of four immunoperoxidase methods. *Journal of Histochemistry & Cytochemistry,* 37**,** 1609-1617.

Miller, D., Arroyo, J. D., Chevillet, J. R., Tewari, M., Knouf, A. E. C., Metzger, M. J. & Mitchell, P. S. 2009. Multiple Integrated Copies and High-Level. *J. Virol,* 83**,** 7353.

Miller, D. C., Hafez, K. S., Stewart, A., Montie, J. E. & Wei, J. T. 2003. Prostate carcinoma presentation, diagnosis, and staging: an update from the National Cancer Data Base. *Cancer: Interdisciplinary International Journal of the American Cancer Society,* 98**,** 1169-1178.

Miller, J. R. 2001. The wnts. *Genome biology,* 3**,** 1-15.

Ming, J., Zhou, Y., Du, J., Fan, S., Pan, B., Wang, Y., Fan, L. & Jiang, J. 2015. Identification of miR-200a as a novel suppressor of connexin 43 in breast cancer cells. *Bioscience reports,* 35**,** e00251.

Mitelman, F., Johansson, B. & Mertens, F. 2007. The impact of translocations and gene fusions on cancer causation. *Nature Reviews Cancer,* 7**,** 233-245.

Miyamoto, H., Hernandez, D. J. & Epstein, J. I. 2009. A pathological reassessment of organ-confined, Gleason score 6 prostatic adenocarcinomas that progress after radical prostatectomy. *Human pathology,* 40**,** 1693-1698.

Miyamoto, K. K., Mcsherry, S. A., Dent, G. A., Sar, M., Wilson, E. M., French, F. S., Sharief, Y. & Mohler, J. L. 1993. Immunohistochemistry of the androgen receptor in human benign and malignant prostate tissue. *The Journal of urology,* 149**,** 1015-1019.

Mogal, A. P., Van Der Meer, R., Crooke, P. S. & Abdulkadir, S. A. 2007. Haploinsufficient prostate tumor suppression by Nkx3. 1: a role for chromatin accessibility in dosage-sensitive gene regulation. *Journal of Biological Chemistry,* 282**,** 25790-25800.

Molenaar, M., Van De Wetering, M., Oosterwegel, M., Peterson-Maduro, J., Godsave, S., Korinek, V., Roose, J., Destrée, O. & Clevers, H. 1996. XTcf-3 transcription factor mediates β-catenin-induced axis formation in Xenopus embryos. *Cell,* 86**,** 391-399.

Molinari, F., Feraco, A., Mirabilii, S., Saladini, S., Sansone, L., Vernucci, E., Tomaselli, G., Marzolla, V., Rotili, D. & Russo, M. A. 2021. SIRT5 Inhibition Induces Brown Fat-Like Phenotype in 3T3-L1 Preadipocytes. *Cells,* 10**,** 1126.

Mollica, J. P., Oakhill, J. S., Lamb, G. D. & Murphy, R. M. 2009. Are genuine changes in protein expression being overlooked? Reassessing Western blotting. *Analytical biochemistry,* 386**,** 270-275.

Montironi, R., Mazzucchelli, R., Lopez-Beltran, A., Cheng, L. & Scarpelli, M. 2007. Mechanisms of disease: high-grade prostatic intraepithelial neoplasia and other proposed preneoplastic lesions in the prostate. *Nature clinical practice Urology,* 4**,** 321-332.

Moore, C. K., Karikehalli, S., Nazeer, T., Fisher, H. A., Kaufman, R. P. & Mian, B. M. 2005. Prognostic significance of high grade prostatic intraepithelial neoplasia and atypical small acinar proliferation in the contemporary era. *The Journal of urology,* 173**,** 70-72.

Moore, K. N., Gunderson, C. C., Sabbatini, P., Mcmeekin, D. S., Mantia-Smaldone, G., Burger, R. A., Morgan, M. A., Kapoun, A. M., Brachmann, R. K. & Stagg, R. 2019. A phase 1b dose escalation study of ipafricept (OMP54F28) in combination with paclitaxel and carboplatin in patients with recurrent platinum-sensitive ovarian cancer. *Gynecologic oncology,* 154**,** 294-301.

Mori, Y., Nagse, H., Ando, H., Horii, A., Ichii, S., Nakatsuru, S., Aoki, T., Miki, Y., Mori, T. & Nakamura, Y. 1992. Somatic mutations of the APC gene in colorectal tumors: mutation cluster region in the APC gene. *Human molecular genetics,* 1**,** 229-233.

Morin, P. J., Sparks, A. B., Korinek, V., Barker, N., Clevers, H., Vogelstein, B. & Kinzler, K. W. 1997. Activation of β-catenin-Tcf signaling in colon cancer by mutations in β-catenin or APC. *Science,* 275**,** 1787-1790.

Moritz, C. P. 2020. 40 years Western blotting: A scientific birthday toast. *Journal of proteomics,* 212**,** 103575.

Moroianu, J., Hijikata, M., Blobel, G. & Radu, A. 1995. Mammalian karyopherin ~ 1 and ~ 2 heterodimers: ~ 1 or ~ 2 subunit binds nuclear localization signal and subunit interacts with peptide repeat-containing nucleoporins. *PROCEEDINGS-NATIONAL ACADEMY OF SCIENCES USA,* 92**,** 6532-6532.

Morrone, S., Cheng, Z., Moon, R. T., Cong, F. & Xu, W. 2012. Crystal structure of a Tankyrase-Axin complex and its implications for Axin turnover and Tankyrase substrate recruitment. *Proceedings of the National Academy of Sciences,* 109**,** 1500-1505.

Mostaghel, E. A., Marck, B. T., Plymate, S. R., Vessella, R. L., Balk, S., Matsumoto, A. M., Nelson, P. S. & Montgomery, R. B. 2011. Resistance to CYP17A1 inhibition with abiraterone in castration-resistant prostate cancer: induction of steroidogenesis and androgen receptor splice variants. *Clinical cancer research,* 17**,** 5913-5925.

Mroue, R., El-Sabban, M. & Talhouk, R. 2011. Connexins and the gap in context. *Integrative Biology,* 3**,** 255-266.

Mueller, M. M. & Fusenig, N. E. 2004. Friends or foes—bipolar effects of the tumour stroma in cancer. *Nature Reviews Cancer,* 4**,** 839-849.

Mukhopadhyay, R. 2012. The men behind Western blotting. *ASBMB Today,* 2012**,** 17-19.

Mulholland, D. J., Cheng, H., Reid, K., Rennie, P. S. & Nelson, C. C. 2002. The androgen receptor can promote β-catenin nuclear translocation independently of adenomatous polyposis coli. *Journal of Biological Chemistry,* 277**,** 17933-17943.

Mulholland, D. J., Read, J. T., Rennie, P. S., Cox, M. E. & Nelson, C. C. 2003. Functional localization and competition between the androgen receptor and T-cell factor for nuclear β-catenin: a means for inhibition of the Tcf signaling axis. *Oncogene,* 22**,** 5602-5613.

Mullins, J. K. & Loeb, S. Environmental exposures and prostate cancer. Urologic Oncology: Seminars and Original Investigations, 2012. Elsevier, 216-219.

Murillo-Garzón, V. & Kypta, R. 2017. WNT signalling in prostate cancer. *Nature Reviews Urology,* 14**,** 683-696.

Musil, L. S., Le, A.-C. N., Vanslyke, J. K. & Roberts, L. M. 2000. Regulation of connexin degradation as a mechanism to increase gap junction assembly and function. *Journal of Biological Chemistry,* 275**,** 25207-25215.

Mutuku, S. M., Trim, P. J., Prabhala, B. K., Irani, S., Bremert, K. L., Logan, J. M., Brooks, D. A., Stahl, J., Centenera, M. M. & Snel, M. F. 2019. Evaluation of small molecule drug uptake in patient-derived prostate cancer explants by mass spectrometry. *Scientific reports,* 9**,** 1-11.

Nadiminty, N., Tummala, R., Liu, C., Lou, W., Evans, C. P. & Gao, A. C. 2015. NF-κB2/p52: c-Myc: hnRNPA1 pathway regulates expression of androgen receptor splice variants and enzalutamide sensitivity in prostate cancer. *Molecular cancer therapeutics,* 14**,** 1884-1895.

Nakane, P. K. & Pierce Jr, G. B. 1966. Enzyme-labeled antibodies: preparation and application for the localization of antigens. *Journal of Histochemistry & Cytochemistry,* 14**,** 929-931.

Nakata, D., Nakayama, K., Masaki, T., Tanaka, A., Kusaka, M. & Watanabe, T. 2016. Growth inhibition by testosterone in an androgen receptor splice variant-driven prostate cancer model. *The Prostate,* 76**,** 1536-1545.

Nakayama, M., Bennett, C. J., Hicks, J. L., Epstein, J. I., Platz, E. A., Nelson, W. G. & De Marzo, A. M. 2003. Hypermethylation of the human glutathione S-transferase-π gene (GSTP1) CpG island is present in a subset of proliferative inflammatory atrophy lesions but not in normal or hyperplastic epithelium of the prostate: a detailed study using laser-capture microdissection. *The American journal of pathology,* 163**,** 923-933.

Nakazato, H., Suzuki, K., Matsui, H., Ohtake, N., Nakata, S. & Yamanaka, H. 2003. Role of genetic polymorphisms of the RNASEL gene on familial prostate cancer risk in a Japanese population. *British journal of cancer,* 89**,** 691-696.

Nan, X., Ng, H.-H., Johnson, C. A., Laherty, C. D., Turner, B. M., Eisenman, R. N. & Bird, A. 1998. Transcriptional repression by the methyl-CpG-binding protein MeCP2 involves a histone deacetylase complex. *Nature,* 393**,** 386-389.

Nasir, A., Copeland, J., Gillespie, J., Chughtai, O., Andrawis, R., Kaiser, H. & Manyak, M. 2002. Preneoplastic lesions of the prostate-clinical, pathological and molecular biological aspects. *In Vivo (Athens, Greece),* 16**,** 557-566.

Nelson, W. J. & Nusse, R. 2004. Convergence of Wnt, ß-catenin, and cadherin pathways. *Science,* 303**,** 1483-1487.

Nguyen, D. X., Bos, P. D. & Massagué, J. 2009. Metastasis: from dissemination to organ-specific colonization. *Nature Reviews Cancer,* 9**,** 274-284.

Nicholson, T. M. & Ricke, W. A. 2011. Androgens and estrogens in benign prostatic hyperplasia: past, present and future. *Differentiation,* 82**,** 184-199.

Nicholson, T. M., Sehgal, P. D., Drew, S. A., Huang, W. & Ricke, W. A. 2013. Sex steroid receptor expression and localization in benign prostatic hyperplasia varies with tissue compartment. *Differentiation,* 85**,** 140-149.

Niehrs, C. 2006. Function and biological roles of the Dickkopf family of Wnt modulators. *Oncogene,* 25**,** 7469-7481.

Nigg, E. A. 1997. Nucleocytoplasmic transport: signals, mechanisms and regulation. *Nature,* 386**,** 779-787.

Noda, D., Itoh, S., Watanabe, Y., Inamitsu, M., Dennler, S., Itoh, F., Koike, S., Danielpour, D., Ten Dijke, P. & Kato, M. 2006. ELAC2, a putative prostate cancer susceptibility gene product, potentiates TGF-β/Smad-induced growth arrest of prostate cells. *Oncogene,* 25**,** 5591-5600.

Nusse, R., Brown, A., Papkoff, J., Scambler, P., Shackleford, G., Mcmahon, A., Moon, R. & Varmus, H. 1991. A new nomenclature for int-1 and related genes: the Wnt gene family. *Cell,* 64**,** 231.

Nusse, R. & Clevers, H. 2017. Wnt/β-catenin signaling, disease, and emerging therapeutic modalities. *Cell,* 169**,** 985-999.

Nüsslein-Volhard, C. & Wieschaus, E. 1980. Mutations affecting segment number and polarity in Drosophila. *Nature,* 287**,** 795-801.

Nüsslein-Volhard, C., Wieschaus, E. & Kluding, H. 1984. Mutations affecting the pattern of the larval cuticle inDrosophila melanogaster. *Wilhelm Roux's archives of developmental biology,* 193**,** 267-282.

Nwosu, V., Carpten, J., Trent, J. M. & Sheridan, R. 2001. Heterogeneity of genetic alterations in prostate cancer: evidence of the complex nature of the disease. *Human molecular genetics,* 10**,** 2313-2318.

O'malley, C. D. & De Cm Saunders, J. 1950. *The illustrations from the works of Andreas Vesalius of Brussels: with annotations and translations, a discussion of the plates and their background, authorship and influence, and a biographical sketch of Vesalius*.

Oertel, H. 1926. An address on involutionary changes in prostate and female breast in relation to cancer development. *Canadian Medical Association Journal,* 16**,** 237.

Olson, A., Le, V., Aldahl, J., Yu, E.-J., Hooker, E., He, Y., Lee, D.-H., Kim, W. K., Cardiff, R. D. & Geradts, J. 2019. The comprehensive role of E-cadherin in maintaining prostatic epithelial integrity during oncogenic transformation and tumor progression. *PLoS genetics,* 15**,** e1008451.

Oosterwegel, M., Van De Wetering, M., Dooijes, D., Klomp, L., Winoto, A., Georgopoulos, K., Meijlink, F. & Clevers, H. 1991. Cloning of murine TCF-1, a T cell-specific transcription factor interacting with functional motifs in the CD3-epsilon and T cell receptor alpha enhancers. *The Journal of experimental medicine,* 173**,** 1133-1142.

Ostrander, E. A. & Stanford, J. L. 2000. Genetics of prostate cancer: too many loci, too few genes. *The American Journal of Human Genetics,* 67**,** 1367-1375.

Pakneshan, P., Xing, R. H. & Rabbani, S. A. 2003. Methylation status of uPA promoter as a molecular mechanism regulating prostate cancer invasion and growth in vitro and in vivo. *The FASEB journal,* 17**,** 1081-1088.

Pakula, H., Xiang, D. & Li, Z. 2017. A tale of two signals: AR and WNT in development and tumorigenesis of prostate and mammary gland. *Cancers,* 9**,** 14.

Pandey, P., Dixit, A., Tanwar, A., Sharma, A. & Mittal, S. 2014. A comparative study to evaluate liquid dish washing soap as an alternative to xylene and alcohol in deparaffinization and hematoxylin and eosin staining. *Journal of laboratory physicians,* 6**,** 84.

Panigrahi, G. K., Praharaj, P. P., Kittaka, H., Mridha, A. R., Black, O. M., Singh, R., Mercer, R., Van Bokhoven, A., Torkko, K. C. & Agarwal, C. 2019. Exosome proteomic analyses identify inflammatory phenotype and novel biomarkers in African American prostate cancer patients. *Cancer medicine,* 8**,** 1110-1123.

Papadopoulos, V. 2004. In search of the function of the peripheral-type benzodiazepine receptor. *Endocrine research,* 30**,** 677-684.

Parekh, N., Lin, Y., Dipaola, R. S., Marcella, S. & Lu-Yao, G. 2010. Obesity and prostate cancer detection: insights from three national surveys. *The American journal of medicine,* 123**,** 829-835.

Paris, P. L., Andaya, A., Fridlyand, J., Jain, A. N., Weinberg, V., Kowbel, D., Brebner, J. H., Simko, J., Watson, J. V. & Volik, S. 2004. Whole genome scanning identifies genotypes associated with recurrence and metastasis in prostate tumors. *Human molecular genetics,* 13**,** 1303-1313.

Parkin, D. M., Bray, F., Ferlay, J. & Jemal, A. 2014. Cancer in africa 2012. *Cancer Epidemiology and Prevention Biomarkers,* 23**,** 953-966.

Paschalis, A., Sharp, A., Welti, J. C., Neeb, A., Raj, G. V., Luo, J., Plymate, S. R. & De Bono, J. S. 2018. Alternative splicing in prostate cancer. *Nature Reviews Clinical Oncology,* 15**,** 663-675.

Patron, J. P., Fendler, A., Bild, M., Jung, U., Müller, H., Arntzen, M. Ø., Piso, C., Stephan, C., Thiede, B. & Mollenkopf, H.-J. 2012. MiR-133b targets antiapoptotic genes and enhances death receptor-induced apoptosis. *PloS one,* 7**,** e35345.

Pawlowski, J. E., Ertel, J. R., Allen, M. P., Xu, M., Butler, C., Wilson, E. M. & Wierman, M. E. 2002a. Liganded androgen receptor interaction with β-catenin nuclear co-localization and modulation of transcriptional activity in neuronal cells. *Journal of Biological Chemistry,* 277**,** 20702-20710.

Pawlowski, J. E., Ertel, J. R., Allen, M. P., Xu, M., Butler, C., Wilson, E. M. & Wierman, M. E. 2002b. Liganded androgen receptor interaction with β-catenin: nuclear co-localization and modulation of transcriptional activity in neuronal cells. *Journal of Biological Chemistry,* 277**,** 20702-20710.

Payne, A. H. & Hales, D. B. 2004. Overview of steroidogenic enzymes in the pathway from cholesterol to active steroid hormones. *Endocrine reviews,* 25**,** 947-970.

Paznekas, W. A., Boyadjiev, S. A., Shapiro, R. E., Daniels, O., Wollnik, B., Keegan, C. E., Innis, J. W., Dinulos, M. B., Christian, C. & Hannibal, M. C. 2003. Connexin 43 (GJA1) mutations cause the pleiotropic phenotype of oculodentodigital dysplasia. *The American Journal of Human Genetics,* 72**,** 408-418.

Perdana, N. R., Mochtar, C. A., Umbas, R. & Hamid, A. 2016. The risk factors of prostate cancer and its prevention: a literature review. *Acta Med Indones,* 48**,** 228-38.

Persad, S., A. Troussard, A., Mcphee, T. R., Mulholland, D. J. & Dedhar, S. 2001. Tumor suppressor PTEN inhibits nuclear accumulation of β-catenin and T cell/lymphoid enhancer factor 1–mediated transcriptional activation. *The Journal of cell biology,* 153**,** 1161-1174.

Pestronk, A. & Lopate, G. 2005. Polyneuropathies and Antibodies to Nervev Components. *Peripheral neuropathy.* Elsevier Inc.

Peters, C. A. & Walsh, P. C. 1987. The effect of nafarelin acetate, a luteinizing-hormone–releasing hormone agonist, on benign prostatic hyperplasia. *New England Journal of Medicine,* 317**,** 599-604.

Pfaffl, M. W. & Berg, W. 2010. Guest editor's introduction: the ongoing evolution of qPCR. *Methods,* 50**,** 215-336.

Pienta, K. J. & Esper, P. S. 1993. Risk factors for prostate cancer. *Annals of internal medicine,* 118**,** 793-803.

Pierorazio, P. M., Walsh, P. C., Partin, A. W. & Epstein, J. I. 2013. Prognostic Gleason grade grouping: data based on the modified Gleason scoring system. *BJU international,* 111**,** 753.

Pillai-Kastoori, L., Schutz-Geschwender, A. R. & Harford, J. A. 2020. A systematic approach to quantitative Western blot analysis. *Analytical biochemistry,* 593**,** 113608.

Planas-Paz, L., Orsini, V., Boulter, L., Calabrese, D., Pikiolek, M., Nigsch, F., Xie, Y., Roma, G., Donovan, A. & Marti, P. 2016. The RSPO–LGR4/5–ZNRF3/RNF43 module controls liver zonation and size. *Nature cell biology,* 18**,** 467-479.

Plante, I., Stewart, M., Barr, K., Allan, A. & Laird, D. 2011. Cx43 suppresses mammary tumor metastasis to the lung in a Cx43 mutant mouse model of human disease. *Oncogene,* 30**,** 1681-1692.

Plotkin, L. I., Manolagas, S. C. & Bellido, T. 2002. Transduction of cell survival signals by connexin-43 hemichannels. *Journal of Biological Chemistry,* 277**,** 8648-8657.

Plum, A., Hallas, G. & Willecke, K. 2002. Expression of the mouse gap junction gene Gjb3 is regulated by distinct mechanisms in embryonic stem cells and keratinocytes. *Genomics,* 79**,** 24-30.

Polak, J. M. & Van Noorden, S. 1997. *Introduction to immunocytochemistry*, BIOS Scientific Publishers Oxford.

Polakis, P. 2000. Wnt signaling and cancer. *Genes & development,* 14**,** 1837-1851.

Polakis, P. 2012. Wnt signaling in cancer. *Cold Spring Harbor perspectives in biology,* 4**,** a008052.

Popadiuk, C. M., Xiong, J., Wells, M. G., Andrews, P. G., Dankwa, K., Hirasawa, K., Lake, B. B. & Kao, K. R. 2006. Antisense suppression of pygopus2 results in growth arrest of epithelial ovarian cancer. *Clinical Cancer Research,* 12**,** 2216-2223.

Possner, M., Heuser, M., Kaulfuss, S., Scharf, J.-G., Schulz, W., Hermann-Ringert, R. & Thelen, P. 2008. Functional analysis of NKX3. 1 in LNCaP prostate cancer cells by RNA interference. *International journal of oncology,* 32**,** 877-884.

Powell, S. M., Zilz, N., Beazer-Barclay, Y., Bryan, T. M., Hamilton, S. R., Thibodeau, S. N., Vogelstein, B. & Kinzler, K. W. 1992. APC mutations occur early during colorectal tumorigenesis. *Nature,* 359**,** 235-237.

Prelich, G. 2012. Gene overexpression: uses, mechanisms, and interpretation. *Genetics,* 190**,** 841-854.

Prendergast, G. C. & Ziff, E. B. 1991. Methylation-sensitive sequence-specific DNA binding by the c-Myc basic region. *Science,* 251**,** 186-189.

Prensner, J. R., Rubin, M. A., Wei, J. T. & Chinnaiyan, A. M. 2012. Beyond PSA: the next generation of prostate cancer biomarkers. *Science translational medicine,* 4**,** 127rv3-127rv3.

Prescott, J. & Coetzee, G. A. 2006. Molecular chaperones throughout the life cycle of the androgen receptor. *Cancer letters,* 231**,** 12-19.

Prescott, J. L., Blok, L. & Tindall, D. J. 1998. Isolation and androgen regulation of the human homeobox cDNA, NKX3. 1. *The Prostate,* 35**,** 71-80.

Puca, L., Bareja, R., Prandi, D., Shaw, R., Benelli, M., Karthaus, W. R., Hess, J., Sigouros, M., Donoghue, A. & Kossai, M. 2018. Patient derived organoids to model rare prostate cancer phenotypes. *Nature communications,* 9**,** 1-10.

Qian, J., Bostwick, D. G., Takahashi, S., Borell, T. J., Herath, J. F., Lieber, M. M. & Jenkins, R. B. 1995. Chromosomal anomalies in prostatic intraepithelial neoplasia and carcinoma detected by fluorescence in situ hybridization. *Cancer research,* 55**,** 5408-5414.

Qian, J., Jenkins, R. B. & Bostwick, D. G. 1997. Detection of chromosomal anomalies and c-myc gene amplification in the cribriform pattern of prostatic intraepithelial neoplasia and carcinoma by fluorescence in situ hybridization. *Modern pathology: an official journal of the United States and Canadian Academy of Pathology, Inc,* 10**,** 1113-1119.

Qian, J., Jiang, Z., Li, M., Heaphy, P., Liu, Y.-H. & Shackleford, G. M. 2003. Mouse Wnt9b transforming activity, tissue-specific expression, and evolution. *Genomics,* 81**,** 34-46.

Qiu, Y. Q., Leuschner, I. & Braun, P. M. 2008. Androgen receptor expression in clinically localized prostate cancer: immunohistochemistry study and literature review. *Asian journal of andrology,* 10**,** 855-863.

Quarmby, V. E., Yarbrough, W. G., Lubahn, D. B., French, F. S. & Wilson, E. M. 1990. Autologous down-regulation of androgen receptor messenger ribonucleic acid. *Molecular endocrinology,* 4**,** 22-28.

Queimado, L., Lopes, C. S. & Reis, A. M. 2007. WIF1, an inhibitor of the Wnt pathway, is rearranged in salivary gland tumors. *Genes, Chromosomes and Cancer,* 46**,** 215-225.

Quinn, M. & Babb, P. 2002. Patterns and trends in prostate cancer incidence, survival, prevalence and mortality. Part I: international comparisons. *BJU international,* 90**,** 162-173.

Rabionet, R., López-Bigas, N., Arbonès, M. L. & Estivill, X. 2002. Connexin mutations in hearing loss, dermatological and neurological disorders. *Trends in molecular medicine,* 8**,** 205-212.

Radmayr, C., Lunacek, A., Schwentner, C., Oswald, J., Klocker, H. & Bartsch, G. 2008. 5-alpha-reductase and the development of the human prostate. *Indian journal of urology: IJU: journal of the Urological Society of India,* 24**,** 309.

Raffo, A. J., Perlman, H., Chen, M.-W., Day, M. L., Streitman, J. S. & Buttyan, R. 1995. Overexpression of bcl-2 protects prostate cancer cells from apoptosis in vitro and confers resistance to androgen depletion in vivo. *Cancer research,* 55**,** 4438-4445.

Ramos, L., Chávez, B., Mares, L., Valdés, E. & Vilchis, F. 2018. Mutational analysis of the androgen receptor (NR3C4) gene in patients with 46, XY DSD. *Gene,* 641**,** 86-93.

Ramos-Vara, J. A., Kiupel, M., Baszler, T., Bliven, L., Brodersen, B., Chelack, B., West, K., Czub, S., Del Piero, F. & Dial, S. 2008. Suggested guidelines for immunohistochemical techniques in veterinary diagnostic laboratories. *Journal of Veterinary Diagnostic Investigation,* 20**,** 393-413.

Rapisuwon, S., Vietsch, E. E. & Wellstein, A. 2016. Circulating biomarkers to monitor cancer progression and treatment. *Computational and structural biotechnology journal,* 14**,** 211-222.

Rawla, P. 2019. Epidemiology of prostate cancer. *World journal of oncology,* 10**,** 63.

Reichsman, F., Smith, L. & Cumberledge, S. 1996. Glycosaminoglycans can modulate extracellular localization of the wingless protein and promote signal transduction. *The Journal of cell biology,* 135**,** 819-827.

Ren, F., Zhang, S., Mitchell, S. H., Butler, R. & Young, C. Y. 2000. Tea polyphenols down-regulate the expression of the androgen receptor in LNCaP prostate cancer cells. *Oncogene,* 19**,** 1924-1932.

Renart, J., Reiser, J. & Stark, G. R. 1979. Transfer of proteins from gels to diazobenzyloxymethyl-paper and detection with antisera: a method for studying antibody specificity and antigen structure. *Proceedings of the National Academy of Sciences,* 76**,** 3116-3120.

Rennert, H., Zeigler-Johnson, C. M., Addya, K., Finley, M. J., Walker, A. H., Spangler, E., Leonard, D. G., Wein, A., Malkowicz, S. B. & Rebbeck, T. R. 2005. Association of susceptibility alleles in ELAC2/HPC2, RNASEL/HPC1, and MSR1 with prostate cancer severity in European American and African American men. *Cancer Epidemiology and Prevention Biomarkers,* 14**,** 949-957.

Rennoll, S. & Yochum, G. 2015. Regulation of MYC gene expression by aberrant Wnt/β-catenin signaling in colorectal cancer. *World journal of biological chemistry,* 6**,** 290.

Reya, T. & Clevers, H. 2005. Wnt signalling in stem cells and cancer. *Nature,* 434**,** 843-850.

Ribas, J., Ni, X., Haffner, M., Wentzel, E. A., Salmasi, A. H., Chowdhury, W. H., Kudrolli, T. A., Yegnasubramanian, S., Luo, J. & Rodriguez, R. 2009. miR-21: an androgen receptor–regulated microRNA that promotes hormone-dependent and hormone-independent prostate cancer growth. *Cancer research,* 69**,** 7165-7169.

Richard, G., Brown, N., Smith, L. E., Terrinoni, A., Melino, G., Mackie, R. M., Bale, S. J. & Uitto, J. 2000. The spectrum of mutations in erythrokeratodermias–novel and de novo mutations in GJB3. *Human genetics,* 106**,** 321-329.

Rijsewijk, F., Schuermann, M., Wagenaar, E., Parren, P., Weigel, D. & Nusse, R. 1987. The Drosophila homology of the mouse mammary oncogene int-1 is identical to the segment polarity gene wingless. *Cell,* 50**,** 649-657.

Rizos, C., Papassava, M., Golias, C. & Charalabopoulos, K. 2010. Alcohol consumption and prostate cancer: a mini review. *Exp Oncol,* 32**,** 66-70.

Robinson, D., Van Allen, E. M., Wu, Y.-M., Schultz, N., Lonigro, R. J., Mosquera, J.-M., Montgomery, B., Taplin, M.-E., Pritchard, C. C. & Attard, G. 2015. Integrative clinical genomics of advanced prostate cancer. *Cell,* 161**,** 1215-1228.

Robinson-Rechavi, M., Garcia, H. E. & Laudet, V. 2003. The nuclear receptor superfamily. *Journal of cell science,* 116**,** 585-586.

Roeder, R. G. 1996. The role of general initiation factors in transcription by RNA polymerase II. *Trends in biochemical sciences,* 21**,** 327-335.

Roehrborn, C. G. 2008. Pathology of benign prostatic hyperplasia. *Int J Impot Res,* 20 Suppl 3**,** S11-8.

Ross, R., Bernstein, L., Judd, H., Hanisch, R., Pike, M. & Henderson, B. 1986. Serum testosterone levels in healthy young black and white men. *Journal of the National Cancer Institute,* 76**,** 45-48.

Roth, K. A. & Perry, A. 2005. Cell and tissue imaging techniques. *Translational and experimental medicine (Schuster D, Powers W, eds)***,** 396-412.

Routledge, D. & Scholpp, S. 2019. Mechanisms of intercellular Wnt transport. *Development,* 146.

Roy, A. K., Tyagi, R. K., Song, C. S., Lavrovsky, Y., Ahn, S. C., Oh, T. S. & Chatterjee, B. 2001. Androgen receptor: structural domains and functional dynamics after ligand-receptor interaction. *Annals of the New York Academy of Sciences,* 949**,** 44-57.

Ruan, K., Fang, X. & Ouyang, G. 2009. MicroRNAs: novel regulators in the hallmarks of human cancer. *Cancer letters,* 285**,** 116-126.

Rubinfeld, B., Souza, B., Albert, I., Muller, O., Chamberlain, S. H., Masiarz, F. R., Munemitsu, S. & Polakis, P. 1993. Association of the APC gene product with beta-catenin. *Science,* 262**,** 1731-1734.

Rubio-Briones, J., Fernández-Serra, A., Calatrava, A., García-Casado, Z., Rubio, L., Bonillo, M. A., Iborra, I., Solsona, E. & López-Guerrero, J. A. 2010. Clinical implications of TMPRSS2-ERG gene fusion expression in patients with prostate cancer treated with radical prostatectomy. *The Journal of urology,* 183**,** 2054-2061.

Sadi, M. V., Walsh, P. C. & Barrack, E. R. 1991. Immunohistochemical study of androgen receptors in metastatic prostate cancer. Comparison of receptor content and response to hormonal therapy. *Cancer,* 67**,** 3057-3064.

Sadler, T. W. 2018. *Langman's medical embryology*, Lippincott Williams & Wilkins.

Said, W., Emaetig, F., El Gehani, K., Eldarat, T., Buhmeida, A., Enattah, N., Elzagheid, A. & Al-Fituri, O. 2017. Over-expression of β-catenin is associated with high grade of prostatic cancer in Libyan patients. *African Journal of Urology,* 23**,** 133-138.

Saitoh, T., Hirai, M. & Katoh, M. 2001. Molecular cloning and characterization of WNT3A and WNT14 clustered in human chromosome 1q42 region. *Biochemical and Biophysical Research Communications,* 284**,** 1168-1175.

Sakr, W. A., Grignon, D. J., Haas, G. P., Heilbrun, L. K., Pontes, J. E. & Crissmana, J. D. 1996. Age and racial distribution of prostatic intraepithelial neoplasia. *European urology,* 30**,** 138-144.

Salic, A., Lee, E., Mayer, L. & Kirschner, M. W. 2000. Control of β-catenin stability: reconstitution of the cytoplasmic steps of the Wnt pathway in Xenopus egg extracts. *Molecular cell,* 5**,** 523-532.

Salmena, L., Carracedo, A. & Pandolfi, P. P. 2008. Tenets of PTEN tumor suppression. *Cell,* 133**,** 403-414.

Samaratunga, H., Delahunt, B., Yaxley, J., Srigley, J. R. & Egevad, L. 2016. From Gleason to International Society of Urological Pathology (ISUP) grading of prostate cancer. *Scandinavian journal of urology,* 50**,** 325-329.

Sandsmark, E., Hansen, A. F., Selnæs, K. M., Bertilsson, H., Bofin, A. M., Wright, A. J., Viset, T., Richardsen, E., Drabløs, F. & Bathen, T. F. 2017. A novel non-canonical Wnt signature for prostate cancer aggressiveness. *Oncotarget,* 8**,** 9572.

Saraon, P., Drabovich, A. P., Jarvi, K. A. & Diamandis, E. P. 2014. Mechanisms of androgen-independent prostate cancer. *Ejifcc,* 25**,** 42.

Sarma, A. & Yang, W. 2011. Calcium regulation of nucleocytoplasmic transport. *Protein & cell,* 2**,** 291-302.

Sasaki, M., Tanaka, Y., Perinchery, G., Dharia, A., Kotcherguina, I., Fujimoto, S. I. & Dahiya, R. 2002. Methylation and inactivation of estrogen, progesterone, and androgen receptors in prostate cancer. *Journal of the National Cancer Institute,* 94**,** 384-390.

Satoh, S., Daigo, Y., Furukawa, Y., Kato, T., Miwa, N., Nishiwaki, T., Kawasoe, T., Ishiguro, H., Fujita, M. & Tokino, T. 2000. AXIN1 mutations in hepatocellular carcinomas, and growth suppression in cancer cells by virus-mediated transfer of AXIN1. *Nature genetics,* 24**,** 245-250.

Sauriol, A., Simeone, K., Portelance, L., Meunier, L., Leclerc-Desaulniers, K., De Ladurantaye, M., Chergui, M., Kendall-Dupont, J., Rahimi, K. & Carmona, E. 2020. Modeling the diversity of epithelial ovarian cancer through ten novel well characterized cell lines covering multiple subtypes of the disease. *Cancers,* 12**,** 2222.

Scardino, P. T., Weaver, R. & M'liss, A. H. 1992. Early detection of prostate cancer. *Human pathology,* 23**,** 211-222.

Schaeffer, E., Marchionni, L., Huang, Z., Simons, B., Blackman, A., Yu, W., Parmigiani, G. & Berman, D. 2008. Androgen-induced programs for prostate epithelial growth and invasion arise in embryogenesis and are reactivated in cancer. *Oncogene,* 27**,** 7180-7191.

Schatzl, G., Madersbacher, S., Gsur, A., Preyer, M., Haidinger, G., Haitel, A., Vutuc, C., Micksche, M. & Marberger, M. 2002. Association of polymorphisms within androgen receptor, 5α-reductase, and PSA genes with prostate volume, clinical parameters, and endocrine status in elderly men. *The Prostate,* 52**,** 130-138.

Schaufele, F., Carbonell, X., Guerbadot, M., Borngraeber, S., Chapman, M. S., Ma, A. a. K., Miner, J. N. & Diamond, M. I. 2005. The structural basis of androgen receptor activation: intramolecular and intermolecular amino–carboxy interactions. *Proceedings of the National Academy of Sciences,* 102**,** 9802-9807.

Schlaberg, R., Choe, D. J., Brown, K. R., Thaker, H. M. & Singh, I. R. 2009. XMRV is present in malignant prostatic epithelium and is associated with prostate cancer, especially high-grade tumors. *Proceedings of the National Academy of Sciences,* 106**,** 16351-16356.

Schmidt, W. & De Lint, J. 1972. Causes of death of alcoholics. *Quarterly Journal of Studies on Alcohol,* 33**,** 171-185.

Schneider, C. A., Rasband, W. S. & Eliceiri, K. W. 2012. NIH Image to ImageJ: 25 years of image analysis. *Nature methods,* 9**,** 671-675.

Schulz, W., Burchardt, M. & Cronauer, M. 2003. Molecular biology of prostate cancer. *Molecular human reproduction,* 9**,** 437-448.

Schütz, S. V., Cronauer, M. V. & Rinnab, L. 2010. Inhibition of glycogen synthase kinase-3β promotes nuclear export of the androgen receptor through a CRM1-dependent mechanism in prostate cancer cell lines. *Journal of cellular biochemistry,* 109**,** 1192-1200.

Schweizer, L., Rizzo, C. A., Spires, T. E., Platero, J. S., Wu, Q., Lin, T.-A., Gottardis, M. M. & Attar, R. M. 2008a. The androgen receptor can signal through Wnt/β-Catenin in prostate cancer cells as an adaptation mechanism to castration levels of androgens. *BMC cell biology,* 9**,** 4.

Schweizer, L., Rizzo, C. A., Spires, T. E., Platero, J. S., Wu, Q., Lin, T.-A., Gottardis, M. M. & Attar, R. M. 2008b. The androgen receptor can signal through Wnt/β-Catenin in prostate cancer cells as an adaptation mechanism to castration levels of androgens. *BMC cell biology,* 9**,** 1-15.

Segawa, N., Mori, I., Utsunomiya, H., Nakamura, M., Nakamura, Y., Shan, L., Kakudo, K. & Katsuoka, Y. 2001. Prognostic significance of neuroendocrine differentiation, proliferation

activity and androgen receptor expression in prostate cancer. *Pathology international,* 51**,** 452-459.

Seifert, J. R. & Mlodzik, M. 2007. Frizzled/PCP signalling: a conserved mechanism regulating cell polarity and directed motility. *Nature Reviews Genetics,* 8**,** 126-138.

Semënov, M., Tamai, K. & He, X. 2005. SOST is a ligand for LRP5/LRP6 and a Wnt signaling inhibitor. *Journal of Biological Chemistry,* 280**,** 26770-26775.

Senda, T., Shimomura, A. & Iizuka-Kogo, A. 2005. Adenomatous polyposis coli (Apc) tumor suppressor gene as a multifunctional gene. *Anatomical science international,* 80**,** 121-131.

Sengüven, B., Baris, E., Oygur, T. & Berktas, M. 2014. Comparison of methods for the extraction of DNA from formalin-fixed, paraffin-embedded archival tissues. *International journal of medical sciences,* 11**,** 494.

Seshagiri, S., Stawiski, E. W., Durinck, S., Modrusan, Z., Storm, E. E., Conboy, C. B., Chaudhuri, S., Guan, Y., Janakiraman, V. & Jaiswal, B. S. 2012. Recurrent R-spondin fusions in colon cancer. *Nature,* 488**,** 660-664.

Sethi, J. K. & Vidal-Puig, A. 2010. Wnt signalling and the control of cellular metabolism. *Biochemical Journal,* 427**,** 1-17.

Shah, R. B., Mehra, R., Chinnaiyan, A. M., Shen, R., Ghosh, D., Zhou, M., Macvicar, G. R., Varambally, S., Harwood, J. & Bismar, T. A. 2004. Androgen-independent prostate cancer is a heterogeneous group of diseases: lessons from a rapid autopsy program. *Cancer research,* 64**,** 9209-9216.

Shah, R. B. & Zhou, M. 2016. Recent advances in prostate cancer pathology: Gleason grading and beyond. *Pathology international,* 66**,** 260-272.

Shao, Q., Wang, H., Mclachlan, E., Veitch, G. I. & Laird, D. W. 2005. Down-regulation of Cx43 by retroviral delivery of small interfering RNA promotes an aggressive breast cancer cell phenotype. *Cancer research,* 65**,** 2705-2711.

Sharma, N. L., Massie, C. E., Ramos-Montoya, A., Zecchini, V., Scott, H. E., Lamb, A. D., Macarthur, S., Stark, R., Warren, A. Y. & Mills, I. G. 2013. The androgen receptor induces a distinct transcriptional program in castration-resistant prostate cancer in man. *Cancer cell,* 23**,** 35-47.

Shen, M. M. & Abate-Shen, C. 2010. Molecular genetics of prostate cancer: new prospects for old challenges. *Genes & development,* 24**,** 1967-2000.

Sheridan, J. & Atkinson, M. 1985. Physiological roles of permeable junctions: some possibilities. *Annual review of physiology,* 47**,** 337-353.

Sherwood, V. & Leigh, I. M. 2016. WNT signaling in cutaneous squamous cell carcinoma: a future treatment strategy? *Journal of Investigative Dermatology,* 136**,** 1760-1767.

Shi, Q. & Jackowski, G. 1998. One-dimensional polyacrylamide gel electrophoresis. *Gel electrophoresis of proteins: A practical approach,* 3**,** 1-52.

Shi, S.-R., Key, M. E. & Kalra, K. L. 1991. Antigen retrieval in formalin-fixed, paraffin-embedded tissues: an enhancement method for immunohistochemical staining based on microwave oven heating of tissue sections. *Journal of Histochemistry & Cytochemistry,* 39**,** 741-748.

Shimizu, H., Ross, R., Bernstein, L., Yatani, R., Henderson, B. & Mack, T. 1991. Cancers of the prostate and breast among Japanese and white immigrants in Los Angeles County. *British journal of cancer,* 63**,** 963-966.

Shtutman, M., Zhurinsky, J., Simcha, I., Albanese, C., D'amico, M., Pestell, R. & Ben-Ze'ev, A. 1999. The cyclin D1 gene is a target of the β-catenin/LEF-1 pathway. *Proceedings of the National Academy of Sciences,* 96**,** 5522-5527.

Shulewitz, M., Soloviev, I., Wu, T., Koeppen, H., Polakis, P. & Sakanaka, C. 2006. Repressor roles for TCF-4 and Sfrp1 in Wnt signaling in breast cancer. *Oncogene,* 25**,** 4361-9.

Siar, C. H., Nagatsuka, H., Han, P. P., Buery, R. R., Tsujigiwa, H., Nakano, K., Ng, K. H. & Kawakami, T. 2012. Differential expression of canonical and non-canonical Wnt ligands in ameloblastoma. *Journal of oral pathology & medicine,* 41**,** 332-339.

Siegel, R. L. 2016. Miller kd and Jemal A: Cancer statistics, 2016. *CA Cancer j Clin,* 66**,** 7-30.

Siegel, R. L., Miller, K. D. & Jemal, A. 2016. Cancer statistics, 2016. *CA: a cancer journal for clinicians,* 66**,** 7-30.

Siemens, H., Neumann, J., Jackstadt, R., Mansmann, U., Horst, D., Kirchner, T. & Hermeking, H. 2013. Detection of miR-34a promoter methylation in combination with elevated expression of c-Met and β-catenin predicts distant metastasis of colon cancer. *Clinical cancer research,* 19**,** 710-720.

Simental, J., Sar, M., Lane, M., French, F. & Wilson, E. 1991. Transcriptional activation and nuclear targeting signals of the human androgen receptor. *Journal of Biological Chemistry,* 266**,** 510-518.

Smith, P. E., Krohn, R. I., Hermanson, G. T., Mallia, A. K., Gartner, F. H., Provenzano, M., Fujimoto, E. K., Goeke, N. M., Olson, B. J. & Klenk, D. 1985. Measurement of protein using bicinchoninic acid. *Analytical biochemistry,* 150**,** 76-85.

Smolich, B. D., Mcmahon, J. A., Mcmahon, A. P. & Papkoff, J. 1993. Wnt family proteins are secreted and associated with the cell surface. *Molecular biology of the cell,* 4**,** 1267-1275.

Soetemans, D. J. 2017. Computer-assisted characterization of prostate cancer on magnetic resonance imaging.

Söhl, G. & Willecke, K. 2003. An update on connexin genes and their nomenclature in mouse and man. *Cell communication & adhesion,* 10**,** 173-180.

Söhl, G. & Willecke, K. 2004. Gap junctions and the connexin protein family. *Cardiovascular research,* 62**,** 228-232.

Song, L.-N., Herrell, R., Byers, S., Shah, S., Wilson, E. M. & Gelmann, E. P. 2003. β-Catenin binds to the activation function 2 region of the androgen receptor and modulates the effects of the N-terminal domain and TIF2 on ligand-dependent transcription. *Molecular and cellular biology,* 23**,** 1674-1687.

Song, M. S., Salmena, L. & Pandolfi, P. P. 2012. The functions and regulation of the PTEN tumour suppressor. *Nature reviews Molecular cell biology,* 13**,** 283-296.

Spagnol, G., Trease, A. J., Zheng, L., Gutierrez, M., Basu, I., Sarmiento, C., Moore, G., Cervantes, M. & Sorgen, P. L. 2018. Connexin43 carboxyl-terminal domain directly interacts with β-catenin. *International journal of molecular sciences,* 19**,** 1562.

Srinivas, M., Verselis, V. K. & White, T. W. 2018. Human diseases associated with connexin mutations. *Biochimica et Biophysica Acta (BBA)-Biomembranes,* 1860**,** 192-201.

Städeli, R., Hoffmans, R. & Basler, K. 2006. Transcription under the control of nuclear Arm/β-catenin. *Current Biology,* 16**,** R378-R385.

Stamos, J. L. & Weis, W. I. 2013. The β-catenin destruction complex. *Cold Spring Harbor perspectives in biology,* 5**,** a007898.

Steger, K., Tetens, F. & Bergmann, M. 1999. Expression of connexin 43 in human testis. *Histochemistry and cell biology,* 112**,** 215-220.

Stehno-Bittel, L., Perez-Terzic, C. & Clapham, D. E. 1995. Diffusion across the nuclear envelope inhibited by depletion of the nuclear Ca2+ store. *Science,* 270**,** 1835-1838.

Stocco, D. 2000. The role of the StAR protein in steroidogenesis: challenges for the future. *Journal of Endocrinology,* 164**,** 247-253.

Stocco, D. M. & Clark, B. J. 1996. Regulation of the acute production of steroids in steroidogenic cells. *Endocrine reviews,* 17**,** 221-244.

Stolz, W., Schmoeckel, C., Landthaler, M. & Braun-Falco, O. 1989. Association of early malignant melanoma with nevocytic nevi. *Cancer,* 63**,** 550-555.

Story, M. T., Livingston, B., Baeten, L., Swartz, S. J., Jacobs, S. C., Begun, F. P. & Lawson, R. K. 1989. Cultured human prostate-derived fibroblasts produce a factor that stimulates their growth with properties indistinguishable from basic fibroblast growth factor. *The Prostate,* 15**,** 355-365.

Stubbs, A., Lalani, E.-N., Stamp, G., Hurst, H., Abel, P. & Waxman, J. 1996. Second messenger up-regulation of androgen receptor gene transcription is absent in androgen insensitive human prostatic carcinoma cell lines, PC-3 and DU-145. *FEBS letters,* 383**,** 237-240.

Suarez, B. K., Gerhard, D. S., Lin, J., Haberer, B., Nguyen, L., Kesterson, N. K. & Catalona, W. J. 2001. Polymorphisms in the prostate cancer susceptibility gene HPC2/ELAC2 in multiplex families and healthy controls. *Cancer research,* 61**,** 4982-4984.

Sugimura, Y., Cunha, G. & Donjacour, A. 1986. Morphogenesis of ductal networks in the mouse prostate. *Biology of reproduction,* 34**,** 961-971.

Suh, E.-K. & Gumbiner, B. M. 2003. Translocation of β-catenin into the nucleus independent of interactions with FG-rich nucleoporins. *Experimental cell research,* 290**,** 447-456.

Sun, F., Indran, I. R., Zhang, Z. W., Tan, M. E., Li, Y., Lim, Z. R., Hua, R., Yang, C., Soon, F.-F. & Li, J. 2015. A novel prostate cancer therapeutic strategy using icaritin-activated arylhydrocarbon-receptor to co-target androgen receptor and its splice variants. *Carcinogenesis,* 36**,** 757-768.

Sun, S., Sprenger, C. C., Vessella, R. L., Haugk, K., Soriano, K., Mostaghel, E. A., Page, S. T., Coleman, I. M., Nguyen, H. M. & Sun, H. 2010. Castration resistance in human prostate cancer is conferred by a frequently occurring androgen receptor splice variant. *The Journal of clinical investigation,* 120**,** 2715-2730.

Svindland, A., Eri, L. & Tveter, K. 1996. Morphometry of benign prostatic hyperplasia during androgen suppressive therapy. Relationships among epithelial content, PSA density, and clinical outcome. *Scandinavian journal of urology and nephrology. Supplementum,* 179**,** 113-117.

Symes, A. J., Eilertsen, M., Millar, M., Nariculam, J., Freeman, A., Notara, M., Feneley, M. R., Patel, H. R., Masters, J. R. & Ahmed, A. 2013. Quantitative analysis of BTF3, HINT1, NDRG1 and ODC1 protein over-expression in human prostate cancer tissue. *PLoS One,* 8.

Szafran, A. T., Stephan, C., Bolt, M., Mancini, M. G., Marcelli, M. & Mancini, M. A. 2017. High-content screening identifies Src family kinases as potential regulators of AR-V7 expression and androgen-independent cell growth. *The Prostate,* 77**,** 82-93.

Szczyrba, J., Niesen, A., Wagner, M., Wandernoth, P. M., Aumüller, G. & Wennemuth, G. 2017. Neuroendocrine cells of the prostate derive from the neural crest. *Journal of Biological Chemistry,* 292**,** 2021-2031.

Tacchelly-Benites, O., Wang, Z., Yang, E., Benchabane, H., Tian, A., Randall, M. P. & Ahmed, Y. 2018. Axin phosphorylation in both Wnt-off and Wnt-on states requires the tumor suppressor APC. *PLoS genetics,* 14**,** e1007178.

Tai, S., Sun, Y., Squires, J. M., Zhang, H., Oh, W. K., Liang, C. Z. & Huang, J. 2011. PC3 is a cell line characteristic of prostatic small cell carcinoma. *The Prostate,* 71**,** 1668-1679.

Taitt, H. E. 2018. Global trends and prostate cancer: a review of incidence, detection, and mortality as influenced by race, ethnicity, and geographic location. *American journal of men's health,* 12**,** 1807-1823.

Takada, R., Satomi, Y., Kurata, T., Ueno, N., Norioka, S., Kondoh, H., Takao, T. & Takada, S. 2006. Monounsaturated fatty acid modification of Wnt protein: its role in Wnt secretion. *Developmental cell,* 11**,** 791-801.

Takahashi, S., Watanabe, T., Okada, M., Inoue, K., Ueda, T., Takada, I., Watabe, T., Yamamoto, Y., Fukuda, T. & Nakamura, T. 2011. Noncanonical Wnt signaling mediates androgen-dependent tumor growth in a mouse model of prostate cancer. *Proceedings of the National Academy of Sciences,* 108**,** 4938-4943.

Takane, K. K. & Mcphaul, M. J. 1996. Functional analysis of the human androgen receptor promoter. *Molecular and cellular endocrinology,* 119**,** 83-93.

Takeda, H., Akakura, K., Masai, M., Akimoto, S., Yatani, R. & Shimazaki, J. 1996. Androgen receptor content of prostate carcinoma cells estimated by immunohistochemistry is related to prognosis of patients with stage D2 prostate carcinoma. *Cancer: Interdisciplinary International Journal of the American Cancer Society,* 77**,** 934-940.

Takeda, H., Nakamoto, T., Kokontis, J., Chodak, G. W. & Chang, C. 1991. Autoregulation of androgen receptor expression in rodent prostate: immunohistochemical and in situ hybridization analysis. *Biochemical and biophysical research communications,* 177**,** 488-496.

Takemaru, K.-I. & Moon, R. T. 2000. The transcriptional coactivator CBP interacts with β-catenin to activate gene expression. *The Journal of cell biology,* 149**,** 249-254.

Talla, S. B. & Brembeck, F. H. 2016. The role of Pygo2 for Wnt/ß-catenin signaling activity during intestinal tumor initiation and progression. *Oncotarget,* 7**,** 80612.

Tamamura, Y., Otani, T., Kanatani, N., Koyama, E., Kitagaki, J., Komori, T., Yamada, Y., Costantini, F., Wakisaka, S. & Pacifici, M. 2005. Developmental regulation of Wnt/β-catenin signals is required for growth plate assembly, cartilage integrity, and endochondral ossification. *Journal of Biological Chemistry,* 280**,** 19185-19195.

Tan, M. E., Li, J., Xu, H. E., Melcher, K. & Yong, E.-L. 2015. Androgen receptor: structure, role in prostate cancer and drug discovery. *Acta Pharmacologica Sinica,* 36**,** 3-23.

Tan, X., Behari, J., Cieply, B., Michalopoulos, G. K. & Monga, S. P. 2006. Conditional deletion of β-catenin reveals its role in liver growth and regeneration. *Gastroenterology,* 131**,** 1561-1572.

Tanegashima, K., Zhao, H. & Dawid, I. B. 2008. WGEF activates Rho in the Wnt–PCP pathway and controls convergent extension in Xenopus gastrulation. *The EMBO journal,* 27**,** 606-617.

Tang, B., Peng, Z.-H., Yu, P.-W., Yu, G. & Qian, F. 2011. Expression and significance of Cx43 and E-cadherin in gastric cancer and metastatic lymph nodes. *Medical Oncology,* 28**,** 502-508.

Taplin, M.-E., Bubley, G. J., Ko, Y.-J., Small, E. J., Upton, M., Rajeshkumar, B. & Balk, S. P. 1999. Selection for androgen receptor mutations in prostate cancers treated with androgen antagonist. *Cancer research,* 59**,** 2511-2515.

Taplin, M. E. & Balk, S. P. 2004. Androgen receptor: a key molecule in the progression of prostate cancer to hormone independence. *Journal of cellular biochemistry,* 91**,** 483-190.

Tarakanov, A. O. & Goncharova, L. B. 2009. Cell-cell nanotubes: tunneling through several types of synapses. *Communicative & Integrative Biology,* 2**,** 359-361.

Taylor, B. S., Schultz, N., Hieronymus, H., Gopalan, A., Xiao, Y., Carver, B. S., Arora, V. K., Kaushik, P., Cerami, E. & Reva, B. 2010. Integrative genomic profiling of human prostate cancer. *Cancer cell,* 18**,** 11-22.

Taylor, C. & Burns, J. 1974. The demonstration of plasma cells and other immunoglobulin-containing cells in formalin-fixed, paraffin-embedded tissues using peroxidase-labelled antibody. *Journal of clinical pathology,* 27**,** 14-20.

Taylor, C. R., Shi, S.-R., Barr, N. & Wu, N. 2013. Techniques of immunohistochemistry: principles, pitfalls, and standardization. *Diagnostic immunohistochemistry,* 2**,** 1-42.

Tepper, C. G., Boucher, D. L., Ryan, P. E., Ma, A.-H., Xia, L., Lee, L.-F., Pretlow, T. G. & Kung, H.-J. 2002. Characterization of a novel androgen receptor mutation in a relapsed CWR22 prostate cancer xenograft and cell line. *Cancer research,* 62**,** 6606-6614.

Terry, S., Yang, X., Chen, M. W., Vacherot, F. & Buttyan, R. 2006. Multifaceted interaction between the androgen and Wnt signaling pathways and the implication for prostate cancer. *Journal of cellular biochemistry,* 99**,** 402-410.

Theodoropoulos, V., Tsigka, A., Mihalopoulou, A., Tsoukala, V., Lazaris, A., Patsouris, E. & Ghikonti, I. 2005. Evaluation of neuroendocrine staining and androgen receptor expression in incidental prostatic adenocarcinoma: prognostic implications. *Urology,* 66**,** 897-902.

Thomson, A. A. 2008. Mesenchymal mechanisms in prostate organogenesis. *Differentiation,* 76**,** 587-598.

Thorne, C. A., Hanson, A. J., Schneider, J., Tahinci, E., Orton, D., Cselenyi, C. S., Jernigan, K. K., Meyers, K. C., Hang, B. I. & Waterson, A. G. 2010. Small-molecule inhibition of Wnt signaling through activation of casein kinase 1α. *Nature chemical biology,* 6**,** 829-836.

Thrasivoulou, C., Millar, M. & Ahmed, A. 2013. Activation of intracellular calcium by multiple Wnt ligands and translocation of β-catenin into the nucleus a convergent model of wnt/ca2+ and wnt/β-catenin pathways. *Journal of Biological Chemistry,* 288**,** 35651-35659.

Timms, B. G. 2008. Prostate development: a historical perspective. *Differentiation,* 76**,** 565-577.

Timms, B. G. & Hofkamp, L. E. 2011. Prostate development and growth in benign prostatic hyperplasia. *Differentiation,* 82**,** 173-183.

Titus, M. A., Schell, M. J., Lih, F. B., Tomer, K. B. & Mohler, J. L. 2005. Testosterone and dihydrotestosterone tissue levels in recurrent prostate cancer. *Clinical cancer research,* 11**,** 4653-4657.

Toivanen, R. & Shen, M. M. 2017. Prostate organogenesis: tissue induction, hormonal regulation and cell type specification. *Development,* 144**,** 1382-1398.

Tokizane, T., Shiina, H., Igawa, M., Enokida, H., Urakami, S., Kawakami, T., Ogishima, T., Okino, S. T., Li, L.-C. & Tanaka, Y. 2005. Cytochrome P450 1B1 is overexpressed and regulated by hypomethylation in prostate cancer. *Clinical cancer research,* 11**,** 5793-5801.

Toko, H., Hariharan, N., Konstandin, M. H., Ormachea, L., Mcgregor, M., Gude, N. A., Sundararaman, B., Joyo, E., Joyo, A. Y. & Collins, B. 2014. Differential regulation of cellular senescence and differentiation by prolyl isomerase Pin1 in cardiac progenitor cells. *Journal of Biological Chemistry,* 289**,** 5348-5356.

Tomlins, S. A., Rhodes, D. R., Perner, S., Dhanasekaran, S. M., Mehra, R., Sun, X.-W., Varambally, S., Cao, X., Tchinda, J. & Kuefer, R. 2005. Recurrent fusion of TMPRSS2 and ETS transcription factor genes in prostate cancer. *science,* 310**,** 644-648.

Toren, P. & Zoubeidi, A. 2014. Targeting the PI3K/Akt pathway in prostate cancer: challenges and opportunities. *International journal of oncology,* 45**,** 1793-1801.

Torres, V. I., Godoy, J. A. & Inestrosa, N. C. 2019. Modulating Wnt signaling at the root: Porcupine and Wnt acylation. *Pharmacology & therapeutics,* 198**,** 34-45.

Toth, Z. E. & Mezey, E. 2007. Simultaneous visualization of multiple antigens with tyramide signal amplification using antibodies from the same species. *Journal of Histochemistry & Cytochemistry,* 55**,** 545-554.

Towbin, H. & Gordon, J. 1984. Immunoblotting and dot immunobinding—current status and outlook. *Journal of immunological methods,* 72**,** 313-340.

Towbin, H., Staehelin, T. & Gordon, J. 1979. Electrophoretic transfer of proteins from polyacrylamide gels to nitrocellulose sheets: procedure and some applications. *Proceedings of the National Academy of Sciences,* 76**,** 4350-4354.

Toyofuku, T., Yabuki, M., Otsu, K., Kuzuya, T., Hori, M. & Tada, M. 1998. Direct association of the gap junction protein connexin-43 with ZO-1 in cardiac myocytes. *Journal of Biological Chemistry,* 273**,** 12725-12731.

Trapman, J., Ris-Stalpers, C., Van Der Korput, J., Kuiper, G., Faber, P., Romijn, J., Mulder, E. & Brinkmann, A. 1990. The androgen receptor: functional structure and expression in transplanted human prostate tumors and prostate tumor cell lines. *The Journal of steroid biochemistry and molecular biology,* 37**,** 837-842.

Travis, A., Amsterdam, A., Belanger, C. & Grosschedl, R. 1991. LEF-1, a gene encoding a lymphoid-specific protein with an HMG domain, regulates T-cell receptor alpha enhancer function [corrected]. *Genes & development,* 5**,** 880-894.

Trosko, J. E. 2007. Gap junctional intercellular communication as a biological “Rosetta stone” in understanding, in a systems biological manner, stem cell behavior, mechanisms of epigenetic toxicology, chemoprevention and chemotherapy. *Journal of Membrane Biology,* 218**,** 93-100.

Truica, C. I., Byers, S. & Gelmann, E. P. 2000. β-Catenin affects androgen receptor transcriptional activity and ligand specificity. *Cancer research,* 60**,** 4709-4713.

Tsai, H., Werber, J., Davia, M. O., Edelman, M., Tanaka, K. E., Melman, A., Christ, G. J. & Geliebter, J. 1996. Reduced connexin 43 expression in high grade, human prostatic adenocarcinoma cells. *Biochemical and biophysical research communications,* 227**,** 64-69.

Tsivian, M., Sun, L., Mouraviev, V., Madden, J. F., Mayes, J. M., Moul, J. W. & Polascik, T. J. 2009. Changes in Gleason score grading and their effect in predicting outcome after radical prostatectomy. *Urology,* 74**,** 1090-1093.

Tyagi, R. K., Lavrovsky, Y., Ahn, S. C., Song, C. S., Chatterjee, B. & Roy, A. K. 2000. Dynamics of intracellular movement and nucleocytoplasmic recycling of the ligand-activated androgen receptor in living cells. *Molecular endocrinology,* 14**,** 1162-1174.

Tzenov, Y. R., Andrews, P. G., Voisey, K., Popadiuk, P., Xiong, J., Popadiuk, C. & Kao, K. R. 2013. Human papilloma virus (HPV) E7-mediated attenuation of retinoblastoma (Rb) induces hPygopus2 expression via Elf-1 in cervical cancer. *Molecular Cancer Research,* 11**,** 19-30.

Ubuka, T., Moriya, S., Soga, T. & Parhar, I. 2018. Identification of transmembrane protease serine 2 and forkhead box A1 as the potential bisphenol A responsive genes in the neonatal male rat brain. *Frontiers in endocrinology,* 9**,** 139.

Van Amerongen, R. 2012. Alternative Wnt pathways and receptors. *Cold Spring Harbor perspectives in biology,* 4**,** a007914.

Van Breemen, R. B. & Pajkovic, N. 2008. Multitargeted therapy of cancer by lycopene. *Cancer letters,* 269**,** 339-351.

Van Gijn, M. E., Daemen, M. J., Smits, J. F. & Blankesteijn, W. M. 2002. The wnt-frizzled cascade in cardiovascular disease. *Cardiovascular research,* 55**,** 16-24.

Van Leenders, G. J., Gage, W. R., Hicks, J. L., Van Balken, B., Aalders, T. W., Schalken, J. A. & De Marzo, A. M. 2003. Intermediate cells in human prostate epithelium are enriched in proliferative inflammatory atrophy. *The American journal of pathology,* 162**,** 1529-1537.

Van Leeuwen, F., Samos, C. H. & Nusse, R. 1994. Biological activity of soluble wingless protein in cultured Drosophila imaginal disc cells. *Nature,* 368**,** 342-344.

Vanslyke, J. K. & Musil, L. S. 2005. Cytosolic stress reduces degradation of connexin43 internalized from the cell surface and enhances gap junction formation and function. *Molecular biology of the cell,* 16**,** 5247-5257.

Veeman, M. T., Axelrod, J. D. & Moon, R. T. 2003. A second canon: functions and mechanisms of β-catenin-independent Wnt signaling. *Developmental cell,* 5**,** 367-377.

Veldscholte, J., Berrevoets, C., Ris-Stalpers, C., Kuiper, G., Jenster, G., Trapman, J., Brinkmann, A. & Mulder, E. 1992. The androgen receptor in LNCaP cells contains a mutation in the ligand binding domain which affects steroid binding characteristics and response to antiandrogens. *The Journal of steroid biochemistry and molecular biology,* 41**,** 665-669.

Vernet, S. G. 1953. *Patología urogenital: Biología y patología de la próstata. Tomo II-Volumen I*, Paz Montalvo.

Verras, M., Brown, J., Li, X., Nusse, R. & Sun, Z. 2004. Wnt3a growth factor induces androgen receptor-mediated transcription and enhances cell growth in human prostate cancer cells. *Cancer research,* 64**,** 8860-8866.

Vijayakumar, S., Winter, K., Sause, W., Gallagher, M. J., Michalski, J., Roach, M., Porter, A. & Bondy, M. 1998. Prostate-specific antigen levels are higher in African-American than in white patients in a multicenter registration study: results of RTOG 94-12. *International Journal of Radiation Oncology* Biology* Physics,* 40**,** 17-25.

Vinken, M., Vanhaecke, T., Papeleu, P., Snykers, S., Henkens, T. & Rogiers, V. 2006. Connexins and their channels in cell growth and cell death. *Cellular signalling,* 18**,** 592-600.

Visakorpi, T., Kallioniemi, A. H., Syvänen, A.-C., Hyytinen, E. R., Karhu, R., Tammela, T., Isola, J. J. & Kallioniemi, O.-P. 1995. Genetic changes in primary and recurrent prostate cancer by comparative genomic hybridization. *Cancer research,* 55**,** 342-347.

Voeller, H. J., Augustus, M., Madike, V., Bova, G. S., Carter, K. C. & Gelmann, E. P. 1997. Coding region of NKX3. 1, a prostate-specific homeobox gene on 8p21, is not mutated in human prostate cancers. *Cancer research,* 57**,** 4455-4459.

Vogt, P. K. 2002. Fortuitous convergences: the beginnings of JUN. *Nature Reviews Cancer,* 2**,** 465-469.

Volinia, S., Calin, G. A., Liu, C.-G., Ambs, S., Cimmino, A., Petrocca, F., Visone, R., Iorio, M., Roldo, C. & Ferracin, M. 2006. A microRNA expression signature of human solid tumors defines cancer gene targets. *Proceedings of the National Academy of Sciences,* 103**,** 2257-2261.

Wallingford, J. B. & Habas, R. 2005. The developmental biology of Dishevelled: an enigmatic protein governing cell fate and cell polarity. *Development,* 132**,** 4421-4436.

Wan, W.-H., Fortuna, M. B. & Furmanski, P. 1987. A rapid and efficient method for testing immunohistochemical reactivity of monoclonal antibodies against multiple tissue samples simultaneously. *Journal of immunological methods,* 103**,** 121-129.

Wan, X., Liu, J., Lu, J.-F., Tzelepi, V., Yang, J., Starbuck, M. W., Diao, L., Wang, J., Efstathiou, E. & Vazquez, E. S. 2012. Activation of β-catenin signaling in androgen receptor–negative prostate Cancer cells. *Clinical cancer research,* 18**,** 726-736.

Wang, B., Lo, U. G., Wu, K., Kapur, P., Liu, X., Huang, J., Chen, W., Hernandez, E., Santoyo, J. & Ma, S. H. 2017. Developing new targeting strategy for androgen receptor variants in castration resistant prostate cancer. *International journal of cancer,* 141**,** 2121-2130.

Wang, F., Flanagan, J., Su, N., Wang, L.-C., Bui, S., Nielson, A., Wu, X., Vo, H.-T., Ma, X.-J. & Luo, Y. 2012. RNAscope: a novel in situ RNA analysis platform for formalin-fixed, paraffin-embedded tissues. *The Journal of molecular diagnostics,* 14**,** 22-29.

Wang, G., Wang, J. & Sadar, M. D. 2008. Crosstalk between the androgen receptor and β-catenin in castrate-resistant prostate cancer. *Cancer research,* 68**,** 9918-9927.

Wang, G., Zhao, D., Spring, D. J. & Depinho, R. A. 2018. Genetics and biology of prostate cancer. *Genes & development,* 32**,** 1105-1140.

Wang, H., Fu, J., Xu, D., Xu, W., Wang, S., Zhang, L. & Xiang, Y. 2016. Downregulation of Pygopus 2 inhibits vascular mimicry in glioma U251 cells by suppressing the canonical Wnt signaling pathway. *Oncology letters,* 11**,** 678-684.

Wang, H., Wang, M. X.-M., Su, N., Wang, L.-C., Wu, X., Bui, S., Nielsen, A., Vo, H.-T., Nguyen, N. & Luo, Y. 2014. RNAscope for in situ detection of transcriptionally active human papillomavirus in head and neck squamous cell carcinoma. *Journal of visualized experiments: JoVE*.

Wang, L., Wang, L., Cybula, M., Drumond-Bock, A. L., Moxley, K. M. & Bieniasz, M. 2020. Multi-kinase targeted therapy as a promising treatment strategy for ovarian tumors expressing sfRon receptor. *Genes & cancer,* 11**,** 106.

Wang, M., Berthoud, V. M. & Beyer, E. C. 2007a. Connexin43 increases the sensitivity of prostate cancer cells to TNFα-induced apoptosis. *Journal of cell science,* 120**,** 320-329.

Wang, M. & Stearns, M. E. 1991. Isolation and characterization of PC-3 human prostatic tumor sublines which preferentially metastasize to select organs in SCID mice. *Differentiation,* 48**,** 115-125.

Wang, Q., Symes, A. J., Kane, C. A., Freeman, A., Nariculam, J., Munson, P., Thrasivoulou, C., Masters, J. R. & Ahmed, A. 2010a. A novel role for Wnt/Ca2+ signaling in actin cytoskeleton remodeling and cell motility in prostate cancer. *PloS one,* 5.

Wang, Q., Symes, A. J., Kane, C. A., Freeman, A., Nariculam, J., Munson, P., Thrasivoulou, C., Masters, J. R. & Ahmed, A. 2010b. A novel role for Wnt/Ca 2+ signaling in actin cytoskeleton remodeling and cell motility in prostate cancer. *PloS one,* 5**,** e10456.

Wang, Q., Williamson, M., Bott, S., Brookman-Amissah, N., Freeman, A., Nariculam, J., Hubank, M., Ahmed, A. & Masters, J. 2007b. Hypomethylation of WNT5A, CRIP1 and S100P in prostate cancer. *Oncogene,* 26**,** 6560-6565.

Wang, W., Bergh, A. & Damber, J. E. 2009. Morphological transition of proliferative inflammatory atrophy to high-grade intraepithelial neoplasia and cancer in human prostate. *The Prostate,* 69**,** 1378-1386.

Wang, Y., Krivtsov, A. V., Sinha, A. U., North, T. E., Goessling, W., Feng, Z., Zon, L. I. & Armstrong, S. A. 2010c. The Wnt/β-catenin pathway is required for the development of leukemia stem cells in AML. *Science,* 327**,** 1650-1653.

Wang, Y.-L., Wu, S., Jiang, B., Yin, F.-F., Zheng, S.-S. & Hou, S.-C. 2015. Role of microRNAs in prostate cancer pathogenesis. *Clinical genitourinary cancer,* 13**,** 261-270.

Wang, Z., Portier, B. P., Gruver, A. M., Bui, S., Wang, H., Su, N., Vo, H.-T., Ma, X.-J., Luo, Y. & Budd, G. T. 2013. Automated quantitative RNA in situ hybridization for resolution of equivocal and heterogeneous ERBB2 (HER2) status in invasive breast carcinoma. *The Journal of molecular diagnostics,* 15**,** 210-219.

Weber, M. J. & Gioeli, D. 2004. Ras signaling in prostate cancer progression. *Journal of cellular biochemistry,* 91**,** 13-25.

Wei, C.-J., Xu, X. & Lo, C. W. 2004. Connexins and cell signaling in development and disease. *Annu. Rev. Cell Dev. Biol.,* 20**,** 811-838.

Weis, W. I. & Nelson, W. J. 2006. Re-solving the cadherin-catenin-actin conundrum. *Journal of biological chemistry,* 281**,** 35593-35597.

Whitaker, H. C., Girling, J., Warren, A. Y., Leung, H., Mills, I. G. & Neal, D. E. 2008. Alterations in β-catenin expression and localization in prostate cancer. *The Prostate,* 68**,** 1196-1205.

White, B. D., Chien, A. J. & Dawson, D. W. 2012. Dysregulation of Wnt/β-catenin signaling in gastrointestinal cancers. *Gastroenterology,* 142**,** 219-232.

Willecke, K., Eiberger, J., Degen, J., Eckardt, D., Romualdi, A., Güldenagel, M., Deutsch, U. & Söhl, G. 2002. Structural and functional diversity of connexin genes in the mouse and human genome.

Willert, K., Brown, J. D., Danenberg, E., Duncan, A. W., Weissman, I. L., Reya, T., Yates, J. R. & Nusse, R. 2003. Wnt proteins are lipid-modified and can act as stem cell growth factors. *Nature,* 423**,** 448-452.

Willert, K. & Nusse, R. 1998. β-catenin: a key mediator of Wnt signaling. *Current opinion in genetics & development,* 8**,** 95-102.

Willert, K. & Nusse, R. 2012. Wnt proteins. *Cold Spring Harbor perspectives in biology,* 4**,** a007864.

Williams, J. L., Yoshimoto, M., Boag, A. H., Squire, J. A. & Park, P. C. 2011. TMPRSS2: ETS gene fusions in prostate cancer. *Atlas of Genetics and Cytogenetics in Oncology and Haematology*.

Wilson, C. M. & Mcphaul, M. J. 1994. A and B forms of the androgen receptor are present in human genital skin fibroblasts. *Proceedings of the National Academy of Sciences,* 91**,** 1234-1238.

Wilson, K. M., Shui, I. M., Mucci, L. A. & Giovannucci, E. 2015. Calcium and phosphorus intake and prostate cancer risk: a 24-y follow-up study. *The American journal of clinical nutrition,* 101**,** 173-183.

Wiren, K. M., Zhang, X., Chang, C., Keenan, E. & Orwoll, E. S. 1997. Transcriptional up-regulation of the human androgen receptor by androgen in bone cells. *Endocrinology,* 138**,** 2291-2300.

Wisdon, R. & Verma, I. M. 1993. Transformation by Fos proteins requires a C-terminal transactivation domain. *Molecular and cellular biology,* 13**,** 7429-7438.

Wong, H.-C., Bourdelas, A., Krauss, A., Lee, H.-J., Shao, Y., Wu, D., Mlodzik, M., Shi, D.-L. & Zheng, J. 2003. Direct binding of the PDZ domain of Dishevelled to a conserved internal sequence in the C-terminal region of Frizzled. *Molecular cell,* 12**,** 1251-1260.

Wu, I. & Modlin, C. S. 2012. Disparities in prostate cancer in African American men: what primary care physicians can do. *Cleve Clin J Med,* 79**,** 313-320.

Wu, J., Ji, A., Wang, X., Zhu, Y., Yu, Y., Lin, Y., Liu, Y., Li, S., Liang, Z. & Xu, X. 2015. MicroRNA-195-5p, a new regulator of Fra-1, suppresses the migration and invasion of prostate cancer cells. *Journal of translational medicine,* 13**,** 1-15.

Wu, L., Runkle, C., Jin, H., Yu, J., Li, J., Yang, X., Kuzel, T. & Lee, C. 2014. CCN3/NOV gene expression in human prostate cancer is directly suppressed by the androgen receptor. *Oncogene,* 33**,** 504-513.

Wünnemann, F., Kokta, V., Leclerc, S., Thibeault, M., Mccuaig, C., Hatami, A., Stheneur, C., Grenier, J.-C., Awadalla, P. & Mitchell, G. A. 2016. Aortic dilatation associated with a de novo mutation in the SOX18 gene: expanding the clinical spectrum of hypotrichosis-lymphedema-telangiectasia syndrome. *Canadian Journal of Cardiology,* 32**,** 135. e1-135. e7.

Xiao, S., Zhou, Y., Jiang, J., Yuan, L. & Xue, M. 2014. CD44 affects the expression level of FOS-like antigen 1 in cervical cancer tissues. *Molecular medicine reports,* 9**,** 1667-1674.

Xing, Y., Takemaru, K.-I., Liu, J., Berndt, J. D., Zheng, J. J., Moon, R. T. & Xu, W. 2008. Crystal structure of a full-length β-catenin. *Structure,* 16**,** 478-487.

Xing, Y., Xiao, Y., Zeng, F., Zhao, J., Xiao, C., Xiong, P. & Feng, W. 2007. Altered expression of connexin-43 and impaired capacity of gap junctional intercellular communication in prostate cancer cells. *Journal of Huazhong University of Science and Technology,* 27**,** 291-294.

Xu, J., Prosperi, J. R., Choudhury, N., Olopade, O. I. & Goss, K. H. 2015. β-Catenin is required for the tumorigenic behavior of triple-negative breast cancer cells. *PloS one,* 10**,** e0117097.

Xu, J., Zheng, S. L., Komiya, A., Mychaleckyj, J. C., Isaacs, S. D., Hu, J. J., Sterling, D., Lange, E. M., Hawkins, G. A. & Turner, A. 2002. Germline mutations and sequence variants of the macrophage scavenger receptor 1 gene are associated with prostate cancer risk. *Nature genetics,* 32**,** 321-325.

Xu, N., Chen, H.-J., Chen, S.-H., Xue, X.-Y., Chen, H., Zheng, Q.-S., Wei, Y., Li, X.-D., Huang, J.-B. & Cai, H. 2016. Reduced Connexin 43 expression is associated with tumor malignant behaviors and biochemical recurrence-free survival of prostate cancer. *Oncotarget,* 7**,** 67476.

Xu, X., Li, W., Huang, G., Meyer, R., Chen, T., Luo, Y., Thomas, M., Radice, G. & Lo, C. 2001. Modulation of mouse neural crest cell motility by N-cadherin and connexin 43 gap junctions. *The Journal of cell biology,* 154**,** 217-230.

Yamamoto, H., Awada, C., Hanaki, H., Sakane, H., Tsujimoto, I., Takahashi, Y., Takao, T. & Kikuchi, A. 2013. The apical and basolateral secretion of Wnt11 and Wnt3a in polarized epithelial cells is regulated by different mechanisms. *Journal of cell science,* 126**,** 2931-2943.

Yamamura, S., Saini, S., Majid, S., Hirata, H., Ueno, K., Deng, G. & Dahiya, R. 2012. MicroRNA-34a modulates c-Myc transcriptional complexes to suppress malignancy in human prostate cancer cells. *PloS one,* 7**,** e29722.

Yang, F., Li, X., Sharma, M., Sasaki, C. Y., Longo, D. L., Lim, B. & Sun, Z. 2002. Linking β-catenin to androgen-signaling pathway. *Journal of Biological Chemistry,* 277**,** 11336-11344.

Yang, J., Mowry, L. E., Nejak-Bowen, K. N., Okabe, H., Diegel, C. R., Lang, R. A., Williams, B. O. & Monga, S. P. 2014. Beta-catenin signaling in murine liver zonation and regeneration: A Wnt-Wnt situation! *Hepatology,* 60**,** 964-976.

Yang, X., Du, W. W., Li, H., Liu, F., Khorshidi, A., Rutnam, Z. J. & Yang, B. B. 2013. Both mature miR-17-5p and passenger strand miR-17-3p target TIMP3 and induce prostate tumor growth and invasion. *Nucleic acids research,* 41**,** 9688-9704.

Yang, X., Guo, Z., Sun, F., Li, W., Alfano, A., Shimelis, H., Chen, M., Brodie, A. M., Chen, H. & Xiao, Z. 2011. Novel membrane-associated androgen receptor splice variant potentiates proliferative and survival responses in prostate cancer cells. *Journal of Biological Chemistry,* 286**,** 36152-36160.

Yao, B., Niu, Y., Li, Y., Chen, T., Wei, X. & Liu, Q. 2020. High-matrix-stiffness induces promotion of hepatocellular carcinoma proliferation and suppression of apoptosis via miR-3682-3p-PHLDA1-FAS pathway. *Journal of Cancer,* 11**,** 6188.

Ye, Y., Li, M., Chen, L., Li, S. & Quan, Z. 2021. Circ-AK2 is associated with preeclampsia and regulates biological behaviors of trophoblast cells through miR-454–3p/THBS2. *Placenta,* 103**,** 156-163.

Yeager, M. & Nicholson, B. J. 1996. Structure of gap junction intercellular channels. *Current opinion in structural biology,* 6**,** 183-192.

Yeap, B. B., Krueger, R. G. & Leedman, P. J. 1999. Differential posttranscriptional regulation of androgen receptor gene expression by androgen in prostate and breast cancer cells. *Endocrinology,* 140**,** 3282-3291.

Yin, H., Sheng, Z., Zhang, X., Du, Y., Qin, C., Liu, H., Dun, Y., Wang, Q., Jin, C. & Zhao, Y. 2017. Overexpression of SOX18 promotes prostate cancer progression via the regulation of TCF1, c-Myc, cyclin D1 and MMP-7. *Oncology reports,* 37**,** 1045-1051.

Yokoyama, N. N., Shao, S., Hoang, B. H., Mercola, D. & Zi, X. 2014. Wnt signaling in castration-resistant prostate cancer: implications for therapy. *American journal of clinical and experimental urology,* 2**,** 27.

Yoshioka, K., Deng, T., Cavigelli, M. & Karin, M. 1995. Antitumor promotion by phenolic antioxidants: inhibition of AP-1 activity through induction of Fra expression. *Proceedings of the National Academy of Sciences,* 92**,** 4972-4976.

Yu, W., Li, L., Zheng, F., Yang, W., Zhao, S., Tian, C., Yin, W., Chen, Y., Guo, W. & Zou, L. 2017. β-catenin cooperates with CREB binding protein to promote the growth of tumor cells. *Cellular Physiology and Biochemistry,* 44**,** 467-478.

Yu, X., Wang, Y., Jiang, M., Bierie, B., Roy-Burman, P., Shen, M. M., Taketo, M. M., Wills, M. & Matusik, R. J. 2009. Activation of β-Catenin in mouse prostate causes HGPIN and continuous prostate growth after castration. *The Prostate,* 69**,** 249-262.

Zeng, X., Huang, H., Tamai, K., Zhang, X., Harada, Y., Yokota, C., Almeida, K., Wang, J., Doble, B. & Woodgett, J. 2008. Initiation of Wnt signaling: control of Wnt coreceptor Lrp6 phosphorylation/activation via frizzled, dishevelled and axin functions.

Zhang, A., Hitomi, M., Bar-Shain, N., Dalimov, Z., Ellis, L., Velpula, K. K., Fraizer, G. C., Gourdie, R. G. & Lathia, J. D. 2015. Connexin 43 expression is associated with increased malignancy in prostate cancer cell lines and functions to promote migration. *Oncotarget,* 6**,** 11640.

Zhang, L. & Barritt, G. J. 2006. TRPM8 in prostate cancer cells: a potential diagnostic and prognostic marker with a secretory function? *Endocrine-related cancer,* 13**,** 27-38.

Zhang, N., Shen, Q. & Zhang, P. 2016. miR-497 suppresses epithelial–mesenchymal transition and metastasis in colorectal cancer cells by targeting fos-related antigen-1. *OncoTargets and therapy,* 9**,** 6597.

Zhang, T.-J., Hoffman, B. G., De Algara, T. R. & Helgason, C. D. 2006. SAGE reveals expression of Wnt signalling pathway members during mouse prostate development. *Gene Expression Patterns,* 6**,** 310-324.

Zhang, Y. & Wang, X. 2020. Targeting the Wnt/β-catenin signaling pathway in cancer. *Journal of hematology & oncology,* 13**,** 1-16.

Zhang, Y.-W., Morita, I., Ikeda, M., Ma, K.-W. & Murota, S. 2001. Connexin43 suppresses proliferation of osteosarcoma U2OS cells through post-transcriptional regulation of p27. *Oncogene,* 20**,** 4138-4149.

Zholos, A. 2010. Pharmacology of transient receptor potential melastatin channels in the vasculature. *British journal of pharmacology,* 159**,** 1559-1571.

Zhou, A., Paranjape, J., Brown, T. L., Nie, H., Naik, S., Dong, B., Chang, A., Trapp, B., Fairchild, R. & Colmenares, C. 1997. Interferon action and apoptosis are defective in mice devoid of 2′, 5′-oligoadenylate-dependent RNase L. *The EMBO journal,* 16**,** 6355-6363.

Zhou, D., Li, Y., Lin, L., Zhou, L., Igarashi, P. & Liu, Y. 2012. Tubule-specific ablation of endogenous β-catenin aggravates acute kidney injury in mice. *Kidney international,* 82**,** 537-547.

Zhou, J. Z. & Jiang, J. X. 2014. Gap junction and hemichannel-independent actions of connexins on cell and tissue functions–an update. *FEBS letters,* 588**,** 1186-1192.

Zhou, Y., Bolton, E. C. & Jones, J. O. 2015. Androgens and androgen receptor signaling in prostate tumorigenesis. *J Mol Endocrinol,* 54**,** R15-R29.

Zhou, Z., Sar, M., Simental, J. A., Lane, M. V. & Wilson, E. M. 1994. A ligand-dependent bipartite nuclear targeting signal in the human androgen receptor. Requirement for the DNA-binding domain and modulation by NH2-terminal and carboxyl-terminal sequences. *Journal of Biological Chemistry,* 269**,** 13115-13123.

Zhu, G., Zhau, H. E., He, H., Zhang, L., Shehata, B., Wang, X., Cerwinka, W. H., Elmore, J. & He, D. 2007. Sonic and desert hedgehog signaling in human fetal prostate development. *The Prostate,* 67**,** 674-684.

National Cancer Intelligence Network and Cancer Research UK, 2009http://www.ncin.org.uk/news_and_events/conferences/2009

APPENDIXES (APPX)

APPX I

1. AR signalling pathway in Castration Resistant Prostate Cancer (CRPC)

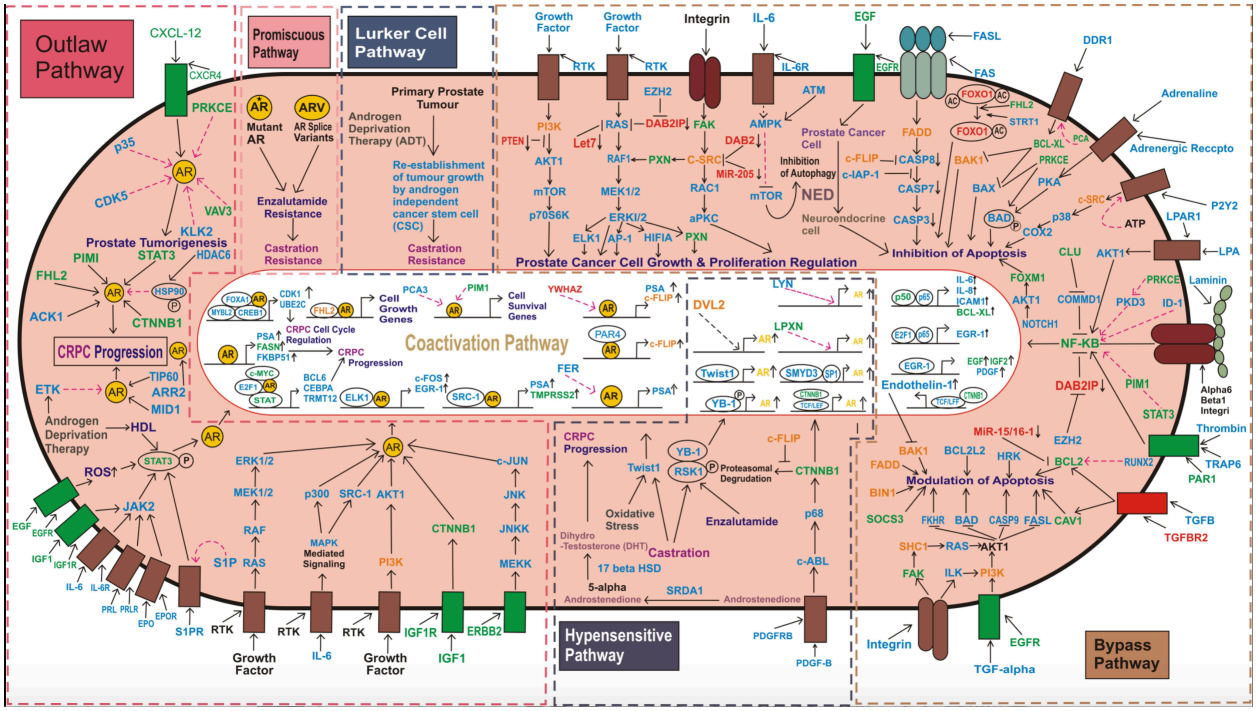

Figure 1.1. Complexity of AR signalling in CRPC (http://saweb2.sabiosciences.com/pathway.php?sn =WNT_Signalling). Five possible pathways for AIPC development. (a) hypersensitive pathway: AR stimulate sensitivity to balance low androgen levels. (b) promiscuous pathway: the ligand binding specificity of AR is extended to allow for the activation by non-androgenic compound present in the circulation. (c) outlaw pathway: Receptor tyrosine kinase (RTKs) are activated and the AR is either phosphorylated by the AKT (protein kinase B) or by the mitogen-activated protein kinase (MAPK) pathway for generating a ligand-independent AR. (d) bypass pathway: parallel survival pathways which includes that containing the BCL2 (B-cell lymphoma 2) anti-apoptotic protein, avoid AR and its ligand. (e) lurker cell pathway: androgen-independent malignant cells that are evident in the prostate throughout its life. Adapted from Feldman and Feldman, (2001).

APPX II

2. Catalogue of Prostate cancer tissue and layout of slide

Paraffin embedded 86 normal prostate tissue and prostate cancer samples with their exam number and block references were obtained from Rui Henrique (Pathologist, Portugal). Following H&E, the samples were categorized in normal prostate tissue (NPT): 36, benign prostatic hyperplasia :10, Gleason grade 3+3: 10, Gleason grade 4+4: 5 and Gleason grade 4+5/5+4: 5 and CRPC: 20 by pathologist using the grading and scoring guideline of the International Society of Urological Pathologists (ISUP). Total 171 cores composed of normal tissue cores: 66, BPH: 10, Gleason grade 3+3: 25, Gleason grade 4+4: 15, Gleason grade 4+5/5+4:15, CRPC cores: 40 were distributed over the 5 slides including RH16, RH17, RH18, RH19 and RH20.

At the first phase of conducting experiment, the prostate cancer tissue of Gleason grade 3+3, Gleason grade 4+4 and Gleason grade 4+5/5+4 was used to construct tissue array slide RH16, RH17 and RH18. The blocks are shown with their exam number and block reference in the following table:

Table 2.1. Catalogue of PCa tissue with different Gleason grades. Gleason grade 3+3 shaded with yellow, grade 4+4 shaded with grey and grade 4+5/5+4 with green. The tissues were examined and categorized by a pathologist.

	Gleason Grade					
	Grade: 3+3		Grade: 4+4		Grade: 4+5/5+4	
	Exam number	Block reference	Exam number	Block reference	Exam number	Block reference
1	H0901804	A A5	H1307652	A D1	H0810764	A1
2	H0912369	A3	H1307856	A A5	H0909375	C1
3	H1103610	A1	H1308297	D2	H1313961	C4
4	H1104892	C4	H1313345	C2	H1400020	A1
5	H1109027	A4	H1505541	A2	H1400073	B1

Three slides RH16, RH17 and RH18 were constructed using the cores of PCa tissue with Gleason grade 3+3, Gleason grade 4+4 and Gleason grade 4+5/5+4 stated in the table 1.1. The slides were prepared using one tumour core and one adjacent control core in the A1 and B1 positions respectively and thus the three slides were constructed.

2.1. Designing of RH16

Table 2.2. Layout of slide RH16 displaying tumour cores (Column: A, C, E) and control cores (Column: B, D, F) remain adjacent. Cores from Gleason grade 3+3 tissue displayed in yellow, Gleason grade 4+4 in grey and Gleason grade 4+5/5+4 in green coloured shade. T: Tumour core, C: Control core

RH16	A	B	C	D	E	F
1	H0901804 - T	H0901804 - C	H0912369 -T	H0912369 - C	H1103610 -T	H1103610 - C
2	H1104892 - T	H1104892 - C	H1109027 - T	H1109027 - C	H1307652 - T	H1307652 - C
3	H1307856 - T	H1307856 - C	H1308297 - T	H1308297 - C	H1313345 - T	H1313345 - C
4	H1505541 - T	H1505541 - C	H0810764 - T	H0810764 - C	H0909375 - T	H0909375 - C
5	H1313961 - T	H1313961 - C	H1400020 - T	H1400020 - C	H1400073 - T	H1400073 - C

The RH16 slide contains 30 cores which are composed of:

Grade 3+3: 10 cores: Grade 3+3: A1 (T), B1 (C), C1 (T), D1 (C), E1 (T), F1 (C), A2 (T), B2 (C), C2 (T), D2 (C)=

5 normal prostate tissue + 5 cancer tissue

Grade 4+4: 10 cores: Grade 4+4: E2 (T), F2 (C), A3 (T), B3 (C), C3 (T), D3 (C), E3 (T), F3 (C), A4 (T), B4 (C) =

5 normal prostate tissue + 5 cancer tissue

Grade 4+5/5+4: 10 cores: C4 (T), D4 (C), E4 (T), F4 (C), A5 (T), B5 (C), C5 (T), D5 (C), E5 (T), F5 (C)= 5

normal prostate tissue + 5 cancer tissue

2.2. Designing of RH17 slide

Table 2.3. Layout of slide RH_17 displaying tumour core (Column: A, C, E) and control core (Column: B, D, F) remain adjacent. Cores from Gleason grade 3+3 tissue displayed in yellow, Gleason grade 4+4 in grey and Gleason grade 4+5/5+4 in green coloured shade. T: Tumour core, C: Control core

RH17	A	B	C	D	E	F
1	H1307652 - T	H1307652 - C	H1307856 - T	H1307856 - C	H1308297 - T	H1308297 - C
2	H1313345 - T	H1313345 - C	H1505541 - T	H1505541 - C	H0810764 - T	H0810764 - C
3	H0909375 - T	H0909375 - C	H1313961 - T	H1313961 - C	H1400020 - T	H1400020 - C
4	H1400073 - T	H1400073 - C	H0901804 - T	H0901804 - C	H0912369 -T	H0912369 - C
5	H1103610 -T	H1103610 - C	H1109027 - T	H1109027 - C	H1104892 - T	H1104892 - C

The RH17 slide contains 30 cores which are composed of:

Grade 3+3: 10 cores: Grade 3+3: C4 (T), D4 (C), E4 (T), F4 (C), A5 (T), B5 (C), C5 (T), D5 (C), E5 (T),

F5 (C)= 5 normal prostate tissue + 5 cancer tissue

Grade 4+4: 10 cores: Grade 4+4: A1 (T), B1 (C), C1 (T), D1 (C), E1 (T), F1 (C), A2 (T), B2 (C), C2

(T), D2 (C)= 5 normal prostate tissue + 5 cancer tissue

Grade 4+5/5+4: 10 cores: Grade 4+5: E2 (T), F2 (C), A3 (T), B3 (C), C3 (T), D3 (C), E3 (T), F3 (C),

A4 (T), B4 (C) = 5 normal nrostate tissue + 5 cancer tissue

2.3. Designing of RH18 slide

Table 2.4. Layout of slide RH_18 displaying tumour core (Column: A, C, E) and control core (Column: B, D, F) remain adjacent. Cores from Gleason grade 3+3 tissue displayed in yellow, Gleason grade 4+4 in grey and Gleason grade 4+5/5+4 in green coloured shade. T: Tumour core, C: Control core

RH18	A	B	C	D	E	F
1	H0810764 - T	H0810764 - C	H0909375 - T	H0909375 - C	H1313961 - T	H1313961 - C
2	H1400020 - T	H1400020 - C	H1400073 - T	H1400073 - C	H0901804 - T	H0901804 - C
3	H0912369 -T	H0912369 - C	H1103610 - T	H1103610 - C	H1104892 - T	H1104892 - C
4	H1109027 - T	H1109027 - C	H1307652 - T	H1307652 - C	H1307856 - T	H1307856 - C
5	H1308297 - T	H1308297 - C	H1313345 - T	H1313345 - C	H1505541 - T	H1505541 - C

The RH18 slide contains 30 cores which are composed of:

Grade 3+3: 10 cores: Grade 3+3: E2 (T), F2 (C), A3 (T), B3 (C), C3 (T), D3 (C), E3 (T), F3 (C), A4 (T), B4 (C)= 5 normal prostate tissue + 5 cancer tissue

Grade 4+4: 10 cores: Grade 4+4: C4 (T), D4 (C), E4 (T), F4 (C), A5 (T), B5 (C), C5 (T), D5 (C), E5 (T), F5 (C)= 5 normal prostate tissue + 5 cancer tissue

Grade 4+5/5+4: 10 cores: Grade 4+5: A1 (T), B1 (C), C1 (T), D1 (T), E1 (T), F1 (C), A2 (T), B2 (C), C2 (T), D2 (C)= 5 normal prostate tissue + 5 cancer tissue

The second phase of experiments was conducted using normal prostate tissue, BPH, grade 3+3 and CRPC tissue and these were used to construct RH19 and RH20_CRPC in which RH19 slide is composed of normal prostate tissue (21 cores), Gleason grade 3+3 (10 cores) and BPH (10 cores) and slide RH20_CRPC consists of CRPC (40 cores: 20 core + 20 repeat).

2.4. Designing of RH19 slide

36 samples were collected from Rui Henrique (Pathologist) of which 21 normal prostate tissue (NPT), 10 BPH (Benign prostatic Hyperplasia), 5 Grade 3+3. The slide made of 41 cores= 21 cores (NPT)+ 10 cores (Grade 3+3: 5 cores and 5 repeats) + 10 cores (BPH)

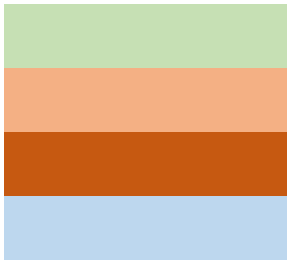

Table 2.5. Layout of slide RH19 displaying the position of normal prostate tissue, BPH and Gleason grade 3+3. Light green coloured font indicating the positions of normal cores, pink coloured font indicating location grade 3+3, brown coloured font indicating the locations of repeat of grade 3+3 and light blue font showing the locations of BPH.

RH19	A	B	C	D	E	F	G
1	12359/10 A B3	8022/06 B3	9394/11B4	9514/11 A B4	2905/10 A B3	3830/11 A B4	7057/12 A B4
2	1804/09 A A5	12369/09 A3	3610/11 A1	9027/11 A1	4892/11 C4	9027/11 A1	12369/09 A3
3	6632/05 B3	A631/12 A B3	3277/11 A PB4	4616/07 A B4	4225/07 AB3	7446/11 A B3	164/C3 C3
4	1804/09 A A5	3610/11 A1	4892/11 C4	8096/16 2	6230/17 B	3721/15 3	3343/15 2
5	975/11 A B3	4864/12 A B3	921/04 B3	1148/11 A B3	8925/10 A B3	1195/06	3630/03 B3
6	6068/13 6	10682/12 4	1566/13 3	4011/14 1	9683/12 B4	11441/12 8	X

The RH19 contains 41cores including:

Normal Core Position: A1, B1, C1, D1, E1, F1, G1, A3, B3, C3, D3, E3, F3, G3, A5, B5, C5, D5, E5, F5, G5: Total 21

BPH: 10 cores: D4, E4, F4, G4, A6, B6, C6, D6, E6, F6 = Total 10,

Grade (3+3): 10 cores: A2, B2, C2, D2, E2, F2 (R), G2 (R), A4 (R), B4 (R), C4 (R)= Total 10

2.5. Designing of RH20_CRPC slide

20 CRPC samples were obtained from Professor Rui Henrique (Pathologist). 20 samples were used to construct the slide RH20_CRPC. The slide contains 40 cores: 20 CRPC + 20 CRPC (repeat). The layout of cores on the slides are given below:

CRPC

CRPC REPEATS

Table 2.6. Layout of slide Rh20_CRPC displaying the position of CRPC and CRPC repeat. Locations of CRPC tissue are indicated with brown coloured font and CRPC repeats indicated with pink coloured font.

RH20_CRPC	A	B	C	D	E	F	G
1	1353/16 1	7402/12 1	12998/15 2	2067/08 1	14281/14 4	4406/15 3	7402/12 1
2	588/13 4	14642/13 1	5652/16 3	6196/01	12528/14 2	4324/16 3	14642/13 1
3	11020/10 5	1875/13 3	5310/16 4	7566/06	6059/15 4	13725/15 3	1875/13 3
4	14281/14 4	2067/08 1	12998/15 2	4406/15 3	1353/16 1	5352/14 1	11845/14 1
5	12528/14 2	6196/01	5652/16 3	4324/16 3	588/13 4	11845/14 1	5352/14 1
6	6059/15 4	7566/06	5310/16 4	13725/15 3	11020/10 5	X	X

The RH20_CRPC slide contains 40 cores, composed of

CRPC: A1, A2, A3, B4, B5, B6, C1, C2, C3, D4, D5, D6, E1, E2, E3, F4, F5, G1, G2, G3,

CRPC (Repeat: R): A4 (R of E1), A5 (R of E2), A6 (R of E3), B1 (R of G1), B2 (R of G2),

B3 (R of G3), C4 (R of C1), C5 (R of C2), C6 (R of C3), D1 (R of B4), D2 (R of B5), D3 (R of B6), E4 (R of A1), E5 (R of A2), E6 (R of A3), F1 (R of D4), F2 (R of D5), F3 (R of D6), G4 (R of F5), G5 (R of F4) = total 40

2.6. Transient expression of AR protein in PC3 cells

Androgen Receptor (AR) (NM_000044) Human Tagged ORF Clone (Cat: RG215316, Origene) was used to transfect PC3 cells.

AR (NM_000044) with 2751bp was inserted into pCMV6-AC-GFP plasmid with ampicillin selection marker for *E. coli* and Neomycin marker in mammalian cell lection marker to express the complete ORF with the expression tag (GFP). The plasmid contains Human cytomegalovirus (CMV) promoter to trigger the expression of the protein.

The following cloning sites was used for ORF insertion.

>RG215316 representing NM_000044
Red=Cloning site Blue=ORF Green=Tags(s)

TTTTGTAATACGACTCACTATAGGGCGGCCGGGAATTCGTCGACTGGATCCGGTACCGAGGAGATCTG
CCGCCGCGATCGCCATGGAAGTGCAGTTAGGGCTGGGAAGGGTCTACCCTCGGCCGCCGTCCAAGAC
CTACCGAGGAGCTTTCCAGAATCTGTTCCAGAGCGTGCGCGAAGTGATCCAGAACCCGGGCCCCAGG
CACCCAGAGGCCGCGAGCGCAGCACCTCCCGGCGCCAGTTTGCTGCTGCTGCAGCAGCAGCAGCAGC
AGCAGCAGCAGCAGCAGCAGCAGCAGCAGCAGCAGCAGCAGCAAGAGACTAGCCCCAGGCAGCAG
CAGCAGCAGCAGGGTGAGGATGGTTCTCCCCAAGCCCATCGTAGAGGCCCCACAGGCTACCTGGTCC
TGGATGAGGAACAGCAACCTTCACAGCCGCAGTCGGCCCTGGAGTGCCACCCCGAGAGAGGTTGCGT
CCCAGAGCCTGGAGCCGCCGTGGCCGCCAGCAAGGGGCTGCCGCAGCAGCTGCCAGCACCTCCGGA
CGAGGATGACTCAGCTGCCCCATCCACGTTGTCCCTGCTGGGCCCCACTTTCCCCGGCTTAAGCAGCT
GCTCCGCTGACCTTAAAGACATCCTGAGCGAGGCCAGCACCATGCAACTCCTTCAGCAACAGCAGCA
GGAAGCAGTATCCGAAGGCAGCAGCAGCGGGAGAGCGAGGGAGGCCTCGGGGGCTCCCACTTCCTC
CAAGGACAATTACTTAGGGGGCACTTCGACCATTTCTGACAACGCCAAGGAGTTGTGTAAGGCAGTGT
CGGTGTCCATGGGCCTGGGTGTGGAGGCGTTGGAGCATCTGAGTCCAGGGGAACAGCTTCGGGGGG
ATTGCATGTACGCCCCACTTTTGGGAGTTCCACCCGCTGTGCGTCCCACTCCTTGTGCCCCATTGGCCG
AATGCAAAGGTTCTCTGCTAGACGACAGCGCAGGCAAGAGCACTGAAGATACTGCTGAGTATTCCCCT
TTCAAGGGAGGTTACACCAAAGGGCTAGAAGGCGAGAGCCTAGGCTGCTCTGGCAGCGCTGCAGCA
GGGAGCTCCGGGACACTTGAACTGCCGTCTACCCTGTCTCTCTACAAGTCCGGAGCACTGGACGAGGC
AGCTGCGTACCAGAGTCGCGACTACTACAACTTTCCACTGGCTCTGGCCGGACCGCCGCCCCCTCCGC
CGCCTCCCCATCCCCACGCTCGCATCAAGCTGGAGAACCCGCTGGACTACGGCAGCGCCTGGGCGGC
TGCGGCGGCGCAGTGCCGCTATGGGGACCTGGCGAGCCTGCATGGCGCGGGTGCAGCGGGACCCGG
TTCTGGGTCACCCTCAGCCGCCGCTTCCTCATCCTGGCACACTCTCTTCACAGCCGAAGAAGGCCAGTT
GTATGGACCGTGTGGTGGTGGTGGGGGTGGTGGCGGCGGCGGCGGCGGCGGCGGCGGCGGCGGCG
GCGGCGGCGGCGGCGGCGAGGCGGGAGCTGTAGCCCCCTACGGCTACACTCGGCCCCCTCAGGGGC
TGGCGGGCCAGGAAAGCGACTTCACCGCACCTGATGTGTGGTACCCTGGCGGCATGGTGAGCAGAGT

GCCCTATCCCAGTCCCACTTGTGTCAAAAGCGAAATGGGCCCCTGGATGGATAGCTACTCCGGACCTT
ACGGGGACATGCGTTTGGAGACTGCCAGGGACCATGTTTTGCCCATTGACTATTACTTTCCACCCCAGA
AGACCTGCCTGATCTGTGGAGATGAAGCTTCTGGGTGTCACTATGGAGCTGTCACATGTGGAAGCTGC
AAGGTCTTCTTCAAAAGAGCCGCTGAAGGGAAACAGAAGTACCTGTGCGCCAGCAGAAATGATTGCA
CTATTGATAAATTCCGAAGGAAAAATTGTCCATCTTGTCGTCTTCGGAAATGTTATGAAGCAGGGATGA
CTCTGGGAGCCCGGAAGCTGAAGAAACTTGGTAATCTGAAACTACAGGAGGAAGGAGAGGCTTCCAG
CACCACCAGCCCCACTGAGGAGACAACCCAGAAGCTGACAGTGTCACACATTGAAGGCTATGAATGT
CAGCCCATCTTTCTGAATGTCCTGGAAGCCATTGAGCCAGGTGTAGTGTGTGCTGGACACGACAACAA
CCAGCCCGACTCCTTTGCAGCCTTGCTCTCTAGCCTCAATGAACTGGGAGAGAGACAGCTTGTACACG
TGGTCAAGTGGGCCAAGGCCTTGCCTGGCTTCCGCAACTTACACGTGGACGACCAGATGGCTGTCATT
CAGTACTCCTGGATGGGGCTCATGGTGTTTGCCATGGGCTGGCGATCCTTCACCAATGTCAACTCCAG
GATGCTCTACTTCGCCCCTGATCTGGTTTTCAATGAGTACCGCATGCACAAGTCCCGGATGTACAGCCA
GTGTGTCCGAATGAGGCACCTCTCTCAAGAGTTTGGATGGCTCCAAATCACCCCCCAGGAATTCCTGT
GCATGAAAGCACTGCTACTCTTCAGCATTATTCCAGTGGATGGGCTGAAAAATCAAAAATTCTTTGATG
AACTTCGAATGAACTACATCAAGGAACTCGATCGTATCATTGCATGCAAAAGAAAAAATCCCACATCC
TGCTCAAGACGCTTCTACCAGCTCACCAAGCTCCTGGACTCCGTGCAGCCTATTGCGAGAGAGCTGCA
TCAGTTCACTTTTGACCTGCTAATCAAGTCACACATGGTGAGCGTGGACTTTCCGGAAATGATGGCAGA
GATCATCTCTGTGCAAGTGCCCAAGATCCTTTCTGGGAAAGTCAAGCCCATCTATTTCCACACCCAG
ACGCGTACGCGGCCGCTCGAG - GFP Tag – GTTTAA

The cloning of AR ORF in pCMV6-AC-GFP:

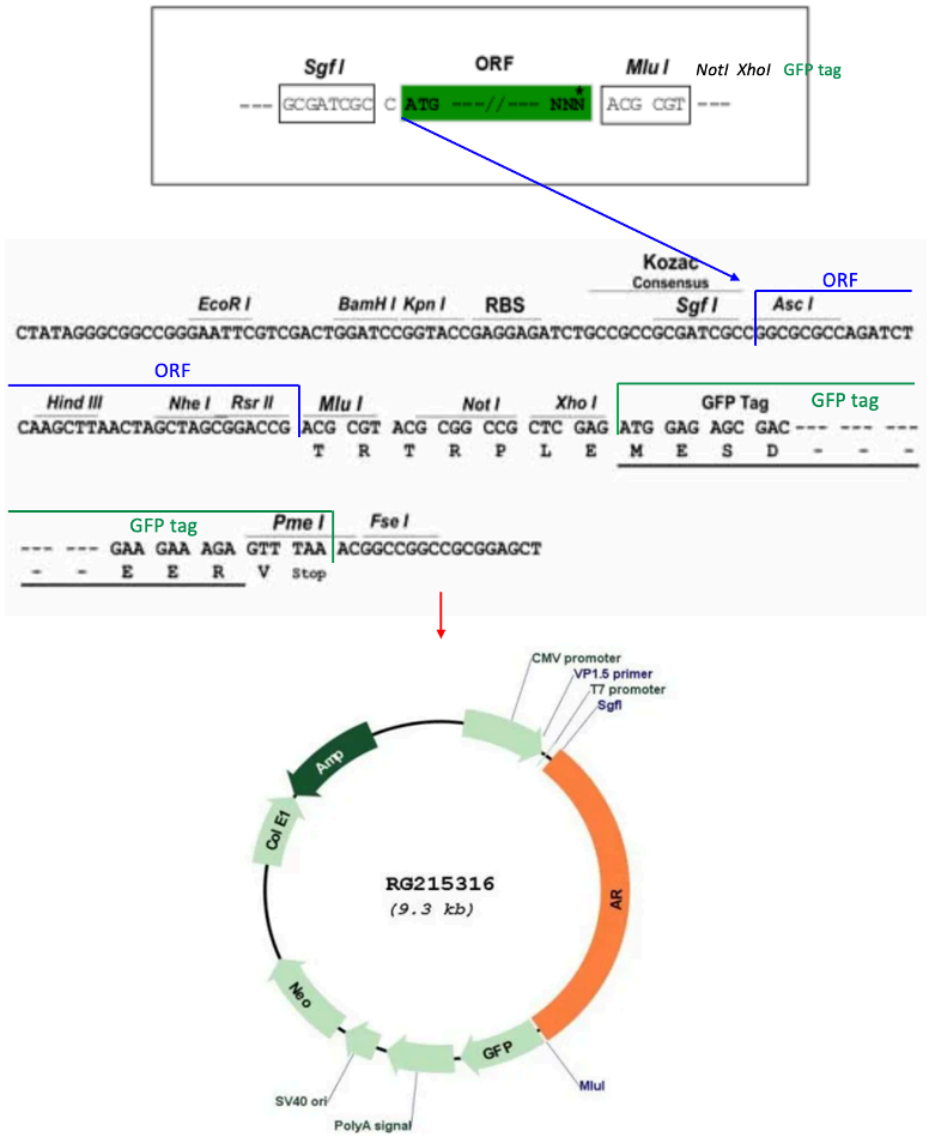

Figure 2.1. Schematic representation of strategy of AR ORF cloning. Red font indicating the cloning site. The restriction site *SgfI* (5' G C G A T C G C 3') and *MluI* (5' A C G C G T 3') were used to clone the AR ORF. Top blue font indicating AR sequence of 2751bp to be cloned.

APPX III

3. Staining and Imaging of the slides

Following staining, the tissue cores were scanned with NanoZoomer-RS Scanner (Type: C10730-02) with resolution 0.23µm/pixel (40x high resolution mode) using. The images were opened using NDP.view 2.3 software.

3.1. Staining with anti-androgen receptor antibody

Tissue cores of Grade 3+3, Grade 4+4 and Grade 4+5/5+4 on RH16, RH17, RH18 were stained with AR.

Figure 3.1. A representation of high Gleason Grade cores stained with anti-AR antibody. 30 cores of Grade 3+3, Grade 4+4 and Grade 4+5/5+4 on each slide stained with Ant-AR antibody to determine the expression of AR.

3.2. Staining with anti-β-catenin antibody

Figure 3.2. Image of anti-β-catenin antibody stained: slides RH16, RH17 and RH18. 30 cores of Grade 3+3, Grade 4+4 and Grade 4+5/5+4 on each slide stained with anti-β-catenin antibody to determine the expression of β-catenin.

3.3. Staining with anti-FRA antibody

Figure 3.3. A representation of high Gleason Grade cores stained with anti-FRA antibody. 30 cores of Grade 3+3, Grade 4+4 and Grade 4+5/5+4 on each slide stained with Ant-FRA-1 antibody to determine the expression of FRA-1.

3.4. Staining with anti-TCF-1 antibody

Figure 3.4. A representation of high Gleason Grade cores stained with anti-TCF-1 antibody. 30 cores of Grade 3+3, Grade 4+4 and Grade 4+5/5+4 on each slide stained with Ant-TCF-1 antibody to determine the expression of TCF-1.

3.5. Staining with anti-PYGO2 antibody

Figure 3.5. A representation of high Gleason Grade cores stained with anti-PYGO2 antibody. 30 cores of Grade 3+3, Grade 4+4 and Grade 4+5/5+4 on each slide stained with Ant-PYGO2 antibody to determine the expression of PYGOPUS2.

3.6. Staining with anti-Cx43 antibody

Figure 3.6. A representation of high Gleason Grade cores stained with anti-Cx43 antibody. 30 cores of Grade 3+3, Grade 4+4 and Grade 4+5/5+4 on each slide stained with Ant-Cx43 antibody to determine the expression of Cx43.

3.7. Binary Logistic Regression Model to identify biomarkers with improved diagnostic potential of NPT Grade 3+3, Grade 4+4 and Grade 4+5/5+4 for AR, β-catenin, FRA-1, PYGO2, TCF-1 and Cx43

Table 3.7.1. Combination of PCa sample: NPT vs Grade 3+3 for AR, β-catenin, FRA-1, PYGO2, TCF-1 and Cx43

Combination of PCa sample: NPT vs Grade 3+3				
Combination of AR and Wnt signalling protein	% cases correctly classified	AUC	Std Error	95% CI
AR and β-cat	91	0.93	0.06	0.7 to 0.9
AR and FRA-1	86	0.89	0.07	0.6 to 0.9
AR and PYGO	96	0.96	0.41	0.8 to 0.9
AR and TCF-1	96	0.96	0.42	0.8 to 0.9
AR and Cx43	96	0.96	0.05	0.8 to 0.9
β-cat and FRA-1	95	0.95	0.05	0.7 to 0.9
β-cat and PYGO2	95	0.95	0.05	0.7 to 0.9
β-cat and TCF-1	95	0.95	0.05	0.7 to 0.9
β-cat and Cx43	86	0.86	0.08	0.6 to 0.9
FRA-1 and PYGO2	90	0.90	0.07	0.7 to 0.9
FRA-1 and TCF-1	90	0.90	0.07	0.7 to 0.9

FRA-1 and Cx43	81	0.81	0.09	0.5 to 0.9
PYGO2 and TCF-1	100	1.00	000	0.8 to 1.0
PYGO2 and Cx43	92	0.92	0.06	0.7 to 0.9
TCF-1 and Cx43	92	0.91	0.06	0.7 to 0.9

Table 3.7.2. Combination of PCa sample: NPT vs Grade 4+4 for AR, β-catenin, FRA-1, PYGO2, TCF-1 and Cx43

Combination of PCa sample: NPT vs Grade 4+4				
Combination of AR and Wnt signalling protein	% cases correctly classified	AUC	Std Error	95% CI
AR and β-cat	92	0.92	0.05	0.7 to 0.9
AR and FRA-1	88	0.89	0.06	0.7 to 0.9
AR and PYGO	96	0.96	0.04	0.8 to 0.9
AR and TCF-1	96	0.96	0.04	0.8 to 0.9
AR and Cx43	96	0.96	0.04	0.8 to 0.9
β-cat and FRA-1	96	0.95	0.04	0.7 to 0.9
β-cat and PYGO2	96	0.96	0.04	0.8 to 0.9
β-cat and TCF-1	96	0.96	0.04	0.8 to 0.9
β-cat and Cx43	88	0.89	0.06	0.7 to 0.9
FRA-1 and PYGO2	92	0.92	0.05	0.7 to 0.9
FRA-1 and TCF-1	92	0.92	0.05	0.7 to 0.9
FRA-1 and Cx43	84	0.85	0.07	0.6 to 0.9
PYGO2 and TCF-1	100	1	0.00	0.8 to 1
PYGO2 and Cx43	92	0.92	0.06	0.7 to 0.9
TCF-1 and Cx43	92	0.92	0.05	0.7 to 0.9

Table:3.7.3. Combination of PCa sample: NPT vs Grade 4+5/5+4 for AR, β-catenin, FRA-1, PYGO2, TCF-1 and Cx43

Combination of PCa sample: NPT vs Grade 4+5				
Combination of AR and Wnt signalling protein	% Cases correctly classified	AUC	Std Error	95% CI
AR and β-cat	95	0.95	0.04	0.7 to 0.9
AR and FRA-1	95	0.95	0.04	0.7 to 0.9
AR and PYGO	96	0.96	0.04	0.8 to 0.9
AR and TCF-1	88	0.90	0.06	0.7 to 0.9
AR and Cx43	96	0.96	0.03	0.8 to 0.9
β-cat and FRA-1	95	0.95	0.05	0.7 to 0.9
β-cat and PYGO2	95	0.95	0.04	0.7 to 0.9
β-cat and TCF-1	95	0.95	0.04	0.7 to 0.9
β-cat and Cx43	86	0.87	0.08	0.6 to 0.9

FRA-1 and PYGO2	91	0.92	0.06	0.7 to 0.9
FRA-1 and TCF-1	91	0.92	0.06	0.7 to 0.9
FRA-1 and Cx43	84	0.85	0.07	0.6 to 0.9
PYGO2 and TCF-1	100	1.00	0.00	0.8 to 1.0
PYGO2 and Cx43	92	0.91	0.06	0.7 to 0.9
TCF-1 and Cx43	92	0.92	0.06	0.7 to 0.9

Table: 3.7.4. Combination of PCa sample: 3+4 vs Grade 4+4 for FRA-1, PYGO2, TCF-1 and Cx43

Combination of PCa sample: Grade 3+3 vs Grade 4+4				
Combination of AR and Wnt signalling protein	% cases correctly classified	AUC	Std Error	95% CI
FRA-1 and PYGO2	91	0.9	0.0	0.7 to 0.9
FRA-1 and TCF-1	92	0.9	0.05	0.7 to 0.9
FRA-1 and Cx43	84	0.85	0.07	0.6 to 0.9
PYGO2 and TCF-1	100	1	000	0.8 to 1
PYGO2 and Cx43	92	0.929	0.05	0.7 to 0.9
TCF-1 and Cx43	92	0.929	0.05	0.7 to 0.9

Table: 3.7.5. Combination of PCa sample: 3+3 vs Grade 4+5/5+4 for FRA-1, PYGO2, TCF-1 and Cx43

Combination of PCa sample: Grade 3+3 vs Grade 4+5/5+4				
Combination of AR and Wnt signalling protein	% cases correctly classified	AUC	Std Error	95% CI
FRA-1 and PYGO2	91	0.923	0.06	0.7 to 0.9
FRA-1 and TCF-1	83	0.846	0.08	0.6 to 0.9
FRA-1 and Cx43	83	0.846	0.08	0.6 to 0.9
PYGO2 and TCF-1	92	0.923	0.06	0.7 to 0.9
PYGO2 and Cx43	92	0.923	0.06	0.7 to 0.9
TCF-1 and Cx43	100	1.000	0.00	0.8 to 1.00

Table: 3.7.6. Combination of PCa sample: 4+4 vs Grade 4+5/5+4 for FRA-1, PYGO2, TCF-1 and Cx43

Combination of PCa sample: Grade 4+4 vs Grade 4+5				
Combination of AR and Wnt signalling protein	% cases correctly classified	AUC	Std Error	95% CI
FRA-1 and PYGO2	100	1	000	0.8 to 1
FRA-1 and TCF-1	100	1	000	0.8 to 1
FRA-1 and Cx43	100	1	000	0.8 to 1
PYGO2 and TCF-1	100	1	000	0.8 to 1
PYGO2 and Cx43	100	1	000	0.8 to 1
TCF-1 and Cx43	100	1	000	0.8 to 1

APPX IV

4. Expression analysis of AR and Wnt signalling pathways in non-CRPC and CRPC tissue

4.1. Negative staining for anti-Cx43 and anti-AR antibodies

Negative staining was performed before proceeding to antibody staining. Secondary antibody antibodies were checked whether they pick any virtual background. No background staining was observed.

Figure 4.1. A Representation of negative staining for Anti-Cx43 and Anti-AR antibodies. Each of the slides contains 30 cores of Grade 3+3, Grade 4+4 and Grade 4+5/5+4 was stained for Cx43 and anti-AR antibodies.

4.2. AR and Wnt signalling protein expression analysis non-CRPC (castration resistant prostate cancer) and CRPC tissue using single label chromogenic (DAB) staining technique

4.2.1. Analysis of AR expression in non-CRPC and CRPC tissue using single label chromogenic (DAB) staining technique

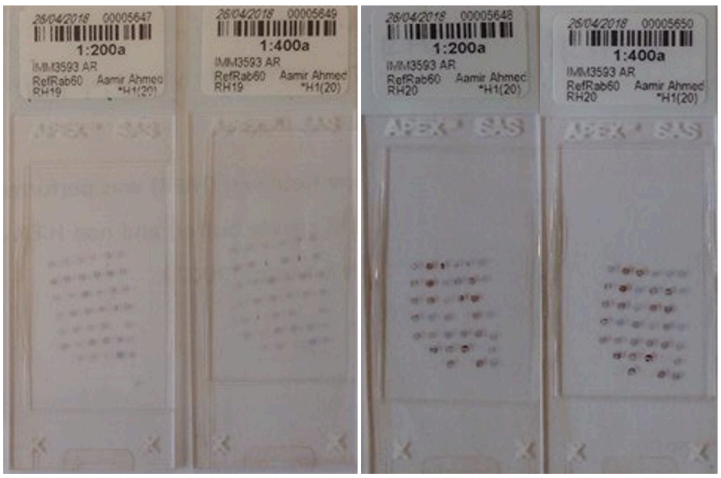

Figure 4.2. A Representation of non-CRPC and CRPC tissue cores stained with anti-AR antibody. Slide: RH19 contain 41 non-CRPC tissue cores composed of 21 NPT+10 BPH+ 10 Grade 3+3 stained with Anti-AR antibody at 1:200 dilution (left), and 1:400 dilution (2nd from left). Slide: RH20_CRPC contains 40 cores of CRPC stained with Ant-AR antibody at 1:200 dilution (3rd from left) and 1:400 dilution (right). The stained cores were imaged and analysed for protein expression.

4.2.2. Analysis of Cx43 expression in non-CRPC and CRPC tissue using single label chromogenic (DAB) staining technique

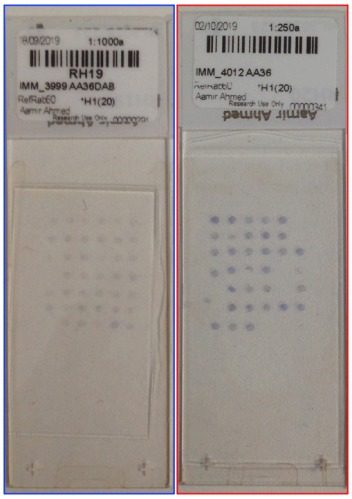

Figure 4.3. A Representation of non-CRPC and CRPC tissue cores stained with anti-Cx43 antibody. Slide: RH19 contain 41 non-CRPC tissue cores composed of 21 NPT+10 BPH+ 10 Grade 3+3 stained with anti-Cx43 antibody at 1:1000 dilution (left). Slide: RH20_CRPC contains 40 cores of CRPC stained with Ant-Cx43 antibody at 1:250 dilution (Right). The stained cores were imaged and analysed for protein expression.

4.3. Expression analysis of AR and Wnt signalling protein in non-CRPC and CRPC using multilabel fluorescence staining technique

The non-CRPC tissue cores on slide RH19 and CRPC tissue cores on slide RH20_CRPC were stained with four antibodies (namely, anti-FRA-1, anti-β-catenin, anti-AR and anti-c-MYC antibodies) for Wnt and AR signalling proteins namely, FRA-1, β-catenin, AR and c-MYC expression.

Figure 4.4. A representation of non-CRPC and CRPC cores on slide: RH19 and RH20_CRPC stained with anti-FRA-1, anti-β-catenin, anti-AR and anti-c-MYC antibodies for FRA-1, β-catenin, AR, c-MYC, respectively, expression. The fluorophores tagged with TSA (Tyramide Signal Amplification) namely, Tyr-Alexa 405, Tyr-FITC, Tyr-Cy3 and Tyr-Cy5 were used to visualise FRA-1, β-catenin, AR, c-MYC protein respectively in non-CRPC and CRPC tissue. Following imaged with AxioScan, protein expression and co-localization were analysed.

4.3.1. Fluorescence imaging of antibodies FRA-1, β-catenin, AR and c-MYC signal

Image of each core of RH19 and RH20 were obtained using Zeiss Axioscan Z.1 slide scanner (Carl Zeiss) at 20x magnification (Arya *et al*., 2015). The fluorescent signals were optimised prior to conducting Axioscan to avoid oversaturation of signal faint for each antibody. For a standardized comparison, the power of Calibri.2 LED lights and integration times of the Hamamatsu ORCA

Flash4 camera (Hamamatsu Photonics) were kept constants for all samples. The imaging of the slides was carried out at the same time sequentially with identical image acquisition settings. Montages of each core were automatically generated and accumulated from multiple 2048x2048 pixel with 16 bit gray level which were compiled locally on the acquisition computer. The images were then segregated categorically.

4.3.2. AxioScan image of normal prostate tissue cores

Image of each individual tissue core was indexed according to its configuration on the tissue array on the slide along with identification of the histological pattern of the NPT, BPH (benign Prostatic Hyperplasia and Grade 3+3) (Chap-4, Sec. 4.4.2.2).

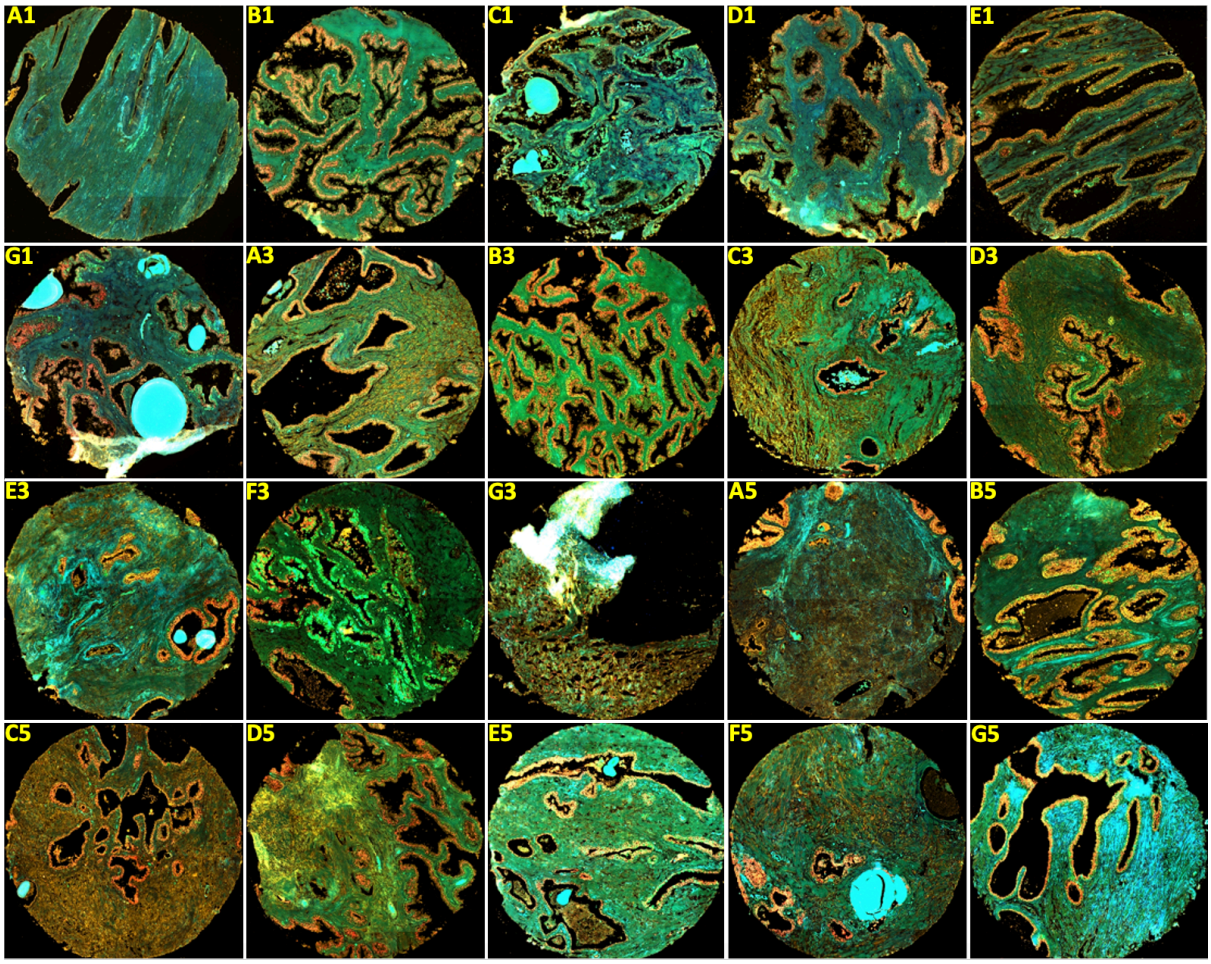

Figure 4.5. A representation of NPT cores used in this study. The tissue cores on the RH19 slide were stained with TSA tagged four fluorophores namely, Tyr-Alexa-405, -FITC, -Cy3, and -Cy5 for FRA-1, β-Catenin, AR and c-MYC respectively and imaged using Zeiss AxioScan Z1 slide scanner. The displayed image of cores is composite (overlay of four fluorophores).

4.3.3. AxioScan image of BPH cores

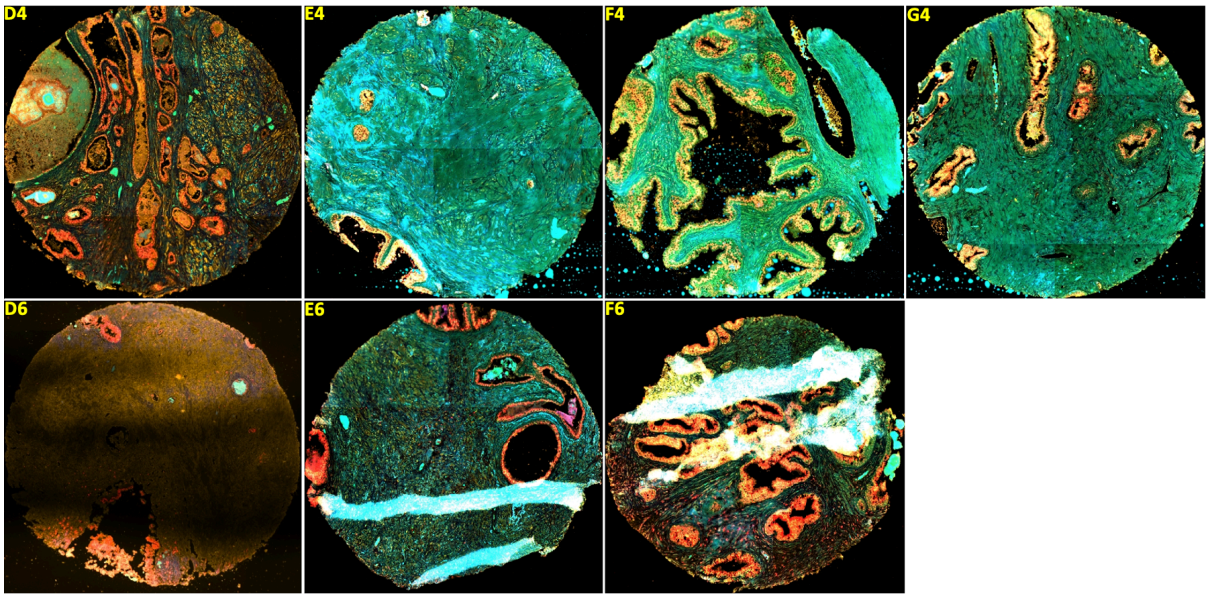

Figure 4.6. A representation of BPHe cores used in this study. The tissue cores on the RH19 slide were stained with TSA tagged four fluorophores namely, Tyr-Alexa-405, -FITC, -Cy3, and -Cy5 for FRA-1, β-Catenin, AR and c-MYC respectively and imaged using Zeiss AxioScan Z1 slide scanner. The displayed image of cores is composite (overlay of four fluorophores).

4.3.4. AxioScan image of Grade 3+3 cores

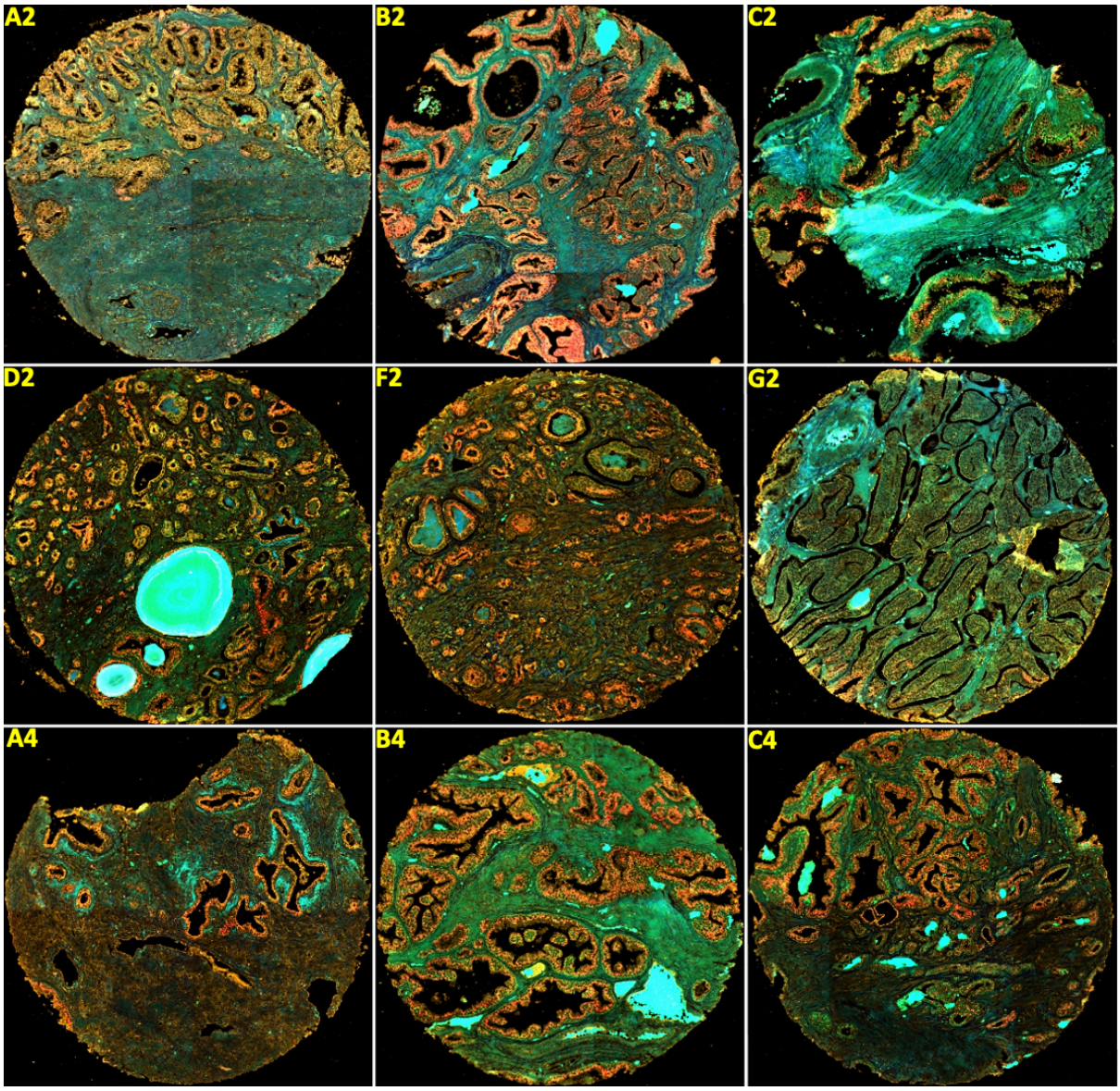

Figure 4.7. A representation of Grade 3+3 cores used in this study. The tissue cores on the RH19 slide were stained with TSA tagged four fluorophores namely, Tyr-Alexa-405, -FITC, -Cy3, and -Cy5 for FRA-1, β-Catenin, AR and c-MYC respectively and imaged using Zeiss AxioScan Z1 slide scanner. The displayed image of cores is composite (overlay oof four fluorophores).

4.3.5. Four antibodies stained individual CRPC tissue cores obtained from RH20_CRPC slide

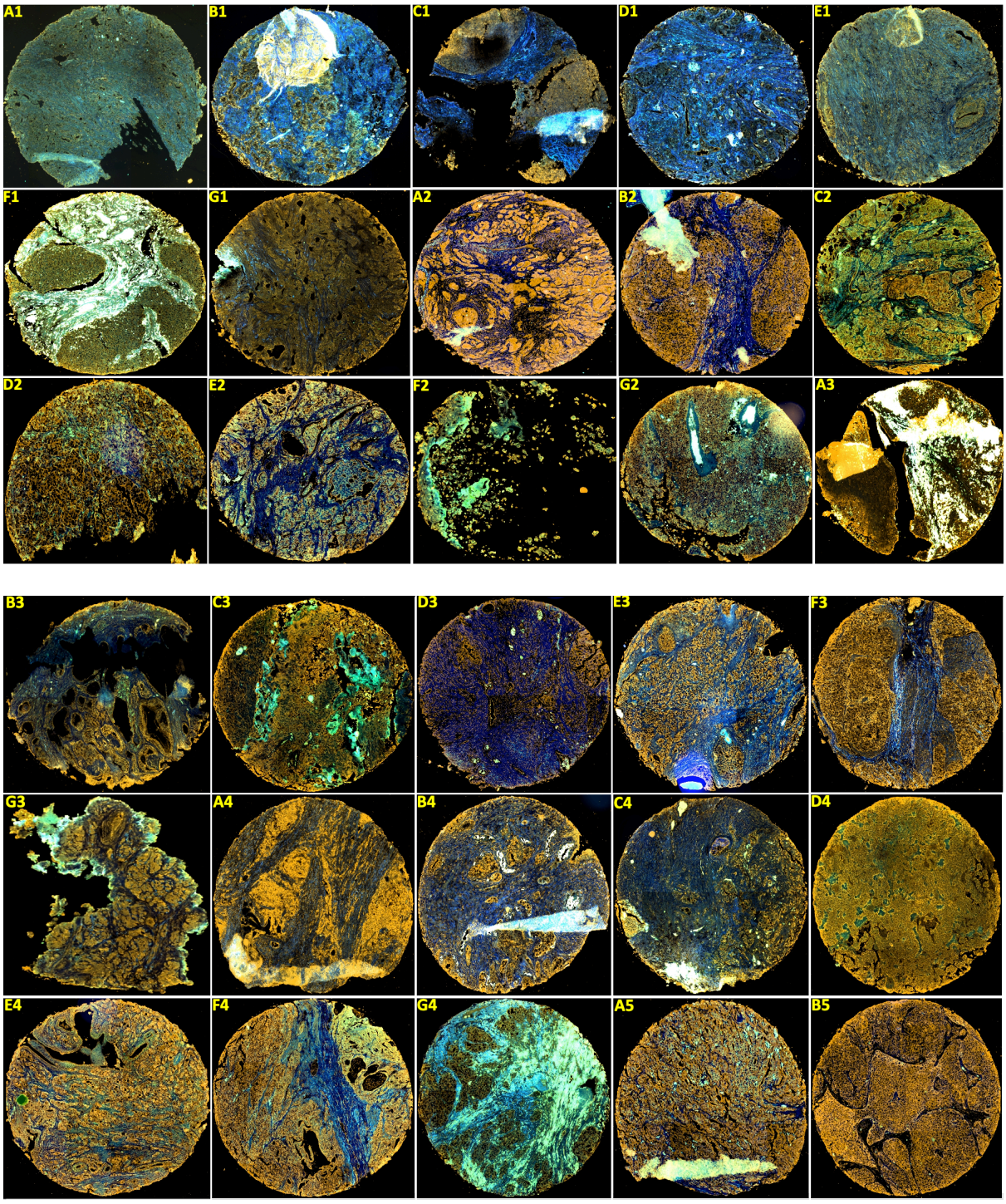

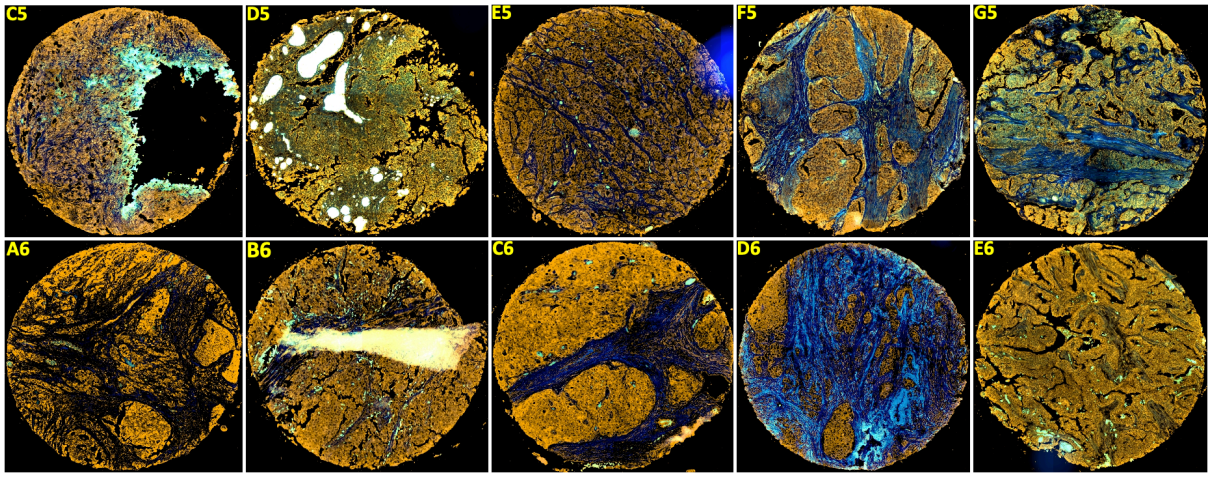

Fig 4.8. A representation of CRPC cores used in this study. The tissue cores on the RH20_CRPC slide were stained with TSA tagged four fluorophores namely, Tyr-Alexa-405, -FITC, -Cy3, and -Cy5 for FRA-1, β-Catenin, AR and c-MYC respectively and imaged using Zeiss AxioScan Z1 slide scanner. The displayed image of cores is composite (overlay of four fluorophores).

APPX V

5. Analysis of expression and interaction of AR and Wnt signalling proteins in PCa cells

5.1. Expression analysis of AR and Wnt signalling proteins in DHT treated LnCAP cells

Three independent experiments were performed to observe the translocation of AR and Wnt signalling target proteins in DHT treated LnCAP cell.

5.1.1. Experiment-1

LnCAP cell was treated with DHT at recommended dilution (Chap-2, Table 5.1). AR, AR (N-ter) and β-catenin translocation were observed.

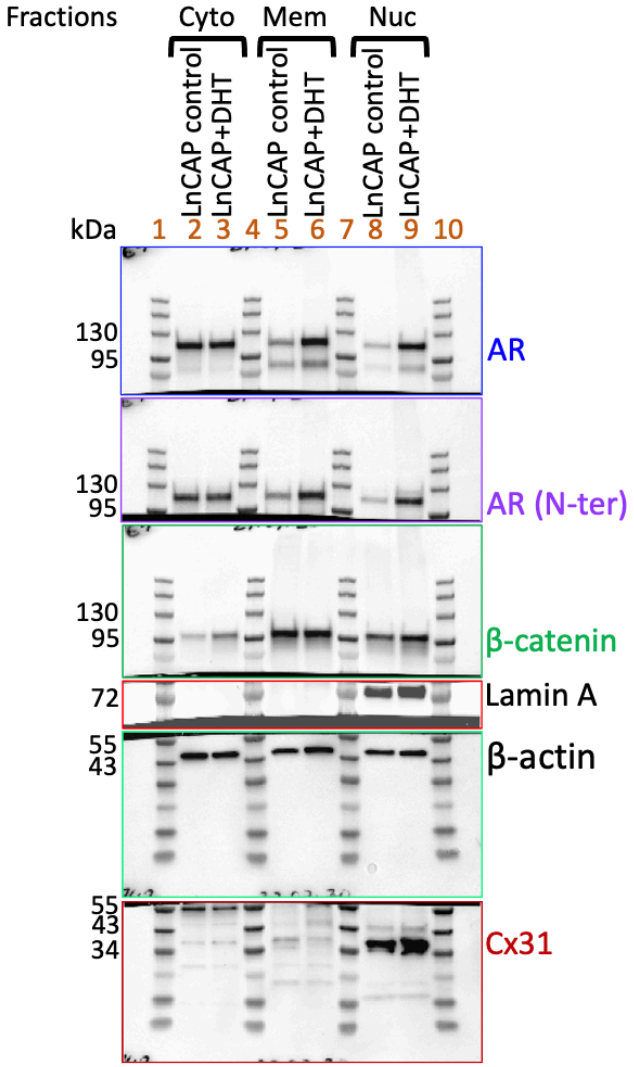

Figure 5.1. A representative WB image showing of multiple use of single PVDF membrane for staining of AR, AR (N-ter), β-catenin and Cx31. 15µg of fractionated protein of LnCAP cells (±DHT) was loaded onto gel, such as cytosolic protein loaded into lane 2 and 3, membrane protein into lane 5 and 6 and nuclear protein in lane 8 and 9. 6µl of Colour Prestained Protein standard, Broad Range (Cat: P7719, NEB) was loaded into lane 1, 4, 7 and 10. The PVDF membrane was cut into two strips of 250 to 57 kDa and 57 to 10kDa and incubated with anti-Lamin A and anti-β actin antibody. Following capturing image with GelDoc system (BioRad), the membranes were stripped off with "Restore™ PLUS Western Blot Stripping buffer (Cat: 46430, Thermo Scientific). The membranes were reprobed with anti-AR, anti-AR (N-ter) and anti-β-catenin and anti-Cx31 antibodies sequentially.

5.1.2. Experiment-2

LnCAP cell of different batch and passage was treated with DHT at recommended dilution (Table 5.1). AR, AR (N-ter) and β-catenin translocation were observed (Fig. 5.2). The stained main PVDF membranes are displayed below:

a. Main PVDF membrane

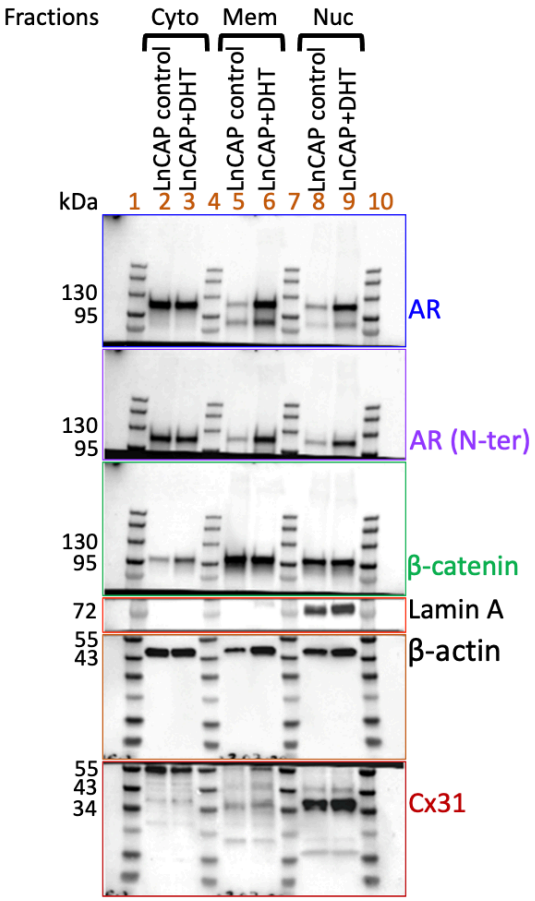

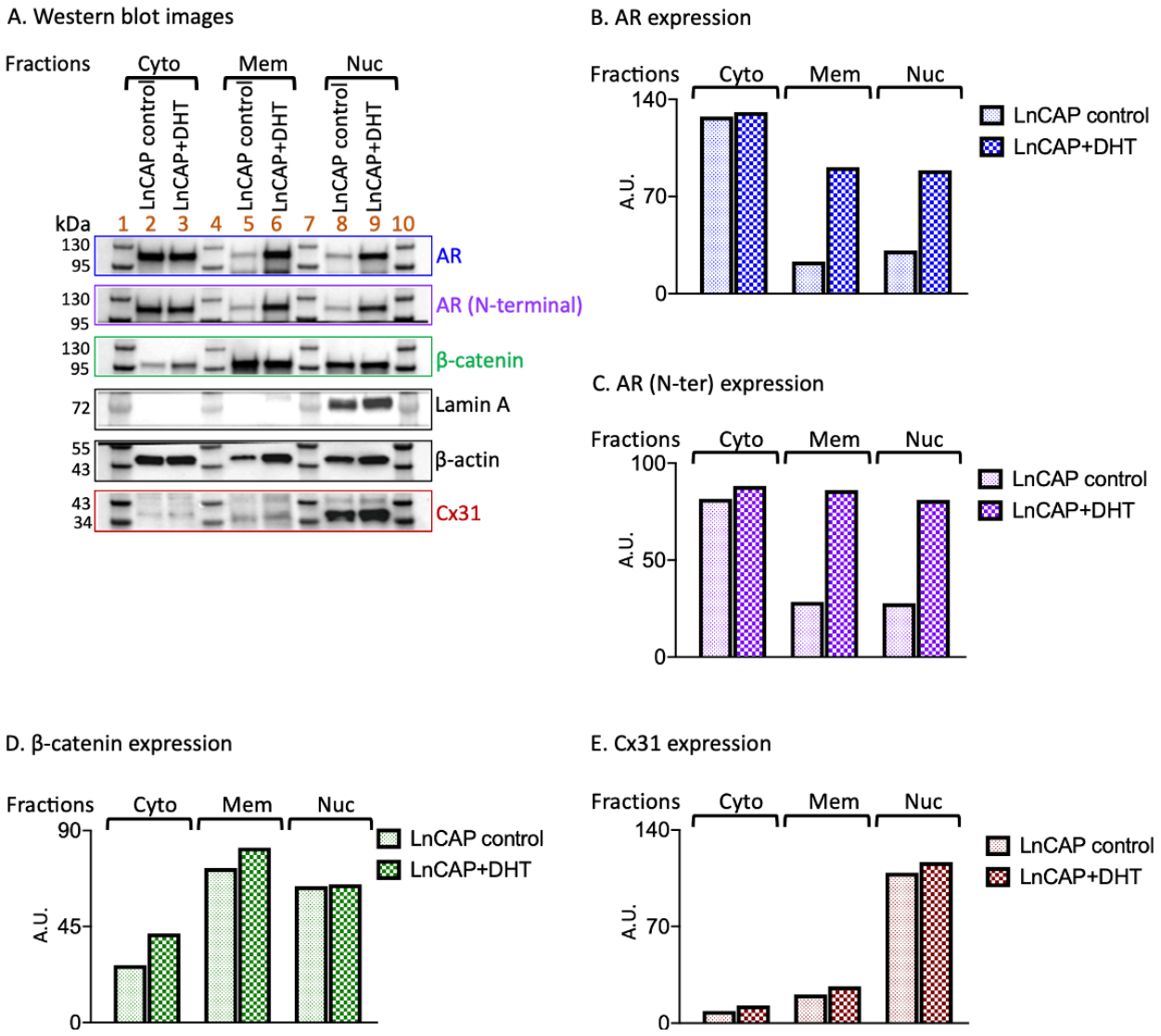

Figure 5.2. A representative WB image for the translocation of AR, AR (N-ter) and β-catenin into nucleus in LnCAP cells treated with DHT. Figure description in details is given in previous section (Sec. 5.1.1, Fig. 5.1). a. The WB images of a single membrane stained with multiple antibodies namely, anti AR, anti AR (N-ter), anti β-catenin and anti-Cx31 antibodies sequentially (Chap-II, Sec. 2.3.4.5). AR, AR (N-ter), β-catenin and Cx31 were translocated into nucleus showed in figs: B, C, D and E respectively in LnCAP cell (±DHT)

5.1.3. Experiment-3

LnCAP cell of different batch and passage was treated with DHT at recommended dilution (Chap-V, Table 5.1). AR, AR (N-ter) and β-catenin translocation were observed (Appx. Fig. 5.3).

a. The main PVDF membrane

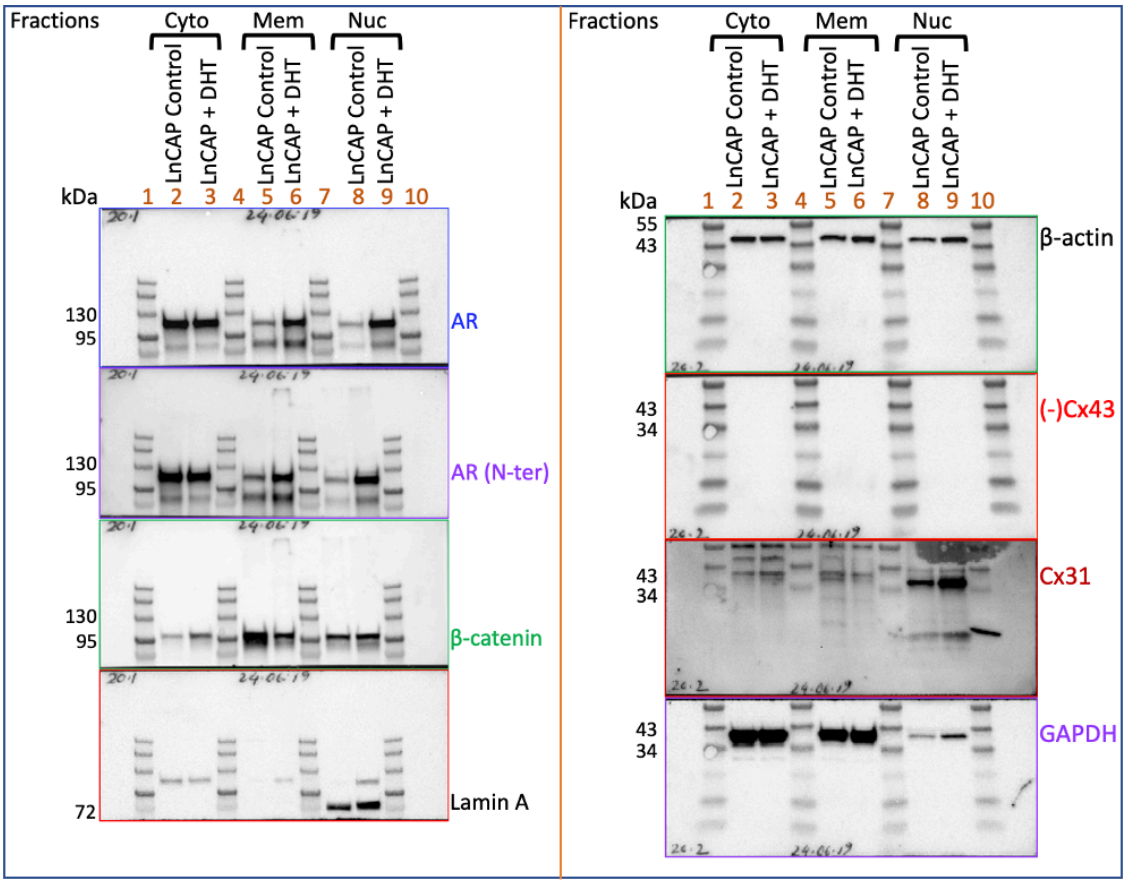

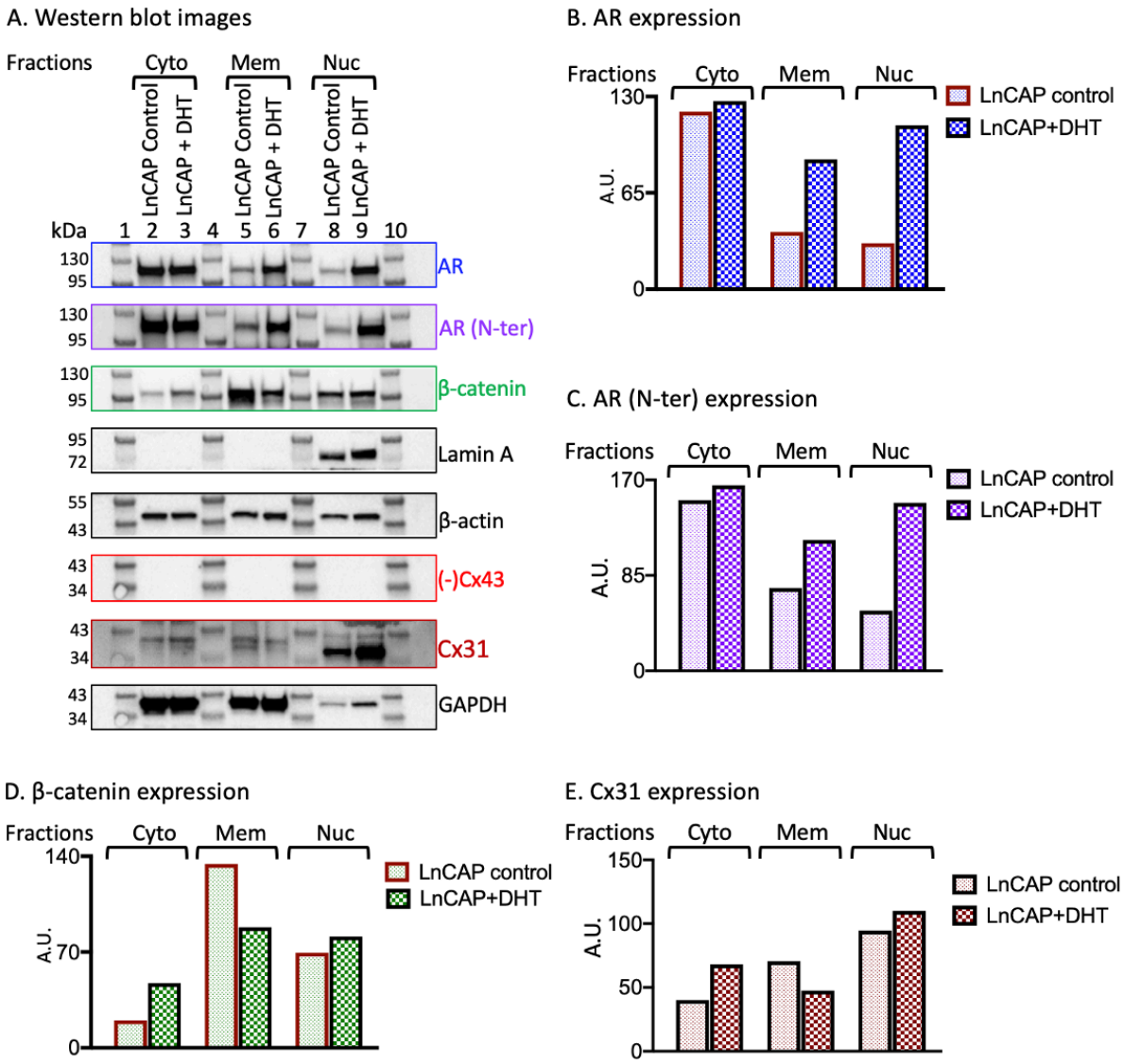

Figure 5.3. A representative WB image for translocation of AR, AR (N-ter) and β-catenin into nucleus in LnCAP cells treated with DHT. Figure description in details is given previously (Fig. 5.2). a. A multiple antibodies staining of a PVDF membrane is showing band intensity of protein expression. B: WB showing intensity of Band indicating level of protein expression. The intensity of bands was quantitated with ImageJ and the results were used to construct bar graph indicating redistribution of AR, AR (N-ter), β-catenin and Cx31 showed in figs: B, C, D and E respectively, in cytosol, membrane and nucleus in LnCAP cell (±DHT)

5.2. Analysis of translocation of AR and Wnt signalling proteins in Wnt3A treated LnCAP cells

5.2.1. Optimization experiment

An optimization experiment was performed with lower concentration of Wnt3A (5nM) which showed β-catenin was translocated (Appx. Fig. 5.4). AR was not translocated.

A. Main PVDF membrane

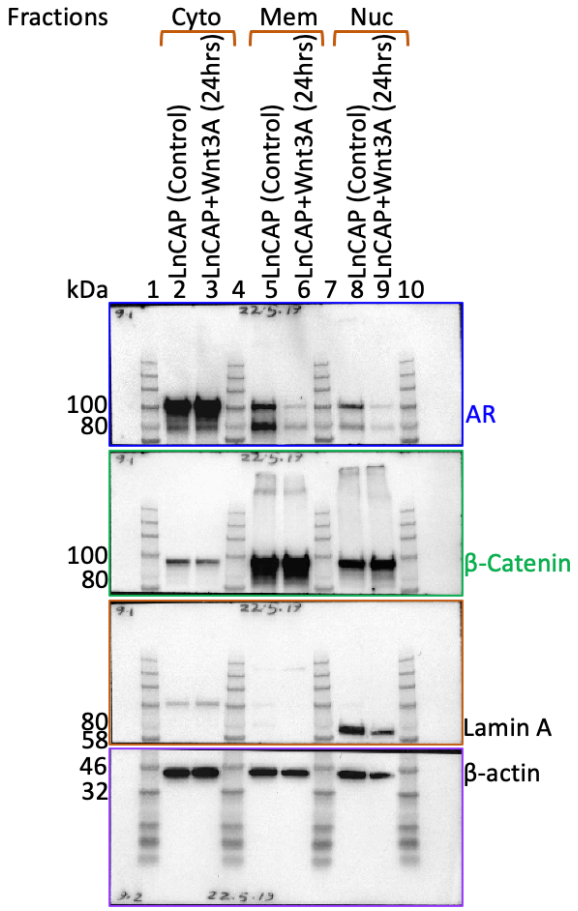

B. WB image

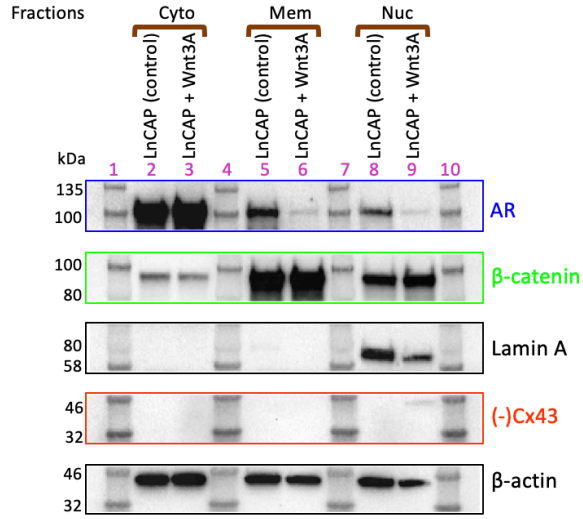

Figure 5.4. A representative WB image for the translocation of β-catenin into nucleus in LnCAP cells treated with Wnt3A. Figure description in details are given previously (Appx. Fig. 5.2). A. showing the

multiple antibodies staining of a single membrane. B WB showing intensity of Band indicating level of protein expression in LnCAP cells treated with Wnt3A.

5.2.2. Experiment-1

LnCAP cell was treated with Wnt3A at recommended dilution (Table 5.1). The result showed AR, AR (N-ter) and β-catenin translocation into nucleus was observed.

A. Western blot image of main PVDF membrane

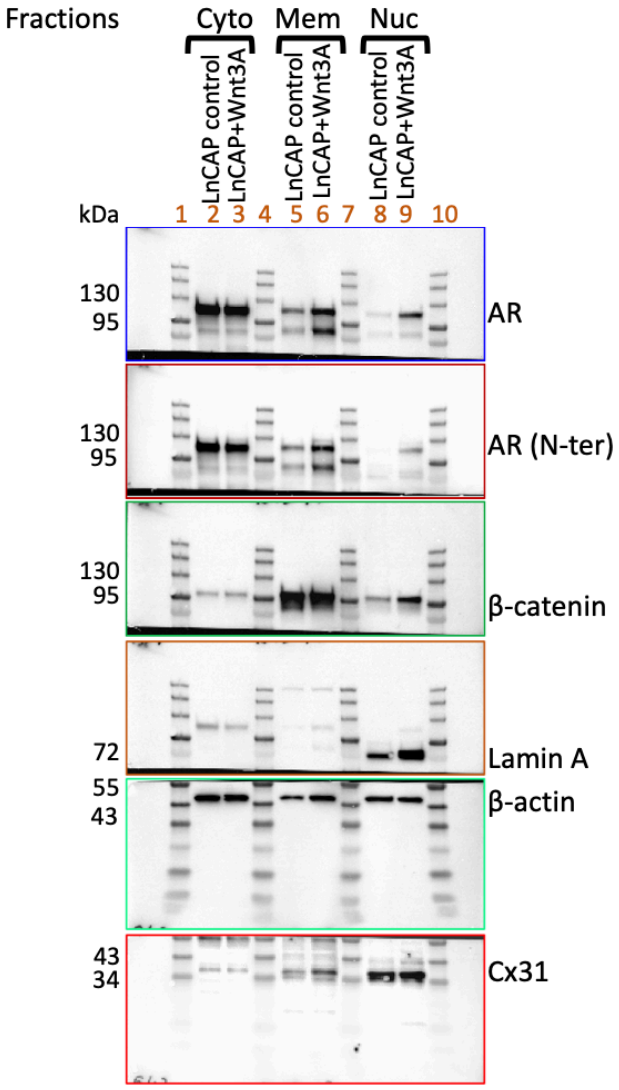

Figure 5.5. A representative WB image for the translocation of AR, AR (N-ter) and β-catenin and Cx31 into nucleus in LnCAP cells treated with Wnt3A. Figure description in details are given (Appx. Fig. 5.2).

5.2.3. Experiment-2

LnCAP cell was treated with Wnt3A at recommended dilution (Table 5.1). The result showed the translocation of AR, AR (N-ter) and β-catenin into nucleus in LnCAP cell treated with Wnt3A.

a. The main PVDF membrane

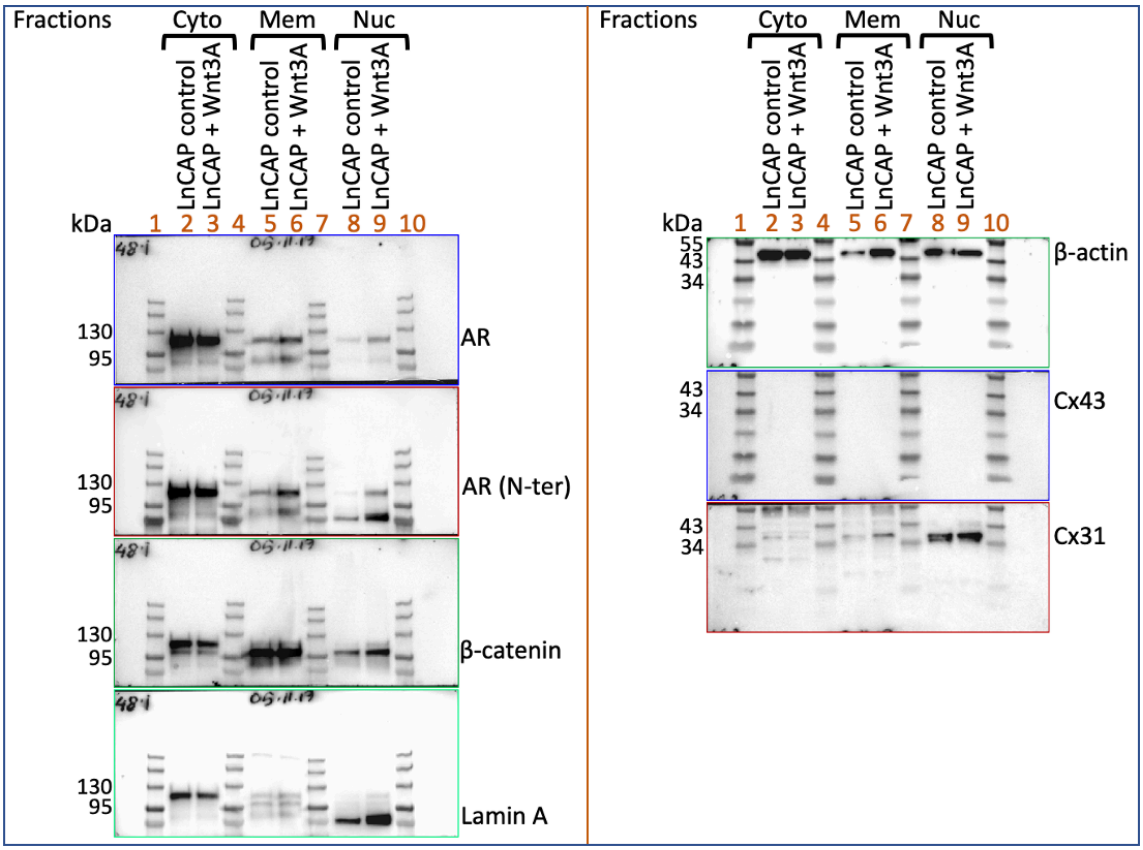

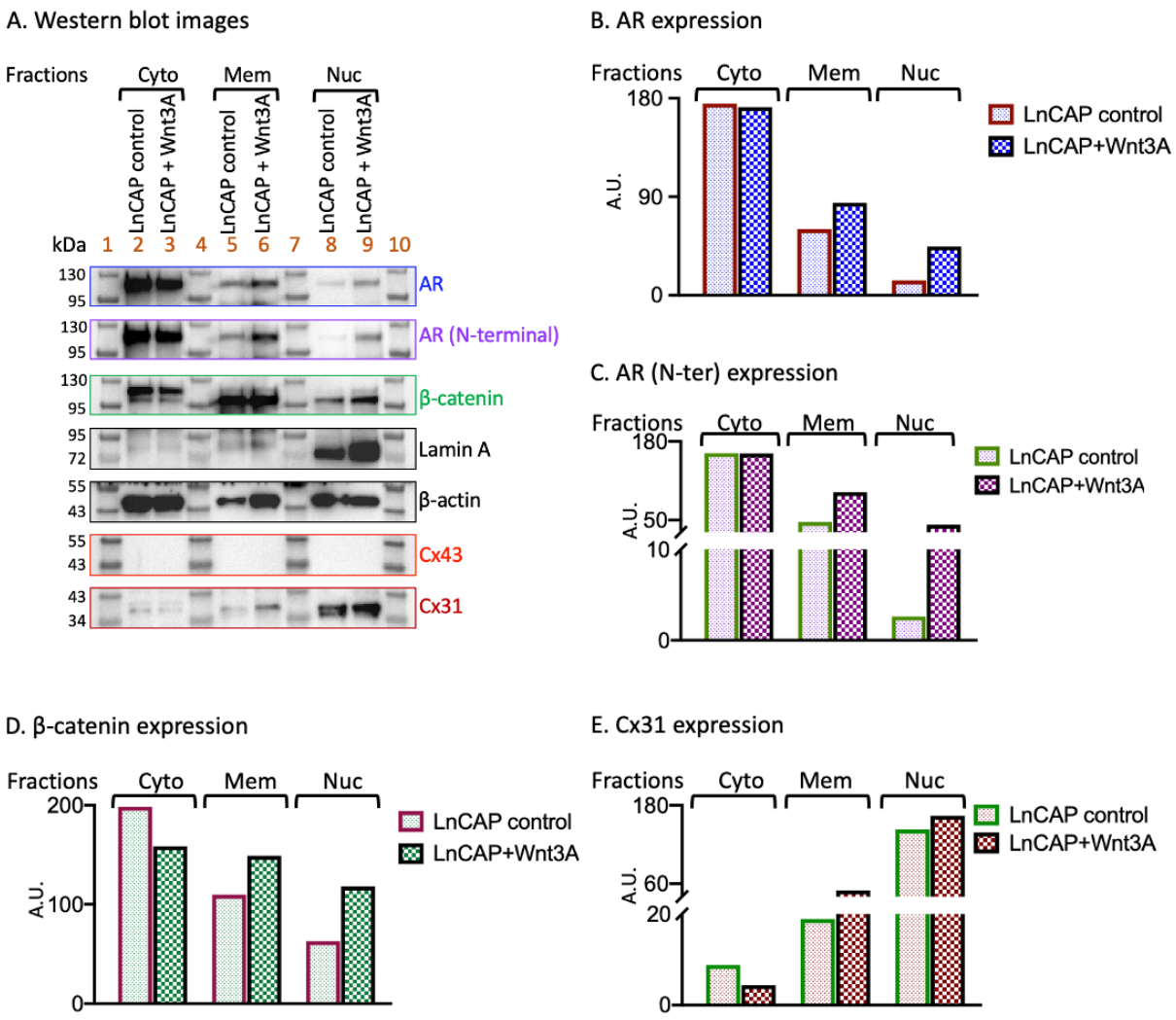

Figure 5.6. A representation of WB displaying translocation of AR, AR (N-ter) and β-catenin and Cx31 into nucleus in LnCAP cells treated with Wnt3A. a. The main PVDF membrane showed the expression of 4 proteins along with marker proteins Lamin A (Nuclear marker protein), β-actin (loading control). Antibody for Cx43 did not produce any band indicating absence of Cx43 protein in LnCAP cells. The selective parts (protein bands) of main PVDF were used to construct the image indicated with A. The intensity of bands was quantitated with ImageJ. B, C, D and E displaying the comparative expression of AR, AR (N-ter), β-catenin and Cx31 respectively, in cytosol, membrane and nucleus in LnCAP cell (±Wnt3A)

5.2.4. Experiment-3

LnCAP cell was treated with Wnt3A at recommended dilution (Table 5.1). The result showed AR, AR (N-ter) and β-catenin translocation into nucleus was observed.

a. Western blot image of main PVDF membrane

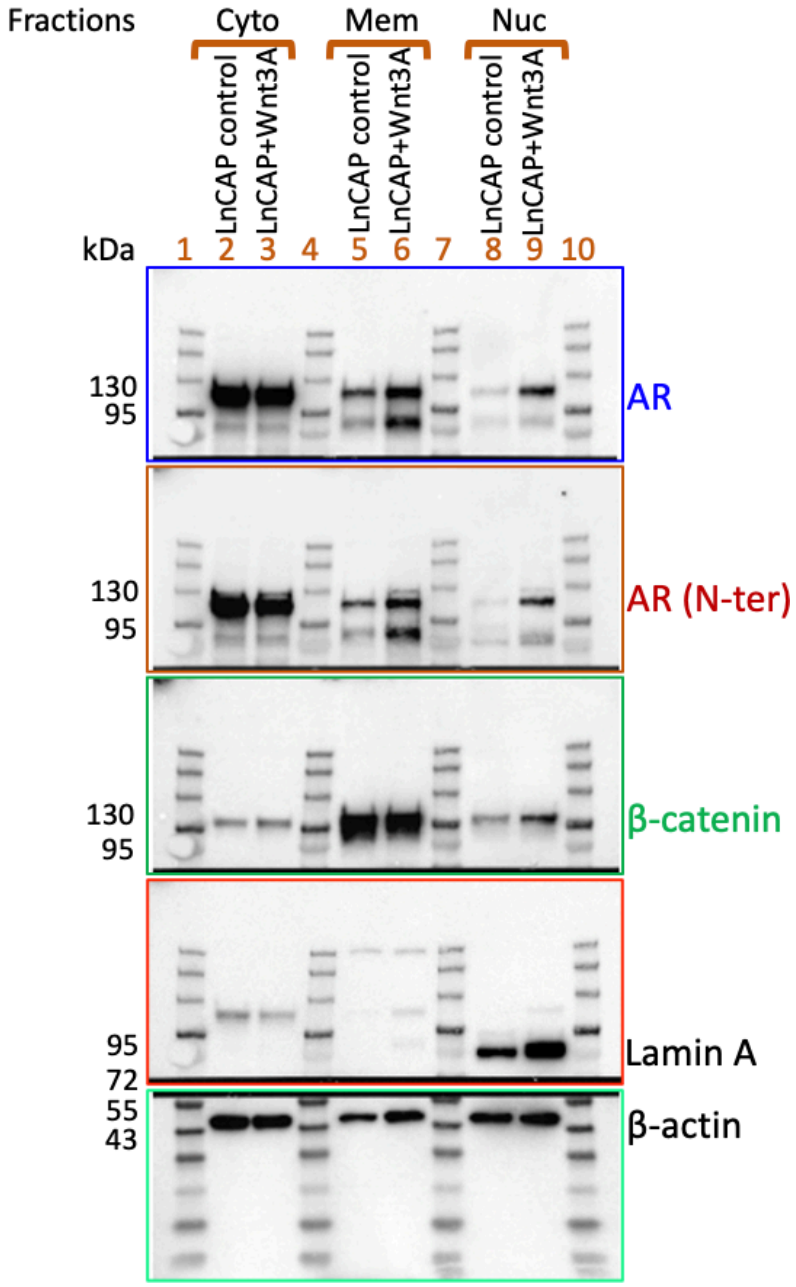

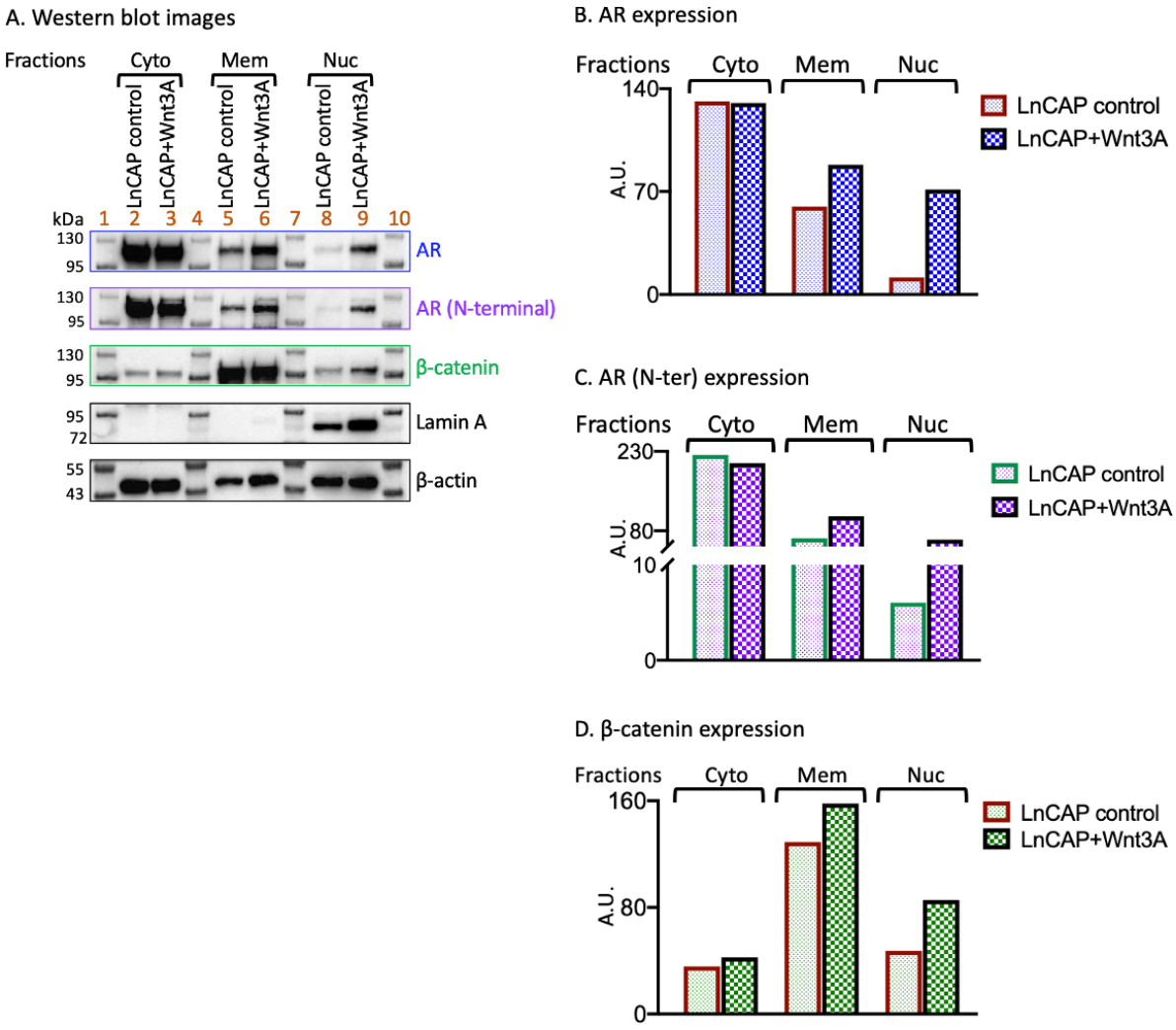

Figure 5.7. A representative WB image for translocation of AR, AR (N-ter) and β-catenin and Cx31 into nucleus in LnCAP cells treated with Wnt3A. a. The main PVDF membrane shows the expression of 4 proteins along with marker protein Lamin A (Nuclear marker protein) and β-actin (loading control). Antibody for Cx43 did not produce any band indicating absence of Cx43 protein in LnCAP cells. The selective parts (protein bands) of main PVDF were used to construct the image indicated with A. The intensity of bands was quantitated with ImageJ which showed redistribution of AR, AR (N-ter) and β-catenin and Cx31 across cytosol, membrane and nucleus showed in B, C, D and E respectively, in LnCAP cell (±Wnt3A).

5.3. Analysis of translocation of AR and Wnt signalling proteins in Wnt5A treated LnCAP cells

5.3.1. Optimization

An optimization experiment was performed with lower concentration of Wnt5A (5 nM) which showed AR was only translocated (Appx. Fig. 5.8) into nucleus. β-catenin was not translocated. Cx43 antibody did not produce any band.

A. Western blot image of main PVDF membrane

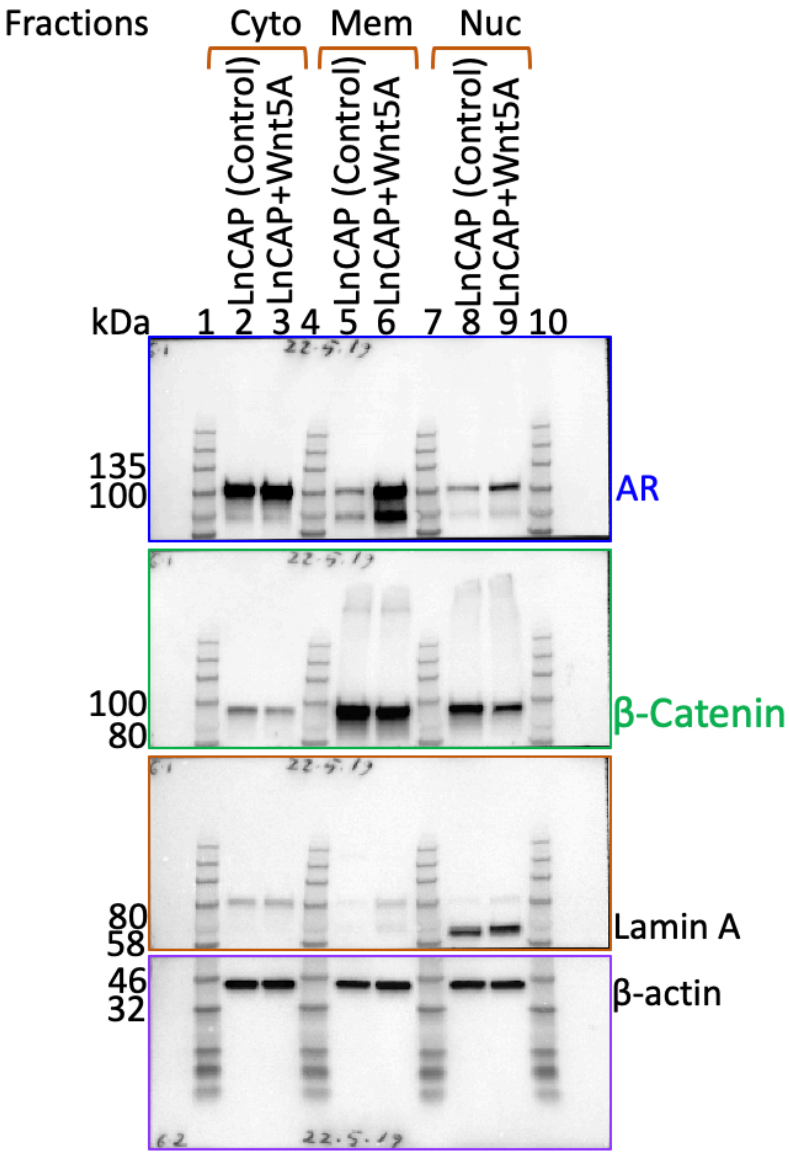

B. WB image

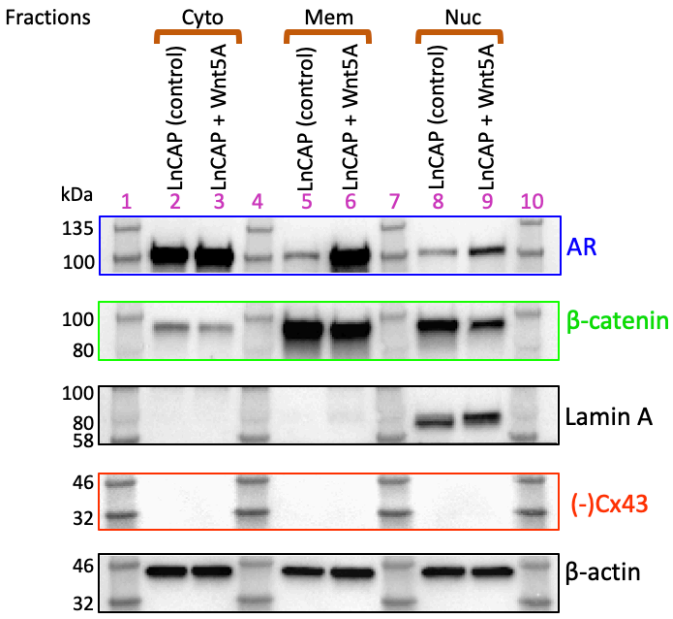

Figure 5.8. A representative WB image for translocation of AR in LnCAP cells treated with Wnt5A. Figure description in details is given previously (Appx. Fig. 5.2). A. The main PVDF membrane stained with five antibodies for AR, β-catenin, β-actin and Lamin A sequentially (Chap-II, Sec. 2.3.4). B WB shows intensity of Bands indicating level of protein expression in LnCAP cells treated with Wnt5A.

5.3.2. Experiment-1

LnCAP cell was treated with Wnt5A at recommended dilution (Table 5.1). The result showed that AR, AR (N-ter), β-catenin and Cx31 were translocated into nucleus.

A. Western blot image of main PVDF membrane

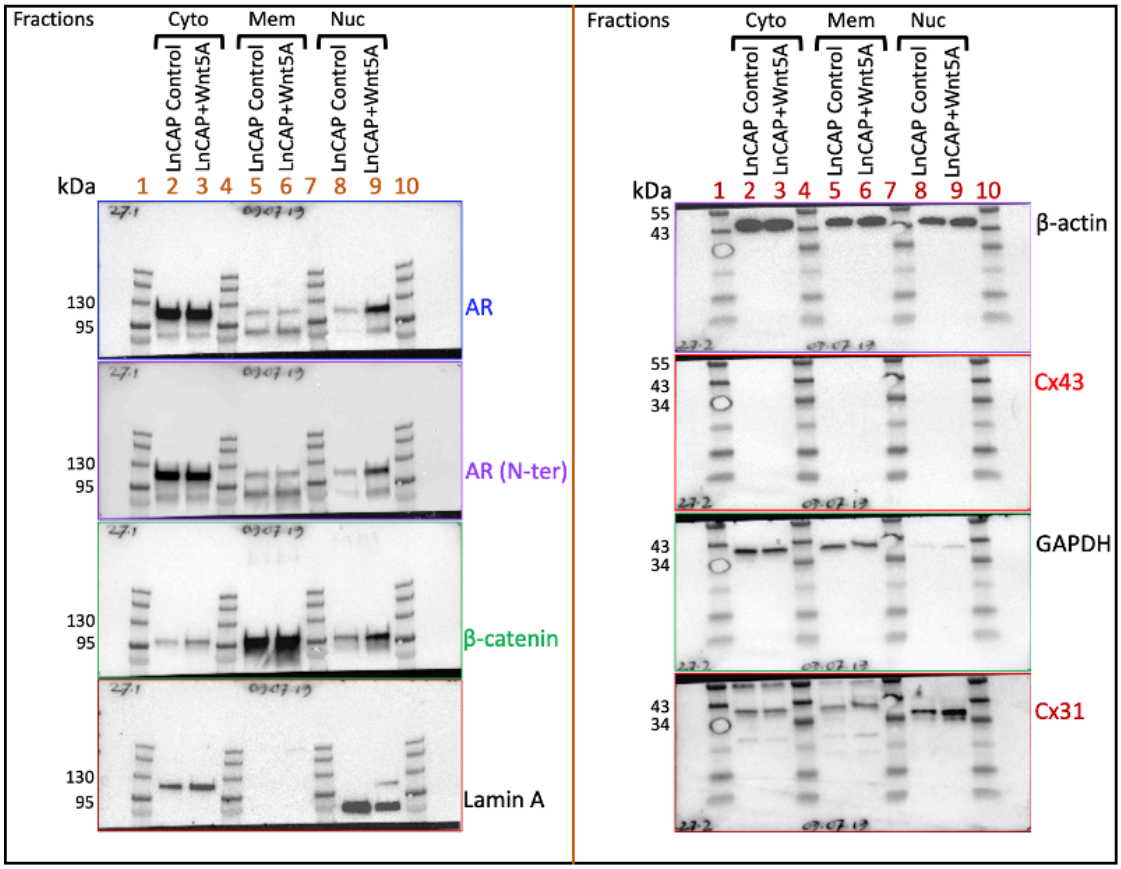

Figure 5.9. A representation of WB for displaying translocation of AR, AR (N-ter), β-catenin and Cx31 into nucleus in LnCAP cells treated with Wnt5A. Figure description in details is given in early figure (Appx. Fig. 5.2).

5.3.3. Experiment-2

LnCAP cell was treated with Wnt5A at recommended dilution (Table 5.1). The result showed that AR, AR (N-ter) and β-catenin were translocated into nucleus.

a. Western blot image of main PVDF membrane

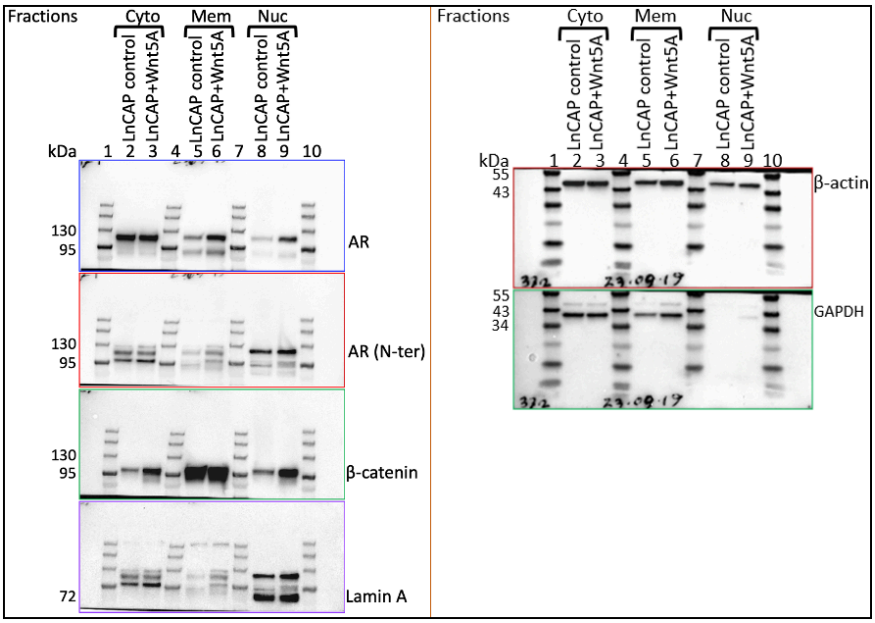

A. Western blot images

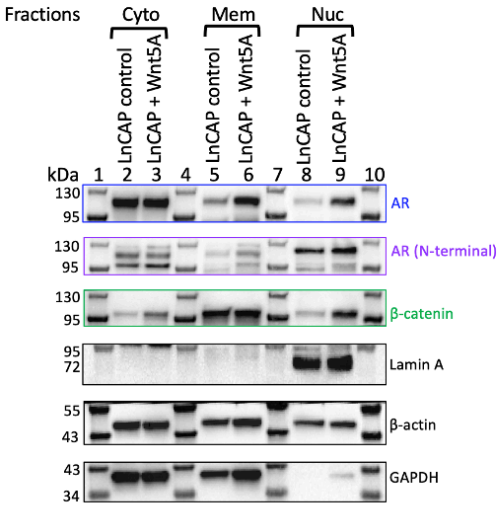

B. AR expression

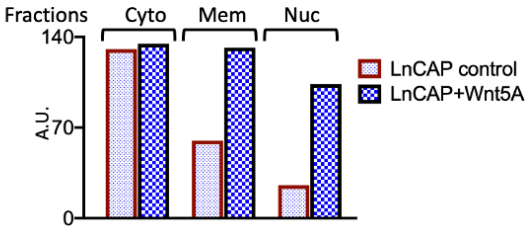

C. AR (N-ter) expression

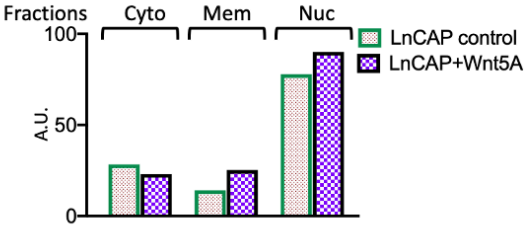

D. β-catenin expression

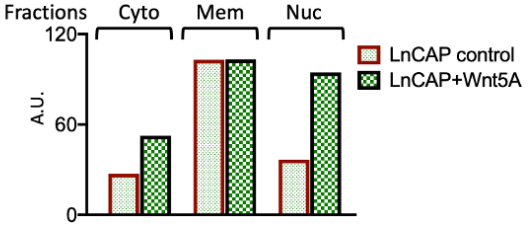

Figure 5.10. A representative WB image for translocation of AR, AR (N-ter) and β-catenin and Cx31 into nucleus in LnCAP cells treated with Wnt5A. a. Shows the multiple antibodies staining of a single PVDF membrane. A. WB shows intensity of bands indicating level of protein expression. The intensity of bands was quantitated with ImageJ. B, C, D and E showed redistribution of AR, AR (N-ter), β-catenin and Cx31 respectively, in cytosol, membrane and nucleus in LnCAP cell (±Wnt5A).

5.3.4. Experiment-3

LnCAP cell was treated with Wnt5A at recommended dilution (Table 5.1). The result showed that AR, AR (N-ter), β-catenin and Cx31 were translocated into nucleus.

a. Western blot image of main PVDF membrane

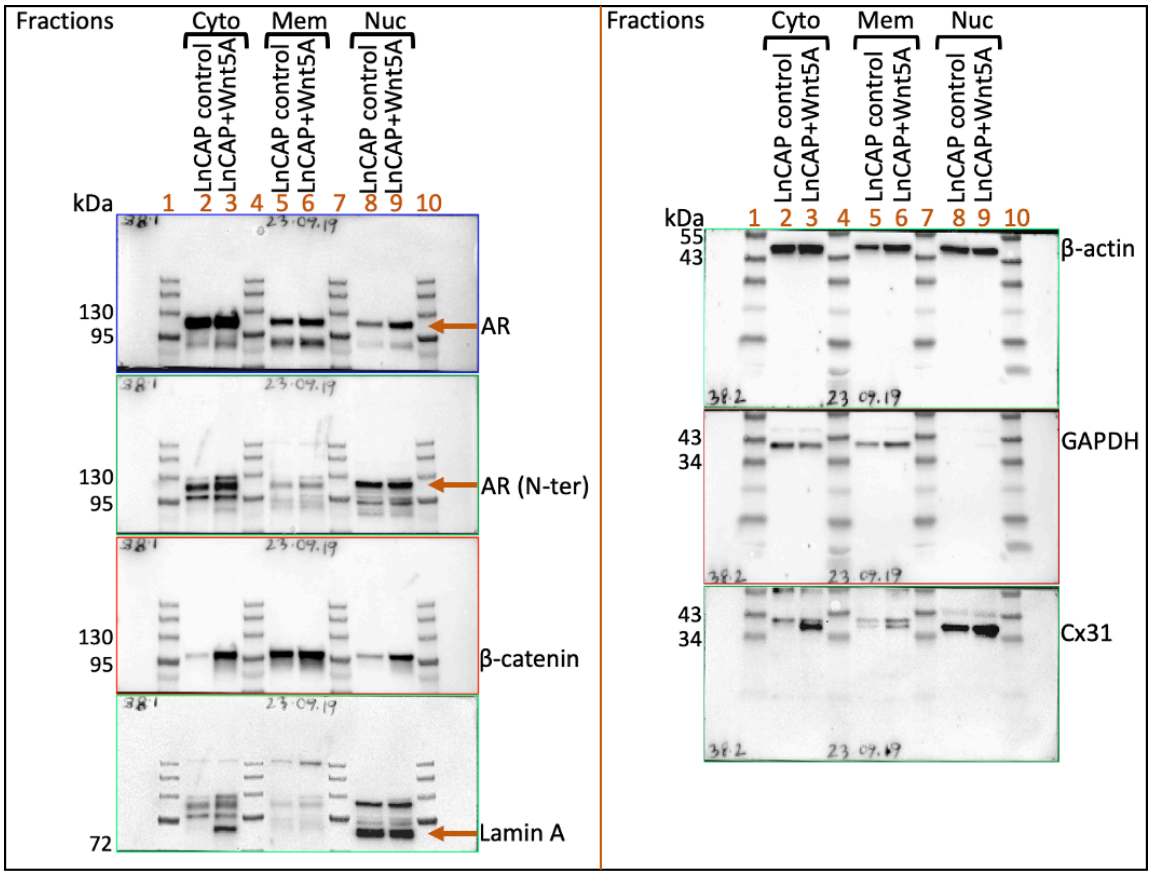

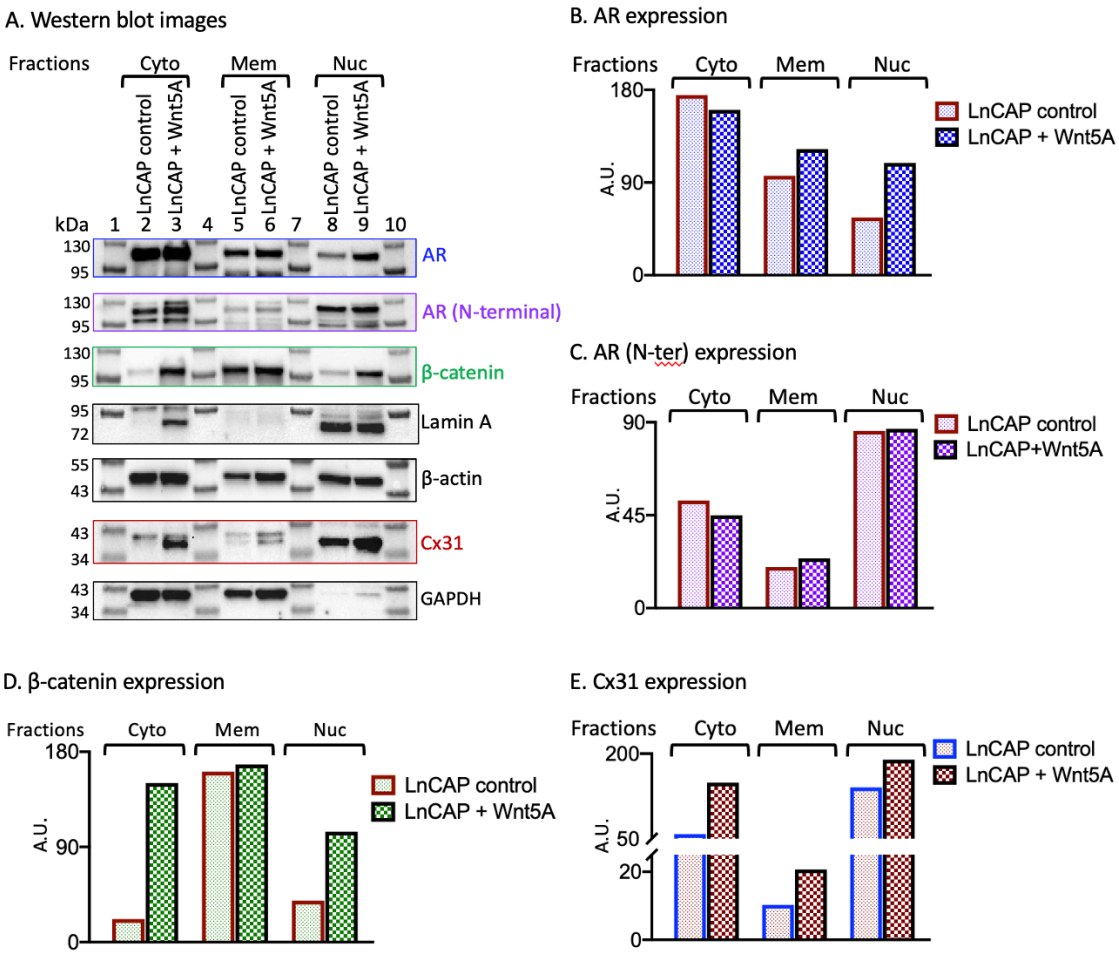

Figure 5.11. A representative WB image for translocation of AR, AR (N-ter) and β-catenin and Cx31 into nucleus in LnCAP cells treated with Wnt5A. a. Shows the multiple antibodies staining of a single membrane. A. WB showing intensity of Band indicating level of protein expression. The intensity of bands was quantitated with ImageJ. B, C, D and E are displaying translocation of AR, AR (N-ter), β-catenin and Cx31 into nucleus in LnCAP cell (±Wnt5A)

5.3.5. Experiment-4

LnCAP cell was treated with Wnt5A at recommended dilution (Table 5.1). The result showed that AR, AR (N-ter) and β-catenin were translocated into nucleus. Cx43 antibody did give any band.

a. Western blot image of main PVDF membrane

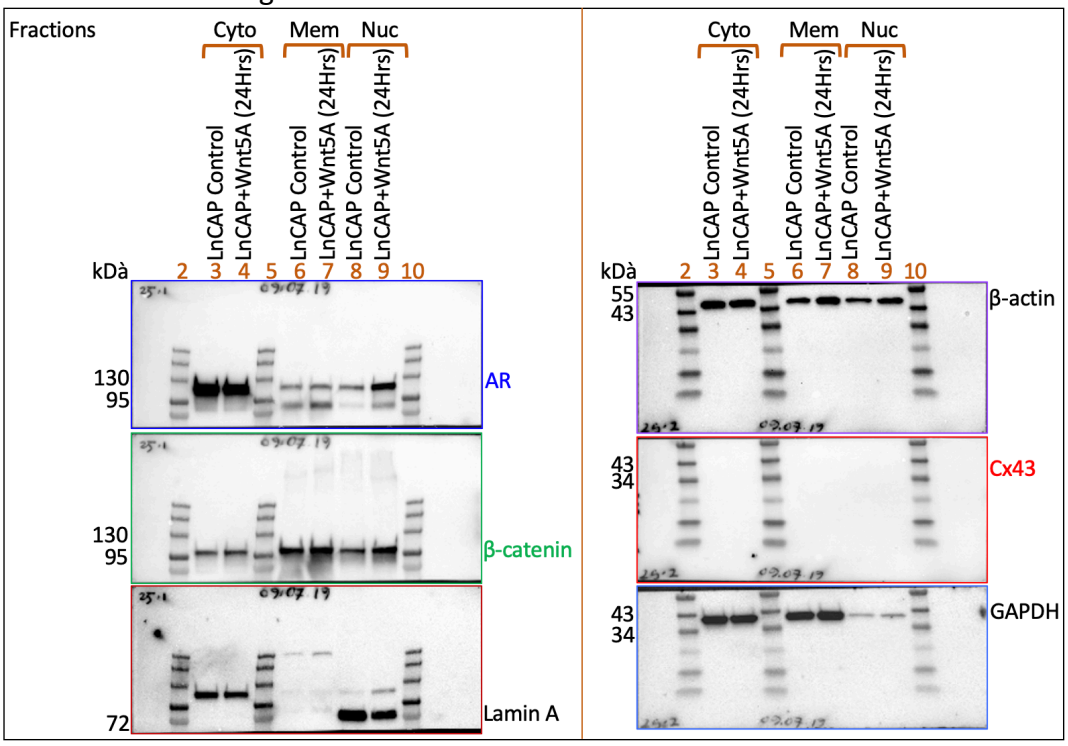

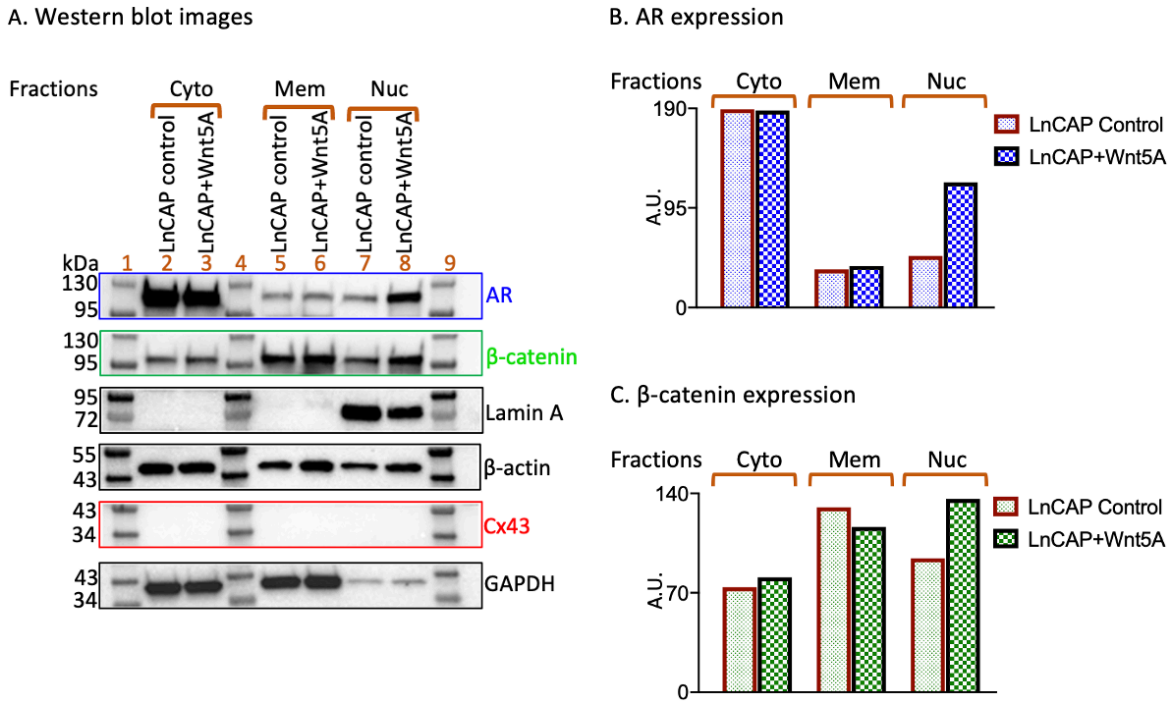

Figure 5.12. A representative WB image for translocation of AR, AR (N-ter) and β-catenin and Cx31 into nucleus in LnCAP cells treated with Wnt5A. a. Shows the multiple antibodies staining of a single membrane. A. WB are showing intensity of Band indicating level of protein expression. The intensity of bands was quantitated with ImageJ. B, C, D and E are displaying the redistribution of AR, AR (N-ter), β-catenin and Cx31 respectively, in cytosol, membrane and nucleus in LnCAP cell (±Wnt5A)

5.4. Analysis of translocation of AR and Wnt signalling proteins in Wnt9B treated LnCAP cells

5.4.1. Optimization

An optimization experiment was performed with lower concentration of Wnt9b (5nM) which showed AR was only translocated (Appx. Fig. 5.13). β-catenin was not translocated. Cx43 did not show any band in LnCAP cell.

A. Western blot image of main PVDF membrane

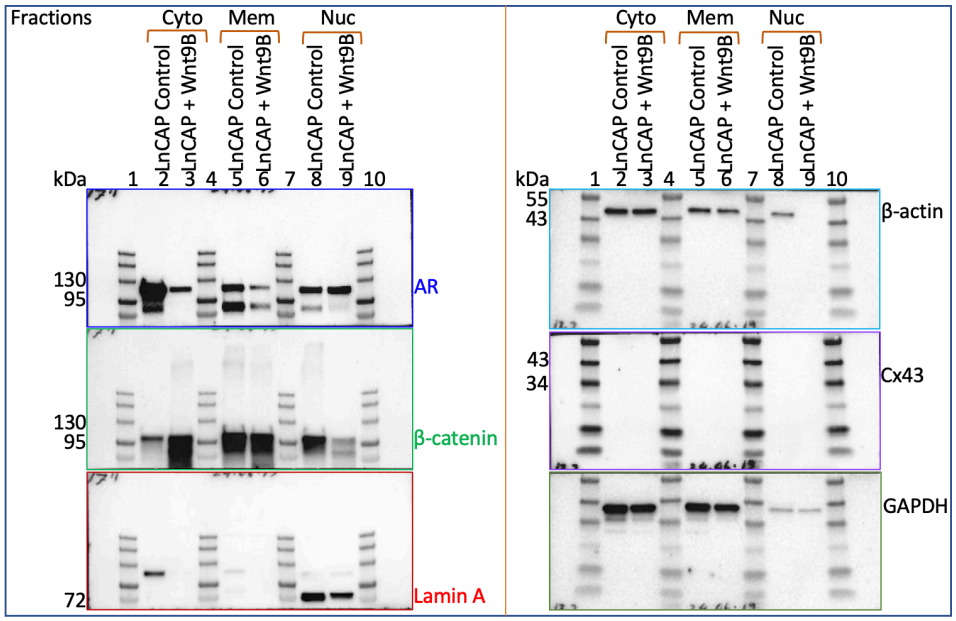

B. WB image

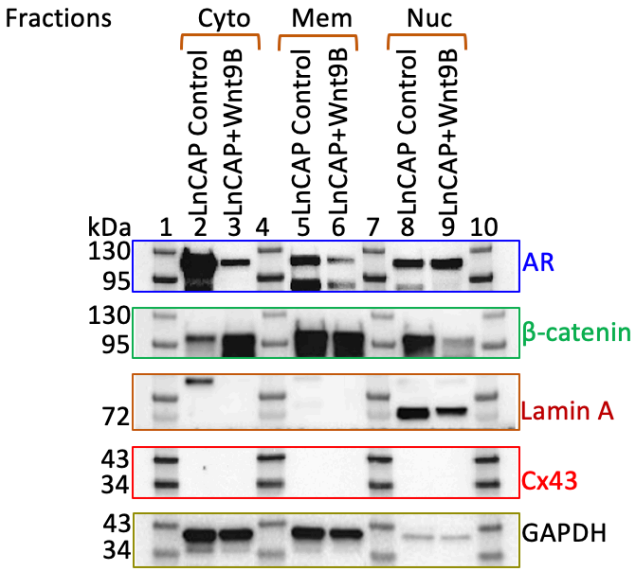

Figure 5.13. A representative WB image for translocation of AR in LnCAP cells treated with Wnt9B. A. Shows the multiple antibodies staining of a single PVDF membrane. B WB is showing intensity of Band indicating level of protein expression in LnCAP cells treated with Wnt9B.

5.4.2. Experiment-1

LnCAP cell was treated with Wnt9B at recommended dilution (Table 5.1). The result showed that AR, AR (N-ter), β-catenin and Cx31 were translocated into nucleus.

a. Western blot image of main PVDF membrane

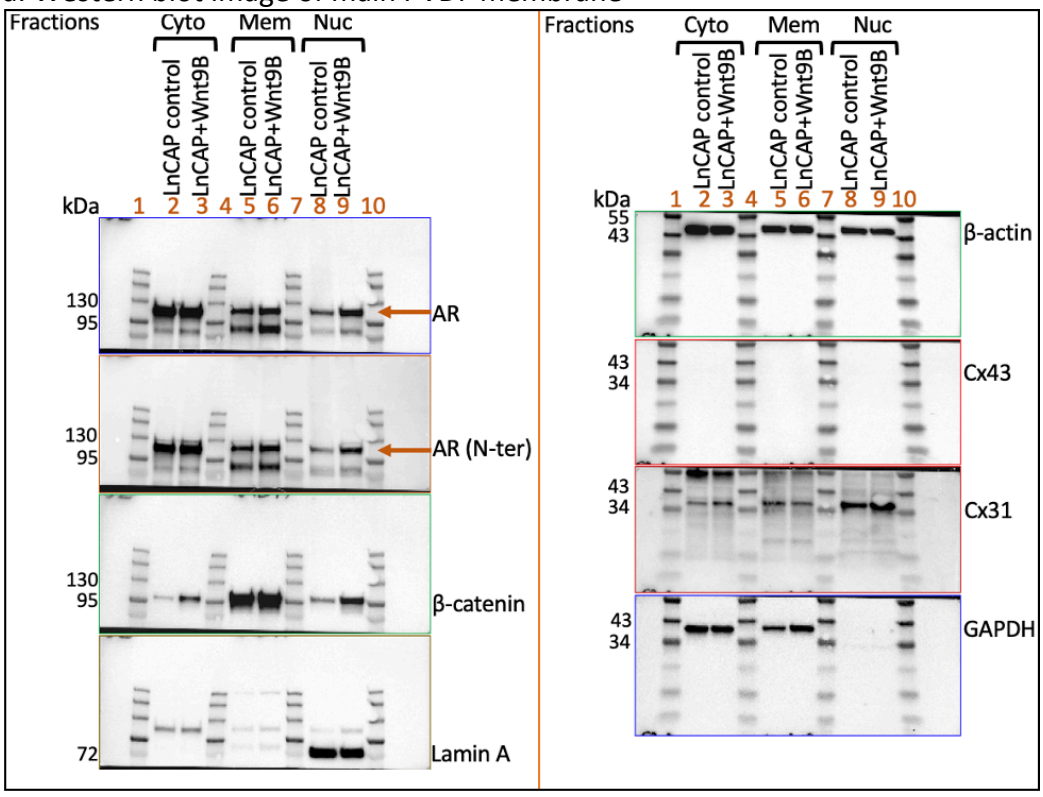

Figure 5.14. A representative WB image for translocation of AR, AR (N-ter), β-catenin and Cx31 into nucleus in LnCAP cells treated with Wnt9B. A. The stained PVDF is showing the translocation of AR, AR (N-ter), β-catenin and Cx31 into nucleus in LnCAP cells treated with Wnt9B. Lamin A is a nuclear marker protein and β-actin and GAPDH are loading control.

5.4.3. Experiment-2

A repeat experiment of LnCAP cell treated with Wnt9B at recommended dilution (Table 5.1) showed that AR, AR (N-ter), β-catenin and Cx31 were translocated into nucleus.

a. Western blot image of main PVDF membrane

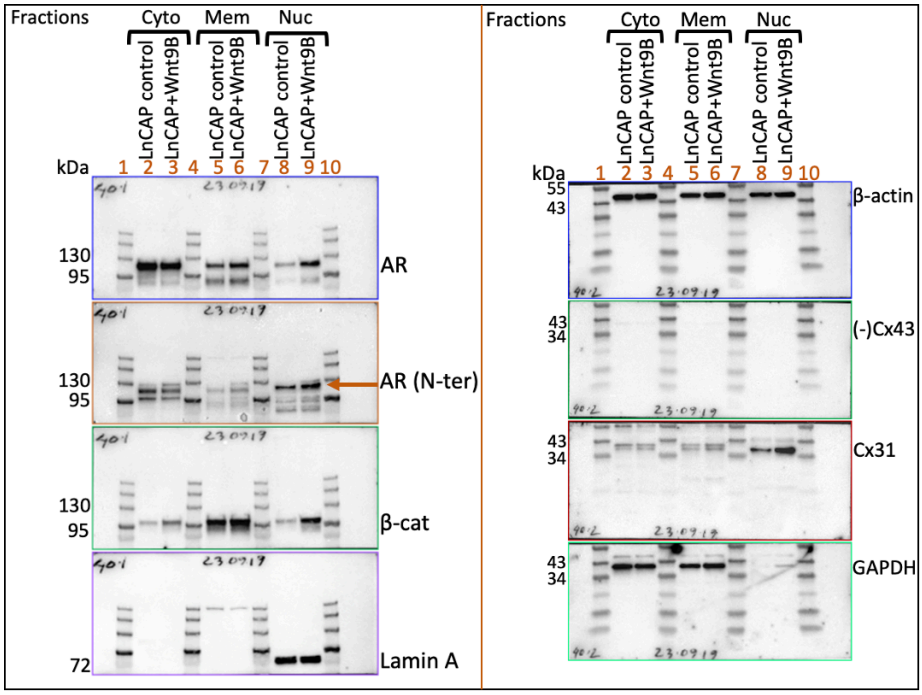

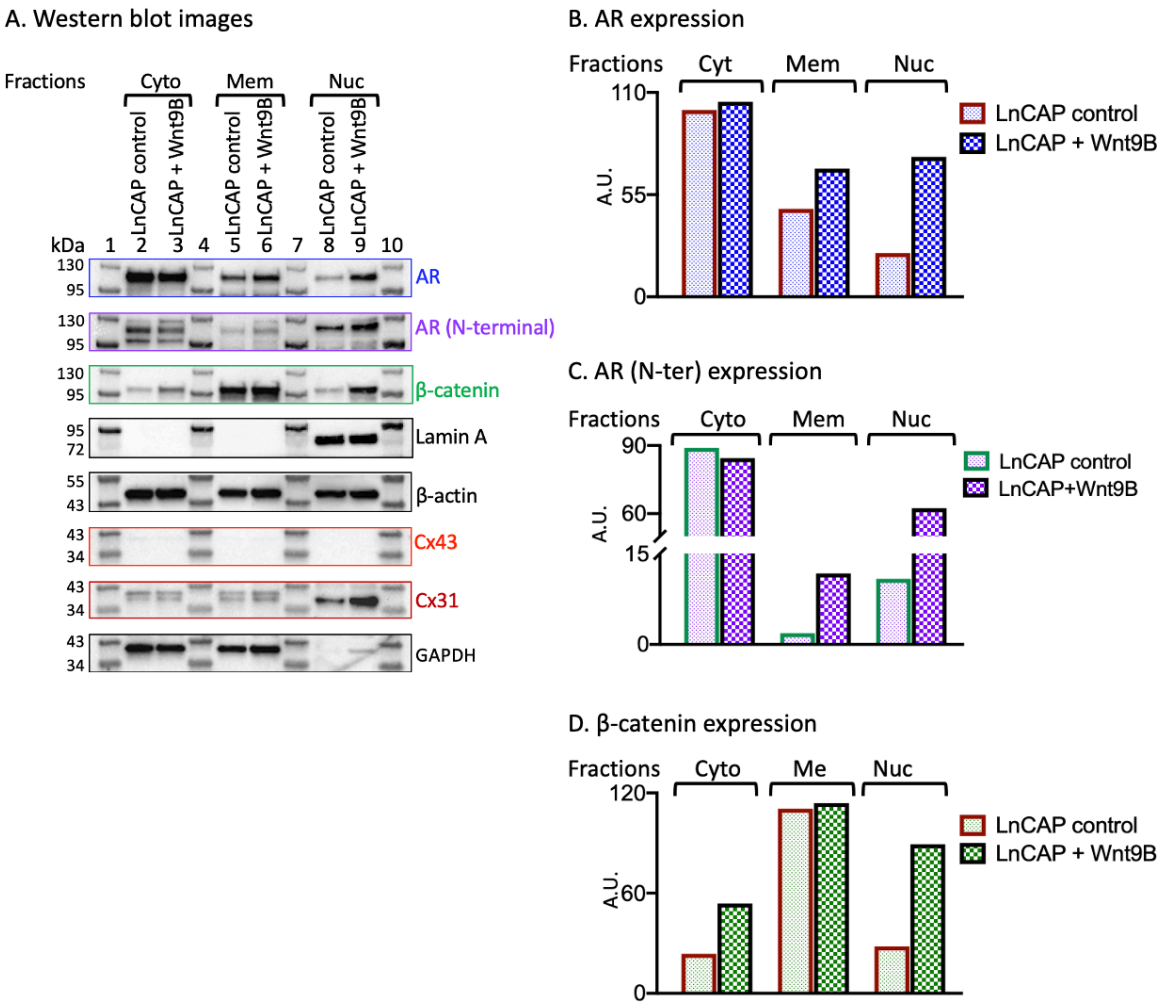

Figure 5.15. A representative WB image for translocation of AR, AR (N-ter) and β-catenin and Cx31 into nucleus in LnCAP cells treated with Wnt9B. a. The main PVDF membrane shows the expression of 4 proteins along with marker proteins Lamin A (Nuclear marker protein) and β-actin (loading control). Antibody for Cx43 did not produce any band, indicating absence of Cx43 protein in LnCAP cells. The selective parts (protein bands) of main PVDF were used to construct the image indicated with A. The intensity of bands was quantitated with ImageJ which showed redistribution of AR, AR (N-ter) and β-catenin and Cx31 across cytosol, membrane and nucleus showed in B, C, D and E respectively, in LnCAP cell (±Wnt9B).

5.4.4. Experiment-3

LnCAP cell was treated with Wnt9B at recommended dilution (Table 5.1). The result showed that AR, AR (N-ter) and β-catenin were translocated into nucleus.

a. Western blot image of main PVDF membrane

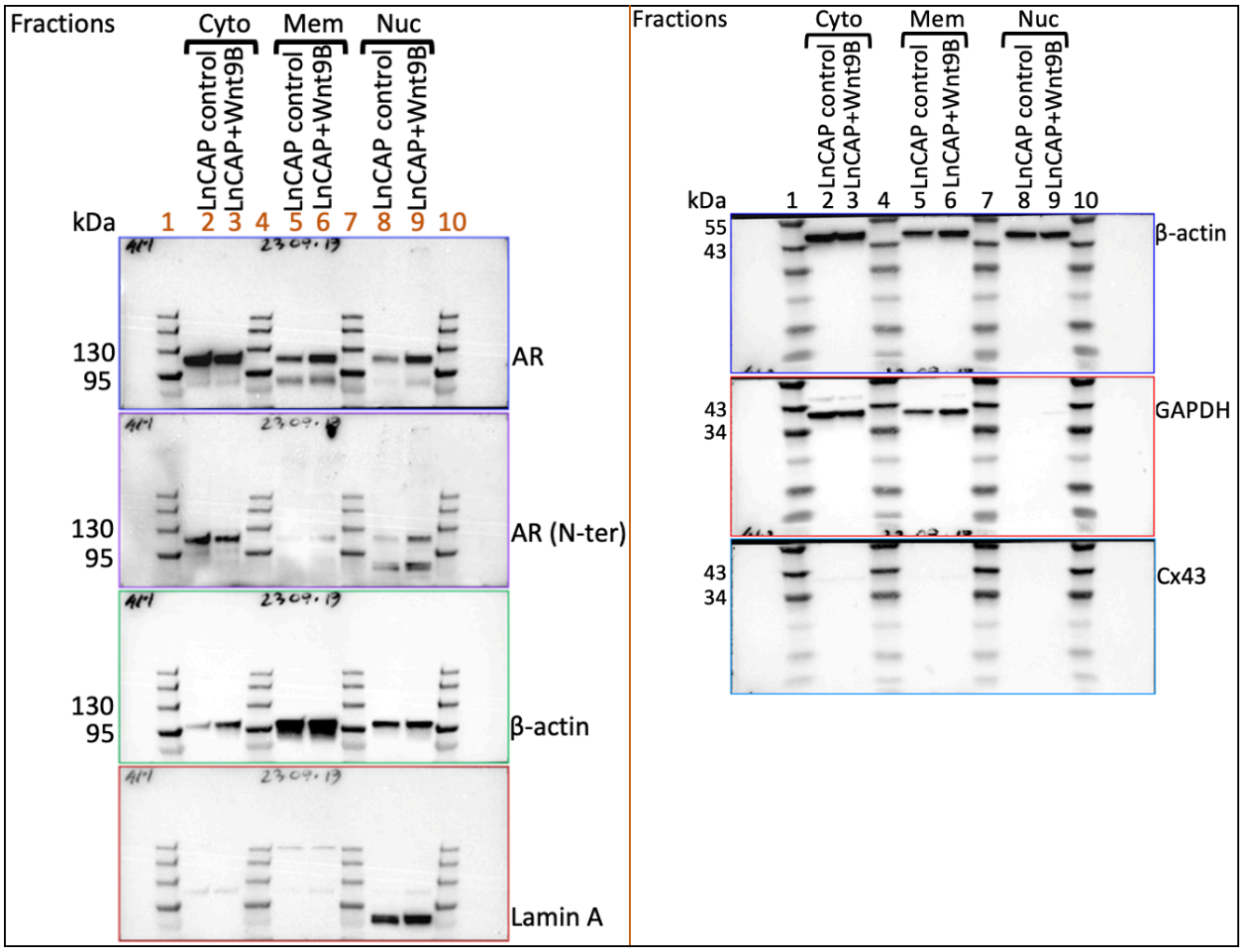
Fractions
Cyto
Mem
Nuc
LnCAP control
LnCAP+Wnt9B
kDa
1 2 3 4 5 6 7 8 9 10
130
95
AR
AR (N-ter)
β-actin
Lamin A
55
43
34
GAPDH
Cx43

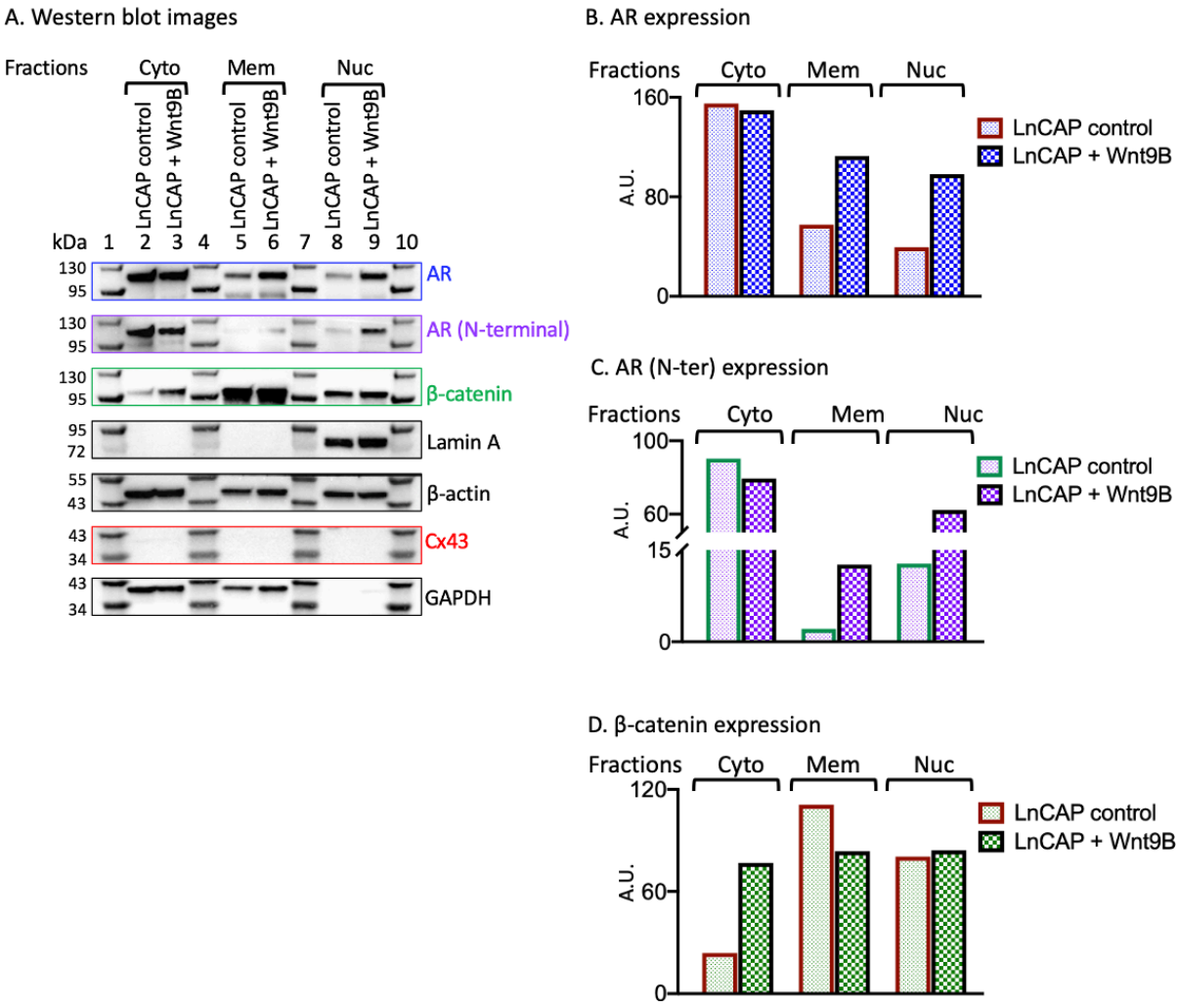

Figure 5.16. A representative WB image for translocation of AR, AR (N-ter) and β-catenin into nucleus in LnCAP cells treated with Wnt9B. a. A multiple stained PVDF membrane shows the proteins indicating expression of the corresponding proteins. Following quantitation, the bar graph was constructed which shows translocation of AR, AR (N-ter) and β-catenin in nucleus in LnCAP (±Wnt9B) cells showed in graphs B, C and D respectively.

5.5. Analysis of translocation of Wnt signalling protein in PC3 cell

PC3 cell was treated with Wnt9B at recommended dilution (Table 5.1). The result showed that β-catenin and Cx43 were translocated into nucleus.

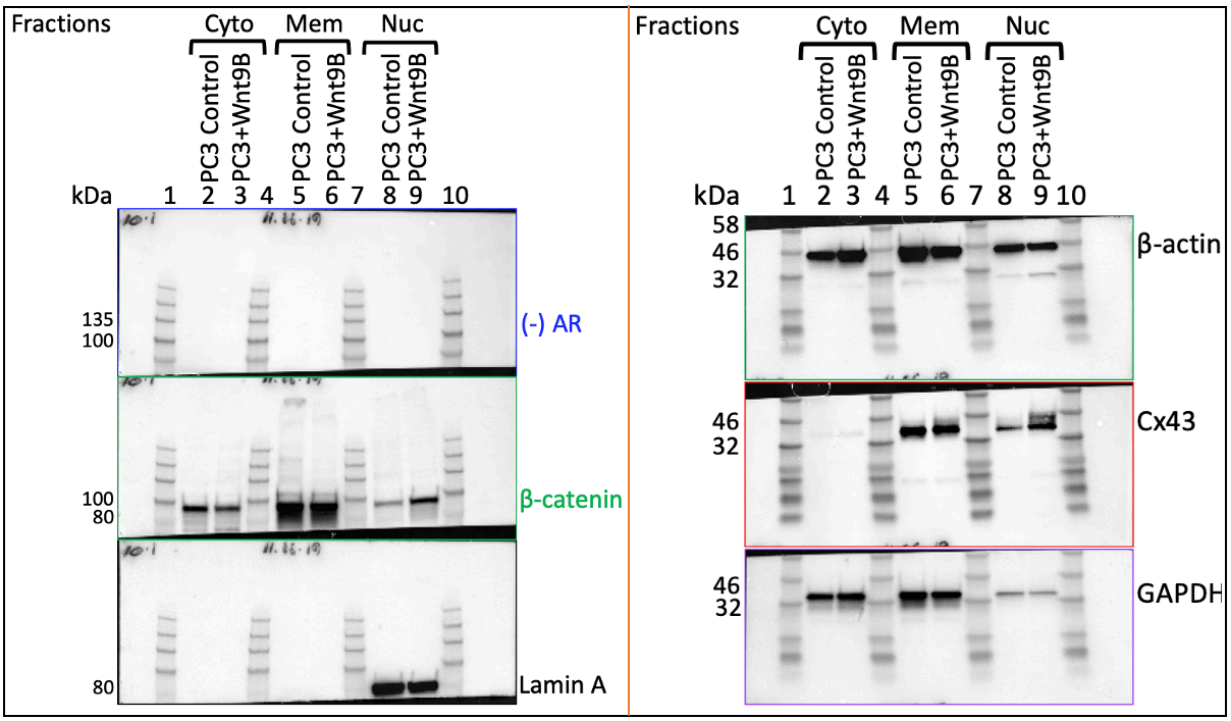

Figure 5.17. A representative WB image for translocation of β-catenin and Cx43 into nucleus in PC3 cells treated with Wnt9B. The image is showing the multiple antibodies staining of a single membrane indicating translocation of β-catenin and Cx43. AR did not show any band, indicating absence AR protein in PC3 cells.

5.6. Analysis of translocation of Wnt signalling proteins in DHT treated PC3 cell

5.6.1. Experiment-1

PC3 cells were treated with DHT at recommended dilution (Table 5.1). The result showed that β-catenin and Cx43 translocation into nucleus were inhibited.

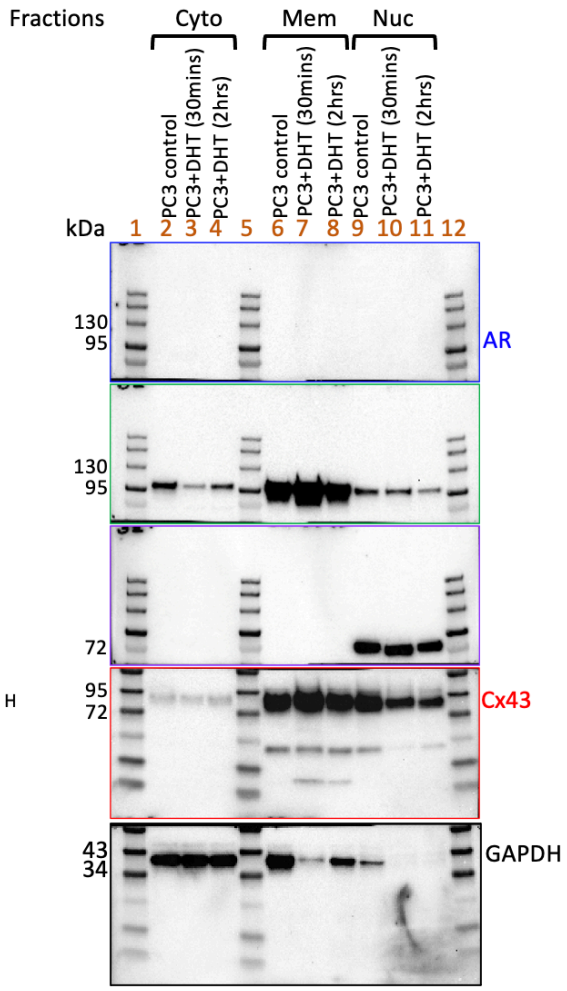

Figure 5.18: A representative WB image for of translocation of β-catenin and Cx43 into nucleus in PC3 cells treated with DHT. A. 15µg of fractionated protein of PC3 cells (±DHT) was loaded onto gels, such as cytosolic protein loaded in lane 2, 3 and 4, membrane protein in lane 6, 7 and 8, and nuclear protein in lane 8, 10 and 11. The resulting shows the inhibition of translocation of β-catenin and Cx43 into nucleus in PC3 (±DHT) cells.

5.6.2. Experiment-2

A repeat experiment was performed of PC3 cells treated with DHT at recommended dilution (Table 5.1). The result showed that β-catenin and Cx43 translocated into nucleus were inhibited.

a. Western blot image of main PVDF membrane

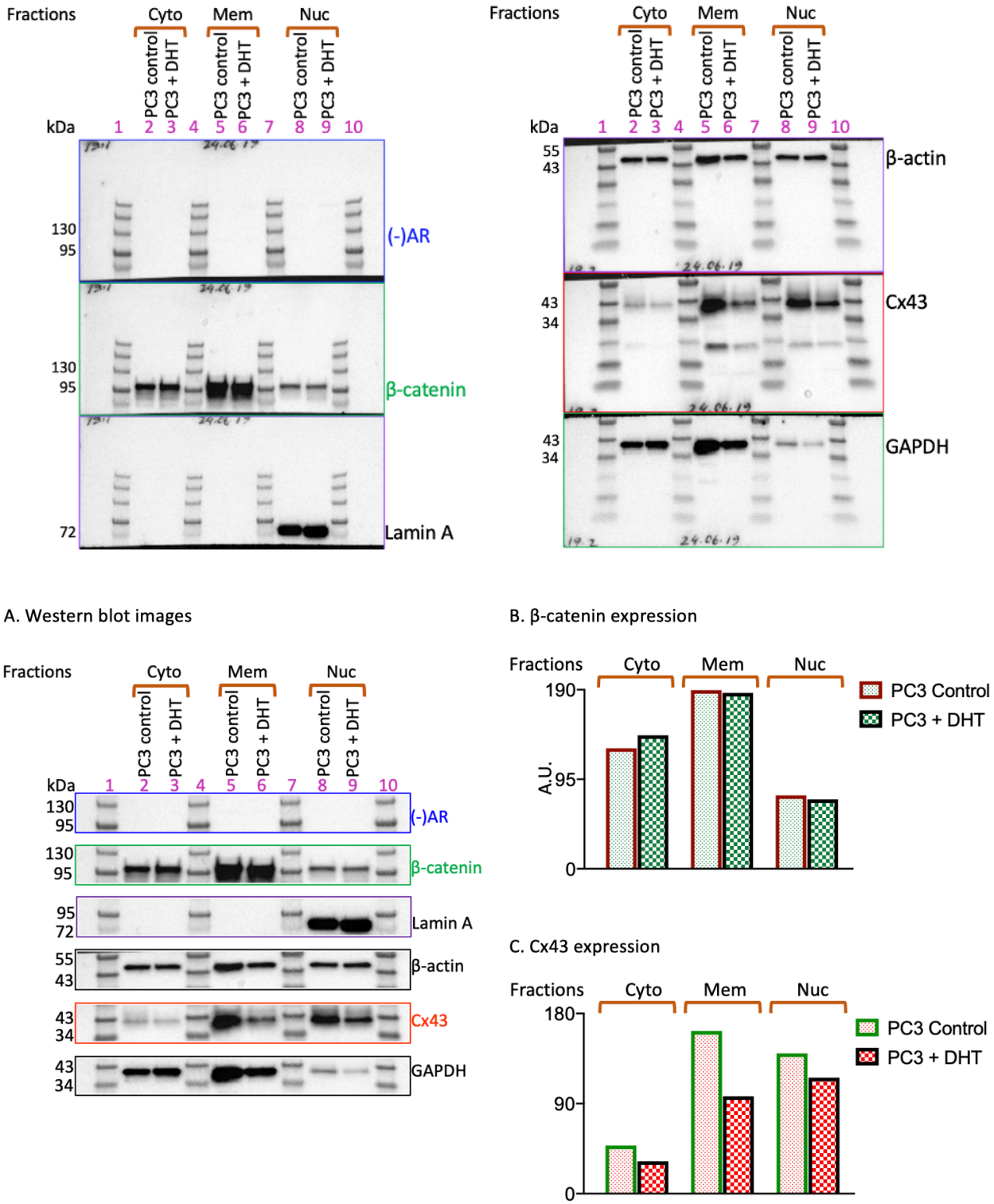

Figure 5.19: A representative WB image for inhibition of translocation of β-catenin and Cx43 into nucleus in PC3 cells treated with DHT. a. A PVDF membrane stained with six antibodies. The bands of the antibodies were cropped and construct the image A. Following quantitation with ImageJ, bar graph for β-catenin and Cx43 were made showed in B and C respectively. This indicated inhibition of β-catenin and Cx43 into nucleus in DHT treated PC3 cells. AR expression was not observed.

5.7. Analysis of translocation of Wnt signalling protein in DHT and Wnt9B treated PC3 cell

5.7.1. Experiment-1

PC3 cell was treated with DHT and Wnt9B at recommended dilution (Table 5.1). Wnt9B treatment to DHT treated PC3 cells showed the translocation of β-catenin and Cx43 into nucleus.

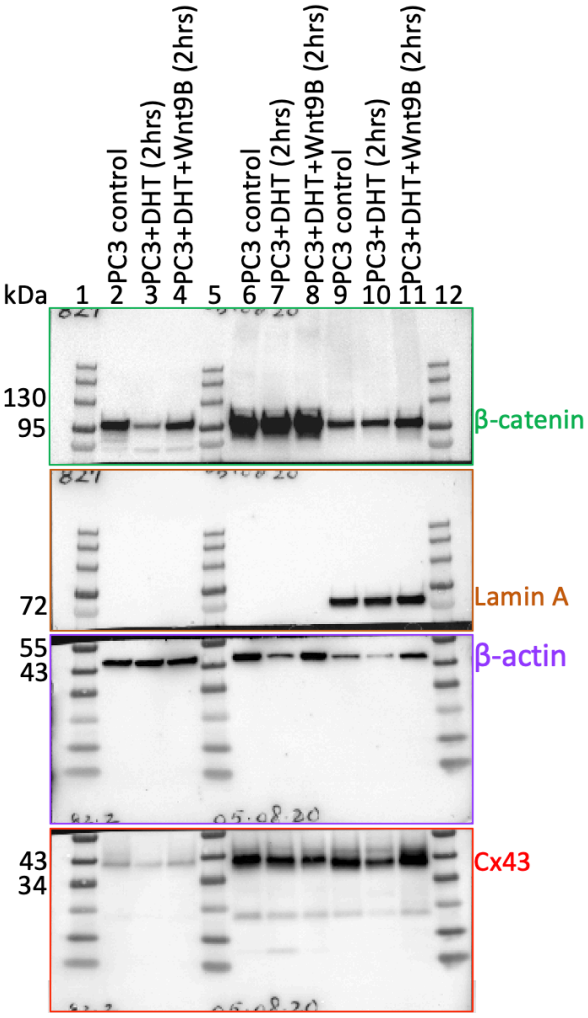

Figure 5.20: A representation of WB displaying the translocation of β-catenin and Cx43 into nucleus in PC3 cells treated with DHT followed by Wnt9B treatment. The image is displaying the PVDF membrane stained with multiple 4 antibodies indicating their corresponding protein expression namely β-catenin and Cx43.

5.7.2. Experiment-2

PC3 cell was treated with DHT followed by Wnt9B at recommended dilution (Table 5.1). The result showed that β-catenin and Cx43 translocated into nucleus. This indicates effect of DHT treatment was altered.

a. The main stained PVDF membrane

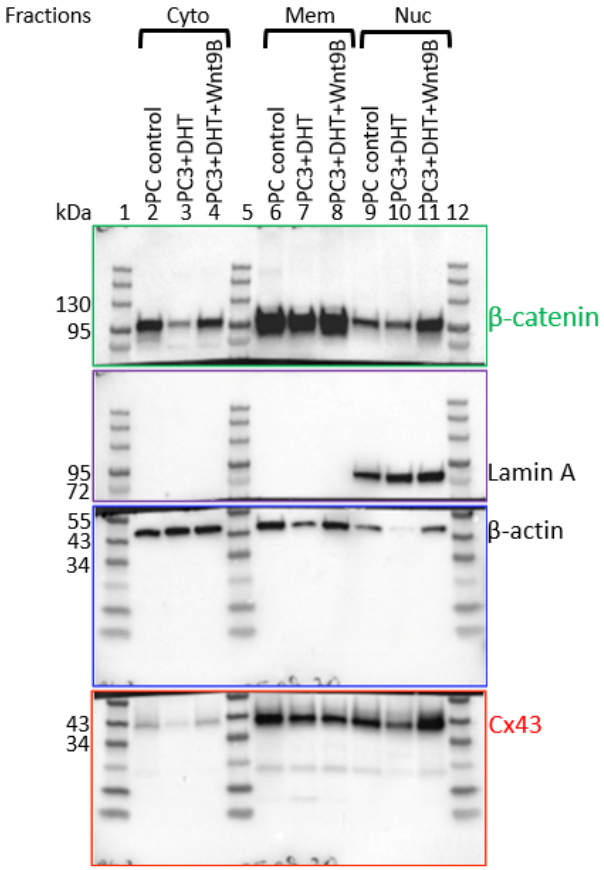

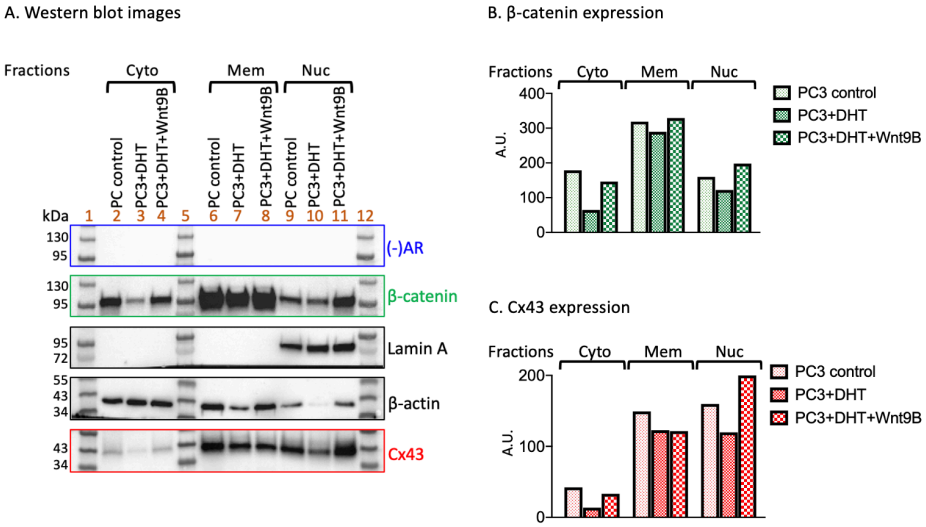

Figure 5.21: A representative WB image for inhibition and translocation of β-catenin and Cx43 into nucleus in PC3 cells treated with DHT or DHT followed by Wnt9B treatment. Figure description in details is given previously (Chap-V, Fig. 5.10). a. The image indicates the multiple antibodies staining of a single membrane. A. WB shows intensity of bands indicating level of protein expression. The intensity of bands was quantitated with ImageJ. B and C displaying the comparative expression of β-catenin and Cx43

respectively, in cytosol, membrane and nucleus in PC3 cell (+DHT) for B and +DHT followed by application of Wnt9B showed in C.

5.8. Analysis of translocation of AR and Wnt signalling proteins in PC3 and PC3$^{(AR+)}$ and PC3$^{(AR+)}$ +DHT

PC3 cells were transfected with AR and treated with DHT to observe the translocation of AR, β-catenin and Cx43. The result showed that AR, β-catenin and Cx43 were translocated

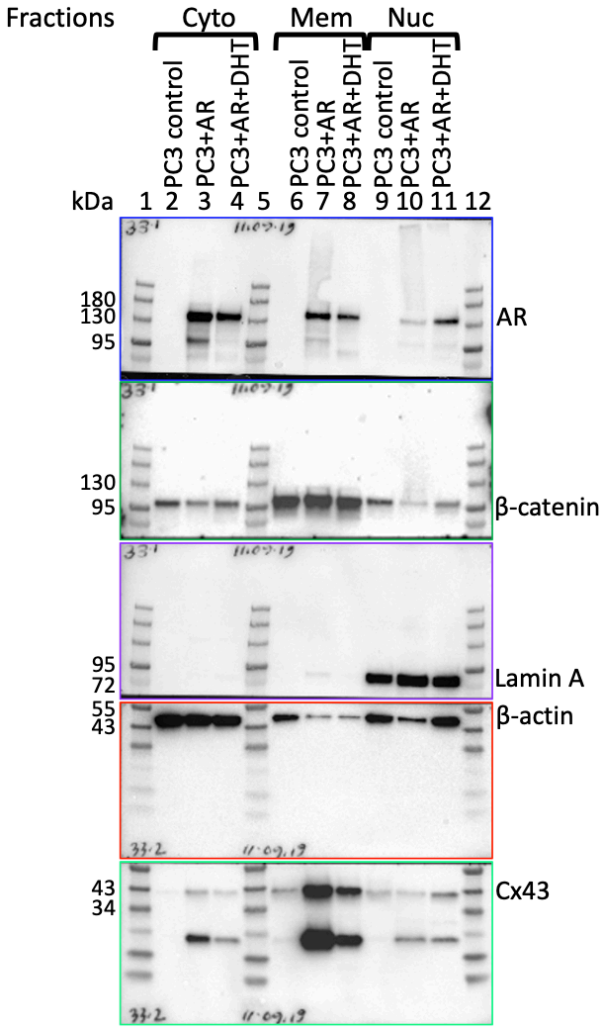

Figure 5.22: A representative WB image for translocation of AR, β-catenin and Cx43 into nucleus in PC3$^{(AR+)}$ and PC3$^{(AR+)}$ +DHT. Figure description is given previously (Chap-V, Fig. 5.12). The image indicating the multiple antibodies stained single membrane.

5.9. Analysis of translocation of AR and Wnt signalling proteins in PC3 and PC3$^{(AR+)}$ and PC3$^{(AR+)}$ +Wnt9B

5.9.1. Experiment-1

PC3 cells were transfected with AR and treated with Wnt9B to observe the translocation of AR, β-catenin and Cx43. The result showed that AR, β-catenin and Cx43 were translocated.

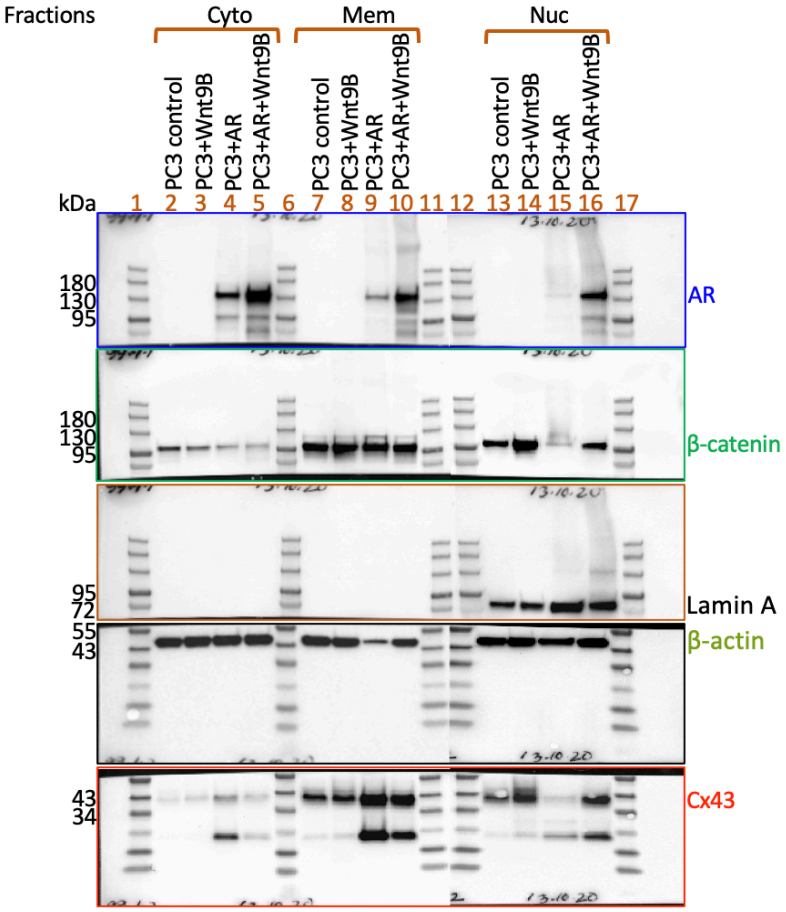

Figure 5.23: A representative WB image for translocation of AR, β-catenin and Cx43 into nucleus in PC3$^{(AR+)}$ and PC3$^{(AR+)}$ +Wnt9B. Figure description is given previously (Chap-V, Fig. 5.13). The image indicating the multiple antibodies stained single membrane.

5.9.2. Experiment-2

PC3 cells were transfected with AR and treated with Wnt9B to observe the translocation of AR, β-catenin and Cx43. The result showed that AR, β-catenin and Cx43 were translocated

a. The main stained PVDF membrane

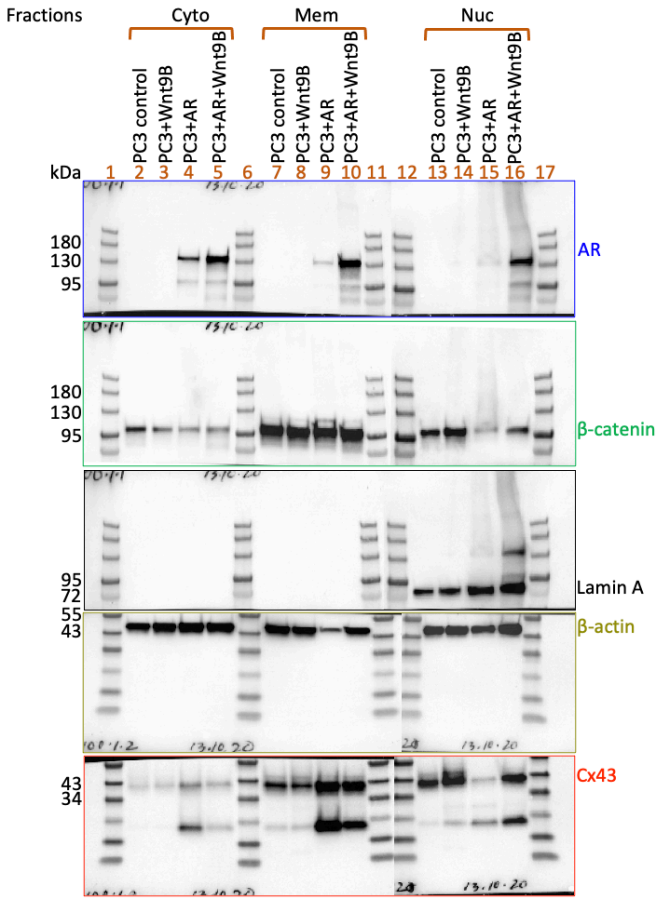

A. Western blot images

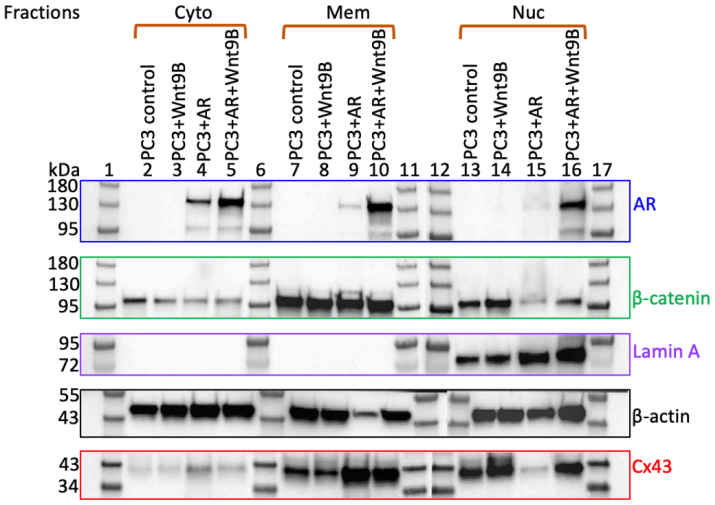

B. AR expression

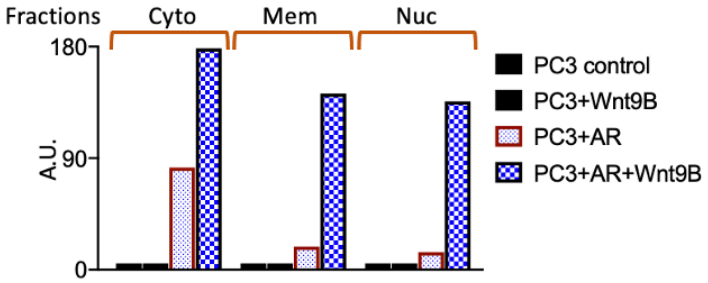

C. β-catenin expression

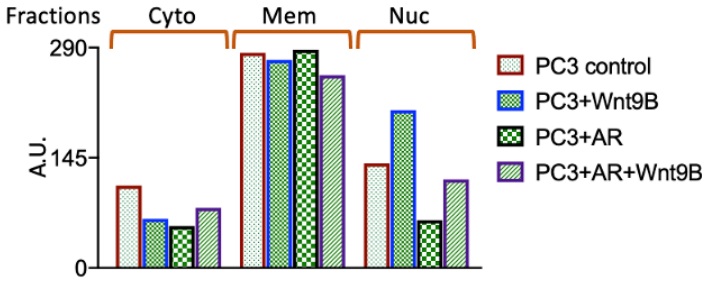

D. Cx43 expression

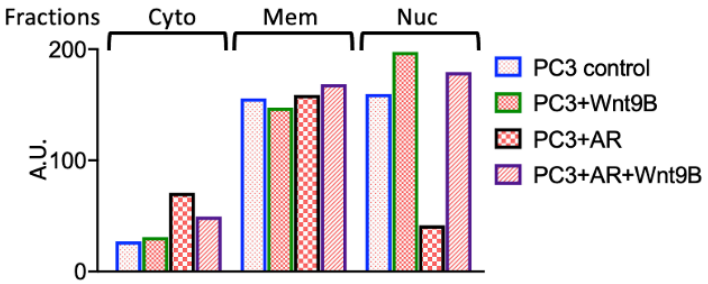

Figure 5.24: A representative WB image for translocation of AR, β-catenin and Cx43 into nucleus in $PC3^{(AR+)}$ and $PC3^{(AR+)}$ +Wnt9B. a. The image indicates the multiple antibodies stained single PVDF membrane. A. WB shows intensity of bands indicating level of protein expression. The intensity of bands was quantitated with ImageJ followed by construction of bar graphs for AR, β-catenin and Cx43 showed in B, C and D respectively.

5.9.3. Experiment-3

PC3 cell were transfected with AR and treated with Wnt9B to observe the translocation of AR, β-catenin and Cx43. The result showed that AR, β-catenin and Cx43 were translocated

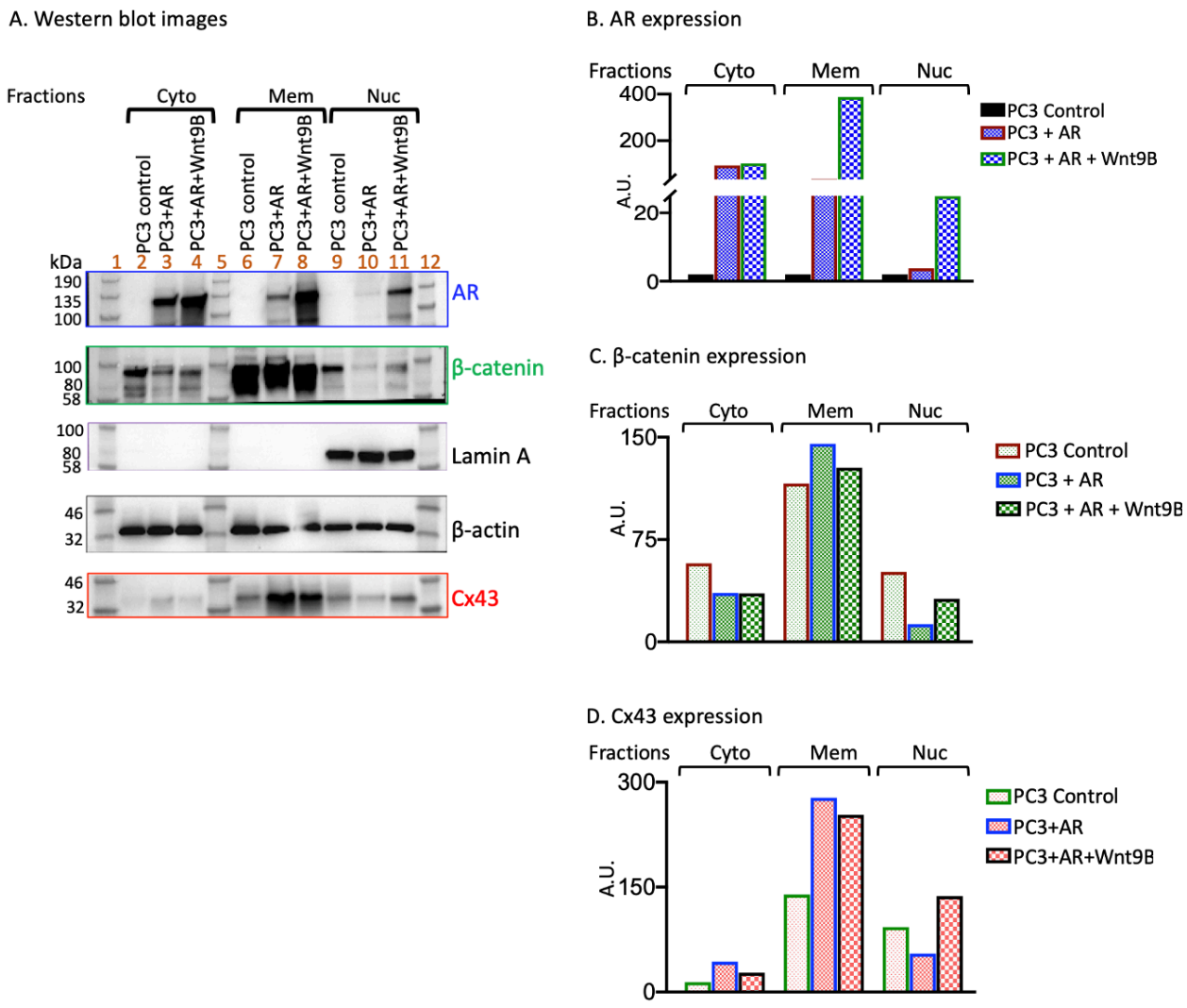

Figure 5.25: A representative WB image for translocation of AR, β-catenin and Cx43 into nucleus in PC3$^{(AR+)}$ and PC3$^{(AR+)}$ +Wnt9B cells. a. A sequential staining of the PVDF membrane with multiple antibodies shows the expression of AR, β-catenin and Cx43. Each of the proteins bands was used to construct the image A, which were used to quantitate the intensity of proteins expression using ImageJ. The results were used to construct the bar graph B, C and D for AR, β-catenin and Cx43, respectively, which indicates the translocation of AR, β-catenin and Cx43 into nucleus in PC3$^{(AR+)}$ and PC3$^{(AR+)}$ +Wnt9B cells.

5.10. Analysis of Expression of AR and Wnt signalling proteins in LnCAP cells treated DHT

5.10.1. Experiment-1: LnCAP cells were treated with DHT to study the expression of AR and Wnt signalling proteins

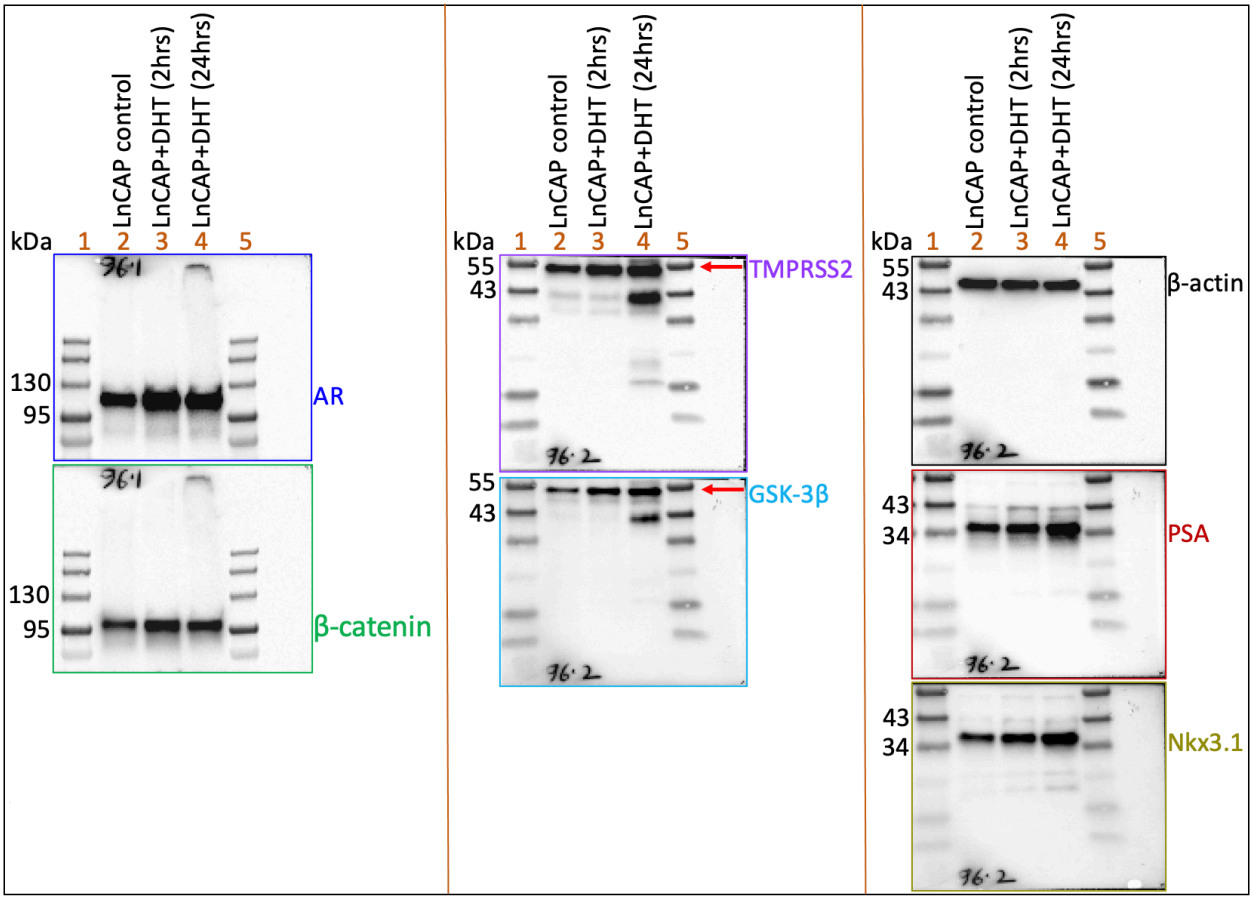

Figure 5.26: A representative WB image for the expression of AR, β-catenin, TMPRSS2, PSA, GSK-3β, Nkx3.1. The main PVDF membrane was used in multiple occasions to stain with Anti-AR antibody, anti-β-catenin antibody, anti-PSA antibody, anti-TMPRSS2 antibody, anti-Nkx3.1. The bar graph for the measurement of the expression of the proteins were incorporated in Chap-V (Fig. 5.19)

5.10.2. Experiment-2: LnCAP cells were treated with DHT to study the expression of AR and Wnt signalling proteins

a. The main stained PVDF membrane

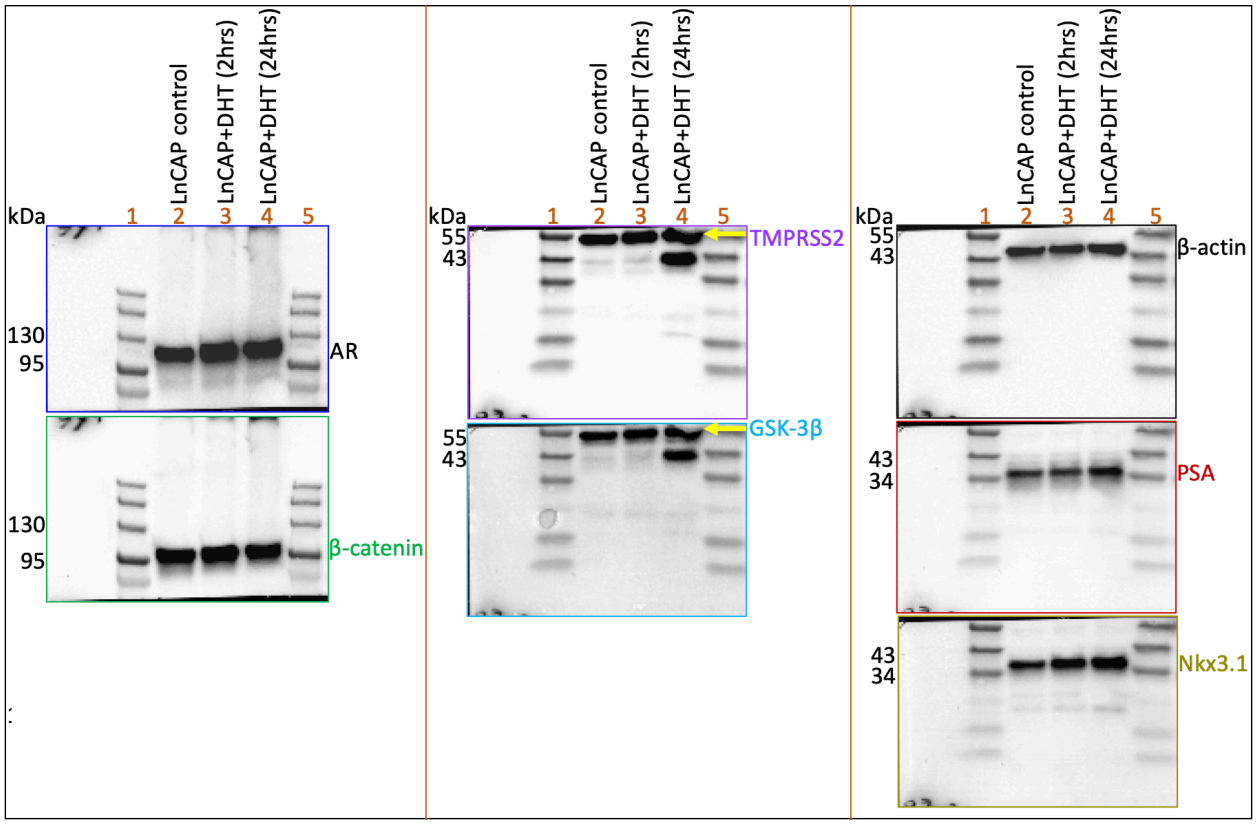

A. Western blot images

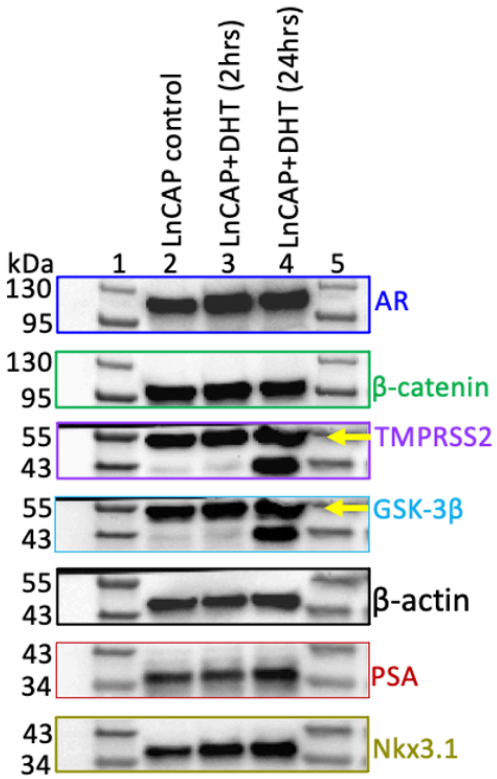

B. AR expression

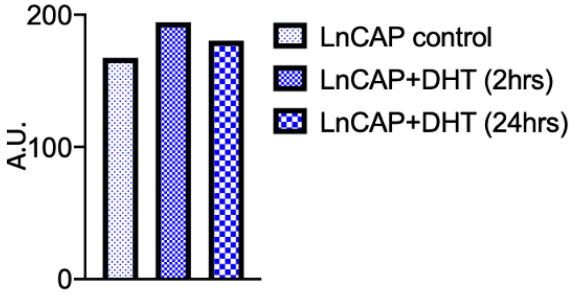

C. β-catenin expression

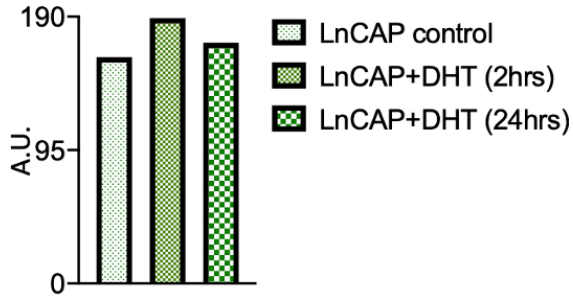

D. PSA expression

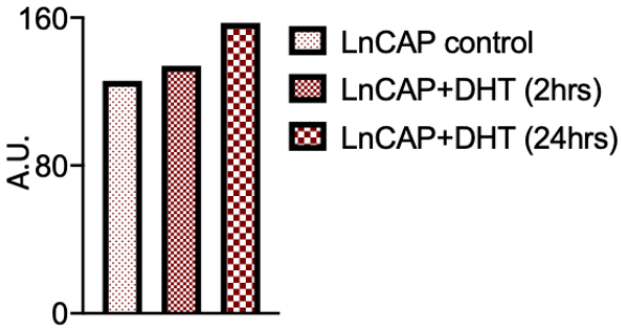

E. Nkx3.1 expression

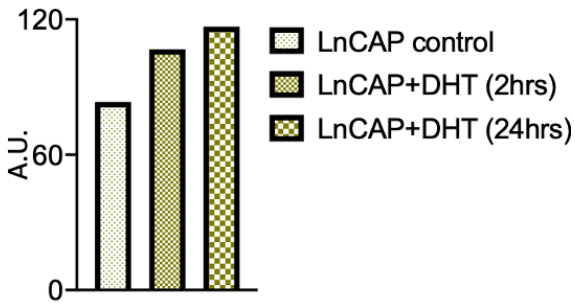

F. TMPRSS2 expression

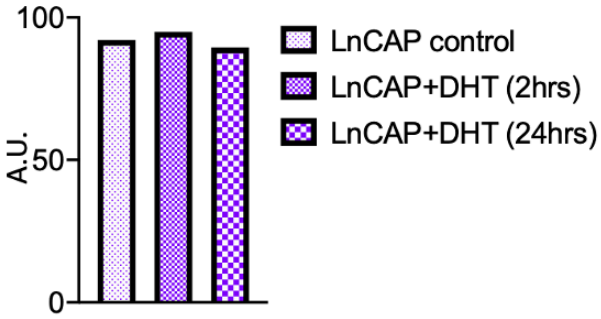

G. GSK-3β expression

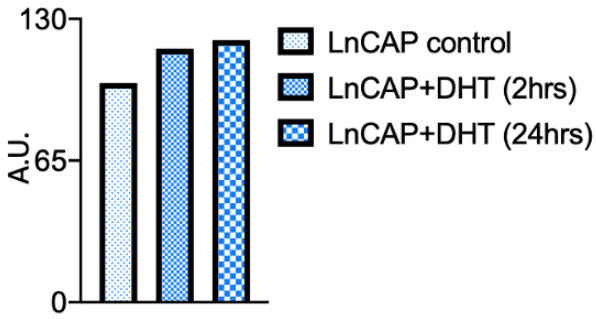

Figure 5.27: Representation of WB displaying the expression of AR, β-catenin, TMPRSS2, PSA, Nkx3.1 and GSK-3β. The main PVDF membrane was used to stain with Anti-AR antibody, anti-β-catenin antibody, antibody, anti-PSA antibody, anti-TMPRSS2 antibody, anti-Nkx3.1 and anti-phospho-GSK-3β antibodies. a. The main PVDF membrane shows the expression of AR, β-catenin, TMPRSS2, PSA, Nkx3.1 and GSK-3β proteins. The protein expression was measured and constructed the bar graphs B, C, D, E, F and G for AR, β-catenin, PSA, Nkx3.1, TMPRSS2 and GSK-3β respectively.

5.10.3. Experiment-3: LnCAP cells were treated with DHT to study the expression of AR and Wnt signalling proteins.

The main stained PVDF membrane

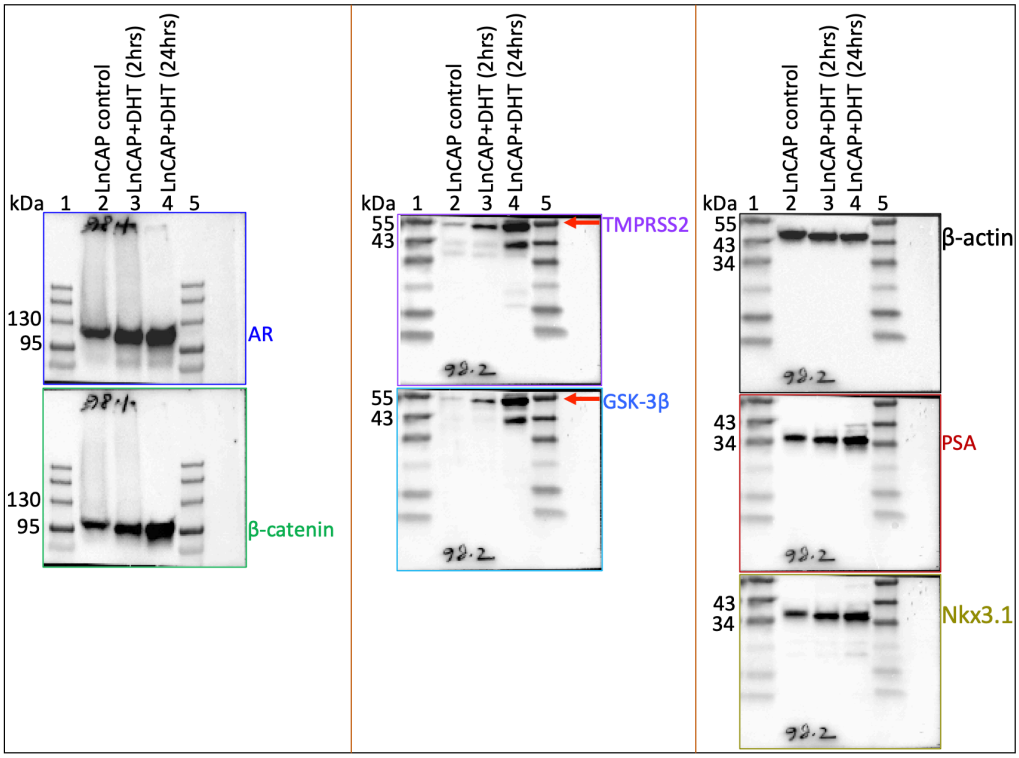

A. Western blot images

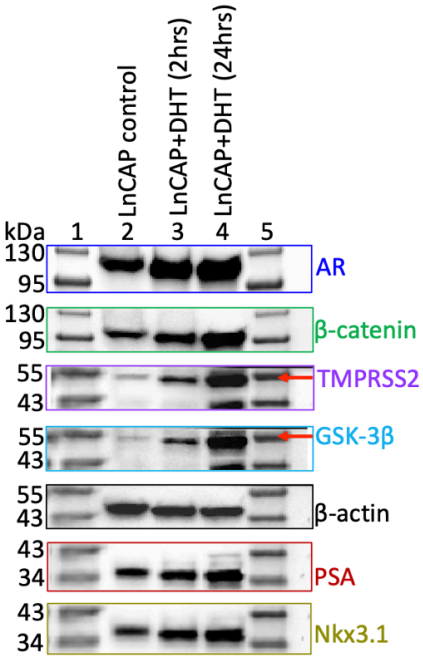

B. β-actin expression

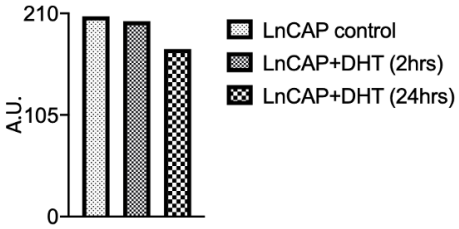

C. AR expression

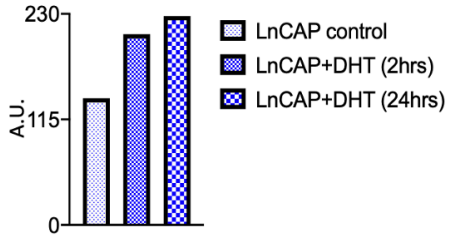

D. β-catenin expression

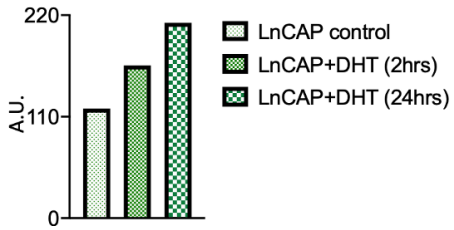

E. Nkx3.1 expression

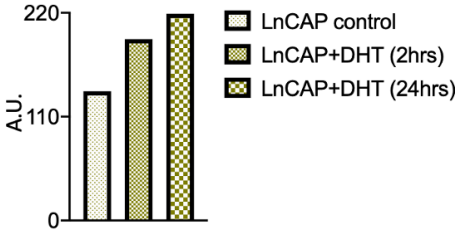

F. TMPRSS2 expression

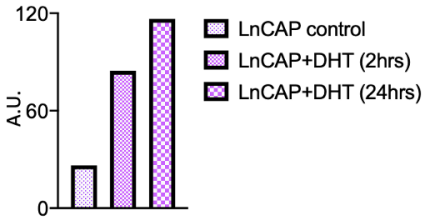

G. GSK-3β expression

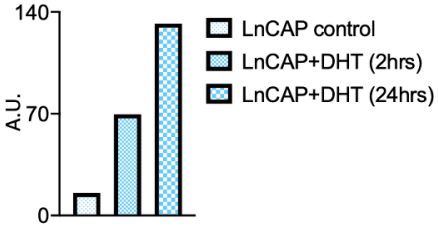

H. PSA expression

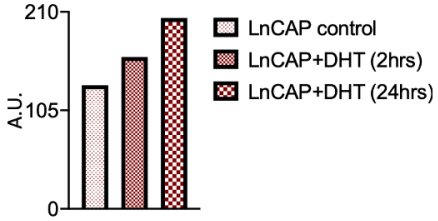

Figure 5.28: A representative WB image for the expression of AR, β-catenin, β-actin, TMPRSS2, PSA, Nkx3.1 and GSK-3β. The main PVDF membrane was used to stain with Anti-AR, -β-actin, -β-catenin, -PSA, -TMPRSS2, -Nkx3.1 and -phospho-GSK-3β antibodies. a. The main PVDF membrane shows the expression of AR, β-catenin, β-actin, TMPRSS2, PSA, Nkx3.1 and GSK-3β proteins. The protein expression was measured and constructed the bar graphs B, C, D, E, F, G and H for β-actin, AR, β-catenin, Nkx3.1, TMPRSS2, GSK-3β and PSA respectively.

5.11. Analysis of Expression of Wnt signalling protein in PC3 cells treated Wnt9B

5.11.1. Experiment-1

PC3 cells were treated with Wnt9B to study the effects of Wnt9B on expression of Wnt signalling proteins.

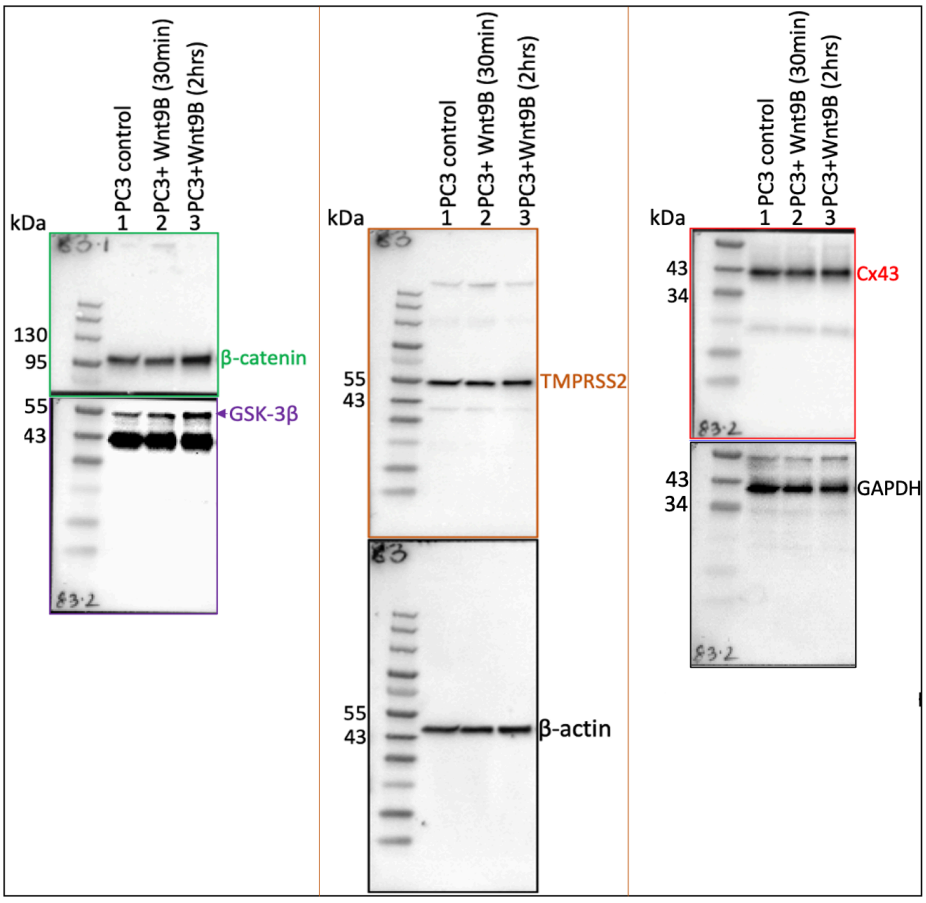

Figure 5.29. Representation of WB displaying the effect of Wnt9B on the expression of Wnt signalling proteins in PC3 cells. a. The PVDF membrane shows the expression of β-catenin, Cx43, TMPRSS2, β-actin, GAPDH was used to stain with multiple antibodies.

5.11.2. Experiment-2

PC3 cells were treated with Wnt9B to study the effect of Wnt9B on expression of Wnt signalling proteins

a. The antibody stained PVDF membrane

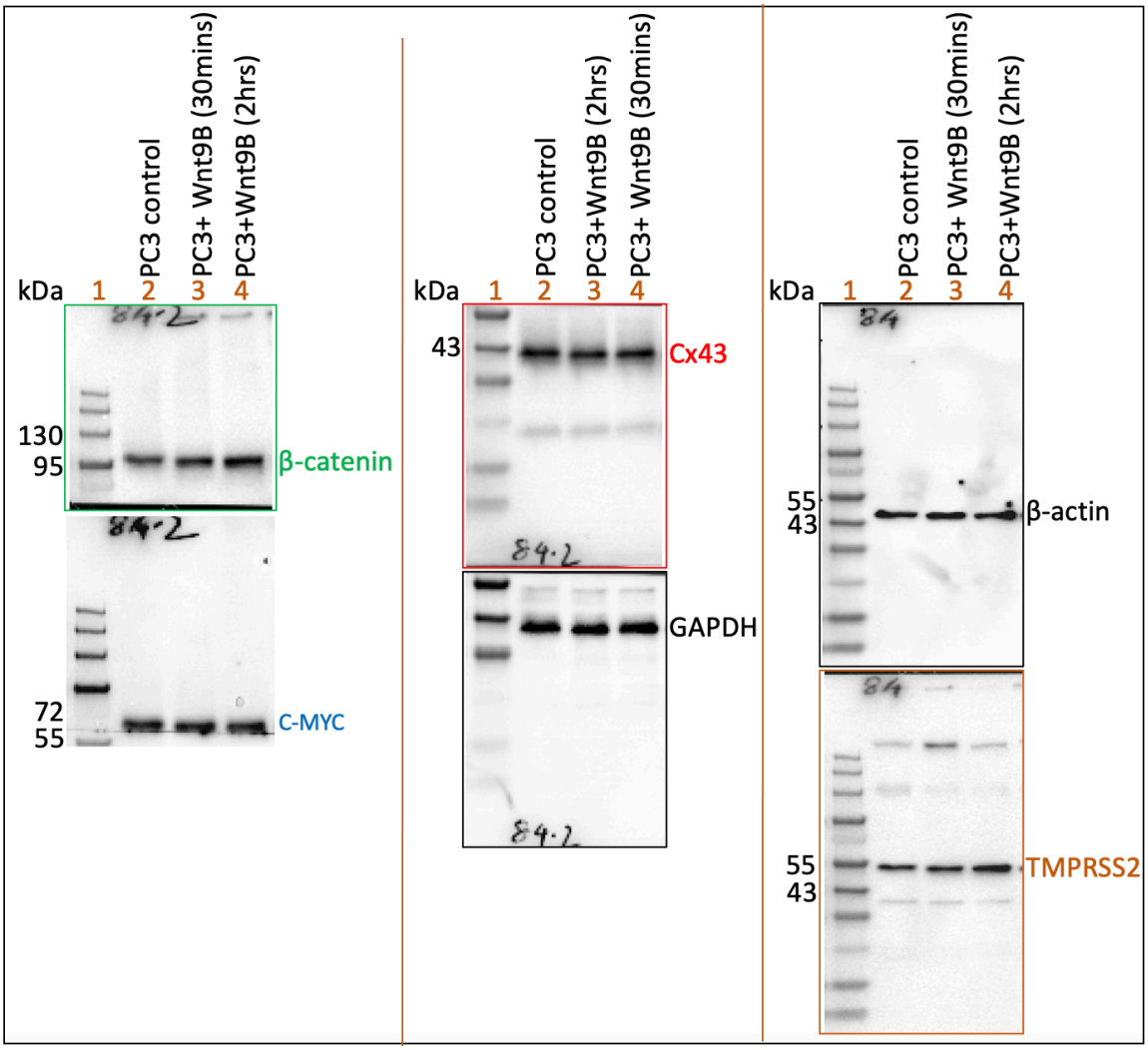

A. Western blot images

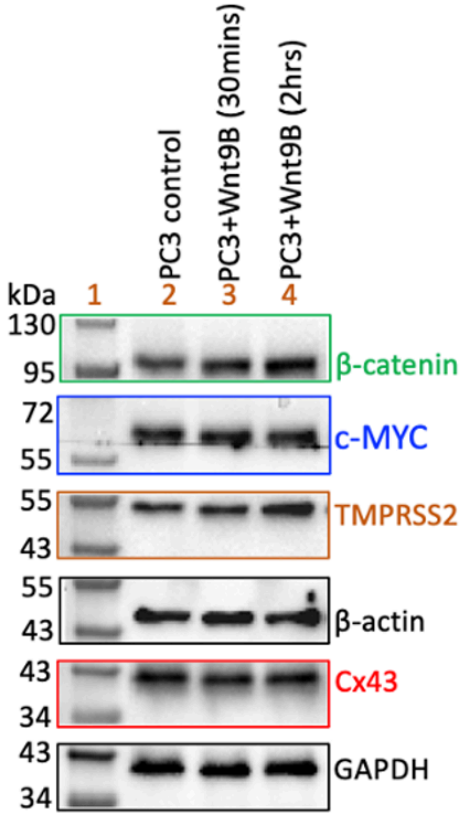

B. β-actin expression

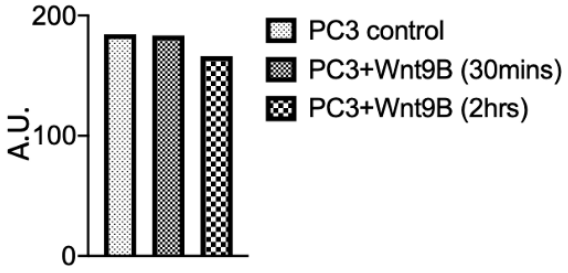

C. β-catenin expression

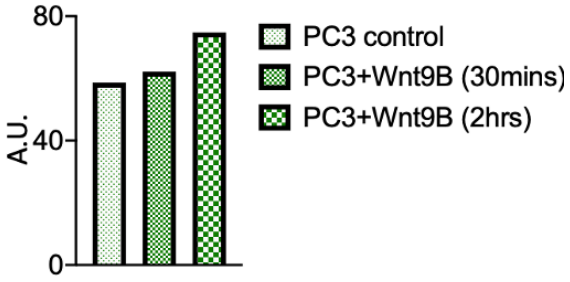

D. c-MYC expression

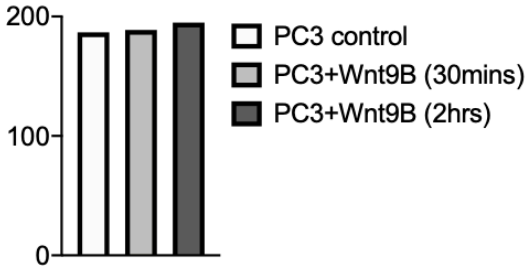

E. Cx43 expression

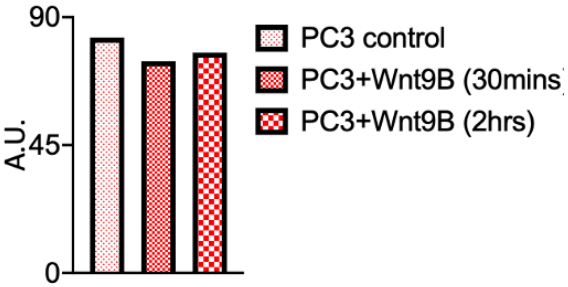

F. TMPRSS2 expression

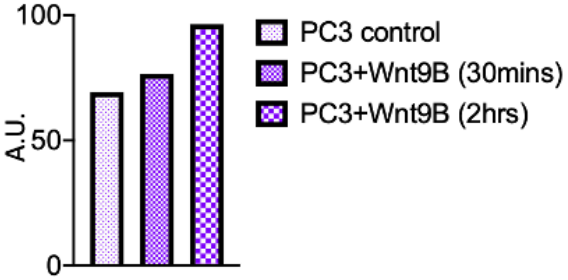

G. GAPDH expression

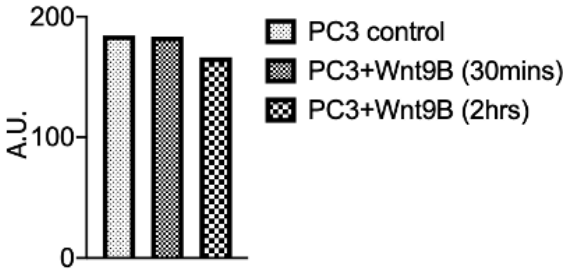

Figure 5.30. A representative WB image for the effect of Wnt9B on the expression of Wnt signalling proteins in PC3 cells. a. The PVDF membrane shows the expression of β-catenin, β-actin, c-MYC, Cx43, TMPRSS2. The protein bands were excised and produced the image A. Following quantitation of the intensity of the bands, the bar graphs B, C, D, E, F and G were constructed to illustrate the expression of β-actin, β-catenin, c-MYC, Cx43, TMPRSS2, GAPDH respectively.

5.11.3. Experiment-3

PC3 cells were treated with Wnt9B to study the effect of Wnt9B on expression of Wnt signalling proteins

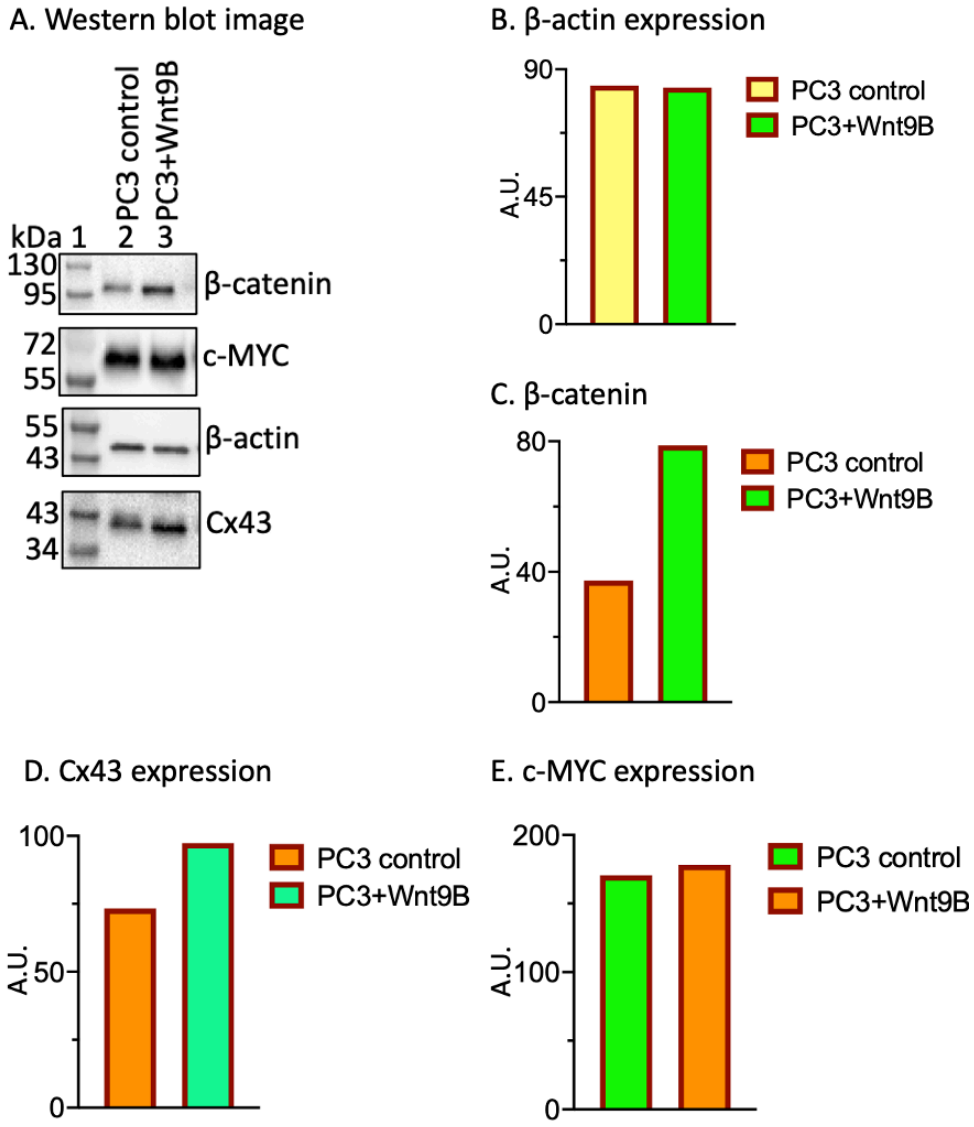

Figure 5.31. Representation of WB displaying the effect of Wnt9B on the expression of Wnt signalling proteins in PC3 cells. A. WB images shows the bands of β-actin, β-catenin, Cx43 and c-MYC which were measured and constructed bar graphs B, C, D and E to illustrate the expression of β-actin, β-catenin, Cx43 and c-MYC respectively.

The PVDF membrane was used for multiple staining sequentially with multiple antibodies. A. WB showing intensity of Band indicating level of protein expression.

5.12. Normalisation of translocation of AR, AR (N-ter), β-catenin and Cx31 into nucleus in LnCAP cells using β-actin

5.12.1. Expression of β-actin in Cytosol, membrane and nucleus in DHT treated LnCAP cells

LnCAP cells were treated with DHT at recommended dilution (Chap-5, Table 5.1). The representative WB image (Fig. 5.32) shows the expression of β-actin of three independent experiments showed in Appx.5.1. β-actin is appeared slightly increased in nucleus. DHT might have also affected the redistribution of β-actin. The redistribution of β-actin by androgen was described in a review paper (Stournaras et al., 2014).

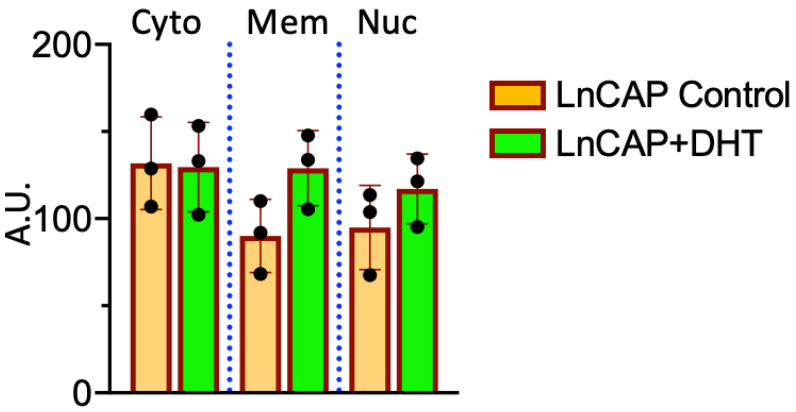

Figure 5.32. A representative WB image for the expression of β-actin in cytosol, membrane and nucleus in LnCAP cells treated with DHT.

5.12.2. Expression of β-actin in Cytosol, membrane and nucleus in Wnt3A treated LnCAP cells

LnCAP cell were treated with Wnt3A at recommended dilution (Chap-5, Table 5.1). The representative WB image (Fig. 5.33) shows the expression of β-actin of three independent experiments showed in Appx.5.1. β-actin expression was not changed in nucleus following treatment with Wnt3A, indicating same amount of protein was loaded.

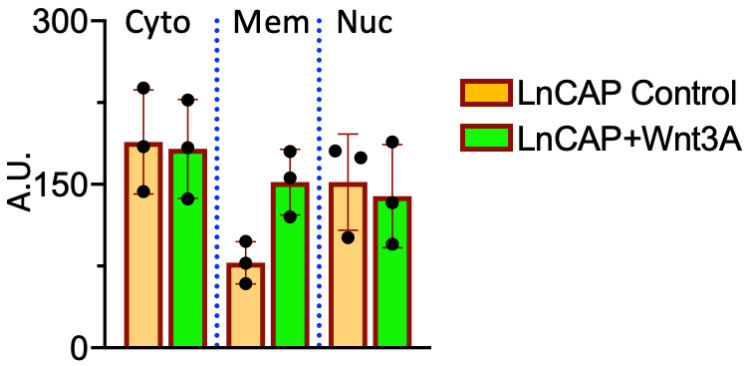

Figure 5.33. A representative WB image for the expression of β-actin in cytosol, membrane and nucleus in LnCAP cells treated with Wnt3A.

5.12.3. Expression of β-actin in Cytosol, membrane and nucleus in Wnt5A treated LnCAP cells

LnCAP cells were treated with Wnt5A at recommended dilution (Chap-5, Table 5.1). The representative WB image (Fig. 3.34) shows the expression of β-actin of three independent experiments showed in Appx.5.1. β-actin expression was not changed in nucleus following treatment with Wnt5A, indicating same amount of protein was loaded.

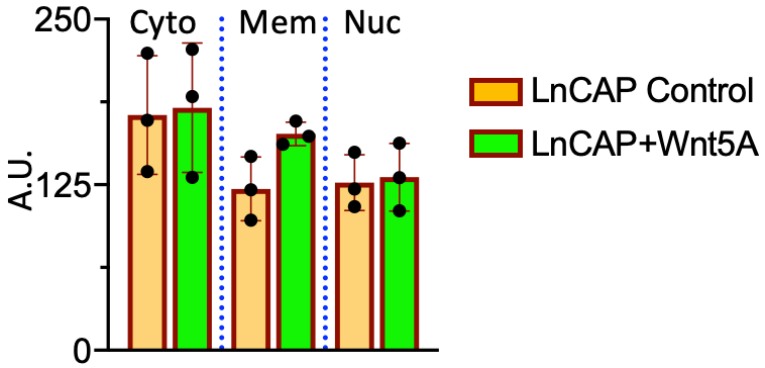

Figure 5.34. A representative WB image for the expression of β-actin in cytosol, membrane and nucleus in LnCAP cells treated with Wnt5A.

5.12.4. Expression of β-actin in Cytosol, membrane and nucleus in Wnt9B treated LnCAP cells

LnCAP cells were treated with Wnt9B at recommended dilution (Chap-5, Table 5.1). The representative WB image (Fig. 5.35) shows the expression of β-actin of three independent experiments showed in Appx.5.1. β-actin expression was not changed in nucleus following treatment with Wnt9B, indicating same amount of protein was loaded.

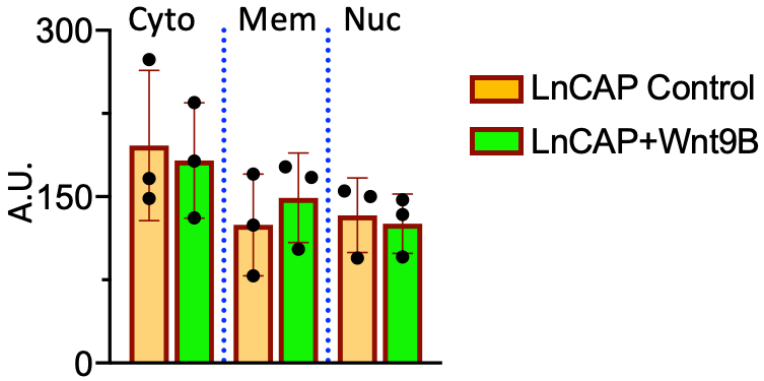

Figure 5.35. A representative WB image for the expression of β-actin in cytosol, membrane and nucleus in LnCAP cells treated with Wnt9B.

5.13. PCa cell lines

There are more PCa cell line normally used in research field.

5.13.1. The original PCa cell lines derived from primary tumours

DU145 cell line

The DU145 cells were the first PCa cell line, isolated from a brain metastatic prostate tumour of a 69-year-old man in 1975 (Mickey et al., 1977). Some of the cytokeratins such as CK-7, CK-8, CK-18 and CK-19 are expressed in DU145, where CK-5, CK14 and CK-20 are not expressed. Meanwhile, later studies showed DU145 also express CK-5. The expression of PAP is low, but AR and PSA mRNA and proteins are not expressed in DU145. Since the majority of prostate tumours express AR, these cells do not trustfully mimic the disease (Li et al., 2008).

1013L

This cell line was derived from primary prostate tumour in 1978 (Williams et al., 1978 and Williams and RD, 1980). These cells do not grow as a monolayer, grow as a small spheroids in stationary suspension cultures (Billström et al., 1995), do not express AR, PSA and urokinase type PA (Hartley-Asp et al., 1989).

E006AA

This cell line is pure epithelial cell line was developed from a 50-year-old African-American (AA) tissue in 2004 which had undergone a radical retropubic prostatectomy for clinically localised

PCa treatment (Koochekpour et al., 2004). The cells express cytokeratin-8, cytokeratin-18, Met proto-oncogene receptor and AR, but low in PSA mRNA expression.

RC-77T/E

This cell line was generated in 2010 from a radical prostatectomy received from a 63-year-old AA patient (Theodore et al., 2010), who had clinical stage T3c adenocarcinoma that was poorly differentiated (Gleason score, 7). These cells show androgen-regulated prostate-specific homeobox gene NKX 3.1, epithelial cell-specific cytokeratin-8, AR, PSA and p16.

5.13.2. Original PCa cell lines originated from Xenograft tumours

LuCAP cell line

This cell line was originated from xenograft tumours obtained from a 63-year-old white man suffering from DI prostate adenocarcinoma at autopsy (Ellis et al., 1996). This cell line has 3 sublines which were isolated from different metastases sites in this patient. The three sublines are LuCaP23.1 and 23.8 isolated from lymph node metastases and LuCAP 23.12 from liver metastases. PSA is highly expressed in these cell lines. Administering of ADT decreases PSA expression and size of xenograft tumour.

LAPC-4

This cell line was originated in 1997 from xenograft model which was the result of a series of subcutaneous xenografting of cells of a femoral PCa metastasis formed in a patient undergoing ADT (Klein et al., 1997). The cell expresses WT AR and PSA. LAPC-4 cells are used as AR-posotive PCa cells (Su et al., 2017 and Masko et al., 2017).

22Rv1 cell line

This cell line is representative of prostate carcinoma which was isolated in 1999 from the xenograft CWR22R which was obtained from a patient suffering from bone metastasis (Klein et al., 1997). The 22Rv1 cells are normally derived by plating on irradiated feeder cells followed by trypsinisation, isolation via CD44 staining. Two consecutive regrowths on feeder cells allow for the isolation of this cell line. The become double from 35-40 hours. It expresses AR and PSA

mRNA and AR proteins but not PSA protein. This cell is EGF sensitive but not inhibited by TGF-β. This cell expresses WT PTEN (Su et al., 2017; Masko et al., 2017 and Sramkoski et al., 1999).

VCAP cell line

This cell line was first originated in 2001 from a vertebral metastatic lesion utilizing a procurement team designed to implement “warm” autopsies (Navone et al., 2000; Ellis et al., 1996). This cell line is androgen sensitive and expresses WT AR and PSA mRNA as well as protein.

KUCAP cell line

The cell line was produced in 2005 from the autopsy of a liver metastasis sample collected from a Japanese 64-year-old male patient who died due to CRPC (Yoshida et al., 2005). The cell expresses AR with a W741L point mutation which is also present in ligand-binding domain in cancerous tissue used for production of KUCAP cells.

PC346

The cell was extracted from the PC346 xenograft tumour generated from a primary prostate tumour transurethral resection (Marques et al., 2006). It is androgen responsive and grows slowly in a steroid-stripped medium (Marques et al., 2006).

Publication

Hou X, Khan MRA, Turmaine M, Thrasivoulou C, Becker DL, Ahmed A. Wnt signalling regulates cytosolic translocation of connexin 43. Am J Physiol Regul Integr Comp Physiol. 2019 Aug 1;317(2): R248-R261.